Evaluation of the effects of coenzyme Q10 and succinate in a rotenone-induced complex I deficient rat model

BY

MARCO ALESSANDRINI, M.Sc.

Thesis submitted in partial fulfilment of the requirements for the degree Philosophiae Doctorae (Ph.D.) in Biochemistry at the North-West University (Potchefstroom Campus)

SUPERVISOR: Professor Antonel Olckers
Centre for Genome Research,
North-West University (Potchefstroom Campus)

CO-SUPERVISOR: Associate Professor Francois van der Westhuizen
Biochemistry,
North-West University (Potchefstroom Campus)

ASSISTANT-SUPERVISOR: Doctor Izelle Smuts
Department of Paediatrics,
University of Pretoria

September 2006

Evaluasie van die effek van koënsiem Q10 en suksinaat in 'n rotmodel met 'n rotenoon-geïnduseerde kompleks I gebrek

DEUR

MARCO ALESSANDRINI, M.Sc.

Proefskrif voorgelê vir gedeeltelike nakoming van die vereistes vir die graad Philosophiae Doctorae (Ph.D.) in Biochemie aan die Noordwes-Universiteit (Potchefstroom Kampus)

STUDIELEIER: Professor Antonel Olckers
Sentrum vir Genomiese Navorsing,
Noordwes-Universiteit (Potchefstroom Kampus)

MEDESTUDIELEIER: Mede Professor Francois van der Westhuizen
Biochemie,
Noordwes-Universiteit (Potchefstroom Kampus)

ASSISTENT-STUDIELEIER: Dokter Izelle Smuts
Departement Kindergeneeskunde,
Universiteit van Pretoria

September 2006

To those who helped me

realise this achievement,

for their support

and

commitment

ABSTRACT

Disorders of the mitochondrial respiratory chain have an incidence ranging from 1 in 2,000 to 1 in 5,000, with the most frequent of these cytopathies resulting from causative alterations within mitochondrial complex I, the first enzyme of the respiratory chain. The biochemical consequences of a complex I deficiency include, amongst others, failure to oxidise reduced nicotinamide adenine dinucleotide (NADH), impairment of the Krebs cycle, elevated blood lactate, lowered adenosine triphosphate (ATP) generation and an increased production of reactive oxygen species (ROS).

The aim of the investigation was to evaluate the effects of CoQ_{10} and succinate in a rotenone-induced animal model. Sprague Dawley rats were dosed with rotenone for a period of 14 days via oesophageal intubation, resulting in the successful establishment of a complex I deficient animal model. Upon optimisation of the rotenone concentration, rat diets were supplemented with high concentrations of either coenzyme Q10 or succinate for two days in an attempt to alleviate the biochemical manifestations of the rotenone-induced complex I deficiency. Five tissue types were collected and assayed for a total of seven biochemical parameters, which enabled the establishment of a biochemical profile of response for each of the tissue groups.

Data generated from the study revealed that rotenone, when dosed in high concentrations, contributed to the alleviation of serum hydroperoxide levels. This result was confirmed by the unexpected finding that rotenone itself harboured an antioxidant capacity equivalent to that of Trolox, the vitamin E analogue generally used for the determination of antioxidant capacity. It was therefore concluded that rotenone was not an ideal inhibitor for the evaluation of complex I deficiency and ROS-related investigations in an animal model. Since this compound is the most widely used inhibitor of complex I, the data from the study affirms the use of alternative complex I inhibition strategies. Finally, the data was suggestive of the fact that both coenzyme Q10 and succinate exclusively improved isolated components of the biochemical profile. Results generated in this study thus support current therapeutic intervention where patients receive a combination of vitamins and cofactors as part of a management strategy for the mitochondrial cytopathies.

OPSOMMING

Afwykings van die mitochondriale respiratoriese ketting het 'n insidensie wat wissel tussen 1 in 2,000 en 1 in 5,000. Die mees algemene afwykings is 'n gevolg van oorsaaklike alterasies in die mitochondriale kompleks I, die eerste ensiem van die respiratoriese ketting. Die biochemiese gevolge van 'n kompleks I gebrek, sluit in die onvermoë om NADH te oksideer, inkorting van die Krebs siklus, verhoogde bloed laktaat, verlaagde ATP generasie en 'n verhoogde produksie van ROS.

Die doel van die studie was om die effekte van ko-ensiem Q10 en suksinaat in 'n rotenoon-geinduseerde diermodel to evalueer. Sprague Dawley rotte was gedoseer met rotenoon vir 'n 14-dag periode deur middel van esofageale intubasie, wat 'n suksesvolle kompleks I gebrek diermodel tot gevolg gehad het. Tydens optimisasie van die rotenoon konsentrasie, was rotte se diëtte aangevul met hoë konsentrasies koensiem Q10 of suksinaat vir twee dae, in 'n poging om die biochemiese gevolge van die rotenoon-geïnduseerde kompleks I gebrek te oorkom. Vyf weefseltipes was versamel en geanaliseer vir 'n totaal van sewe biochemiese parameters, waarmee 'n biochemiese reaksie profiel vir elkeen van die weefsel groepe bepaal is.

Data het aangedui dat rotenoon, wanneer dit in hoë dosisse gedoseer is, bydra tot die verligting van serum hidroperoksiedvlakke. Hierdie resultaat was bevestig deur die onverwagte bevinding dat rotenoon self 'n antioksidant kapasiteit het, soortgelyk aan die van Trolox, die vitamien E analoog wat gewoonlik gebruik word vir die bepaling van antioksidant kapasiteit. Die gevolgtrekking was dus dat rotenoon nie 'n ideale inhibeerder vir die evaluasie van 'n kompleks I gebrek en ROS-verwante ondersoeke in 'n diermodel is nie. Aangesien hierdie verbinding mees algemeen gebruik word as inhibeerder van kompleks I, bevestig die data van hierdie studie die gebruik van alternatiewe kompleks I inhibisie strategieë. Ten slotte het die data aangedui dat beide ko-ensiem Q10 en suksinaat uitsluitlik geïsoleerde komponente van die biochemiese profiel verbeter het. Hierdie bevindinge ondersteun dus die huidige terapeutiese intervensie, waartydens pasiënte 'n kombinasie van vitamiene en ko-faktore ontvang, as deel van die bestuursstrategie van mitochondriale afwykings.

TABLE OF CONTENTS

LIST OF ABBREVIATIONS AND SYMBOLS i
LIST OF EQUATIONS ix
LIST OF FIGURES xi
LIST OF TABLES xiii
ACKNOWLEDGEMENTS xix

CHAPTER ONE
INTRODUCTION 1

CHAPTER TWO
MITOCHONDRIA AND ENERGY PRODUCTION 3

2.1 MITOCHONDRIA 3
2.1.1 Structure of mitochondria 4
2.1.2 The mitochondrial genome 4
2.1.3 Biogenesis of mitochondria 7
2.1.3.1 Transcription of mitochondrial DNA 8
2.1.3.2 Mitochondrial protein synthesis 10
2.1.3.3 Replication of mitochondrial DNA 11
2.2 ENERGY PRODUCTION IN EUKARYOTIC CELLS 12
2.2.1 Oxidative phosphorylation 13
2.2.2 Mitochondrial complex I 15
2.2.2.1 Subunit composition of complex I 15
2.2.2.2 Functional properties of the complex I subunits 20
2.2.3 Inhibitors of the respiratory chain 21
2.2.3.1 Rotenone 22

CHAPTER THREE
PATHOLOGY OF THE MITOCHONDRIA 25

3.1 MITOCHONDRIAL CYTOPATHIES 26
3.1.1 Chronic Progressive External Opthalmoplegia 26
3.1.2 Pearson Syndrome 27
3.1.3 Kearns-Sayre Syndrome 28
3.1.4 Myoclonus Epilepsy with Ragged-Red Fibres 28
3.1.5 Mitochondrial Myopathy, Encephalomyopathy, Lactic Acidosis and Stroke like episodes 29
3.1.6 Leber's Hereditary Optic Neuropathy 29
3.1.7 Leigh and Leigh-like Syndrome 30
3.1.8 Other mitochondrial cytopathies 31
3.2 PRESENTATION OF THE MITOCHONDRIAL CYTOPATHIES 32

3.2.1 Clinical and histological features 33
3.2.2 Biochemical consequences 35
3.2.2.1 Reactive oxygen species 36
3.2.3 Genetic aspects 38
3.3 ANIMAL MODELS FOR THE MITOCHONDRIAL CYTOPATHIES 40
3.4 COMPLEX I DEFICIENCY 41
3.5 TREATMENT OF MITOCHONDRIAL CYTOPATHY 42
3.6 AIMS OF THE STUDY 44

CHAPTER FOUR
MATERIALS AND METHODS 45

4.1 RAT PILOT STUDY 46
4.2 RAT MAIN STUDY 47
4.3 RODENT EXPERIMENTATION 48
4.3.1 Rodent husbandry and determination of rat body weights 49
4.3.2 Oesophageal intubation and dosing 49
4.4 TISSUE COLLECTION AND BIOCHEMICAL ASSAYS 50
4.4.1 Tissue and blood collection 50
4.4.2 Sample preparation and homogenisation 50
4.4.3 Mitochondrial enzyme analysis 51
4.4.3.1 Isolation of mitochondria 51
4.4.3.2 Protein concentration 52
4.4.3.3 Citrate synthase activity 52
4.4.3.4 Complex I activity 53
4.4.4 Serum hydroperoxide concentrations 54
4.4.5 Antioxidant capacity 55
4.4.6 GSH/GSSG ratio determination 56
4.4.7 Lactate/Pyruvate ratio determination 57
4.4.8 ATP/ADP ratio determination 58
4.4.9 NAD/NADH ratio determination 59
4.5 STATISTICAL EVALUATION OF DATA 60
4.5.1 Outlier analysis and basic statistics 62
4.5.2 Analysis of variance 63
4.5.2.1 Factorial analysis of variance 64
4.5.3 Multiple comparison and biological significance testing 64

CHAPTER FIVE
RESULTS AND DISCUSSION 67

5.1 METHOD OPTIMISATION AND EVALUATION 67
5.1.1 Dosage procedure 67
5.1.2 Rat body weights 69
5.1.3 Rat behaviour 71
5.1.4 Determination of complex I activity 72
5.1.5 Determination of citrate synthase activity 73
5.1.6 Protein concentration analysis 76

5.1.7 Hydroperoxide concentration analysis 77
5.1.8 Oxygen radical absorbance capacity (ORAC) analysis 77
5.1.9 Lactate and pyruvate concentrations 79
5.1.10 Glutathione assay 82
5.1.11 Concentrations of adenylates 84
5.1.12 Assay for pyridine concentrations 87
5.2 RAT BODY WEIGHTS 88
5.2.1 Rat pilot study body weights 89
5.2.2 Rat main study body weights 94
5.2.2.1 Rat main study total body weight gains and losses 95
5.2.2.2 Rat main study body weights for days 15-17 102
5.2.2.3 Rat main study body weights for days 1-15 107
5.3 RAT BLOOD DATA 113
5.3.1 Serum hydroperoxide concentrations 113
5.3.1.1 Rat pilot study serum hydroperoxide data 113
5.3.1.2 Rat main study serum hydroperoxide data 118
5.3.1.3 Comparative analysis of serum hydroperoxide data generated from the rat pilot and main studies 126
5.3.2 Plasma antioxidant capacity 129
5.3.2.1 Evaluation of the antioxidant capacity of rotenone 136
5.3.3 GSH/GSSG ratios in blood 138
5.3.4 Lactate/pyruvate ratios in blood 146
5.3.5 ATP/ADP ratios in blood 153
5.3.6 NAD/NADH ratios in blood 163
5.3.7 Blood profile of the rat main study 168
5.3.7.1 Impact of coenzyme Q10 and succinate on the rat blood profile 181
5.4 RAT HEART MUSCLE DATA 183
5.4.1 Heart organ weights 184
5.4.1.1 Rat pilot study heart weights 185
5.4.1.2 Rat main study heart weights 188
5.4.1.3 Comparative analysis of heart weight data generated from the rat pilot and main studies 193
5.4.2 Complex I activity in heart muscle 195
5.4.2.1 Pilot study complex I activity in heart muscle 195
5.4.2.2 Main study complex I activity generated from heart muscle 199
5.4.2.3 Comparative analysis of heart muscle complex I data generated from the rat pilot and main studies 207
5.4.3 Antioxidant capacity in heart muscle 209
5.4.4 Lactate/pyruvate ratios in heart muscle 214
5.4.5 ATP/ADP ratios in heart muscle 219
5.4.6 Heart muscle profile of the rat main study 226
5.4.6.1 Impact of coenzyme Q10 and succinate on rat heart muscle 230
5.5 RAT BRAIN DATA 232
5.5.1 Brain organ weights 233
5.5.1.1 Rat pilot study brain weights 233
5.5.2 Complex I activity in brain 235
5.5.2.1 Pilot study complex I activity in brain tissue 236

5.5.2.2 Main study complex I activity in brain tissue 239
5.5.2.3 Comparative analysis of brain tissue complex I data generated from the rat pilot and main studies 245
5.5.3 Antioxidant capacity in brain tissue 247
5.5.4 Lactate/pyruvate ratios in brain tissue 252
5.5.5 Brain tissue profile of the rat main study 259
5.5.5.1 Impact of coenzyme Q10 and succinate on rat brain 263
5.6 RAT SKELETAL MUSCLE DATA 265
5.6.1 Complex I activity in skeletal muscle 265
5.6.1.1 Pilot study complex I activity in skeletal muscle 265
5.6.1.2 Main study complex I activity in skeletal muscle 268
5.6.1.3 Comparative analysis of skeletal muscle complex I data generated from the rat pilot and main studies 272
5.6.2 Antioxidant capacity in skeletal muscle 274
5.6.3 Lactate/pyruvate ratios in skeletal muscle 279
5.6.4 ATP/ADP ratios in skeletal muscle 283
5.6.5 NAD/NADH ratios in skeletal muscle 290
5.6.6 Skeletal muscle profile of the rat main study 295
5.6.6.1 Impact of coenzyme Q10 and succinate on rat skeletal muscle 299
5.7 RAT LIVER DATA 301
5.7.1 Liver weights 301
5.7.1.1 Rat pilot study liver weights 301
5.7.1.2 Rat main study liver weights 305
5.7.1.3 Comparative analysis of the liver weight data generated from the rat pilot and main studies 311
5.7.2 Complex I activity in liver 313
5.7.2.1 Pilot study complex I activity in liver tissue 313
5.7.2.2 Main study complex I activity in liver tissue 316
5.7.2.3 Comparative analysis of the liver complex I data generated from the rat pilot and main studies 322
5.7.3 Antioxidant capacity in liver tissue 325
5.7.4 Lactate/pyruvate ratios in liver tissue 330
5.7.5 GSH/GSSG ratios in liver tissue 336
5.7.6 ATP/ADP ratios in liver tissue 343
5.7.7 NAD/NADH ratios in liver tissue 350
5.7.8 Liver tissue profile of the rat main study 356
5.7.8.1 Impact of coenzyme Q10 and succinate on rat liver tissue 361
5.8 COLLECTIVE PRESENTATION OF RAT PILOT AND MAIN STUDIES 363
5.8.1 Rat pilot study collective summary of data 363
5.8.2 Rat main study collective summary of data 368

CHAPTER SIX

CONCLUSIONS 375

6.1 SELECTION OF ANIMAL MODEL 378
6.2 MODEL OF STUDY DESIGN 380
6.3 MODEL OF OBSERVED EFFECTS 381

6.3.1 Respiratory chain 384
6.3.2 Cellular level 384
6.3.3 Organ level 385
6.3.4 Blood and circulation 386
6.3.5 Rat organism 387
6.4 IMPLICATIONS OF THE STUDY DESIGN 388
6.5 ROTENONE AS A COMPLEX I INHIBITOR 391
6.6 COENZYME Q10 AND SUCCINATE AS THERAPEUTIC AGENTS 392
6.7 FUTURE DIRECTIONS IN MITOCHONDRIAL MEDICINE 394

CHAPTER SEVEN
REFERENCE LIST 397

APPENDIX A
RAT WEIGHT DATA 409

APPENDIX B
COMPLEX I ACTIVITY DATA 413
B.1 RAT PILOT STUDY COMPLEX I DATA 413
B.2 RAT MAIN STUDY COMPLEX I DATA 418

APPENDIX C
ANTIOXIDANT CAPACITY DATA 425

APPENDIX D
GLUTATHIONE CONCENTRATION DATA 433

APPENDIX E
LACTATE AND PYRUVATE DATA 437

APPENDIX F
ADENYLATE DATA 445

APPENDIX G
PYRIDINE DATA 453

LIST OF ABBREVIATIONS AND SYMBOLS

Symbols and abbreviations are listed in alphanumerical order.

LIST OF SYMBOLS

α	alpha
β	beta
Δ	delta, denoting change
γ	gamma
f	fluorescence
λ	lambda
μ	mu, denoting micro (10^{-6})
®	registered trademark
™	trademark
$\bar{x}$	mean statistic
°C	degrees Centigrade
%	percent
=	equal to
<	less than
$\sqrt{}$	square root
*	asterisk, indicating dose group and data with an excluded extreme outlier
■	median data point in a box-whisker plot
+	outlier data point in a box-whisker plot
•	extreme outlier data point in a box-whisker plot
---	missing data point
:	colon, indicating ratio

LIST OF ABBREVIATIONS

1α	alpha sub-complex of human complex I
1β	beta sub-complex of human complex I
1γ	gamma sub-complex of human complex I
1λ	lambda sub-complex of human complex I
3'	3 prime
5'	5 prime
28S	28 Svedberg unit
39S	39 Svedberg unit
55S	55 Svedberg unit
12S rRNA	12 Svedberg unit ribosomal ribonucleic acid
16S rRNA	16 Svedberg unit ribosomal ribonucleic acid
A	adenine
A_1	initial absorbency
A_2	final absorbency
A_{rs}	rotenone sensitive absorbency
A_{ri}	rotenone insensitive absorbency
AAPH	2,2'-azobis(2-amidinopropane) dihydrochloride
AC	antioxidant capacity
AC.prot^{-1}	antioxidant capacity in terms of protein
ADH	alcohol dehydrogenase

ADP	adenosine diphosphate
Ala	alanine
ANOVA	analysis of variance
Arg	arginine
Asn	asparagine
Asp	aspartic acid
ATP	adenosine triphosphate
ATP 6	ATP synthase subunit 6
ATP 8	ATP synthase subunit 8
ATP/ADP	ratio of adenosine triphosphate to adenosine diphosphate
AUC	area under the curve
BCA	bicinchoninic acid
BSA	bovine serum albumin
bp	base pair
C	carbon (in chemical structures and formulae)
C	cytosine (in DNA sequence)
C	Factor-2 dose code representing a CoQ_{10} treatment
C57BL	parent mouse strain originating from the mating of female 57 with male 52
C57BL/6	black mouse strain originating from C57 parent strain
CARR U	Carratelli units
CGR	Centre for Genome Research
CIA	complex I activity
$CIA.prot^{-1}$	complex I activity in relation to protein content
$CIA.UCS^{-1}$	complex I activity per units citrate synthase
cm	centimetre: 10^{-2} metre
CO	carbon monoxide
CO_2	carbon dioxide
CO I	cytochrome c oxidase I
CO II	cytochrome c oxidase II
CO III	cytochrome c oxidase III
CoA	coenzyme A
Conc	concentration
CoQ_1	coenzyme Q1
CoQ_{10}	coenzyme Q10
COX10	cytochrome c oxidase subunit 10
COX15	cytochrome c oxidase subunit 15
CPEO	Chronic Progressive External Opthalmoplegia
CRS	Cambridge Reference Sequence
CSA	citrate synthase activity
$CSA.prot^{-1}$	citrate synthase activity in relation to protein content
CSB I	conserved sequence blocks I
CSB II	conserved sequence blocks II
CSB III	conserved sequence blocks III
Cu^{+}	copper ion
Cu^{2+}	copper II ion
$CuSO_4.5H_2O$	copper (II) sulphate pentahydrate
Cys	cysteine
cyt b	cytochrome b
cyt c	cytochrome c
d	effect size value representing biological significance
ddH_2O	double distilled water
DCCD	dicyclohexylcarbodimide
D-loop	displacement loop
DMSO	dimethylsulphoxide
DNA	deoxyribonucleic acid
d-ROMs	Diacron reactive oxygen metabolites
DTNB	5,5'dithio-bis(2-nitrobenzoic acid)
E	enhancer element
EDTA	ethylenediamine tetraacetic acid: $C_{10}H_{16}N_2O_8$
EOs	extreme outliers

ER	excluding rotenone
et al.	*et alii* (and others)
EtOH	ethanol: CH_3CH_2OH
EXCL	excluded data point
F	F-statistic
F1	Factor-1
F2	Factor-2
F1*F2	interaction between Factor-1 and Factor-2
f_0	initial fluorescence
f_i	fluorescence at time i
Factor-1	dose regimen received by rats of the main study from day 1 to day 14
Factor-2	dose regimen received by rats of the main study on days 15 and 16
Fe_2S_2	binuclear iron-sulphur
Fe_4S_4	tetranuclear iron-sulphur
FMN	flavin mononucleotide
g	gram
G	guanine
G6PD	glucose-6-phosphate dehydrogenase
$g.day^{-1}$	grams per day
Gln	glutamine
Glu	glutamic acid
Gly	glycine
GR	glutathione reductase
GRACILE	Growth Retardation, Aminoaciduria, Cholestasis, Iron overload, Lactic acidosis and Early death
GPT	glutamate-pyruvate transaminase
GSH	reduced glutathione
GSH/GSSG	ratio of reduced to oxidised glutathione
GSSG	oxidised glutathione
GTP	guanosine triphosphate
H	hydrogen molecule (in chemical structures and formulae)
H^+	hydrogen ion (proton)
H_2O	water
H_2O_2	hydrogen peroxide
HCl	hydrochloric acid
HeLa	Henrietta Lacks cancer cell-line
His	histidine
HP	hydrophobic protein fraction of complex I
HPs	hydroperoxides
H-strand	heavy strand
HSD	Honestly Significant Difference (of Tukey multiple comparison procedure)
HSP	H-strand promoter
i.e.	*id est* (that is)
Ile	isoleucine
IP	iron-sulphur protein fraction of complex I
IQR	inter-quartile range
IR	including rotenone
IT_{H1}	H-strand transcription initiation site 1
IT_{H2}	H-strand transcription initiation site 2
IT_L	L-strand transcription initiation site
kb	kilo (10^3) base pair
kDa	kilo-Dalton
KCl	potassium chloride
KCN	potassium cyanide
K_2HPO_4	dibasic potassium phosphate
KH_2PO_4	monobasic potassium phosphate
K_3PO_4	tribasic potassium phosphate
KSS	Kearns-Sayre Syndrome
Leu^{CUN}	leucine with anticodon CUN
Leu^{UUR}	leucine with anticodon UUR

L	litre
L/P	ratio of lactate to pyruvate
LCI	lower 95% confidence interval data point
LDAO	lauryldimethylamine oxide
LDH	lactate dehydrogenase
LHON	Leber's Hereditary Optic Neuropathy
L-strand	light strand
LSP	L-strand promoter
Lys	lysine
µg	microgram
$\mu g.\mu L^{-1}$	microgram per microlitre
$\mu g.mL^{-1}$	microgram per millilitre
µL	microlitre
µM	micromolar concentration
$\mu M.\mu g^{-1}$	micromolar per microgram
µM TE	micromolar Trolox equivalents
$\mu M\ TE.\mu g^{-1}$	micromolar Trolox equivalents per microgram
$\mu mol.L^{-1}$	micromole per litre
$\mu mol.min^{-1}$	micromole per minute
$\mu mol.min^{-1}.\mu g^{-1}$	micromole per minute per microgram
M	molar concentration
M2EP	1-methyl-2-(2 thioethyl) pyridinium
M2VP	1-methyl-2-vinyl-pyridinium trifluoromethane sulphonate
Max	maximum
MELAS	Mitochondrial myopathy, Encephalomyopathy, Lactic Acidosis and Stroke-like episodes
MERRF	Myoclonus Epilepsy with Ragged-Red Fibres
Met	methionine
mg	milligram
$mg.mL^{-1}$	milligram per millilitre
$MgCl_2$	magnesium chloride
$mg.kg^{-1}$	milligram per kilogram
$mg.kg^{-1}.day^{-1}$	milligram per kilogram per day
min	minute
Min	minimum
mL	millilitres
$mL.kg^{-1}$	millilitre per kilogram
mm	millimetre
mM	millimolar concentration
$mM^{-1}.cm^{-1}$	per millimolar per centimetre
$mmol.min^{-1}$	millimole per minute
MNGIE	Mitochondrial Neuro-Gastro-Intestinal Encephalomyopathy
mRNA	messenger RNA
MSE	mean square of the error
mtDNA	mitochondrial DNA
mtIF 2	mitochondrial initiation factor-2
mtRNase P	mitochondrial ribonuclease P
MTT	thiazolyl blue tetrazolium bromide
MTT-(H)	reduced thiazolyl blue tetrazolium bromide
mtTERF	mitochondrial transcription terminating factor
mtTERM	mitochondrial transcription terminating site
mtTFA	mitochondrial transcription factor
n	cohort size when referring to a sample
n	non-significant when referring to statistical significance
N	dose code representing a no dose treatment
N	normality (when referring to a concentration)
N/A	not applicable
NAD	oxidised nicotinamide adenine dinucleotide
NAD/NADH	ratio of oxidised to reduced nicotinamide adenine dinucleotide
NADH	reduced nicotinamide adenine dinucleotide

NADP	oxidised nicotinamide adenine dinucleotide phosphate
NADPH	reduced nicotinamide adenine dinucleotide phosphate
$NaHCO_3$	sodium bicarbonate
Na_2CO_3	sodium carbonate
NaH_2PO_4	anhydrous monobasic sodium phosphate
$nmol.min^{-1}.UCS^{-1}$	nanomole per minute per unit citrate synthase
NaOH	sodium hydroxide
$NaPO_4$	sodium phosphate
NARP	Neurogenic muscle weakness, Ataxia and Retinitis Pigmentosa
ND	NADH dehydrogenase
ND1-6	NADH dehydrogenase subunits 1-6
NDH2	NADH dehydrogenase 2
NDI1	*Saccharomyces cerevisiae* NADH dehydrogenase enzyme
nDNA	nuclear DNA
NDUFA1-13	NADH-ubiquinone oxidoreductase alpha (α) sub-complex units 1 to 13
NDUFAB1	NADH-ubiquinone oxidoreductase acyl carrier protein of the beta (β) sub-complex unit 1
NDUFB1-11	NADH-ubiquinone oxidoreductase beta (β) sub-complex units 1 to 11
NDUFC1-2	NADH-ubiquinone oxidoreductase lambda (λ) sub-complex units 1 to 2
NDUFS1-6	NADH-ubiquinone oxidoreductase iron-sulphur proteins 1 to 6
NDUFV1-3	NADH-ubiquinone oxidoreductase flavoproteins 1 to 3
NN	dose group of the rat main study that received a no dose Factor-1 and Factor-2 treatment
NO	nitric oxide
nm	nanometre
nM	nanomolar concentration
$nM.\mu g^{-1}$	nanomolar per microgram
$nmol.\mu g^{-1}$	nanomole per microgram
$nmol.min^{-1}.UCS^{-1}$	nanomole per minute per unit citrate synthase
$nmol.min^{-1}.\mu g^{-1}$	nanomole per minute per microgram
O	oxygen atom
O_2	molecular oxygen
O_2^-	superoxide
OG_{CON}	oxidised glutathione concentration
$OG.prot^{-1}$	oxidised glutathione in terms of protein
O_H	H-strand origin of replication
OH^-	hydroxyl radicals
O_L	L-strand origin of replication
OMIM	online Mendelian inheritance in man
$ONOO^-$	peroxynitrite
$OP.prot^{-1}$	oxidised pyridines in terms of protein
ORAC	oxygen radical absorbance capacity
OXPHOS	oxidative phosphorylation
p	p-value: in a statistical context
p	short arm of chromosome: in a genetic context
P_{CON}	protein concentration
P_{CIA}	amount of protein used in the assay for complex I activity
P_{CSA}	amount of protein used in the assay for citrate synthase activity
PBS	phosphate buffered saline
PCA	perchloric acid
PDH	pyruvate dehydrogenase
PEG	polyethylene glycol
PES	phenazine ethosulphate
PES-(H)	reduced phenazine ethosulphate
pH	power of hydrogen, indicating acidity: numerically equal to the negative logarithm of H^+ concentration expressed in molarity
Phe	phenylalanine
PK	pyruvate kinase
Pro	praline
(Pty) Ltd	proprietary limited

q	long arm of a chromosome
R	dose code representing rotenone treatment
r^2	square of the Pearson product moment correlation coefficient
R3	dose group of the rat pilot study that received rotenone 3 $mg.kg^{-1}.day^{-1}$
R6	dose group of the rat pilot study that received rotenone 6 $mg.kg^{-1}.day^{-1}$
R9	dose group of the rat pilot study that received rotenone 9 $mg.kg^{-1}.day^{-1}$
R12	dose group of the rat pilot study that received rotenone 12 $mg.kg^{-1}.day^{-1}$
R15	dose group of the rat pilot study that received rotenone 15 $mg.kg^{-1}.day^{-1}$
RC	dose group of the rat main study that received a rotenone Factor-1 and CoQ_{10} Factor-2 treatment
$RG.prot^{-1}$	reduced glutathione in terms of protein
RN	dose group of the rat main study that received a rotenone Factor-1 and no dose Factor-2 treatment
RNA	ribonucleic acid
Rnase MRP	mitochondrial RNA processing endonuclease
ROS	reactive oxygen species
rotenone sensitive	including rotenone: indicating total activity of complex I, thus already corrected by the subtraction of the measurable complex I activity that can not be inhibited by rotenone
rotenone insensitive	excluding rotenone
RP_{CON}	reduced pyridine concentration
$RP.prot^{-1}$	reduced pyridines in terms of protein
rRNA	ribosomal ribonucleic acid
RS	dose group of the rat main study that received a rotenone Factor-1 and succinate Factor-2 treatment
RV	dose group of the rat main study that received a rotenone Factor-1 and vehicle Factor-2 treatment
RX	dose group of the rat main study that received a rotenone Factor-1 and sacrifice Factor-2 treatment
s	significant
S	dose code representing succinate treatment
SCO1	*Saccharomyces* cytochrome oxidase homolog subunit 1
SCO2	*Saccharomyces* cytochrome oxidase homolog subunit 2
SD	standard deviation
SD_{max}	maximum standard deviation between two means
Ser^{AGY}	serine with anticodon AGY
Ser^{UCN}	serine with anticodon UCN
SET buffer	0.25 M sucrose, 2 mM EDTA and 10 mM Tris-HCl buffer (pH = 7.4)
SURF1	surfeit locus 1
t	time
T	thymine
TGA	thymine-guanine-adenine
TAS	termination associated sequence
TCA	tricarboxylic acid
TE	Trolox equivalents
TG_{CON}	total glutathione concentration
$TG.prot^{-1}$	total glutathione in terms of protein
Thr	threonine
TNB	thionitrobenzoic acid
TP_{CON}	total pyridine concentration
$TP.prot^{-1}$	total pyridines in terms of protein
tRNA	transfer RNA
$tRNA^{fMet}$	transfer RNA N-formyl-methionyl
$tRNA^{Leu(UUR)}$	transfer RNA for leucine with anticodon UUR
$tRNA^{Lys}$	transfer RNA for lysine
$tRNA^{Met}$	transfer RNA for methionine
$tRNA^{Ser(UCN)}$	transfer RNA for serine with anticodon UCN
$tRNA^{Phe}$	transfer RNA for phenylalanine
$tRNA^{Pro}$	transfer RNA for proline
Tris-HCl	2-amino-2-2(hydroxymethyl)-1,3-propanediol hydrochloride: $C_4H_{11}NO_3.H_2O$
Triton X-100	t-octylphenoxypolyethoxyethanol: $C_{14}H_{22}O(C_2H_4O)_n$

Trp	tryptophan
Tyr	tyrosine
U	uridine
$U.\mu L^{-1}$	units per microlitre
UCI	upper 95% confidence interval data point
UCS	units citrate synthase
UHDBT	5-n-undecyl-6-hydroxy-4,7-dioxobenzothiazol
UQ	ubiquinone
UQH_2	ubiquinol
v	sample volume
V	total reaction volume: when referring to analytical data
V	dose code representing vehicle treatment: when referring to study design
Val	valine
VC	dose group of the rat main study that received a vehicle Factor-1 and CoQ_{10} Factor-2 treatment
VN	dose group of the rat main study that received a vehicle Factor-1 and no dose Factor-2 treatment
VS	dose group of the rat main study that received a vehicle Factor-1 and succinate Factor-2 treatment
VV	dose group of the rat main study that received a vehicle Factor-1 and vehicle Factor-2 treatment
VX	dose group of the rat main study that received a vehicle Factor-1 and sacrifice Factor-2 treatment
w/v	weight to volume ratio
X	dose code representing a sacrifice treatment
x	number of isoprenoid side-chains (in chemical structures and formulae)
x g	gravitational force

LIST OF EQUATIONS

Equation	Heading	Page
Equation 4.1	Citrate synthase activity	53
Equation 4.2	Complex I activity	54
Equation 4.3	Calculation of d ROMs Carratelli Units (CARR U)	54
Equation 4.4	Calculation of antioxidant capacity	55
Equation 4.5	GSH/GSSG ratio calculation	57
Equation 4.6	Calculation for the ratio of lactate to pyruvate	58
Equation 4.7	Calculation for the ratio of ATP to ADP	59
Equation 4.8	Calculation for the ratio of NAD to NADH	60
Equation 4.9	Test for biological significance	65

LIST OF FIGURES

Figure	Heading	Page
Figure 2.1	Electron microscopic view of a mammalian mitochondrion	4
Figure 2.2	Diagrammatic representation of the mitochondrial genome	6
Figure 2.3	Diagrammatic representation of the transcriptional elements involved in mitochondrial transcription	9
Figure 2.4	Diagrammatic representation of mitochondrial H strand replication	11
Figure 2.5	Diagrammatic representation of oxidative phosphorylation	14
Figure 2.6	Diagrammatic representation of mitochondrial complex I	18
Figure 2.7	Schematic representations of the chemical structures of rotenone and coenzyme Q	23
Figure 3.1	Photographic representation of the ragged-red fibre appearance of muscle obtained from patients with mitochondrial defects	34
Figure 4.1	Flow chart illustrating the design of the rat pilot study	46
Figure 4.2	Flow chart illustrating the design of the rat main study	48
Figure 4.3	Flow chart illustrating the statistical strategy adopted for the rat pilot and main studies	61
Figure 4.4	Schematic representation of a box whisker plot and outlier ranges	62
Figure 5.1	Photographic representations of dosage needles and oesophageal intubation in rodents	68
Figure 5.2	Schematic representation of the biochemical relationship between lactate and pyruvate	79
Figure 5.3	Diagrammatic representation of the GSH/GSSG assay	82
Figure 5.4	Diagrammatic representation of the ATP/ADP assay	84
Figure 5.5	Spectrophotometric data generated by assaying concentrations of adenylates	85
Figure 5.6	Diagrammatic representation of the NAD/NADH assay	87
Figure 6.1	Model of study design for the rat main study	380
Figure 6.2	Model representing a network of effects of therapeutic regimens in the presence of a rotenone induced Complex I deficiency in rats	382

LIST OF TABLES

Table	Heading	Page
Table 2.1	The nuclear encoded subunits of complex I	16
Table 2.2	Listing of the most common inhibitors of the respiratory chain	22
Table 3.1	Primary characteristics of mitochondrial cytopathies	34
Table 3.2	Biochemical consequences of respiratory chain defects	35
Table 3.3	Reported mutations within complex I subunit genes	41
Table 3.4	Reported therapeutic intervention strategies for complex I deficiency	43
Table 4.1	List of basic descriptive statistics utilised in the study to define central tendency and variation	63
Table 5.1	Daily recording of rat pilot study body weights	70
Table 5.2	Spectrophotometric data generated via the analysis of complex I activity	72
Table 5.3	Spectrophotometric data generated via the optimisation of citrate synthase activity	74
Table 5.4	Graphic representation of a linear standard curve generated for the determination of protein concentration	76
Table 5.5	Spectrophotometric data generated via the determination of sample antioxidant capacity	78
Table 5.6	Spectrophotometric data generated by assaying varied concentrations of lactate and pyruvate	80
Table 5.7	Spectrophotometric data generated by assaying varied concentrations of glutathione	83
Table 5.8	Spectrophotometric data generated by assaying varied concentrations of nicotinamide adenine dinucleotide	88
Table 5.9	Box whisker representation and descriptive statistics of the rat body weight data generated from the rat pilot study	90
Table 5.10	Multiple comparison statistics of body weight data generated from the rat pilot study	92
Table 5.11	Box whisker representation and descriptive statistics of the total rat weight data generated from the main study	96
Table 5.12	Multiple comparison statistics of total body weight data generated from the rat main study	98
Table 5.13	Graphic and tabulated summary of the rat main study total body weight data analysed via a two-way ANOVA	100
Table 5.14	Box whisker representation and descriptive statistics of the day 15 to 17 body weight data generated from the rat main study	104
Table 5.15	Multiple comparison statistics of day 15 to 17 body weight data generated from the rat main study	106
Table 5.16	Box whisker representation and descriptive statistics of the day 1 to 15 rat weight data generated from the main and pilot studies	109
Table 5.17	Multiple comparison statistics of day 1 to 15 body weight data generated from the rat pilot and main studies	110
Table 5.18	Oxidative stress severity in humans according to the d ROMs kit	113
Table 5.19	Box whisker representation and descriptive statistics of the serum hydroperoxide data generated from the rat pilot study	114
Table 5.20	Multiple comparison statistics of the serum hydroperoxide data generated from the rat pilot study	116
Table 5.21	Box whisker representation and descriptive statistics of the serum hydroperoxide data generated from the rat main study	120
Table 5.22	Multiple comparison statistics of the serum hydroperoxide data generated from the rat main study	122
Table 5.23	Graphic and tabulated summary of the hydroperoxide data analysed via a two-way ANOVA	125
Table 5.24	Summary of serum hydroperoxide data generated from comparative dose groups of the rat pilot and main studies	127

Table 5.25 Box whisker representation and descriptive statistics of the plasma antioxidant capacity data generated from the main study 130
Table 5.26 Multiple comparison statistics of the plasma antioxidant capacity data generated from the rat main study 131
Table 5.27 Graphic and tabulated summary of the plasma antioxidant capacity data analysed via a two-way ANOVA 135
Table 5.28 Fluorescent decay curves and antioxidant capacity of rotenone in relation to Trolox 137
Table 5.29 Box whisker representation and descriptive statistics of the blood GSH/GSSG ratio data generated from the main study 138
Table 5.30 Multiple comparison statistics of the blood GSH/GSSG ratio data generated from the rat main study 141
Table 5.31 Graphic and tabulated summary of the blood GSH/GSSG ratio data analysed via a two-way ANOVA 145
Table 5.32 Box whisker representation and descriptive statistics of the blood L/P ratio data generated from the main study 148
Table 5.33 Multiple comparison statistics of the blood L/P ratio data generated from the rat main study 149
Table 5.34 Graphic and tabulated summary of the blood L/P ratio data analysed via a two-way ANOVA 150
Table 5.35 Box whisker representation and descriptive statistics of the blood ATP/ADP ratio data generated from the main study 154
Table 5.36 Multiple comparison statistics of the blood ATP/ADP ratio data generated from the rat main study 158
Table 5.37 Graphic and tabulated summary of the blood ATP/ADP ratio data analysed via a two-way ANOVA 162
Table 5.38 Box whisker representation and descriptive statistics of the blood NAD/NADH ratio data generated from the main study 164
Table 5.39 Multiple comparison statistics of the blood NAD/NADH ratio data generated from the rat main study 166
Table 5.40 Graphic and tabulated summary of the blood NAD/NADH ratio data analysed via a two-way ANOVA 167
Table 5.41 Data categorisation according to assumed beneficial and harmful effects in relation to the environmental control rat group NN 170
Table 5.42 Blood profile of response generated from the rat main study indicating the beneficial and harmful effects of dose regimens 172
Table 5.43 Box whisker representation and descriptive statistics of the rat heart weight data generated from the pilot study 185
Table 5.44 Multiple comparison statistics of heart weight data generated from the rat pilot study 186
Table 5.45 Box whisker representation and descriptive statistics of the heart weight data generated from the main study 189
Table 5.46 Multiple comparison statistics of heart weight data generated from the rat main study 190
Table 5.47 Graphic and tabulated summary of the heart weight data analysed via a two-way ANOVA 192
Table 5.48 Summary of comparative dose groups of the rat pilot and main study heart weight data 194
Table 5.49 Box whisker representation and descriptive statistics of the complex I data generated from heart muscle during the rat pilot study 196
Table 5.50 Multiple comparison statistics of heart muscle complex I activity data generated from the rat pilot study 198
Table 5.51 Box whisker representation and descriptive statistics of the complex I data generated from heart muscle during the rat main study 200
Table 5.52 Multiple comparison statistics of heart muscle complex I data generated from the rat main study 202
Table 5.53 Graphic and tabulated summary of heart muscle complex I data analysed via a two-way ANOVA 206
Table 5.54 Summary of comparative dose groups of the rat pilot and main study heart muscle complex I data 208

Table 5.55 Box whisker representation and descriptive statistics of the heart muscle antioxidant capacity data generated from the main study 210
Table 5.56 Multiple comparison statistics of heart muscle antioxidant capacity data generated from the rat main study 211
Table 5.57 Graphic and tabulated summary of the heart muscle antioxidant capacity data analysed via a two-way ANOVA 213
Table 5.58 Box whisker representation and descriptive statistics of the heart muscle L/P data generated from the main study 215
Table 5.59 Multiple comparison statistics of heart muscle L/P data generated from the rat main study 217
Table 5.60 Graphic and tabulated summary of the heart muscle L/P data analysed via a two-way ANOVA 218
Table 5.61 Box whisker representation and descriptive statistics of the heart muscle ATP/ADP ratio data generated from the main study 220
Table 5.62 Multiple comparison statistics of heart muscle ATP/ADP ratio data generated from the rat main study 223
Table 5.63 Graphic and tabulated summary of the heart muscle ATP/ADP ratio data analysed via a two-way ANOVA 224
Table 5.64 Heart muscle profile of response generated from the rat main study indicating the beneficial and harmful effects of dose regimens 227
Table 5.65 Box whisker representation and descriptive statistics of the rat brain weight data generated from the pilot study 234
Table 5.66 Multiple comparison statistics of brain weight data generated from the rat pilot study 235
Table 5.67 Box whisker representation and descriptive statistics of the complex I data generated from brain tissue during the rat pilot study 236
Table 5.68 Multiple comparison statistics of brain tissue complex I activity data generated from the rat pilot study 238
Table 5.69 Box whisker representation and descriptive statistics of the complex I data generated from brain tissue during the rat main study 240
Table 5.70 Multiple comparison statistics of brain tissue complex I activity data generated from the rat main study 241
Table 5.71 Graphic and tabulated summary of the brain tissue complex I data analysed via a two-way ANOVA 243
Table 5.72 Summary of comparative dose groups of the rat pilot and main study brain tissue complex I data 246
Table 5.73 Box whisker representation and descriptive statistics of the brain tissue antioxidant capacity data generated from the main study 248
Table 5.74 Multiple comparison statistics of brain tissue antioxidant capacity data generated from the rat main study 250
Table 5.75 Graphic and tabulated summary of the brain tissue antioxidant capacity data analysed via a two-way ANOVA 251
Table 5.76 Box whisker representation and descriptive statistics of the brain tissue L/P data generated from the main study 253
Table 5.77 Multiple comparison statistics of brain tissue L/P data generated from the rat main study 255
Table 5.78 Graphic and tabulated summary of the brain tissue L/P ratio data analysed via a two-way ANOVA 257
Table 5.79 Brain tissue profile of response generated from the rat main study indicating the beneficial and harmful effects of the dose regimens 260
Table 5.80 Box whisker representation and descriptive statistics of the complex I data generated from skeletal muscle during the rat pilot study 266
Table 5.81 Multiple comparison statistics of the skeletal muscle complex I activity data generated from the rat pilot study 267
Table 5.82 Box whisker representation and descriptive statistics of the complex I data generated from skeletal muscle during the rat main study 268
Table 5.83 Multiple comparison statistics of the skeletal muscle complex I data generated from the rat main study 270
Table 5.84 Graphic and tabulated summary of the skeletal muscle complex I data analysed via a two-way ANOVA 271

Table 5.85 Summary of comparative dose groups of the rat pilot and main study skeletal muscle complex I data 273
Table 5.86 Box whisker representation and descriptive statistics of the skeletal muscle data generated from the main study 275
Table 5.87 Multiple comparison statistics of the skeletal muscle antioxidant capacity data generated from the rat main study 276
Table 5.88 Graphic and tabulated summary of the skeletal muscle antioxidant capacity data analysed via a two-way ANOVA 278
Table 5.89 Box whisker representation and descriptive statistics of the skeletal muscle L/P ratio data generated from the rat main study 280
Table 5.90 Multiple comparison statistics of the skeletal muscle L/P ratio data generated from the rat main study 281
Table 5.91 Graphic and tabulated summary of the skeletal muscle L/P ratio data analysed via a two-way ANOVA 282
Table 5.92 Box whisker representation and descriptive statistics of the skeletal muscle ATP/ADP ratio data generated from the main study 284
Table 5.93 Multiple comparison statistics of the skeletal muscle ATP/ADP ratio data generated from the rat main study 286
Table 5.94 Graphic and tabulated summary of the skeletal muscle ATP/ADP ratio data analysed via a two-way ANOVA 288
Table 5.95 Box whisker representation and descriptive statistics of the skeletal muscle NAD/NADH ratio data generated from the main study 290
Table 5.96 Multiple comparison statistics of the skeletal muscle NAD/NADH ratio data generated from the rat main study 292
Table 5.97 Graphic and tabulated summary of the skeletal muscle NAD/NADH ratio data analysed via a two-way ANOVA 294
Table 5.98 Skeletal muscle profile of response generated from the rat main study indicating the beneficial and harmful effects of the dose regimens 296
Table 5.99 Box whisker representation and descriptive statistics of the rat liver weight data generated from the pilot study 302
Table 5.100 Multiple comparison statistics of the liver organ weight data generated from the rat pilot study 304
Table 5.101 Box whisker representation and descriptive statistics of the liver weight data generated from the main study 305
Table 5.102 Multiple comparison statistics of the liver organ weight data generated from the rat main study 308
Table 5.103 Graphic and tabulated summary of the liver weight data analysed via a two-way ANOVA 310
Table 5.104 Summary of comparative dose groups of the rat pilot and main study liver weight data 312
Table 5.105 Box whisker representation and descriptive statistics of the complex I data generated from liver tissue during the rat pilot study 314
Table 5.106 Multiple comparison statistics of the liver complex I data generated from the rat pilot study 315
Table 5.107 Box whisker representation and descriptive statistics of the complex I data generated from liver tissue during the rat main study 317
Table 5.108 Multiple comparison statistics of the liver complex I data generated from the rat main study 319
Table 5.109 Graphic and tabulated summary of the liver tissue complex I data analysed via a two-way ANOVA 321
Table 5.110 Summary of comparative dose groups of the rat pilot and main study liver tissue complex I data 324
Table 5.111 Box whisker representation and descriptive statistics of the liver antioxidant capacity data generated from the main study 326
Table 5.112 Multiple comparison statistics of the liver antioxidant capacity data generated from the rat main study 328
Table 5.113 Graphic and tabulated summary of the liver tissue antioxidant capacity data analysed via a two-way ANOVA 329
Table 5.114 Box whisker representation and descriptive statistics of the liver tissue L/P ratio data generated from the main study 332

Table 5.115 Multiple comparison statistics of the liver L/P ratio data generated from the rat main study 333
Table 5.116 Graphic and tabulated summary of the liver tissue L/P ratio data analysed via a two-way ANOVA 335
Table 5.117 Box whisker representation and descriptive statistics of the liver GSH/GSSG ratio data generated from the main study 336
Table 5.118 Multiple comparison statistics of the liver GSH/GSSG ratio data generated from the rat main study 339
Table 5.119 Graphic and tabulated summary of the liver tissue GSH/GSSG ratio data analysed via a two-way ANOVA 342
Table 5.120 Box whisker representation and descriptive statistics of the liver tissue ATP/ADP ratio data generated from the main study 344
Table 5.121 Multiple comparison statistics of the liver ATP/ADP ratio data generated from the rat main study 346
Table 5.122 Graphic and tabulated summary of the liver ATP/ADP ratio data analysed via a two-way ANOVA 348
Table 5.123 Box whisker representation and descriptive statistics of the liver tissue NAD/NADH ratio data generated from the main study 351
Table 5.124 Multiple comparison statistics of the liver tissue NAD/NADH ratio data generated from the rat main study 353
Table 5.125 Graphic and tabulated summary of the liver tissue NAD/NADH ratio data analysed via a two-way ANOVA 354
Table 5.126 Liver tissue profile of response generated from the rat main study indicating the beneficial and harmful effects of the dose regimens 358
Table 5.127 Graphic and tabulated representation of data generated from the rat pilot study 364
Table 5.128 Graphic representation and correlation statistics generated from the rat pilot study 367
Table 5.129 Collective summary of rat main study median percentages in relation to environmental controls 369
Table A.1 Daily recordings of body weight in the rat pilot study 409
Table A.2 Daily recordings of body weight in the rat main study 411
Table B.1 Heart muscle complex I data generated from the rat pilot study 414
Table B.2 Brain tissue complex I data generated from the rat pilot study 415
Table B.3 Skeletal muscle complex I data generated from the rat pilot study 416
Table B.4 Liver tissue complex I data generated from the rat pilot study 417
Table B.5 Heart muscle complex I data generated from the rat main study 418
Table B.6 Brain tissue complex I data generated from the rat main study 420
Table B.7 Skeletal muscle complex I data generated from the rat main study 421
Table B.8 Liver tissue complex I data generated from the rat main study 423
Table C.1 Heart muscle antioxidant capacity data generated from the rat main study 425
Table C.2 Brain tissue antioxidant capacity data generated from the rat main study 427
Table C.3 Skeletal muscle antioxidant capacity data generated from the rat main study 428
Table C.4 Liver tissue antioxidant capacity data generated from the rat main study 430
Table D.1 Blood glutathione data generated from the rat main study 433
Table D.2 Liver tissue glutathione data generated from the rat main study 435
Table E.1 Blood lactate and pyruvate data generated from the rat main study 437
Table E.2 Heart muscle lactate and pyruvate data generated from the rat main study 439
Table E.3 Brain tissue lactate and pyruvate data generated from the rat main study 440
Table E.4 Skeletal muscle lactate and pyruvate data generated from the rat main study 442
Table E.5 Liver tissue lactate and pyruvate data generated from the rat main study 443
Table F.1 Blood adenylate data generated from the rat main study 445
Table F.2 Heart muscle adenylate data generated from the rat main study 447
Table F.3 Skeletal muscle adenylate data generated from the rat main study 448
Table F.4 Liver tissue adenylate data generated from the rat main study 450
Table G.1 Blood pyridine data generated from the rat main study 453
Table G.2 Skeletal muscle pyridine data generated from the rat main study 455
Table G.3 Liver tissue pyridine data generated from the rat main study 457

ACKNOWLEDGEMENTS

I would like to thank the following people and organisations for help in realising this achievement. This investigation would not have been possible without your contributions.

Professor Antonel Olckers, for your supervision and support throughout this journey. Your insight into research, quality of training and commitment to students makes the Centre for Genome Research (CGR) a prestigious entity from which to qualify. I truly believe that the many skills I have attained from your training programme will serve me well in the years ahead. **Professor Francois van der Westhuizen**, for accepting me into the Mitochondrial Laboratory and guiding me throughout the practical phase of the study. Your continued willingness to help is greatly appreciated. It was a privilege to gain experience in mitochondrial biochemistry under your supervision. **Doctor Izelle Smuts**, for sharing your clinical expertise.

Professor Doug Wallace, for inspiring me to explore the field of mitochondrial biology. Your contributions to mitochondrial genetics are truly remarkable and I am yet to meet another man who is as enthusiastic about his research as you are.

The **CGR** of **North-West University**, for providing the opportunity to further my studies and for financial support in the form of bursaries. **DNAbiotec (Pty) Ltd**, for funding. Both entities for providing exceptional facilities. The **National Research Foundation (NRF)** of South Africa for the Prestigious Doctoral Scholarship award that enabled the completion of my studies.

To the **CGR** and **DNAbiotec team**, the times spent with you will always be remembered. **Annelize van der Merwe**, your friendship, endless support and professionalism will always be a part of my memories at the CGR. **Wayne Towers**, for enduring the late nights with me 'solving the statistics', for proofreading all the chapters and being available whenever I needed clarification of concepts. Only a friend and committed team member would have been able to fulfil these roles. **Tumi Semete**, it was always great to have a fellow team-member like you around in Potchefstroom while working the late nights. **Estie Kotzé**, for your unconditional willingness to help, devotion and care for my needs.

Michelle Freeman, **Desiré-Lee Dalton**, **Dan Isabirye** and **Delia Tanner**, sharing an office with you was always a pleasure for me. **Tshireletso Mataboge**, **Kenneth Nkadimeng** and **Leonard Mdluli**, for adding humour to my life and assisting wherever possible. **Martha Sebogoli**, for maintaining a comfortable environment to work in.

The people I met at **North-West University (Potchefstroom Campus)**, for your support. Students and employees of the **Mitochondrial Laboratory**, your acceptance of me into your laboratory and helping wherever possible is greatly appreciated. **Oksana Levanets**, your reliability and precision-orientated assistance while dosing the animals was invaluable. **Cristal Huysamen**, for your incredible commitment to assisting and encouraging me during the toughest of practical sessions. There are few people who would have been able to be there for me the way you were. **Fanie Rautenbach** and **Martin Brits**, for helping me with countless aspects of working with an animal model and for your practical guidance in the Mitochondrial Laboratory. **Cor Bester**, **Antoinette Fick**, **Rynand van den Berg** and other members of the **Animal Experimentation Centre**, for your consideration, sense of humour and friendship throughout the animal experimentation phase and my time in Potchefstroom. **Deirdré and CJ Claasen**, for your friendship and our peaceful times together. **Dr Suria Ellis** of the Statistical Consultation Service for assisting me in the construction of a sound strategy to analyse the data.

My **Friends**, the encouragement you provided me from day one is often what heightened my determination to realise this dream. **Wimpie Prozesky**, **Peter Beskyd**, **Monica Calvo**, **Stefano Sellarione**, **Alexis Oosthuizen**, **Michelle Clüver**, **Chris Pavlou**, **Jurek Pietrzak**, **Fabio Marsura**, **Marco Palladino**, **Jason Olivier**, **Emiliano Casanovus**, **Marize Botha**, **Angela and Michelle Abouchabki**, I am honoured to have such special people in my life.

To my extended **Family**, for continuously supporting me throughout this challenging period. In particular, to **Nice Alessandrini**, my nonna, I will always remember and love you for the generous care that you gave me. **Emilio Alessandrini**, for relieving me of responsibilities and becoming the man you are today, you have had a wonderful impact in my life. **Denyse**, **Tawny**, **Deanne** and **Gabriella Alessandrini**, thank you for being there and providing me with the feeling of family. **Anton and Crystelle Jacobsz**, your compassion in the past years contributed a great deal to my success.

To my **Parents**, for the unconditional support and the countless opportunities that you have made available for me. Your love and concern for my well-being throughout the years is truly appreciated. It is your devotion that made the achievement of this goal possible, I will be eternally grateful.

CHAPTER ONE

INTRODUCTION

The mitochondrion is one of the most vital organelles in all eukaryotic cells due to its central role in energy production processes and aerobic respiratory pathways. The respiratory chain consists of five enzyme complexes associated with the inner mitochondrial membrane as well as various redox intermediates, which function in unity to ultimately produce the majority of the total energy required by the cell in the form of ATP. The membrane-bound enzyme complexes of mitochondria, designated complex I to V, consist of over 70 different polypeptides that are subject to expression via a dual genetic system, namely the nuclear and self-contained mitochondrial genomes. It is therefore understandable that an intricate control system exists to ensure that mitochondrial functioning is successfully coordinated. Alterations in either mitochondrial DNA (mtDNA) or nuclear DNA (nDNA) encoded subunits of these enzymes, whether inherited or sporadic, result in impaired respiratory chain functioning and consequently decreased energy production.

Complex I is the first and most complex enzyme of the respiratory chain. The enzyme is composed of 46 polypeptide subunits (Carroll *et al.*, 2002) encoded by both the nuclear and mitochondrial genomes. The overall function of this enzyme is to transfer electrons from NADH to ubiquinone, while transferring protons from the mitochondrial matrix into an inter-membrane space. Disorders of the mitochondrial respiratory chain have an incidence ranging between 1 in 2,000 to 1 in 5,000 live births (Naviaux, 2004), of which the most frequent result from causative mutations within complex I. Patients with Complex I deficiency present with a great variety of symptoms, which primarily manifest as Leigh and Leigh-like syndromes, slowly or highly progressive encephalomyopathy, or fatal infantile lactic acidosis (Loeffen *et al.*, 2000). Patients often suffer from fatigue, exercise intolerance and lactic acidaemia. On a biochemical level, a deficiency of complex I activity results in failure to oxidise NADH, impairment of the Krebs cycle and elevated blood lactate. Consequent lowered ATP generation, altered mitochondrial membrane potential and increased production of ROS is also observed.

Previously, therapeutic interventions have been explored via the use of cofactors, which included coenzyme Q derivatives, niacin, thiamine, and riboflavin, electron donors like

succinate and menadione, as well as vitamins acting as free radical scavengers. Pharmacological agents have also been investigated in the past, not to mention attempts at gene therapy (Schon and DiMauro, 2003). However, the minority of studies have reported improvements, whilst the majority represent a lack of response (Chinnery and Turnbull, 2001). Moreover, few studies have investigated Complex I deficiency itself (Bar-Meir *et al.*, 2001).

Even though the field of mitochondrial medicine has progressed considerably in the past decade, a satisfactory understanding of the molecular complexities and pathogenicity of the mitochondrial disorders is still to be gained. Therefore, the trend has shifted to a more 'supportive' approach of improving the phenotypic management of patients affected by the mitochondrial cytopathies. It is thus vital that successful animal models be developed, which accurately portray the complex I deficient phenotype and hence enable reliable intervention and therapeutic experimentation.

The aim of the proposed investigation was to determine the effectiveness of therapeutic intervention in a rotenone-induced complex I deficient animal model. Since no animal model harbouring a genetically induced Complex I deficiency has been reported to date, it was required that the deficiency be induced by a potent inhibitor of complex I. It is for this reason that rotenone was selected, the most widely used and accepted inhibitor of complex I (Miyoshi, 1998). Experimentation was performed in C57BL/6 mice, originating from parent strain C57, and Sprague Dawley rats, with a successfully induced Complex I deficiency being induced in the latter animal model. To follow, the therapeutic benefits of coenzyme Q10 (CoQ_{10}) and succinate were evaluated in five tissue groups in order to establish a biochemical profile of response. The tissue profiles were composed of data generated from a total of seven biochemical analysis types, investigating redox and oxidative stress components in each of the tissues.

The data was evaluated via a thorough and comprehensive statistical strategy including both parametric and non-parametric test procedures. Data sets were investigated for the presence of outliers and further analysed via the use of descriptive statistics, analysis of variance (ANOVA) and multiple comparison procedures. Furthermore, effect sizes were calculated in order to determine the biological significance of differences between the various rat dose groups included in the investigation.

CHAPTER TWO

MITOCHONDRIA AND ENERGY PRODUCTION

The mitochondrion has become the most investigated organelle of eukaryotic cells due to its pivotal role in energy generation and cell maintenance. The fact that diverse groups of neurological and muscular defects can inexorably be linked to deficiencies in mitochondrial processes has resulted in an inevitable paradigm shift in the disorder classification process. Defects in mtDNA result in disorders that have a reported prevalence of 1 in 10,000 in the general population (Graff *et al.*, 2002). These disorders primarily refer to a subset of conditions that result from disturbances in the respiratory chain, which is the principal biochemical pathway involved in the production of energy. The five enzyme complexes that constitute the respiratory chain each have essential roles in the production of energy. This chapter focuses on the mitochondrion, its role in energy production and primarily on enzyme complex I as well as defects associated with this enzyme.

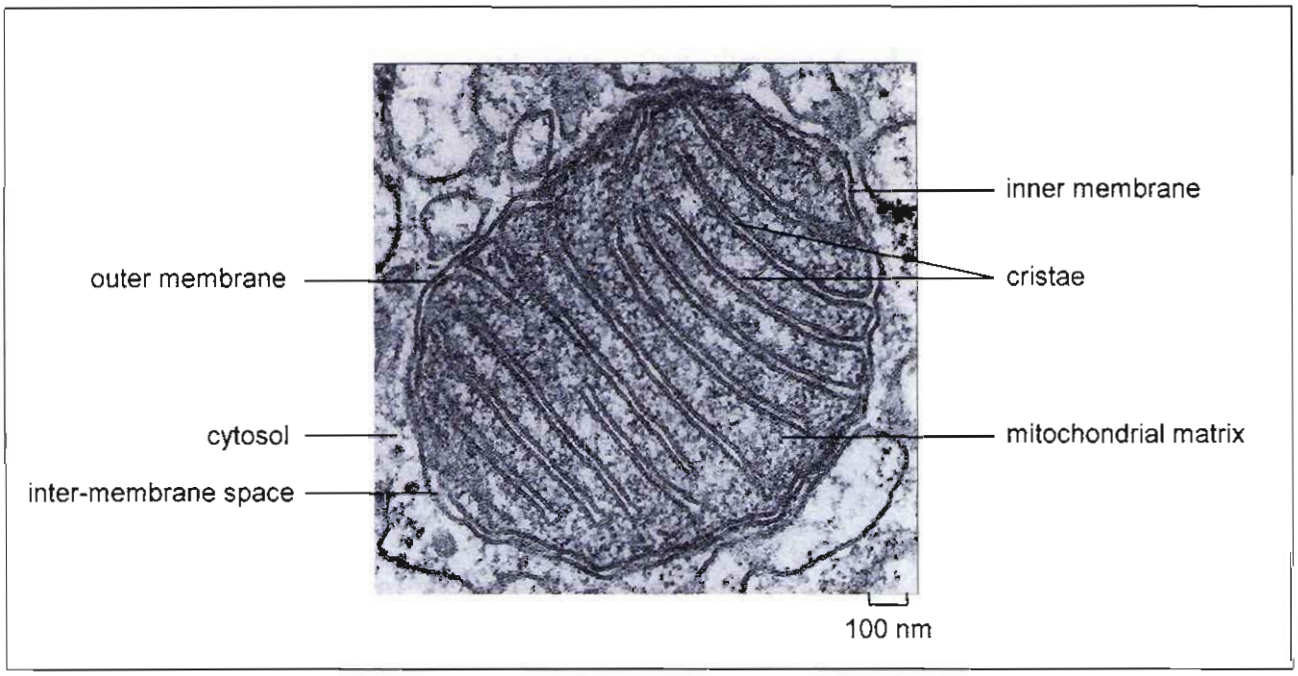
2.1 MITOCHONDRIA

It is hypothesised that mitochondria originated more than a billion years ago when a predecessor of present day eukaryotic cells engulfed a free-living aerobic bacterium (Scheffler, 2000). A symbiotic relationship evolved over time resulting in a loss of redundant genes and a simultaneous transfer of genes from the bacterium to the eukaryotic nucleus. Today, the mitochondrion is no longer autonomous and depends largely on the nuclear genome for biogenesis. The fact that mitochondria are today an essential feature of most eukaryotic cells clarifies that this endosymbiotic event was indeed beneficial to both organisms. The reason mitochondria are of benefit to the eukaryotic cell is of course its ability to harness energy from the oxidation and conversion of food molecules, such as sugars, to produce the cell's basic chemical fuel, ATP. The mitochondria are unique in the sense that they function and are regulated by proteins encoded by two genomes, the mitochondrial and nuclear genomes. The inter-relationship of the two genomes will be highlighted throughout this chapter.

2.1.1 Structure of mitochondria

The mitochondria are a vital component and of the most conspicuous organelles present in eukaryotic cells. They are distinctive in structure and easily recognisable via electron microscopy, as depicted in Figure 2.1. Mitochondria are visually characterised by their distinctive double membranes, consisting of an inner and outer membrane. The outer membrane separates the mitochondrion from the cytosol, whilst the inner membrane folds into the mitochondrial matrix to form cristae. The forming of cristae by the inner membrane is said to have evolved in order to increase the surface area for respiration, as will be discussed in Section 2.2. The respiratory chain, with its five enzyme complexes, is embedded in the inner membrane.

Figure 2.1 Electron microscopic view of a mammalian mitochondrion



The abbreviation nm = nanometre. Adapted from Alberts *et al.* (1997).

Mitochondria are unique from the other organelles in that they harbour their own genetic information or genome, referred to as the mtDNA. Even though the mitochondrial genome encodes less than five percent of the total amount of proteins that are functional within mitochondria, it still encodes polypeptides that are essential for the functioning of the organelle as well as for respiration.

2.1.2 The mitochondrial genome

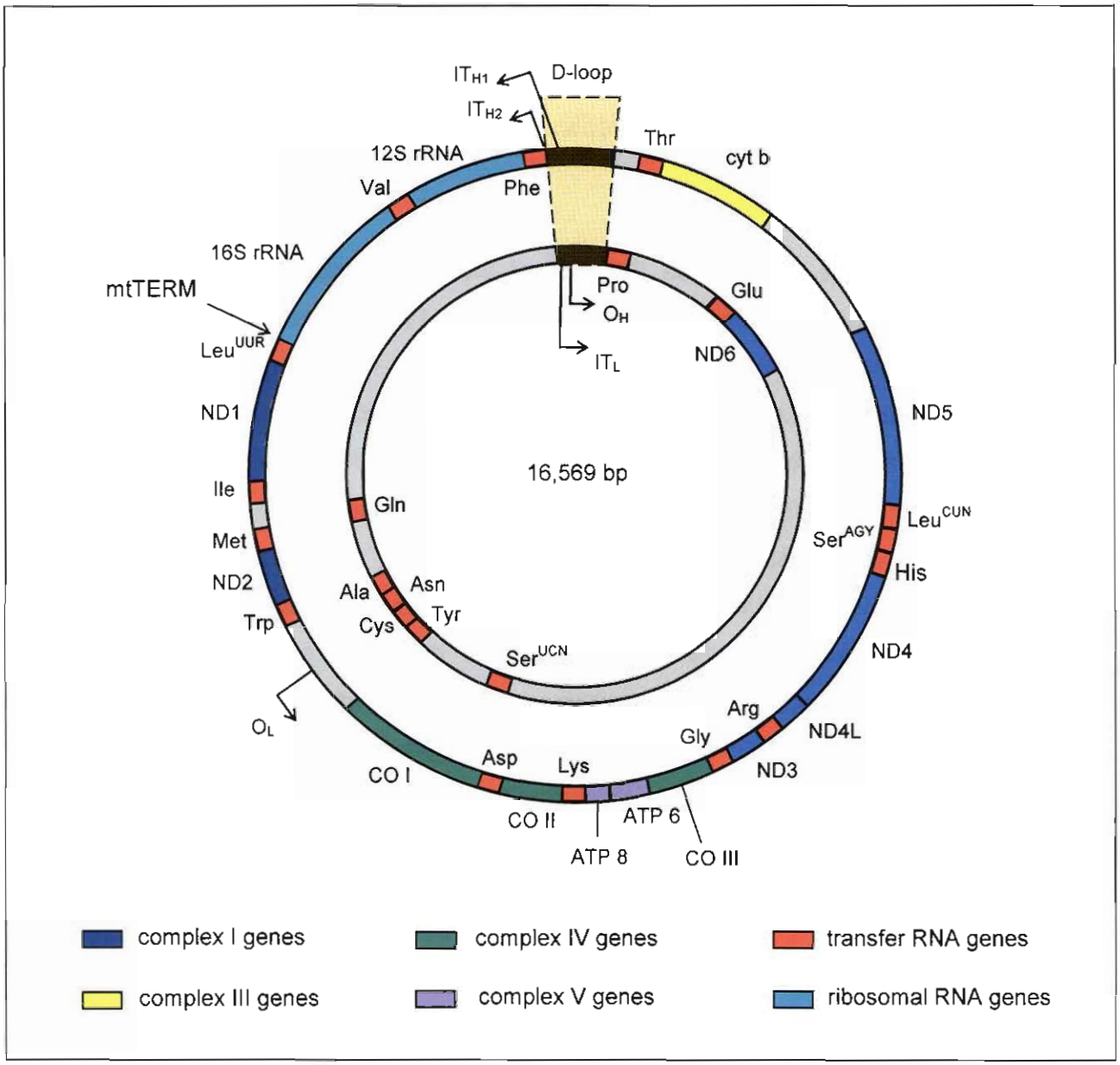
Every living human cell contains 1,000 to 10,000 copies of mtDNA, with the exception of spermatozoa, which have approximately 100. Each mitochondrion generally harbours two

to ten copies of mtDNA. During the mitochondrion's evolution into the present day energy generator of all eukaryotic cells, it transferred many of its essential genes to the nuclear chromosomes. As a consequence, the mitochondria combine both their own machinery as well as that of the human cell to replicate, transcribe and synthesise the proteins encoded within.

The human mtDNA sequence was the first of the mitochondrial genomes to be fully sequenced and was documented by Anderson *et al.* in 1981. This sequence is referred to as the Cambridge Reference Sequence (CRS) and was derived from sequence information of various sources including a European individual, Henrietta Lacks (HeLa) cancer cell line and *Bos taurus* (bovine) mtDNA. Once further mammalian mitochondrial genomes were sequenced, it became clear that mtDNA structure and gene organisation is highly conserved across eukaryotic organisms. However, deviations from the standard genetic code and even variations in codon use have been reported in mitochondria from different species (Osawa *et al.*, 1992). For example, the thymine-guanine-adenine (TGA) codon, encodes a stop codon in some species, whereas in others it codes for the amino acid tryptophan. The CRS was more recently revised (Andrews *et al.*, 1999) by sequencing the original European individual's mtDNA. The data revealed eight sequencing errors and seven rare polymorphisms. The errors were corrected and polymorphisms retained in order to maintain the sequence as a true reference and not a consensus sequence.

The human mtDNA genome, as presented in Figure 2.2, is a closed circular, double-stranded DNA molecule of 16,569 nucleotide base pairs (bp). The complete genome encodes 13 polypeptide coding genes, which are translated by 22 transfer ribonucleic acids (tRNAs) and two ribosomal RNAs (rRNAs), for which the mitochondrial genome also codes. All 13 polypeptide products function as enzyme subunits in the respiratory chain, which will be discussed in Section 2.2.1. The two strands of the DNA duplex are referred to as the heavy strand (H-strand) and the light strand (L-strand) respectively. The H-strand consists of primarily guanine (G) residues and the L-strand mainly cytosine (C), the strands could be differentiated from each other based on their different buoyant densities (Kasamatsu and Vinograd, 1974). The H-strand represents the majority of the genome and functions as a template for both mitochondrial encoded rRNAs, 12 of the 13 polypeptides and 14 of the 22 tRNAs. The light L-strand codes for the remaining eight tRNAs and a single polypeptide.

Figure 2.2 Diagrammatic representation of the mitochondrial genome



The outer circle represents the H-strand and the inner circle the L-strand. The displacement loop (D-loop) is indicated by the light orange-filled dashed trapezium. The right-angled arrows indicate the direction of DNA/RNA synthesis. 12S rRNA and 16S rRNA = 12 and 16 Svedberg unit ribosomal RNA, Arg = arginine, Ala = alanine, Asn = asparagine, Asp = aspartic acid, ATP 6 and ATP 8 = ATP synthase subunits 6 and 8, bp = base pairs, CO I – III = cytochrome *c* oxidase I – III, Cys = cysteine, cyt b = cytochrome b, Gln = glutamine, Glu = glutamic acid, Gly = glycine, His = histidine, Ile = isoleucine, IT_{H1} and IT_{H2} = heavy strand initiation of transcription sites 1 and 2, IT_L = light strand initiation of transcription site, Leu^{CUN} = leucine with anticodon CUN, Leu^{UUR} = leucine with anticodon UUR, Lys = lysine, Met = methionine, mtTERM = binding site for the mitochondrial transcription terminator, ND1-6 = NADH dehydrogenase subunits 1-6, O_H = heavy strand origin of replication, O_L = light strand origin of replication, Phe = phenylalanine, Pro = proline, Ser^{AGY} = serine with anticodon AGY, Ser^{UCN} = serine with anticodon UCN, Thr = threonine, Trp = tryptophan, Tyr = tyrosine, Val = valine. Adapted from Taanman (1999).

Mammalian mtDNA genomes are highly compact and display exceptional economy of organisation (Taanman, 1999). Mitochondrial genes lack intronic DNA and the genome consists of minimal intergenic DNA. There is only one non-coding region, which contains the displacement loop (D-loop) and origin of replication, discussed in Section 2.1.3.3. Each strand has its own principal promoter and both of the encoded rRNAs as well as the 22 tRNA molecules are considerably smaller than those present within the nuclear genome. Some of the polypeptide coding genes are overlapping and, in many cases, part

of the termination codons are not encoded by the template itself, but are generated post-transcriptionally by polyadenylation of the messenger RNA (mRNA) molecules.

In addition, since only 22 tRNAs function in codon translation in the mitochondrial genetic system, as opposed to the 32 tRNAs of nuclear DNA, the mitochondria utilises a simplified coding mechanism. The reduction in the number of tRNAs is achieved by the use of a single tRNA with uridine (U) in the first anticodon position, referred to as the wobble position. This allows for the recognition of all codons of a four-codon family. The mechanism prevents misreading of two codon families with a pyrimidine in the third position and is considered to be conserved in vertebrate mitochondria. This would imply that 24 tRNA species are required to decode mtDNA. In addition, in vertebrates the AGR codons, where R represents either an adenine (A) or G, indicate a stop with the corresponding tRNA gene absent. Furthermore, a single tRNA species, with a modified C in the first anticodon position followed by AU, functions for initiation via N-formylmethionyl-tRNA ($tRNA^{fMet}$) as well as elongation via methionine tRNA ($tRNA^{Met}$), and pairs with codon AUA in addition to AUG. Hence, the 22 tRNA species encoded by human mtDNA are sufficient to translate all 13 mitochondrial polypeptide genes.

2.1.3 Biogenesis of mitochondria

In vertebrate cells, a large proportion of the mtDNA duplexes contain a short three-stranded structure, the so-called D-loop, in which a short nucleic acid strand of 1,118 bp, complementary to the L-strand, displaces the H-strand. This region has evolved as the major control site for mtDNA expression, containing the leading-strand origin of replication and the major promoters for transcription, depicted in Figure 2.2.

Mitochondria are not self-supporting entities within the cell. Replication and transcription depend upon trans-acting nuclear encoded factors. Mitochondrial tRNAs are modified via imported aminoacyl-tRNA synthases and, in the majority of cases, all mitochondrial ribosomal proteins are encoded and synthesised outside the organelle. Nuclear DNA encodes enzymes of the various catabolytic pathways located in the mitochondria, as well as the components of the mitochondrial import machinery. Even the enzyme complexes of the respiratory chain are of hybrid genetic origin. All nuclear-encoded polypeptides destined to function in the mitochondria are synthesised on cytosolic ribosomes, usually with a cleavable, N-terminal pre-sequence for mitochondrial targeting and are

subsequently imported into mitochondria. Hence, the biogenesis of this organelle depends on an intricate communication and coordinated expression of the two genomes.

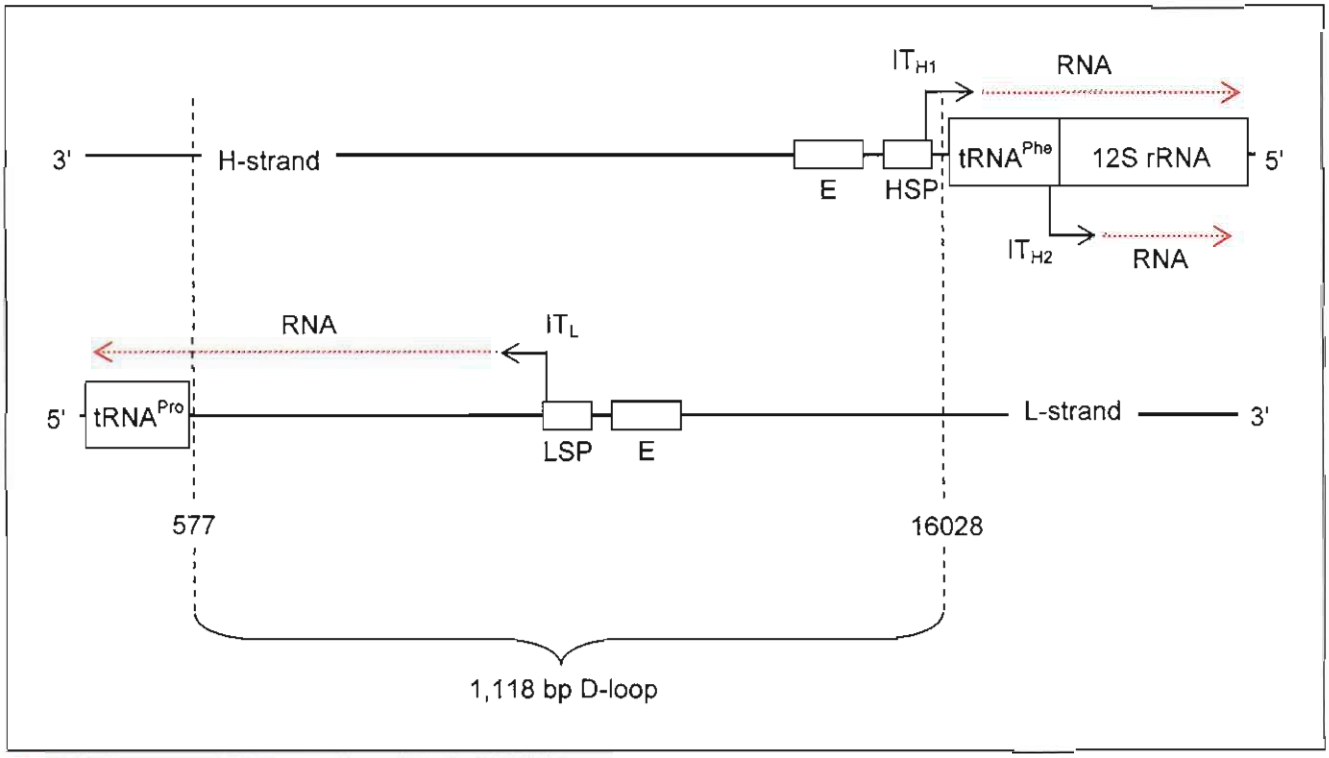
2.1.3.1 Transcription of mitochondrial DNA

Human mtDNA requires a mitochondrial specific RNA polymerase, mitochondrial transcription factors and transacting nuclear encoded factors in order to transcribe its sequences. Transcription initiation sites and promoter regions have been determined using a variety of techniques, namely 5'-end mapping (Montoya *et al.*, 1982; Montoya *et al.*, 1983), deletion experiments (Chang and Clayton, 1984; Bogenhagen *et al.*, 1984) site directed mutagenesis (Hixson and Clayton, 1985) and linker substitution analyses (Topper and Clayton, 1989). The two major transcription initiation sites for the mitochondria are both situated in the D-loop and are referred to as IT_{H1} and IT_L, the H-strand transcription initiation site one and L-strand transcription initiation site, respectively, as illustrated in Figure 2.3. H-strand transcription starts at IT_{H1} located within the H-strand promoter and immediately adjacent to the phenylalanine tRNA ($tRNA^{Phe}$) gene, whereas the L-strand transcription starts at IT_L located within the L-strand promoter. A less frequently utilised transcription initiation site, referred to as IT_{H2}, is located within the $tRNA^{Phe}$ gene. Additional upstream enhancer elements are required for optimal transcription (denoted E) and are known to bind a nuclear encoded mitochondrial transcription factor (mtTFA). This transcription factor is said to bind and induce mtDNA conformational changes that allow the core RNA polymerase access to the template for initiation of transcription (Antoshechkin *et al.*, 1997). Additional mitochondrial transcription factors have been identified.

Transcription of the mtDNA genome is initiated at the respective promoter sequences, termed the H-strand promoter (HSP) and L-strand promoter (LSP), by the binding of mtTFA. Both of the transcriptional promoters in human mitochondria are located in the D-loop and can function bi-directionally. However, the binding of mtTFA to the upstream enhancer ensures transcription initiation in a unidirectional fashion. The L-strand is transcribed via the core RNA polymerase into a single polycistronic RNA, encompassing all of the genetic information encoded by this strand. The presence of two transcription initiation sites, IT_{H1} and IT_{H2}, makes for a more complicated mechanism on the H-strand. Transcription starts at IT_{H1} and terminates at a termination site at the end of the 16 Svedberg unit ribosomal RNA (16S rRNA) gene, called mtTERM for the mitochondrial termination site (Figure 2.2). As mentioned above, the activity of IT_{H1} is much greater than

IT_{H2}, and consequently the rRNAs are synthesised at a much higher rate. Transcription at IT_{H2} results in the synthesis of a polycistronic molecule containing all the mRNAs and most of the tRNAs, in a similar fashion to the L-strand. The intricacy of H-strand transcription coordination is, however, not fully understood.

Figure 2.3 Diagrammatic representation of the transcriptional elements involved in mitochondrial transcription



Red dotted arrows indicate newly synthesised RNA in a 5' to 3' direction. 12S rRNA = 12 Svedberg unit ribosomal RNA, D-loop = displacement loop, E = Enhancer element, H-strand = heavy strand, HSP = H-strand promoter, IT_{H1} and IT_{H2} = H-strand transcription initiation sites 1 and 2, IT_L = L-strand transcription initiation site, L-strand = light strand, LSP = L-strand promoter, RNA = ribose nucleic acid, $tRNA^{Pro}$ = tRNA Proline, $tRNA^{Phe}$ = tRNA Phenylalanine. Adapted from Taanman (1999).

Transcription termination of both the H and L-strands occurs at mtTERM. The mitochondrial termination factor (mtTERF) protein, which binds to the mtTERM site, induces bending of the mtDNA helix and forms a physical barrier for the mitochondrial RNA polymerase. This binding and bending of the DNA by mtTERF inhibits any further transcription by the polymerase on the L-strand in a region where no encoded genes are present.

As no intronic and minimal intergenic sequences are present in the nascent polycistronic RNA strands, a different and simplified processing model has been proposed for mitochondrial RNA species than for transcribed nuclear RNA. The process is referred to as the tRNA punctuation model of mitochondrial RNA processing (Ojala *et al.*, 1981). The majority of tRNAs, rRNAs and mRNAs are correctly processed by endolytic cleavage and excision at their sequence boundaries. The excision is based upon the recognition of the

tRNA secondary structures. Since tRNA genes flank both of the rRNAs and almost all of the protein coding genes, precise endolytic cleavage and excision of the tRNAs yields correctly processed rRNAs as well as the majority of mRNAs. In cases where this organisation is not present, a separate model for processing is proposed.

The RNA molecules are subsequently matured for future functioning in the mitochondria. Maturation occurs via cleavage at the 5' and 3'-ends of the molecule by an enzyme referred to as mitochondrial ribonuclease P (mtRNase P), followed by the addition of CCA nucleotides to the 3'-end via a tRNA nucleotidyltransferase. The mRNAs are polyadenylated by mitochondrial poly (A) polymerase during or immediately after cleavage, whilst the rRNAs are post-transcriptionally modified.

2.1.3.2 Mitochondrial protein synthesis

The translation machinery of the mitochondria is unique from that of the rest of the cell. The mitochondrial ribosomes, or mitoribosomes, are located on the matrix side of the mitochondrial inner membrane. These mitoribosomes have an unusually low RNA content and relatively high protein content. It is reported that no more than 100 mitoribosomes function in the mitochondria (Taanman, 1999). Translation of mitochondrial mRNAs begins at the N-formylmethionine codon. This system is unique from that of cytoplasmic translation in that the mitochondrially encoded mRNAs do not contain upstream leader sequences nor do they contain 7-methylguanylate caps to facilitate binding of the ribosomes. A disparate recognition process probably exists.

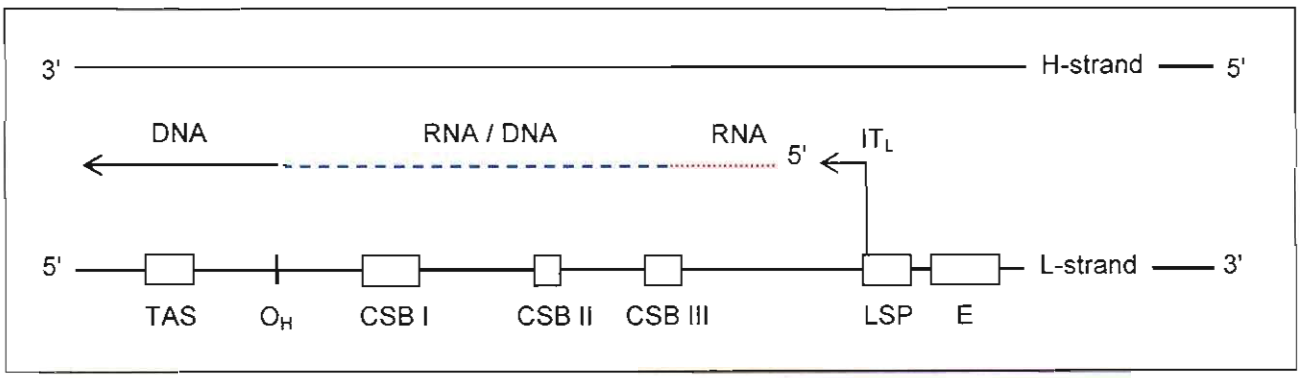
The small 28 Svedberg unit (28S) ribosomal subunit binds tightly to the mRNA in a sequence independent manner and moves to the 5'-end of the mRNA without any assistance from initiation factors. A mitochondrial initiation factor, mtIF 2, binds $tRNA^{fMet}$ to the small ribosomal subunit as well as to the mRNA template in the presence of guanosine triphosphate (GTP). The hydrolysis of GTP allows for the release of mtIF 2 and subsequent recruitment of the large 39 Svedberg unit (39S) subunit to form a 55 Svedberg unit (55S) translation initiation complex. Polypeptide elongation proceeds in the presence of numerous mitochondrial elongation factors.

2.1.3.3 Replication of mitochondrial DNA

Kasamatsu and Vinograd (1974) initially described the process of replication of circular DNA in eukaryotic cells. Today, it is clear that coordination of mitochondrial genome replication is closely linked to transcription. Short mitochondrial transcripts originating from IT_L are utilised as primers in the initiation of H-strand synthesis. The RNA precursor primers continue to extend, followed by RNA to DNA synthesis transition at three distinct sites called conserved sequence blocks (CSB I, II and III), as illustrated in Figure 2.4. The primary transcript is enzymatically processed to yield the mature primer RNA 3'-termini. The three CSBs are said to direct the precise cleavage of primary transcripts to provide the appropriate primer species. The cleavage is performed by a ribonucleoprotein, mitochondrial RNA processing endonuclease (Rnase MRP). A second nuclease, endonuclease G, has been implicated in processing of the precursor RNA primers for H-strand synthesis. However, both of the aforementioned enzymes have also been determined to function in the nucleus and precise involvements in the eukaryotic cell as a whole are yet to be assigned.

Soon after replication has been initiated and approximately 1 kilobase (kb) has been synthesised, the process is halted. The nascent strand remains annealed to the L-strand and forms the triplex D-loop structure. The synthesis arrest takes place approximately 50 nucleotides downstream from a termination-associated sequence (TAS). Replication may continue over the entire length of the mitochondrial genome, or it may simply remain halted indefinitely. Nuclear encoded transacting proteins have been reported in bovine mitochondria to bind to TAS and have hence been suggested to regulate mitochondrial replication and copy number (Madsen *et al.*, 1993).

Figure 2.4 Diagrammatic representation of mitochondrial H-strand replication



The red dotted line indicates newly synthesised RNA in a 5' to 3' direction, while the blue dashed line indicates the RNA/DNA transition. The black straight arrow = fully transformed DNA and direction of synthesis. CSB I, II and III = conserved sequence blocks I, II and III, E = Enhancer element, H-strand = heavy strand, IT_L = L-strand transcription initiation site, L-strand = light strand, LSP = L-strand promoter, O_H = origin of replication of H-strand, TAS = termination associated element. Adapted from Taanman (1999).

Replication of the L-strand can only begin once the parental H-strand has been displaced by the nascent H-strand. The displaced strand, which contains the L-strand origin of replication (O_L), forms a stem-loop structure and is recognised by mitochondrial DNA primase enzyme, which provides a short RNA primer for L-strand synthesis (Clayton, 1991). The RNA to DNA transition occurs at the base of the hairpin, after which the synthesis continues via DNA polymerase gamma (γ) in the opposite direction. This polymerase is the only DNA polymerase reported to function in the mitochondria (Bolden *et al.*, 1977) and consists of two activities, a 5' to 3' DNA polymerase as well as a 3' to 5' proof reading exonuclease. The initiation of DNA synthesis is preceded by the unwinding of the double stranded mtDNA via a trans-acting DNA helicase. Finally, the primers are removed and the completed DNA circles are ligated by a DNA ligase to form continuous strands.

2.2 ENERGY PRODUCTION IN EUKARYOTIC CELLS

A constant supply of energy is required to generate and maintain biological order in any living cell. This chemical energy is in the form of ATP. In all animal cells, this form of energy is generated from the ingestion of food and subsequent breakdown into smaller molecules. Animal cells generate ATP via two pathways. The first process occurs in the cytoplasm of the cell and results in the partial oxidation of food molecules, producing ATP and other activated carrier molecules. The second takes place in the mitochondria where the activated carrier molecules, generated in the cytoplasm, are converted into ATP. The amount of ATP generated in the mitochondria is far greater than that in the cytoplasm.

Ingested food, in the form of proteins, polysaccharides and fats, is digested by enzymes to form amino acids, sugars, and triglycerides respectively. These monomers are then transported into the cytosol of cells where they will be oxidised (Alberts *et al.* 1997). Specific metabolic pathways convert the sugars and amino acids into pyruvate and at the same time form ATP and NADH, which are activated carrier molecules of the cell. The pyruvate is transported into the mitochondria and is converted to carbon dioxide (CO_2) and a two-carbon acetyl group. The two-carbon acetyl group is subsequently joined to coenzyme A (CoA) to form acetyl CoA, another activated carrier molecule. The fatty acids from lipid breakdown are also transported into the mitochondria and utilised to form acetyl CoA. Once in the mitochondria, the acetyl group is transferred to oxaloacetate and enters the citric acid cycle where several NADH molecules are generated. Amino acids derived

from protein breakdown also join the citric acid cycle directly via other metabolic pathways. Finally, the electrons from NADH are transferred to the electron transport system, or respiratory chain, in the inner mitochondrial membrane where the transferred energy will ultimately result in the consumption of oxygen and release of ATP. The process that takes place in the mitochondrial inner membrane is known as oxidative phosphorylation (OXPHOS).

2.2.1 Oxidative phosphorylation

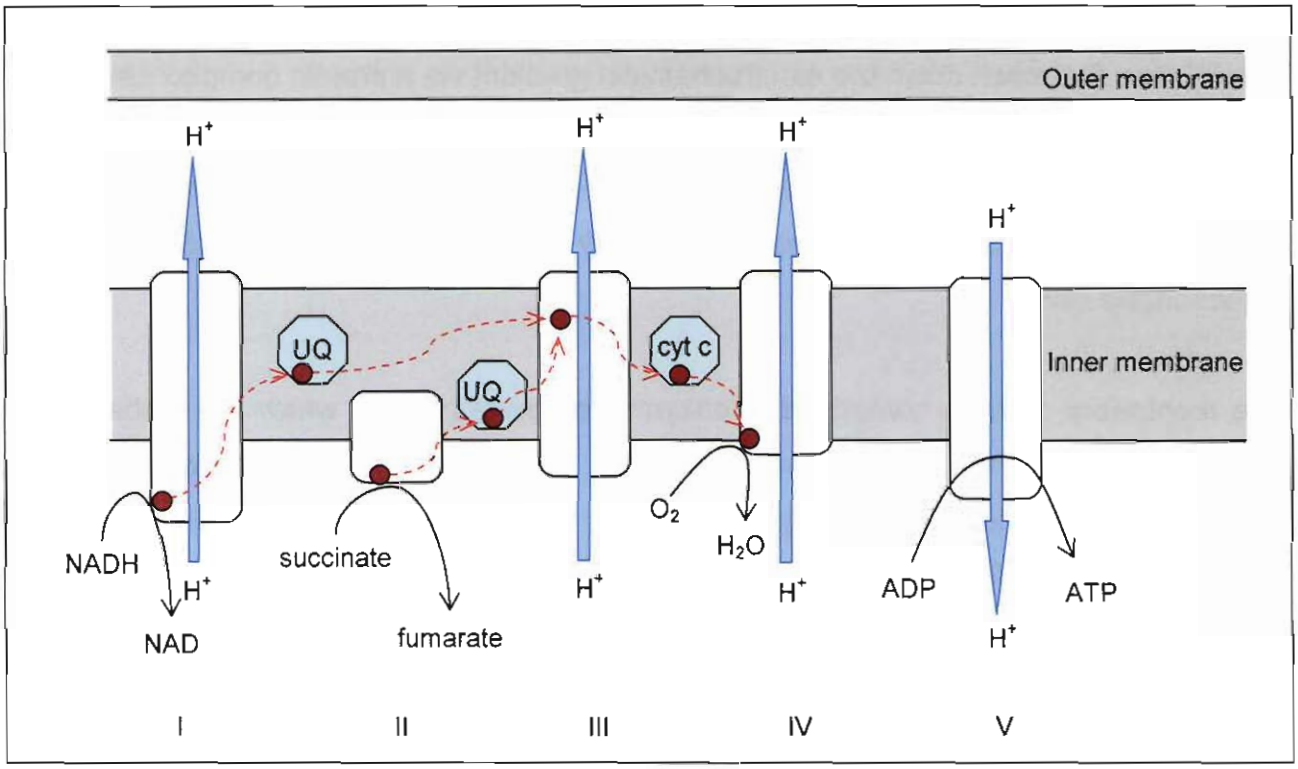
As depicted in Figure 2.5, the respiratory chain of eukaryotes, which is embedded in the mitochondrial inner membrane, provides the most efficient means by which an organism can extract energy from nutrients. The main function of the respiratory chain is to coordinate the transfer of electrons and protons, which ultimately leads to the production of ATP. The electron transport system allows for energy release that is utilised to transfer protons (H^+) across the inner membrane, thus generating an electrochemical gradient. The H^+ ions flow back down the electrochemical gradient via a protein complex called ATP synthase (or complex V), which in turn catalyses the energy-requiring synthesis of ATP. The majority of generated ATP is transported out of the mitochondria and utilised for diverse cellular functions, whereas the minority is used for general functioning in the mitochondria itself.

The respiratory chain is comprised of enzyme complexes I to V, which are embedded in the mitochondrial inner membrane as well as two electron carriers, ubiquinone (also known as coenzyme Q10) and cytochrome c. As depicted in Figure 2.5, high-energy electrons are transferred from both NADH and succinate on the left hand side of the respiratory chain to molecular oxygen (O_2) at the other end. The initial electron transfer from NADH and succinate, with ubiquinone (UQ) as the acceptor, is generated via respiratory complexes I and II, respectively.

One of the major products of the citric acid cycle, NADH, is oxidised to form oxidised nicotinamide adenine dinucleotide (NAD) whilst simultaneously transferring an electron (e^-) into complex I. The complex then reduces UQ, allowing it to take on H^+ ions to form ubiquinol (UQH_2), hence the name NADH: UQ oxidoreductase. In the process, the two-electron transfer is coupled to the translocation of four protons across the inner membrane. Complex II accepts electrons from succinate, another product of the citric acid cycle, which is converted to fumarate via oxidation and the simultaneous transfer of

electrons to UQ to form UQH_2. Ubiquinol is oxidised and transfers its electrons to complex III. Electrons subsequently relocate to cytochrome c (cyt c) after which they are transferred to the final electron acceptor, complex IV. At this point, O_2 is reduced to form water (H_2O). Every time electrons are transferred to either of the complexes, free energy is harnessed by the enzyme complexes and consequently couples the movement of H^+ ions from the mitochondrial matrix, across the inner membrane and into the inter-membrane space, as indicated by the blue block arrows. This generates a proton gradient, which is used to drive the production of ATP by complex V. Whilst harnessing the energy generated by the electron transport chain, complex V pumps protons along the electrochemical gradient back into the mitochondrial matrix. The process involves the consumption of O_2 and phosphorylation of adenosine diphosphate (ADP) to ATP, and is hence referred to as oxidative phosphorylation.

Figure 2.5 Diagrammatic representation of oxidative phosphorylation



The five enzyme complexes are indicated in Roman numerals. The blue block arrows indicate the direction of H^+ ion pumping through each of the enzyme complexes. Red dashed arrows (- - -) indicate the flow of electrons (●). ADP = adenosine diphosphate, ATP = adenosine triphosphate, cyt c = cytochrome c, H^+ = protons, H_2O = water, NAD = oxidised nicotinamide adenine dinucleotide, NADH = reduced nicotinamide adenine dinucleotide, O_2 = molecular oxygen, UQ = ubiquinone.

Each of the complexes within the respiratory chain have important roles in mitochondrial energy production. Complex I, by linking redox chemistry to vectorial proton translocation, converts up to 40% of the energy used in mitochondria to make ATP, more efficient than any of the other complexes (Zickermann *et al.*, 2003). Therefore, it is understandable that any defects occurring within the structure of complex I, severely affects its energy

metabolism. Investigations performed by Davey *et al.* (1998) clearly illustrated the vital roles of complex I in mitochondria of synaptic origin. Their experiments demonstrated, via inhibition of each of the proton-translocating complexes (I, III and IV) with their respective inhibitors at a range of concentrations, that threshold levels could be determined at specific stages where major changes in rates of oxygen consumption and ATP synthesis were observed (Davey *et al.*, 1998). The results revealed that by inhibiting the action of complex I by just 25%, as opposed to 80% and 70% for complexes III and IV respectively, severe impairment in mitochondrial energy metabolism was observed. This clearly illustrates the imperative role that complex I has in neuronal cells, one of the highest energy demanding tissues within the body.

2.2.2 Mitochondrial complex I

There has been growing interest in complex I due to its role in ROS generation, in addition to the increasing number of diseases that are caused by defects in or related to complex I (Robinson, 1998). As mentioned previously, complex I catalyses the first step in the respiratory electron transport chain. The enzyme performs the crucial function of oxidising NADH, providing electrons for the reduction of ubiquinone to ubiquinol and pumping of protons across the inner mitochondrial membrane.

Complex I has been the most difficult of the enzyme complexes to investigate in the mitochondrial membrane for various reasons. The complexity of the enzyme concerning subunit composition and function is superior to most existing enzymes in eukaryotes. Protein chemistry and molecular analyses have been hampered due to the high level of hydrophobicity and number of subunits with N-termini modifications, complicating direct sequencing experiments. Complex I is still the only respiratory chain complex for which no X-ray structure is available. This is mainly due to the iron-sulphur prosthetic group clusters that have no characteristic spectra in the visible region (Brandt *et al.*, 2003). Mutagenic studies in order to determine structure-function relationships of complex I have also been few and far between.

2.2.2.1 Subunit composition of complex I

Complex I originating from bovine heart mitochondria is currently the most investigated type of mammalian complex I. The bovine enzyme has been adopted as a model for human complex I and has become essential in experimentation aimed at elucidating

pathogenesis resulting from defects in this enzyme. Due to the homology with mammalian complex I, the nuclear DNA sequences of bovine derived subunits have been used to map complex I subunits within the human genome. The mammalian counterpart of complex I has been identified to consist of 45 fully characterised subunits (Brandt *et al.*, 2003) with, despite exhaustive efforts, an unsequenced 46th subunit (Carroll *et al.*, 2002). The full complement of nuclear encoded subunits classified according to sequence homology and human chromosomal location is listed in Table 2.1. Subunit masses and sequence references are also listed. The 'core' of the enzyme consists of 14 subunits, which is conserved not only in complex I of mammalian mitochondria, but also in the bacterial form of the enzyme (Friedrich *et al.*, 1998). The remaining subunits are referred to as 'supernumerary' or 'peripheral'. The core subunits have provided important clues to understanding the redox and proton translocating activities of the protein. Seven of the 14 core subunits are, in most cases, encoded by the mitochondrial genome in eukaryotes, as discussed in Section 2.1.2. These subunits, designated 'ND' units for NADH dehydrogenase, are highly hydrophobic proteins and contain several putative transmembrane helices. The seven nuclear encoded subunits contain all of the known redox prosthetic groups, namely a flavin mononucleotide (FMN) and eight to nine iron-sulphur clusters.

Table 2.1 The nuclear encoded subunits of complex I

Human subunit	Human chromosomal location	Molecular weight (kDa)	Reference
NDUFV1	11q13	48.5	Patel *et al.* (1991)
NDUFV2	18p11.31-p11.2	23.8	Chomyn and Lai (1989)
NDUFV3	21q22.3	8.4	Skehel *et al.* (1991)
NDUFS1	2q33-q34	77.0	Runswick *et al.* (1989)
NDUFS2	1q23	49.2	Fearnley *et al.* (1989)
NDUFS3	11p11.11	30.4	Pilkington *et al.* (1991)
NDUFS4	5q11.1	15.3	Walker *et al.* (1992)
NDUFS5	1p34.2-p33	12.5	Walker *et al.* (1992)
NDUFS6	5p15.33	10.5	Walker *et al.* (1992)
NDUFS7	19p13	20.1	Arizmendi *et al.* (1992b)
NDUFS8	11q13	20.2	Dupuis *et al.* (1991b)
NDUFA1	Xp24	8.1	Walker *et al.* (1992)
NDUFA2	5q31	11.0	Walker *et al.* (1992)
NDUFA3	19q13.42	9.3	Walker *et al.* (1992)
NDUFA4	7p21.3	9.3	Walker *et al.* (1992)
NDUFA5	7q32	13.2	Walker *et al.* (1992)
NDUFA6	22q13.2-q13.31	15.0	Walker *et al.* (1992)
NDUFA7	19p13.2	12.6	Arizmendi *et al.* (1992a)
NDUFA8	9q33.2-q34.11	20.0	Dupuis *et al.* (1991a)
NDUFA9	12p13.3	39.1	Fearnley *et al.* (1991)
NDUFA10	2q37.3	36.7	Fearnley *et al.* (1991)

Table 2.1 Continued...

Human subunit	Human chromosomal location	Molecular weight (kDa)	Reference
NDUFA11	19p13.3	14.8	Carroll *et al.* (2002)
NDUFA12	12q21.33	17.1	Skehel *et al.* (1998)
NDUFA13	19p13.2	16.6	Fearnley *et al.* (2001)
NDUFB1	14q32.12	7.0	Walker *et al.* (1992)
NDUFB2	7q34	8.5	Walker *et al.* (1992)
NDUFB3	2q31.3	11.1	Walker *et al*, (1992)
NDUFB4	3q13.33	15.1	Walker *et al.* (1992)
NDUFB5	3q27.1	16.7	Walker *et al.* (1992)
NDUFB6	9p13.3	15.4	Walker *et al.* (1992)
NDUFB7	19p13.12-p13.11	16.5	Walker *et al.* (1992)
NDUFB8	10q23.2-q23.33	18.7	Walker *et al.* (1992)
NDUFB9	8q13.3	21.7	Walker *et al.* (1992)
NDUFB10	16p13.3	20.8	Walker *et al.* (1992)
NDUFB11	Xp11.23	14.5	Carroll *et al.* (2002)
NDUFAB1	16p12.3	10.7	Runswick *et al.* (1991)
NDUFC1	4q28.2-q31.1	5.8	Walker *et al.* (1992)
NDUFC2	11q13.3	14.1	Arizmendi *et al.* (1992a)

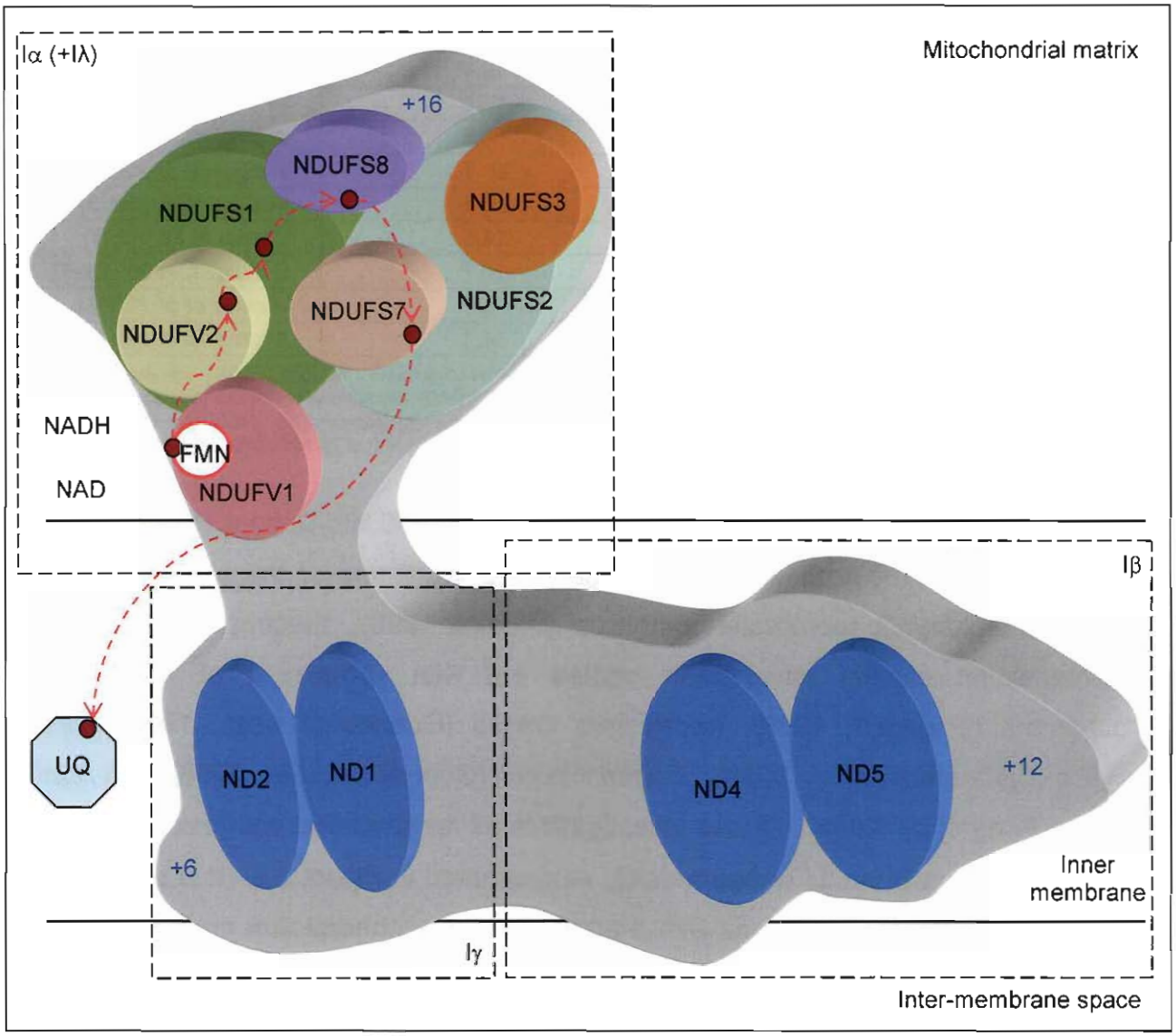
NDUFV = NADH-ubiquinone oxidoreductase flavoprotein, NDUFS = NADH-ubiquinone oxidoreductase iron-sulphur protein, NDUFA = NADH-ubiquinone oxidoreductase alpha (α) sub-complex, NDUFAB = NADH-ubiquinone oxidoreductase acyl carrier protein of the beta (β) sub-complex, NDUFB = NADH-ubiquinone oxidoreductase beta (β) sub-complex, NDUFC = NADH-ubiquinone oxidoreductase lambda (λ) subcomplex, p = 'petit' or short arm of chromosome, q = long arm of chromosome, kDa = kilo-Dalton.

The complete enzyme has a total mass of approximately 980 kilo-Daltons (kDa), assuming that only one copy of each subunit is present, making it one of the biggest and most complicated eukaryotic membrane complexes (Videira, 1998). Electron microscopic and two-dimensional studies have been carried out with complex I of bovine heart mitochondria (Grigorieff, 1998), *Neurospora crassa* (Guenebaut *et al.*, 1998), *Yirowia lipolytica* (Djafarzadeh *et al.*, 2000), *Escherichia coli* (Guenebaut *et al.*, 1998), and *Aquifex aeolicus* (Peng *et al.*, 2003). These investigations all reported that complex I is generally shaped in the form of an 'L' or boomerang, as presented in Figure 2.6. It is embedded in the inner mitochondrial membrane with a perpendicular peripheral arm protruding into the mitochondrial matrix, or cytoplasm in the case of bacteria. The assignment of the subunits to either the trans-membrane or protruding arms of the complex was based on the dual genetic control of the mitochondrial and nuclear genomes, the characterisation and chaotropic fractioning of sub-complexes, as well as modules of common evolutionary origin (Brandt *et al.*, 2003).

The subunit composition can be attributed primarily to two experimental approaches. The first approach was to separate the complex into several smaller sub-complexes, allowing for simplified complex analyses. Secondly, subunit fractionation was achieved by exploiting the physical and chemical properties of the various subunits, followed by protein

analyses via mass spectrometry. These methods led to the identification of the hypothesised full complement of 46 subunits for complex I (Carroll *et al.*, 2002). The complex can be experimentally fragmented using chaotropic agents or, as more recently described, via sucrose gradient centrifugation (Finel *et al.*, 1994) and ion exchange chromatography (Finel *et al.*, 1992 and Sazanov *et al.*, 2000).

Figure 2.6 Diagrammatic representation of mitochondrial complex I



The three human sub-complexes, Iα, Iβ and Iγ have been indicated within the dashed quadrants. It should be noted that the Iα sub-complex can be further fractionated to form Iλ, which contains 15 subunits. The added values in blue refer to the amount of additional subunits, which have not been assigned within the sub-complexes. The sum of the indicated subunits amounts to 45, since ND6 has not been reported to fractionate with any of the sub-complexes. The dark red dots and red dashed arrows represent the flow of electrons. Blue shaded subunits indicate those encoded by the mitochondrial genome. FMN = flavin mononucleotide, NAD = oxidised nicotinamide adenine dinucleotide, NADH = reduced nicotinamide adenine dinucleotide, ND1 to ND5 = NADH dehydrogenase subunits 1 to 5, UQ = ubiquinone, NDUFV = NADH-ubiquinone oxidoreductase flavoprotein, NDUFS = NADH-ubiquinone oxidoreductase iron-sulphur protein. Adapted from Brandt *et al.* (2003), Carroll *et al.* (2003), Grigorieff (1998) and Sazanoz *et al.* (2000).

Treatment with chaotropic agents as well as other detergents result in the separation of complex I into three fractions namely, flavoprotein, iron-sulphur protein (IP) and hydrophobic protein (HP) fractions. The bovine flavoprotein fraction is made up of three

subunits, 51, 24 and 10 kDa in size respectively referred to as NADH-ubiquinone oxidoreductase flavoproteins 1, 2 and 3 (NDUFV1, NDUFV2 and NDUFV3) in humans (see Table 2.1). It is postulated that NDUFV1 is the binding site for NADH (Chen and Beattie, 1981 and Deng *et al.*, 1990). This subunit harbours the FMN prosthetic group, which catalyses the electron transport reactions. The FMN functions as an electron converter between the donor, NADH, and the electron transferring iron-sulphur clusters in adjacent complex I subunits. It is postulated that this 51 kDa subunit also harbours an iron-sulphur cluster. The NDUFV2 subunit contains a binuclear iron-sulphur (Fe_2S_2) prosthetic group, while NDUFV3 does not contain any known redox centres. The IP fraction consists of seven subunits, which includes the NADH-ubiquinone oxidoreductase iron-sulphur proteins (NDUFS1, NDUFS2, NDUFS3, NDUFS4, NDUFS5, NDUFS6) and NADH-ubiquinone oxidoreductase alpha subunit 5 (NDUFA5). The molecular weight of each of the IP subunits is listed in Table 2.1. NDUFS1 is said to contain both tetranuclear (Fe_4S_4) and Fe_2S_2 iron-sulphur clusters. The final fraction of complex I, HP, is a large group of subunits containing 24 nuclear and seven mitochondrially encoded subunits. Unlike the other sub-fractions, this membranous portion of the complex does not contain any iron-sulphur clusters (Finel *et al.*, 1992). Unfortunately, little is known about the functional properties of the subunits in the HP fraction. It is speculated that this fraction may participate in the transport of protons from the mitochondrial matrix to the inter-membrane space (Belogrudov and Hatefi, 1994).

Complex I can also be fractionated via alternative means, for example via treatment with lauryldimethylamine oxide (LDAO), which renders three sub-complexes Iα, Iβ and Iγ (Finel *et al.*, 1992 and Sazanov *et al.*, 2000). The Iα sub-complex constitutes 21 primarily hydrophilic subunits and constitutes approximately 55% of the total enzyme mass. Sub-complex Iα contains all the redox centres of the enzyme, which can be further fractionated to form sub-complex Iλ (Finel *et al.* 1994). Since the majority of subunits in Iα are hydrophilic, it forms the peripheral arm and part of the membrane domain of complex I. Sub-complex Iβ contains 14 hydrophobic subunits, except for ND6, which has been fractionated into sub-complex Iγ (Sazanov *et al.*, 2000). Figure 2.6 depicts the three sub-complexes within dashed quadrants. During chromatography experiments subunits ND1 and ND2 were always determined to be associated with each other, the same being true for subunits ND4 and ND5. Since the pairs were observed to separate into different sub-complexes, Sazanov *et al.* (2000) hypothesised that these subunits are located in different regions of the hydrophobic membrane arm. Electron microscope analyses

indicated that ND5 and ND4 could be localised distal to the membrane arm, whilst ND1 and ND2 reside near the junction of the membrane and peripheral arm.

2.2.2.2 Functional properties of the complex I subunits

Little is known about the exact functional properties of each of the subunits. The mitochondrially encoded subunit ND1 has been indicated via photoaffinity labelled experiments of rotenone and ubiquinone analogues that it may very well be the terminal acceptor for quinone reduction within the membrane portion of complex I (Earley *et al.*, 1987). Patients with mutations in ND1 have also been demonstrated to have defective electron transport (Majander *et al.*, 1991). Additional functional properties based on clues from patients affected with mutations in complex I subunits, have also been inferred to other subunits. Defects in ND4 resulted in the inability to synthesise ATP from NAD linked substrates, thus implying that ND4 may be involved in proton translocation (Majander *et al.*, 1991). Since a high degree of homology exists between ND2, ND4 and ND5, it is probable that the other two subunits might also be involved in the transfer of protons across the inner mitochondrial membrane (De Vries *et al.*, 1996). A deficiency in electron flow was also reported to be due to the presence of mutations in ND6 (Jun *et al.*, 1994).

Several complex I investigations have been performed in prokaryotic lineages in order to determine structure-function relationships of the subunits. However, investigations have been complicated due to the fact that even the corresponding prokaryotic form of the enzyme is a large 500 kDa protein, a factor contributing to its lack of stability. Until recently, only two intact forms of complex I have been purified, the first from *Escherichia coli* (Leif *et al.*, 1995) and second from the closely related *Klebsiella pneumoniae* (Krebs *et al.*, 1999).

Molecular biology's classical investigative organism, *Saccharomyces cerevisiae*, cannot be utilised in application studies since it does not harbour a complex I. Consequently, studies on complex I have primarily been undertaken in mitochondria from *Escherichia coli, Neurospora crassa* and bovine heart muscle. However, since successful functional studies based on mutagenesis have been scarce due to organismal complications, different investigational models have been explored. One of the most popular and established experimental genetic systems for investigating complex I is that of *Yarrowia lipolytica* (Djafarzadeh *et al.*, 2000, Kerscher *et al.*, 2002). This powerful new model is a

strictly aerobic yeast organism and has proven valuable since it is one of the first organisms to have its complex I manipulated successfully for structure-function studies. As it is an obligate aerobe, it has the unique capability to utilise aliphatic carbon sources, including fatty acids and alkanes. Therefore, this form of yeast will always undergo aerobic respiration to utilise glucose, as opposed to *Saccharomyces cerevisiae* that prefers the fermentation of ethanol. Moreover, the *Yarrowia lipolytica* respiratory chain is a great deal more similar to that of the mammalian system than other yeast species. Complex I is essential for the survival of this yeast and any subunit deletions results in death. In order to perform functional studies on complex I, this limitation was overcome by constructing transgenic strains of *Yarrowia lipolytica* that possess mitochondrial matrix facing NADH: UQ oxidoreductase. Most yeast strains encode alternative forms of complex I, namely NADH dehydrogenase 2 (NDH2). These alternatives, however, lack the ability to pump protons across the membrane and hence do not contribute to the proton gradient. In contrast to *Saccharomyces cerevisiae*, the *Yarrowia lipolytica* alternative form does not project internally to the mitochondrial matrix, but is externally oriented. Thus, the protein cannot replace the role of electron transfer of complex I if mutations arise within it. By fusing a mitochondrial targeting sequence to *Yarrowia lipolytica* NDH2, successful import and orientation of the trans-gene was achieved. This allowed for subsequent functional studies on complex I, with the strain surviving to high levels of inhibition and mutagenic investigations of complex I.

Site directed mutations, employing the various techniques of DNA recombinant technology, have been induced in several of the core subunits of complex I of *Yarrowia lipolytica*. To date, it has been proven that unless the induced mutations result in assembly defects or instabilities of complex I, reduction in expression levels of the enzyme have not been observed.

2.2.3 Inhibitors of the respiratory chain

Inhibitors of the respiratory chain result in a 'block' in electron transfer and hence an accumulation of reduced compounds before the blocked point (Campbell, 1995). The inclusion of inhibitors in research has great value when performing functional studies with specific cellular processes in mind. Although respiratory chain inhibitors have been reported for all five of the enzyme complexes, the most commonly used are those that bind complexes I, III and IV. A listing of some commonly used inhibitors of the mitochondrial respiratory chain is presented in Table 2.2.

Table 2.2 Listing of the most common inhibitors of the respiratory chain

Enzyme	Inhibitor
Complex I	Rotenone, amytyl, acetogenins, piercidin, vanilloids
Complex II	Atpenins, thenoyltrifluoroacetone, carboxanilides
Complex III	Antimycin A, myxathiazol, 5-n-undecyl-6-hydroxy-4,7-dioxobenzothiazol (UHDBT)
Complex IV	Cyanide, carbon monoxide (CO), azide
Complex V	oligomycin, dicyclohexylcarbodimide (DCCD)

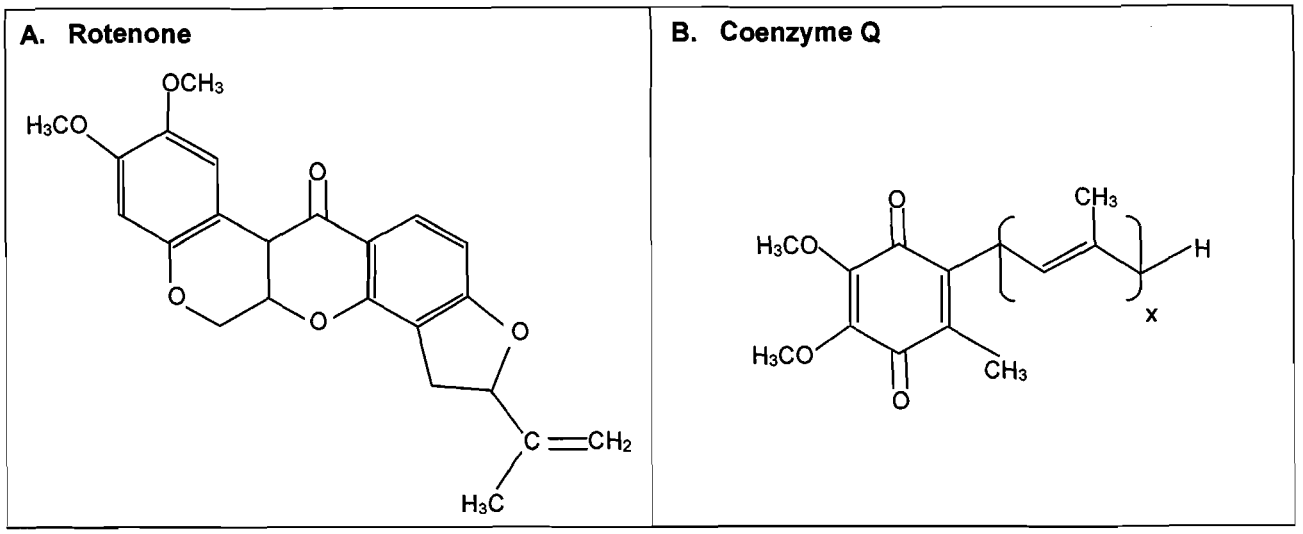
It should be noted that only some of the inhibitors for the various complexes are listed in Table 2.2. Each of the respiratory chain complexes are subject to a far greater amount of inhibitors, such as complex I that has been reported to be inhibited by over 60 different compounds (Degli Esposti, 1998). Since one of the specific aims of the study, as listed in Chapter Three, was to establish a complex I deficient animal model, literature regarding the inhibitor of choice for the investigation, that is rotenone, will be presented in the subsequent section. The remainder of respiratory chain inhibitors will not be discussed as it is beyond the scope of the study to do so.

2.2.3.1 Rotenone

Enzyme inhibitors of complex I are mostly similar in structure to that of ubiquinone, also referred to as coenzyme Q. These compounds are composed of a cyclic 'head' and hydrophobic 'tail', as presented in Figure 2.7. As a consequence, the inhibitors of complex I that share structure similarity with coenzyme Q, are in direct competition for the same binding site within the mitochondrial inter-membrane space.

Rotenone and the rotenoids, which are a family of the isoflavanoids, are extracts from legume plants and have been used in the field of mitochondrial research for years. Rotenone is the most widely used and accepted inhibitor of complex I, so much so that the site where both coenzyme Q and rotenone bind is often referred to in the literature as the 'rotenone site' (Degli Esposti *et al.*, 1996).

Figure 2.7 Schematic representations of the chemical structures of rotenone and coenzyme Q



C = carbon, H = hydrogen, O = oxygen, x = refers to number of isoprenoid side-chains.

Even though rotenone binds complex I irreversibly (Grivennikova *et al.*, 1997), it does not fully inhibit complex I and therefore results in a leaking of electrons and hence ROS formation (Krishnamoorthy and Hinkle, 1988). Rotenone, as presented in Figure 2.7.A, consists of a five-ring structure, while coenzyme Q is comprised of a single ring, or cyclic head. Both structures present with a hydrophobic tail, as mentioned previously in this section. The 'x' depicted in Figure 2.7.B indicates the number of isoprenoid side chains.

CHAPTER THREE

PATHOLOGY OF THE MITOCHONDRIA

Mitochondrial disorders were first described in the 1960's when a 30-year-old woman was diagnosed with severe hypermetabolism, but not due to a thyroid dysfunction (DiMauro, 2004a). The patient presented with extremely high perspiration, an unusually high caloric intake, muscular weakness and a basal metabolic rate of more than 180%. To the surprise of the researchers, the thyroid function of the woman was normal (Luft, 1994). Experiments that followed implicated the mitochondria as the primary cause of the hypermetabolism due to biochemical verification of 'loosely coupled' respiration and morphological abnormalities of the mitochondria from skeletal muscle. These biochemical findings, namely the deficiency in respiratory control, resulting in an energy leakage and the inability of the mitochondria to sufficiently maintain ATP synthesis correlated superlatively with the clinical expression of the disorder. The electron microscopic proof of mitochondrial structural abnormalities in muscle became a key characteristic feature initially utilised in the diagnostic process of mitochondrial cytopathies. The disorder was coined Luft Syndrome, named after Rolf Luft who made this staggering finding (Luft *et al.*, 1962) along with coworkers Lars Ernster and Bjorn Afzelius.

Following the completion of the sequence of the human mitochondrial genome (Anderson *et al.*, 1981), the first of the pathogenic mtDNA rearrangements were reported (Holt *et al.*, 1988 and Wallace *et al.*, 1988). Holt and colleagues reported large-scale single deletions in patients with mitochondrial myopathies, while Wallace *et al.* published the first report of a point mutation in subunit four of complex I (ND4) of the respiratory chain resulting in the clinical phenotype of an optic neuropathy. In the most recent of publications (Servidei, 2004) a listing of 118 pathogenic point mutations can be viewed. However, it should be noted that this publication lists only point mutations and not single deletions or duplications, increasing the number of DNA rearrangements resulting in mitochondrial deficiencies closer to a figure of 200.

Today, mitochondrial biology is one of the fastest growing disciplines in science. The interest in this field of work has shifted from that of a speciality discipline to a major focus within the scope of research. This is due to several factors, but above all due to the fact that recent epidemiological reports indicate the prevalence of mitochondrial disorders to

range somewhere between 1 in 2,000 and 1 in 5,000 (Schaefer *et al.*, 2004; Naviaux, 2004). That is to say that this is the amount of children that will be born and diagnosed with some form of mitochondrial disorder in their lifetimes. Approximately half of these children will start showing symptoms in their first decades of life, while the other half will have a delayed onset. The mitochondrial disorders were previously assumed to affect roughly one in a million people, but today it is one of the most prevalent human disorders (Schaefer *et al.*, 2004).

Despite the burst of research in the field of mitochondrial medicine, our understanding of the pathogenesis of mitochondrial cytopathy is still poor. Several therapy regimens have been attempted, but few have shown responsive results, be it biochemically or clinically. The fact that we are still so overwhelmed by the diverse variation in expression of these disorders most certainly complicates the development of rational therapeutic regimens.

3.1 MITOCHONDRIAL CYTOPATHIES

Disorders of the respiratory chain have, in the past, been classified as solely neuromuscular and to originate from structural or functional abnormalities in the mitochondria. This was chiefly due to the fact that mitochondrial disorders were traditionally diagnosed via the histologic detection of abnormally proliferating mitochondria on skeletal muscle biopsies (Fadic and Johns, 1996). In addition, it was historically thought that since a defect in the respiratory chain results in a decrease in the overall output of ATP, the tissues that would predominantly be affected, based on energy requirement, would include that of the central nervous system, skeletal muscle and cardiac muscle. These simplified views of mitochondrial biology have however evolved considerably over the years. The disorders are today clearly multi-systemic and highly variable.

3.1.1 Chronic Progressive External Opthalmoplegia

Chronic Progressive External Opthalmoplegia (CPEO) is the most common of the mitochondrial disorders. The age of onset ranges between 20 and 30 years of age, but has been reported to occur later in life. In the majority of cases, CPEO initially presents with ptosis and symmetrical weakness of the extraocular muscles. Proximal limb myopathy usually accompanies the opthalmoplegia. The progression of CPEO is benign

in nature with rare developments of additional tissue or organ failure. Patients seldom end up with a disability (Leonard and Schapira, 2000). The genetic causes of CPEO are usually sporadic in origin, but can follow other forms of inheritance. Maternally inherited CPEO occurs in association with a point mutation in position 3243 in the tRNA gene for leucine ($tRNA^{Leu(UUR)}$) of mtDNA. The autosomal dominant form of CPEO is associated with multiple mtDNA deletions, probably due to a nuclear gene defect resulting in defective mtDNA replication and repair (Soumalainen and Kaukonen, 2001).

3.1.2 Pearson Syndrome

Pearson Syndrome was originally defined as a disorder presenting with sideroblastic anaemia, vacuolisation of marrow precursors and pancreatic dysfunction (Pearson *et al.*, 1979). It was, however, only classified as a mitochondrial disorder some years later due to findings of abnormal oxidative phosphorylation in lymphocytes (Rötig *et al.*, 1990), and confirmed by the presence of primarily large deletions of mtDNA (Rötig *et al.*, 1995). Patients have more recently been reported to present with Pearson syndrome lacking pancreatic (Rötig *et al.*, 1995) or marrow (Morris, 1999) involvement. Similar to most of the mitochondrial cytopathies, a multi-organ involvement profile has also been associated with Pearson syndrome. Patients suffer from transfusion-dependent anaemia, neutropenia and thrombocytopenia. Precursor vacuolisation principally includes erythroid and myeloid precursors, probably due to cellular degenerations and death. Haemosiderosis and ringed sideroblasts are also featured. Skeletal muscle biopsies may or may not reveal ragged-red fibres. The pancreatic involvement may be exocrine or endocrine, with chronic diarrhoea, failure to thrive and diabetes mellitus often being present (Gillis and Kaye, 2002). Splenic, hepatic and other gastrointestinal involvements are not uncommon. No neurological symptoms are associated with this mitochondrial cytopathy. Most patients do not survive beyond four years of age, and those that do often develop Kearns-Sayre syndrome (KSS), as discussed in Section 3.1.3. A variety of sporadically occurring mtDNA duplications and deletions has been identified to be causative of Pearson Syndrome. However, the most common of rearrangements are large deletions of approximately 5 kb in size. Identical mtDNA deletions have been reported in CPEO, KSS and Pearson Syndrome, even though they may present phenotypically different. The tissue distribution of the mutated mtDNA does differ between these cytopathies (Poulton *et al.*, 1994).

3.1.3 Kearns-Sayre Syndrome

Kearns-Sayre syndrome, a subtype and more malignant form of CPEO, presents with pigmentary retinopathy and a cardiac conduction defect. Patients usually present with progressive symmetrical ptosis and limited eye movement. It is often accompanied by ataxia and/or raised cerebrospinal fluid protein content. Other central nervous system related signs may include slowly progressing dementia and seizures (Vedanarayanan, 2003). Skeletal muscle biopsies reveal ragged-red fibres. In addition, patients may develop deafness, diabetes, endocrine dysfunction and behavioural disorders. The onset of KSS generally occurs before 20 years of age. The course of the disorder is also progressive, but with few patients surviving into the fourth decade of life (Leonard and Schapira, 2000). Sporadically occurring, large-scale mtDNA deletions (Holt *et al.*, 1988 and Zeviani *et al.*, 2003), as well as duplications (Poulton, 1992), result in the manifestation of this syndrome. These rearrangements are present in muscle and therefore may be overlooked by analysing blood samples alone. It should also be noted that no nuclear DNA defects exist for KSS, unlike in CPEO. Therefore, no autosomal dominant or recessive inheritance patterns exist. As mentioned in Section 3.1.2, children surviving Pearson Syndrome may develop KSS due to progressive accumulation of mutant mtDNA in brain, skeletal muscle and heart (McShane *et al.*, 1991).

3.1.4 Myoclonus Epilepsy with Ragged-Red Fibres

Myoclonus Epilepsy with Ragged-Red Fibres (MERRF) presents symptomatically in early childhood as myoclonic epilepsy, progressive ataxia and muscle weakness. A generalised deterioration in intellectuality is observed. These symptoms are often accompanied with signs of recurrent headaches, sensorineural deafness, opthalmoplegia, optic atrophy, polyneuropathy, cardiomyopathy, high-arched feet, involuntary movements, spastic paraparesis and multiple symmetrical lipomatosis (Vedanarayanan, 2003). The cytopathy is clinically highly variable between individuals, even from the same family. The myoclonus is induced by noise, activity or photic stimulation. Drop attacks, focal as well as photosensitive tonic-clonic seizures are common. Truncal and appendicular muscle ataxia are prominent with ragged-red fibres often being identified too. The majority of cases arise from a mtDNA mutation in position 8344 of the tRNA lysine gene ($tRNA^{Lys}$) (Shoffner *et al.*, 1990), where a change of nucleotides from adenine to guanine takes place, resulting in deficient protein synthesis of mitochondrial proteins. An additional mutation of importance is the T8356C, which has, in addition (Zeviani *et al.* 1993), been

observed in cases where a family presented with an overlapping phenotype between MERRF and another of the mitochondrial cytopathies, namely Mitochondrial myopathy, Encephalomyopathy, Lactic acidosis and Stroke-like episodes (MELAS), discussed in Section 3.1.5. These mutations are maternally inherited. However, there is also a report of the MERRF phenotype resulting from sporadic multiple deletions of mtDNA (Blumenthal *et al.*, 1998). It is suspected that this manifestation is due to a nuclear DNA rearrangement that has not been identified as yet.

3.1.5 Mitochondrial Myopathy, Encephalomyopathy, Lactic Acidosis and Stroke-like episodes

The MELAS phenotype is characterised by cognitive impairment associated with migraine-like intermittent hemicranial headaches and vomiting. Normal early growth of children takes place followed by growth failure, focal and generalised seizures and recurrent focal neurological deficits that resemble strokes. Lesions have been identified in the occipital and parietal lobes of the brain and have been determined to extend beyond defined vascular territories (Vedanarayanan, 2003). Elevated serum and cerebrospinal fluid lactate is present and remains high until recovery. Intellectual impairment often results. Children also present with recurrent vomiting, muscle weakness and short stature. Myoclonus, sensory neuropathy, heart block, opthalmoplegia and pigmentary retinopathy are generally absent, but have been reported on few occasions. A large degree of clinical variation is often observed in patients with MELAS encompassing features of psychomotor retardation, limb weakness, diabetes mellitus, deafness, cardiomyopathy and CPEO. In addition, ragged-red fibre appearances in skeletal biopsies have been identified, but not consistently. The primary genetic defect associated with MELAS, accounting for approximately 80% of patients, is the A3243G mutation in $tRNA^{Leu(UUR)}$ of mtDNA. This mutation results in suboptimal protein synthesis of subunits of the respiratory chain. An additional 10 mtDNA aberrations have been reported to date (Servidei, 2004). In most cases, the cytopathy is maternally inherited, presents symptomatically towards the end of the first decade of life and is progressive in nature.

3.1.6 Leber's Hereditary Optic Neuropathy

One of the most common causes of sudden visual loss and of the mitochondrial disorders is the maternally inherited Leber's Hereditary Optic Neuropathy (LHON), a disorder characterised by acute or subacute bilateral visual loss predominantly affecting young men. Onset takes place in adolescence or early adulthood, with a normal growth and

maturity pattern until this point. The disorder is usually accompanied by peripapillary microangiopathy and most commonly cardiovascular abnormalities (DiMauro *et al.*, 2001). Skeletal muscle is not affected. The three most prevalent mutations resulting in the disorder occur in the subunits of complex I. These include G3460A, G11778A and T14484C in subunits ND1, ND4 and ND6 respectively. However, only 10% of women and 50% of males with either of these mutations develop symptoms of this disorder (Bhattacharya *et al.*, 2003). The fact that the majority of clinically affected patients are male may indicate that an X-linked susceptibility factor may be involved in the phenotypic expression of LHON.

3.1.7 Leigh and Leigh-like Syndrome

Leigh Syndrome, also referred to as subacute necrotizing encephalomyelopathy, is of the most common of the mitochondrial disorders of childhood. It typically presents with psychomotor retardation. The initial signs begin with retarded development, hypotonia, ataxia, poor motor control and generalised weakness (Vedanarayanan, 2003). Children suffer from vomiting, other systemic complications and develop a failure to thrive along with respiratory complications. Lactic acidosis is often a feature accompanied by ocular atrophy, seizures and an altered mental status. The clinical expression is also highly variable with several organs coming into play. As children get older, regression may occur along with focal neurological symptoms. The course of the disorder varies considerably with some patients remaining stable for several years, whilst others deteriorate considerably rapidly. Neuro-imaging of these children often reveals necrotic lesions in posterior regions of the spinal cord, brain stem and thalamus illustrating an incomplete recovery from each relapsing seizure (Bhattacharya *et al.*, 2003).

Several DNA mutations, both nuclear and mitochondrial, have been reported to be associated with Leigh Syndrome. The majority of mtDNA mutations occur in the ATPase 6 gene. The biochemical profiles generally include a deficiency of complex I and IV of the respiratory chain, pyruvate dehydrogenase and biotinidase. Complex I deficiency results from mutations in nuclear and mitochondrially encoded polypeptide subunits. Complex IV deficiency is chiefly due to mutations in a variety of proteins involved in the assembly of complex IV, namely the surfeit locus 1 (SURF1), *Saccharomyces* cytochrome oxidase homolog subunits 1 and 2 (SCO1 and SCO2), and cytochrome c oxidase subunits 10 and 15 (COX10 and COX15). However, these ancillary proteins have also been identified to be associated with various other clinical phenotypes. Leigh Syndrome, along with another

disorder referred to as GRACILE (Growth Retardation, Aminoaciduria, Cholestasis, Iron overload, Lactic acidosis and Early death), is also associated with a mutation within assembly proteins of complex III, encoded by the nuclear genome (De Lonlay *et al.*, 2001). A deficiency in pyruvate dehydrogenase, an enzyme involved in pyruvate metabolism, is largely due to mutations in one of its subunits encoded for by a gene located on the X-chromosome. Therefore, the mode of inheritance of Leigh Syndrome may be maternal, autosomal recessive or X-linked recessive.

Neurogenic muscle weakness, Ataxia and Retinitis Pigmentosa (NARP) is a disorder that presents with seizures, ataxia, sensorimotor neuropathy and intellectual impairment or dementia. This defect is also referred to as a 'Leigh-like' syndrome and children that develop this disorder often adopt a true Leigh syndrome phenotype with time when specific mutations, namely T8993G and T8993C, become more and more homoplasmic (Rahman *et al.*, 1996).

3.1.8 Other mitochondrial cytopathies

Mitochondrial Neuro-Gastro-Intestinal Encephalomyopathy (MNGIE) is one of the more rare forms of the mitochondrial cytopathies that displays clinical signs of peripheral neuropathy, progressive leukoencephalopathy accompanied by intermittent diarrhoea and gastrointestinal dysmotility (Hirano *et al.*, 1994). Pseudo obstruction of the intestinal tract may also occur. This defect follows an autosomal recessive mode of inheritance and results from deletions in a nuclear gene known as thymidine phosphorylase located at the terminal end of chromosome 22q. This gene is involved in maintaining the integrity of mtDNA with an aberration resulting in multiple mtDNA deletions (Gills and Kaye, 2002).

Friedreich ataxia is an autosomal recessive disorder manifesting from a triplet nucleotide repeat expansion in the frataxin gene. The protein product of this gene is localised to the mitochondria and functions to control iron homeostasis and possibly the assembly of iron-sulphur subunits of the respiratory chain. The repeat expansion results in a decrease in mRNA transcripts of frataxin and consequently iron accumulation in tissue. The clinical signs include spinocerebellar ataxia, neuropathy and hypertrophic cardiomyopathy (Calabresse *et al.*, 2005).

Barth Syndrome is defined by skeletal myopathy, cardiomyopathy, growth retardation and cyclic neutropenia. It has been classified as a disorder of the inner mitochondrial

membrane and manifests due to a deficiency in cardiolipin, one of the phospholipids constituting the membrane. Barth Syndrome follows an X-linked recessive mode of inheritance and is caused by mutations in a gene encoding a family of proteins known as the 'tafazzins'. These proteins are homologous to phospholipid acyltransferases and it is hypothesised that the syndrome may result from a defect in a mitochondrial specific acyltransferase. This theory is indirectly supported by the fact cardiolipin is in paucity.

The mitochondria have also been associated with late onset neurodegenerative disorders that include Parkinson disease, Huntington disease, Alzheimer disease and amyotrophic lateral sclerosis. The precise role that the mitochondria and environmental factors have on the pathogenesis of these disorders remains to be well defined (DiMauro, 2004a).

3.2 PRESENTATION OF THE MITOCHONRIAL CYTOPATHIES

The diagnosis of mitochondrial cytopathies has been more complicated than previously assumed. The spectrum seems to be broadening with each publication. It appears that any organ may be implicated or at least involved in the phenotypic manifestation of one or other mitochondrial cytopathy. There are several factors that may influence the severity of a mitochondrial defect, ranging from a variety of genetic factors to dietary and medical contributions, not to forget environmental influences.

Defects of the mitochondria result in disorders that are clinically, biochemically and genetically heterogeneous. The pathophysiological events that are the consequence of these defects are complex and symptomatic management is challenging. Since the functioning of the mitochondria depends on an intricate coordination of two genetic entities, that is nuclear and mitochondrial, it is understandable that a complex pathogenic expression is observed. The clinical manifestation of the disorders may be fatal, progressive or even regress with age. Symptomatic presentation may occur at any stage of life and as the disorder progresses, it is expected that an increasing number of seemingly unrelated organs may become involved. Furthermore, the mitochondrial cytopathies follow any mode of inheritance.

The diagnostic process for the mitochondrial cytopathies involves the integration of clinical, biochemical and genetic parameters obtained from the patient, in addition to the classical approach of determining a thorough medical and family history, as well as

physical and neurological characteristics. Four systemic approaches for the diagnosis of mitochondrial disorders have been developed in the past and used with success (Naviaux, 2004). These are the Modified Walker Criteria, the Nijmegen Criteria, the Nonaka Criteria and the Wolfson Criteria. These Criteria predominantly use a clinical and biochemical profile to classify a patient as a 'likely', 'unlikely', 'probable', 'possible' or 'definite' candidate. No method is perfect, as there are most certainly patients that fall into the grey areas somewhere between 'unlikely' and 'definite'. The sensitivity and specificity of these criteria still needs to be fine-tuned before physicians can diagnose patients with absolute certainty. However, due to extreme diversity in the pathogenesis of these disorders, complete sensitivity and specificity of diagnosis may be a difficult concept to accept for several physicians.

3.2.1 Clinical and histological features

Since every living cell in the body is dependent on the mitochondria and respiratory chain to produce energy, a defect in this process can potentially affect each cell, tissue and organ of the human body. As a consequence, the categorisation of these disorders has shifted from the classical mitochondrial 'encephalomyopathies' and 'myopathies' to that of the mitochondrial 'cytopathies'. This shift in classification has been validated on several occasions with the literature unequivocally reporting a diverse spectrum of clinical presentation. Therefore, a key characteristic of patients typically affected by a respiratory chain defect is that of a profile presenting with a combination of neuromuscular and non-neuromuscular symptoms. Diagnosis may be straightforward with patients presenting with clear-cut clinical symptoms associated with the various mitochondrial cytopathies. However, this scenario is in the minority (Bhattacharya *et al.*, 2003). A few distinctive syndromes have been assigned, as discussed in Section 3.1. However, several patients present with overlapping pathological expression, making the diagnostic process extremely challenging. The diversity of reported clinical symptoms of patients harbouring mitochondrial defects include neurological, muscular, cardiac, renal, nutritional, hepatic, endocrine, haematological, sensorineural hearing loss, opthalmological, dermatological and facial dysmorphism involvement (Munnich *et al.*, 1992). Table 3.1 lists the primary symptoms associated with the mitochondrial cytopathies.

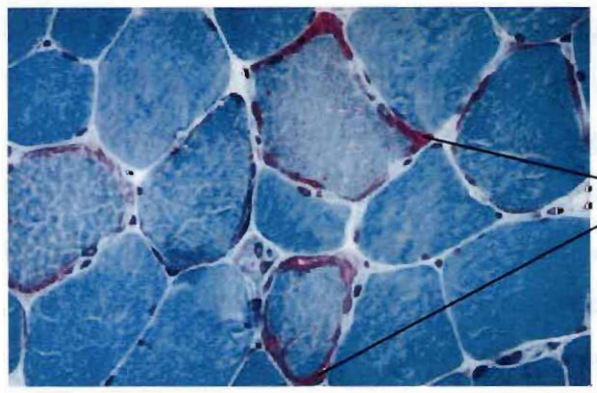
Table 3.1 Primary characteristics of mitochondrial cytopathies

System/ Tissue	Symptom
General systemic	Failure to thrive, irritability, recurrent and episodic vomiting
Neurological	Seizures, ataxia, myoclonus, psychomotor retardation and regression, acute encephalopathy, migraine-like headaches, hypotonia, hypertonia and dystonia, hemiparesis/ hemianopia, cortical disease, developmental delay and regression, stroke-like episodes, peripheral neuropathy
Muscle	Weakness/ exercise intolerance, opthalmoplegia, ptosis, rhabdomyolysis, ragged-red fibres (histological)
Cardiac	Conduction defects, cardiomyopathy
Pulmonary	Respiratory abnormalities
Eye and ear	Progressive external opthalmoplegia, pigmentary retinopathy, optic atrophy, cataracts, retinal degeneration, sensorineural hearing loss
Bone marrow	Sideroblastic anaemia, thrombocytopenia, neutropenia
Endocrine	Diabetes mellitus, growth hormone insufficiency, hypoparathyroidism, hypoadrenalism, hypothyroidism
Gastrointestinal	Exocrine pancreatic dysfunction, intestinal pseudo-obstruction, chronic diarrhoea
Liver	Liver dysfunction, hepatomegaly, fulminant liver failure
Kidney	Proximal tubulopathy, tubulointerstitial nephritis
Cutaneous	Hypertrichosis
Metabolic and histological	Lactic acidosis, hypoglycaemia

Adapted from DiMauro and Schon (2001) and Bhattacharya *et al.* (2003).

Traditionally, clinicians diagnosed the mitochondrial disorders based on morphology of skeletal muscle mitochondria. Abnormal deposits of enlarged mitochondria were detected via light microscopy and a modification of the Gomori trichrome histochemical stain, as can be seen in Figure 3.1. The subsarcolemmal region of abnormal muscle fibres were stained red by Gomori trichrome, resulting in a 'ragged-red' appearance of the muscle.

Figure 3.1 Photographic representation of the ragged-red fibre appearance of muscle obtained from patients with mitochondrial defects



Adapted from DiMauro (2004a).

Ragged-red fibres became a signature for the then referred to mitochondrial myopathies (Shanske and DiMauro, 1997). With time, it became evident that the ragged-red fibre

diagnostic tool could not be used to exclusively diagnose these disorders. A good example of this fact is Leigh syndrome, a mitochondrial encephalomyopathy of infancy, which is rarely accompanied by ragged-red fibres (DiMauro, 2004a). A number of reports that followed indicated that this morphology was not specific to the primary mitochondrial myopathies, nor was it present in all the mitochondrial cytopathies (DiMauro *et al.*, 2001).

3.2.2 Biochemical consequences

The field of mitochondrial medicine evolved to characterise various syndromes of mitochondrial pathology, as discussed in Section 3.1. However, several overlapping features between these syndromes exist, making clear-cut diagnoses challenging. The biochemical component of the diagnostic process has also become an explicit feature. Key biochemical consequences of the mitochondrial cytopathies are listed in Table 3.2.

Table 3.2 Biochemical consequences of respiratory chain defects

Consequence	Reason
1. Elevated NADH/NAD ratio	Impaired electron transfer from NADH to complex I
2. Impaired Krebs cycle	Due to excess NADH
3. Elevated lactate/pyruvate ratio	Functional impairment of Krebs cycle and β-oxidation
4. Elevation of ketone body formation	Functional impairment of Krebs cycle (conversion of acetyl CoA to ketone bodies)
5. Decreased mitochondrial ATP production	Inadequate formation of an electrochemical gradient
6. Superoxide formation	Increased reduction of oxygen

ATP = adenosine triphosphate, β = beta, CoA = coenzyme A, NAD = oxidised nicotinamide adenine dinucleotide, NADH = reduced nicotinamide adenine dinucleotide.

The respiratory chain is composed of a multi-enzyme system that functions via an oxidation-reduction model in order to transfer electrons across a chain of enzymes to create an electrochemical gradient that ultimately enables the production of ATP, as discussed in Section 2.2.1 of Chapter Two. In the majority of diagnostic laboratories, ATP output used to be the primary biochemical parameter measured. In 60% of cases, where there is a decreased ATP level, patients harbour at least one respiratory chain enzyme deficiency (Van den Heuvel *et al.*, 2004). Therefore, it is today regarded that the most valuable biochemical tests are those performed on the respiratory chain enzymes. However, caution should be taken since these may be compromised by threshold effects and mutant mitochondrial load in a specific tissue, resulting in a lack of reproducibility and inaccurate diagnoses.

Aberrations in the respiratory chain will most certainly affect the oxidation-reduction status of the cell. In most cases excess NADH collects in the cell due to insufficient oxidation via complex I. As a consequence, the Krebs cycle is negatively affected, accompanied by an altered ratio of lactate to pyruvate due to secondary elevation of lactate. An increase in the formation of ketone bodies after meals is also an indicator since acetyl CoA is shifted to ketogenesis (Rötig *et al.*, 1990). Therefore, primary metabolic indicators in patients are that of the NAD/NADH status, lactate/pyruvate ratios and ketone bodies (Munnich *et al.*, 1992). It should, however, be noted that increased lactate levels may not be specifically due to impairment of the respiratory chain. It may also arise from a range of other metabolic disorders, such as pyruvate dehydrogenase deficiency and organic acidaemias, or from secondary causes such as tissue hypoxia and hepatic failure (Morris *et al.*, 1995).

A defect in the respiratory chain will inevitably result in an increased formation of ROS due to a leakage of electrons. The harmful effects of ROS, by targeting various components of the cell, may result in a further production of ROS, coinciding with exacerbated biochemical and molecular aberrations. Ultimately, the fate of cells under such oxidative stress is an unsurprising death. The increased production of superoxides, as indicated in Table 3.2, is discussed further in the section to follow.

3.2.2.1 Reactive oxygen species

Defects in the respiratory chain also result in an increase in the formation of ROS, which have deleterious effects in the cell. In the final step of oxidative phosphorylation and ATP production, oxygen is reduced to form water as a by-product. However, oxygen molecules are also capable of accepting additional electrons to create superoxide (O_2^-), a more reactive form of oxygen. Ubisemiquinone, an intermediate state of ubiquinone and ubiquinol and involved in electron transport of the respiratory chain, is a supplier of electrons to oxygen and thus superoxide formation.

Although debatable, it is thought that the majority of superoxide production stems from complex I of the respiratory chain, with the contribution of the other enzyme complexes being significantly lower. Each of the electron transferring centres within complex I have been implicated, although there is a lack of consensus as to exactly which sites are primary to the production of ROS. However, the most likely contributor to superoxide production would be the iron-sulphur centre corresponding to the binding site of ubiquinone (Brand *et al.*, 2004). Complex III is also said to harbour sites for superoxide

production, secondary in rate to complex I, followed by complex II, whose contribution is in the minority.

A family of enzymes known as the superoxide dismutases are involved in maintaining low levels of superoxide by converting them to hydrogen peroxide (H_2O_2). Hydrogen peroxide is not a free radical *per se*, since it does not contain a free electron. However, it is important to note that this molecule can readily diffuse across the mitochondrial membranes and be converted to hydroxyl radicals (OH^-) via contact with ferric and cupric ions. Hydroxyl ions are the most reactive of radicals and have the potential for peroxidative damage to proteins, lipid membranes and DNA of the cell. When a cell reaches this stage of cellular damage, it is said to be suffering from 'oxidative stress'. This state is the consequence of the inherent antioxidant capacity of the cell not being high enough to scavenge all the ROS produced by the respiratory chain. It can also be translated as an imbalance of two opposing forces, namely ROS formation and antioxidant capacity, where the formation of ROS predominates (Kirkinezos and Moraes, 2001).

Superoxides also have the ability to react with nitric oxide (NO) to form another highly reactive free radical, namely peroxynitrite ($ONOO^-$). This form of ROS has several targets and has the potential to have a multitude of deleterious effects. Peroxynitrite targets respiratory chain complexes I, II, IV and V, mitochondrial membranes, mtDNA, superoxide dismutase and other enzymes functioning in the mitochondria. The peroxynitrite induces its deleterious functions by oxidising amino acids, mainly tryptophan and cysteine, as well as by nitrating tyrosine residues of proteins.

Reactive oxygen species have several deleterious outcomes to the cell. They can attack the iron-sulphur centres of complex I and II releasing the iron and consequently obliterating the catalytic activities of these enzymes. This attack from ROS results in decreased activity of these vital enzymes and consequently lowered levels of oxidative phosphorylation and ATP production. An increased generation of lactic acid is often present. These consequences are supported by experiments where mice deficient in superoxide dismutase develop lactic acidaemia, cardiomyopathy and abnormalities of the central nervous system (Lebovitz *et al.*, 1996).

Reactive oxygen species have also been implicated to play a role in apoptosis, or programmed cell death. Apoptosis is a natural mechanism in all living animals that regulates the removal of damaged and unwanted cells. The apoptotic fate of cells may

contribute to our understanding of tissue specific decrease in ATP generation, a scenario often identified in patients suffering from mitochondrial defects. Several cascade pathways initiated by ROS lead to this form of cell death.

There have been reports of increased expression of the superoxide dismutases in patients with respiratory chain deficiencies, in particular complex I deficiency (Robinson, 1998). In a healthy cell, most of the hydrogen peroxide is converted to oxygen and water by antioxidant enzymes such as catalase and glutathione peroxidase in the cytosol and mitochondrial matrix respectively. Furthermore, several antioxidant compounds, such as vitamin E and CoQ_{10}, aid in the prevention of oxidative stress.

3.2.3 Genetic aspects

Genetic defects are the predominant origin of mitochondrial cytopathies. Since the bioenergetic role of mitochondria in the cell depends on the precise coordination of proteins synthesised from both the nuclear and mitochondrial genomes, a potentially large number of critical steps could be genetically altered and result in biochemical turmoil. Due to this dual genetic control, mitochondrial disorders can genetically be classified into two categories, namely defects due to alterations of mtDNA and secondly nuclear DNA. These genetic defects can occur in the genes that influence the activity of the respiratory chain, or alternatively they can arise in genes that code for proteins involved in the house keeping of the mitochondria as well as other metabolic functions of this organelle.

Genetic alterations of mtDNA have been reported to include single or multiple deletions, duplications and point mutations. In addition, although rare, deletions in conjunction with duplications have also been reported (Superti Furga *et al.*, 1993). The deletions and duplications are generally very large, involving approximately 5 kb of the mitochondrial genome. These normally arise sporadically and can occur at any age. The syndromes resulting from single or multiple deletions and duplications, or in combination, of mtDNA include CPEO, KSS and Pearson Syndrome.

Single nucleotide alterations of mtDNA can be subdivided into those that impair mitochondrial protein synthesis, namely in rRNA and tRNA genes, and those that directly alter structural polypeptides that form the respiratory chain. These point mutations may be sporadic or maternally inherited and may result in variety of disease phenotypes, potentially affecting any system of the body. However, even though the point mutations

can be genetically classified into two classes, the clinical expression for both remains highly variable. The syndromes that chiefly manifest from these single nucleotide alterations include MERRF, MELAS and LHON.

The molecular pathogenesis of mitochondrial cytopathies was originally focused essentially on characterising pathogenic genetic alterations in mtDNA. However, with the realisation of the importance of the nuclear component in the overall functioning of the mitochondria, the focus rapidly expanded to encompass investigations in nuclear DNA. Genetic alterations have been reported in several nuclear genes encoding subunits of the enzyme complexes involved in the respiratory chain. These alterations are considerably more prevalent due to the large amount of nuclear proteins and factors involved in the assembly, maintenance and overall functioning of the mitochondria. In addition, for the mitochondria to function as effectively as possible, it is necessary that efficient mtDNA and nuclear DNA coordination take place. The nuclear genome plays a large role in each of the aforementioned characteristics.

A large number of mutations have been identified in genes encoding polypeptides that form a functional part of the respiratory chain. Coenzyme Q10, also referred to as UQ in Figure 2.5 and one of the electron transporters of the respiratory chain, has also been reported to be in deficiency. It is imperative that factors encoded by the nuclear genome coordinate appropriate assembly of the respiratory chain enzyme complexes, maintain mtDNA integrity and efficient replication thereof, and ensure that nuclear proteins targeted to the mitochondria be transported appropriately. Causative mutations in nuclear genes that direct these processes have also been reported. The clinical manifestations that result are usually multi-systemic and, as with all the other mitochondrial disorders, highly variable. In addition, there have also been reports of alterations in genes contributing to the formation and stability of the mitochondrial inner membrane as well as in genes involved in mitochondrial motility.

If a patient presents with one of the classic syndromes, discussed in Section 3.1, it may be worthwhile to attempt screening for reported mtDNA mutations specific to each of the syndromes. However, in most cases, since more and more nuclear genes are being implicated and that the clinical variation is so immense, the safer and more cost effective route would be to perform respiratory chain enzyme analysis.

3.3 ANIMAL MODELS FOR THE MITOCHONDRIAL CYTOPATHIES

Animal models for the mitochondrial disorders have exclusively been established in mice. Three notable mouse models have been reported to date, all of which present with biochemical and physiological features resembling the mitochondrial cytopathies. The first of the 'mito-mice' harboured a deficiency in superoxide dismutase, which was generated via homologous recombination (Li *et al.*, 1995; Lebovitz *et al.*, 1996). These mice presented with neonatal lethality as well as with defects in the heart, liver, bone marrow and brain. A second mouse model established with a mitochondrial disorder lacked one of the adenine nucleotide translocator genes, namely ANT1 (Graham *et al.*, 1997). This protein is responsible for the transportation of ADP and ATP into and out of the mitochondria, respectively. The ANT1 knockout presented with hypertrophic cardiomyopathy and ragged-red fibres, typical of a mitochondrial myopathy. Furthermore, the mice suffered from increased levels of H_2O_2 in mitochondria isolated from skeletal muscle. The third knockout mouse to present with features of a mitochondrial cytopathy harboured an inactivation of mitochondrial transcription factor A (Tfam), responsible for the regulation of mtDNA replication and transcription. These mice developed myopathy with ragged-red fibres, cardiomyopathy, abnormal accumulation of mitochondria and decreased activity of the respiratory chain (Wang *et al.*, 1999 and Wredenberg *et al.* 2002).

In addition to the development of knockout mice for the investigation of the mitochondrial cytopathies, trans-mitochondrial animal models have also been established via the use of cybrid technologies. A trans-mitochondrial mouse model expressing the phenotype of a mitochondrial cytopathy was reported for the first time by Sligh *et al.* (2000). These mice harboured a pathogenic point mutation and presented with a variety of ocular abnormalities, which included congenital cataracts, decreased retinal function and hamaratomas of the optic nerve. Mice progeny presented with further complications, such as growth retardation, myopathy, dilated cardiomyopathy and perinatal or *in utero* lethality. Skeletal and heart muscle mitochondria of these mice were enlarged and atypical with inclusions (Sligh *et al.*, 2000). In the same year, Inoue *et al.* reported cybrid mice with large-scale mtDNA deletions, presenting with cytochrome oxidase deficiency and ragged-red fibres, as well as lactic acidosis (Inoue *et al.*, 2000). In addition, the mice appeared to suffer from renal dysfunction, a feature not typical of a mitochondrial disorder. More recently, McKenzie *et al.* (2004) and Kasahara *et al.* (2006) reported the successful generation trans-mitochondrial mouse models harbouring homoplasmic mtDNA.

3.4 COMPLEX I DEFICIENCY

Isolated Complex I deficiency is the most common and clinically severe reported mitochondrial cytopathy (Smeitink *et al.*, 2004). The deficiency generally manifests itself as Leigh and Leigh-like syndromes, MELAS, LHON as well as other forms of encephalomyopathies. Patients often suffer from fatigue, exercise intolerance and lactic acidaemia. However, additional symptoms, as listed in Table 3.1, often accompany the phenotypes of the above-mentioned syndromes. Causative alterations have been reported in several of the genes that encode subunits of the five enzyme complexes of the respiratory chain as well as in tRNA and rRNA genes. However, new mutations are still being discovered (DiMauro, 2004b). The journal Neuromuscular Disorders published a tabulated section, maintained by Servidei (2004), which listed all of the reported mutations that have been determined to be causative in any of the mitochondrial disorders. Pathogenic alterations, resulting in complex I deficiency, have been reported in 16 genes encoding subunits for complex I, as listed in Table 3.3. The table also briefly lists the clinical phenotypes reported in association with the list of genetic alterations. References to the original publication reports for each mutation are listed in the footer of Table 3.3.

Table 3.3 Reported mutations within complex I subunit genes

Subunit	DNA rearrangement		Clinical phenotypes
ND1	T3308C[1]	G3316A[2]	LHON, MELAS, CPEO, LHON/ MELAS overlap, bilateral striatal necrosis/ MELAS overlap, adult onset dystonia, mitochondrial myopathy
	G3376A[3]	T3394C[4]	
	G3460A[5]	G3496T[6]	
	G3497T[6]	G3635A[7]	
	G3697A[8]	G3700A[9]	
	G3733A[10]	A3796G[11]	
	G3946A[8]	T3949C[8]	
	A4136G[12]	T4160C[12]	
	C4171A[13]	T4216C[14]	
	7 bp inversion starting from 3902[15]		
ND2	C4640A[7]	A4917G[14]	LHON
	G5244A[4]	2 bp deletion from 5132 to 5134[16]	
ND3	T10158C[17]	T10191C[17]	Leigh syndrome, Leigh-like syndrome, LHON
	T10237C[18]		
ND4L	T10663C[19]		LHON
ND4	A11084G[20]	T11232C[21]	MELAS, CPEO, LHON, Leigh syndrome, exercise intolerance
	T11253C[22]	G11696A[23]	
	C11777A[24]	G11778A[25]	
	G11832A[26]		
ND5	T12706C[27]	A12770G[28]	Leigh syndrome, MELAS, LHON, MELAS/ LHON/ Leigh syndrome overlap, LHON-like
	C12848T[29]	A13045C[28]	
	G13051A[30]	A13084T[31]	
	G13513A[32]	A13514G[33]	
	A13528G[34]	G13708A[14]	
	G13730A[35]		

Table 3.3 Continued...

Subunit	DNA rearrangement		Clinical phenotypes
ND6	G14279A[36]	G14325T[35]	LHON, MELAS, dystonia, Leigh syndrome, sensorineural hearing loss
	C14340T[37]	G14453A[38]	
	G14459A[39]	C14482A[40]	
	C14482G[41]	T14484C[42]	
	T14487C[43]	T14495G[44]	
	T14498C[45]	C14568T[46]	
	A14596T[23]		
NDUFV1	C1268T[47]	C175T[47]	Leigh syndrome, leukodystrophy, myoclonic epilepsy, lactic acidosis
	C1022T[47]	G640A[48]	
NDUFV2	4 bp deletion in intron 2 (5-8)[49]		Hypertrophic cardiomyopathy and hypotonia
NDUFS1	3 bp deletion in exon 8 (664-666)[47]	A755G in exon 9[47]	Leigh syndrome, leukodystrophy, lactic acidosis, growth retardation, dystonia
	C691G in cDNA[50]		
NDUFS2	G683A[51]	C686A[51]	Lactic acidosis, cardiomyopathy, encephalomyopathy, respiratory insufficiency
	T1237C[51]		
NDUFS3	C434T in exon 5[52]	C595T in exon 6[52]	Leigh syndrome
NDUFS4	5 bp duplication (466-470 in cDNA)[53]	G deletion (289 or 290 in cDNA)[54]	Fatal multi-system complex I deficiency, lactic acidosis, encephalomyopathy, cardiomyopathy, Leigh syndrome
	C316T in cDNA[54]	G44A in cDNA[55]	
	G-A inversion at splice acceptor site of intron 1[49]		
NDUFS6	T to A transversion at splice donor site of exon 2[8]		Lethal infantile mitochondrial disease
	4.175 kb deletion encompassing exon 3 and exon 4[8]		
NDUFS7	G364A[56]		Leigh syndrome
NDUFS8	C236T in cDNA[57]	G305A in cDNA[57]	Leigh syndrome
	C254T/ G413A compound heterozygote[58]		Leigh syndrome

Adapted from Servidei (2004), Online Mendelian Inheritance in Man (OMIM) and MITOMAP. The numbered superscripts refer to the original report for a specific alteration: [1] = Campos *et al.*(1997), [2] = Nakagawa *et al.* (1995), [3] = Blakely *et al.* (2005), [4] = Brown *et al.* (1992), [5] = Huoponen *et al.* (1991), [6] = Matsumoto *et al.* (1999), [7] = Brown *et al.* (2001), [8] = Kirby *et al.* (2004), [9] = Fauser *et al.* (2002), [10] = Valentino *et al.* (2004), [11] = Simon (2003), [12] = Howell *et al.* (1991), [13] = Kim *et al.* (2002), [14] = Johns and Berman (1991), [15] = Musumeci *et al.* (2000), [16] = Schwartz and Vissing (2002), [17] = Lebon *et al.* (2003), [18] = Horvath *et al.* (2002), [19] = Brown *et al.* (1995), [20] = Letrit *et al.* (1992), [21] = Pulkes *et al.* (2003), [22] = Kosel *et al.* (1998), [23] = De Vries *et al.* (1996), [24] = Komaki *et al.* (2003), [25] = Wallace *et al.* (1988), [26] = Andreu *et al.* (1999), [27] = Taylor *et al.* (2002), [28] = Liolitsa *et al.* (2003), [29] = Mayorov *et al.* (2005), [30] = Howell *et al.* (2003), [31] = Crimi *et al.* (2003), [32] = Santorelli *et al.* (1997), [33] = Corona *et al.* (2001), [34] = Batandier *et al.* (2000), [35] = Howell *et al.* (1993), [36] = Zhadanov *et al.* (2005), [37] = Wang *et al.* (2005), [38] = Ravn *et al.* (2001), [39] = Jun *et al.* (1994), [40] = Valentino *et al.* (2002), [41] = Howell *et al.* (1998), [42] = Johns *et al.* (1992), [43] = Solano *et al.* (2003), [44] = Chinnery *et al.* (2001), [45] = Leo-Kotler *et al.* (1996), [46] = Wissenger *et al.* (1997), [47] = Schuelke *et al.* (1999), [48] = Benit *et al.* (2001), [49] = Benit *et al.* (2003), [50] = Martin *et al.* (2005), [51] = Loeffen *et al.* (2001), [52] = Benit *et al.* (2004), [53] = Van den Heuvel *et al.* (1998), [54] = Budde *et al.* (2000), [55] = Petruzzella *et al.* (2001), [56] = Triepels *et al.* (1999), [57] = Loeffen *et al.* 1998, [58] = Procaccio and Wallace (2004). A = adenine, bp = base pair, C = cytosine, cDNA = complementary DNA, CPEO = chronic progressive external opthalmoplegia, G = guanine, kb = kilobase, LHON = Leber's hereditary optic neuropathy, MELAS = mitochondrial encephalomyopathy, lactic acidosis and stroke-like episodes, ND 1-6 = NADH dehydrogenase subunits 1 to 6, NDUFV = NADH-ubiquinone oxidoreductase flavoprotein, NDUFS = NADH-ubiquinone oxidoreductase iron-sulphur protein, T = thymine.

3.5 TREATMENT OF MITOCHONDRIAL CYTOPATHY

Various treatment regimens have been prescribed in the past to patients affected with mitochondrial disorders. However, truly successful therapeutic interventions are not yet available. Despite numerous treatments that have been utilised to date, only isolated cases of improvements have been demonstrated. In the majority of cases, a lack of

response seems to be the trend. Patients suffering from mitochondrial disorders, as well as other *in vitro* and *in vivo* models, have been treated with cofactors including coenzyme Q derivatives, niacin, thiamine, and riboflavin, electron donors like succinate and menadione as well as vitamins and plant extracts acting as free radical scavengers. However, as mentioned above, isolated cases of improvements have been reported, along with lack of response and hard evidence supporting their use. Furthermore, few of the mentioned studies have dealt with complex I deficiency itself (Bar-Meir *et al.*, 2001). Table 3.4 lists some of the reported therapeutic intervention compounds utilised in attempts to alleviate the adverse effects induced by a complex I deficiency.

Table 3.4 Reported therapeutic intervention strategies for complex I deficiency

Treatment	Proposed mechanisms	Reference
CoQ_{10}	Sustain electron transfer, stabilise the subunits of the respiratory chain, oxygen free radical scavenging, redox bypass of complex I	Ogasahara *et al.* (1986), Abe *et al.* (1991), Bendehan *et al.* (1992), Gold *et al.* (1996), Ihara *et al.* (1989), Nishikawa *et al.* (1989), Bresolin *et al.* (1990), Shoffner *et al.* (1989)
Idebenone	Redox bypass of complex I, oxygen free radical scavenging	Ihara *et al.* (1989), Cortelli *et al.* (1997), Mashima *et al.* (1992)
Succinate	Donates electrons to complex II (circumventing complex I)	Shoffner *et al.* (1989)
Riboflavin	Flavin precursor for complex I and II	Bernsen *et al.* (1993), Penn *et al.* (1992), Matthews *et al.* (1993)
Bilobalide (Gingo Biloba)	Delays hypoxia induced decrease in ATP content (based on *in vitro* investigations), prevents development of peroxide formation, increases activity of complex I, permits respiratory activity and ATP regeneration	Janssens *et al.* (1995), Janssens *et al.* (1999)

ATP = adenosine triphosphate, CoQ_{10} = coenzyme Q10.

Furthermore, attempts at gene therapy have also been explored (Chinnery, 2003). However, few occurrences of success have been reported with consistency. The most promising of strategies is that which uses the human complex I equivalent from *Saccharomyces cerevisiae*, namely *NDI1*. The enzyme is encoded by a single subunit and transfers electrons from NADH to ubiquinone (Yagi *et al.*, 2006). In addition, *NDI1* is rotenone insensitive and projects into the inner mitochondrial matrix. Research has proven that this enzyme is successfully transported and functions effectively in Chinese hamster cells (Seo *et al.*, 1998), human embryonal kidney cells (Seo *et al.*, 1999), human osteosarcoma (Seo *et al.*, 2000) as well as dopaminergic cell lines (Seo *et al.*, 2002). Furthermore, it has also been illustrated that these cells presented with lowered levels of ROS (Yagi *et al.*, 2006).

As noted previously in this section, the minority of therapeutic studies report improvements, whilst the majority represent a lack of response. Instead, the trend has shifted to a supportive approach of improving the 'management' of patients affected by mitochondrial disorders. This supportive strategy includes accurate diagnosis, improved genetic counselling, alerting clinicians to the complications of mitochondrial disorders and continued management of symptoms where possible.

3.6 AIMS OF THE STUDY

Several therapeutic strategies for mitochondrial related disorders have been explored in the past, ranging from patient supplementation with vitamins and pharmaceutical compounds (Shoffner and Wallace, 1994) to various attempts at gene therapy (Chinnery, 2003). However, progress in the development of therapies has not been encouraging. The study was aimed at delineating the beneficial effects of selected compounds, namely succinate and CoQ_{10} in a rotenone-induced complex I deficient animal model. Therefore, the hypothesis stated that succinate and CoQ_{10} alleviates the complex I deficient phenotype. The investigation first required that the complex I deficient animal model be established successfully, followed by the optimisation of a dose concentration that would induce the deficiency to an acceptable degree. In an attempt to circumvent the deficient complex I, upon administration of additional electron-donating succinate, an electron fuelling effect for complex II is produced, which in turn allows for increased electron transfer to UQ. Administration of CoQ_{10} was explored in an attempt to sustain electron transfer within the inner mitochondrial membrane, stabilise the subunits of the respiratory chain and aid in oxygen free radical scavenging (Shoffner and Wallace, 1994). The effectiveness of the therapeutic regimens was evaluated via the assaying of selected biochemical parameters and the subsequent establishment of tissue-specific biochemical profiles.

CHAPTER FOUR

MATERIALS AND METHODS

The investigation presented was approved by the Ethics Committee of North-West University (Potchefstroom Campus), with the approval number 04D05. All dosing experimentation was performed in the Animal Experimentation Centre, whilst biochemical analyses were undertaken in the Mitochondrial Laboratory at the School for Chemistry and Biochemistry. Reagents purchased for the study were obtained from Sigma-Aldrich®[1], Fluka Riedel-de Haën®[2] and Roche®[3].

Complex I deficiency was induced in rats via oesophageal intubation of rotenone, a natural compound and the most widely used inhibitor of complex I. The study initially undertook to induce Complex I deficiency in a commonly used mouse strain, C57BL/6, which was black in colour and originated from the mating of female 57 with male 52 by C.C. Little in 1921 (Silver, 1995). However, as discussed in Chapter Five, it was observed that unfavourable inhibition levels were obtained as the mice apparently overcame the effects of rotenone. Therefore, the study shifted its focus to a rat model rather than a murine model. In 2004, Rautenbach reported on an investigation where Sprague Dawley rats were administered with a range of rotenone doses in order to evaluate the differential tissue response. The Rautenbach (2004) study served as a useful guide for experiments performed in this investigation.

An initial pilot study was performed in which rats were treated with various doses of rotenone in order to establish and optimise dose-inhibition responses, similar to that of Rautenbach (2004). In the main study of the project, rats were dosed with the selected rotenone concentration to inhibit complex I activity to acceptable levels, followed by the administration of two therapeutic compounds, succinate and CoQ_{10}. Therapeutic relief was evaluated by measuring a selection of biochemical parameters.

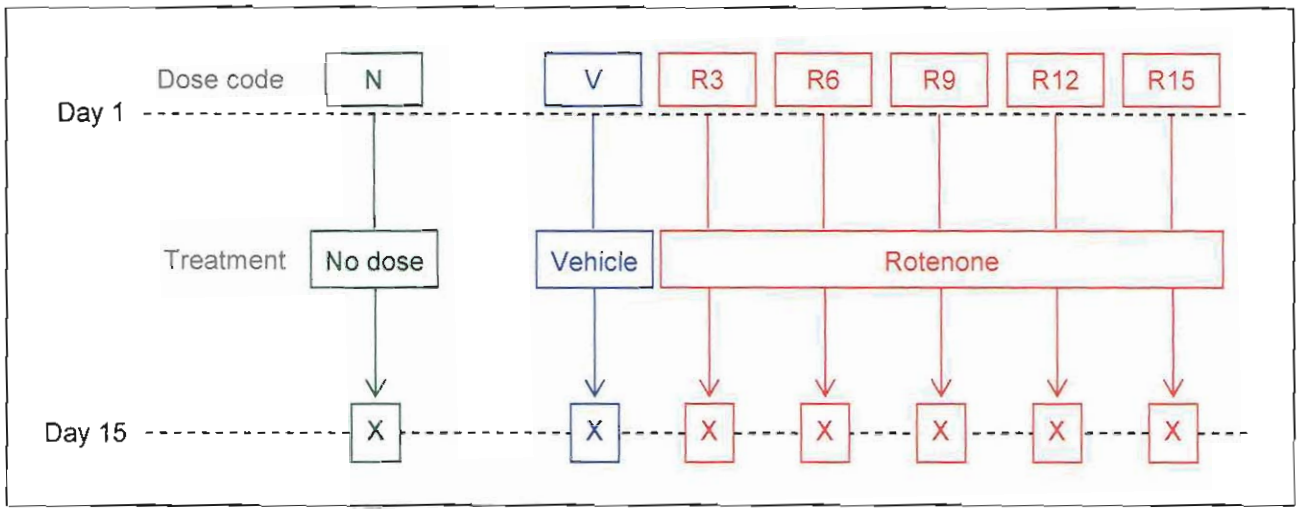
[1] Sigma-Aldrich® is a registered trademark of the Sigma-Aldrich Corporation, St Louis, MO, USA.
[2] Fluka Riedel-de Haën® is a registered trademark of Sigma-Aldrich Corporation, St Louis, MO, USA.
[3] Roche® is a registered trademark of Roche Molecular Biochemicals, Indianapolis, IN, USA.

4.1 RAT PILOT STUDY

The primary goal of the pilot study was to establish rotenone dose and complex I inhibition relationships in Sprague Dawley rats. Based on the results obtained from the Rautenbach study (2004), it was expected that varying degrees of inhibition would be obtained correlating to the concentration of rotenone administered. Moreover, the aforementioned study also confirmed varied inhibition levels in different tissue types. Therefore, the activities of complex I for the respective tissues, namely brain, liver, heart and skeletal muscle, were independently investigated.

The rats were dosed orally with the various concentrations of rotenone over a period of 14 days, after which the rats were sacrificed via decapitation. The body weights of the rats were recorded every day prior to dosing and on day 15 when the rats were sacrificed. Finally, whole brain, heart and liver organ weights were recorded upon sacrificing the rats and the activities of complex I as well as the levels of serum hydroperoxides measured. A flow diagram of the rat pilot study is illustrated in Figure 4.1.

Figure 4.1 Flow chart illustrating the design of the rat pilot study



A total cohort size (n) of 42 rats (n = 6 per group) were dosed with either no dose (N), vehicle (V) or rotenone (R) every morning over a period of 14 days after which they were sacrificed (X) on day 15 via decapitation and the four tissue groups prepared for evaluation of complex I activities. R3 = rotenone 3 $mg.kg^{-1}.day^{-1}$, R6 = rotenone 6 $mg.kg^{-1}.day^{-1}$, R9 = rotenone 9 $mg.kg^{-1}.day^{-1}$, R12 = rotenone 12 $mg.kg^{-1}.day^{-1}$ and R15 = rotenone 15 $mg.kg^{-1}.day^{-1}$.

The rats were dosed with rotenone concentrations of 3, 6, 9, 12 and 15 milligrams per kilogram ($mg.kg^{-1}$). A number of six rats (n = 6) was included in each experimental dose category. Two additional rat groups were also included, namely no dose (N) and vehicle (V). The first group was referred to as the environmental controls, since rats in this group were simply housed and maintained in the same environment as the rats that were dosed on a daily basis. This group was assigned the dose code N, since this group received no

dose for 14 days. The N rat group enabled an evaluation of the effects of the vehicle, as well as the various concentrations of rotenone. The second group of control rats were dosed with only the vehicle, namely sunflower oil. The vehicle treated rats, assigned to dose group V, served to enable the evaluation of the various concentrations of rotenone eliminating any additional effects that the sunflower oil vehicle may contribute. Dose volumes utilised in the rat pilot and main studies are described in Section 4.3.2.

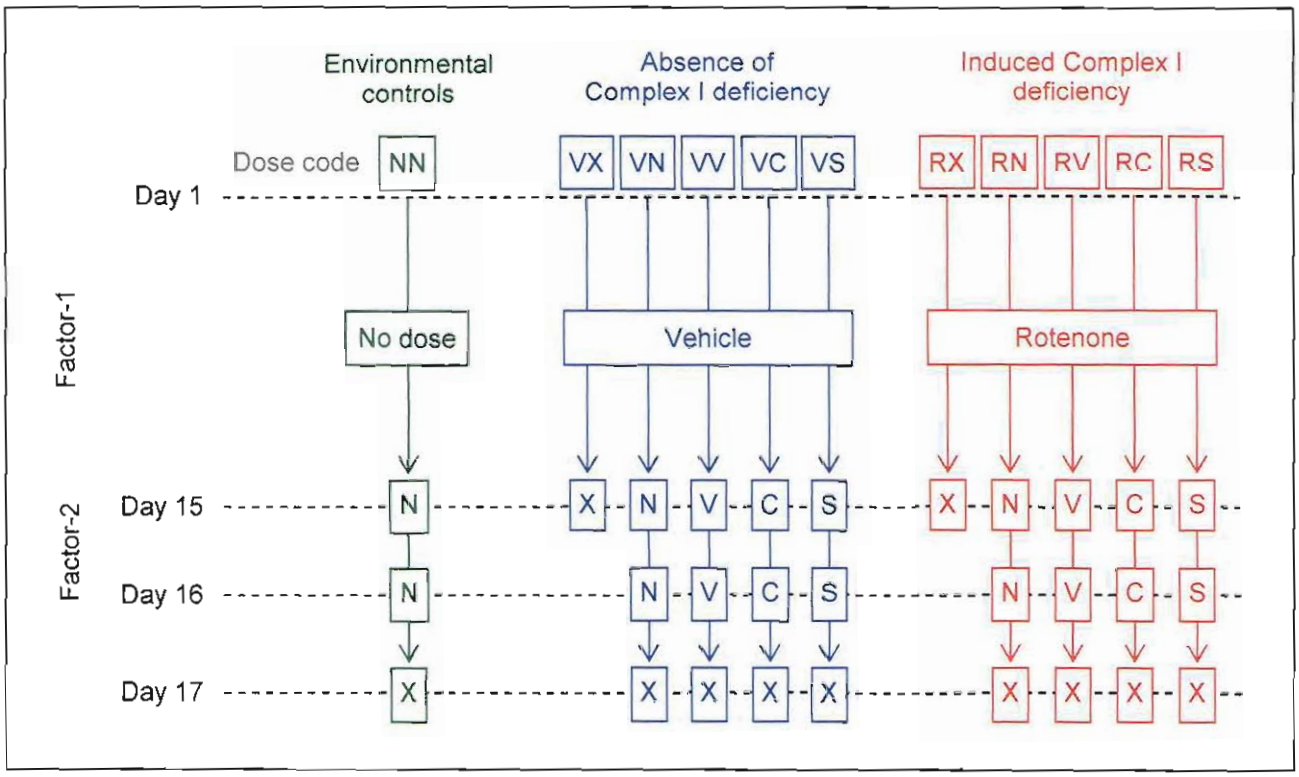
4.2 RAT MAIN STUDY

Results obtained from the rat pilot study enabled the establishment of the rotenone dose concentrations required to inhibit complex I to the highest degree possible. After comparable 14-day rotenone dosing, the rotenone-treated rats were supplemented with either of the two therapeutic compounds, namely succinate or CoQ_{10}, for a period of two days. Succinate was dosed in a concentration of 30 $mg.kg^{-1}.day^{-1}$, while CoQ_{10} was dosed in a concentration of 150 milligrams per kilogram per day ($mg.kg^{-1}.day^{-1}$). These regimens were referred to as Factor-2 dose regimens, while doses received form days 1 to 14 were referred to as the Factor-1 dose regimens. In addition, a further nine rat dose groups were included into the experiment to serve as controls and to evaluate the effects of CoQ_{10} and succinate in the absence of Complex I deficiency. All dose groups are indicated in the experimental flow diagram of the rat main study in Figure 4.2.

The dosage periods for rats were either 14 or 16 days. This time period depended on which dose group the rats were designated to, as indicated in Figure 4.2. Rat sacrificing always took place the day after a dose group received its final dose. Therefore, groups VX and RX were sacrificed on day 15, while the other nine groups were sacrificed on day 17. Subsequently, the rat tissues were prepared appropriately and biochemical analyses performed.

The rat main study was categorised into three subgroups of dosing. The first subgroup contained only the environmental controls, which received no dose over a full 16-day period. This dose group was coded **NN**, since rats received a no dose Factor-1 regimen from day 1 to 14, followed by a no dose Factor-2 regimen on days 15 and 16.

Figure 4.2 Flow chart illustrating the design of the rat main study



A total of 66 rats (n = 6 per dose group) were dosed every morning after which they were sacrificed via decapitation. Dosing was initiated on day 1 and rats were sacrificed either on days 15 or 17, depending on which dose group the rats were designated. Each dose group was assigned an abbreviated dose code, representing the Factor-1 and Factor-2 treatments received. Rats were treated with NN = no dose regimen, VX = vehicle and sacrificed, VN = vehicle and no dose, VV = vehicle and vehicle, VC = vehicle and CoQ_{10}, VS = vehicle and succinate, RX = rotenone and sacrificed, RN = rotenone and no dose, RV = rotenone and vehicle, RC = rotenone and CoQ_{10}, RS = rotenone and succinate. C = CoQ_{10}, N = no dose, R = rotenone, S = succinate, V = vehicle, X = sacrificed.

The second subgroup, referred to as the absence of Complex I deficiency group, consisted of five vehicle Factor-1 treated rat groups. Each of the five dose groups received sunflower oil vehicle from day 1 to 14 after which they received a Factor-2 regimen on days 15 and 16. The Factor-2 regimens included no dose, vehicle, CoQ_{10} (C) or succinate (S). The combined coding of VN, VV, VC and VS was thus assigned respectively. The dose group designated VX, was sacrificed (X) on day 15 after it had received vehicle for 14 consecutive days.

The third subgroup, with induced Complex I deficiency, also consisted of five dose groups. All five groups received rotenone Factor-1 regimens from days 1 to 14, after which they received Factor-2 treatments corresponding to that of subgroup two. Therefore, their combined treatment codes were RX, RN, RV, RC and RS, as indicated in Figure 4.2.

4.3 RODENT EXPERIMENTATION

The mouse strain that was selected for the initial investigation was of the C57BL inbred strains, in particular C57BL/6. However, as will be discussed in Chapter Five, mice did not

respond with complex I inhibition and the study was consequently altered to make use of Sprague Dawley rats as the animal model of choice. Nonetheless, rodent experimentation protocols remained unchanged for both the mice and rats.

4.3.1 Rodent husbandry and determination of rat body weights

The C57BL/6 inbred mouse strains as well as the Sprague Dawley rats were purchased from the Animal Unit of the South African Vaccine producers (Pty) Ltd and transported to the Animal Experimentation Centre, North-West University (Potchefstroom campus), where they were acclimatised for a minimum of three days. The rodents were maintained in a pathogen free environment, housed individually in cages and kept in a room maintained at a constant temperature of 22 degrees Centigrade (°C), 50 to 60% humidity and a 12/12 hour light/dark cycle (07h00-19h00). The animals had free access to rat and mouse dry feed [Epol®[1]] and water.

4.3.2 Oesophageal intubation and dosing

The mice and rats were dosed via oesophageal intubation every morning for a period of 14 or 16 days, depending on the dose regimen received. Due to the poor solubility of rotenone in water, the compound was administered to the rodents in a sunflower oil suspension. For consistency, sunflower oil was therefore also used as the vehicle of choice when CoQ_{10} was dosed. However, since succinate is extremely hydrophilic and thus inappropriate for dosage as a suspension in sunflower oil, it was dissolved in ultra-pure Milli-Q®[1] water and administered accordingly.

The maximum doses for mice and rats are 0.5 millilitre (mL) and 2 mL respectively (Poole, 1999). Therefore, mice were dosed between 0.1 and 0.15 mL, in order to limit any danger of reaching the maximum dose as well as to prevent any biological side effects that the sunflower oil might have. Rats were dosed volumes of 1 millilitre per kilogram ($mL.kg^{-1}$), which is well below the specified maximum dose.

Prior to oral dosing, all rodents were weighed and the dose volumes calculated accordingly. All mice were selected at weights ranging between 25 and 30 grams (g). Rats were dosed after it had been established that they weighed between 260 and 300 g.

[1] Epol® is a registered trademark of Epol Animal Feed Manufacturers, Johannesburg, Gauteng, South Africa.

The procedure of oral dosing was optimised by utilising a thin pipe with a diameter of approximately 1 millimetre (mm). Once the rodent had been positioned correctly, the dosage pipe was fed down the oesophagus to just above the stomach valve and the dose injected. Photographic representations and discussion of the oesophageal intubation process is presented in Section 5.1.1 of Chapter Five.

4.4 TISSUE COLLECTION AND BIOCHEMICAL ASSAYS

Several biochemical parameters were assayed in the rat main study in order to obtain a comprehensive biochemical profile. The full profile of analyses were not utilised for the pilot investigation as it was only required that rotenone inhibition of complex I be determined. However, an additional analysis that measures the levels of hydroperoxides, and hence ROS formation, in blood serum was also employed. In the rat main study, biochemical profiles were generated from blood, brain, liver, heart and skeletal muscle tissue, all of which were collected and prepared appropriately from the rodents after their respective dosage periods.

4.4.1 Tissue and blood collection

Due to the fact that the rat main study design required the analysis of up to six biochemical parameters in each of the tissues collected, the collection process was performed with caution, so as to ensure that adequate amounts of tissue were collected. Upon sacrificing the rats, whole organ weights of brain, liver and heart were recorded to evaluate whether rotenone administration might have influenced organ weights over the 14 or 16-day dosage period.

4.4.2 Sample preparation and homogenisation

The homogenates were prepared using a rotor-stator homogeniser and tight fitting Potter-Elvehjam tissue grinder. The rotor was set to 500 revolutions per minute with the glass pestle suspended in ice water while homogenising. Heart and skeletal muscle tissues were sliced on a cold glass plate prior to homogenisation to enable the preparation of a more homogeneous lysate. In addition, heart and skeletal muscle tissues were homogenised using 20 strokes as opposed to 15 utilised for brain and liver. All tissues

[1] Milli-Q® is a registered trademark of the Millipore Corporation, Billerica, MA, USA.

were homogenised with the appropriate buffer solutions in a 10% weight to volume ratio (w/v).

4.4.3 Mitochondrial enzyme analysis

The activities of complexes I were evaluated in brain, liver, heart and skeletal muscle collected from the treated rodents. Respiratory chain enzymes were not assayed from circulating lymphocytes due to the large volume of blood required to assay them accurately. In order to assay the activity of complex I, mitochondria were isolated and an enriched extract appropriately prepared. Citrate synthase, a general enzyme of the mitochondria involved in the tricarboxylic acid (TCA) cycle was also assayed as a reference enzyme for each of the mitochondrial preparations. In addition, the protein concentration of each mitochondrial preparation was determined and utilised when calculating the final activities of these enzymes.

Preparation and storage of crude mitochondrial extracts was imperative to ensure rich mitochondrial preparations and enable accurate and reproducible analysis of the enzyme complexes. The various tissues were initially homogenised and mitochondria isolated, as described in subsequent sections.

4.4.3.1 Isolation of mitochondria

The tissue biopsies were collected (Fernandez-Vizarra *et al.*, 2002) in SET buffer [0.25 molar (M) sucrose, 2 millimolar (mM) ethylenediamine tetra-acetic acid (EDTA) and 10 mM Tris-HCl, adjusted to a power of hydrogen (pH) of 7.4)] and were homogenised at 4°C in the same buffer and on the same day of the collection. Mitochondria were isolated by centrifugation at 600 x g (gravitational force) for 10 minutes (min) at 4°C, after which the mitochondria containing supernatant was removed and aliquotted into a separate tube. A crude mitochondrial preparation was obtained by centrifugation at 10,000 x g for 10 min at 4°C followed by resuspension in 100 microlitres (µL) hypotonic buffer [25 mM monobasic (KH_2PO_4) and dibasic (K_2HPO_4) potassium phosphate buffer (pH 7.2), and 5 mM magnesium chloride ($MgCl_2$)] and storage at -70°C until required for analyses. Prior to performing any of the OXPHOS analyses, the enriched mitochondrial preparations were freeze-thawed three times. This step, along with the hypotonic buffer resuspension, facilitated the rupturing of the mitochondrial membrane and release of its contents.

4.4.3.2 Protein concentration

A reagent mix was initially prepared containing bicinchoninic acid (BCA) and copper (II) sulphate pentahydrate ($CuSO_4.5H_2O$) in a ratio of 50:1 respectively (Smith *et al.*, 1985). Optimised volumes of 2 to 5 μL of the mitochondrial preparations were aliquotted into a microplate and the volumes made up to 10 μL with double-distilled water (ddH_2O). Subsequently, 200 μL of the reagent mix was added to each well and the microplate incubated at 37°C for 20 min in the preheated FL 600 Microplate Fluorescence Reader [Bio-Tek Instruments]. A single spectrophotometric reading was subsequently recorded at a wavelength of 560 nanometre (nm). A concentration series of bovine serum albumin (BSA) ranging from 0 to 10 microgram per microlitre ($\mu g.\mu L^{-1}$) was included in the assay, in duplicate, allowing for the generation of a standard curve from which the protein concentrations of the various samples could be inferred.

4.4.3.3 Citrate synthase activity

According to the protocol (Trounce *et al.*, 1996), mitochondrial preparations were resuspended in a 1 mL spectrophotometric cuvette along with a citrate synthase assay reagent containing 50 μL of 0.45 mM 5,5'-dithio-bis (2-nitrobenzoic acid) or DTNB, 2 μL of 10% Triton X-100®[1] and 5 μL of 6 mM acetyl-coenzyme A. The reaction mix was subsequently made up to a volume of 475 μL with ddH_2O. Spectrophotometric analyses were performed utilising a UVKON UV-Vis double beam spectrophotometer [Bio-Tek Instruments].

After recording the absorbency at 412 nm for a period of 3 min (A_1), the reaction was started via the addition of 25 μL of 10 mM oxaloacetate, followed by the measurement of the sharpened graphic linear increase for an additional two to three min (A_2). The activity of citrate synthase was calculated according to Equation 4.1. The activity was finally expressed in terms of protein by dividing the reaction rate by the amount of protein utilised in each reaction.

[1] Triton X-100 is a registered trademark of Union Carbide Chemicals and Plastics Co., Inc., Swampscott, MA, USA.

Equation 4.1 Citrate synthase activity

$$\text{Citrate synthase activity} = \frac{(A_1 - A_2) \times (V/v \times 1000)}{13.6}$$

$$= \mu mol.min^{-1}$$

$$\text{Citrate synthase activity.protein}^{-1} = \mu mol.min^{-1}.\mu g^{-1}$$

Equation as stated by Bergmeyer (1987). The equation is divided by 13.6 units per millimolar per centimetre ($mM^{-1}.cm^{-1}$) to compensate for the extinction coefficient of thionitrobenzoic acid (TNB). A_1 = initial absorbancy at 412 nm, A_2 = final absorbancy at 412 nm, $\mu mol.min^{-1}$ = micromole per minute, $\mu mol.min^{-1}.\mu g^{-1}$ = micromole per minute per microgram, V = total reaction volume (µL), v = volume of crude mitochondrial extract (µL).

4.4.3.4 Complex I activity

Complex I analysis focuses directly on the quantification of electron transfer from NADH to Coenzyme Q_1 (CoQ_1) the primary function of this enzyme. The protocol described was obtained via personal communication from Dr David Thornburn where the rotenone sensitive and insensitive activities of complex I are assayed in separate cuvettes (Murdoch Childrens Research Institute, Melbourne, Australia). The oxidation of NADH was measured at a wavelength of 340 nm utilising a UVKON UV-Vis double beam spectrophotometer [Bio-Tek Instruments].

Optimised volumes of the crude mitochondrial extract, ranging from 5 to 20 µL, and ddH_2O prewarmed to 37°C was added to the two 1 mL cuvettes and the mitochondria exposed to hypotonic shock by incubation for a period of 3 min. Subsequent to the incubation, 2.5 µL of 10 mM CoQ_1 was added to both cuvettes, followed by the addition of 5 µL of 0.75 mM rotenone in pure ethanol (EtOH) to one cuvette for rotenone insensitive quantification and 5 µL of pure EtOH to the second cuvette for rotenone sensitive quantification.

The reaction was initiated by the addition of 87.5 µL of a complex I assay reagent containing 50 µL of 0.5 M potassium phosphate buffer (pH 7.2), 12.5 µL of 2 mM NADH, 10.0 µL of 50 mM potassium cyanide (KCN) in 100 mM potassium phosphate buffer, 10 µL of 0.5 mM antimycin A in EtOH and 5 µL of 10% BSA (w/v). Spectrophotometric readings were recorded for a maximum period of 20 min at the specified wavelength of 340 nm. The initial reaction rates over a 2 to 3 min period for the duplicate samples were determined and utilised in Equation 4.2 to calculate the final activity of complex I.

As with citrate synthase, the activity of complex I was expressed in terms of the protein in the reaction. Complex I activity was finally expressed in terms of the units citrate synthase, as indicated in the final line of Equation 4.2.

Equation 4.2 Complex I activity

$$\text{Complex I activity} = \frac{(A_1 - A_2) \times (V/v \times 1000)}{6.81}$$

$$= \mu\text{mol.min}^{-1}$$

$$\text{Complex I activity.protein}^{-1} = \mu\text{mol.min}^{-1}.\mu\text{g}^{-1}$$

$$\text{Complex I activity.UCS}^{-1} = \mu\text{mol.min}^{-1}.\text{UCS}^{-1}$$

Equation as stated by Bergmeyer (1987). A_1 = initial absorbancy at 412 nm, A_2 = final absorbancy at 412 nm, $\mu\text{mol.min}^{-1}$ = micromole per minute, $\mu\text{mol.min}^{-1}.\mu\text{g}^{-1}$ = micromole per minute per microgram, $\mu\text{mol.min}^{-1}.\text{UCS}^{-1}$ = micromole per minute per unit citrate synthase, V = total reaction volume (µL), v = volume of crude mitochondrial extract (µL), UCS = units citrate synthase. The equation in line one is divided by 6.81 units per millimolar per centimetre ($\text{mM}^{-1}.\text{cm}^{-1}$), the sum of the extinction coefficients of NADH and CoQ_1.

4.4.4 Serum hydroperoxide concentrations

The method performed was according to that described in the Diacron reactive oxygen metabolites (d-ROMs) test kit [Diacron International]. Dipotassium salt EDTA treated blood was centrifuged at 4,000 x g and 4°C for 30 min to collect serum. Four microlitres of freshly prepared serum was aliquotted into wells of a microplate, followed by the addition of a mixture of 2 µL of Reagent 1, the chromogenic substrate, and 200 µL of Reagent 2, the buffer (pH 4.8). The microplate was incubated for one minute at 37°C in the preheated FL 600 Microplate Fluorescence Reader [Bio-Tek Instruments], and spectrophotometric readings recorded at a wavelength of 485 nm immediately and every 2 min for 15 min. A serum standard, assigned a value of 250 Carratelli units (CARR U), as well as a blank control was included into the assay run. Finally, the absorbance values of the reagent blank were subtracted from those of the standard and the samples, and CARR U calculated according to Equation 4.3.

Equation 4.3 Calculation of d-ROMs Carratelli Units (CARR U)

$$\text{CARR U} = (\Delta A/t \text{ of sample}) / (\Delta A/t \text{ of standard}) \times 250$$

Equation as stated by Iorio (2002). CARR U = Carratelli Units, A = absorbency reading at 485 nm, t = time, 250 = standard CARR U.

4.4.5 Antioxidant capacity

Sample antioxidant capacity was determined via the oxygen radical absorbance capacity (ORAC) assay, as described by Ou *et al.* (2001). Blood was collected and coagulation prevented by treatment with dipotassium salt EDTA and placed on ice until prepared for assaying. Serum was collected via centrifugation of the blood sample at 4,000 x g and 4°C for 30 min. Tissues were collected on ice and homogenised in 10% (w/v) ice-cold 75 mM phosphate buffer [1 M K_2HPO_4, 1 M anhydrous monobasic sodium phosphate (NaH_2PO_4), pH 7.4]. An aliquot of the tissue homogenates was stored for protein determination, as described in Section 4.4.3.2, which was required for accurate ORAC value calculation in terms of protein. Recovered serum and tissue homogenates were deproteinised by centrifugation for 10 min at 16,000 x g and 4°C after addition of an equal volume of 0.5 M perchloric acid (PCA). The deproteinised supernatants were recovered and subsequently stored at -70°C until assayed.

Prior to analysis and in order to minimise protein interference in the assay, prepared supernatants were diluted a further 10 fold by aliquotting 2 µL into microplate wells and made up to 20 µL with 75 mM phosphate buffer. Subsequently, 160 µL of a 56 nanomolar (nM) fluorescein solution in buffer was added to each well and the microplate incubated for 15 min at 37°C in the preheated FL 600 Microplate Fluorescence Reader [Bio-Tek Instruments]. The generation of reactive oxygen species in the form of peroxyl radicals was initiated by the addition of 20 µL of 240 mM 2,2'-Azobis(2-amidinopropane) dihydrochloride (AAPH) and the decrease in fluorescence recorded spectrophotometrically at a wavelength of 520 nm every 5 min for 2 hours.

A standard curve was generated via the inclusion of diluted concentrations of Trolox, a powerful antioxidant and vitamin E analogue, undergoing the same reaction assay. Blank assay samples were also included. The area under the curve (AUC) was calculated according to Equation 4.4.

Equation 4.4 Calculation of antioxidant capacity

$$AUC = (0.5 + f_5/f_0 + f_{10}/f_0 + f_{15}/f_0 + \ldots\ldots f_i/f_0) \times 5$$

Equation as stated from Ou *et al.* (2001). AUC = area under the curve, f_0 = initial fluorescence, f_i = fluorescence at time i, 5 = time period between reading points in minutes.

Graphic representations of the data were established according to a 2nd order polynomial slope ($y = ax^2 + bx + c$). The antioxidant capacity of a sample, expressed in terms of micromolar (μM), was calculated by solving for the x-value and multiplying by the dilution factor. In addition, tissue antioxidant capacities were expressed in terms of the protein utilised for each reaction set.

4.4.6 GSH/GSSG ratio determination

Blood was collected in dipotassium salt EDTA and stored on ice until preparation. For oxidised glutathione (GSSG) analysis, blood was aliquotted and treated with 30 mM of 1-methyl-2-vinyl-pyridinium trifluoromethane sulphonate (M2VP), dissolved in 0.1 normal (N) hydrochloric acid (HCl), to a final concentration of 3 mM, after which the sample was snap frozen and stored at -70°C until assayed. The remainder of the EDTA treated blood was also stored at -70°C for reduced glutathione (GSH) analysis.

Tissue samples were collected and placed on ice until preparation. The tissue was homogenised in 10% (w/v) ice-cold phosphate buffer and the homogenate split for separate analysis of GSH and GSSG, as described by Asensi *et al.* (1990). As for blood, the homogenate used to assay GSSG concentrations was immediately treated with M2VP to a final concentration of 3 mM. Prepared tissue homogenates were stored at -70°C until assayed. The protein concentration of homogenates were also determined, as described in Section 4.4.3.2, upon assaying for glutathione concentrations in order to express the GSH/GSSG ratio in terms of protein content.

Prepared blood samples were thawed for 2-10 min and mixed by resuspension prior to analysis. The GSSG and GSH blood samples were subsequently diluted to 1/4 and 1/8, respectively, with ice cold 5% metaphosphoric acid and mixed by vortexing. Both were centrifuged for 10 min at 10,000 x g and 4°C. The GSSG extracts were further diluted to 1/15 with a buffer containing 500 mM sodium phosphate ($NaPO_4$) and 1 mM EDTA (pH 7.5), whilst the GSH extracts were diluted to 1/61 with the same buffer.

The prepared tissue homogenates were thawed on ice and immediately centrifuged for 5 min at 15,000 x g and 4°C. The supernatants were subsequently diluted appropriately to enable the assaying of glutathione concentrations.

Fifty microlitres of the GSH or GSSG dilutions were aliquotted into microplate wells, followed by the addition of 50 µL of 0.3 mM DTNB in assay buffer and 50 µL of 0.02 units per microlitre ($U.\mu L^{-1}$) glutathione reductase (GR) in assay buffer. The microplate was incubated for 5 min at 25°C in the preheated FL 600 Microplate Fluorescence Reader [Bio-Tek Instruments], after which the reactions were started by the addition of 50 µL reduced nicotinamide adenine dinucleotide phosphate (NADPH). The formation of thionitrobenzoic acid (TNB) was monitored spectrophotometrically at a wavelength of 412 nm every minute for 5 min. The concentrations of glutathione were calculated via the use of a standard curve generated from a range of GSH concentrations. Blank control samples were also included in each of the assays. The GSH to GSSG ratio was calculated according to Equation 4.5.

Equation 4.5 GSH/GSSG ratio calculation

$$\text{Glutathione ratio} = (\text{Total glutathione} - 2\text{GSSG}) / \text{GSSG}$$

Equation as stated by Asensi *et al.* (1990). GSSG = oxidised glutathione.

4.4.7 Lactate/Pyruvate ratio determination

Blood was collected in two volumes of ice-cold 2 M perchloric acid, mixed thoroughly and stored on ice until preparation for the assaying of lactate and pyruvate concentrations, as described by Wijburg *et al.* (1990). The collection was centrifuged for 15 min at 1,000 x g and 4°C, the supernatant removed and pH neutralised to between 7.6 and 8.0 with 2 M tribasic potassium phosphate (K_3PO_4). The precipitate was removed via centrifugation for 5 min at 5,000 x g and 4°C and supernatants were stored at -80°C until assayed.

Tissues were collected and immediately snap frozen until prepared for assaying. Homogenisation was performed on ice in 10% (w/v) solution of 1.66 M perchloric acid and the homogenate centrifuged for 15 min at 1000 x g and 4°C. The supernatants were neutralised and stored as described above for blood. The spectrophotometric analyses for the determination of lactate and pyruvate concentrations were performed via a UVKON UV-Vis double beam spectrophotometer [Bio-Tek Instruments]. Blank samples and a standard series of lactate and pyruvate concentrations were also assayed for every set of samples.

In order to determine sample lactate concentrations, 20 µL of the deproteinised extract was aliquotted into a 1 mL cuvette containing 220 µL of 0.1 M glutamate in 0.6 M glycylglycine buffer (pH 10), 44 µL of 50 mM NAD and 200 µL of ddH_2O. Subsequently, 4.4 µL of 0.1 milligram per millilitre ($mg.mL^{-1}$) glutamate-pyruvate transaminase (GPT) was added, the reaction contents resuspended and the initial absorbance (A_1) recorded at a wavelength of 340 nm. Lactate was subsequently converted to pyruvate by the addition of 4.4 µL of 0.1 $mg.mL^{-1}$ lactate dehydrogenase (LDH). The reaction contents were incubated for a minimum of three hours when a final spectrophotometric reading (A_2) was recorded at the same wavelength of 340 nm.

Pyruvate was assayed by initially adding 220 µL of 5 mM EDTA in 0.5 M triethanolamine, 44 µL of 7 mM NADH, 160 µL of ddH_2O and 40 µL of the neutralised extract to a 1 mL cuvette. After resuspending the reaction contents and an incubation period of 5 min, the initial spectrophotometric reading (A_1) was recorded at a wavelength of 340 nm. The endogenous pyruvate was converted to lactate by the addition of 4.4 µL of 0.1 $mg.mL^{-1}$ LDH and the decrease in absorbance recorded after 30 min incubation period.

The final concentrations of sample lactate and pyruvate were determined via the use of standard curves generated from a series of lactate and pyruvate concentrations. The lactic and pyruvic acid standard concentrations were assayed in conjunction with the sample preparations via identical protocols, as described above. Finally, the ratios of lactate to pyruvate were calculated according to Equation 4.6 for each of the respective tissue types.

Equation 4.6 Calculation for the ratio of lactate to pyruvate

L/P ratio = lactate concentration / pyruvate concentration

Equation as stated by Wijburg *et al.* (1990). L/P = ratio of lactate to pyruvate.

4.4.8 ATP/ADP ratio determination

Blood and tissue was collected and prepared in the same manner as for the lactate and pyruvate assay, described in Section 4.4.7. Preparations were stored at -80°C until assayed. The total adenylates (ATP + ADP) was quantified by converting the sample ADP to ATP (Lust *et al.*, 1981). This was achieved by the addition of a sample equivalent volume of ATP/ADP Buffer A [50 mM Imidazole-HCl (pH 7.0), 2 mM $MgCl_2$, 75 mM

potassium chloride (KCl) and 3 mM phosphoenolpyruvate] and 5 μL of 1.5 $\mu g.mL^{-1}$ pyruvate kinase (PK). The original ATP content of the samples was similarly quantified in a separate reaction except that PK was replaced with 5 μL of ATP/ADP Buffer A. eactions were incubated at room temperature for 60 min. Pyruvate kinase was inactivated by the addition of 5 μL 1 M sodium hydroxide (NaOH) and incubating at 60°C for 10 min.

Optimised volumes, ranging from 70 to 85 μL, of the sample preparations were subsequently transferred to 1 mL spectrophotometer cuvettes and 350 μL of ATP/ADP Buffer B [50 mM Tris-HCl (pH 8.1), 100 μM glucose, 0.08 $\mu g.mL^{-1}$ glucose-6-phosphate dehydrogenase (G6PD), 1 microgram per millilitre ($\mu g.mL^{-1}$) hexokinase] added. The absorbance was recorded spectrophotometrically at a wavelength of 340 nm (A_1), after which the reaction was started by the addition of 5 μL of 1 mM oxidised nicotinamide adenine dinucleotide phosphate (NADP). After approximately 30 min reaction time at 37°C, a final absorbance reading was recorded (A_2) at the same wavelength of 340 nm. The sample concentrations of adenylates were calculated according to a standard curve generated from a range of ATP concentrations. The ATP/ADP ratios were calculated according to Equation 4.7.

Equation 4.7 Calculation for the ratio of ATP to ADP

ATP/ADP ratio = ATP concentration / ADP concentration

Equation according to Lust *et al.* (1981). ATP/ADP = ratio of adenosine triphosphate to adenosine diphosphate.

4.4.9 NAD/NADH ratio determination

Blood was collected in a fluoride tube reagent, which inhibits relative metabolic pathways ensuring that the pyridine status is not altered until analysis. As described by Zerez *et al.* (1987), the blood was subsequently diluted 1:100 in NADH buffer [10 mM nicotinamide, 20 mM sodium bicarbonate ($NaHCO_3$) and 100 mM sodium carbonate (Na_2CO_3) (pH 7.5)] and directly snap frozen and stored at -80°C until assayed. Tissue samples were collected, snap frozen and stored at -80°C until assayed. Prior to analysis, the stored blood samples were thawed quickly in a room temperature waterbath and immediately chilled on ice. The sample was split into two for separate analysis of total pyridine and NADH alone. By incubating the NADH analysis tube for 30 min at 60°C, the oxidised NAD was destroyed. The mixture was promptly chilled on ice. Tissue was prepared by

homogenising in 10% (w/v) NADH buffer and centrifuged for 20 min at 3,000 x g and 4°C. The supernatants were prepared as for blood and stored at -80°C.

The assays were performed utilising a FL 600 Microplate Fluorescence Reader [Bio-Tek Instruments]. Upon assaying the samples, 146 µL of a reaction premix containing 25 µL of 1 M Tris-HCl (pH 8.0), 5 µL of 100 mM phenazine ethosulphate (PES), 12.5 µL of 10 mM thiazolyl blue tetrazolium bromide (MTT), 7 µL of 29.4 $mg.mL^{-1}$ alcohol dehydrogenase (ADH) and 96.5 µL ddH_2O was aliquotted into each of the wells of a microplate. Subsequently, 80 µL of the sample preparations was added to the wells and the plate incubated for 5 min at 37°C. The reaction was started by the addition of 24 µL of ethanol. Spectrophotometric readings were recorded at 560 nm every minute for 4 min. A blank sample reaction as well as a NADH standard series was included in the reactions to generate a standard curve and allow for inference of pyridine concentrations. The concentrations of NAD were determined by subtracting the concentration of NADH from that of the total pyridine concentration. Finally, the ratio of NAD to NADH was determined according to Equation 4.8.

Equation 4.8 Calculation for the ratio of NAD to NADH

NAD/NADH ratio = NAD concentration / NADH concentration

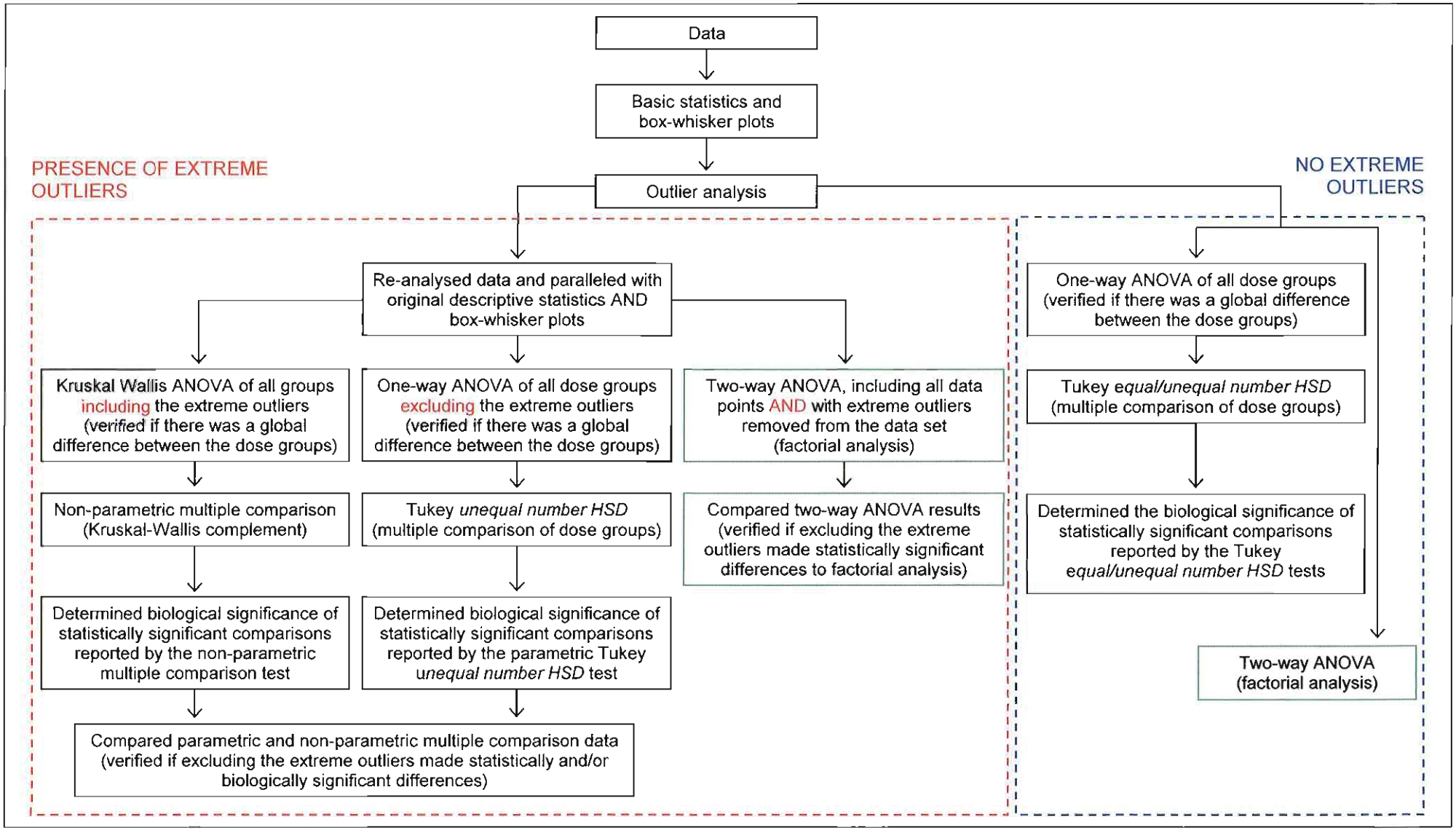
Equation as stated by Zerez *et al.* (1987). NAD/NADH = ratio of oxidised to reduced nicotinamide adenine dinucleotide.

4.5 STATISTICAL EVALUATION OF DATA

The data generated via the rat pilot and main studies were initially captured in Microsoft®[1] Excel®[2] and exported to the STATISTICA™[3] programme, version 7 [Statsoft (2004)]. For the rat main study, the random number generator of STATISTICA™ was used to exclude two additional rats from dose group RX and one from RV so that each dose group contained a total of six rats, as discussed in Appendix A. Descriptive statistics, ANOVA, multiple comparison procedures as well as biological significance calculations were included to evaluate the data effectively. An overview of the statistical strategy is diagrammatically represented in Figure 4.3. This strategy was consistently adhered to for the analysis of all data sets. In addition, descriptions of the statistical methods used in this study are discussed in subsequent sections.

[1] Microsoft® is a registered trademark of the Microsoft Corporation, Seattle, WA, USA.
[2] Excel® is a registered trademark of the Microsoft Corporation in the United States and/or other countries.
[3] STATISTICA™ is a trademark of StatSoft, Inc., Tulsa, OK, USA.

Figure 4.3 Flow chart illustrating the statistical strategy adopted for the rat pilot and main studies

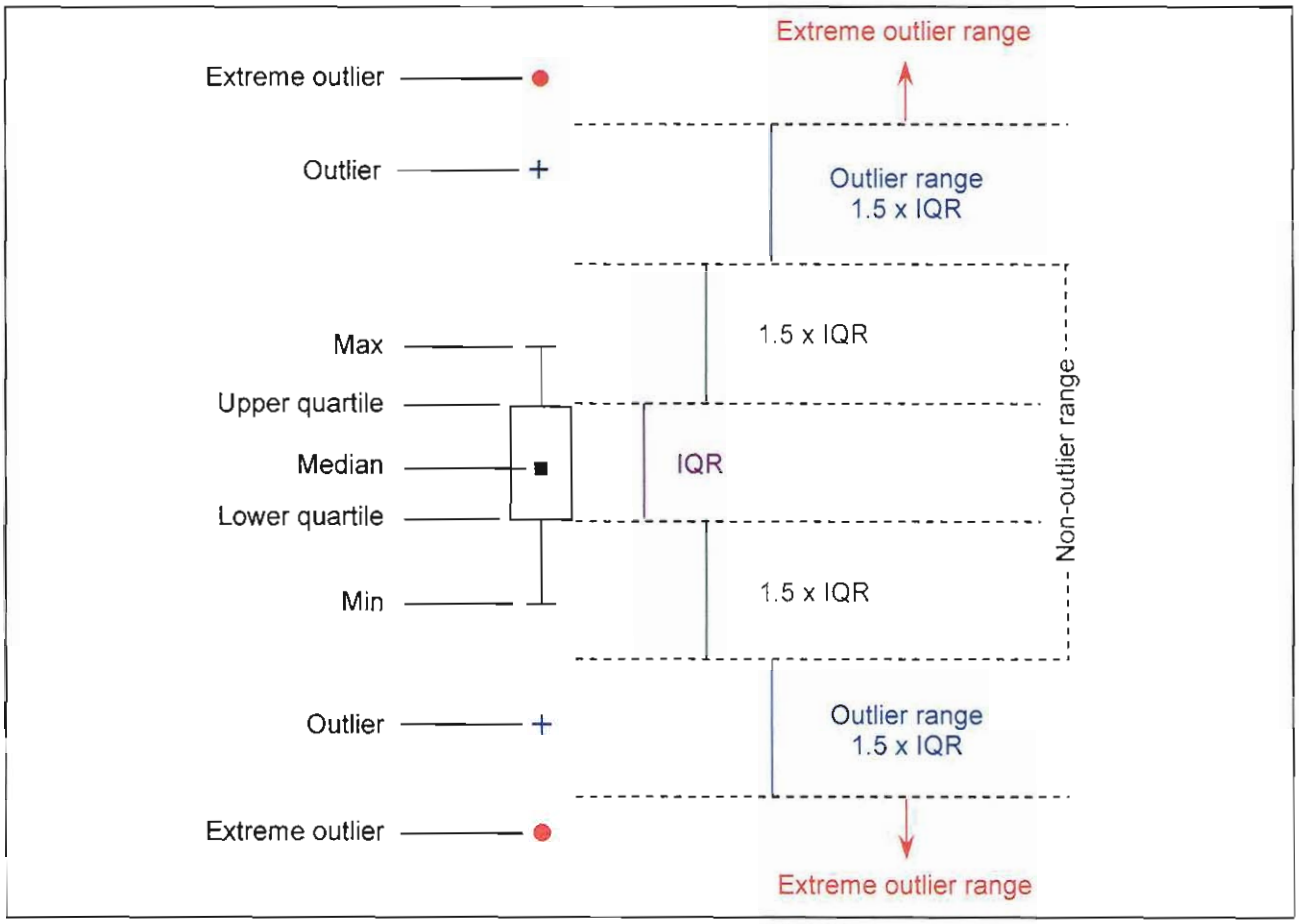


The excerpt of flow chart enclosed in the red dashed block indicates the strategy that was adopted when extreme outliers were detected in the data sets, while the excerpt in the blue dashed section represents the strategy adopted in the absence of extreme outliers. The two-way ANOVA strategies, surrounded by the green blocks, were applied for the rat main study only. *HSD* = Honestly Significant Difference.

4.5.1 Outlier analysis and basic statistics

The data were captured in STATISTICA™, the distributions for each dose group depicted graphically by means of box-whisker plots, after which outlier analysis was performed, and the extreme outliers excluded. Outliers and extreme outliers were determined via the use of an outlier coefficient of 1.5. Data points thus positioned more than 1.5 times the inter-quartile range (IQR) above or below the upper or lower quartiles respectively, were classified as either an outlier or extreme outlier, as indicated in Figure 4.4. A data point was regarded as an extreme outlier if it was positioned in a range beyond double that of the outlier coefficient of 1.5, thus having a coefficient of 3.0. The diagrammatic representation of the aforementioned ranges in Figure 4.4 is not drawn to scale.

Figure 4.4 Schematic representation of a box-whisker plot and outlier ranges



Adapted from the STATISTICA™ 7 Electronic Manual. Data points were excluded if they were positioned within the extreme outlier ranges. IQR = inter-quartile range, Max = maximum data point, Min = minimum data point.

The outlier coefficient of 1.5 was deemed a realistic coefficient based on the design of the proposed study. Since small sample sizes of six data points were generated per dose group, it could certainly be argued that data point exclusion may not be an optimal strategy. This is primarily due to the fact that a data point may be classified as an outlier,

even though it may truly represent within the normal distribution of data, had a larger sample size been utilised. Therefore, a more conservative approach was adopted whereby the non-parametric IQR statistic was used to define the variation of the central tendency, and the outlier and extreme outlier ranges determined accordingly for the exclusion of only the extreme outliers. Furthermore, as illustrated in the statistical strategy in Figure 4.3, the data was consistently analysed via non-parametric and parametric test procedures for the inclusion and exclusion of extreme outliers respectively.

A selection of basic descriptive statistics was included to accompany the box-whisker plots in order to define the central tendency and variation inherent to each data set. The basic statistics selected for the study were composed of parametric and non-parametric tests to compensate for exaggeration of statistics due to the presence of outliers and extreme outliers. The basic statistics and definitions utilised in the study are listed in Table 4.1.

Table 4.1 List of basic descriptive statistics utilised in the study to define central tendency and variation

Basic statistic	Definition
Sample size	Number of data points in a data set
Minimum	Lowest ranked data point of a sample ranked in ascending order
Maximum	Highest ranked data point of a sample ranked in ascending order
Range	Difference between the minimum and maximum statistics
Upper quartile	75th percentile data point in a distribution
Lower quartile	25th percentile data point in a distribution
Inter-quartile range	Difference between the upper and lower quartile statistics
Mean	Average score in a distribution
Median	Middle score in a distribution
Standard deviation	Defines the standard variation of a sample

Definitions obtained from Sheskin (2004).

If extreme outliers were present in data sets, these were excluded and data sets analysed via parametric statistics, as indicated in Figure 4.3. However, since small sample sizes of six were utilised in the study, the statistics generated via the inclusion and exclusion of extreme outliers was consistently presented in parallel.

4.5.2 Analysis of variance

Data sets generated from both the rat pilot and main study were analysed via an ANOVA in order to determine the global variation and difference among dose groups. In the presence of outliers and extreme outliers, the data sets were analysed with the inclusion and exclusion of the extreme outliers. The non-parametric Kruskal-Wallis ANOVA was

used prior to the exclusion of extreme outliers, while the parametric one-way ANOVA was used for data sets where the extreme outliers were excluded. In addition, the parametric one-way ANOVA was applied in the analysis of data sets that did not contain any extreme outliers.

4.5.2.1 Factorial analysis of variance

A factorial ANOVA was performed on data sets generated from the rat main study in order to delineate the effects of the various dose regimens. Since the rat main study was designed to treat rats with two dose regimens, followed by an evaluation of the impact of both regimens on physiological and biochemical parameters, the data was analysed via two-way ANOVA. As mentioned earlier, and outlined in Figure 4.2, treatments received from days 1 to 14 were referred to as Factor-1 regimens, while those received on days 15 and 16 were designated Factor-2 regimens. The statistics generated via the factorial ANOVA analyses were in addition depicted graphically and 95% confidence intervals determined. Furthermore, if extreme outliers were determined to be present in a data set, the two-way ANOVA was performed via the inclusion and exclusion of the extreme outliers. The data was subsequently presented in parallel to view the effects of extreme outlier exclusion. Fisher statistics (F-statistics) generated from the factorial ANOVA were presented in combination with the respective p-values for statistical significance.

4.5.3 Multiple comparison and biological significance testing

Individual differences among dose groups in response to the various dose regimens were evaluated with the use of multiple comparison procedures. Data sets that presented with no extreme outliers were analysed via the parametric Tukey *Honestly Significant Difference* (*HSD*) multiple comparison procedures. When complete data sets were recorded for a parameter, the Tukey *equal number HSD* multiple comparison procedure was used. However, when missing data points were listed for a parameter, the Tukey *unequal number HSD* multiple comparison procedure was applied. When data sets included extreme outliers, the non-parametric multiple comparison test that complements the Kruskal-Wallis ANOVA was used, as presented in Figure 4.3. Finally, effect sizes were calculated in order to determine the biological significance of statistically significant differences. Biological significance, as indicated by the d-value, indicates not only significance on the statistical level, but also indicates whether observed differences are

significant on the biological level. The equations for the determination of effect size (Ellis and Steyn, 2003) in parametric and non-parametric data sets are listed in Equation 4.9.

Equation 4.9 Test for biological significance

A: Parametric data (excluding EOs)	B: Non-parametric data (including EOs)
$d = \frac{\lvert \bar{x}_1 - \bar{x}_2 \rvert}{\sqrt{MSE}}$	$d = \frac{\lvert \bar{x}_1 - \bar{x}_2 \rvert}{SD_{\max}}$

Equations obtained from Ellis and Steyn (2003). d = d-value indicating biological significance, EOs = extreme outliers, $\bar{x}$ = mean statistic for a dose group, $\sqrt{MSE}$ = square root of the mean square error for the entire parameter data set, SD_{max} = maximum standard deviation of the two means being compared.

Dose groups were determined to differ by a biologically significant degree if the effect sizes, or d-values, were calculated to be greater than or equal to 0.8 (Ellis and Steyn, 2003). If extreme outliers were present in data sets, biological significance was determined with the inclusion and exclusion of the extreme outliers.

CHAPTER FIVE

RESULTS AND DISCUSSION

The primary goal of the study was to evaluate possible therapeutic intervention strategies for mitochondrial Complex I deficiency in an *in vivo* animal model. The initial investigation consisted of developing a mouse model with the deficiency induced by the complex I inhibitor rotenone. As the investigation progressed, it was observed that the inhibitor did not have the desired effects on mice. It was unexpected that the C57BL/6 mice did not present with a decrease of complex I activity. Consequently, an alternative animal model had to be utilised, one that would manifest with a phenotype of Complex I deficiency, induced by rotenone. Therefore, a similar study was performed in Sprague Dawley rats, which was eventually proven as a successful animal model.

Chapter Five focuses on the results generated from experiments included in the study, aimed at evaluating several biochemical and physiological aspects of the rotenone-induced Complex I deficiency as well as the therapeutic benefits of CoQ_{10} and succinate. Discussions regarding biochemical data and statistical evaluations thereof form the bulk of the chapter. The methods utilised are discussed, followed by interpretations of the data generated from the rat pilot and main studies. Finally, the data is collectively summarised to enable the establishment of tissue-specific biochemical profiles in response to the various dose regimens.

5.1 METHOD OPTIMISATION AND EVALUATION

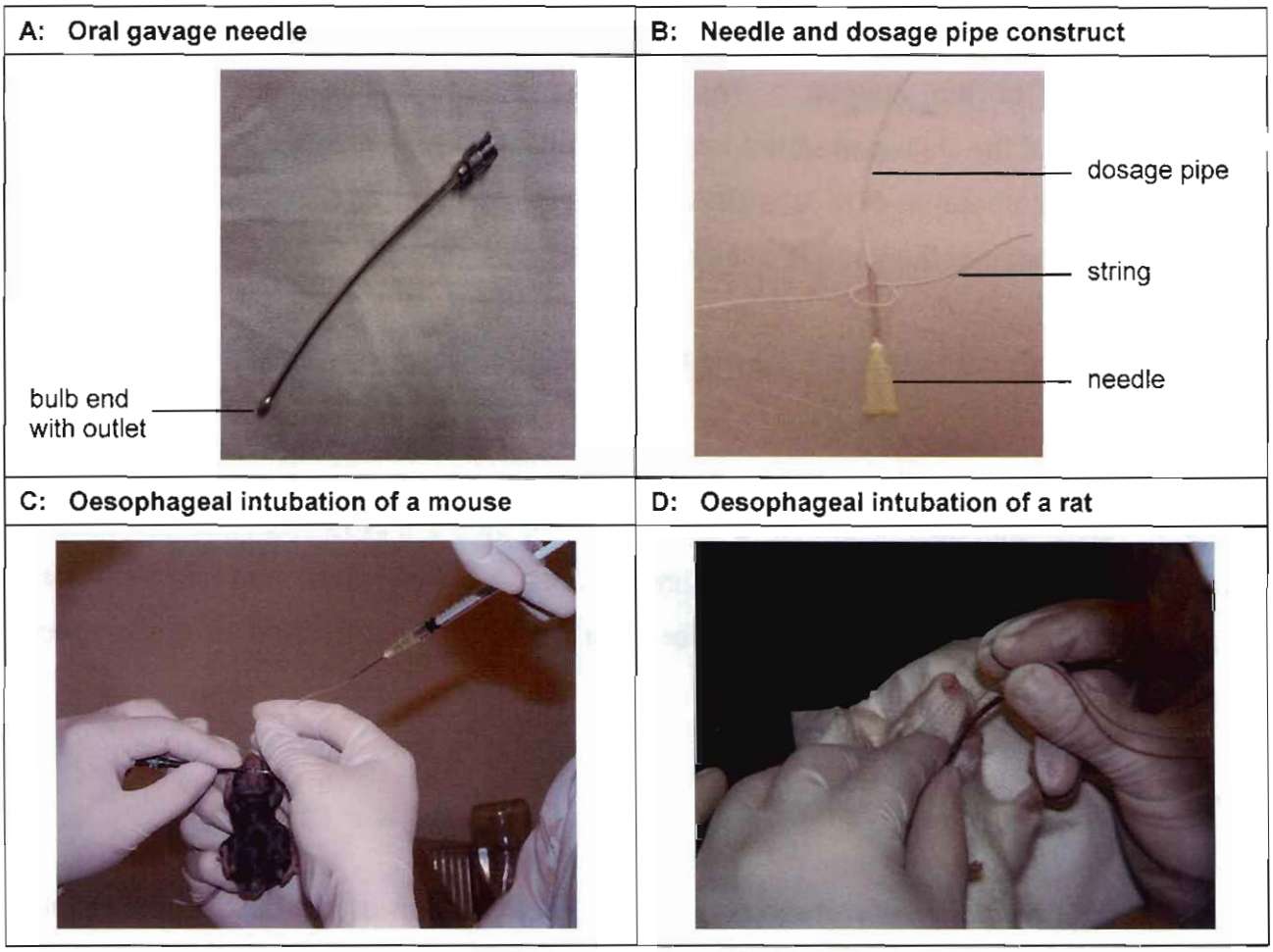
An evaluation of the methods utilised in the investigation is undertaken in the following section. Successful optimisation and typical data outputs are presented and discussed for each of the analysis protocols, in conjunction with the theoretical and practical use of each. The reader may refer to Chapter Four for further clarification of the respective protocols.

5.1.1 Dosage procedure

Since the study was initially attempted in mice, optimisation of the dosage procedure is discussed in view of experimentation with C57BL/6 mice and Sprague Dawley rats. On

each day that the rodents were dosed, body weights were recorded and dose volumes calculated according to these measurements. Rodents were originally dosed orally utilising the typical gavage needle, as presented in Figure 5.1.A, which is curved and has a bulging end with an outlet. The bulb-like end has a diameter of approximately 0.8 mm. Dosing with this gavage required positioning the bulb at the back of the throat of rodents, at the oesophageal opening, and injection of the dose directly into the oesophagus. This procedure proved to be problematic, resulting in incomplete dosage and superfluous dose volumes remaining and spilling out from the mouths of rodents. Furthermore, dosage via the use of the gavage needle resulted in almost instantaneous death in a majority of the mice. The reasons for the deaths in mice were not conclusive, but hypothesised to be due to the high viscosity of the sunflower vehicle. Since the sunflower oil was not injected directly down the throats of the animals on all occasions, it appeared as if the highly viscous dose medium might have entered the lungs on several dosage attempts, resulting in the aspiration of the oil. The residual dose volumes were observed to leak from the sides of both mouse and rat oral cavities.

Figure 5.1 Photographic representations of dosage needles and oesophageal intubation in rodents



The complications encountered when using the traditional gavage needle required the adaptation of the dosage procedure to that of oesophageal intubation, as presented in Figure 5.1.C for mice and Figure 5.1.D for rats. A needle and dosage pipe construct, illustrated in Figure 5.1.B, was designed so that it could be fed down the oesophagus and the dose injected directly into the stomach. Dosage via oesophageal intubation was very successful and significantly improved the accuracy of the dosage procedure. Occasional rodent deaths were however encountered due to unintentional intubation of the trachea and dosage aspiration. The optimised method ensured that both rats and mice received complete dose volumes and that minimal deaths were encountered.

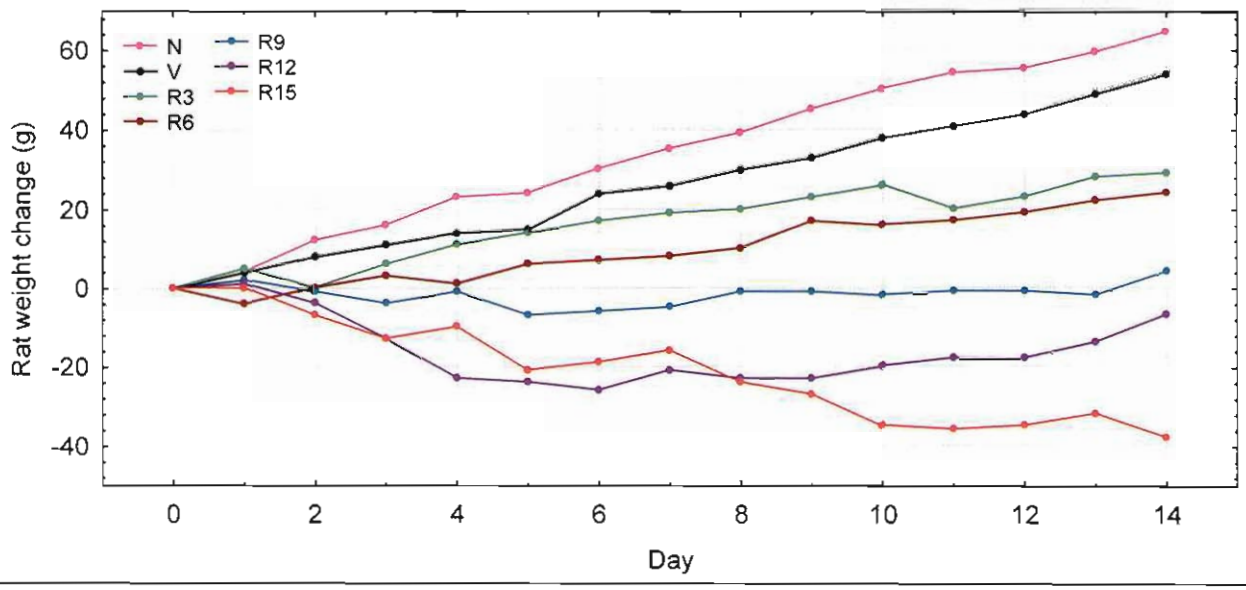
In addition to the advantage of rodents receiving complete dose volumes, it was evident that a decrease in discomfort was experienced when utilising the intubation technique, particularly in rats. An irritation of having the original gavage needle positioned at the oesophagus entry point was often observed. In contrast, dosage via oesophageal intubation resulted in far less irritation, particularly in rats. The ease of oesophageal intubation in rats was greater than in mice due to obvious diameter restrictions in mice. Dosing rats with the adapted procedure enabled the elimination of physical stress factors that may have additionally influenced biochemical parameters when using the original gavage needle and dosage procedure.

5.1.2 Rat body weights

The body weights of rats and mice were recorded prior to dosing and preceding tissue collection. The collection of body weight data proved a very valuable practice as it was the only day-to-day monitoring of rat response over the 14 or 16-day periods of dosing. In Table 5.1, typical gains and losses in body weight recordings of rats from each of the dose groups in the rat pilot study are presented. For the sake of simplicity, weight gains and losses of one rat from each dose group was selected for presentation. However, it should be noted that the mean weight gains and losses are presented as cumulative from day 0, the day that rats received the first of their respective dose regimens.

Table 5.1 Daily recording of rat pilot study body weights

A: Graphic representation of day-to-day weight gains and losses



B: Mean rate and standard deviation of weight gains and losses (g.day^{-1})

	Dose group	N	V	R3	R6	R9	R12	R15
Body weight	Mean	3.31	3.18	1.90	1.58	0.66	0.14	-1.84
	SD	0.77	0.43	0.27	0.64	0.94	0.77	0.86

Rats were treated with N = no dose, V = vehicle, R3 = rotenone 3 mg.kg^{-1}.day^{-1}, R6 = rotenone 6 mg.kg^{-1}.day^{-1}, R9 = rotenone 9 mg.kg^{-1}.day^{-1}, R12 = rotenone 12 mg.kg^{-1}.day^{-1}, R15 = rotenone 15 mg.kg^{-1}.day^{-1}. g = grams, g.day^{-1} = grams per day, mg = milligrams, kg = kilograms, SD = standard deviation.

The graphic representation and data in Table 5.1 illustrates a dose dependent decrease in weight gain. As the concentration of rotenone increased from 3 mg.kg^{-1}.day^{-1} to 15 mg.kg^{-1}.day^{-1}, it was observed that the day-to-day weight gain decreased from a mean of 3.31 g.day^{-1} to an overall mean loss of 1.84 g.day^{-1}, as reported in Table 5.1.B. In addition, it can be observed from the standard deviation (SD) statistics that the rat groups that received higher dose concentrations of rotenone presented with an increased variation in the daily weight gains or losses. With the exception of dose group N, it was determined that rat groups V and R3 presented with the least variation when compared to R6, R9, R12 and R15. However, as discussed in Section 5.2.1, dose group N presented with an extreme outlier data point, which of course contributed considerably to the elevation of the SD for this dose group. A more in-depth discussion regarding the pilot study rat weight data is presented in Section 5.2.1. Analogous to dose group R15, where rats received 15 mg.kg^{-1}.day^{-1} rotenone, rats in the main study lost equivalent amounts of weight over the first 14 days that rotenone was dosed, as presented in Section 5.2.2. The rat groups of the main study that received a Factor-2 dose regimen on days 15 and 16 presented with generally increased weight gains as the rats were relieved of the rotenone

Factor-1 regimens. A statistical evaluation of the rat weight recordings from the pilot and main study is presented in Section 5.2.

5.1.3 Rat behaviour

No protocols investigating rodent behaviour were applied in the study. Therefore, the only form of behavioural observation that can be reported is that which was subjectively observed on a daily basis. There was a clear distinction between the behaviour patterns of rats receiving rotenone doses as opposed to vehicle regimens. Rats receiving vehicle were complacent and receptive. The rats were positioned appropriately and the dosage tube was inserted without any difficulty. Rats were unresponsive to the intubation and therefore did not react negatively to receiving the dose. However, rats that were dosed with rotenone were not as receptive. Resistance was often encountered which was identified by rats either subtly moving their heads away to avoid intubation or by abrupt movements in an attempt to escape the grip and positioning. In the pilot study, this behaviour was not always present upon dosage with low rotenone concentrations, as was the case in dose groups R3 and R6, but became more frequent as the rotenone concentrations increased to 9, 12 and 15 $mg.kg^{-1}.day^{-1}$. As expected, these difficulties were also experienced in the rat main study amongst the rotenone-treated rats, namely dose groups RX, RN, RV, RC and RS.

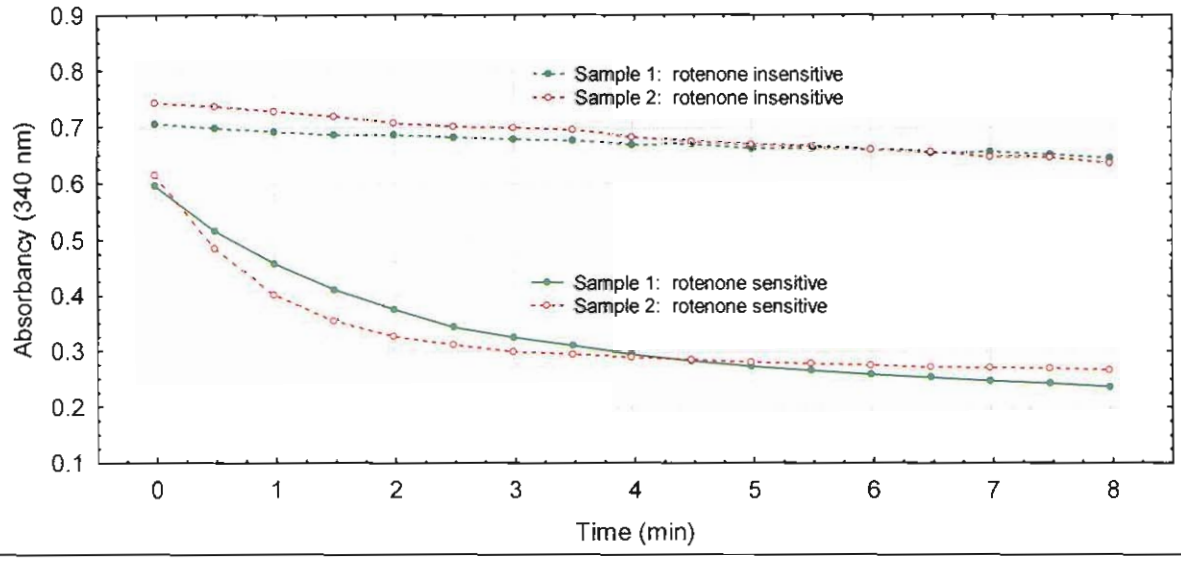
Characteristic irritation patterns were observed in the rats directly after they were dosed with rotenone. Kicking at the vermiculite in the cage and circular movements were the predominant signs of irritation. This behaviour stopped within approximately 3 min after the dose had been received, followed by a sedated and subdued demeanour. After approximately two to four hours had passed, rats generally appeared to have recovered to normal. The period of recovery depended largely on the dose that was received by the rodent. In the pilot study, rats that received the highest doses of 12 and 15 $mg.kg^{-1}.day^{-1}$ took longer to recover than those that received the lower concentrations. In the main study, all complex I deficient rats that received rotenone presented in a similar manner. In both the pilot and main studies, rats that received vehicle as opposed to rotenone presented with no signs of discomfort or adverse responses. These rats simply received the vehicle dose and continued with regular patterns of behaviour.

5.1.4 Determination of complex I activity

The activity of complex I was determined in mitochondrial preparations from whole brain, liver, heart and skeletal muscle. This spectrophotometric assay measures the decrease in NADH at a wavelength of 340 nm as a function of complex I activity, which transfers electrons from NADH to the electron acceptor coenzyme Q_1. The assay was performed via the use of two separate cuvettes for the determination of rotenone sensitive and rotenone insensitive complex I activity respectively. A graphic representation of the typical reaction data generated via the sample analysis of complex I activity is presented in Table 5.2. The table also contains corresponding calculations of complex I activity.

Table 5.2 Spectrophotometric data generated via the analysis of complex I activity

A: Graphic representation of reaction data



B: Equation for the calculation of complex I activity

Complex I activity ($\mu mol.min^{-1}$) = $(\Delta A_{rs}/\Delta t_{rs} - \Delta A_{ri}/\Delta t_{ri}) \times (V/v \times 1000)/6.81$

C: Corresponding calculation of complex I activities

Sample	Cuvette	$\Delta A/\Delta t$	V (μL)	v (μL)	$\Delta A_{rs}/\Delta t_{rs} - \Delta A_{ri}/\Delta t_{ri}$	Complex I activity ($\mu mol.min^{-1}$)
1	rotenone sensitive (ER)	-0.1221	500	5	-0.1090	1,601
	rotenone insensitive (IR)	-0.0131	500	5		
2	rotenone sensitive (ER)	-0.1729	500	5	-0.1565	2,298
	rotenone insensitive (IR)	-0.0164	500	5		

A: Each plot represents the oxidation of NADH in four cuvettes, that is, the activities of complex I. B: The equation for calculation of complex I activity was obtained from Equation 4.2 of Chapter Four. C: A tabulated format for the calculation of the corresponding complex I activities is presented. $\Delta A_{rs}/\Delta t_{rs}$ = reaction rate determined from rotenone sensitive mitochondria, $\Delta A_{ri}/\Delta t_{ri}$ = reaction rate determined from rotenone insensitive mitochondria, extinction coefficient of NADH = 6.81 $mM^{-1}.cm^{-1}$, ER = excluding rotenone, IR = including rotenone, μL = microlitre, $\mu mol.min^{-1}$ = micromole per minute activity, min = minute, nm = nanometre, V = total reaction volume, v = sample volume used in reaction.

Table 5.2 presents the rate of NADH oxidation via mitochondrial complex I. Four oxidation curves are presented representing two mitochondrial samples, along with the required

data for the calculation of complex I activities. Each sample reaction was performed in duplicate. The first cuvette, used to determine rotenone sensitive complex I activity [excluding rotenone (ER)], contained an optimised mitochondrial preparation volume as well as assay reagents that enabled the determination of the actual sample complex I activity, in the absence of a rotenone inhibitor. Mitochondrial preparation volumes and assay reagents were equivalent in the duplicate cuvette, except that rotenone was included to inhibit NADH oxidation irreversibly via complex I. The duplicate therefore facilitated the determination of rotenone insensitive complex I activity [including rotenone (IR)]. Mitochondrial preparations were initially exposed to 3 min of hypotonic shock in ddH_2O, followed by the addition of NADH and the remaining assay reagents to initiate the reactions. As indicated by the rotenone sensitive curves of the two samples in Table 5.2.B, NADH oxidation takes place rapidly and finally plateaus as all of the substrate is oxidised. In contrast, NADH oxidation in the presence of rotenone insensitive mitochondria presented with a marked decrease in the substrate oxidation rate.

Calculation of complex I activity via the equation indicated in Table 5.2.B required the determination of the initial linear rate of NADH oxidation of both the rotenone sensitive and rotenone insensitive mitochondrial preparations, as well as total reaction and sample volumes. The data requirements and calculated complex I activities for the presented samples are listed in Table 5.2.C. The biochemical calculation of complex I activity requires that a linear representation of NADH oxidation for the rotenone sensitive and rotenone insensitive mitochondrial preparations be utilised. Therefore, since rotenone sensitive NADH oxidation occurred at a high initial rate, complex I activities in the study were calculated over the first two to three minutes of each reaction. Therefore, since absorbency values were recorded every 30 seconds, a minimum of five data points were utilised per reaction. Based on the data presented in Table 5.2.C, the complex I activities for the two samples presented were calculated to oxidise NADH at a rate of 1.6 and 2.3 micromole per minute ($\mu mol.min^{-1}$) respectively. Finally, complex I activities were divided by the amount of protein used in each reaction and expressed in terms of corresponding citrate synthase activities.

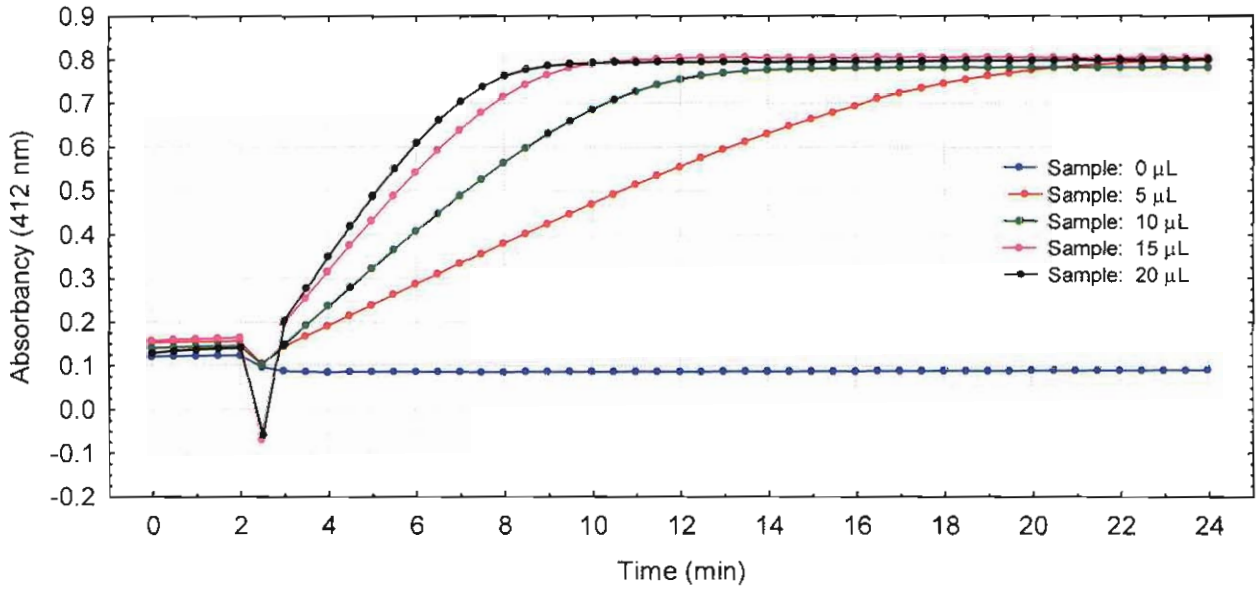
5.1.5 Determination of citrate synthase activity

Citrate synthase activities were determined from mitochondria as a standard enzyme utilised in the expression of complex I activities. The inclusion of such an assay enables normalisation of complex I activity to express it relative to the amount of mitochondria in

the sample, as represented by the citrate synthase activity. The enzyme functions in the Krebs cycle and utilises oxaloacetate as a substrate to convert acetyl-coenzyme A to citrate and sulfhydryl compounds. The assay reaction contains DTNB reagent, which binds to the newly formed sulfhydryl compounds and simultaneously converted to TNB. Generated TNB results in a colour change, which is recorded spectrophotometrically at a wavelength of 412 nm. Tissue specific optimisation was performed by establishing a dilution series of mitochondrial preparations, as presented in Table 5.3.

Table 5.3 Spectrophotometric data generated via the optimisation of citrate synthase activity

A: Graphic representation of reaction data



B: Equation for the calculation of citrate synthase activity

Citrate synthase activity ($\mu mol.min^{-1}$) = $(\Delta A_2/\Delta t_2 - \Delta A_1/\Delta t_1) \times (V/v \times 1000)/13.6$

C: Corresponding calculation of citrate synthase activities

Sample volume (µL)	$\Delta A_1/\Delta t_1$	$\Delta A_2/\Delta t_2$	V (µL)	v (µL)	$\Delta A_1/\Delta t_1 - \Delta A_2/\Delta t_2$	Citrate synthase ($\mu mol.min^{-1}$)
0	0.0013	0.0001	500	0	0	0
5	0.0015	0.0472	500	0.25	0.0457	6,720
10	0.0025	0.0871	500	0.50	0.0845	6,215
15	0.0035	0.1183	500	0.75	0.1148	5,628
20	0.0057	0.1420	500	1.00	0.1363	5,013

A: Each of the plots represents the citrate synthase activity of a single sample dilution. B: The equation for calculation of citrate synthase activity was obtained from Equation 4.1 of Chapter Four. C: A tabulated format for the calculation of the corresponding citrate synthase activities is presented. $\Delta A_1/\Delta t_1$ = reaction rate determined prior to the addition of the oxaloacetate substrate, $\Delta A_2/\Delta t_2$ = reaction rate determined after the addition of the oxaloacetate substrate, extinction coefficient of TNB = 13.6 $mM^{-1}.cm^{-1}$, µL = microlitre, $\mu mol.min^{-1}$ = micromole per minute activity, min = minute, nm = nanometre, V = total reaction volume, v = sample volume used in reaction.

The graphic representation in Table 5.3.A illustrates the activities of citrate synthase for four different mitochondrial preparation volumes ranging from five to 20 µL. Mitochondrial preparations were initially incubated for a period of two minutes, after which the

oxaloacetate substrate was added and the reactions initiated. The decrease in absorbencies, observed from 2 min to 3 min, is due to opening of the spectrophotometer lid in order to add the substrate to cuvettes. As expected, since no mitochondria were included in the 0 μL reaction, the absorbency remained unchanged when oxaloacetate was added. The slight decrease in absorbency from above 0.1 to just below the same value is due to the addition of 25 μL oxaloacetate, which in turn decreases the initial concentration of TNB. Since DTNB reacts freely with sulphur groups that are made available in the mitochondrial preparation, a steady state formation of TNB is expected. This is confirmed by the positive $\Delta A_1/\Delta t_1$ values, i.e. reaction rates, listed in Table 5.3.C. Furthermore, it can be determined that as the volume of mitochondrial preparations increased in each of the reactions, so did the $\Delta A_1/\Delta t_1$ values, indicating an increased formation of TNB. Upon the addition of oxaloacetate, it can be observed that the slope of each of the curves increased accordingly with the volume of mitochondrial preparations, indicating the increased rate of TNB formation and hence citrate synthase activity. A plateau is reached when no more oxaloacetate substrate is available for the enzyme. If a higher concentration of oxaloacetate were utilised in the reactions, it would be expected that the curve plateau would be achieved after a longer time interval and at a higher absorbency level. Since a constant concentration of the substrate was utilised in all reactions, the plateau was consistently reached at an absorbency of approximately 0.8.

Calculations of citrate synthase activities were determined according to the equation in Table 5.3.B. The data in Table 5.3.C indicates that which is required for the calculation of citrate synthase activity. It should be noted that the total reaction volumes were equilibrated accordingly with ddH_2O to 500 μL as the sample volumes increased. Upon optimisation of the citrate synthase assay, it was observed that a 1:20 dilution of mitochondrial preparations was required as substrate utilisation was too rapid to be recorded from the original sample. Therefore, a dilution factor was implemented into the calculation of citrate synthase activity, resulting in the adjusted sample volumes (v) in Table 5.3.C. However, even though the equation takes into account sample volume, it can be noticed that a variation in the $\mu mol.min^{-1}$ citrate synthase activities was calculated. This is primarily because the increase in $\Delta A_2/\Delta t_2$ values was not directly proportional to the increase in sample volumes. The slope for the 5 μL sample after initiation of the reaction was 0.0472 and increased by an order of 1.8 to 0.0871 when 10 μL of the sample preparation was used. Moreover, the slope was only 1.6 times greater when 20 μL of the sample preparation was used. For this reason, the optimisation of citrate synthase

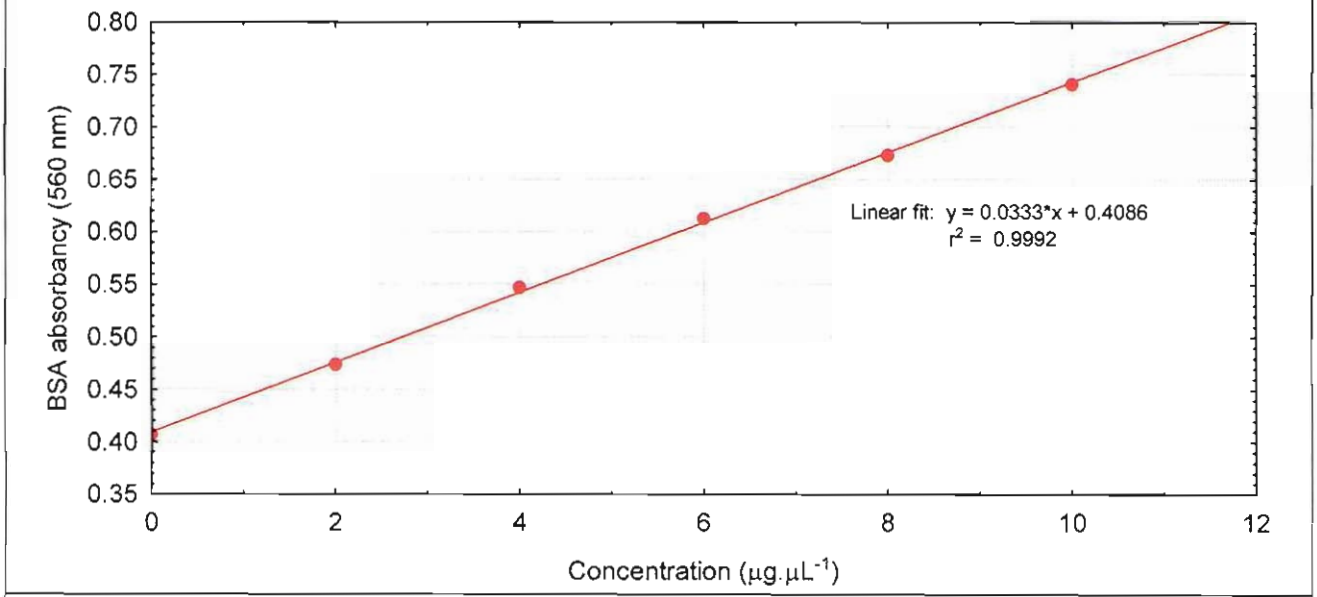
reactions were performed prior to the analysis of a specific tissue group and an optimal mitochondrial volume selected, which was utilised consistently for all samples.

5.1.6 Protein concentration analysis

The protein concentration of tissue preparations was determined for several assays requiring expression in terms of protein content. The protocol utilised (Smith *et al.*, 1985) in this study exploits the chemical properties of BCA, which forms a complex with copper ions (Cu^{+}) in an alkaline environment. The peptide bonds of the protein sample reduce copper II ions (Cu^{2+}) to that of Cu^{+}, providing the substrate for BCA to bind. The purple colour produced from the reaction is stable and correlates directly with the protein concentration in the sample aliquot. Samples were assayed in duplicate and protein concentrations determined via the use of linear standard curve analysis, generated from a range of BSA standard concentrations. An example of a linear standard curve generated from BSA is presented in Table 5.4, along with the list of corresponding absorbencies, recorded at a wavelength of 560 nm.

Table 5.4 Graphic representation of a linear standard curve generated for the determination of protein concentration

A: Graphic representation



B: Absorbency data

BSA concentration	0	2	4	6	8	10
Corresponding absorbency	0.406	0.474	0.547	0.613	0.673	0.740

BSA = bovine serum albumin, $\mu g.\mu L^{-1}$ = microgram per microlitre concentration, nm = nanometre, r^2 = square of the Pearson product moment correlation coefficient, signifying curve linearity.

The mean of duplicate absorbencies was determined and corresponding protein concentrations calculated by substituting 'y' with the mean absorbency and solving for 'x' in the linear-fit equation indicated in Table 5.4.A. The r^2 value indicated on the graph is representative of the linearity of the standard curve. The r^2 value is determined from the Pearson correlation coefficient, where a value of 1.0, is indicative of complete correlation. In contrast, an r^2 value of zero indicates no correlation. Therefore, since an r^2 value of 0.9992 was reported for the protein standard curve, it can be concluded that an almost complete correlation in the increase in BSA concentration and absorbency was present. All protein concentrations throughout the study were determined via this simplistic procedure discussed above without encountering complications.

5.1.7 Hydroperoxide concentration analysis

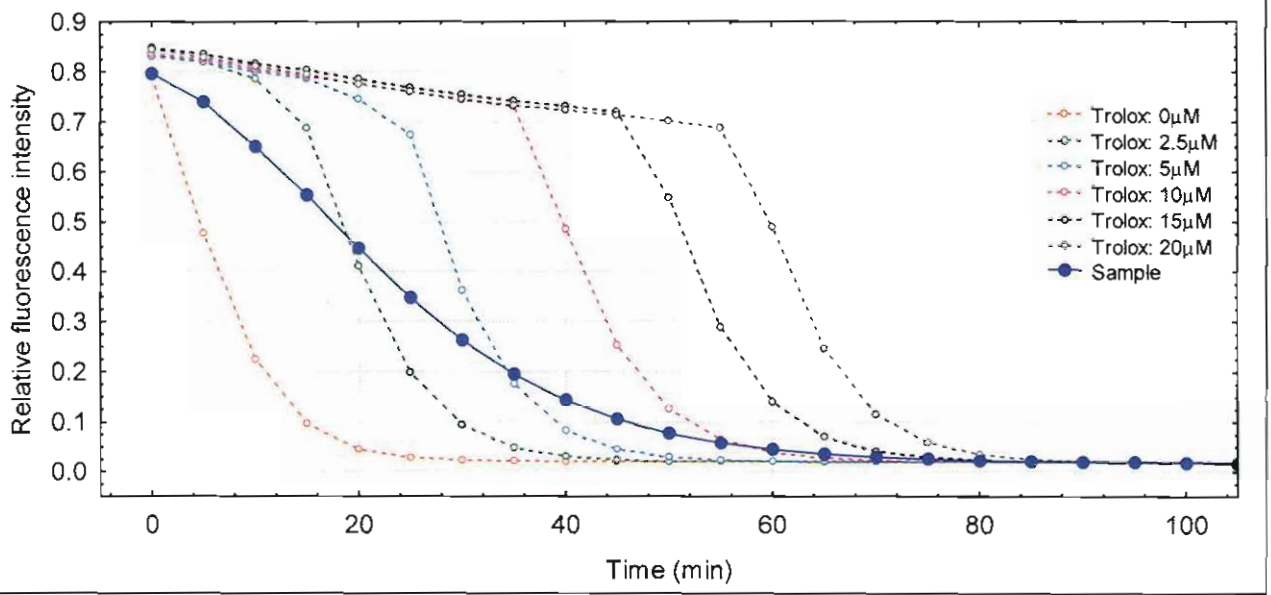
The concentration of hydroperoxides in blood serum was assayed via the use of the d-ROMs kit. The hydroperoxides are detected utilising a chromogenic substrate, which is monitored spectrophotometrically at a wavelength of 485 nm. The colour intensities, which correlate directly with the concentration of hydroperoxides, are expressed in terms of CARR U, where one CARR U corresponds to 0.8 nanograms of hydrogen peroxide in 1 mL of serum. Blood serum was appropriately collected and assayed in conjunction with a serum standard supplied by the d-ROMs kit. According to the manufacturer's specifications, the standard was assigned a hydroperoxide concentration of 250 CARR U and was utilised as a reference to determine hydroperoxide concentrations of serum samples.

5.1.8 Oxygen radical absorbance capacity (ORAC) analysis

Antioxidant capacity was measured in blood and the various tissue preparations by use of the ORAC assay. The protocol (Ou *et al.*, 2001) measures the decrease in the fluorescence of fluorescein in response to peroxyl radicals. A decrease in the decay of fluorescein, or alternatively inhibition of peroxyl radical action, due to the effect of an antioxidant is referred to as the antioxidant capacity of a sample. This capacity is calculated by use of an AUC technique, accounting for both inhibition time and percentage of reactive species endogenous to the sample. The antioxidant capacity of a sample is finally calculated in relation to Trolox, a vitamin E analogue. An example of fluorescein decay in the presence of a Trolox standard series, as well as a sample, is presented in Table 5.5.

Table 5.5 Spectrophotometric data generated via the determination of sample antioxidant capacity

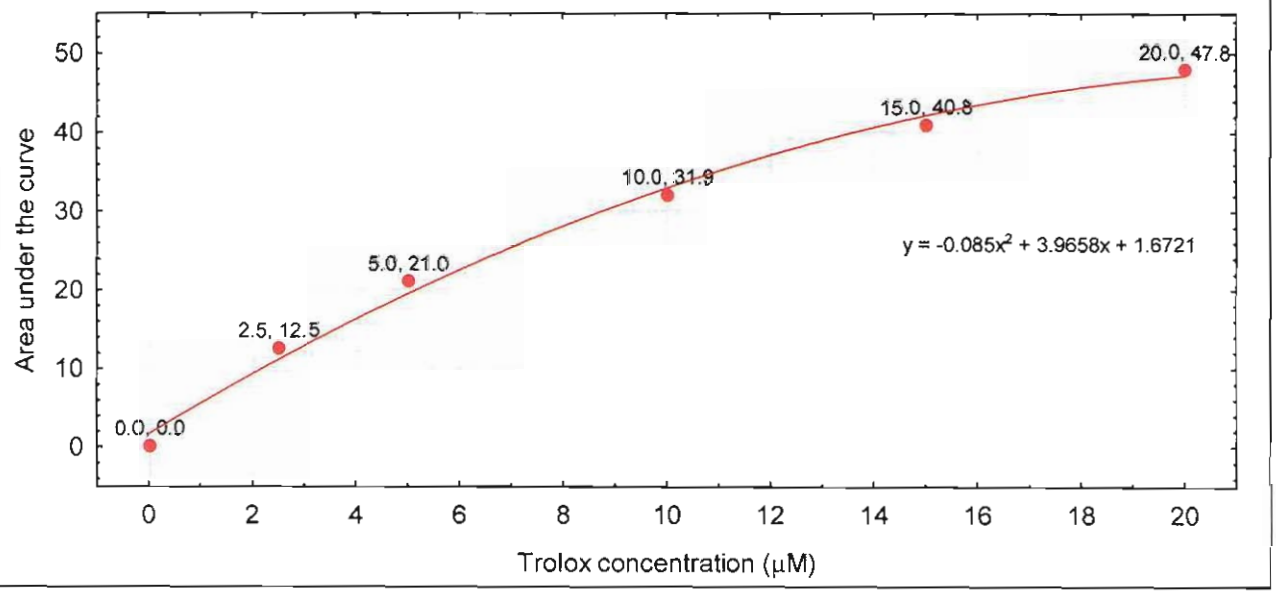
A: Graphic representation of fluorescein decay



B: Data required for the determination of antioxidant capacity

Trolox			Sample			
Concentration (µM)	AUC	AUC – blank	AUC	AUC – blank	AC (µM TE)	AC x dilution factor (µM TE)
0	10.2	0	26.7	16.5	4.25	849
2.5	22.7	12.5				
5	31.2	21.0				
10	42.2	41.9				
15	51.1	40.8				
20	58.0	47.8				

C: Trolox standard curve



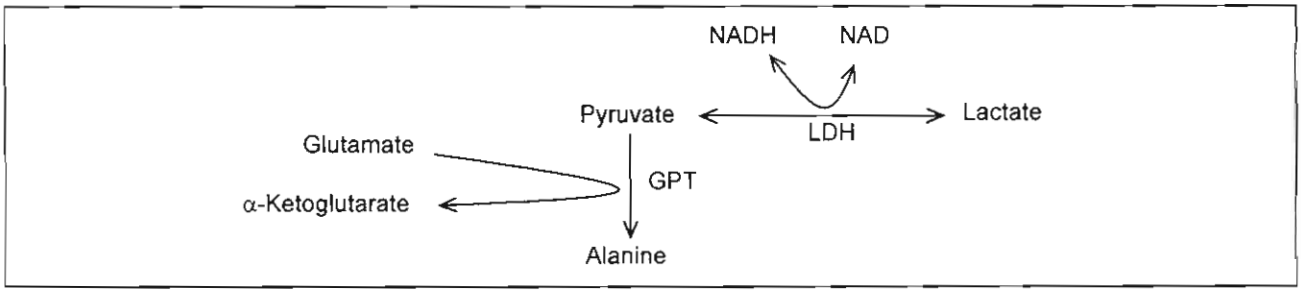
A: Fluorescein decay curves in the presence of Trolox are represented by open circular data points and dashed curve lines, while the filled circular data points and a solid line curve represents the sample. B: Antioxidant capacity of the sample is calculated utilising the AUC data generated from the various Trolox concentrations. C: Utilising the AUC data, a Trolox standard curve is generated, with X and Y-coordinates indicated at each data point. AUC = area under the curve, AC = antioxidant capacity, µM = micromolar concentration, min = minute, TE = Trolox equivalents.

As can be observed from Table 5.5.A, the decrease in the fluorescence of fluorescein in the presence of various concentrations of Trolox corresponds to the length of the lag phase. As the concentration of Trolox increases, the time of the lag phase increases. The fluorescein decay curve in the presence of a random sample is also presented in the aforementioned graph, superimposed over the Trolox fluorescein decay curves. Area under each of the curves was calculated, as presented in Table 5.5.B. By subtracting the AUC calculated for fluorescein decay in the presence of 0 μL Trolox, i.e. the blank sample, from that calculated in the presence of the various Trolox concentrations, a net AUC value was determined. The net AUC values were utilised to generate a second order polynomial standard curve, as presented in Table 5.5.C. In order to determine the Trolox equivalent (TE) antioxidant capacity of a sample, the net AUC value of the sample was substituted for 'y' in the polynomial equation, as indicated on the graph, and μM antioxidant capacity determined by solving for 'x'. In the case of the sample in Table 5.5, the net AUC of 16.5 was substituted into the polynomial equation and a 4.25 micromolar Trolox equivalents (μM TE) antioxidant capacity calculated. Finally, the sample dilution was taken into consideration, resulting in an 849 μM TE antioxidant capacity recording for the original sample. The ORAC assay was performed successfully in all sample preparations obtained from rat blood, heart muscle, brain tissue, liver tissue and skeletal muscle. Sample protein concentrations for the latter four tissue groups were also determined and the antioxidant capacity data expressed in terms of protein content.

5.1.9 Lactate and pyruvate concentrations

The concentrations of lactate and pyruvate were determined via the protocol described in Section 4.4.7 of Chapter Four. The principle of the reaction relies upon the inter-conversion of pyruvate to lactate and the simultaneous formation of NADH or NAD. A schematic representation of lactate-pyruvate inter-conversion is displayed in Figure 5.2.

Figure 5.2 Schematic representation of the biochemical relationship between lactate and pyruvate

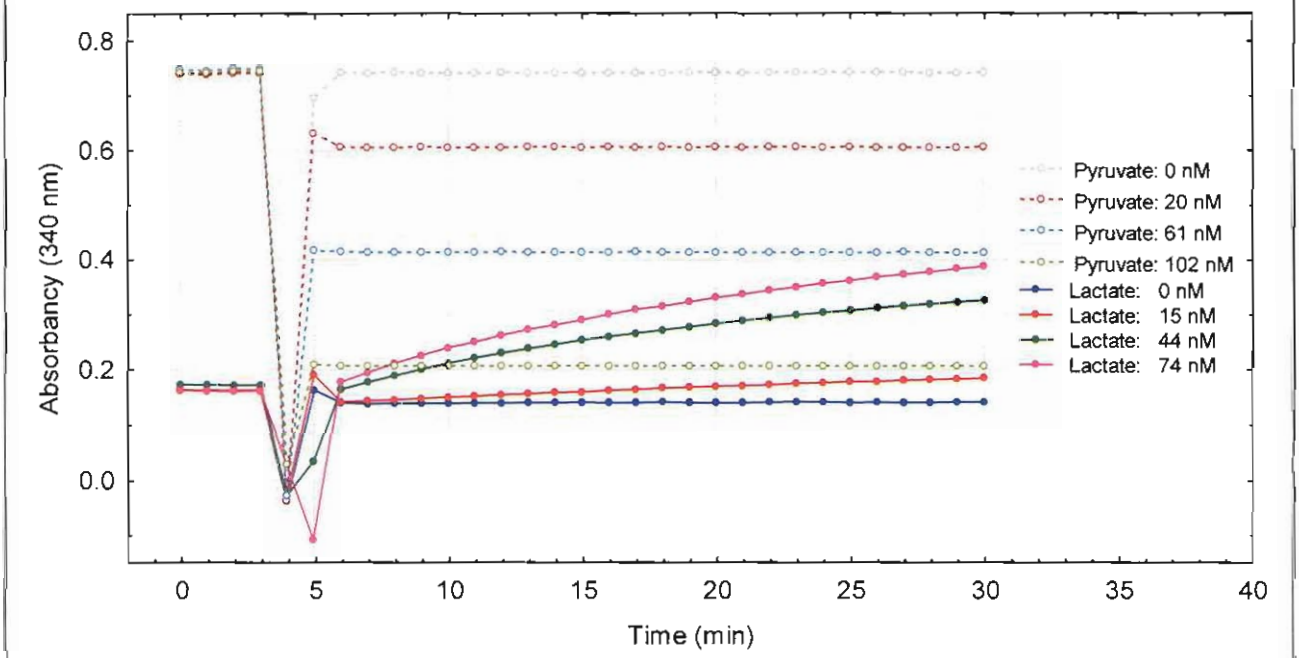


GPT = Glutamate-pyruvate transaminase, LDH = Lactate dehydrogenase, NADH = reduced nicotinamide adenine dinucleotide, NAD = oxidised nicotinamide adenine dinucleotide, α = alpha.

Pyruvate concentration assays were based on the reduction of pyruvate to lactate in the presence of LDH, and spectrophotometric measurement of the oxidation of NADH at a wavelength of 340 nm. Lactate concentrations were determined via the conversion of lactate to pyruvate in the presence of LDH. The reduction of NAD to NADH was recorded spectrophotometrically at 340 nm. Since the reaction favours the formation of lactate, the pyruvate formed was immediately converted to alanine in the presence of glutamate and GPT. The formation of alanine is irreversible, preventing false pyruvate quantification. A summary of the data generated when assaying known lactate and pyruvate concentrations is presented in Table 5.6.

Table 5.6 Spectrophotometric data generated by assaying varied concentrations of lactate and pyruvate

A: Graphic representation of absorbency data



B: Lactate and pyruvate standard curve data

	Lactate				Pyruvate			
Concentration (nM)	0	15	44	74	0	20	61	102
A_1	0.162	0.161	0.172	0.163	0.745	0.740	0.747	0.745
A_2	0.177	0.275	0.435	0.538	0.745	0.607	0.418	0.208
A_1-A_2	0.015	0.114	0.263	0.376	0.000	0.133	0.329	0.536
Standard curve slope	0.0048				0.0052			
Standard curve r^2	0.988				0.997			

A: The absorbency pattern corresponding to four lactate and pyruvate concentration assays is presented. B: Data determined from the reaction plots and standard calculations are listed. A_1 = initial absorbency, A_2 = final absorbency, nm = nanometre wavelength, nM = nanomolar concentration, r^2 = square of the Pearson product moment correlation coefficient, signifying curve linearity.

Table 5.6.A contains a graphic representation of the change in absorbency due to the reduction and oxidation of nicotinamide adenine dinucleotide when assaying different concentrations of lactate and pyruvate respectively. The plot represents standard

concentrations that were routinely used in the study to generate lactate and pyruvate standard curves. Lactate and pyruvate concentrations were assayed in two separate reaction runs and the data superimposed to generate the graphic representation in Table 5.6.A. However, it should be noted that two concentrations were excluded from both the lactate and pyruvate standard series in order to simplify the presentation of data. For both assay types, a mean A_1 data point was determined from a minimum of three absorbency values. The A_1 data recorded for the various lactate concentrations were narrowly distributed, with mean absorbency values ranging from 0.161 to 0.172, as listed in Table 5.6.B. The sharp decrease in the curves at the 3 min point is due to the opening of the spectrophotometer lid and removal of cuvettes to add LDH. Upon initiation, it can be observed that the curves for the reactions containing lactate started to increase at a slow steady rate. The increase is due to the reduction of NAD reagent to NADH, as indicated in Figure 5.2. As the concentration of lactate increased in reactions, so did the reaction rates, indicating a greater production rate of NADH. As expected, the 0 nM lactate absorbency remained unchanged throughout the 30 min period. It can also be determined from Table 5.6 that the A_2 recordings listed in section B do not correspond to that which is observed on the graphic representation. The reason for this is, since an endpoint method of analysis was utilised, it was required that the reactions continued to completion. Therefore, the A_2 values listed in Table 5.6.B indicate absorbencies recorded after a period of approximately 180 minutes, a period optimised for this study. At this point, reactions were completed and absorbency recordings for the highest lactate concentration of 74 nM were determined to remain unchanged.

Pyruvate concentrations were assayed in a similar fashion as described above. Initial absorbency recordings (A_1) were determined and mean statistics calculated. Similar to the lactate samples, pyruvate A_1 readings were collected within a narrow data range of 0.007. The higher A_1 readings for pyruvate analyses, in contrast to lactate assays, were due to the presence of NADH substrate amongst the initial reaction constituents. Reactions were similarly initiated via the addition of LDH after approximately three minutes of A_1 recordings. In contrast to the lactate assay, however, the pyruvate analyses continued to completion within seconds. As indicated in the graphic representation of Table 5.6.A, absorbency readings after the addition of LDH decreased immediately in proportion to the concentration of pyruvate in each reaction. The fact that absorbency recordings remained unchanged for the following 24 minutes indicated that the reactions had already continued to completion. In order to provide an improved opportunity to visualise the rapid rate of NADH oxidation, more sophisticated instrumentation could be utilised to dispense LDH via automated technology coupled to simultaneous absorbency

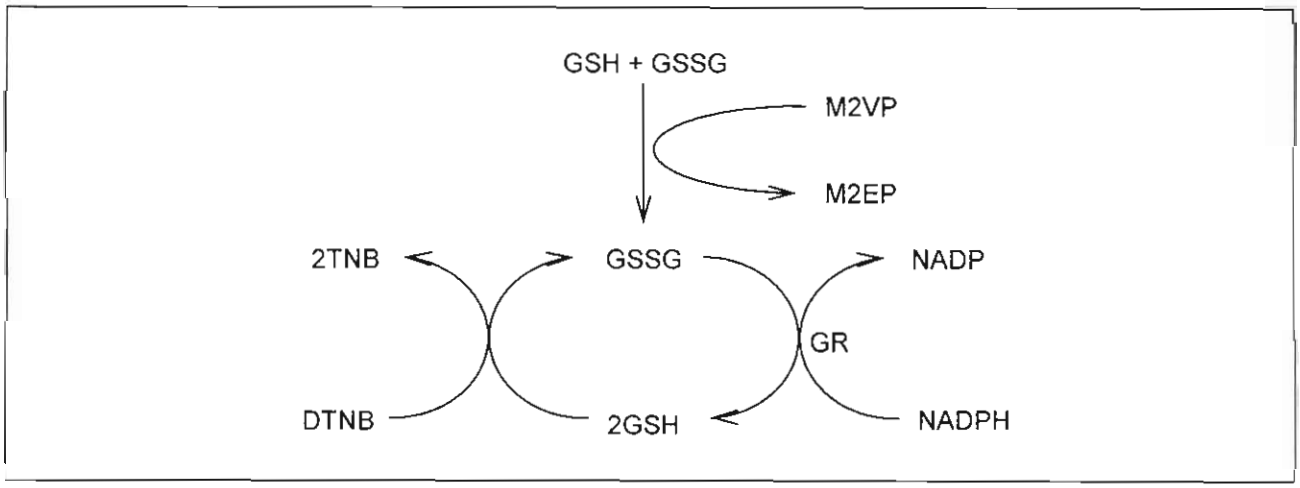
recordings. The rapid reaction rates observed for the pyruvate analyses made it possible to determine A_2 absorbency levels within minutes after initiating the reactions, in contrast to assaying lactate concentrations that required 180 minutes.

Lactate and pyruvate standard curves were determined according to the calculations presented in Table 5.6.B. The difference between A_1 and A_2 absorbencies were calculated and the values utilised in conjunction with lactate or pyruvate concentrations to generate a linear standard curve, as presented in Section 5.1.6 for the determination of protein concentration. In addition, Table 5.6.B lists the slope of the lactate and pyruvate standard curves and r^2 values as a reflection of the linearity of the standard curves. The r^2 values of 0.988 and 0.997 confirm that the standard curve data points were indeed positioned in a linear fashion. Lactate and pyruvate concentrations of samples assayed in the study were subsequently determined by use of the standard curve data.

5.1.10 Glutathione assay

The GSH/GSSG ratio is an important indicator of oxidative stress in a cell since the reduced form, GSH, is a major antioxidant in all living cells. Reduced glutathione is a tripeptide with a free thiol group, which is converted to disulphide GSSG in the presence of oxidants. The method used was an adaptation of that originally described by Tietze (1968). A schematic representation of the GSH/GSSG procedure is presented in Figure 5.3.

Figure 5.3 Diagrammatic representation of the GSH/GSSG assay

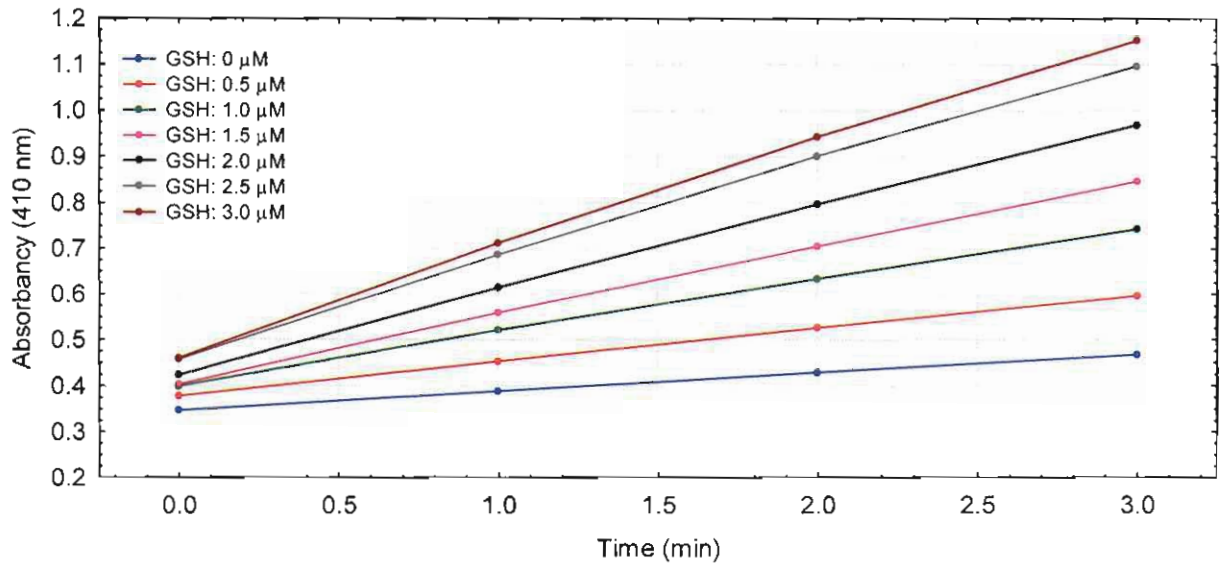


GSH = reduced glutathione, GSSG = oxidised glutathione, M2VP = 1-methyl-2(thioethyl) pyridinium, M2EP = 1-methyl-2(2-thioethyl) pyridinium, GR = glutathione reductase, DTNB = 5,5'-Dithio-bis(2-nitrobenzoic acid), TNB = thionitrobenzoic acid, NADPH = reduced nicotinamide adenine dinucleotide phosphate, NADP = oxidised nicotinamide adenine dinucleotide phosphate.

During the preparation of tissue, autoxidation of GSH to GSSG is often encountered, resulting in altered GSH/GSSG ratios. Therefore, the use of suitable agents, such as M2VP to derivatise or trap GSH was included. The addition of M2VP results in scavenging of the free thiol group of GSH and formation of M2EP, as indicated in Figure 5.3. In the final reaction, GSH is recycled from GSSG in the presence of glutathione reductase and NADPH. The autoxidation of GSH to GSSG and simultaneous formation of TNB is monitored spectrophotometrically at a wavelength of 412 nm. The determination of glutathione status therefore required that two assays be performed for each sample. The first determined total glutathione, since all existing GSH is expected to be autoxidised to GSSG while in the second reaction, the M2VP-captured GSH results in the determination of GSSG only. Both sample preparations were assayed in the same analysis run and glutathione concentrations determined via the use of a standard curve generated from a range of GSH concentrations. The change in absorbencies, i.e. reaction rates, of the GSH standard concentrations were utilised as data points in constructing the standard curve. An example of the typical change in absorbencies generated from the GSH standard series is presented in Table 5.7.

Table 5.7 Spectrophotometric data generated by assaying varied concentrations of glutathione

A: Graphic representation of the change in absorbency data



B: Glutathione standard curve data

GSH concentration (µM)	0	0.5	1.0	1.5	2.0	2.5	3.0
Reaction rate	0.042	0.075	0.118	0.152	0.188	0.223	0.243
r^2	1.000	1.000	1.000	1.000	1.000	1.000	0.999
Standard curve slope	0.069						
Standard curve r^2	0.994						

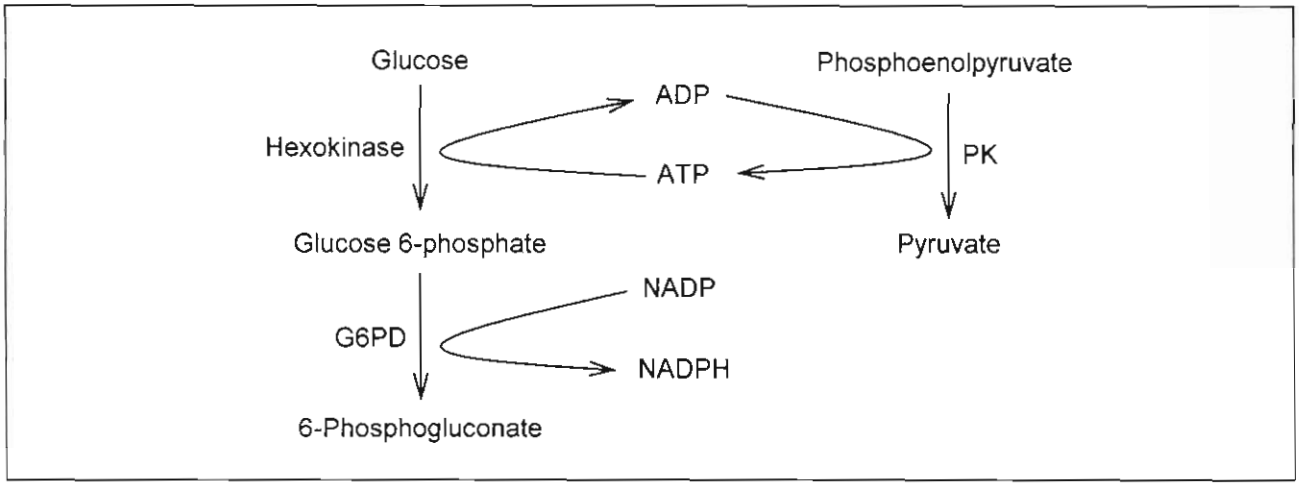
A: The increase in absorbency at varied concentrations of GSH is presented, along with reaction rate and r^2 values. B: Data determined from the reaction plots and standard calculations are listed. GSH = reduced glutathione, min = minute, nm = nanometre wavelength, µM = micromolar concentration, r^2 = square of the Pearson product moment correlation coefficient, signifying curve linearity.

The change in absorbency curves in Table 5.7.A indicate that a consistency in relation to GSH concentrations exists. As the concentration of GSH increased, so did the conversion of DTNB to TNB, resulting in a proportional increase in reaction rates. Moreover, a consistency in the formation of TNB was observed, as confirmed by the respective r^2 values listed below the graphic representation. The reaction rates for each of the glutathione concentrations were utilised to generate a linear standard curve, a procedure similar to that presented in Section 5.1.6, where the protein concentration assay was described. As indicated in Table 5.7.B, the slope of the glutathione standard curve was calculated to be 0.069, with an r^2 value of 0.994, indicating an almost complete correlation between GSH concentration and reaction rates. Samples were assayed in conjunction with the GSH standard series and the concentrations of glutathione calculated according to standard curve data. Finally, GSH levels were calculated from the determined total glutathione and GSSG concentrations. Furthermore, tissue preparations were assayed for protein concentration, as presented in Section 5.1.6, and the respective glutathione data presented in terms of protein content.

5.1.11 Concentrations of adenylates

The ATP/ADP ratio was calculated in two separate assays for the determination of total adenylates and ATP respectively. The concentrations of ADP were mathematically calculated by subtracting the determined ATP amount from that of total adenylates. The assay (Lust *et al.*, 1981) evaluates ATP/ADP status of treated samples based on the conversion of ATP to ADP in the presence of hexokinase and glucose, as indicated in Figure 5.4.

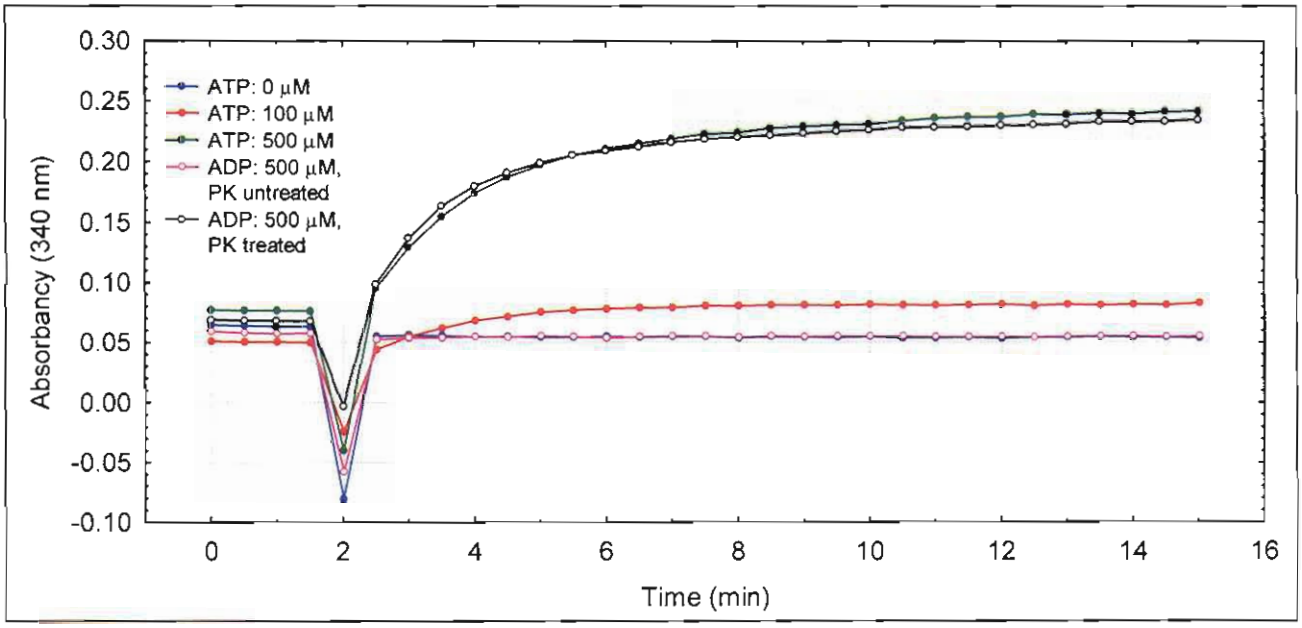
Figure 5.4 Diagrammatic representation of the ATP/ADP assay



ATP = adenosine triphosphate, ADP = adenosine diphosphate, G6PD = glucose 6-phosphate dehydrogenase, NADP = oxidised nicotinamide adenine dinucleotide phosphate, NADPH = reduced nicotinamide adenine dinucleotide phosphate, PK = pyruvate kinase.

Hexokinase converts glucose to glucose 6-phosphate. To follow, the latter is converted to 6-phosphogluconate in the presence of G6PD and NADP. The simultaneously formed NADPH was monitored spectrophotometrically at a wavelength of 340 nm. In order to determine total adenylate content of a sample, ADP was initially converted to ATP in the presence of phosphoenolpyruvate and PK. For a single sample, the analysis of adenylate content was performed in duplicate and via a two-step procedure. Sample preparations were divided into two equal volumes for the analysis of total adenylates and ATP only. As mentioned already in the previous paragraph, the first step was implemented to enable the conversion of ADP to ATP via the use of PK and hence determine total adenylate content of a sample. The duplicate samples, used to determine ATP concentrations only, were assayed with buffer instead of PK. In the second step of the method, all the ATP present in the sample is converted to ADP in order to allow for the downstream monitoring of NADPH formation. Since PK was initially used in the total adenylates reaction to convert ADP to ATP, it is essential that the enzyme be destroyed before initiating the second step of the method and hence recycling of ATP. This would result in a cycling of adenylates and elevated concentrations. To destroy PK activity and prevent adenylate cycling, a 10 min incubation period at 60°C in the presence of NaOH was implemented. Optimisation of the assay was performed with known concentrations of adenylates, as illustrated in Figure 5.5.

Figure 5.5 Spectrophotometric data generated by assaying concentrations of adenylates



The absorbency pattern corresponding to four adenylate concentration assays is presented. The sharp decrease in absorbency at 2 min is due to the removal of cuvettes from the spectrophotometer to initiate reactions via the addition of hexokinase. nm = nanometre wavelength, µM = micromolar concentration.

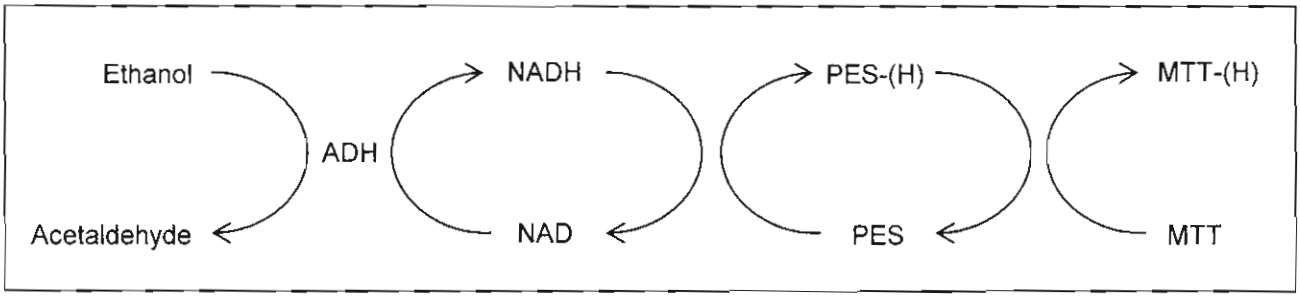
The graphic representation in Figure 5.5 indicates the change in absorbency for five concentrations of adenylates over a period of 15 min. The first reaction contained no ATP and hence presented with no change in absorbency after the reaction was initiated with hexokinase. The second reaction contained 100 μM ATP that resulted in an immediate increase in the formation of NADPH, and consequently a positive increase in the curve slope. The reaction was completed after approximately 10 minutes, where the graph is presented to plateau. At this point, all of the ATP in the reaction, i.e. 100 μM, had been converted to ADP. The third cuvette contained 500 μM ATP and resulted in a rapid increase in the reaction rate as soon as hexokinase was introduced, followed by a marked decrease in NADPH formation. Although not presented, the absorbency was observed to plateau completely and remain unchanged after a period of approximately 120 min. At this point, 500 μM of ATP had been converted to ADP and the reactions completed. Similarly, the cuvette containing 500 μM ADP, which was initially treated with PK, increased and stabilised at an absorbency equivalent to that of the 500 μM ATP sample. It should be noticed that the fifth and final reaction that contained 500 μM ADP, which was not treated with PK, presented with absorbencies that remained unaltered after the addition of hexokinase. This illustrated that PK was indeed effective in the conversion of ATP to ADP. Furthermore, the fact that similar reaction rates and final absorbencies for the 500 μM ATP and 500 μM ADP samples were observed, illustrates that no PK activity was present in the second step of the method, precluding the cycling of adenylates.

As can be observed in Figure 5.5, the adenylate absorbency data resembled that generated for the determination of lactate concentrations, presented in Section 5.1.9. Similar to the standard series used for lactate assays, the varied concentrations of ATP too presented with positive reaction rates and final absorbencies that increased as the concentrations of ATP increased. Therefore, endpoint analysis methods were also utilised to calculate adenylate concentrations. A linear standard curve was established by calculating the difference between A_1 and A_2 absorbencies of the various adenylate concentrations. The linearity was further confirmed by r^2 values that consistently illustrated that the change in absorbency was almost completely correlated to ATP concentrations. Finally, the concentrations of sample adenylates were calculated utilising the linear standard curve data.

5.1.12 Assay for pyridine concentrations

The principle behind the protocol described to evaluate the levels of NADH and NAD (Zerez *et al.*, 1987) is based on a cycling reaction, as illustrated in Figure 5.6. The enzyme ADH functions in the reaction to reduce the endogenous NAD to NADH. The reduced pyridine is subsequently oxidised by PES, which is in turn re-oxidised by MTT. The reaction mixture undergoes a colour change that can be monitored spectrophotometrically at a wavelength of 570 nm. Sample preparations were split into two and assayed for total pyridine concentrations and NADH only. Oxidised nicotinamide adenine dinucleotide was thermally destroyed in the latter sample assay to enable determination of NADH only.

Figure 5.6 Diagrammatic representation of the NAD/NADH assay



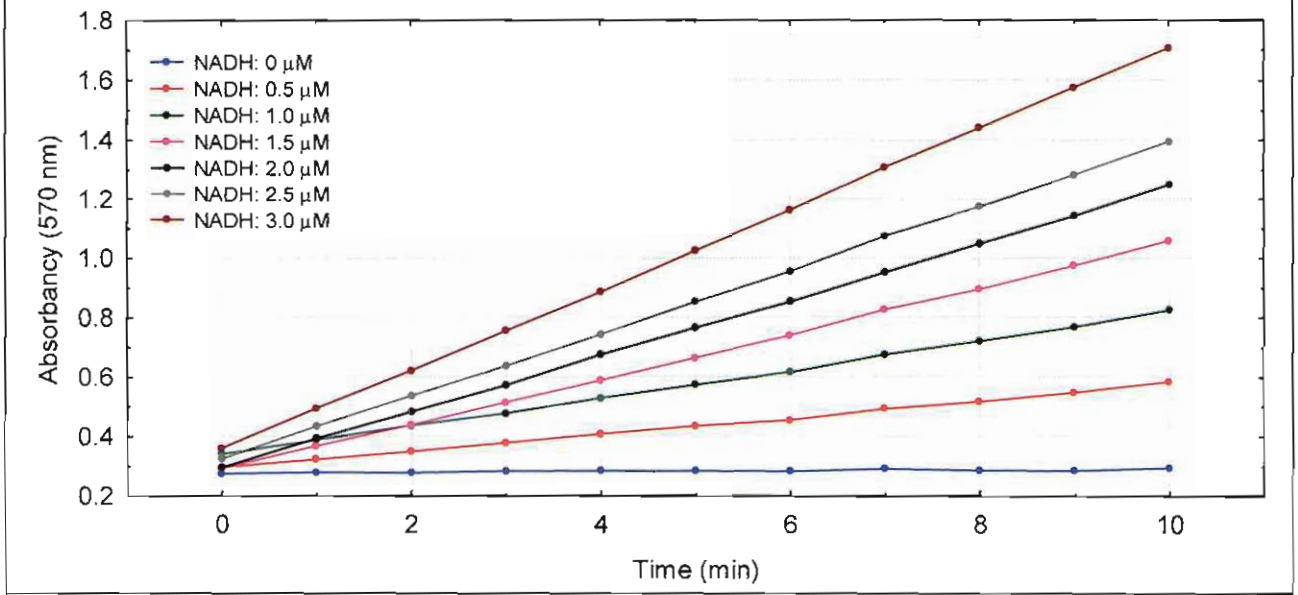
ADH = alcohol dehydrogenase, NADH = reduced nicotinamide adenine dinucleotide, NAD = oxidised nicotinamide adenine dinucleotide, PES = phenazine ethosulphate, PES-(H) = reduced phenazine ethosulphate, MTT = thiazolyl blue tetrazolium bromide, MTT (H) = reduced thiazolyl blue tetrazolium bromide.

Pyridine sample preparations were assayed in conjunction with a standard series of NADH concentrations. The reaction rates for each concentration of NADH were collectively utilised to generate a standard curve, a process identical to that of the glutathione assays presented in Section 5.1.10. The typical reaction rates for various concentrations of NADH are presented in Table 5.8.

As can be observed from the graphic representation, reaction rates for the NADH standard series correlated with the increase in NADH concentrations. Furthermore, a consistent linear increase for each of the curves was attained. This is confirmed by the r^2 values that are all very near to 1.0. The blank sample, i.e. 0 μM concentration, presented with an r^2 value of 0.730, which is irrelevant since there was no increase in absorbency over the 10 min period.

Table 5.8 Spectrophotometric data generated by assaying varied concentrations of nicotinamide adenine dinucleotide

A: Graphic representation of the change in absorbency data



B: NADH standard curve data

NADH concentration (µM)	0	0.5	1.0	1.5	2.0	2.5	3.0
Reaction rate	0.002	0.027	0.049	0.073	0.093	0.106	0.131
r^2	0.730	0.998	0.999	0.999	0.999	0.999	0.999
Standard curve slope	0.021						
Standard curve r^2	0.994						

A: The increase in absorbency at varied concentrations of NADH is presented, along with reaction rates and r^2 values. B: Data determined from the reaction rates and standard calculations are listed. NADH = reduced nicotinamide adenine dinucleotide, nm = nanometre wavelength, µM = micromolar concentration, r^2 = square of the Pearson product moment correlation coefficient, signifying curve linearity.

As mentioned previously in this section, a linear standard curve was generated from the series of NADH reaction rates and the pyridine concentration of samples determined via the use of the linear equation. The process was identical to that utilised in the determination of glutathione concentrations, as presented in Section 5.1.10. As indicated in Table 5.8.B, the slope and r^2 value of the corresponding linear standard curve were calculated to be 0.021 and 0.994 respectively. The calculated NADH concentration was subtracted from the total pyridine amount in order to determine NAD levels. Finally, protein concentrations of the sample preparations were determined and NAD/NADH ratios calculated accordingly.

5.2 RAT BODY WEIGHTS

Body weights of rats were determined in both the rat pilot and main studies. Rats were weighed every day prior to dosing as well as on the days that they were sacrificed for tissue collection. The daily weight measurements were captured and analysed in Excel®

format, followed by statistical evaluation utilising the STATISTICA™ programme. The day-to-day weight recordings for both the rat pilot and main studies are listed in Appendix A for reference.

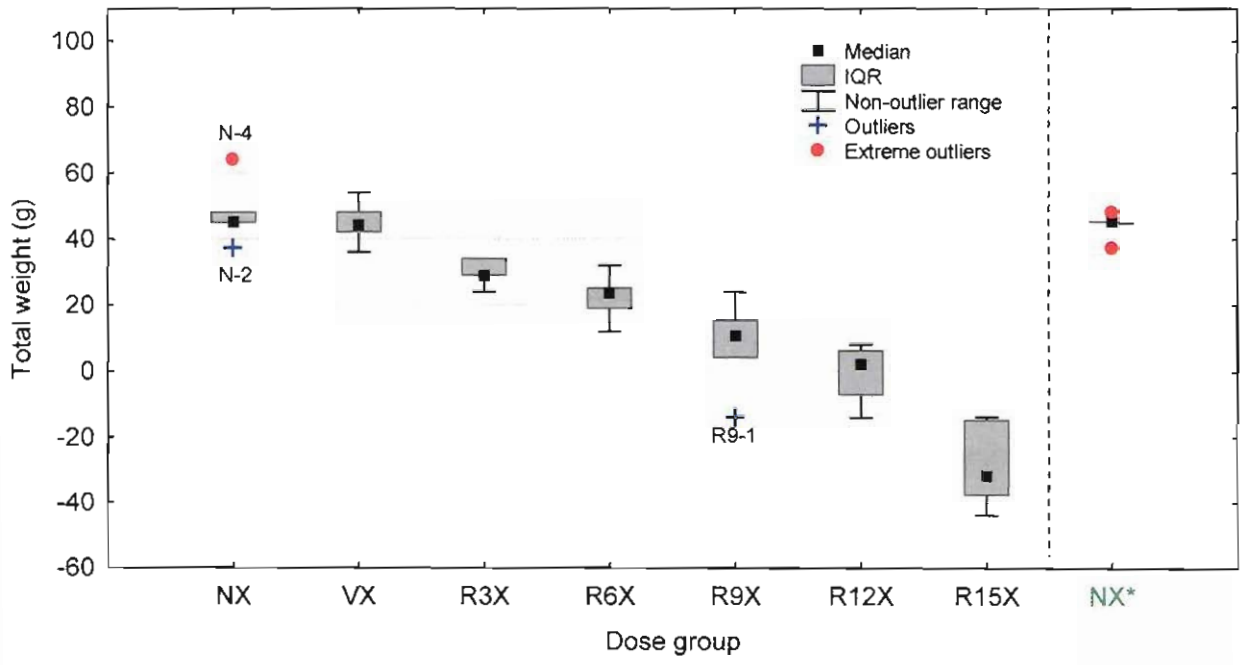
5.2.1 Rat pilot study body weights

Body weight data was collected during the rat pilot study and statistically evaluated in terms of total weight gains and losses over the complete 15-day period. This data is presented in Table 5.9 via the use of box-whisker representations and descriptive statistics. The graphic representation of rat weight data illustrates a decrease in the gain of body weight as the concentrations of dosed rotenone increased. Only one extreme outlier was determined from the original data set, as indicated by the red dot (•) and corresponding rat number, namely N-4. The final box-whisker plot, for dose group N*, is a representation of the distribution of data points after the exclusion of the extreme outlier N-4 from the original data set N. The appearance of two additional extreme outliers in dose group N* is due to the narrowing of the IQR after the extreme outlier was excluded from 3 g to 0 g, as confirmed in Table 5.9.B. It is for this very reason that there is no 'box' in the box-whisker plot of dose group N*, which has been replaced by a horizontal line that represents the 0 g IQR. The exclusion of N-4 from the dose group results in the adjusted mean statistic of 44.0 g, from the original 47.3 g in dose group N. An adjustment of more than a half is also made to the SD, which decreased from 8.96 g to 4.12 g. These adjustments to the N dose group resulted in comparative descriptive statistics as those obtained for V, the dose group that received the sunflower oil vehicle for 14 days. This suggests that the rats did not gain additional weight when dosed with the vehicle.

In addition to N-4 being classified as an extreme outlier in the N dose group, N-2 is illustrated to be an outlier (+), as indicated in Table 5.9.A. Again, since the data points in this dose group are clustered into a narrow IQR, even in the presence of the extreme outlier, the N-2 data point falls outside the non-outlier range. Based on Figure 4.4 presented in Chapter Four, the upper non-outlier boundary for dose group N is positioned at 49.5 g, therefore qualifying the weight gain for N-2 as an outlier. The box-whisker representation also illustrates the presence of a second outlier in dose group R9, with a corresponding weight loss of 14 g. This value can be confirmed in the list of weight gain data points in Table 5.9.A and the minimum statistic in Table 5.9.B. However, as discussed in the statistical strategy in Section 4.5 of Chapter Four, only the extreme outliers in the original set of data per dose group were excluded for subsequent analyses.

Table 5.9 Box-whisker representation and descriptive statistics of the rat body weight data generated from the rat pilot study

A: Box-whisker plots and data points according to rat groups



Rat	N	V	R3	R6	R9	R12	R15	N*
1	45	36	29	12	+ -14	-7	-15	45
2	+ 37	42	29	25	10	0	-32	37
3	48	54	34	23	4	8	-32	48
4	• 64	45	—	19	15	6	-44	EXCL
5	45	48	34	24	11	-14	-38	45
6	45	43	24	32	24	4	-14	45

B: Descriptive statistics

Dose group	Sample size	Mean	SD	Median	Min	Max	Range	Lower quartile	Upper quartile	IQR
N	6	47.3	8.96	45.0	37	64	27	45	48	3
N*	5	44.0	4.12	45.0	37	48	11	45	45	0
V	6	44.7	6.06	44.0	36	54	18	42	48	6
R3	5	30.0	4.18	29.0	24	34	10	29	34	5
R6	6	22.5	6.66	23.5	12	32	20	19	25	6
R9	6	8.33	12.8	10.5	-14	24	38	4	15	11
R12	6	-0.50	8.48	2.00	-14	8	22	-7	6	13
R15	6	-29.2	12.2	-32.0	-44	-14	30	-38	-15	23

Rat codes for outliers and extreme outliers are located above or below the respective blue crosses (+) and red dots (•), which correspond to data point values listed in the table directly below the graph. The vertical dashed line in the box-whisker graphic representation separates original dose group box-whiskers from those that have had the extreme outliers excluded, which are also indicated by the asterisk (*) following the dose group code. Data sets with excluded data points are designated in green text. Rats were treated with N = no dose, V = vehicle, R3 = rotenone 3 $mg.kg^{-1}.day^{-1}$, R6 = rotenone 6 $mg.kg^{-1}.day^{-1}$, R9 = rotenone 9 $mg.kg^{-1}.day^{-1}$, R12 = rotenone 12 $mg.kg^{-1}.day^{-1}$, R15 = rotenone 15 $mg.kg^{-1}.day^{-1}$. '—' = missing data point due to death of rat R3-4, EXCL = excluded data point, g = grams, IQR = inter-quartile range, Min = minimum data point value, Max = maximum data point value, SD = standard deviation.

The evident downward trend observed from the rat weight box-whisker plots strongly suggests that rotenone harmfully affected the rats. Moreover, it appears that as the dose concentration increased the severity of weight loss increased. At concentrations of 9, 12 and 15 $mg.kg^{-1}.day^{-1}$, certain rats started to present with lower final body weights than

what they had before dosing was even initiated. Lapointe *et al.* (2004) reported that rotenone-treated rats lost considerable amounts of weight and suffered severe damage to rat peripheral organs, in particular the stomach. Undigested food was demonstrated to compact in stomachs, which were in turn increased in size to double that of the vehicle-treated rats. Furthermore, pathological investigation of the stomach revealed severe loss in muscle mass as well as a diagnosis of achlorhydria, a condition preventing the production of gastric acid and hence digestion of food (Lapointe *et al.*, 2004). Although dietary intake and physiological evaluation of the stomach was not performed in this study, it was hypothesised that rotenone comparable effects occurred, resulting in compromised digestive patterns and supporting the pattern of weight loss.

It should also be noted that as the rotenone dose concentrations increased so did the distribution of data points, as can be inferred from the IQR statistics, listed in Table 5.9.B. The IQRs increased in a near proportional manner from 6.0 g to 23.0 g, as the rotenone concentrations increased from 6 $mg.kg^{-1}.day^{-1}$ to 15 $mg.kg^{-1}.day^{-1}$. The IQRs for dose groups V, R3 and R6 were constant at 6 g, 5 g and 6 g respectively. However, these increased to 11 g, 13 g and 23 g for dose groups R9, R12 and R15 respectively. In addition, with the exclusion of extreme outlier N-4 and ensuing IQR of 0 g, it would indicate that the dosage procedure itself contributed to the variation in body weight variation. However, as discussed in Section 5.1.3, oesophageal intubation was performed without resistance or complications in the dose groups receiving vehicle and low concentrations of rotenone. Therefore, even though the IQRs may reflect a difference, the variation in data is not congruent with the physical responses observed in the rats while dosing was performed. Nonetheless, the increased variation in rat weight data, in addition to the proportional increase in weight loss, confirms that a difference between the environmental control dose group N and experimental groups existed.

In order to evaluate the statistical significance of the differences in total weight gains and losses, the rat weight data was analysed via both parametric and non-parametric procedures. As specified by the statistical strategy in Section 4.5 of Chapter Four, the parametric tests were performed on the data upon exclusion of the extreme outlier N-4, while the non-parametric tests were used to analyse the original set of data. The ANOVA and multiple comparison procedure statistics, as well as the biological significance of statistically significant differences, are presented in Table 5.10.

Table 5.10 Multiple comparison statistics of body weight data generated from the rat pilot study

A: Non-parametric (original data set) and parametric (excluding extreme outliers) p-values

Dose group	N	V	R3	R6	R9	R12	R15
N		1.000	1.000	0.713	0.045	0.005	< 0.001
		1.000	0.171	0.007	< 0.001	< 0.001	< 0.001
V	1.000		1.000	1.000	0.084	0.010	< 0.001
	1.000		0.135	0.002	< 0.001	< 0.001	< 0.001
R3	1.000	1.000		1.000	1.000	0.746	0.044
	0.171	0.135		0.812	0.006	< 0.001	< 0.001
R6	0.713	1.000	1.000		1.000	1.000	0.208
	0.007	0.002	0.812		0.097	0.001	< 0.001
R9	0.045	0.084	1.000	1.000		1.000	1.000
	< 0.001	< 0.001	0.006	0.097		0.576	< 0.001
R12	0.005	0.010	0.746	1.000	1.000		1.000
	< 0.001	< 0.001	< 0.001	0.001	0.576		< 0.001
R15	< 0.001	< 0.001	0.044	0.208	1.000	1.000	
	< 0.001	< 0.001	< 0.001	< 0.001	< 0.001	< 0.001	

B: ANOVA p-values

Kruskal-Wallis p-value < 0.001	One-way ANOVA p-value < 0.001

C: Statistical and biological significance

Comparison		Statistical significance (p)		Biological significance (d)	
		Including EOs	Excluding EOs	Including EOs	Excluding EOs
N	R6	0.713	0.007	N/A	2.488
N	R9	0.045	< 0.001	3.049	4.128
N	R12	0.005	< 0.001	5.338	5.149
N	R15	< 0.001	< 0.001	6.265	8.467
V	R6	1.000	0.002	N/A	2.565
V	R9	0.084	< 0.001	N/A	4.205
V	R12	0.010	< 0.001	5.327	5.227
V	R15	< 0.001	< 0.001	6.048	8.545
R3	R9	1.000	0.006	N/A	2.508
R3	R12	0.746	< 0.001	N/A	3.529
R3	R15	0.044	< 0.001	4.846	6.847
R6	R12	1.000	0.001	N/A	2.662
R6	R15	0.208	< 0.001	N/A	5.979
R9	R15	1.000	< 0.001	N/A	4.339
R12	R15	1.000	< 0.001	N/A	3.318

A: All comparison statistics are indicated as p-values. The upper p-value is the non-parametric multiple comparison test statistic, generated from the original set of data. The lower p-value was generated via the parametric Tukey *unequal number HSD* (Honestly Significant Difference) test, after the exclusion of extreme outliers. P-values indicated in red are statistically significant at the pre-determined significance level of 0.05. P-values in black text represent those that are not statistically significant, but have complementary p-values that are statistically significant. The remainder of p-values are listed in grey. The comparisons surrounded by the **bold** black line are those that were determined to be statistically significant by both the non-parametric and parametric multiple comparison procedures. The turquoise shaded blocks represent statistically significant comparisons that were also determined to be of biological significance. B: P-values for the non-parametric Kruskal-Wallis ANOVA and parametric one-way ANOVA are listed, with significant p-values, less than the 0.05 significance level, indicated in red. C: List of comparisons determined to be statistically significant with corresponding biological significance. A d-value greater than or equal to 0.8 signifies biological significance, indicated in red. Rats were treated N = no dose, V = vehicle, R3 = rotenone 3 $mg.kg^{-1}.day^{-1}$, R6 = rotenone 6 $mg.kg^{-1}.day^{-1}$, R9 = rotenone 9 $mg.kg^{-1}.day^{-1}$, R12 = rotenone 12 $mg.kg^{-1}.day^{-1}$, R15 = rotenone 15 $mg.kg^{-1}.day^{-1}$. < = less than, ANOVA = analysis of variance, EOs = extreme outliers, N/A = not applicable.

The multiple comparison grid in Table 5.10.A reveals six comparisons that were determined to be statistically significant by both the non-parametric multiple comparison procedure and parametric Tukey *unequal number HSD*, as indicated by the bold lining. Furthermore, all six comparisons were determined to differ with biological significance,

indicated by the turquoise shading. The calculated d-values for biological significance are listed in Table 5.10.B. Three of these significant differences in rat weights include dose group N, when compared to R9, R12 and R15. According to the mean weight gains and losses, presented in Table 5.9.B, the rats in N* gained on average 44.0 g and 47.3 g if the extreme outlier was not excluded, while rats in R9 gained 8.3 g. The mean differences between the groups were also determined to be biologically significant with d-values of 3.049 and 4.128 for comparisons including and excluding extreme outliers, respectively. It should be noted that the biological significance increased when the extreme outlier was excluded from the N data set. Since the test for biological significance relies predominantly on the SD of two data sets in relation to a mean data point, the exclusion of extreme outliers would have a definitive effect on the test result. As the variance and SD increases in a data set, the probability of confirming biological significance decreases. In other words, the nearer the data points are clustered within a data set, decreasing the variation and improving accuracy of the central tendency statistics, the better the chance that the comparison will yield biological significance when there truly is a difference. Since the data is well clustered according to the various dose groups, it is therefore not unexpected that the weight gains and losses for dose groups R12 and R15 also differed biologically significantly from dose group N.

When rat weights of dose groups R12 and R15 were compared to those of V, statistically significant differences were reported by both the parametric and non-parametric multiple comparison procedures, as presented in Table 5.10. Furthermore, these differences were determined to be of biological significance. Rat weights of dose groups V and R9 were determined to differ statistically significantly only upon the exclusion of extreme outlier N-4. The difference was also determined to differ on a biological level, as indicated in Table 5.10.B, with a d-value of 4.205. This result is not unexpected since it was illustrated in Table 5.9.B that the central tendency statistics for dose groups V and N* were very similar to each other. Since dose group N differed significantly from R9, regardless if the extreme outlier was excluded or not, it is understandable that the aforementioned dose group differed significantly from N*. The comparison of rat weights between dose groups R3 and R15 was the final comparison that was determined to be of statistical significance, prior to and after the exclusion of the extreme outlier. Furthermore, the aforementioned dose groups also differed biologically significantly from each other. The mean weight gain for R3 was 30 g, whereas dose group R15 lost a mean weight of 29.2 g. It was therefore not unexpected that these groups differed significantly.

The parametric Tukey *unequal number HSD* test, which was performed on the data upon exclusion of the extreme outlier, resulted in the generation of 15 statistically significant p-values. Furthermore, all 15 comparisons were determined to differ with biological significance. Dose group R15 differed significantly from all the other groups in the study, even R12. The fact that there was a statistically significant difference between R12 and R15 suggests that even the 3 $mg.kg^{-1}.day^{-1}$ difference in rotenone concentration affected the rats significantly in terms of weight loss. However, this was not the case on all occasions, that is, R12 did not statistically differ significantly from R9, nor did R9 from R6 and so with R3 and V. It should be noted though that a statistically significant difference was indeed observed over the 6 $mg.kg^{-1}.day^{-1}$ dose ranges and higher. In other words, any comparison between dose groups that differed by 6 $mg.kg^{-1}.day^{-1}$ or more in dose concentration, for example R9 and R3, was demonstrated to present with body weight discrepancies that differed significantly.

Finally, it should be noted that the high percentage of statistically significant differences that were observed in the multiple comparison grid, namely 6 out of 21 (28.6%) for the non-parametric test and 15 out of 21 (71.4%) for the Tukey *unequal number HSD*, were confirmed by the highly significant p-values recorded when performing the ANOVAs. The Kruskal-Wallis and one-way ANOVA p-values listed in Table 5.10.B were both highly significant with p-values of < 0.001.

5.2.2 Rat main study body weights

The rat body weights were recorded daily as in the pilot study. The rat main study design, as presented in Figure 4.2 of Chapter Four, included 11 dose groups. Five dose groups received a 15 $mg.kg^{-1}.day^{-1}$ rotenone Factor-1 dose regimen for 14 days, followed by one of five Factor-2 treatment regimens, which included either sacrificing on day 15, or no dose, vehicle, CoQ_{10} or succinate for a period of two days. Therefore, the dose group codes were assigned as RX, RN, RV, RC and RS respectively. The dose groups that received two-day regimens, namely RN, RV, RC and RS, were consequently sacrificed for tissue collection on day 17. An additional five dose groups received the sunflower oil vehicle as a Factor-1 regimen for 14 days, followed by one of the five Factor-2 regimens discussed above. Similarly, dose groups were assigned the codes VX, VN, VV, VC and VS respectively. A final dose group, referred to as the environmental controls, received no dose for a period of 16 consecutive days and was sacrificed on day 17 for tissue collection. This group was assigned the dose code NN.

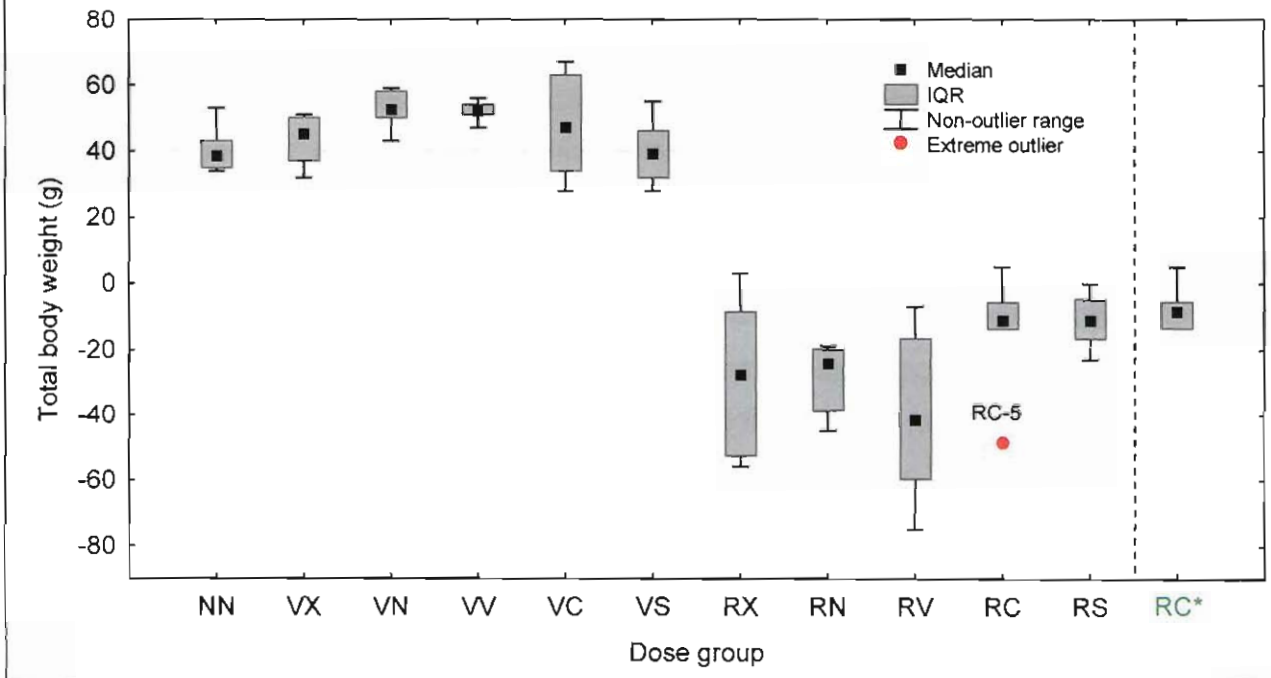
Body weight data generated from the rat main study was analysed in three separate data sets. The first was via a total weight gain or loss analysis, which was the difference in weight from day 1 to the final day of sacrificing, a period of either 15 or 17 days. As mentioned in the previous paragraph, the two dose groups VX and RX were dosed for a period of 14 days and sacrificed on day 15, as opposed to the other nine groups that were dosed for 16 days and sacrificed on day 17. However, dose groups VX and RX were still included in the overall rat weight statistical analyses as the sacrificing of these rats was regarded as a statistical 'treatment', and hence a Factor-2 regimen. These two groups were thus included to represent the rat status on day 15. The second form of statistical evaluation of the body weight data was performed via analysis of the weight gain or loss that took place from days 15 to 17, for it was of interest to evaluate if rat weights would respond more favourably over the last two days depending on the Factor-2 regimens they received. Finally, the weight gains and losses from days 1 to 15 were analysed comparatively to that of the rat pilot study in order to confirm consistency between the two study groups.

5.2.2.1 Rat main study total body weight gains and losses

The overall body weight recordings were analysed and total weight gains and losses evaluated. Box-whisker plots and descriptive statistics of the total weight changes are presented in Table 5.11. In addition, the day-to-day rat weight recordings are listed in Table A.2 in Appendix A. As expected, the total weight gain and loss differences between the rotenone and vehicle dosed rats are large. Data presented in Section 5.2.1 illustrated that a drastic loss in weight can be observed in the rats that received high dose concentrations of rotenone, whereas a consistent weight gain can be observed in the rats that received vehicle or no dose. As indicated in Table 5.11.A, a single extreme outlier in dose group RC was present in the entire total body weight gains and losses data set. The exclusion of RC-5 resulted in an increase in the mean body weight for dose group RC from -14.5 g to -7.60 g, as listed in Table 5.11.B. The SD decreased from 18.3 g to 7.83 g. The range statistic strongly supports the exclusion of RC-5 as an extreme outlier showing a considerable decrease from 54 g to 19 g. The non-parametric descriptive statistics were once again found to be more robust to the presence and exclusion of extreme outliers. The median weight for dose group RC decreased minimally from -11.5 g to -9.00 g, while the lower and upper quartile values as well as the IQR remained unchanged.

Table 5.11 Box-whisker representation and descriptive statistics of the total rat weight data generated from the main study

A: Box-whisker plots and data points according to rat groups



Rat	NN	VX	VN	VV	VC	VS	RX	RN	RV	RC	RS	RC*
1	53	49	54	51	67	28	-9	-28	-50	-9	-10	-9
2	36	37	43	54	28	46	-38	-21	-7	5	-23	5
3	43	32	58	56	49	42	3	-19	-17	-14	-5	-14
4	34	51	51	52	34	32	-56	-39	-60	-14	0	-14
5	41	50	50	52	45	55	-53	-20	-75	• -49	-13	EXCL
6	35	41	59	47	63	36	-18	-45	-34	-6	-17	-6

B: Descriptive statistics

Dose group	Sample size	Mean	SD	Median	Min	Max	Range	Lower quartile	Upper quartile	IQR
NN	6	40.3	7.15	38.5	34	53	19	35	43	8
VX	6	43.3	7.87	45.0	32	51	19	37	50	13
VN	6	52.5	5.89	52.5	43	59	16	50	58	8
VV	6	52.0	3.03	52.0	47	56	9	51	54	3
VC	6	47.7	15.4	47.0	28	67	39	34	63	29
VS	6	39.8	9.89	39.0	28	55	27	32	46	14
RX	6	-28.5	24.2	-28.0	-56	3	59	-53	-9	44
RN	6	-28.7	11.0	-24.5	-45	-19	26	-39	-20	19
RV	6	-40.5	26.0	-42.0	-75	-7	68	-60	-17	43
RC	6	-14.5	18.3	-11.5	-49	5	54	-14	-6	8
RC*	5	-7.60	7.83	-9.00	-14	5	19	-14	-6	8
RS	6	-11.3	8.26	-11.5	-23	0	23	-17	-5	12

Rat codes for the extreme outliers are located above or below the red dots (•), which correspond to data point values listed in the table directly below the graph. The vertical dashed line in the box-whisker graphic representation separates original dose group box-whiskers from those that have had the extreme outliers excluded, which are also indicated by the asterisk (*) following the dose group code. Data sets with excluded data points are designated in green text. Rats were treated with NN = no dose regimen, VX = vehicle and sacrificed, VN = vehicle and no dose, VV = vehicle and vehicle, VC = vehicle and CoQ_{10}, VS = vehicle and succinate, RX = rotenone and sacrificed, RN = rotenone and no dose, RV = rotenone and vehicle, RC = rotenone and CoQ_{10}, RS = rotenone and succinate. EXCL = excluded data point, g = grams, IQR = inter-quartile range, Min = minimum data point value, Max = maximum data point value, SD = standard deviation.

The fact that rats RC-3 and RC-4 both lost 14 g over the 17-day period, as presented in Table 5.11.A, meant that the extreme outlier RC-5, which suffered a total weight loss of 49 g, lost 35 g more than its closest ranked data points. However, it should be noted that although there were rats in dose groups RX and RV that lost more weight than RC-5, they were not regarded as extreme outliers in their respective dose groups due to the wider distribution of data points in the RX and RV data sets. This may be the first indication that the CoQ_{10} response, observed in five of the six rats in the RC group, was indeed beneficial and made a difference to weight gain over the last two days that the rats were dosed with the CoQ_{10} Factor-2 regimen. The significance of this difference as well as other differences between dose groups are discussed further below, in conjunction with the multiple comparison data. P-values generated from parametric and non-parametric multiple comparison procedures are presented in Table 5.12, along with corresponding biologically significant d-values.

As observed from the pilot study, it is clear that a marked difference in the rat weights between the rotenone-treated rats and those that received a vehicle Factor-1 regimen exists. This is evident when referring to the box-whisker plots and descriptive statistics in Table 5.11. However, not all differences observed were of statistical significance. When the non-parametric multiple comparison test was performed on the original set of data, thus without the exclusion of the extreme outlier RC-5, not all the dose groups that received vehicle Factor-1 regimens were shown to differ statistically significantly from the groups that were dosed a rotenone Factor-1 regimen. However, this was the case when RC-5 was excluded, which is clearly indicated in the multiple comparison grid of Table 5.12. The exclusion of RC-5 from the data set resulted in all 30 of the comparisons between rotenone-treated and vehicle Factor-1 dose groups being statistically significant when analysed via the Tukey *unequal number HSD* multiple comparison test. In contrast, only eight of the 30 comparisons were determined to differ significantly when the non-parametric multiple comparison test was used. The p-values surrounded by the bold lines in Table 5.12.B indicates these eight comparisons, which of course also indicates those which were determined to be statistically significant by both the parametric and non-parametric multiple comparison tests.

Table 5.12 Multiple comparison statistics of total body weight data generated from the rat main study

A: Non-parametric (original data set) and parametric (excluding extreme outliers) p-values

Dose group	NN	VX	VN	VV	VC	VS	RX	RN	RV	RC	RS
NN		1.000	1.000	1.000	1.000	1.000	0.569	0.271	0.190	1.000	1.000
		1.000	0.895	0.918	0.997	1.000	< 0.001	< 0.001	< 0.001	< 0.001	< 0.001
VX	1.000		1.000	1.000	1.000	1.000	0.290	0.131	0.090	1.000	1.000
	1.000		0.983	0.989	1.000	1.000	< 0.001	< 0.001	< 0.001	< 0.001	< 0.001
VN	1.000	1.000		1.000	1.000	1.000	0.008	0.003	0.002	0.079	0.092
	0.895	0.983		1.000	1.000	0.869	< 0.001	< 0.001	< 0.001	< 0.001	< 0.001
VV	1.000	1.000	1.000		1.000	1.000	0.008	0.003	0.002	0.079	0.092
	0.918	0.989	1.000		1.000	0.895	< 0.001	< 0.001	< 0.001	< 0.001	< 0.001
VC	1.000	1.000	1.000	1.000		1.000	0.092	0.038	0.025	0.607	0.690
	0.997	1.000	1.000	1.000		0.995	< 0.001	< 0.001	< 0.001	< 0.001	< 0.001
VS	1.000	1.000	1.000	1.000	1.000		0.582	0.277	0.194	1.000	1.000
	1.000	1.000	0.869	0.895	0.995		< 0.001	< 0.001	< 0.001	< 0.001	< 0.001
RX	0.569	0.290	0.008	0.008	0.092	0.582		1.000	1.000	1.000	1.000
	< 0.001	< 0.001	< 0.001	< 0.001	< 0.001	< 0.001		1.000	0.903	0.366	0.522
RN	0.271	0.131	0.003	0.003	0.038	0.277	1.000		1.000	1.000	1.000
	< 0.001	< 0.001	< 0.001	< 0.001	< 0.001	< 0.001	1.000		0.910	0.355	0.508
RV	0.190	0.090	0.002	0.002	0.025	0.194	1.000	1.000		1.000	1.000
	< 0.001	< 0.001	< 0.001	< 0.001	< 0.001	< 0.001	0.903	0.910		0.014	0.019
RC	1.000	1.000	0.079	0.079	0.607	1.000	1.000	1.000	1.000		1.000
	< 0.001	< 0.001	< 0.001	< 0.001	< 0.001	< 0.001	0.366	0.355	0.014		1.000
RS	1.000	1.000	0.092	0.092	0.690	1.000	1.000	1.000	1.000	1.000	
	< 0.001	< 0.001	< 0.001	< 0.001	< 0.001	< 0.001	0.522	0.508	0.019	1.000	

B: ANOVA p-values

Kruskal-Wallis p-value < 0.001	One-way ANOVA p-value < 0.001

C: Statistical and biological significance

Comparison		Statistical significance (p)		Biological significance (d)	
		Including EOs	Excluding EOs	Including EOs	Excluding EOs
NN	RX	0.569	< 0.001	N/A	5.066
NN	RN	0.271	< 0.001	N/A	5.081
NN	RV	0.190	< 0.001	N/A	5.950
NN	RC	1.000	< 0.001	N/A	3.527
NN	RS	1.000	< 0.001	N/A	3.800
VX	RX	0.290	< 0.001	N/A	5.287
VX	RN	0.131	< 0.001	N/A	5.302
VX	RV	0.090	< 0.001	N/A	6.171
VX	RC	1.000	< 0.001	N/A	3.748
VX	RS	1.000	< 0.001	N/A	4.020
VN	RX	0.008	< 0.001	3.347	5.964
VN	RN	0.003	< 0.001	7.382	5.979
VN	RV	0.002	< 0.001	3.577	6.848
VN	RC	0.079	< 0.001	N/A	4.425
VN	RS	0.092	< 0.001	N/A	4.698
VV	RX	0.008	< 0.001	3.326	5.928
VV	RN	0.003	< 0.001	7.336	5.942
VV	RV	0.002	< 0.001	3.558	6.811
VV	RC	0.079	< 0.001	N/A	4.389
VV	RS	0.092	< 0.001	N/A	4.661
VC	RX	0.092	< 0.001	N/A	5.611
VC	RN	0.038	< 0.001	4.961	5.626
VC	RC	0.607	< 0.001	N/A	4.072
VC	RS	0.690	< 0.001	N/A	4.344

Table 5.12 Continued...

Comparison		Statistical significance (p)		Biological significance (d)	
		Including EOs	Excluding EOs	Including EOs	Excluding EOs
VS	RX	0.582	< 0.001	N/A	5.029
VS	RN	0.277	< 0.001	N/A	5.044
VS	RV	0.194	< 0.001	N/A	5.913
VS	RC	1.000	< 0.001	N/A	3.490
VS	RS	1.000	< 0.001	N/A	3.763
RV	RC	1.000	0.014	N/A	2.423
RV	RS	1.000	0.019	N/A	2.150

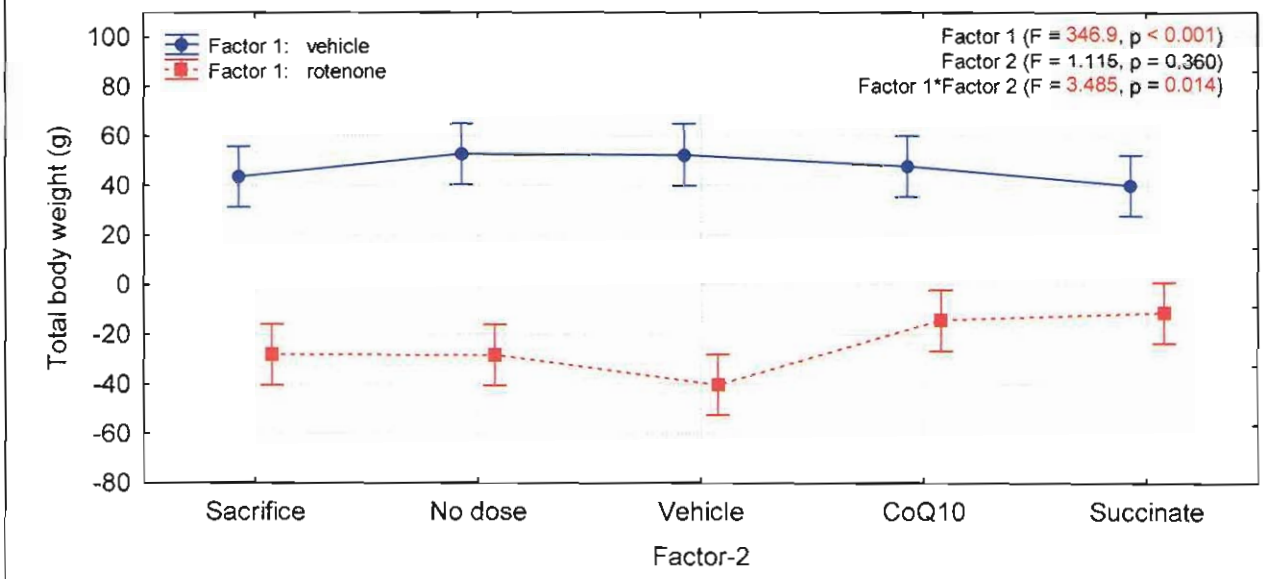
A: All comparison statistics are indicated as p-values. The upper p-value is the non-parametric multiple comparison test statistic, generated from the original set of data. The lower p-value was generated via the parametric Tukey *unequal number HSD* (Honestly Significant Difference) test, after the exclusion of extreme outliers. P-values indicated in red are statistically significant at the pre-determined significance level of 0.05. P-values in black text represent those that are not statistically significant, but have complementary p-values that are statistically significant. The remainder of p-values are listed in grey. The comparisons surrounded by the **bold** black line are those that were determined to be statistically significant by both the non-parametric and parametric multiple comparison procedures. The turquoise shaded blocks represent statistically significant comparisons that were also determined to be of biological significance. B: P-values for the non-parametric Kruskal-Wallis ANOVA and parametric one-way ANOVA are listed, with significant p-values, less than the 0.05 significance level, indicated in red. C: List of comparisons determined to be statistically significant with corresponding biological significance. A d-value greater than or equal to 0.8 signifies biological significance, indicated in red. Rats were treated with NN = no dose regimen, VX = vehicle and sacrificed, VN = vehicle and no dose, VV = vehicle and vehicle, VC = vehicle and CoQ_{10}, VS = vehicle and succinate, RX = rotenone and sacrificed, RN = rotenone and no dose, RV = rotenone and vehicle, RC = rotenone and CoQ_{10}, RS = rotenone and succinate. < = less than, ANOVA = analysis of variance, EOs = extreme outliers, N/A = not applicable.

The fact that 22 comparisons, which were expected to differ significantly, were only statistically significant after the extreme outlier was excluded strengthens the argument that the test for extreme outliers should indeed be performed and presented in parallel with the analysis results generated from the complete original data set. The paralleled presentation of results enables the reader to evaluate the data sets from their critical point of view. In this scenario, it is argued that the presence of the extreme outlier RC-5 may have masked statistically significant differences.

For rat weights, this is certainly a founded argument since a marked physical difference was observed between the rotenone-treated rats and those that received vehicle. Furthermore, the fact that the data analysed in this section encompasses the weight gains incurred on days 15 and 16, when rats were relieved from rotenone regimens, does raise concern as to the direct comparison of 'total' weight differences from days 1 to 17. It is for this reason that the factorial analysis of dose groups was performed for all data sets. Total rat weight gains and losses was analysed via a two-way ANOVA and results presented in Table 5.13.

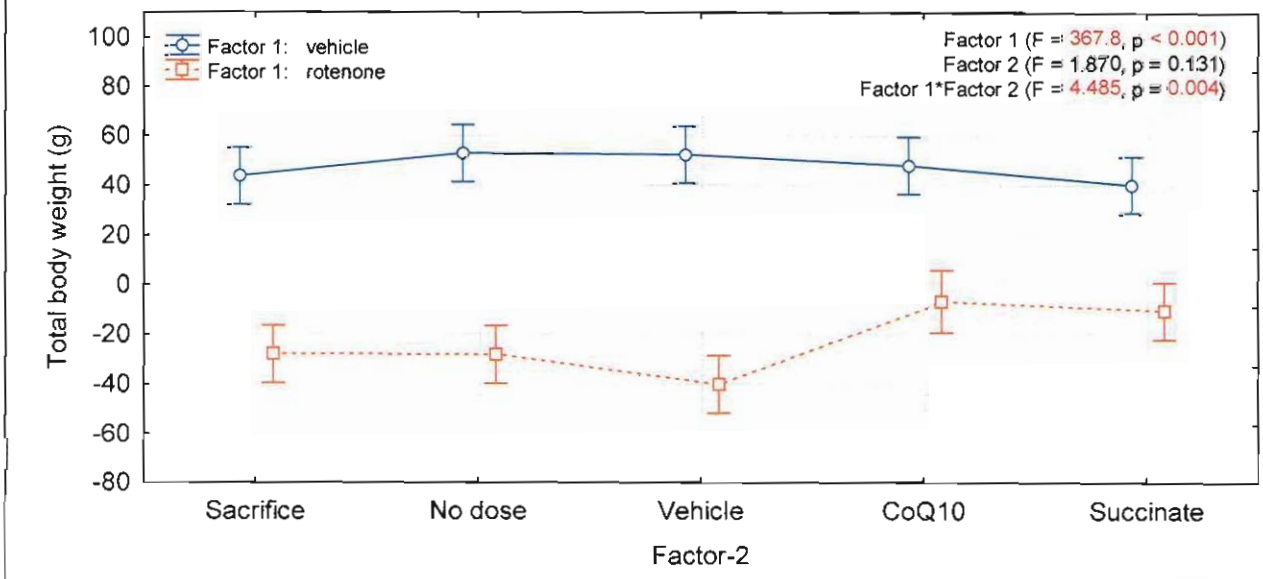
Table 5.13 Graphic and tabulated summary of the rat main study total body weight data analysed via a two-way ANOVA

A: Data set including extreme outliers



Description		VX	VN	VV	VC	VS	RX	RN	RV	RC	RS
With extreme outliers	UCI	55.6	64.7	64.2	59.9	52.1	-16.3	-16.4	-28.3	-2.26	0.90
	mean	43.3	52.5	52.0	47.7	39.8	-28.5	-28.7	-40.5	-14.5	-11.3
	LCI	31.1	40.3	39.8	35.4	27.6	-40.7	-40.9	-52.7	-26.7	-23.6

B: Data set excluding extreme outliers



Description		VX	VN	VV	VC	VS	RX	RN	RV	RC	RS
Without extreme outliers	UCI	54.9	64.1	63.6	59.2	51.4	-17.0	-17.1	-29.0	5.05	0.21
	mean	43.3	52.5	52.0	47.7	39.8	-28.5	-28.7	-40.5	-7.60	-11.3
	LCI	31.8	41.0	40.5	36.1	28.3	-40.1	-40.2	-52.1	-20.3	-22.9

The plot legends for each graph are indicated in the top left corners of the respective graphs, while the two-way ANOVA F-statistics (F) and p-values (p) for Factor-1, Factor-2 and Factor-1*Factor-2 are located in the top right corner, with the statistically significant values indicated in red. The vertical whiskers at each mean data point represent 95% confidence intervals for the respective data sets. The mean values in green text, located in the data point summary tables below the graphs, indicate those that were adjusted due to the exclusion of extreme outliers. < = less than, g = grams, LCI = lower 95% confidence interval data point, UCI = upper 95% confidence interval data point. Rats were treated with NN = no dose regimen, VX = vehicle and sacrificed, VN = vehicle and no dose, VV = vehicle and vehicle, VC = vehicle and CoQ_{10}, VS = vehicle and succinate, RX = rotenone and sacrificed, RN = rotenone and no dose, RV = rotenone and vehicle, RC = rotenone and CoQ_{10}, RS = rotenone and succinate.

Two additional comparisons were also shown to differ significantly by the Tukey *unequal number* HSD test. These were between RV and RC, as well as between RV and RS. Both RC and RS are groups that received therapeutic interventions in the presence of the rotenone-induced Complex I deficiency, whereas RV received only the vehicle for the last two days. Since the mean body weights for both RC and RS were higher than for RV, it may well be argued that CoQ_{10} and succinate contributed more than the vehicle alone to weight gain and recovery over the last two days. The body weight means for RC and RS were also higher than RX and RN. Since the RX group did not have a final two-day recovery period from rotenone, as RN, RC and RS had, it is understandable that a lowered mean body weight was recorded. As was the case with RV, it appears that the CoQ_{10} and succinate compounds made the difference when compared to RN, which received no dose for the last two days. It should also be noted that all 32 comparisons that were determined to differ statistically significantly were also determined to differ with biological significance. The d-values for biological significance are listed in Table 5.12.C, indicating that all values exceeded the 0.8 d-value threshold, with the lowest being 2.150.

According to the statistical strategy discussed in Section 4.5 of Chapter Four, the factor analysis was also performed via the inclusion and exclusion of extreme outliers. Two-way ANOVA results obtained from the raw data set, including the extreme outlier RC-5, are presented in Table 5.13.A, while the results generated via the exclusion of RC-5 are presented in Table 5.13.B. Data is summarised in the form of a graphic representation and the value of each data point on the graph indicated in a table directly below the graph. The factor analysis F-statistics and p-values are indicated in the top right corner of each graph.

The effect of excluding the extreme outlier from the data can be visualised by referring to the 95% confidence intervals, represented as vertical whiskers, at each of the mean data points indicated in Table 5.13. The upper and lower confidence interval data values (UCI and LCI) can also be referred to directly below the two-way ANOVA plots. In Table 5.13.A, prior to the exclusion of the extreme outlier, the 95% confidence interval for the data set extended 24.5 g above and below the mean data points. However, upon the exclusion of RC-5, the 95% confidence interval decreased to 23.1 g. These intervals can be calculated by subtracting the LCI values from that of the UCI values listed in Table 5.13. Therefore, the exclusion of just one extreme outlier data point from the whole data set resulted in an overall decrease in 95% confidence interval ranges of approximately 1.4 g.

The two-way ANOVA F-statistics and p-values presented in Table 5.13 indicated that an interaction effect was indeed present, whether the extreme outlier of RC-5 was excluded or not. However, the Factor-1 plots do not appear to diverge to a large extent. In this scenario, the highly significant main effect of Factor-1 is argued to induce the interaction effect. The F-statistics for Factor-1 are both in excess of 300, whether the extreme outlier is excluded from the data set or not. The differences in the effects of vehicle and rotenone over the first 14 days of dosing were highly statistically significant, with p-values well below the pre-determined 0.05 significance level. This is confirmed by the large differences in the F-statistics between Factor-1 and Factor-2. The Factor-2 F-statistics were a mere 1.115 and 1.870 for the data set including and excluding the extreme outlier respectively. Therefore, Factor-1 undoubtedly contributed by far the most with its main effect 'spilling over' and affecting the Factor-1*Factor-2 statistics. This statement is supported by the behaviour patterns observed in rats, which evidently illustrated that rotenone harmfully affected weight gain from the first day that it was dosed. The fact that rats lost such a significant amount of weight while receiving rotenone, as confirmed in Section 5.2.1 of the pilot study, certainly contributed to the way they responded upon receiving the Factor-2 dose regimens. There was no doubt that the inhibitor was the primary dose factor that resulted in the total weight gains and losses in the data set.

With the exclusion of dose group RX that was sacrificed on day 15, the rotenone-treated rats lost weight continuously for 15 days followed by a gain upon receiving their Factor-2 treatments. The graphic representations in Table 5.13 revealed that CoQ_{10} and succinate might have contributed to improved weight gains in rats harbouring the rotenone-induced Complex I deficiency. However, as mentioned previously in this section, the overwhelming impact of rotenone on the total rat body weight cannot be ignored. It could certainly be argued that simply the relief from rotenone might have contributed to the improved gain in weight. Nonetheless, the data is suggestive of improved response to both CoQ_{10} and succinate in the presence of an induced Complex I deficiency, where this was not observed to be the case when rats received no dose or vehicle Factor-2 regimens.

5.2.2.2 Rat main study body weights for days 15-17

A statistical evaluation of body weight gains and losses that were recorded for rats receiving Factor-2 dose regimens from days 15 to 17 are presented. It was of interest to determine whether the therapeutic compounds, CoQ_{10} and succinate, would improve body weight gains more so than the no dose and vehicle Factor-2 regimens. The weight gains

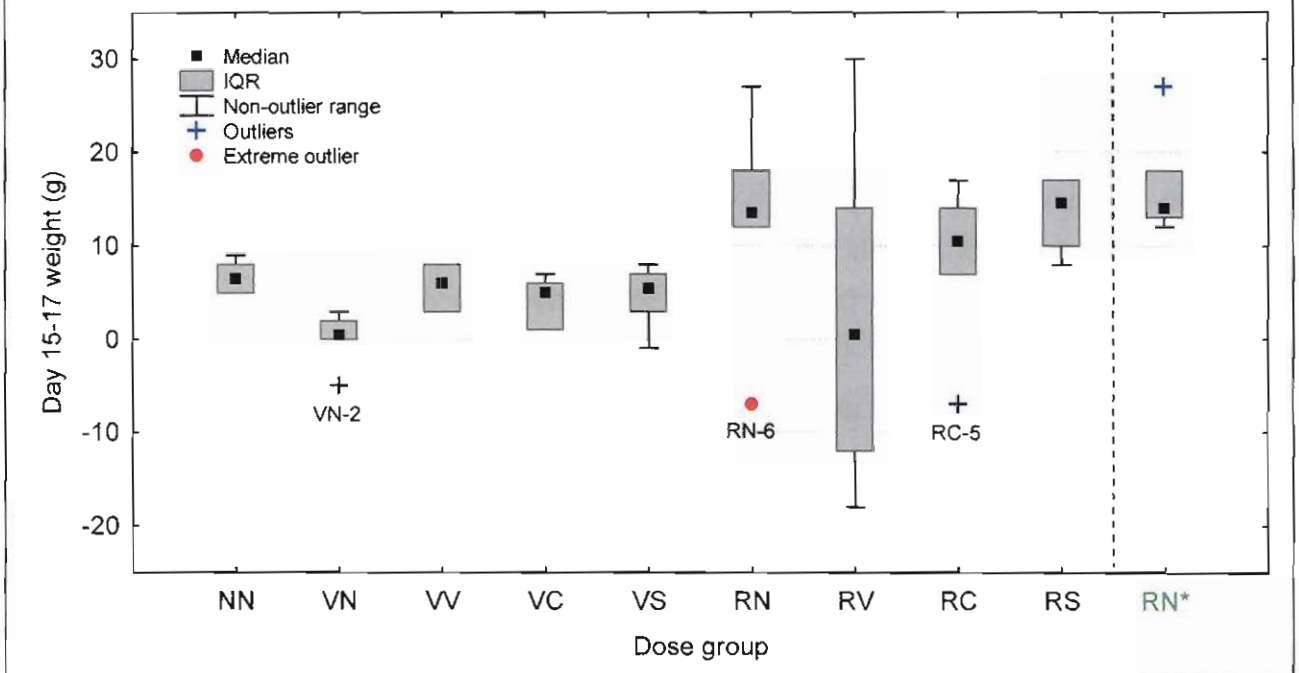
and losses from days 15 to 17 as well as descriptive statistics are presented in Table 5.14. Dose groups VX and RX are not presented since the rats in these groups were sacrificed on day 15, as illustrated by the flow chart in Figure 4.2.

The box-whisker representations in Table 5.14.A display a trend that indicates a greater weight gain over the last two days of dosing for the groups that received rotenone from days 1 to 14. Excluding dose group RV, all the rotenone-treated groups gained weight. In the RV group, three of the six rats continued to lose weight, even though the rotenone dosing had ended. The rats that received rotenone from days 1 to 14 continuously lost weight for the full period of 15 days, whereas those that received a vehicle Factor-1 regimen continuously gained weight for 15 days. This may suggest why the weight gain was greater in the groups that received rotenone as their first dose factor, since they were alleviated from rotenone and its direct effect on dietary intake. If the increased weight gains were due to therapeutic administration, then the gains encountered in the RC and RS groups would be greater than the RN and RV groups. In addition, it would be expected that VC and VS would present with higher weight gains than VN and VV. However, the two mentioned scenarios were not observed and consequently it would not be possible to conclude that CoQ_{10} and succinate contributed to increased weight gains.

Upon outlier analysis, only one extreme outlier was observed in the RN dose group. Rat RN-6 was the only rat to have lost weight from days 15 to 17 in this group. RN-6 lost 7 g, whereas the other five rats gained on average 16 g. This is a considerable difference from the rest of the group and it should be noted that even though it received no dose over this period it still suffered, in terms of weight. It may be that the effects of rotenone were still ongoing in the rat causing an exaggerated disruption in the dietary intake of these specific rats. A box-whisker plot for the RN data set with the exclusion of RN-6, denoted RN*, is presented on the right of the vertical dashed line in the graphic presentation of Table 5.14.A. Descriptive statistics of all the groups, including RN*, are listed in Table 5.14.B. The mean weight gain increased from 12.8 to 16.8 g, the SD decreased from 11.2 to 6.14 g, and the range more than halved from 34 g to 15 g. The non-parametric descriptive statistics varied little with the median changing from 13.5 g to 14.0 g and the IQR narrowing from 6 g to 5 g.

Table 5.14 Box-whisker representation and descriptive statistics of the day 15 to 17 body weight data generated from the rat main study

A: Box-whisker plots and data points according to rat groups



Rat	NN	VN	VV	VC	VS	RN	RV	RC	RS	RN*
1	8	3	3	5	-1	14	-10	14	8	14
2	9	+ -5	6	1	5	18	14	7	17	18
3	5	0	8	5	7	13	11	11	10	13
4	5	0	6	7	6	27	-12	10	13	27
5	7	1	8	1	8	12	-18	+ -7	17	12
6	6	2	3	6	3	• -7	30	17	16	EXCL

B: Descriptive statistics

Dose group	Sample size	Mean	SD	Median	Min	Max	Range	Lower quartile	Upper quartile	IQR
NN	6	6.67	1.63	6.50	5	9	4	5	8	3
VN	6	0.17	2.79	0.50	-5	3	8	0	2	2
VV	6	5.67	2.25	6.00	3	8	5	3	8	5
VC	6	4.17	2.56	5.00	1	7	6	1	6	5
VS	6	4.67	3.27	5.50	-1	8	9	3	7	4
RN	6	12.8	11.2	13.5	-7	27	34	12	18	6
RN*	5	16.8	6.14	14.0	12	27	15	13	18	5
RV	6	2.50	18.7	0.50	-18	30	48	-12	14	26
RC	6	8.67	8.41	10.5	-7	17	24	7	14	7
RS	6	13.5	3.83	14.5	8	17	9	10	17	7

Rat codes for outliers and extreme outliers are located above or below the respective blue crosses (+) and red dots (•), which correspond to data point values listed in the table directly below the graph. The vertical dashed line in the box-whisker graphic representation separates original dose group box-whiskers from those that have had the extreme outliers excluded, which are also indicated by the asterisk (*) following the dose group code. Data sets with excluded data points are designated in green text. Rats were treated with NN = no dose regimen, VX = vehicle and sacrificed, VN = vehicle and no dose, VV = vehicle and vehicle, VC = vehicle and CoQ_{10}, VS = vehicle and succinate, RX = rotenone and sacrificed, RN = rotenone and no dose, RV = rotenone and vehicle, RC = rotenone and CoQ_{10}, RS = rotenone and succinate. EXCL = excluded data point, g = grams, IQR = inter-quartile range, Min = minimum data point value, Max = maximum data point value, SD = standard deviation.

The test for outliers also revealed the presence of an outlier in the RC dose group. Rat RC-5 was the only rat in this group that continued to lose weight after the rotenone dosing had switched to the second treatment of receiving no dose over the last two days. As

presented in Section 5.2.2.1, this same rat was also determined to be an extreme outlier in the total body weight gains and losses section. The fact that the rat continued to lose weight, 7 g in total, from days 15 to 17 is the most likely reason for it being regarded an extreme outlier in the aforementioned section. By referring to Table 5.14.A, it can be determined that the remaining five rats in RC all gained on average more than 10 g over the last two days. As mentioned in Section 5.2.2.1, RC-5 may have been affected more by the initial Factor-1 dose regimen of rotenone. However, the day-to-day rat weight recordings in Table A.2 of Appendix A, indicates that RC-5 gained 1 g of weight from day 15 to 16 and then lost 8 g from day 16 to 17. Therefore, it may be argued that the 8 g loss may have been due to other unknown factors that affected RC-5 itself, and not due to the first dose factor rotenone. Nonetheless, since RC-5 was determined to be an outlier and not an extreme outlier, it will not be excluded from the data set for future statistical analyses. The indication of a second outlier, referring to rat RN-4 in the RN* group, is only due to the exclusion of RN-6 from the original data set. This rat gained more weight than all the other rats in the group, but will not be excluded since it was only considered to be an outlier after the first round of outlier analysis was performed.

The presence of an extreme outlier in the day 15 to 17 rat weight data set, required that the data be analysed via parametric and non-parametric multiple comparison procedures for the exclusion and inclusion of RN-6 respectively. The multiple comparison data as well as the biological significance of these comparisons are presented in Table 5.15.

There was only one comparison, between VN and RN, that was determined to be statistically significant by both the parametric and non-parametric multiple comparison procedures. Furthermore, the difference between VN and RN was also determined to be of biological significance, as listed in Table 5.15.C. This significant difference confirms that rats receiving no dose from days 15 to 17 in the presence of Complex I deficiency gained more weight than those that were not subject to rotenone-induced deficiency. As mentioned previously, it is expected that rats that received rotenone from days 1 to 14 would gain a considerable amount of weight from days 15 to 17 as exposure to the inhibitor was discontinued. Rats that were not exposed to rotenone, namely in groups NN, VX, VN, VC and VS, constantly gained weight at a relatively consistent rate. In contrast, the rotenone-treated rats lost weight at an almost constant rate for 15 days, followed by a marked weight gain when Factor-2 dose regimens were introduced. It can therefore be argued that relieving the rats of the rotenone Factor-1 dose contributed largely to the significant weight gain from days 15 to 17. However, if this were to be the primary cause

of increased weight gain amongst the rotenone-treated rats, it would be expected that all of these dose groups differ significantly from rat groups that were not dosed with the rotenone Factor-1 regimen. As presented in Table 5.15, this was not the case.

Table 5.15 Multiple comparison statistics of day 15 to 17 body weight data generated from the rat main study

A: Non-parametric (original data set) and parametric (excluding extreme outliers) p-values

Dose group	NN	VN	VV	VC	VS	RN	RV	RC	RS
NN		1.000	1.000	1.000	1.000	1.000	1.000	1.000	1.000
		0.851	1.000	1.000	1.000	0.467	0.988	1.000	0.813
VN	1.000		1.000	1.000	1.000	0.038	1.000	0.259	0.008
	0.851		0.936	0.991	0.980	0.027	1.000	0.580	**0.079**
VV	1.000	1.000		1.000	1.000	1.000	1.000	1.000	1.000
	1.000	0.936		1.000	1.000	0.341	0.998	0.999	0.679
VC	1.000	1.000	1.000		1.000	0.804	1.000	1.000	0.245
	1.000	0.991	1.000		1.000	0.194	1.000	0.980	0.455
VS	1.000	1.000	1.000	1.000		1.000	1.000	1.000	0.528
	1.000	0.980	1.000	1.000		0.237	1.000	0.991	0.529
RN	1.000	0.038	1.000	0.804	1.000		1.000	1.000	1.000
	0.467	0.027	0.341	0.194	0.237		0.092	0.737	0.999
RV	1.000	1.000	1.000	1.000	1.000	1.000		1.000	1.000
	0.988	1.000	0.998	1.000	1.000	0.092		0.884	0.245
RC	1.000	0.259	1.000	1.000	1.000	1.000	1.000		1.000
	1.000	0.580	0.999	0.980	0.991	0.737	0.884		0.969
RS	1.000	0.008	1.000	0.245	0.528	1.000	1.000	1.000	
	0.813	**0.079**	0.679	0.455	0.529	0.999	0.245	0.969	

B: ANOVA p-values

Kruskal-Wallis p-value = 0.006	One-way ANOVA p-value = 0.015

C: Statistical and biological significance

Comparison		Statistical significance (p)		Biological significance (d)	
		Including EOs	Excluding EOs	Including EOs	Excluding EOs
VN	RN	0.038	0.027	1.125	2.207
VN	RS	0.008	0.079	3.500	N/A

A: All comparison statistics are indicated as p-values. The upper p-value is the non-parametric multiple comparison test statistic, generated from the original set of data. The lower p-value was generated via the parametric Tukey *unequal number HSD* (Honestly Significant Difference) test, after the exclusion of extreme outliers. P-values indicated in red are statistically significant at the pre-determined significance level of 0.05. P-values in black text represent those that are not statistically significant, but have complementary p-values that are statistically significant. The remainder of p-values are listed in grey. The comparisons surrounded by the **bold** black line are those that were determined to be statistically significant by both the non-parametric and parametric multiple comparison procedures. The turquoise shaded blocks represent statistically significant comparisons that were also determined to be of biological significance. B: P-values for the non-parametric Kruskal-Wallis ANOVA and parametric one-way ANOVA are listed, with significant p-values, less than the 0.05 significance level, indicated in red. C: List of comparisons determined to be statistically significant with corresponding biological significance. A *d*-value greater than or equal to 0.8 signifies biological significance, indicated in red. Rats were treated with NN = no dose regimen, VX = vehicle and sacrificed, VN = vehicle and no dose, VV = vehicle and vehicle, VC = vehicle and CoQ_{10}, VS = vehicle and succinate, RX = rotenone and sacrificed, RN = rotenone and no dose, RV = rotenone and vehicle, RC = rotenone and CoQ_{10}, RS = rotenone and succinate. ANOVA = analysis of variance, EOs = extreme outliers, N/A = not applicable.

The comparison between dose groups VN and RS was also demonstrated to be statistically significant before the exclusion of the extreme outlier RN-6. However, upon removal of RN-6 from the data set, this comparison was no longer determined to differ significantly on a statistical level. This significance is probably due to the narrowing of the data after the extreme outlier exclusion. It should also be noted that the groups do differ

significantly between the 0.05 and 0.01 significance levels, since it has a p-value of 0.079. Nonetheless, it is not less than the pre-determined 0.05 significance level and is therefore not regarded to be significant in the context of this study. Another factor that should be taken into account is that two different multiple comparison procedures are used. The original data sets, including extreme outliers, were analysed via a non-parametric procedure in an attempt to avoid having to violate assumptions of the parametric Tukey multiple comparison procedure. The non-parametric tests are, in general, not as stringent regarding the distribution of data being compared. It may also be due to this leniency of analysis that resulted in a statistically significant p-value for the comparison between VN and RS. The determined biological significance of d = 3.500 indicates that in practice the differences between these two groups are significant. Nonetheless, since too many dose factors differed between the aforementioned dose groups, an inference is not possible. Firstly, the VN group received a vehicle Factor-1 regimen, whereas RS was treated with rotenone. Secondly, VN received no dose over the last two days while RS received succinate, which was diluted in Milli-Q® water as its vehicle. These differences prohibit a meaningful comparison between these two dose groups.

5.2.2.3 Rat main study body weights for days 1-15

The body weight data was also evaluated over the period that rats received Factor-1 dose regimens only, namely from days 1 to 15. In addition to the data presented from the main study, three dose groups from the pilot study were also included to evaluate the consistency in results between the two studies. The three groups from the pilot included dose groups N, V and R15, as presented in Section 5.2.1. The remainder of the groups from the pilot study were not included since none of them could be paralleled with any groups in the main study due to experimentation with various rotenone dose concentrations. The day 1-15 weight gain in dose group N from the pilot study could be paralleled with the day 1-15 weight gain of NN from the main study. Rat groups that received vehicle Factor-1 regimens, namely VX, VN, VC and VS could be matched to dose group V of the pilot study. Dose group R15 from the pilot study was also paralleled with all the groups in the main study that received rotenone Factor-1 regimens, namely RX, RN, RV, RC and RS. Box-whisker plots and descriptive statistics of main and pilot studies are presented in Table 5.16.

As with the data presented in Section 5.2.2.1 where the total rat body weight gains and losses were analysed, the box-whisker plots in Table 5.16 illustrate a clear distinction between the rotenone-treated rat groups and those that received either a vehicle or no

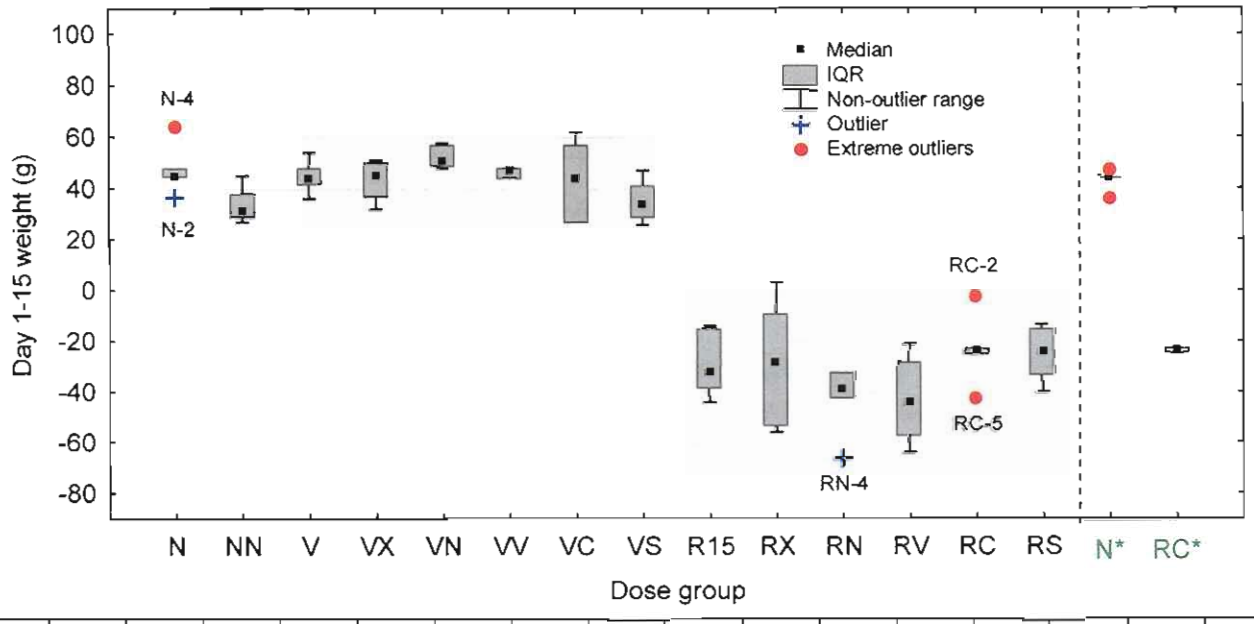
dose Factor-1 regimen. The distinction was more evident here since the weight gains and losses from days 1 to 15 are presented, which was the period where only dose Factor-1 was received by the rats. Therefore, weight changes that occurred from days 15 to 17 are not incorporated. The weight changes in Section 5.2.2.1 included that incurred in the presence of Factor-2 dosing, where a majority of the rotenone-treated rats displayed marked weight gains as soon as the rotenone Factor-1 dosing regimens were completed. Pilot study dose groups were also observed to be in similar weight gain and loss ranges to those from the main study when the box-whisker plots were visually inspected.

Upon outlier analysis of the original 14 dose groups, three extreme outliers were observed to be present. The additional two extreme outliers in the N* group will not be considered for discussion since they were assigned only after the extreme outlier N-4 was excluded from the dose group N. Moreover, dose groups N, V and R15 have already been discussed in Section 5.2.1. The remaining two extreme outliers are both located within the RC data set. The reason for there being two rats in this group that were excluded is due to the close grouping of the internal four data points that constitute the IQR. This range was distributed over only 2 g and since the non-outlier range is calculated from the IQR, data points outside of the IQR were subject to an extremely conservative non-outlier range that extends only 1 g above and below the IQR box.

As illustrated by the box-whisker plot for RC in Table 5.16.A, there are no whiskers above or below the IQR box due to the highest and lowest data points being indicated by the red extreme outlier dots. Nevertheless, by referring to the descriptive statistics for RC and RC* in Table 5.16.B, it can be demonstrated that, even though two data points were excluded from a small sample size of six rats, the mean weight loss increased by only 0.6 g from 23.2 to 23.8 g. The median weight loss for dose group RC remained unchanged at 23.5 g, as would be expected if the highest and lowest data points were excluded from a data set. Rat RC-5, one of the extreme outliers of dose group RC, was also determined to be an extreme outlier in the total rat weight data as well as an outlier in the day 15 to 17 analyses, presented in Sections 5.2.2.1 and 5.2.2.2 respectively. It is apparent that RC-5 responded in a different manner to the dose factors than all the other rats in its group, supporting not only the criteria for excluding it as an extreme outlier, but also the notion that it should be excluded based on its aberrant body weight response profile.

Table 5.16 Box-whisker representation and descriptive statistics of the day 1 to 15 rat weight data generated from the main and pilot studies

A: Box-whisker plots and data points according to rat groups



Rat	N	NN	V	VX	VN	VV	VC	VS	R15	RX	RN	RV	RC	RS	N*	RC*
1	45	45	36	49	51	48	62	29	-15	-9	-42	-40	-23	-18	45	-23
2	+ 37	27	42	37	48	48	27	41	-32	-38	-39	-21	• -2	-40	37	EXCL
3	48	38	54	32	58	48	44	35	-32	3	-32	-28	-25	-15	48	-25
4	• 64	29	45	51	51	46	27	26	-44	-56	+ -66	-48	-24	-13	EXCL	-24
5	45	34	48	50	49	44	44	47	-38	-53	-32	-57	• -42	-30	45	EXCL
6	45	29	43	41	57	44	57	33	-14	-18	-38	-64	-23	-33	45	-23

B: Descriptive statistics

Dose group	Sample size	Mean	SD	Median	Min	Max	Range	Lower quartile	Upper quartile	IQR
N	6	47.3	8.96	45.0	37	64	27	45	48	3
N*	5	44.0	4.12	45.0	37	48	11	45	45	0
NN	6	33.7	6.86	31.5	27	45	18	29	38	9
V	6	44.7	6.06	44.0	36	54	18	42	48	6
VX	6	43.3	7.87	45.0	32	51	19	37	50	13
VN	6	52.3	4.18	51.0	48	58	10	49	57	8
VV	6	46.3	1.97	47.0	44	48	4	44	48	4
VC	6	43.5	14.6	44.0	27	62	35	27	57	30
VS	6	35.2	7.76	34.0	26	47	21	29	41	12
R15	6	-29.2	12.2	-32.0	-44	-14	30	-38	-15	23
RX	6	-28.5	24.2	-28.0	-56	3	59	-53	-9	44
RN	6	-41.5	12.6	-38.5	-66	-32	34	-42	-32	10
RV	6	-43.0	16.6	-44.0	-64	-21	43	-57	-28	29
RC	6	-23.2	12.7	-23.5	-42	-2	40	-25	-23	2
RC*	4	-23.8	0.96	-23.5	-25	-23	2	-24.5	-23	1.5
RS	6	-24.8	11.0	-24.0	-40	-13	27	-33	-15	18

Rat codes for outliers and extreme outliers are located above or below the respective blue crosses (+) and red dots (•), which correspond to data point values listed in the table directly below the graph. The vertical dashed line in the box-whisker graphic representation separates original dose group box-whiskers from those that have had the extreme outliers excluded, which are also indicated by the asterisk (*) following the dose group code. Data sets with excluded data points are designated in green text. Rats were treated with N = no dose (pilot study), NN = no dose (main study), V = vehicle (pilot study), VX = vehicle (main study), VN = vehicle and no dose, VV = vehicle and vehicle, VC = vehicle and CoQ_{10}, VS = vehicle and succinate, R15 = rotenone 15 $mg.kg^{-1}.day^{-1}$ (pilot study), RX = rotenone (15 $mg.kg^{-1}.day^{-1}$) and sacrificed, RN = rotenone and no dose, RV = rotenone and vehicle, RC = rotenone and CoQ_{10}, RS = rotenone and succinate. EXCL = excluded data point, g = grams, IQR = inter-quartile range, Min = minimum data point value, Max = maximum data point value, SD = standard deviation.

An additional outlier was observed in the day 1 to 15 data set. Rat RN-4 lost 66 g over the rotenone-dosing period, more than all the other rats in its group. The next closest rat, RN-1, lost 42 g over this same period. Despite the added weight loss, the RN-4 data point will not be excluded since it is not an extreme outlier. Determination of the statistical significance of the differences observed in the box-whisker plots was performed including and excluding the extreme outliers. The multiple comparison grid of p-values generated from the parametric and non-parametric multiple comparison procedures, together with biological significance d-values are presented in Table 5.17.

Table 5.17 Multiple comparison statistics of day 1 to 15 body weight data generated from the rat pilot and main studies

A: Non-parametric (original data set) and parametric (excluding extreme outliers) p-values

Dose group	N	NN	V	VX	VN	VV	VC	VS	R15	RX	RN	RV	RC	RS
N		1.000 0.975	1.000 1.000	1.000 1.000	1.000 0.996	1.000 1.000	1.000 1.000	1.000 0.994	0.135 < 0.001	0.141 < 0.001	0.016 < 0.001	0.015 < 0.001	0.309 < 0.001	0.287 < 0.001
NN	1.000 0.975		1.000 0.920	1.000 0.969	1.000 0.235	1.000 0.808	1.000 0.965	1.000 1.000	1.000 < 0.001	1.000 < 0.001	1.000 < 0.001	1.000 < 0.001	1.000 < 0.001	1.000 < 0.001
V	1.000 1.000	1.000 0.920		1.000 1.000	1.000 0.996	1.000 1.000	1.000 1.000	1.000 0.973	0.315 < 0.001	0.328 < 0.001	0.044 < 0.001	0.040 < 0.001	0.681 < 0.001	0.634 < 0.001
VX	1.000 1.000	1.000 0.969	1.000 1.000		1.000 0.983	1.000 1.000	1.000 1.000	1.000 0.993	0.271 < 0.001	0.281 < 0.001	0.037 < 0.001	0.034 < 0.001	0.591 < 0.001	0.550 < 0.001
VN	1.000 0.996	1.000 0.235	1.000 0.996	1.000 0.983		1.000 1.000	1.000 0.985	1.000 0.358	0.006 < 0.001	0.006 < 0.001	< 0.001 < 0.001	< 0.001 < 0.001	0.015 < 0.001	0.014 < 0.001
VV	1.000 1.000	1.000 0.808	1.000 1.000	1.000 1.000	1.000 1.000		1.000 1.000	1.000 0.911	0.138 < 0.001	0.144 < 0.001	0.017 < 0.001	0.015 < 0.001	0.315 < 0.001	0.292 < 0.001
VC	1.000 1.000	1.000 0.965	1.000 1.000	1.000 1.000	1.000 0.985	1.000 1.000		1.000 0.991	0.475 < 0.001	0.493 < 0.001	0.071 < 0.001	0.065 < 0.001	0.996 < 0.001	0.931 < 0.001
VS	1.000 0.994	1.000 1.000	1.000 0.973	1.000 0.993	1.000 0.358	1.000 0.911	1.000 0.991		1.000 < 0.001	1.000 < 0.001	0.931 < 0.001	0.869 < 0.001	1.000 < 0.001	1.000 < 0.001
R15	0.135 < 0.001	1.000 < 0.001	0.315 < 0.001	0.271 < 0.001	0.006 < 0.001	0.138 < 0.001	0.475 < 0.001	1.000 < 0.001		1.000 1.000	1.000 0.834	1.000 0.700	1.000 1.000	1.000 1.000
RX	0.141 < 0.001	1.000 < 0.001	0.328 < 0.001	0.281 < 0.001	0.006 < 0.001	0.144 < 0.001	0.493 < 0.001	1.000 < 0.001	1.000 1.000		1.000 0.779	1.000 0.631	1.000 1.000	1.000 1.000
RN	0.016 < 0.001	1.000 < 0.001	0.044 < 0.001	0.037 < 0.001	< 0.001 < 0.001	0.017 < 0.001	0.071 < 0.001	0.931 < 0.001	1.000 0.834	1.000 0.779		1.000 1.000	1.000 0.632	1.000 0.406
RV	0.015 < 0.001	1.000 < 0.001	0.040 < 0.001	0.034 < 0.001	< 0.001 < 0.001	0.015 < 0.001	0.065 < 0.001	0.869 < 0.001	1.000 0.700	1.000 0.631	1.000 1.000		1.000 0.502	1.000 0.272
RC	0.309 < 0.001	1.000 < 0.001	0.681 < 0.001	0.591 < 0.001	0.015 < 0.001	0.315 < 0.001	0.996 < 0.001	1.000 < 0.001	1.000 1.000	1.000 1.000	1.000 0.632	1.000 0.502		1.000 1.000
RS	0.287 < 0.001	1.000 < 0.001	0.634 < 0.001	0.550 < 0.001	0.014 < 0.001	0.292 < 0.001	0.931 < 0.001	1.000 < 0.001	1.000 1.000	1.000 1.000	1.000 0.406	1.000 0.272	1.000 1.000	

B: ANOVA p-values

Kruskal-Wallis p-value	One-way ANOVA p-value
< 0.001	< 0.001

C: Statistical and biological significance

Comparison		Statistical significance (p)		Biological significance (d)	
		Including EOs	Excluding EOs	Including EOs	Excluding EOs
N	R15	0.135	< 0.001	N/A	6.410
N	RX	0.141	< 0.001	N/A	6.349
N	RN	0.016	< 0.001	7.048	7.488
N	RV	0.015	< 0.001	5.440	7.619
N	RC	0.309	< 0.001	N/A	5.937

Table 5.17 Continued…

Comparison		Statistical significance (p)		Biological significance (d)	
		Including EOs	Excluding EOs	Including EOs	Excluding EOs
N	RS	0.287	< 0.001	N/A	6.025
NN	R15	1.000	< 0.001	N/A	5.508
NN	RX	1.000	< 0.001	N/A	5.447
NN	RN	1.000	< 0.001	N/A	6.586
NN	RV	1.000	< 0.001	N/A	6.717
NN	RC	1.000	< 0.001	N/A	5.035
NN	RS	1.000	< 0.001	N/A	5.123
V	R15	0.315	< 0.001	N/A	6.472
V	RX	0.328	< 0.001	N/A	6.410
V	RN	0.044	< 0.001	6.841	7.549
V	RV	0.040	< 0.001	5.283	7.680
V	RC	0.681	< 0.001	N/A	5.999
V	RS	0.634	< 0.001	N/A	6.086
VX	R15	0.271	< 0.001	N/A	6.349
VX	RX	0.281	< 0.001	N/A	6.288
VX	RN	0.037	< 0.001	6.730	7.426
VX	RV	0.033	< 0.001	5.199	7.558
VX	RC	0.591	< 0.001	N/A	5.876
VX	RS	0.550	< 0.001	N/A	5.964
VN	R15	0.005	< 0.001	6.680	7.137
VN	RX	0.006	< 0.001	3.339	7.076
VN	RN	< 0.001	< 0.001	7.444	8.214
VN	RV	< 0.001	< 0.001	5.741	8.346
VN	RC	0.015	< 0.001	5.945	6.664
VN	RS	0.014	< 0.001	7.009	6.752
VV	R15	0.138	< 0.001	N/A	6.612
VV	RX	0.144	< 0.001	N/A	6.550
VV	RN	0.017	< 0.001	6.968	7.689
VV	RV	0.015	< 0.001	5.380	7.820
VV	RC	0.315	< 0.001	N/A	6.139
VV	RS	0.292	< 0.001	N/A	6.226
VC	R15	0.475	< 0.001	N/A	6.367
VC	RX	0.493	< 0.001	N/A	6.305
VC	RN	0.071	< 0.001	N/A	7.444
VC	RV	0.065	< 0.001	N/A	7.575
VC	RC	0.996	< 0.001	N/A	5.167
VC	RS	0.931	< 0.001	N/A	5.254
VS	R15	1.000	< 0.001	N/A	5.640
VS	RX	1.000	< 0.001	N/A	5.578
VS	RN	0.931	< 0.001	N/A	6.717
VS	RV	0.869	< 0.001	N/A	6.848
VS	RC	1.000	< 0.001	N/A	5.167
VS	RS	1.000	< 0.001	N/A	5.254

A: All comparison statistics are indicated as p-values. The upper p-value is the non-parametric multiple comparison test statistic, generated from the original set of data. The lower p-value was generated via the parametric Tukey *unequal number HSD* (Honestly Significant Difference) test, after the exclusion of extreme outliers. P-values indicated in red are statistically significant at the pre-determined significance level of 0.05. P-values in black text represent those that are not statistically significant, but have complementary p-values that are statistically significant. The remainder of p-values are listed in grey. The comparisons surrounded by the **bold** black line are those that were determined to be statistically significant by both the non-parametric and parametric multiple comparison procedures. The turquoise shaded blocks represent statistically significant comparisons that were also determined to be of biological significance. B: P-values for the non-parametric Kruskal-Wallis ANOVA and parametric one-way ANOVA are listed, with significant p-values, less than the 0.05 significance level, indicated in red. C: List of comparisons determined to be statistically significant with corresponding biological significance. A d-value greater than or equal to 0.8 signifies biological significance, indicated in red. Rats were treated with N = no dose (for 14 days), NN = no dose (for 16 days), V = vehicle for 14 days (and sacrificed), VX = vehicle and sacrificed, VN = vehicle and no dose, VV = vehicle and vehicle, VC = vehicle and CoQ_{10}, VS = vehicle and succinate, R15 = 15 $mg.kg^{-1}.day^{-1}$ (and sacrificed), RX = rotenone and sacrificed, RN = rotenone and no dose, RV = rotenone and vehicle, RC = rotenone and CoQ_{10}, RS = rotenone and succinate. < = less than, ANOVA = analysis of variance, EOs = extreme outliers, N/A = not applicable.

The multiple comparison grid reveals that when the extreme outliers were excluded, all the rats that were dosed with rotenone for the first 14 days differed significantly from those that received the sunflower oil vehicle. However, once again, as presented in Section 5.2.2.1, this was not the case with the non-parametric comparison of the mentioned groups. Only 14 of the 48 rotenone Factor-1 versus vehicle and no dose Factor-1 comparisons were determined to be statistically significant via the non-parametric multiple comparison procedure. These are indicated by the bold line, surrounding p-values in Table 5.17.A. The exclusion of extreme outliers results in a marked decrease in variance in the respective groups, which is a factor that weighs heavily in ANOVA testing, and the determination of statistically significant comparisons. It is for this reason that the less sensitive non-parametric multiple comparison procedure was used to analyse the original data including the extreme outliers. The 48 statistically significant comparisons were further determined to be of biological significance, with d-values greater than 0.8. A listing of the biological significance d-values can be referred to in Table 5.17.C.

The most important information to gather from this set of analyses is that among the rat groups that could be paralleled, of both the rat pilot and main studies, no statistically significant differences were determined. Therefore, the result confirms that the Factor-1 dose phase, namely from days 1 to 14, resulted in comparatively equivalent rat weight data within and between the rat pilot and main studies. All 30 rats in the main study that were dosed 15 $mg.kg^{-1}.day^{-1}$ rotenone were losing weight at comparable rates. Furthermore, the weight loss observed for rat group R15 of the pilot study was comparable to that of the five rotenone-treated dose groups in the main study. The same was true for the 30 rats that received the vehicle Factor-1 regimen. All these rats gained weights equivalently among themselves, as well as when compared to dose group V of the pilot study. In addition, the multiple comparison grid reveals that both dose groups N and NN gained weights similarly to all the rats that received vehicle from days 1 to 14.

The incorporation of pilot study groups N, V and R15 into the ANOVA and multiple comparison testing enabled the confirmation that experimental procedures were consistent and that results could be compared to those generated in the main study. Dose group N did not differ significantly from the 14-day weight gain observed for NN of the main study. Dose group V gained equivalent weights to VX, VN, VV, VC and VS over 14 days with no statistically significant differences. Finally, R15 from the pilot study lost similar amounts of weight to RX, RN, RV, RC and RS of the main study. The data

presented here forms a solid foundation and endorses, with confidence, that the pilot study itself and the experimental procedures were optimised sufficiently enough to enable accurate reproducibility of results.

5.3 RAT BLOOD DATA

Blood was collected upon sacrificing the rats and prepared appropriately for each of the respective assays to be performed. In the rat main study, a total of six blood related data sets were generated. These are presented in subsequent sections and a biochemical profile for blood established. A single blood-related data set was generated from the rat pilot study, namely blood hydroperoxides, as presented in Section 5.3.1.2. Raw data generated from blood during the rat main study is presented in Appendix Chapters D to G.

5.3.1 Serum hydroperoxide concentrations

The d-ROMs assay was performed on the same days that the rats were sacrificed to determine hydroperoxide levels. Blood serum was isolated and prepared from both the pilot and main study rats and assayed via the d-ROMs kit according to the manufacturer's specifications. In order to infer oxidative stress levels from the serum hydroperoxide data, a reference scale was provided by Diacron International, as presented in Table 5.18.

Table 5.18 Oxidative stress severity in humans according to the d-ROMs kit

Hydroperoxide concentration (CARR U)	Oxidative stress level
300 to 320	Borderline range
321 to 340	Low
341 to 400	Middle
401 to 500	High
more than 500	Very high

Adapted from Iorio, 2002. CARR U = Carratelli units, d-ROMs = Diacron Reactive Oxygen Metabolites.

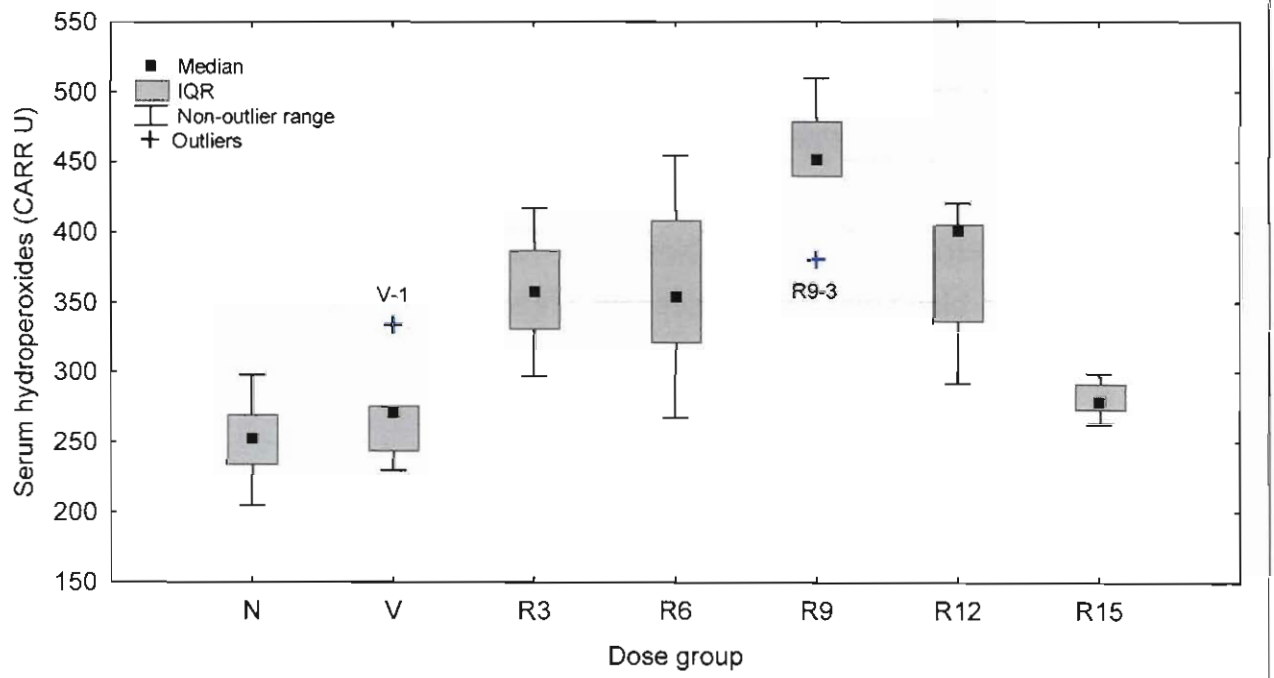
5.3.1.1 Rat pilot study serum hydroperoxide data

The rat pilot study was performed to establish which rotenone dose concentration to use in order to inhibit complex I to a desired percentage and mimic a Complex I deficiency. Complex I was assayed to evaluate the relationships between rotenone dose concentrations and complex I inhibition. To complement the complex I data, the d-ROMs assay was performed to determine the blood-related oxidative stress levels in rats.

Table 5.19 displays the distribution of hydroperoxide data by means of box-whisker plots and a table of descriptive statistics.

Table 5.19 Box-whisker representation and descriptive statistics of the serum hydroperoxide data generated from the rat pilot study

A: Box-whisker plots and data points according to rat groups



Rat	N	V	R3	R6	R9	R12	R15
1	268	+ 334	417	454	510	404	262
2	234	230	297	267	439	292	298
3	237	274	357	321	+ 380	397	272
4	269	275	—	407	448	420	290
5	205	268	330	327	478	335	279
6	297	243	386	379	453	401	278

B: Descriptive statistics

Dose group	Sample size	Mean	SD	Median	Min	Max	Range	Lower quartile	Upper quartile	IQR
N	6	252	32.8	253	205	298	92.9	234	269	35.1
V	6	271	35.9	271	230	334	104	243	275	31.5
R3	5	357	46.8	357	297	417	120	330	386	55.6
R6	6	360	67.4	353	267	454	187	321	407	86.3
R9	6	451	43.4	451	380	510	130	439	478	38.8
R12	6	375	50.2	399	292	420	129	335	404	68.8
R15	6	280	12.7	279	262	298	36.0	272	290	17.5

Rat codes for the outliers are located above or below the respective blue crosses (+). '—' = missing data point due to death of rat R3-4. Rats were treated with N = no dose, V = vehicle, R3 = rotenone 3 $mg.kg^{-1}.day^{-1}$, R6 = rotenone 6 $mg.kg^{-1}.day^{-1}$, R9 = rotenone 9 $mg.kg^{-1}.day^{-1}$, R12 = rotenone 12 $mg.kg^{-1}.day^{-1}$, R15 = rotenone 15 $mg.kg^{-1}.day^{-1}$. CARR U = Carratelli units, IQR = inter-quartile range, Min = minimum data point value, Max = maximum data point value, SD = standard deviation.

The box-whisker plots illustrate the presence of two outliers, one of which is present in dose group V, the other in R9. The values of these outliers are indicated in the data point table below the box-whisker plots in Table 5.19.A. The outlier V-1 has a hydroperoxide

value of 334 CARR U, while outlier R9-3 had an oxidative stress level of 380 CARR U. Both outliers occur in dose groups that have relatively narrow IQRs with respect to the other IQRs in the pilot study, as can be observed in the IQR column in Table 5.19.B. There it can be expected that if these outliers were to be excluded from their respective data sets, then minor adjustments would occur in the statistics that define the central tendency. However, since V-1 and R9-3 are not positioned within their respective extreme outlier ranges, these data points will not be excluded.

The graphic presentation of data in Table 5.19.A illustrates that there was an upward trend in the formation of hydroperoxides up to and including R9, the dose group that received 9 $mg.kg^{-1}.day^{-1}$ rotenone for 14 days. The aforementioned group presented with a mean hydroperoxide concentration of 451 CARR U, which is classified as a value of 'high' oxidative stress according to Table 5.18. However, it should be noted that the control dose groups N and V harboured mean hydroperoxide values of 252 and 271 CARR U, respectively. Both these values fall well below the 300 to 320 CARR U borderline range specified by the manufacturers.

Unexpectedly, dose group R12 harboured lower hydroperoxide levels when compared to R9, while the R15 group presented with an even greater decrease to a mean value of 280 CARR U. Reasons for this unexpected decrease in serum hydroperoxide levels in the two dose groups that received the highest concentrations of rotenone were difficult to explain. To the knowledge of the author, there are no similar reports in the literature that describe such a trend, which may be the result of a reduced state of oxidative stress, either through less ROS production or higher antioxidant status.

The data was further investigated via one-way ANOVA and the Tukey *unequal number HSD* multiple comparison procedure to determine statistically significant differences between the various dose groups. The ANOVA, multiple comparison data and the biological significance of the statistically significant comparisons are presented in Table 5.20.

Table 5.20 Multiple comparison statistics of the serum hydroperoxide data generated from the rat pilot study

A: Parametric Tukey *unequal number HSD* p-values

Dose group	N	V	R3	R6	R9	R12	R15
N		0.988	0.010	0.003	< 0.001	0.001	0.920
V	0.988		0.053	0.022	< 0.001	0.004	1.000
R3	0.010	0.053		1.000	0.029	0.996	0.111
R6	0.003	0.022	1.000		0.015	0.996	0.052
R9	< 0.001	< 0.001	0.029	0.015		0.068	< 0.001
R12	0.001	0.004	0.996	0.996	0.068		0.011
R15	0.920	1.000	0.111	0.052	< 0.001	0.011	

B: ANOVA p-values

One-way ANOVA p-value < 0.001

C: Statistical and biological significance

Comparison		Statistical significance (p)	Biological significance (d)
N	R3	0.010	2.397
N	R6	0.003	2.439
N	R9	< 0.001	4.525
N	R12	0.001	2.793
V	R6	0.022	2.008
V	R9	< 0.001	4.094
V	R12	0.004	2.362
R3	R9	0.029	2.128
R6	R9	0.015	2.086
R9	R15	< 0.001	3.882
R12	R15	0.011	2.150

A: All comparison statistics are indicated as p-values generated via the Tukey *unequal number HSD* (Honestly Significant Difference) test. The p-values indicated in red are statistically significant at a significance level of 0.05, while all other p-values are in grey. The turquoise shaded blocks represent statistically significant comparisons that were also determined to be biologically significant. B: The parametric one-way ANOVA with significant p-values less than $\alpha = 0.05$ indicated in red text. C: List of comparisons found to be statistically significant with corresponding biological significance. The test for biological significance was only performed on comparisons that were shown to be statistically significant. A comparison is regarded to be biologically significant, indicated in red, if the calculated d-value is greater than or equal to 0.8. Rats were treated N = no dose, V = vehicle, R3 = rotenone 3 $mg.kg^{-1}.day^{-1}$, R6 = rotenone 6 $mg.kg^{-1}.day^{-1}$, R9 = rotenone 9 $mg.kg^{-1}.day^{-1}$, R12 = rotenone 12 $mg.kg^{-1}.day^{-1}$, R15 = rotenone 15 $mg.kg^{-1}.day^{-1}$. < = less than, ANOVA = analysis of variance.

The Tukey *unequal number HSD* test revealed that 11 of the 21 comparisons performed were statistically significant. In addition, all of the 11 statistically significant comparisons were also determined to be biologically significant, as presented in Table 5.20.C. According to the p-values presented in Table 5.20.A, all of the dose groups that received rotenone Factor-1 doses, excluding R15, were demonstrated to differ significantly from the environmental control dose group N. In addition, rats that were dosed 6, 9 and 12 $mg.kg^{-1}.day^{-1}$ rotenone, also presented with statistically significant p-values when compared to rat group V. Dose group R9, which harboured the highest mean hydroperoxides level of 451 CARR U, differed significantly from all the other groups, except for R12.

The most surprising of results stems from the hydroperoxide concentrations obtained for the two rat groups R12 and R15, which were dosed with the highest concentrations of rotenone. Although debatable, it can be argued that complex I is the primary enzyme in the respiratory chain that produces ROS (Ježek and Hlavatá, 2005), followed by complex III. A deficiency in the enzyme would theoretically result in an excessive formation of ROS. The fact that rotenone concentrations beyond 9 $mg.kg^{-1}.day^{-1}$ resulted in improvements in the hydroperoxide levels of serum was certainly unforeseen. Dose group R12 still harboured hydroperoxide levels that were significantly higher than both rat groups N and V. However, dose group R15 did not differ statistically significantly from the two latter mentioned dose groups. As discussed in Sections 5.2.1 and 5.1.3, rats from R15 lost considerable amounts of weight and presented with signs of discomfort, respectively. Furthermore, dose group R15 displayed statistically significant complex I inhibition in all organs investigated, except for skeletal muscle, as presented in subsequent sections. Yet, the hydroperoxide recordings were not determined to differ statistically significantly from the environmental controls **NN**, not to mention dose group V.

Since rotenone is an inhibitor of complex I, it possesses a modular similarity to that of the electron acceptor ubiquinone (Degli Esposti, 1998), or CoQ_{10}. Therefore, it could be argued that the resemblance in structure, as presented in Figure 2.7 of Chapter Two, may enable inference as to the chemical properties of rotenone. CoQ_{10} plays a major role in the transfer of electrons from complex I and II to complex III. However, it also functions to stabilise the enzyme complexes of the respiratory chain, not to mention its functionality as an antioxidant (Shoffner and Wallace, 1994). Rotenone binds to complex I in a similar manner as CoQ_{10}, except that it binds irreversibly to the site of action (Grivennikova *et al.*, 1997), preventing CoQ_{10} from returning to the site to retrieve more electrons for further transfer to complex III. However, as far as it is known to the author, there are no reports that state that rotenone can act as an antioxidant. Since the inhibitor is analogous in structure to that of coenzyme Q, the suggestion that it may act as an antioxidant in its unbound form cannot be excluded.

The formation of hydroperoxides increased to 357 and 360 mean CARR U when rats were dosed with 3 and 6 $mg.kg^{-1}.day^{-1}$ rotenone respectively, after which the sharp increase to 451 CARR U occurred when 9 $mg.kg^{-1}.day^{-1}$ was used. If rotenone indeed displays antioxidant properties, it may be argued that a saturation threshold was reached at the 9 $mg.kg^{-1}.day^{-1}$ dose concentration. The availability of complex I enzymes throughout the rat organism may be a limiting factor for rotenone to bind to beyond the 9 $mg.kg^{-1}.day^{-1}$ concentration. Most of the enzymes may already be bound in the various organs of the

rat, or alternatively cellular permeability may be preventing access to complex I. This may in turn lead to excess rotenone being transported in the circulatory system. Consequently, if the antioxidant properties of rotenone can be assumed, it resulted in the scavenging of ROS that was produced initially due to the overall deficiency in complex I. This analogy may explain the decreased hydroperoxide levels in R12 and even more so in R15, where the increase in dose concentration resulted in increased rotenone excess in the blood flow, which in turn scavenges the majority of the ROS formed due to the inhibition of complex I. This appears to be the case in the R15 group that presented with a mean hydroperoxide concentration of 280 CARR U, which is only slightly higher than the 271 CARR U of dose group V.

An alternative view may be that the excessive rotenone concentrations beyond 9 $mg.kg^{-1}.day^{-1}$ resulted in a considerable increase in the expression of transcripts that contribute to maintaining oxidative stress levels. Van der Westhuizen *et al.* (2003) reported putative defensive responses to Complex I deficiency in a study where transcriptional responses in fibroblasts, harbouring common Complex I deficiency mutations, were investigated. The publication reported that the production of ROS appears to play a role in the induction of genes that may protect against ROS itself. The most significant increases in expression were of genes encoding the metallothioneins, which are cysteine-rich proteins induced by several oxidant related compounds, most notably ROS. In support of this, Reinecke *et al.* (2006) reported that metallothionein induction increased rapidly when complex I activity was inhibited by rotenone to levels below 50% in HeLa cells. The described mechanism may be postulated to have effects in the rat models investigated here. It could therefore certainly be argued that the induction of defensive transcripts, similar in function to that of metallothionein, occurred after the 9 $mg.kg^{-1}.day^{-1}$ rotenone threshold, induced by the corresponding levels of ROS production.

5.3.1.2 Rat main study serum hydroperoxide data

Table 5.21 contains a summary of the distribution of hydroperoxide data in terms of box-whisker representations and a tabulated format. The first 11 box-whisker plots, representing dose groups NN to RS, are illustrated with the presence of one outlier and two extreme outliers. The final two box-whisker plots, RV* and RC*, are those groups where the extreme outliers have been excluded from the data sets. The box-whisker representation is accompanied by a table listing all of the six data points per dose group as well as a table of descriptive statistics. Two extreme outliers were determined to be

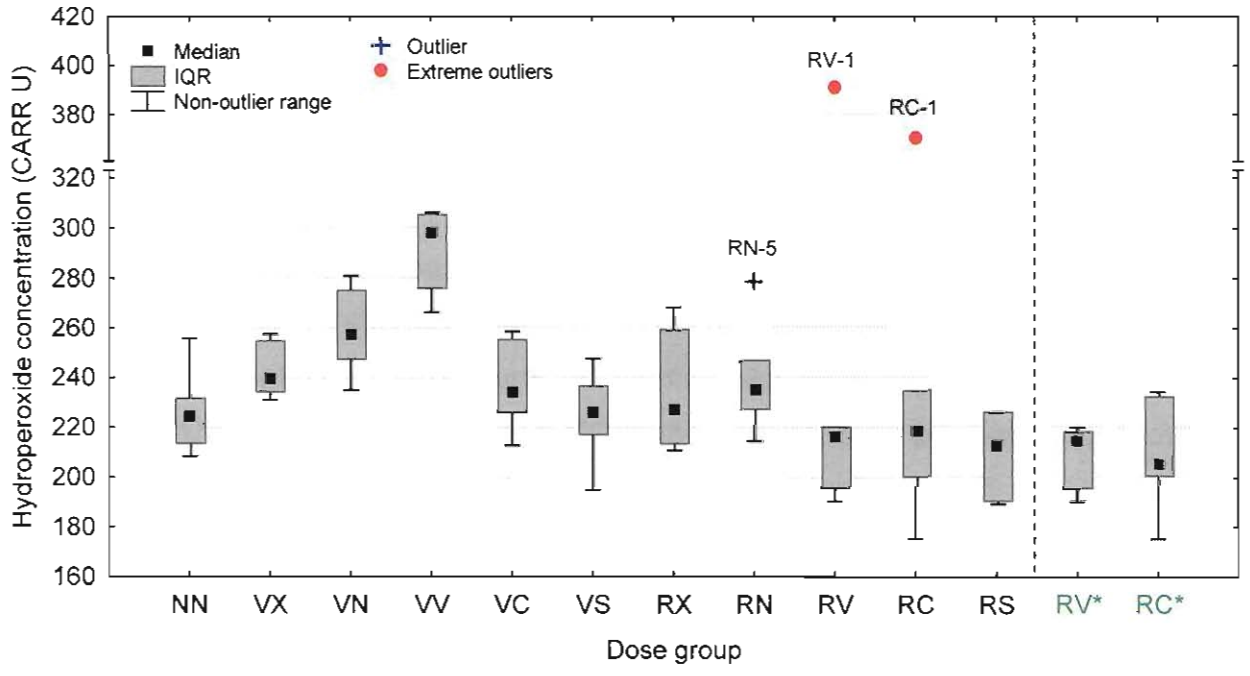
present in the serum hydroperoxide data set, namely RV-1 and RC-1, along with a single outlier, RN-5. Since RN-5 is not an extreme outlier, it was not excluded from the data set and will therefore no longer be discussed. The upper outlier boundaries for RV and RC are at 293 and 337 CARR U respectively. Hence it is evident that RV-1, being 391 CARR U, and RC-1, being 370 CARR U, are regarded to be extreme and were therefore excluded from their respective data sets.

The exclusion of these extreme outliers from the hydroperoxide data set had definitive effects on certain of the descriptive statistics. The most notable of adjustments are within the parametric descriptive statistics, namely the means and standard deviations. The mean for RV diminished from 238 to 208 CARR U, and the standard deviation from 75.7 to 13.8 CARR U. The same is true for dose group RC, where the mean decreased from 236 to 209 CARR U, and the standard deviation from 69.3 to 24.5 CARR U. As expected, the maximum values and range statistics also changed considerably. However, it should be noted that the non-parametric descriptive statistics, namely the median, lower and upper quartiles and IQR were not altered as much as the means and standard deviations. The median for RV was adjusted only slightly from 216 to 215 CARR U, and the IQR from 24.5 to 22.5 CARR U. The median for RC changed from 219 to 205 CARR U, while the IQR decreased from 34.2 to 31.7 CARR U. Even though the decrease in median for RC is approximately 14 CARR U, it is still almost half the difference observed in the means, which was approximately 27 CARR U.

The aforementioned examples illustrate the robustness of non-parametric descriptive statistics versus its parametric counterparts, even with small sample sizes of five and six data points per group. The hydroperoxide data also confirms that using lower and upper quartile statistics, as opposed to standard deviations, to determine the presence of outliers and extreme outliers is most certainly a better option. If standard deviations were to be used in the cases of RV and RC, which were 75.7 and 69.3 CARR U respectively, it would be very difficult to assign any outliers and extreme outliers in a data set. Since the standard deviation is severely exaggerated due to the presence of extreme outliers, it was not considered for use in outlier analysis.

Table 5.21 Box-whisker representation and descriptive statistics of the serum hydroperoxide data generated from the rat main study

A: Box-whisker plots and data points according to rat groups



Rat	NN	VX	VN	VV	VC	VS	RX	RN	RV	RC	RS	RV*	RC*
1	214	258	248	276	255	226	268	230	• 391	• 370	189	EXCL	EXCL
2	218	231	235	306	258	236	211	227	196	232	190	196	232
3	231	255	264	266	213	217	214	239	190	200	226	190	200
4	232	237	281	305	230	226	259	215	215	175	220	215	175
5	208	242	252	291	238	248	216	+ 278	218	205	226	218	205
6	256	235	275	305	226	195	238	247	220	234	205	220	234

B: Descriptive statistics

Dose group	Sample size	Mean	SD	Median	Min	Max	Range	Lower quartile	Upper quartile	IQR
NN	6	226	17.2	225	208	256	47.6	214	232	17.9
VX	6	243	11.0	240	231	258	26.7	235	255	20.2
VN	6	259	17.5	258	235	281	46.1	248	275	27.5
VV	6	292	16.9	298	266	306	39.5	276	305	28.9
VC	6	237	17.4	234	213	258	45.3	226	255	28.9
VS	6	225	17.9	226	195	248	52.8	217	236	19.1
RX	6	234	24.9	227	211	268	57.6	214	259	45.3
RN	6	239	22.1	235	215	278	64.0	227	247	19.5
RV	6	238	75.7	216	190	391	200	196	220	24.5
RV*	5	208	13.8	215	190	220	29.7	195	218	22.5
RC	6	236	69.3	219	175	370	195	200	234	34.2
RC*	5	209	24.5	205	175	234	59.1	200	232	31.7
RS	6	209	16.9	213	189	226	36.5	190	226	35.2

Rat codes for outliers and extreme outliers are located above or below the respective blue crosses (+) and red dots (•), which correspond to data point values listed in the table directly below the graph. The vertical dashed line in the box-whisker graphic representation separates original dose group box-whiskers from those that have had the extreme outliers excluded, which are also indicated by the asterisk (*) following the dose group code. Data sets with excluded data points are designated in green text. A scale break was implemented on the Y-axis between 320 and 380 CARR U. Rats were treated with NN = no dose regimen, VX = vehicle and sacrificed, VN = vehicle and no dose, VV = vehicle and vehicle, VC = vehicle and CoQ_{10}, VS = vehicle and succinate, RX = rotenone and sacrificed, RN = rotenone and no dose, RV = rotenone and vehicle, RC = rotenone and CoQ_{10}, RS = rotenone and succinate. CARR U = Carratelli units, EXCL = excluded data point, IQR = inter-quartile range, Min = minimum data point value, Max = maximum data point value, SD = standard deviation.

The hydroperoxide data of the pilot study, presented in Section 5.3.1.1, are well supported by the results obtained in the rat main study. The box-whisker plots in Table 5.21.A portray that the rotenone treatment appeared to lower oxidative stress levels in rats when compared to vehicle. Due to the presence of extreme outliers in the rat main study serum hydroperoxide data set, a statistical comparison of the data including and excluding the extreme outliers was required. Table 5.22 presents the multiple comparison data generated from serum hydroperoxide data, analysed via parametric and non-parametric test procedures. The statistically significant comparisons were also tested for their biological significance, as presented in section C of the same table.

Only two comparisons between rat groups were determined to be statistically significant by both the parametric and non-parametric multiple comparison procedures, as indicated by the values surrounded by **bold** lining in Table 5.22. These are the comparisons between VV and RV as well as VV and RS. Although it is not possible to infer single effects from these comparisons, the data strongly supports the fact that the serum hydroperoxide levels between these rat groups indeed differed. However, the data in Table 5.22.C indicates that the comparison between VV and RV was only determined to be biologically significant after the extreme outliers were excluded. If the test for extreme outliers were not performed, it would have resulted in an uncertainty as to whether a difference in response indeed existed between these groups.

The exclusion of extreme outliers RV-1 and RC-1 resulted in statistically significant differences between an additional 10 dose group comparisons. Upon the exclusion, VV was determined to differ significantly from nine of the other dose groups, excluding dose group VN. The fact that VV differed significantly from NN, VX, VC and VS strongly suggests that the vehicle Factor-2 regimen contributed to oxidative stress in rats. The environmental controls NN received no dose for 16 days, while VV received sunflower oil for the same time period. Since the vehicle utilised in this study is a vegetable oil, it is composed of high levels of polyunsaturated fat. It has been reported in the past that a high polyunsaturated fat content is responsible for increasing susceptibility to lipid peroxidation (Mataix *et al.*, 1998) and inducing oxidative stress (Turpeinen *et al.*, 1998). These reports are in congruence with the serum hydroperoxide data presented here for dose group VV. Furthermore, although not determined to be of statistical significance, the aforementioned reports are also in support of the remaining four rat groups that received vehicle Factor-1 doses, where the majority of these hydroperoxide data points were higher than those recorded in the environmental controls NN.

Table 5.22 Multiple comparison statistics of the serum hydroperoxide data generated from the rat main study

A: Non-parametric (original data set) and parametric (excluding extreme outliers) p-values

Dose group	NN	VX	VN	VV	VC	VS	RX	RN	RV	RC	RS
NN		1.000	1.000	0.113	1.000	1.000	1.000	1.000	1.000	1.000	1.000
		0.901	0.113	< 0.001	0.997	1.000	1.000	0.979	0.878	0.931	0.881
VX	1.000		1.000	1.000	1.000	1.000	1.000	1.000	1.000	1.000	0.720
	0.901		0.915	0.002	1.000	0.827	0.999	1.000	0.122	0.170	0.091
VN	1.000	1.000		1.000	1.000	1.000	1.000	1.000	0.607	1.000	0.064
	0.113	0.915		0.112	0.592	0.076	0.448	0.763	0.003	0.004	0.001
VV	0.113	1.000	1.000		1.000	0.119	0.533	1.000	0.027	0.075	0.002
	< 0.001	0.002	0.112		< 0.001	< 0.001	< 0.001	0.001	< 0.001	< 0.001	< 0.001
VC	1.000	1.000	1.000	1.000		1.000	1.000	1.000	1.000	1.000	1.000
	0.997	1.000	0.592	< 0.001		0.988	1.000	1.000	0.353	0.446	0.310
VS	1.000	1.000	1.000	0.119	1.000		1.000	1.000	1.000	1.000	1.000
	1.000	0.827	0.076	< 0.001	0.988		0.998	0.948	0.932	0.967	0.938
RX	1.000	1.000	1.000	0.533	1.000	1.000		1.000	1.000	1.000	1.000
	1.000	0.999	0.448	< 0.001	1.000	0.998		1.000	0.475	0.577	0.438
RN	1.000	1.000	1.000	1.000	1.000	1.000	1.000		1.000	1.000	1.000
	0.979	1.000	0.763	0.001	1.000	0.948	1.000		0.228	0.302	0.187
RV	1.000	1.000	0.607	0.027	1.000	1.000	1.000	1.000		1.000	1.000
	0.878	0.122	0.003	< 0.001	0.353	0.932	0.475	0.228		1.000	1.000
RC	1.000	1.000	1.000	0.075	1.000	1.000	1.000	1.000	1.000		1.000
	0.931	0.170	0.004	< 0.001	0.446	0.967	0.577	0.302	1.000		1.000
RS	1.000	0.720	0.064	0.002	1.000	1.000	1.000	1.000	1.000	1.000	
	0.881	0.091	0.001	< 0.001	0.310	0.938	0.438	0.187	1.000	1.000	

B: ANOVA p-values

Kruskal-Wallis p-value = 0.0014	One-way ANOVA p-value < 0.001

C: Statistical and biological significance

Comparison		Statistical significance (p)		Biological significance (d)	
		Including EOs	Excluding EOs	Including EOs	Excluding EOs
NN	VV	0.113	< 0.001	N/A	3.505
VX	VV	1.000	0.002	N/A	2.618
VN	RV	0.607	0.003	N/A	2.760
VN	RC	1.000	0.004	N/A	2.664
VN	RS	0.064	0.001	N/A	4.421
VV	VC	1.000	< 0.001	N/A	2.959
VV	VS	0.119	< 0.001	N/A	3.602
VV	RX	0.533	< 0.001	N/A	3.083
VV	RN	1.000	0.001	N/A	2.806
VV	RV	0.027	< 0.001	0.704	4.513
VV	RC	0.075	< 0.001	N/A	4.417
VV	RS	0.002	< 0.001	4.848	4.421

A: All comparison statistics are indicated as p-values. The upper p-value is the non-parametric multiple comparison test statistic, generated from the original set of data. The lower p-value was generated via the parametric Tukey *unequal number HSD* (Honestly Significant Difference) test, after the exclusion of extreme outliers. P-values indicated in red are statistically significant at the pre-determined significance level of 0.05. P-values in black text represent those that are not statistically significant, but have complementary p-values that are statistically significant. The remainder of p-values are listed in grey. The comparisons surrounded by the **bold** black line are those that were determined to be statistically significant by both the non-parametric and parametric multiple comparison procedures. The turquoise shaded blocks represent statistically significant comparisons that were also determined to be of biological significance. B: P-values for the non-parametric Kruskal-Wallis ANOVA and parametric one-way ANOVA are listed, with significant p-values, less than the 0.05 significance level, indicated in red. C: List of comparisons determined to be statistically significant with corresponding biological significance. A d-value greater than or equal to 0.8 signifies biological significance, indicated in red. Rats were treated with NN = no dose regimen, VX = vehicle and sacrificed, VN = vehicle and no dose, VV = vehicle and vehicle, VC = vehicle and CoQ_{10}, VS = vehicle and succinate, RX = rotenone and sacrificed, RN = rotenone and no dose, RV = rotenone and vehicle, RC = rotenone and CoQ_{10}, RS = rotenone and succinate. ANOVA = analysis of variance, EOs = extreme outliers, N/A = not applicable.

Dose group VX received sunflower oil for 14 days as opposed to VV that received the oil for 16 days. The p-value of 0.002 for the comparison between VX and VV indicates that the two additional days of oil dosing resulted in a significant increase in oxidative stress, further supporting the notion that vehicle may have an adverse effect on serum hydroperoxide levels in rats. The hydroperoxide measurements for VV also exceeded that for VN, the group that received a no dose Factor-2 regimen. This difference was however not determined to be statistically significant. Both groups VC and VS also harboured serum hydroperoxide levels significantly lower than VV. These indicate that CoQ_{10} and succinate significantly improved the oxidative stress levels in rats over groups that received vehicle on days 15 and 16 of dosing. It may appear that VS presented with slightly greater improvements in oxidative stress from days 15 to 16 as opposed to VC. However, as discussed in Section 4.3.2 of Chapter Four, it should be noted that succinate was dosed in a Milli-Q® water vehicle whereas CoQ_{10} was dosed in sunflower oil. Based on the Mataix *et al.* (1998) and Turpeinen *et al.* (1998) publications, it can certainly be argued that the high polyunsaturated fat content of sunflower oil might have contributed to the fact that VC harboured higher hydroperoxide levels. Nonetheless, the difference between the groups was not of statistical significance.

By referring to the groups that harboured the induced Complex I deficiency, that is, the groups that received rotenone Factor-1 regimens, it is evident that all the groups on average presented with improved oxidative stress levels when compared to the rat groups that were dosed vehicle or no dose. Dose group RN harboured slightly elevated hydroperoxide recordings compared to the other groups that received rotenone. If the vehicle were to contribute to serum hydroperoxide levels, it would be expected that group RV would have the highest recordings. However, this was not determined to be the case. Similar to RN, the distribution of data points in RX also appeared to be elevated when compared to the remaining rotenone-treated rats. This is reflected in the mean hydroperoxide value for RX at 234 CARR U, which is, upon exclusion of the extreme outliers, at least 24 CARR U higher than the means for RV, RC and RS. As with the rat groups receiving vehicle Factor-1 doses, the rats that received CoQ_{10} and succinate both presented with the lowest of oxidative stress levels, suggesting that the therapeutic regimens may have improved serum hydroperoxide levels. The fact that no statistically significant differences were observed to be present among any of the rotenone-treated rat groups, little emphasis was placed on these discrepancies. The hydroperoxide data was finally analysed via the use of a two-way ANOVA, in the presence and absence of the

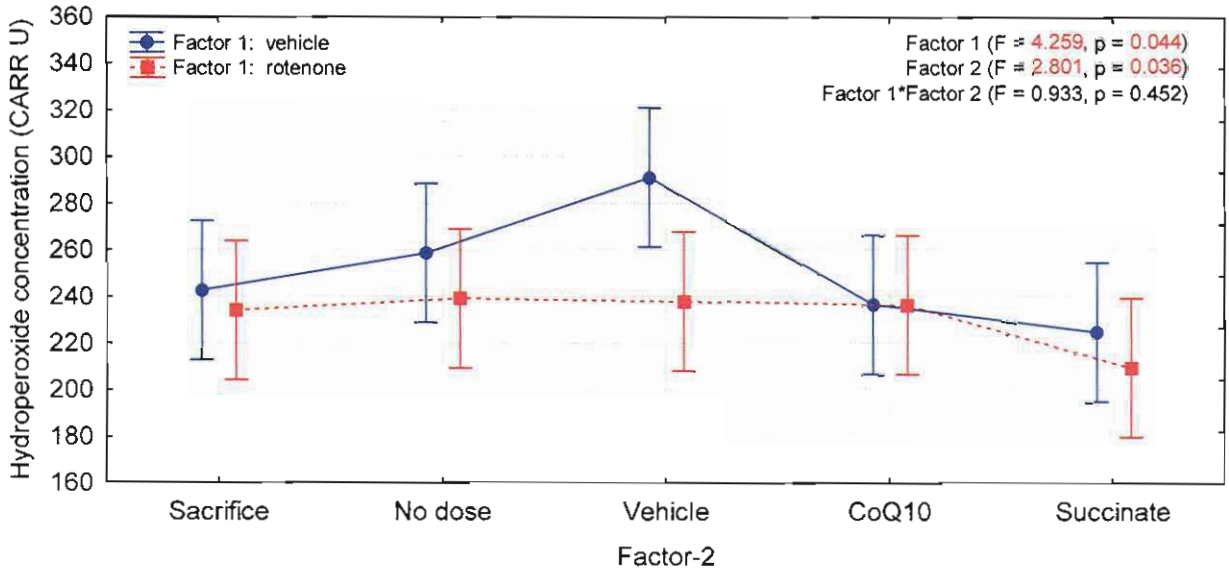
extreme outliers. Table 5.23 presents the results generated from the factorial ANOVA by means of graphic representations, F-statistics and p-values.

The exclusion of RV-1 and RC-1 as extreme outliers evidently had an impact on the two-way ANOVA results. The graphic representations of the data sets display noticeable differences. The overall effect of extreme outliers on the experiments is exemplified by the marked decrease in confidence intervals from 59.7 to 30.7 CARR U. This is a substantial adjustment considering that only two extreme outliers were present in the complete data set. The change in means due to exclusion of RV-1 and RC-1 is also evident on the graphs by observing the decrease in vehicle and CoQ_{10} data points on the rotenone plots. The mean hydroperoxide recordings as well as the UCI and LCI boundaries are listed in the tables directly below each of the graphic representations, with the adjusted means indicated in green in Table 5.23.B.

The marked impact that RV-1 and RC-1 had on the hydroperoxide data set is further exemplified by evaluating the F-statistics and p-values in each of the graphs. Factor-1 regimens, namely vehicle or rotenone, resulted in statistically significant p-values whether the extreme outliers were included or not. The same was true for dose Factor-2, that is, the exclusion of RV-1 and RC-1 similarly yielded statistically significant p-values. However, attention is drawn towards the F-statistics. The F-statistic for Factor-1 sharply increased from 4.259 to 39.19, while it only increased from 2.801 to 7.367 for dose Factor-2. Furthermore, the exclusion also resulted in two-way ANOVA rendering a highly statistically significant interaction effect with a p-value of less than 0.001. This can be confirmed by the increased divergence of the Factor-1 plots, indicated in Table 5.23.B, when compared to the graph in section A of the same table. Since the rat main study hydroperoxide data evidently illustrated that data points RV-1 and RC-1 were positioned well beyond the remaining data points in their respective data sets, and hence undoubtedly classified as extreme outliers, it can be argued that the factorial ANOVA results generated after the exclusion of RV-1 and RC-1 is a more reliable interpretation of the serum hydroperoxide data.

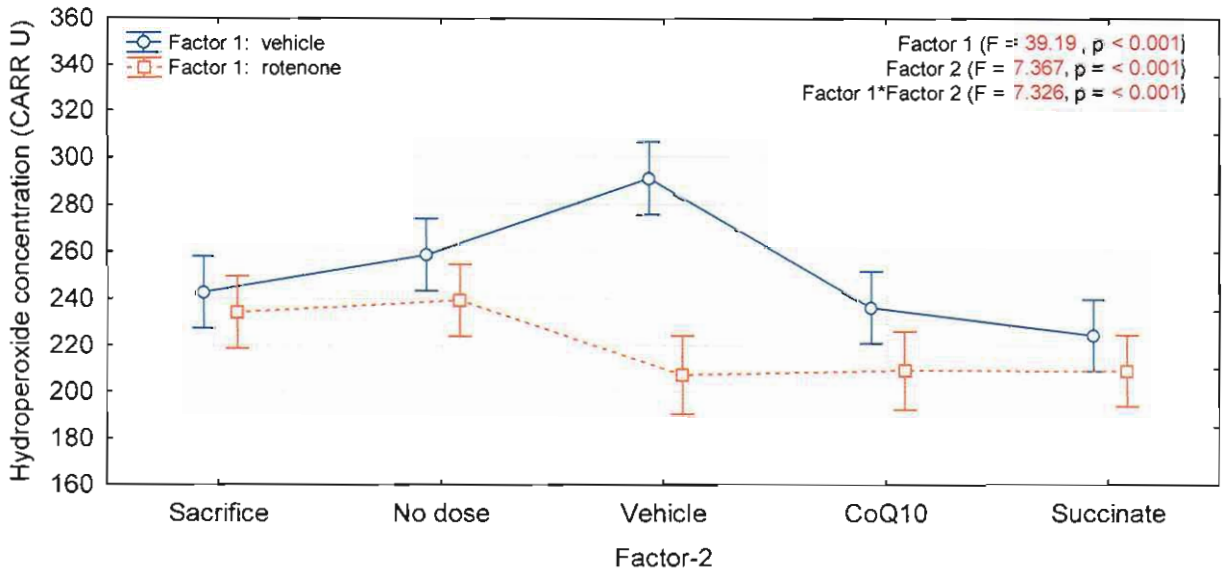
Table 5.23 Graphic and tabulated summary of the hydroperoxide data analysed via a two-way ANOVA

A: Data set including extreme outliers



Description		VX	VN	VV	VC	VS	RX	RN	RV	RC	RS
With extreme outliers	UCI	272.7	288.8	321.3	266.4	254.4	264.1	269.2	268.0	266.1	239.2
	mean	242.8	258.9	291.5	236.5	224.6	234.2	239.4	238.1	236.2	209.3
	LCI	213.0	229.0	261.6	206.6	194.7	204.3	209.5	208.3	206.4	179.5

B: Data set excluding extreme outliers



Description		VX	VN	VV	VC	VS	RX	RN	RV	RC	RS
Without extreme outliers	UCI	258.2	274.3	306.8	251.9	239.9	249.6	254.7	224.5	226.2	224.7
	mean	242.8	258.9	291.5	236.5	224.6	234.2	239.4	207.6	209.4	209.3
	LCI	227.5	243.5	276.1	221.1	209.2	218.8	224.0	190.8	192.6	194.0

The plot legends for each graph are indicated in the top left corners of the respective graphs, while the two-way ANOVA F-statistics (F) and p-values (p) for Factor-1, Factor-2 and Factor-1*Factor-2 are located in the top right corner, with the statistically significant values indicated in red. The vertical whiskers at each mean data point represent 95% confidence intervals for the respective data sets. The mean values in green text, located in the data point summary tables below the graphs, indicate those that were adjusted due to the exclusion of extreme outliers. < = less than, CARR U = Carratelli units, LCI = lower 95% confidence interval data point, UCI = upper 95% confidence interval data point. Rats were treated with NN = no dose regimen, VX = vehicle and sacrificed, VN = vehicle and no dose, VV = vehicle and vehicle, VC = vehicle and CoQ_{10}, VS = vehicle and succinate, RX = rotenone and sacrificed, RN = rotenone and no dose, RV = rotenone and vehicle, RC = rotenone and CoQ_{10}, RS = rotenone and succinate.

The graphic representation in Table 5.23.B indicates that the vehicle Factor-1 plot consistently presented with higher mean data points than those determined from the rotenone-treated rats. This is supportive of the statistically significant Factor-1 generated from the two-way ANOVA, confirming that serum hydroperoxide levels were indeed contrasted by the type of Factor-1 regimen received, namely vehicle or rotenone. It is also evident from the vehicle Factor-1 plot, as well as the statistically significant Factor-2, that CoQ_{10} and succinate lowered serum hydroperoxide levels. However, the same is true for the rotenone-treated rats, suggesting that both the Factor-1 rotenone regimen as well as the Factor-2 CoQ_{10} and succinate doses contributed to the overall lowered hydroperoxide concentrations. This validates the statistically significant interaction effect that was generated via the two-way ANOVA.

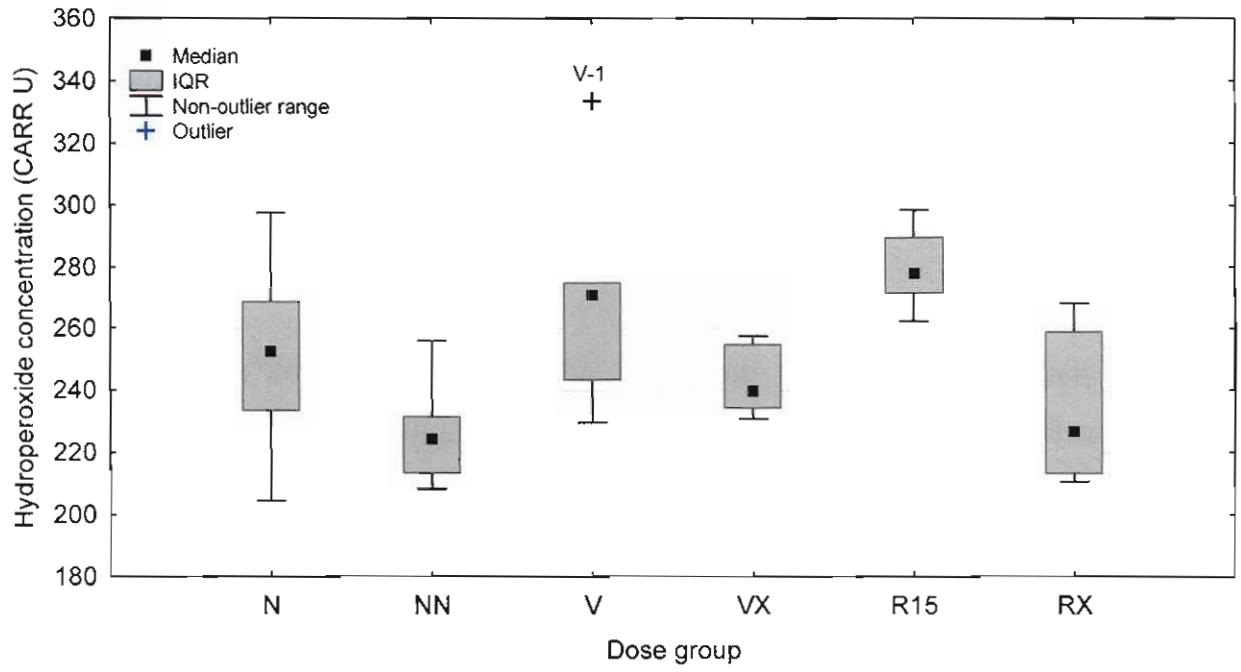
Therefore, it can be concluded that the therapeutic regimens in combination with rotenone resulted in statistically significant improvements in the serum hydroperoxide levels in rats. These statistics are also in support of previous speculations that rotenone had an antioxidant effect, contributing to the scavenging of ROS, a characteristic that will additionally be confirmed in Section 5.3.2.1. Furthermore, since the environmental control dose group NN presented with a mean hydroperoxide value of 226 CARR U, which was lower than four of the five means from the vehicle dosed groups, it can be confidently argued that the high polyunsaturated fat content of sunflower oil contributed to increasing hydroperoxide levels. This further supports the notion that the Factor-1 dose regimens induced contrasting effects to the blood-related oxidative stress levels in rats.

5.3.1.3 Comparative analysis of serum hydroperoxide data generated from the rat pilot and main studies

The hydroperoxide data from both the pilot and main studies were compared for the consistency in results and experimentation protocols. These are presented in Table 5.24. The outlier, V-1, was discussed previously in Table 5.19. Table 5.24 illustrates some unanticipated discrepancies between the paralleled dose groups. The most important feature to notice is the statistically significant difference between R15 and RX. Even though there appears to be visual differences between the environmental control dose group N and NN, as well as between V and VX, these groups were not determined to differ significantly from each other.

Table 5.24 Summary of serum hydroperoxide data generated from comparative dose groups of the rat pilot and main studies

A: Box-whisker plots and data points according to rat groups



B: Descriptive statistics

Dose group	Sample size	Mean	SD	Median	Min	Max	Range	Lower quartile	Upper quartile	IQR
N	6	252	32.8	253	205	298	92.9	234	269	35.1
NN	6	226	17.2	225	208	256	47.6	214	232	17.9
V	6	271	35.9	271	230	334	104.1	243	275	31.5
VX	6	243	11.0	240	231	258	26.7	235	255	20.2
R15	6	280	12.7	279	262	298	36.0	272	290	17.5
RX	6	234	24.9	227	211	268	57.6	214	259	45.3

C: Tukey *equal number HSD* p-values

Dose group	N	NN	V	VX	R15	RX
N		0.485	0.754	0.989	0.358	0.815
NN	0.485		0.040	0.847	0.008	0.993
V	0.754	0.040		0.380	0.985	0.131
VX	0.989	0.847	0.380		0.119	0.989
R15	0.358	0.008	0.985	0.119		0.031
RX	0.815	0.993	0.131	0.989	0.031	

All comparison statistics are indicated as p-values. The p-values indicated in red are statistically significant at a significance level of 0.05, while all other p-values are in grey. Rats were dosed N = no dose (pilot study), NN = no dose (main study), V = vehicle (pilot study), VX = vehicle (main study), R15 = rotenone 15 $mg.kg^{-1}.day^{-1}$ (pilot study), RX = rotenone 15 $mg.kg^{-1}.day^{-1}$ (main study). CARR U = Carratelli units.

The box-whisker plots tend to illustrate a pattern of difference between the pilot and main study. All of the hydroperoxide recordings for groups in the pilot study appear to harbour higher measurements than their main study equivalents. These inconsistencies may be explained by an increase in the hydroperoxide levels present in the control or 'standard' serum supplied in the d-ROMs kit. Although data is not presented here, it has been confirmed in the past that hydroperoxide levels of the control serum between newly

purchased and existing d-ROMs kits have differed (personal communication with Prof Francois van der Westhuizen). The measurements displayed an increase in absorbency recordings of the existing or older control serum, suggesting a cumulative increase in hydroperoxide over time. Since a single d-ROMs kit was utilised throughout the pilot and main studies, it is possible that an increase in hydroperoxide concentration of the reference sample occurred due to sublimation of the standard, which can take place even at -80°C. In turn, this may have had an increasing effect on serum hydroperoxide concentrations.

Based on the calculations that determine sample hydroperoxide concentrations, as presented in Equation 4.3 of Chapter Four, it can be confirmed that an increase in the absorbency of the standard will result in a decrease in the hydroperoxide levels for all rat samples. This scenario may explain the lowered main study oxidative stress levels and does unfortunately complicate interpretation of paralleled experimentation protocols. The only way of monitoring the equivalence in experimental procedures is by evaluating the oxidative stress relationships between dose groups within each of the sub-studies.

As presented in Table 5.24.C, dose groups N, V and R15 of the pilot study did not differ significantly from each other, nor did NN, VX and RX of the main study differ. This can be confirmed further by referring to multiple comparison p-values presented in Table 5.20 and Table 5.22 ahead for the pilot and main studies respectively. The additional statistically significant comparisons between dose groups NN and V as well as between NN and R15 are of lesser importance as the purpose of the statistical evaluation here was to verify consistency between paralleled groups of the pilot and main study.

The implications of accumulated hydroperoxide levels in the standard serum sample may be suggestive of the fact that the implications extend further into both the pilot and main studies since not all the rats were sacrificed and assayed for hydroperoxide levels on the same day. The pilot study spanned a period of two weeks and the main study four weeks. However, it is unlikely that hydroperoxide accumulation would occur over such short periods. The serum is stored at -20°C in aliquots, which were each discarded after being thawed for use. The longer time period that elapsed between the pilot and main study may however have been a determining factor. Therefore, interpretation of the hydroperoxide data within each of the sub-studies was regarded to be acceptable and more reliable.

There is no reported data on oxidative stress threshold levels in rats. Based on the hydroperoxide concentrations presented for the rat pilot and main studies, a tentative interpretation of oxidative stress levels in rats was required. The maximum hydroperoxide recording in the rat main study, excluding extreme outliers, was for a rat in the VV dose group. Rat VV-2 has a hydroperoxide measurement of 306 CARR U. It can also be observed from Table 5.21.A that there were few data points recorded beyond those in the VV dose group. According the d-ROMs kit specifications, indicated in Table 5.18, a hydroperoxide measurement of 306 CARR U is classified to be only 'borderline' oxidative stress. The mean for dose group VV was 292 CARR U, the median 298 CARR U, both of which are the highest of all the dose groups. In addition, the range of data points in this group is a narrow 39.5 CARR U with a standard deviation of only 16.9 CARR U. The data was well clustered and no outliers or extreme outliers were present.

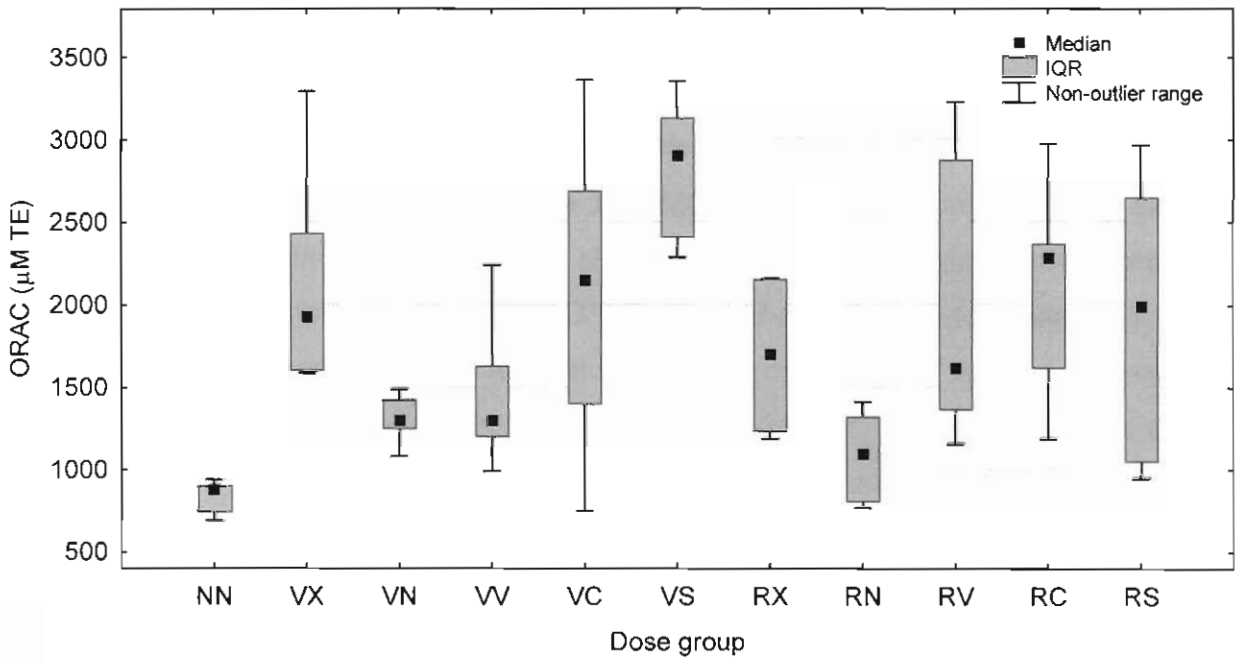
It was initially unexpected that the VV group would have the highest oxidative stress levels of all the dose groups, especially considering that no statistically significant difference was previously reported between dose groups N and V of the pilot study, as presented in Section 5.3.1.1. It would be expected that the groups that were receiving rotenone would suffer most from oxidative stress due to the partial block and electron leakage via complex I. This was true up to a certain extent or threshold level. In support of the pilot study, the data presented for the rat main study indicated that all the rat groups receiving rotenone dose regimens collectively harboured lower hydroperoxide measurements than those receiving no dose or the sunflower oil vehicle.

5.3.2 Plasma antioxidant capacity

Plasma was prepared from the collected blood and assayed for antioxidant capacity. As with the previous data sets evaluated to date, the antioxidant capacity data was captured in Excel® format and statistically evaluated in STATISTICA™. Table 5.25 presents the plasma antioxidant capacity data in terms of box-whisker plots and descriptive statistics. This blood-related data set did not present with any outliers or extreme outliers and could therefore be analysed via a simplified statistical evaluation not requiring comparative presentation of parametric and non-parametric statistical results.

Table 5.25 Box-whisker representation and descriptive statistics of the plasma antioxidant capacity data generated from the main study

A: Box-whisker plots and data points according to rat groups



Rat	NN	VX	VN	VV	VC	VS	RX	RN	RV	RC	RS
1	693	1601	1488	1623	2681	2933	2157	1312	1740	2320	1047
2	900	2424	1327	992	2683	2860	1941	802	2871	2977	1339
3	860	2216	1421	1241	3364	2287	1187	769	3233	2358	2970
4	896	3299	1082	1344	747	2408	2150	1075	1156	1188	2627
5	744	1586	1258	1196	1398	3359	1237	1102	1360	2227	2638
6	941	1635	1246	2240	1605	3126	1451	1412	1486	1615	949

B: Descriptive statistics

Dose group	Sample size	Mean	SD	Median	Min	Max	Range	Lower quartile	Upper quartile	IQR
NN	6	839	98.3	878	693	941	249	744	900	156
VX	6	2127	676	1926	1586	3299	1713	1601	2424	824
VN	6	1304	144	1293	1082	1488	406	1246	1421	175
VV	6	1439	443	1293	992	2240	1248	1196	1623	427
VC	6	2080	984	2143	747	3364	2617	1398	2683	1286
VS	6	2829	413	2897	2287	3359	1071	2408	3126	718
RX	6	1687	449	1696	1187	2157	970	1237	2150	913
RN	6	1079	260	1088	769	1412	643	802	1312	510
RV	6	1974	864	1613	1156	3233	2077	1360	2871	1511
RC	6	2114	627	2274	1188	2977	1789	1615	2358	743
RS	6	1928	912	1983	949	2970	2021	1047	2638	1591

Rats were treated with NN = no dose regimen, VX = vehicle and sacrificed, VN = vehicle and no dose, VV = vehicle and vehicle, VC = vehicle and CoQ_{10}, VS = vehicle and succinate, RX = rotenone and sacrificed, RN = rotenone and no dose, RV = rotenone and vehicle, RC = rotenone and CoQ_{10}, RS = rotenone and succinate. ORAC = oxygen radical absorbance capacity, IQR = inter-quartile range, µM TE = micromolar Trolox equivalents, Min = minimum data point value, Max = maximum data point value, SD = standard deviation.

The box-whisker plots in Table 5.25 do not present a particular pattern concerning plasma antioxidant capacity. It can be argued that rats that received CoQ_{10} and succinate in both the vehicle and rotenone Factor-1 treated groups benefited most from the dose regimens.

Dose groups VC and VS presented with improved antioxidant capacities when referring to medians in Table 5.25.B. However, the means suggest that VX and VC have very similar capacities at 2127 and 2080 μM TE respectively. Similar to VC and VS, dose groups RC and RS also appeared to have higher antioxidant capacities than the remaining groups that received rotenone. Table 5.25.B does however also list a mean antioxidant capacity statistic for RV similar to that of RS at 1974 μM and 1928 μM TE respectively. It is surprising to see that NN had the lowest antioxidant capacity of all the groups, suggesting that all dose regimens improved antioxidant status in plasma. The statistical significance of the aforementioned comparisons as well as the remaining dose group comparisons was determined via the Tukey *equal number HSD* multiple comparison procedure. The p-values are presented in Table 5.26, followed by the one-way ANOVA p-value and biological significance of statistically significant comparisons.

Table 5.26 Multiple comparison statistics of the plasma antioxidant capacity data generated from the rat main study

A: Tukey *equal number HSD* p-values

Dose group	NN	VX	VN	VV	VC	VS	RX	RN	RV	RC	RS
NN		0.021	0.960	0.823	0.031	< 0.001	0.375	1.000	0.068	0.024	0.094
VX	0.021		0.419	0.676	1.000	0.649	0.973	0.123	1.000	1.000	1.000
VN	0.960	0.419		1.000	0.506	0.003	0.990	1.000	0.707	0.442	0.786
VV	0.823	0.676	1.000		0.760	0.009	1.000	0.994	0.905	0.699	0.945
VC	0.031	1.000	0.506	0.760		0.559	0.988	0.166	1.000	1.000	1.000
VS	< 0.001	0.649	0.003	0.009	0.559		0.065	< 0.001	0.364	0.625	0.291
RX	0.375	0.973	0.990	1.000	0.988	0.065		0.811	0.999	0.978	1.000
RN	1.000	0.123	1.000	0.994	0.166	< 0.001	0.811		0.298	0.134	0.372
RV	0.068	1.000	0.707	0.905	1.000	0.364	0.999	0.298		1.000	1.000
RC	0.024	1.000	0.442	0.699	1.000	0.625	0.978	0.134	1.000		1.000
RS	0.094	1.000	0.786	0.945	1.000	0.291	1.000	0.372	1.000	1.000	

B: ANOVA p-values

One-way ANOVA p-value < 0.001

C: Statistical and biological significance

Comparison		Statistical significance (p)	Biological significance (d)
NN	VX	0.021	2.120
NN	VC	0.031	2.042
NN	VS	< 0.001	3.275
NN	RC	0.024	2.099
VN	VS	0.003	2.510
VV	VS	0.009	2.287
VS	RN	< 0.001	2.880

A: All comparison statistics are indicated as p-values generated via the parametric Tukey *equal number HSD* (Honestly Significant Difference) test. P-values indicated in red are statistically significant at the pre-determined significance level of 0.05, while the remainder of p-values are listed in grey. B: P-value for the parametric one-way ANOVA is listed, with significance below the 0.05 significance level indicated in red. The turquoise shaded blocks represent statistically significant comparisons that were also determined to be of biological significance. C: List of comparisons determined to be statistically significant with corresponding biological significance. A d-value greater than or equal to 0.8 signifies biological significance, indicated in red. Rats were treated with NN = no dose regimen, VX = vehicle and sacrificed, VN = vehicle and no dose, VV = vehicle and vehicle, VC = vehicle and CoQ_{10}, VS = vehicle and succinate, RX = rotenone and sacrificed, RN = rotenone and no dose, RV = rotenone and vehicle, RC = rotenone and CoQ_{10}, RS = rotenone and succinate. < = less than, ANOVA = analysis of variance.

The one-way ANOVA yielded a statistically significant p-value of < 0.001, indicating that a difference exists between at least one of the comparisons of the plasma antioxidant capacity data set. This significance was confirmed by the presence of seven statistically significant p-values in the Tukey *equal number HSD* multiple comparison procedure output, presented in Table 5.26.A. These comparisons were also illustrated to differ on a biological level, as indicated by the turquoise shading and d-values in Table 5.26.A and Table 5.26.C respectively. The multiple comparison grid confirms the improved antioxidant capacities in VC and VS when compared to dose group NN. An additional two groups differed significantly from NN, namely VX and RC. Dose group RS, even though it appears in the box-whisker plot to be very different from NN, did not differ significantly on a statistical level. Since VX, VC, VS and RC differ significantly from NN, it suggests that these dose group regimens improved the antioxidant capacity in rats. However, if VX differed significantly from NN, indicating that the vehicle improved plasma antioxidant capacity, it would be expected that VN too would have a higher antioxidant capacity than NN. In addition, VV would be expected to harbour a capacity very similar to VX, since the only difference between these groups is the additional two days of vehicle for VV. The former scenario is true with VN having a mean antioxidant capacity of 1304 μM TE compared with the mean of 839 μM TE for NN. However, the mean and median VV antioxidant capacities of 1439 μM and 1293 μM TE are both approximately 700 μM TE lower than that of VX. This appears to be a relatively large difference, but due to the wide and overlapping data distributions, these groups were not determined to differ significantly from each other.

The fact that dose group RC differed significantly from NN is suggestive of the fact that rotenone in combination with CoQ_{10} was beneficial to the rats in terms of antioxidant capacity. It can be recalled from the previous section, where serum hydroperoxide levels were presented, that both rotenone and CoQ_{10}, as well as in combination, proved to be beneficial by lowering hydroperoxide concentrations. However, if rotenone were to improve antioxidant status in plasma directly, it would be expected that all the rotenone-treated rats would present with improved antioxidant capacity levels. This cannot be conclusively reported as it can be visualised in Table 5.21.A that there is no clear distinction between rat groups that received vehicle and rotenone Factor-1 regimens. In fact, the data suggests that CoQ_{10} and succinate contributed most to the increase in antioxidant capacity, as was the case with the serum hydroperoxide data. All four groups that received CoQ_{10} or succinate, namely VC, VS, RC and RS, presented with the highest

antioxidant capacity levels, irrespective of whether they received rotenone or vehicle Factor-1 doses.

Table 5.25 indicates that both VX and RX harboured higher antioxidant capacities than NN. In addition, since there is a minimal difference in antioxidant capacities between dose groups VX and RX, it suggests not only that rotenone did not improve antioxidant capacity, but also that vehicle itself is the prime dose factor that improved antioxidant capacity in all rat groups. Moreover, all of the rat groups that received vehicle Factor-1 regimens harboured increased plasma antioxidant capacities when compared to the environmental controls NN. As presented in Section 5.3.1.2, serum hydroperoxide levels were increased in the vehicle Factor-1 treated rat groups, which was argued to result from the high polyunsaturated fat content of sunflower oil. This is in contrast to the antioxidant capacity data presented here. Since sunflower oil is known to be composed of high levels of vitamin E, it is understandable that the vehicle might have improved antioxidant status, even though oxidative stress was also induced by sunflower oil.

Furthermore, the ORAC assay standard curve is generated from a vitamin E analogue, Trolox, which is a powerful scavenger of ROS (Ou *et al.*, 2001). This scenario reveals that the vehicle Factor-1 treated rats presented with improved antioxidant capacities, in the presence of elevated hydroperoxide concentrations, suggesting a shift in the balance of blood-related redox status. In support of the proposed antioxidant capacity of rotenone, it should be noted that rotenone did induce Complex I deficiency, as presented in subsequent sections, which in turn results in the formation of ROS. It can be recalled from the hydroperoxide data of the rat pilot study in Section 5.3.1.1 that an increase in rotenone concentrations did indeed result in an increase in ROS formation up to a certain threshold point, after which a decline in ROS to approximately normal ranges was recorded for the highest doses of rotenone. This was supported by hydroperoxide data generated from the main study, as discussed in Section 5.3.1.2. It was therefore postulated that rotenone, in its unbound state, scavenged the ROS that was being formed by the induced Complex I deficiency. In light of this, it can be speculated that both the sunflower oil vehicle and rotenone may contribute to improving antioxidant capacity, even though these compounds may be harmful in other aspects. Therefore, in combination, the rotenone in sunflower oil vehicle is argued to re-establish antioxidant capacity to a range equivalent to that of dose group VX.

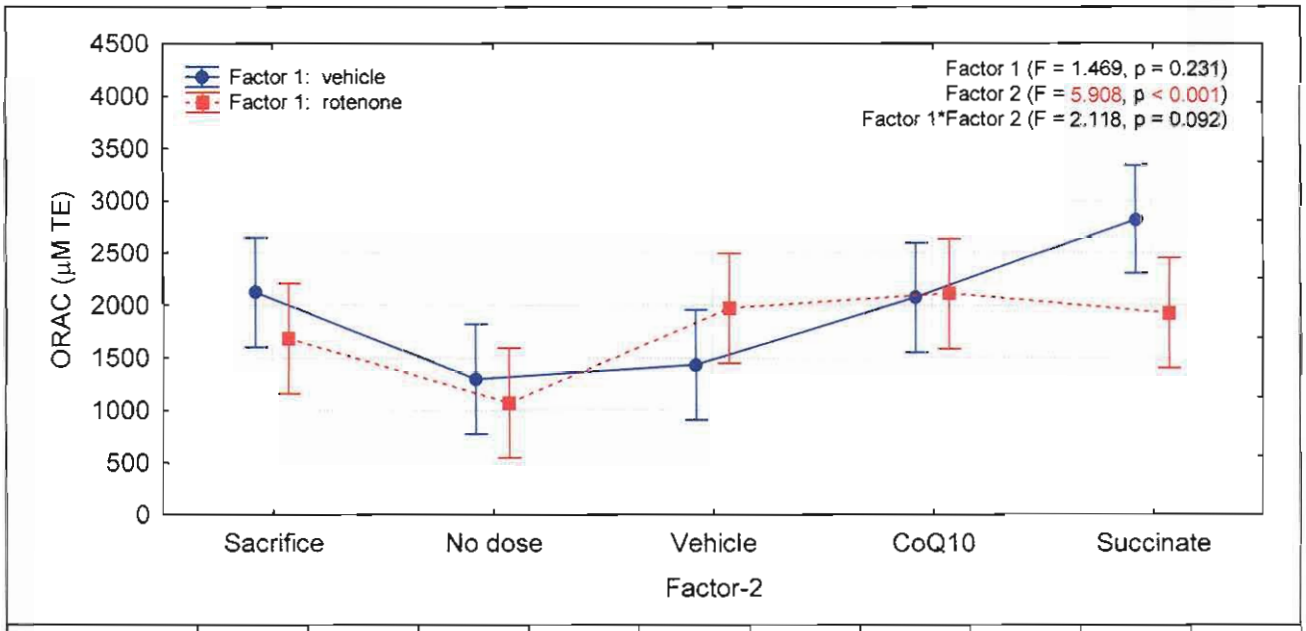
The multiple comparison grid in Table 5.26.A also indicated statistically significant p-values for comparisons between dose groups VS and VN, as well as for VS and VV. This suggests that succinate improved antioxidant capacity significantly more than in rats that received no dose or vehicle Factor-2 regimens. Succinate was dosed in a Milli-Q® water vehicle, as opposed to CoQ_{10} and rotenone, which were dosed in sunflower oil. Milli-Q® water is purified and de-ionised water, which is not expected to influence antioxidant capacity or any other biochemical parameter. Therefore, since succinate was dosed in a Milli-Q® water vehicle, alterations in the antioxidant capacities, as observed for VS and RS, are as a result of succinate alone. The data therefore indicates that succinate improved antioxidant capacity in plasma, building on the initially established antioxidant capacity generated by sunflower oil and rotenone in the respective dose groups.

The final two rat groups to differ statistically significantly from each other were dose groups VS and RN. These two groups are not comparative, as too many dose factor differences exist between these two groups. However, it is noticeable that the trend in the rotenone-treated rat groups is very similar to that observed in the dose groups that received a vehicle Factor-1 dose, where the two dose groups that received a no dose Factor-2 regimen presented with the lowest of the plasma antioxidant capacities. This indicates that the rats that received no dose on days 15 and 16 lost the antioxidant capacity gained over the first 14 days, which was argued in the previous paragraph to be improved by the sunflower oil vehicle and rotenone dose regimens. This argument is strengthened by observing that both VN and RN harboured comparative antioxidant capacities to dose group NN. The plasma antioxidant capacity data set was further analysed via two-way ANOVA to investigate the contributions from Factor-1 and Factor-2 dose regimens. A graphic summary of the two-way ANOVA results is presented in Table 5.27.

As mentioned previously in this section, it is apparent that a similarity in trends between the rat groups that received vehicle and rotenone Factor-1 dose regimens. The plots in Table 5.27 confirm this concordance. The vehicle and rotenone Factor-1 plots both display a drop in means when the no dose Factor-2 treatment was received, followed by an increase in antioxidant capacities when the other Factor-2 doses were administered. The F-statistics and p-values in the top right corner of the graphic summary indicate that Factor-2 doses significantly contributed to the antioxidant capacity levels observed in the different rat groups. The F-statistic of 5.908 was determined to be highly significant with a p-value of < 0.001. This Factor-2 main effect generated by the two-way ANOVA suggests

that Factor-2 doses had the greatest impact on the antioxidant capacity responses in rats. These results support the notion that CoQ_{10} and succinate improved the capacity in plasma. Both the vehicle and rotenone Factor-1 plots displayed the highest mean antioxidant capacities when CoQ_{10} and succinate were administered. These improvements for VC, VS, RC and RS are strongly supported by the more robust median statistics, which are of the highest among the dose groups, as listed in Table 5.25.B.

Table 5.27 Graphic and tabulated summary of the plasma antioxidant capacity data analysed via a two-way ANOVA



Data points	VX	VN	VV	VC	VS	RX	RN	RV	RC	RS
UCI	2649	1826	1961	2602	3351	2209	1600	2496	2636	2450
mean	2127	1304	1439	2080	2829	1687	1079	1974	2114	1928
LCI	1605	782	917	1558	2307	1165	557	1452	1592	1406

The plot legend is indicated in the top left corner of the graph, while the two-way ANOVA F-statistics (F) and p-values (p) for Factor-1, Factor-2 and Factor-1*Factor-2 interaction are located in the top right corner, with the statistically significant values indicated in red. The vertical whiskers at each mean data point represent 95% confidence intervals. Rats were treated with NN = no dose regimen, VX = vehicle and sacrificed, VN = vehicle and no dose, VV = vehicle and vehicle, VC = vehicle and CoQ_{10}, VS = vehicle and succinate, RX = rotenone and sacrificed, RN = rotenone and no dose, RV = rotenone and vehicle, RC = rotenone and CoQ_{10}, RS = rotenone and succinate. < = less than, LCI = lower 95% confidence interval data point, µM TE = micromolar Trolox equivalents, ORAC = oxygen radical absorbance capacity, UCI = upper 95% confidence interval data point.

The CoQ_{10} and succinate comparatively improved plasma antioxidant capacities and since no statistically significant differences were determined to exist between VC and VS as well as between RC and RS, it cannot be concluded that rats responded better to either of the doses. An important result to note is that a rotenone Factor-1 dose did not adversely affect the antioxidant capacity. Even though it was not possible to assay complex I activities in blood, complex I activities were indeed inhibited by rotenone in all the other tissue groups investigated, as presented in subsequent sections. The fact that the two-way ANOVA reports no statistically significant main effect for Factor-1, even though

overall suppression was evident in the rotenone-treated rats, may suggest that rotenone was indeed contributing to a higher antioxidant capacity the blood rather than lowering it.

The antioxidant capacity of a tissue defines the ability to restore ROS levels to normal ranges. A decrease in capacity is expected to be the result of increased ROS levels. The hydroperoxide data in Section 5.3.1 evidently reported a decrease in ROS levels, primarily due to the postulated scavenging capabilities of rotenone. This was further supported by speculations in this section that rotenone might have been maintaining antioxidant capacity, even though complex I inhibition was induced.

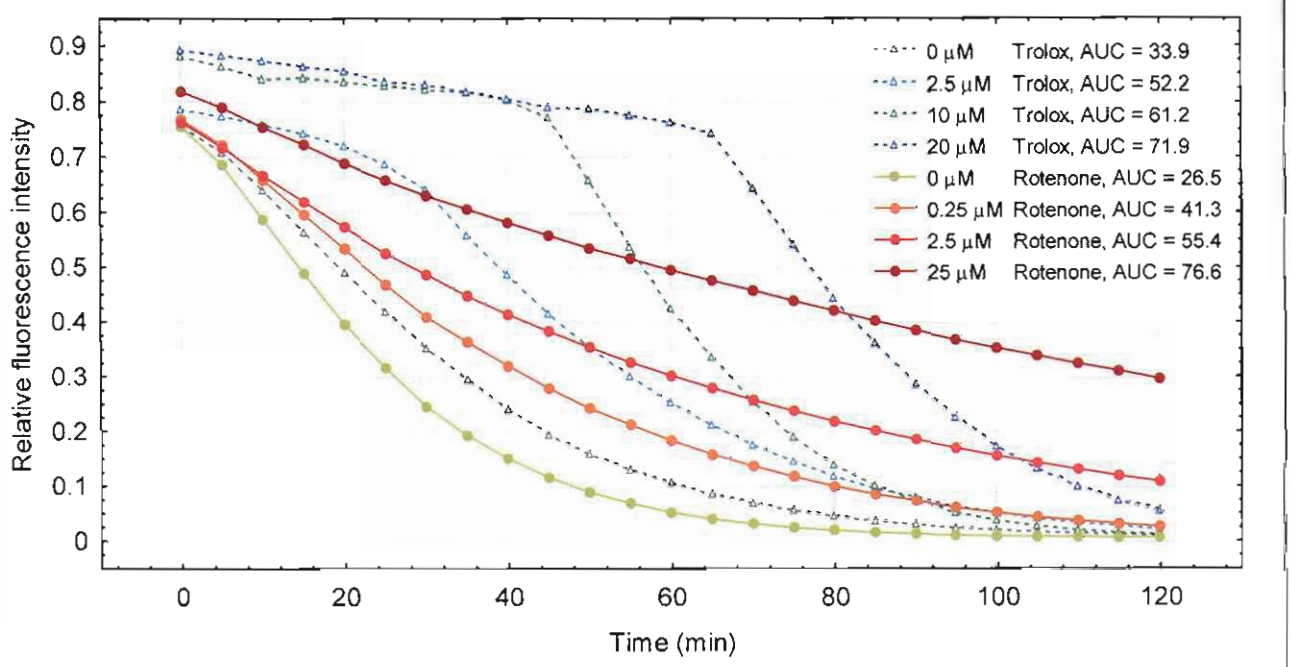
5.3.2.1 Evaluation of the antioxidant capacity of rotenone

Based on the serum hydroperoxide and plasma antioxidant capacity data generated from the rat blood samples, investigation of the antioxidant capacity of rotenone utilising the ORAC assay seemed a most prudent strategy. Rotenone was dissolved in pure ethanol and three concentrations assayed utilising the vitamin E analogue, Trolox, as a standard. The fluorescent decay plots and AUC data is presented in Table 5.28.

The graphic representation in Table 5.28 is representative of the decay of fluorescein in the presence of various concentrations of rotenone and the Trolox standard. Solid line curves and circular data points represent fluorescein decay in the presence of rotenone, while the dashed lines and triangular data points represent decay in the presence of Trolox. Fluorescence decreases in all samples from time zero, after which it either decreases steadily or encounters a sudden rapid decrease. In the case of Trolox, as the concentration of the antioxidant increases, the longer it takes before the curve reaches the rapid decrease point. This is typical of the fluorescent decay in the presence of Trolox, indicating that the antioxidant is scavenging peroxyl radicals at almost the same rate that it is being formed via the decomposition of AAPH, until the concentration threshold of Trolox is reached. At this point, the fluorescence starts to decrease rapidly, as indicated by the rapid drop in curve shape. In contrast, fluorescein decay in the presence of rotenone is more gradual and consistent. Even though the data is not presented, this curve shape was encountered for the majority of sample preparations assayed in the study.

Table 5.28 Fluorescent decay curves and antioxidant capacity of rotenone in relation to Trolox

A: Fluorescent decay curves



B: Trolox and rotenone area under the curve and antioxidant capacity data

Trolox			Rotenone			
Concentration (μM)	AUC	AUC – blank	Concentration (μM)	AUC	AUC – blank	AC (μM TE)
0	34.4	0	0	27.7	0	0
2.5	53.7	19.3	0.25	44.2	16.4	4.84
10	62.1	27.7	2.5	57.9	30.1	9.78
20	83.7	49.2	25	78.7	50.9	22.3

AUC = area under the curve, AC = antioxidant capacity, μM = micromolar concentration, min = minute, TE = Trolox equivalents.

As per normal, the Trolox standard curves presented with an initial lag phase, followed by the rapid fluorescein decay that is delayed as a function of the Trolox concentration. Consequently, the higher the concentration of Trolox used in the reaction, the greater the AUC. The fact that rotenone too presented with increased AUC values, as the concentration increased, was indicative of the fact that rotenone itself harboured peroxyl scavenging properties and hence an antioxidant capacity. As presented in Table 5.28.B, the AUC value calculated for the 2.5 μM rotenone concentration, namely 57.9, was similar to that of the 2.5 μM Trolox standard of 53.7. However, after taking the AUC of the respective blank samples as well as the Trolox standard curve data into account, a 2.5 μM rotenone concentration was calculated to harbour an antioxidant capacity of 9.78 μM TE. In addition, the 20 μM Trolox and 25 μM rotenone AUC values were also similar at 83.7 and 78.7, respectively. Consequently, a 25 μM concentration of rotenone was determined to have an antioxidant capacity of 22.3 μM TE. Therefore, it can be stated that rotenone

itself indeed harboured an antioxidant capacity that is similar to or even higher than that of Trolox.

The antioxidant capacity data reported here for rotenone certainly adds credence to previous speculations that the complex I inhibitor may have contributed to decreasing serum hydroperoxide concentrations as well as to maintaining antioxidant status, as presented in Sections 5.3.1 and 5.3.2, respectively. It should therefore be expected that these properties would influence the redox status of all tissue groups in the rat. The scavenging potential of rotenone was one of the most notable results obtained from the study. These properties were therefore taken into consideration when analysing the data generated from several of the parameters investigated in the study.

5.3.3 GSH/GSSG ratios in blood

Blood was collected from the rats and prepared appropriately for the analysis of glutathione concentrations. The sample preparations per rat were subsequently assayed in parallel and the data captured in Excel® spreadsheets, where the ratios of GSH to GSSG were calculated accordingly. Dose group ratios were further analysed for statistically significant differences via STATISTICA™. The distribution and overview of glutathione data generated from blood is presented in Table 5.29.

Table 5.29 Box-whisker representation and descriptive statistics of the blood GSH/GSSG ratio data generated from the main study

A: Box-whisker plots and data points according to rat groups

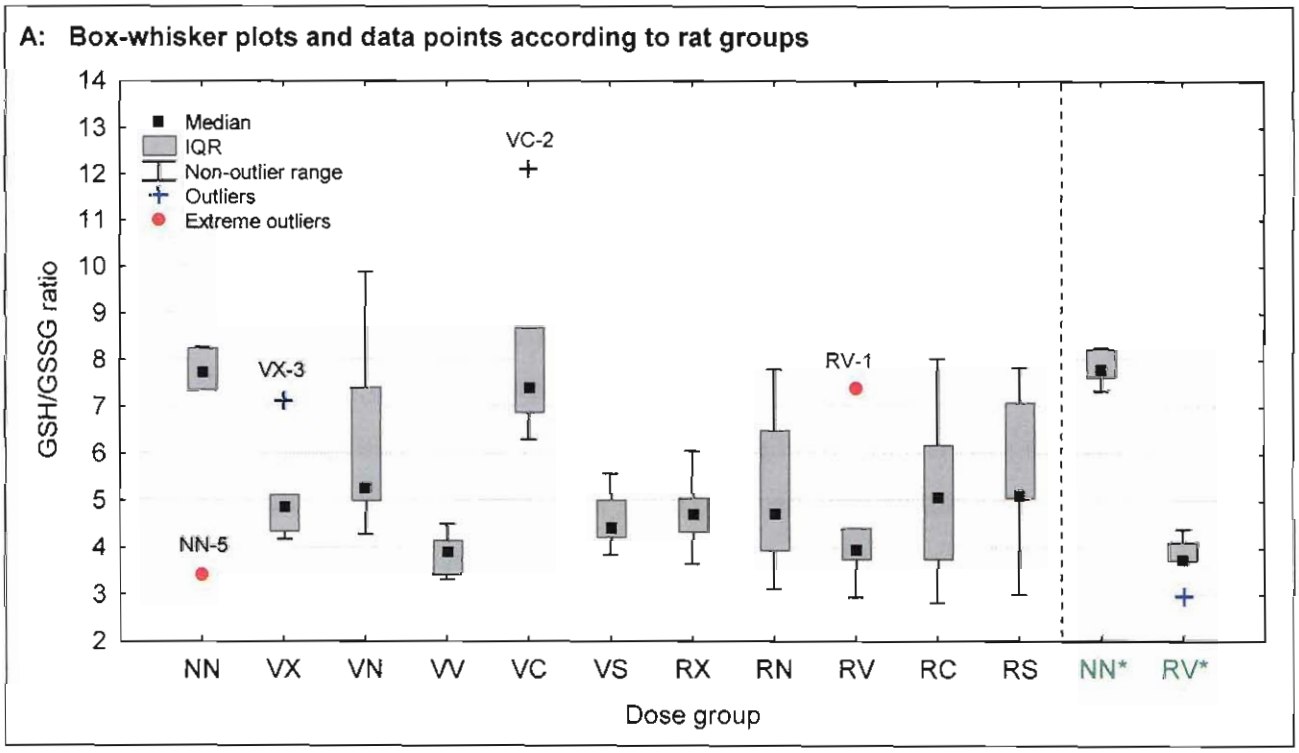


Table 5.29 Continued...

Rat	NN	VX	VN	VV	VC	VS	RX	RN	RV	RC	RS	NN*	RV*
1	8.23	5.07	5.12	3.67	8.67	4.53	3.65	3.13	• 7.37	8.04	5.05	8.23	EXCL
2	8.26	5.10	4.29	4.13	+ 12.1	3.85	6.06	5.24	4.12	3.74	7.85	8.26	4.12
3	7.34	+ 7.11	9.89	3.42	6.30	4.98	4.82	7.80	3.74	2.83	5.13	7.34	3.74
4	7.79	4.33	5.41	4.50	7.24	4.20	4.32	4.16	2.95	5.08	3.01	7.79	2.95
5	• 3.38	4.17	7.39	3.31	7.52	4.28	5.03	3.93	4.40	6.16	7.07	EXCL	4.40
6	7.62	4.64	4.99	4.12	6.87	5.58	4.56	6.47	3.75	5.02	5.08	7.62	3.75

B: Descriptive statistics

Dose group	Sample size	Mean	SD	Median	Min	Max	Range	Lower quartile	Upper quartile	IQR
NN	6	7.10	1.86	7.71	3.38	8.26	4.88	7.34	8.23	0.89
NN*	5	7.85	0.40	7.79	7.34	8.26	0.92	7.62	8.23	0.60
VX	6	5.07	1.07	4.85	4.17	7.11	2.95	4.33	5.10	0.77
VN	6	6.18	2.10	5.26	4.29	9.89	5.60	4.99	7.39	2.41
VV	6	3.86	0.47	3.89	3.31	4.50	1.19	3.42	4.13	0.71
VC	6	8.12	2.10	7.38	6.30	12.1	5.79	6.87	8.67	1.80
VS	6	4.57	0.62	4.40	3.85	5.58	1.73	4.20	4.98	0.78
RX	6	4.74	0.80	4.69	3.65	6.06	2.41	4.32	5.03	0.71
RN	6	5.12	1.75	4.70	3.13	7.80	4.67	3.93	6.47	2.55
RV	6	4.39	1.54	3.93	2.95	7.37	4.42	3.74	4.40	0.66
RV*	5	3.79	0.55	3.75	2.95	4.40	1.45	3.74	4.12	0.38
RC	6	5.15	1.83	5.05	2.83	8.04	5.21	3.74	6.16	2.42
RS	6	5.53	1.71	5.11	3.01	7.85	4.84	5.05	7.07	2.03

Rat codes for outliers and extreme outliers are located above or below the respective blue crosses (+) and red dots (•), which correspond to data point values listed in the table directly below the graph. The vertical dashed line in the box-whisker graphic representation separates original dose group box-whiskers from those that have had the extreme outliers excluded, which are also indicated by the asterisk (*) following the dose group code. Data sets with excluded data points are designated in green text. Rats were treated with NN = no dose regimen, VX = vehicle and sacrificed, VN = vehicle and no dose, VV = vehicle and vehicle, VC = vehicle and CoQ_{10}, VS = vehicle and succinate, RX = rotenone and sacrificed, RN = rotenone and no dose, RV = rotenone and vehicle, RC = rotenone and CoQ_{10}, RS = rotenone and succinate. EXCL = excluded data point, GSH/GSSG = ratio of reduced to oxidised glutathione, IQR = inter-quartile range, Min = minimum data point value, Max = maximum data point value, SD = standard deviation.

In view of the GSH/GSSG ratios generated from rat blood, it was noted that ratios are considerably lower than that obtained from human blood, which are generally greater than 100 (Berkow, 1992). However, several studies in the past have reported the lowered ratios for these animals in their respective contexts (Bayorh *et al.*, 2004; Hussain, 2004; Kadiiska *et al.*, 2000). The box-whisker plots in Table 5.29.A indicate the presence of three outliers and two extreme outliers. Rat NN-5, which harboured a GSH/GSSG ratio determined to be an extreme outlier, presented with a data point ratio of 3.38. The mean and median ratios for NN were calculated to be 7.10 and 7.71 respectively, which were raised to 7.85 and 7.79 when the extreme outlier NN-5 was excluded. The SD decreased from 1.86 to 0.40, while the IQR decreased from 0.89 to 0.60. The box-whisker plot for dose group NN illustrates the close grouping of five data points and one extreme outlier. Due to the narrow grouping of five of the six data points, the exclusion of NN-5 resulted in minor alterations to central tendency statistics, as discussed previously. The second extreme outlier was reported for dose group RV. An exclusion of RV-1 results in a mean decrease from 4.39 to 3.79, while the median decreased far less from 3.93 to 3.75. The

SD decreased from 1.54 to 0.55, and the IQR from 0.66 to 0.38. As with several previous data sets the non-parametric descriptive statistics of median and IQR were altered considerably less than their parametric mean and SD counterparts. Outlier VX-3 harboured a blood GSH/GSSG ratio of 7.11, which was positioned very near to the upper outlier boundary at a ratio of 7.41. Therefore, if it were to be excluded, it is expected that a substantial difference in the central tendency statistics would be observed. In contrast, an exclusion of the outlier in dose group VC would have less impact on the descriptive statistics. Even though rat VC-2 harboured the highest GSH/GSSG ratio of all the rats, the data point is situated well within the outlier boundary. With the upper outlier boundary being at 14.1, the 12.1 ratio for VC-2 is measured to be a comfortable 2.0 units from being classified an extreme outlier. The fact that dose group VC presents with an IQR of 1.80, allows for wider non-outlier and outlier ranges than when compared to dose group VX, which had more narrowly clustered data points and an IQR of 0.77. The third outlier, indicated for RV*, was revealed only after the extreme outlier RV-1 was excluded.

The box-whisker representation in Table 5.29 indicates that all rat groups receiving a dose regimen, excluding VC, appeared to present with lowered blood GSH/GSSG ratios. This is suggestive of the vehicle itself having an adverse effect on glutathione redox ratios. When extreme outlier NN-5 is excluded, the majority of data points within the overall blood GSH/GSSG data set appear to be positioned below all five data points indicated for NN*. With the exclusion of VS, it could certainly be argued that the CoQ_{10} and succinate Factor-2 doses contributed to improving the GSH/GSSG ratios. In order to determine the statistical significance of the differences observed from the box-whisker plots of Table 5.29, the data was analysed via ANOVA and multiple comparison procedures. P-values generated from the aforementioned statistical analyses of the blood GSH/GSSG data, including and excluding extreme outliers, is presented in Table 5.30. A list of biologically significant comparisons accompanies the statistical data.

Kruskal-Wallis and one-way ANOVA p-values generated from the blood GSH/GSSG data are both highly significant below the 0.05 significance level. The exclusion of the extreme outliers resulted in a marked decrease in the p-values from 0.005 to < 0.001, as indicated in Table 5.30.B. Although the ANOVA tests differ conceptually from each other, the large increase in significance strongly supports the exclusion of extreme outliers NN-5 and RV-1. This marked increase in significance of the ANOVA p-value after the exclusion of extreme outliers is well complemented by the increase in the number of statistically significant comparisons determined from the multiple comparison procedures.

Table 5.30 Multiple comparison statistics of the blood GSH/GSSG ratio data generated from the rat main study

A: Non-parametric (original data set) and parametric (excluding extreme outliers) p-values

Dose group	NN	VX	VN	VV	VC	VS	RX	RN	RV	RC	RS
NN		1.000	1.000	0.054	1.000	1.000	1.000	1.000	0.357	1.000	1.000
		0.090	0.729	0.002	1.000	0.021	0.035	0.104	0.002	0.110	0.272
VX	1.000		1.000	1.000	1.000	1.000	1.000	1.000	1.000	1.000	1.000
	0.090		0.951	0.916	0.017	1.000	1.000	1.000	0.932	1.000	1.000
VN	1.000	1.000		0.428	1.000	1.000	1.000	1.000	1.000	1.000	1.000
	0.729	0.951		0.164	0.395	0.658	0.789	0.964	0.233	0.969	0.999
VV	0.054	1.000	0.428		0.007	1.000	1.000	1.000	1.000	1.000	1.000
	0.002	0.916	0.164		< 0.001	0.998	0.990	0.893	1.000	0.882	0.609
VC	1.000	1.000	1.000	0.007		0.409	0.690	1.000	0.064	1.000	1.000
	1.000	0.017	0.395	< 0.001		0.003	0.005	0.021	0.001	0.022	0.078
VS	1.000	1.000	1.000	1.000	0.409		1.000	1.000	1.000	1.000	1.000
	0.021	1.000	0.658	0.998	0.003		1.000	1.000	0.998	1.000	0.981
RX	1.000	1.000	1.000	1.000	0.690	1.000		1.000	1.000	1.000	1.000
	0.035	1.000	0.789	0.990	0.005	1.000		1.000	0.991	1.000	0.996
RN	1.000	1.000	1.000	1.000	1.000	1.000	1.000		1.000	1.000	1.000
	0.104	1.000	0.964	0.893	0.021	1.000	1.000		0.914	1.000	1.000
RV	0.357	1.000	1.000	1.000	0.064	1.000	1.000	1.000		1.000	1.000
	0.002	0.932	0.233	1.000	0.001	0.998	0.991	0.914		0.905	0.676
RC	1.000	1.000	1.000	1.000	1.000	1.000	1.000	1.000	1.000		1.000
	0.110	1.000	0.969	0.882	0.022	1.000	1.000	1.000	0.905		1.000
RS	1.000	1.000	1.000	1.000	1.000	1.000	1.000	1.000	1.000	1.000	
	0.272	1.000	0.999	0.609	0.078	0.981	0.996	1.000	0.676	1.000	

B: ANOVA p-values

Kruskal-Wallis p-value = 0.005	One-way ANOVA p-value < 0.001

C: Statistical and biological significance

Comparison		Statistical significance (p)		Biological significance (d)	
		Including EOs	Excluding EOs	Including EOs	Excluding EOs
NN	VV	0.054	0.002	N/A	2.838
NN	VS	1.000	0.021	N/A	2.333
NN	RX	1.000	0.035	N/A	2.212
NN	RV	0.357	0.002	N/A	2.888
VX	VC	1.000	0.017	N/A	2.170
VV	VC	0.007	< 0.001	2.029	3.031
VC	VS	0.409	0.003	N/A	2.525
VC	RX	0.690	0.005	N/A	2.404
VC	RN	1.000	0.021	N/A	2.134
VC	RV	0.064	0.001	N/A	3.080
VC	RC	1.000	0.022	N/A	2.113

A: All comparison statistics are indicated as p-values. The upper p-value is the non-parametric multiple comparison test statistic, generated from the original set of data. The lower p-value was generated via the parametric Tukey *unequal number HSD* (Honestly Significant Difference) test, after the exclusion of extreme outliers. P-values indicated in red are statistically significant at the pre-determined significance level of 0.05. P-values in black text represent those that are not statistically significant, but have complementary p-values that are statistically significant. The remainder of p-values are listed in grey. The comparisons surrounded by the **bold** black line are those that were determined to be statistically significant by both the non-parametric and parametric multiple comparison procedures. The turquoise shaded blocks represent statistically significant comparisons that were also determined to be of biological significance. B: P-values for the non-parametric Kruskal-Wallis ANOVA and parametric one-way ANOVA are listed, with significant p-values, less than the 0.05 significance level, indicated in red. C: List of comparisons determined to be statistically significant with corresponding biological significance. A d-value greater than or equal to 0.8 signifies biological significance, indicated in red. Rats were treated with NN = no dose regimen, VX = vehicle and sacrificed, VN = vehicle and no dose, VV = vehicle and vehicle, VC = vehicle and CoQ_{10}, VS = vehicle and succinate, RX = rotenone and sacrificed, RN = rotenone and no dose, RV = rotenone and vehicle, RC = rotenone and CoQ_{10}, RS = rotenone and succinate. ANOVA = analysis of variance, EOs = extreme outliers, GSH/GSSG = ratio of reduced to oxidised glutathione, N/A = not applicable.

Prior to exclusion, only the comparison between VV and VC differed significantly, whereas a total of 11 statistically significant comparisons were determined to be present after the exclusion. In addition, all of the statistically significant comparisons, indicated in the multiple comparison grid, were determined to be of biological significance, as listed in Table 5.30.C. A statistically significant difference between dose groups VV and VC was also determined after the extreme outliers were excluded. Therefore, based on the data presented here, it can be concluded with confidence that the blood GSH/GSSG ratios for VV and VC differed from each other and that CoQ_{10} certainly contributed beneficially. However, as noted prior to multiple comparison analyses, the environmental control dose group NN appeared to harbour the highest GSH/GSSG ratio, suggesting that the sunflower oil vehicle may have induced oxidative stress and GSH depletion. The 7.85 GSH/GSSG mean ratio for dose group NN, after the exclusion of NN-5, is similar to the 8.12 mean ratio for dose group VC. Therefore, it could be argued that CoQ_{10} was the only Factor-2 dose that was able to re-establish glutathione status amongst the rats receiving a vehicle Factor-1 dose regimen. Dose group VN included two ratio data points that were in a similar range to that of dose group VC, but on average presented with lowered mean and median GSH/GSSG ratios.

After the exclusion of NN-5 and RV-1 as extreme outliers, an additional four dose groups differed statistically and biologically significantly from the environmental controls NN. Since these four groups presented with lowered GSH/GSSG ratios, they could therefore be interpreted to consist of rats that were affected most by their respective dose regimens. Dose groups VV, VS, RX and RV together harboured median GSH/GSSG ratios between 3.89 and 4.70, as opposed to the 7.79 ratio of NN. Dose groups VX and RN had similar median ratios of 4.85 and 4.70 respectively. However, these groups presented with larger SDs and did consist of data points overlapping with those in dose group NN. It should be noted that VX may well have differed significantly from NN if the outlier VX-3 was excluded. As mentioned previously, data point VX-3 was positioned a mere 0.30 ratio units below the upper outlier boundary of 7.41. Nonetheless, the criteria for determining extreme outliers were well defined, with extreme outlier boundaries established according to size of the IQR statistic and an outlier coefficient of 1.5 for each data set, as discussed in Section 4.5.1 of Chapter Four.

Of the four dose groups that differed statistically significantly from the environmental controls NN, two received a vehicle Factor-1 dose, namely VV and VS, while the other two, RX and RV, received rotenone. This may be suggestive of rotenone not having an

influence on GSH/GSSG ratios in blood. If rotenone were to affect blood ratios adversely, it would be expected that greater GSH depletions be present. However, box-whisker representations for the rotenone-treated rats, as indicated in Table 5.29.A, do not appear to present with lowered blood GSH/GSSG ratios when compared to the rats receiving vehicle Factor-1 dose regimens. Based on the blood-related hydroperoxide and antioxidant capacity data, presented in Sections 5.3.1.1 and 5.3.2, it can certainly be argued that rotenone was also contributing to the maintenance of blood GSH/GSSG ratios. The reported antioxidant capacity of rotenone itself, as discussed in Section 5.3.2.1, further strengthens the argument that unbound rotenone was scavenging the ROS produced by the induced Complex I deficiency. The fact that VV differed significantly from NN suggests that receiving sunflower oil for a period of 16 days compromises glutathione status in blood. As discussed previously in this section, if the VX-3 data point were to be excluded, it may well have resulted in VX also differing statistically significantly from NN, which would in turn further support the notion that sunflower oil adversely affected glutathione ratios in blood. Moreover, the box-whisker plot for dose group VN indicates that improvements were indeed observed in some of the rats that received a no dose Factor-2 regimen.

In a previous discussion in this section, it was proposed that CoQ_{10} was the only Factor-2 dose regimen that re-established glutathione status in rats that did not harbour the rotenone-induced Complex I deficiency. This was supported by the fact that neither the non-parametric nor the Tukey *unequal number HSD* multiple comparison procedures rendered statistically significant p-values when dose groups NN and VC were compared. The multiple comparison data does however indicate that succinate contributed very little, if at all, to improving GSH/GSSG ratios in rats that received a vehicle Factor-1 dose. The distribution of ratio data points for dose group VS was similar to that of VX and VV, rat groups that exclusively received vehicle Factor-1 regimens for 14 and 16 days respectively. Dose group VS did not differ statistically significantly from VX, VN and VV, but did differ significantly when compared to VC, the group that was argued to have re-established glutathione status. It should also be noted that dose group VC differed significantly from VX, whereas NN failed to. Furthermore, blood GSH/GSSG ratios of dose group VC also differed significantly from dose groups RX, RN, RV and RC. Although single factors cannot be measured when comparing blood glutathione ratios of VC with that of the rotenone-treated rats, it appears that CoQ_{10} improved glutathione status in rats receiving vehicle Factor-1 regimens. Therefore, it may be argued that CoQ_{10} was indeed significantly beneficial in alleviating GSH depletion, and hence re-establishing blood

GSH/GSSG ratios in rats that were compromised by the effects of the sunflower oil vehicle.

Among the rotenone-treated rats, no statistically significant differences were determined. All groups that received the rotenone Factor-1 dose presented with overlapping data distributions, suggesting equivalent response patterns regardless of the Factor-2 dose regimens. However, as mentioned previously, RX and RV were the only two rotenone-treated dose groups to differ significantly from the environmental controls NN after the extreme outliers were excluded. Dose groups RC and RS presented with, on average, slightly higher GSH/GSSG ratios than RX and RN, as well as of the widest IQRs. The aforementioned data characteristics contributed to the lack of statistically significant differences upon comparison of NN to both RC and RS.

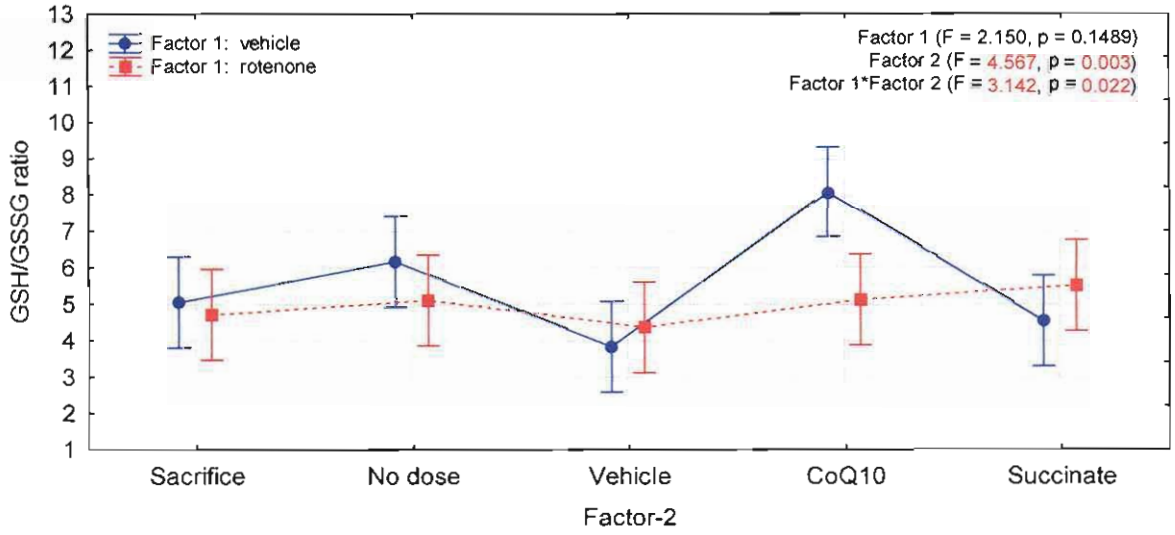
It was discussed earlier that rotenone appeared to have no effect on the blood GSH/GSSG ratios in rats. Dose groups VX and RX harboured similar ratios, which were comparatively lower than the environmental controls NN. Moreover, not only did the majority of dose groups present with data points lower than those in NN*, but they were also distributed within a similar range, with the exception of VC, which was elevated. To elucidate the contributions of Factor-1 and Factor-2 dose regimens further, a factorial ANOVA was performed on the blood GSH/GSSG data. Since two extreme outliers were identified in the data set, the two-way ANOVA was performed via the inclusion and exclusion thereof, as presented in Table 5.31.

The exclusion of RV-1 from the complete data set resulted in minor adjustments to the graphic representations and F-statistics generated from the data. Inclusion and exclusion of the extreme outlier resulted in statistically significant contributions from Factor-2 dose regimens as well as for an interaction effect between the factors. The fact that Factor-1 statistics were not significant strongly supports previous arguments that rotenone did not further influence glutathione ratios. The statistical significance of Factor-2 doses increased upon the exclusion of extreme outlier RV-1, with p-values decreasing from 0.003 to < 0.001, as presented in Table 5.31.A and Table 5.31.B, respectively. However, p-values for the interaction effect remained constant at 0.022 and 0.026 for the inclusion and exclusion of extreme outliers respectively. This implies that the RV-1 extreme outlier contributed minimally to global variation in the blood GSH/GSSG data set. The interaction effect can be confirmed by the intersection and divergence of Factor-1 plots. The vehicle

Factor-1 plots were also demonstrated to deviate over a wider range of GSH/GSSG ratios than that of the rotenone plots, which presented with a greater consistency throughout.

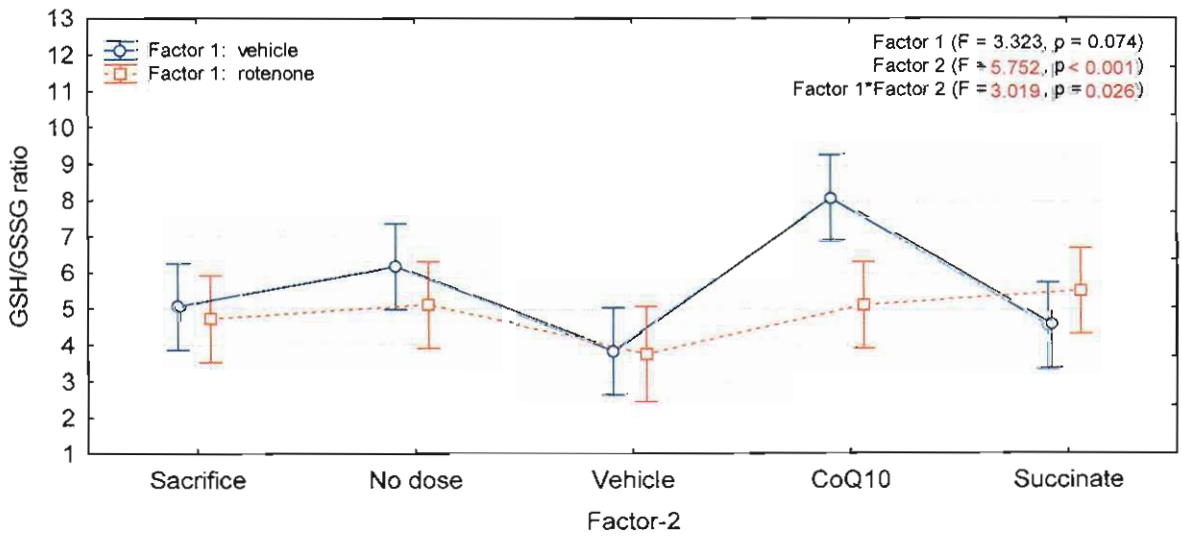
Table 5.31 Graphic and tabulated summary of the blood GSH/GSSG ratio data analysed via a two-way ANOVA

A: Data set including extreme outliers



Description		VX	VN	VV	VC	VS	RX	RN	RV	RC	RS
With extreme outliers	UCI	6.31	7.42	5.10	9.36	5.81	5.98	6.36	5.63	6.39	6.77
	mean	5.07	6.18	3.86	8.12	4.57	4.74	5.12	4.39	5.15	5.53
	LCI	3.83	4.94	2.62	6.87	3.33	3.50	3.88	3.14	3.90	4.29

B: Data set excluding extreme outliers



Description		VX	VN	VV	VC	VS	RX	RN	RV	RC	RS
Without extreme outliers	UCI	6.27	7.38	5.05	9.31	5.76	5.94	6.32	5.10	6.34	6.73
	mean	5.07	6.18	3.86	8.12	4.57	4.74	5.12	3.79	5.15	5.53
	LCI	3.87	4.98	2.66	6.92	3.37	3.54	3.93	2.48	3.95	4.34

The plot legends for each graph are indicated in the top left corners of the respective graphs, while the two-way ANOVA F-statistics (F) and p-values (p) for Factor-1, Factor-2 and Factor-1*Factor-2 are located in the top right corner, with the statistically significant values indicated in red. The vertical whiskers at each mean data point represent 95% confidence intervals for the respective data sets. The mean values in green text, located in the data point summary tables below the graphs, indicate those that were adjusted due to the exclusion of extreme outliers. < = less than, GSH/GSSG = ratio of reduced to oxidised glutathione, LCI = lower 95% confidence interval data point, UCI = upper 95% confidence interval data point. Rats were treated with NN = no dose regimen, VX = vehicle and sacrificed, VN = vehicle and no dose, VV = vehicle and vehicle, VC = vehicle and CoQ_{10}, VS = vehicle and succinate, RX = rotenone and sacrificed, RN = rotenone and no dose, RV = rotenone and vehicle, RC = rotenone and CoQ_{10}, RS = rotenone and succinate.

Since an interaction effect between Factor-1 and Factor-2 dose regimens has been determined to be present, it is required that the contribution of Factor-2 be discussed with caution. The graphic representations in Table 5.31 indicate that the vehicle Factor-1 plots, on average, appear to present with consistently higher blood GSH/GSSG ratios. This is more apparent in Table 5.31.B when RV-1 was excluded as an extreme outlier. The interaction effect may be explained by the more consistent response pattern recorded for rats that received a rotenone Factor-1 dose regimen.

The improvements in glutathione ratios, observed when rats received no dose and CoQ_{10} Factor-2 regimens, were greater when rats were initially dosed vehicle Factor-1 regimens, as opposed to rotenone. Therefore, it may be argued that rotenone indeed adversely affected rats by suppressing their ability to recover from their Factor-1 dose regimens. It was unexpected that the sunflower oil vehicle would result in GSH depletion. However, this was strongly supported by the data, presented in this section, with the environmental controls NN harbouring of the highest GSH/GSSG ratios. Results from the factorial ANOVA therefore support the concept of an interaction effect between a rotenone Factor-1 regimen and Factor-2 dose regimens, ultimately culminating in a suppression of blood GSH/GSSG ratios.

5.3.4 Lactate/pyruvate ratios in blood

Blood samples were collected and assayed for lactate and pyruvate concentrations. The ratios were consequently calculated and analysed for statistically significant variation between the different dose groups. Table 5.32 presents the blood L/P ratio data distributions by means of box-whisker plots and a table of descriptive statistics. In addition, a listing of the lactate and pyruvate concentrations generated from blood can be referred to in Table E.1 of Appendix E. As with blood GSH/GSSG ratios generated from rats, L/P ratios are considerably lower than that obtained from humans. From reports by Bayorh *et al.* (2004), Hussain (2004) and Kadiiska *et al.* (2000), it was confirmed that rat blood L/P ratios are comparable to those presented here.

Table 5.32 reveals the presence of two extreme outliers and three outliers. Two of the three outliers, indicated for RS*, will not be discussed since they were classified after the extreme outlier was excluded from the original RS dose group. The third outlier, VS-5, results in a slight elevation of the L/P ratio for dose group VS, which, with the inclusion of VS-5, appears as a group with of the lowest L/P ratios. The exclusion of VS-5 would lower

the mean and median descriptive statistics further. However, marked changes in the descriptive statistics for VS would not be expected since the inner four data points in the group are gathered within a narrow IQR of 0.19. Regardless, VS-5 is only an outlier and will not be excluded.

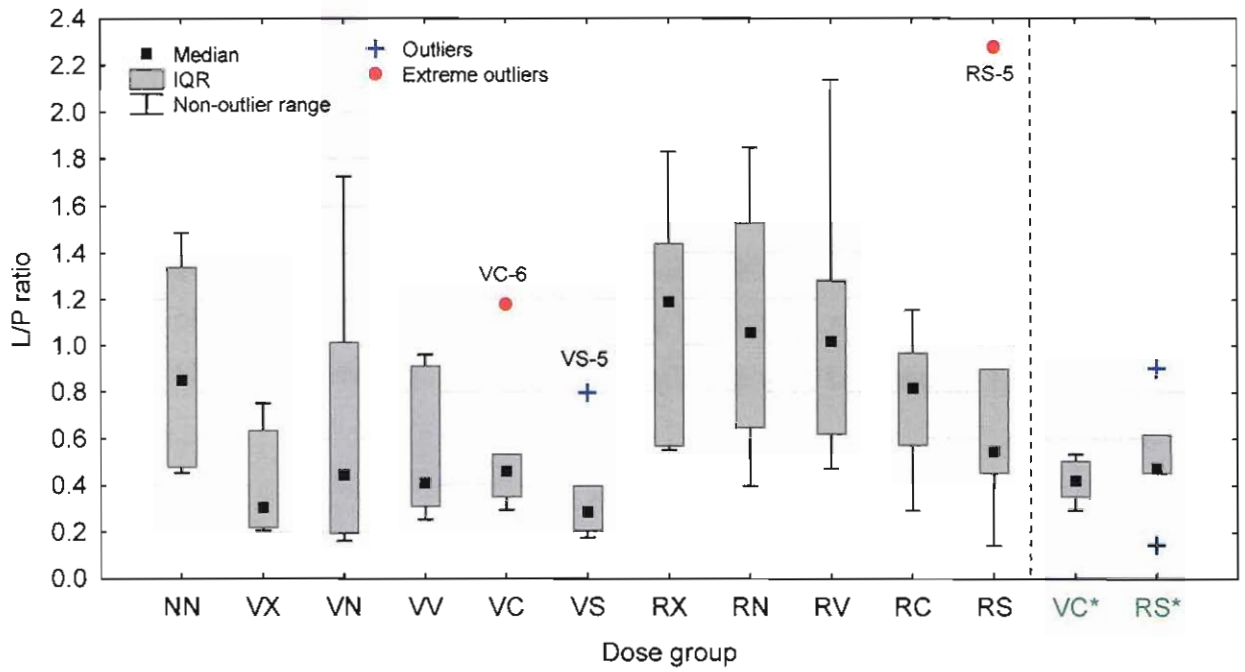
The first of the extreme outliers VC-6 harbours an L/P ratio of 1.18, while the remaining five data points in the group range from 0.29 to 0.53. The exclusion of VC-6 results in a decrease in the mean ratio from 0.54 to 0.42 for dose group VC. The complementing SD decreased by approximately a third from 0.32 to 0.10. The non-parametric counterparts, namely the median decreased only slightly from 0.46 to 0.42, while the IQR was adjusted to 0.15 from 0.18.

The second extreme outlier was determined to be present in dose group RS. The L/P ratio for rat RS-5 was calculated to be 2.28, with the nearest ratio in the group being that of RS-1, that was 0.90. The RS-5 ratio was also the highest calculated for all the rats in the blood data set. The exclusion of RS-5 results in considerable mean and SD declines from 0.81 to 0.52 and from 0.76 to 0.27 respectively. The median for RS remained relatively constant and decreased only moderately from a ratio 0.54 to 0.48. However, the IQR for the same dose group diminished considerably from 0.44 to 0.16, indicating the extremity of RS-5 in the group. The exclusion of both extreme outliers from the blood L/P ratio data set does indeed make an impact on the basic statistics, supporting the inclusion of outlier analysis in the proposed statistical strategy.

The box-whisker plots in Table 5.32 appear to indicate that all the rat groups that received a vehicle Factor-1 dose, namely VX through to VS, displayed lowered L/P ratios when compared to the environmental controls NN. In addition, it appears that the groups that received the rotenone Factor-1 dose harboured higher L/P ratios than NN, with the exclusion of dose groups RC and RS. The latter mentioned groups harboured lowered ratios than RX, RN and RV, which is suggestive of the fact that both CoQ_{10} and succinate contributed to lowering the blood L/P ratios in complex I deficient rats. In fact, the blood L/P ratios for dose groups RC and RS improved to similar and lowered ratios than the environmental controls NN respectively. As a whole, the blood L/P ratio data indicates that both rotenone and the vehicle affected the ratios.

Table 5.32 Box-whisker representation and descriptive statistics of the blood L/P ratio data generated from the main study

A: Box-whisker plots and data points according to rat groups



Rat	NN	VX	VN	VV	VC	VS	RX	RN	RV	RC	RS	VC*	RS*
1	0.48	0.33	1.72	0.96	0.50	0.24	1.44	1.53	0.85	1.15	0.90	0.50	0.90
2	0.92	0.22	1.01	0.50	0.29	0.34	1.00	0.40	1.18	0.96	0.48	0.29	0.48
3	0.78	0.75	0.16	0.25	0.53	0.39	1.83	1.85	0.47	0.87	0.14	0.53	0.14
4	0.45	0.21	0.25	0.91	0.35	0.18	0.55	0.93	2.14	0.29	0.45	0.35	0.45
5	1.49	0.63	0.63	0.32	0.42	+ 0.79	1.37	1.18	1.28	0.75	• 2.28	0.42	EXCL
6	1.34	0.29	0.20	0.31	• 1.18	0.21	0.56	0.64	0.62	0.57	0.61	EXCL	0.61

B: Descriptive statistics

Dose group	Sample size	Mean	SD	Median	Min	Max	Range	Lower quartile	Upper quartile	IQR
NN	6	0.91	0.43	0.85	0.45	1.49	1.03	0.48	1.34	0.86
VX	6	0.40	0.23	0.31	0.21	0.75	0.54	0.22	0.63	0.41
VN	6	0.66	0.61	0.44	0.16	1.72	1.56	0.20	1.01	0.82
VV	6	0.54	0.32	0.41	0.25	0.96	0.71	0.31	0.91	0.60
VC	6	0.54	0.32	0.46	0.29	1.18	0.88	0.35	0.53	0.18
VC*	5	0.42	0.10	0.42	0.29	0.53	0.24	0.35	0.50	0.15
VS	6	0.36	0.23	0.29	0.18	0.79	0.61	0.21	0.39	0.19
RX	6	1.13	0.51	1.19	0.55	1.83	1.28	0.56	1.44	0.87
RN	6	1.09	0.54	1.05	0.40	1.85	1.45	0.64	1.53	0.88
RV	6	1.09	0.60	1.01	0.47	2.14	1.67	0.62	1.28	0.66
RC	6	0.77	0.30	0.81	0.29	1.15	0.86	0.57	0.96	0.39
RS	6	0.81	0.76	0.54	0.14	2.28	2.13	0.45	0.90	0.44
RS*	5	0.52	0.27	0.48	0.14	0.90	0.75	0.45	0.61	0.16

Rat codes for outliers and extreme outliers are located above or below the respective blue crosses (+) and red dots (•), which correspond to data point values listed in the table directly below the graph. The vertical dashed line in the box-whisker graphic representation separates original dose group box-whiskers from those that have had the extreme outliers excluded, which are also indicated by the asterisk (*) following the dose group code. Data sets with excluded data points are designated in green text. Rats were treated with NN = no dose regimen, VX = vehicle and sacrificed, VN = vehicle and no dose, VV = vehicle and vehicle, VC = vehicle and CoQ_{10}, VS = vehicle and succinate, RX = rotenone and sacrificed, RN = rotenone and no dose, RV = rotenone and vehicle, RC = rotenone and CoQ_{10}, RS = rotenone and succinate. EXCL = excluded data point, IQR = inter-quartile range, L/P = ratio of lactate to pyruvate, Min = minimum data point value, Max = maximum data point value, SD = standard deviation.

The data was subsequently analysed via ANOVA and multiple comparison procedures to investigate the statistical significance of the aforementioned differences between dose groups. Table 5.33 presents parametric and non-parametric p-values of the evaluation. The ANOVA p-values for both the one-way and Kruskal-Wallis tests indicate that a difference exists between groups of the blood L/P data set. However, it is not supported by the complementing multiple comparison data. There were no dose group comparisons determined to differ significantly from each other, even when the extreme outliers were excluded from the data sets.

Table 5.33 Multiple comparison statistics of the blood L/P ratio data generated from the rat main study

A: Non-parametric and parametric p-values											
Dose group	**NN**	**VX**	**VN**	**VV**	**VC**	**VS**	**RX**	**RN**	**RV**	**RC**	**RS**
NN		1.000	1.000	1.000	1.000	0.924	1.000	1.000	1.000	1.000	1.000
		0.585	0.994	0.904	0.739	0.454	0.998	1.000	1.000	1.000	0.916
VX	1.000		1.000	1.000	1.000	1.000	0.428	0.607	0.816	1.000	1.000
	0.585		0.991	1.000	1.000	1.000	0.124	0.176	0.171	0.911	1.000
VN	1.000	1.000		1.000	1.000	1.000	1.000	1.000	1.000	1.000	1.000
	0.994	0.991		1.000	0.997	0.970	0.705	0.801	0.794	1.000	1.000
VV	1.000	1.000	1.000		1.000	1.000	1.000	1.000	1.000	1.000	1.000
	0.904	1.000	1.000		1.000	0.999	0.374	0.476	0.467	0.997	1.000
VC	1.000	1.000	1.000	1.000		1.000	1.000	1.000	1.000	1.000	1.000
	0.739	1.000	0.997	1.000		1.000	0.238	0.312	0.305	0.960	1.000
VS	0.924	1.000	1.000	1.000	1.000		0.160	0.235	0.326	1.000	1.000
	0.454	1.000	0.970	0.999	1.000		0.078	0.114	0.111	0.827	1.000
RX	1.000	0.428	1.000	1.000	1.000	0.160		1.000	1.000	1.000	1.000
	0.998	0.124	0.705	0.374	0.238	0.078		1.000	1.000	0.919	0.444
RN	1.000	0.607	1.000	1.000	1.000	0.235	1.000		1.000	1.000	1.000
	1.000	0.176	0.801	0.476	0.312	0.114	1.000		1.000	0.961	0.542
RV	1.000	0.816	1.000	1.000	1.000	0.326	1.000	1.000		1.000	1.000
	1.000	0.171	0.794	0.467	0.305	0.111	1.000	1.000		0.958	0.534
RC	1.000	1.000	1.000	1.000	1.000	1.000	1.000	1.000	1.000		1.000
	1.000	0.911	1.000	0.997	0.960	0.827	0.919	0.961	0.958		0.997
RS	1.000	1.000	1.000	1.000	1.000	1.000	1.000	1.000	1.000	1.000	
	0.916	1.000	1.000	1.000	1.000	1.000	0.444	0.542	0.534	0.997	
B: ANOVA p-values											
Kruskal-Wallis p-value = 0.017						One-way ANOVA p-value = 0.005					

A: All comparison statistics are indicated as p-values. The upper p-value is the non-parametric multiple comparison test statistic, generated from the original set of data. The lower p-value was generated via the parametric Tukey *unequal number HSD* (Honestly Significant Difference) test, after the exclusion of extreme outliers. B: P-values for the non-parametric Kruskal-Wallis ANOVA and parametric one-way ANOVA are listed, with significant p-values, less than the 0.05 significance level, indicated in red. Rats were treated with NN = no dose regimen, VX = vehicle and sacrificed, VN = vehicle and no dose, VV = vehicle and vehicle, VC = vehicle and CoQ_{10}, VS = vehicle and succinate, RX = rotenone and sacrificed, RN = rotenone and no dose, RV = rotenone and vehicle, RC = rotenone and CoQ_{10}, RS = rotenone and succinate. ANOVA = analysis of variance, L/P = ratio of lactate to pyruvate.

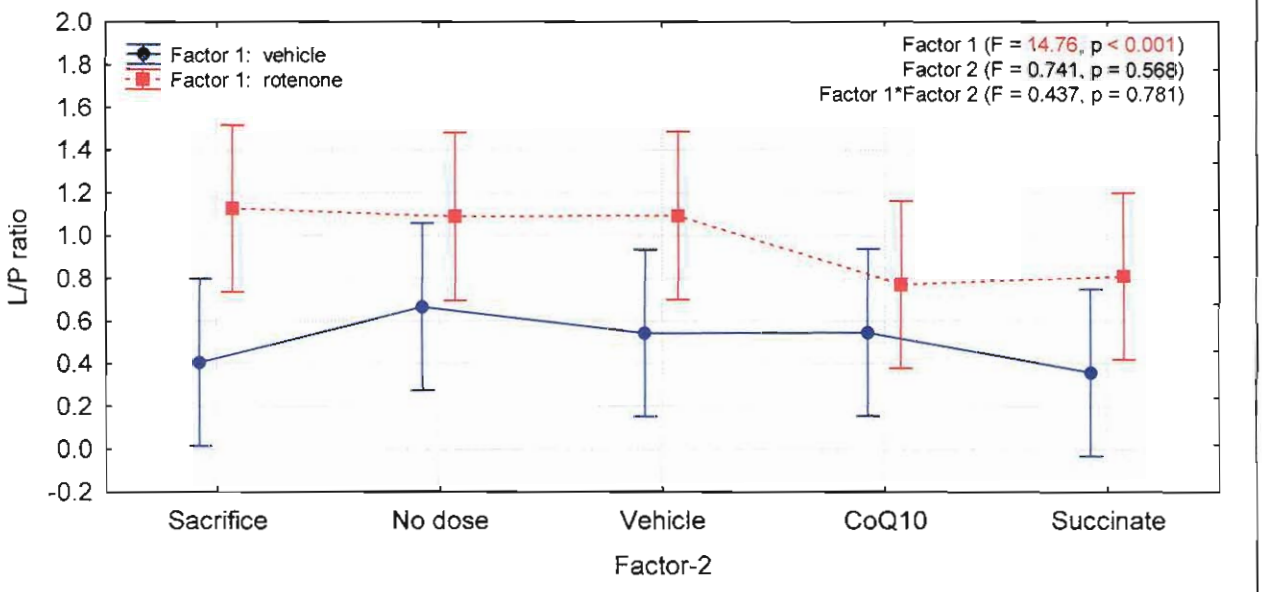
The ANOVA p-values do suggest that significant differences between groups increased when the extreme outliers were excluded. The one-way ANOVA p-value was significant below the 0.01 significance level, whereas the Kruskal-Wallis test was only significant below 0.05. Since the Kruskal-Wallis ANOVA is designed to evaluate a data set in a

non-parametric manner, as opposed to the parametric one-way ANOVA, stringency of the two test procedures differs. The Kruskal-Wallis test, being non-parametric based, is designed to be less stringent with no assumptions as to the distribution and variance of data. The one-way ANOVA assumes that the data is normally distributed with homoscedasticity in variance. Therefore, it could be argued that the difference in p-values may be an underestimate and that if a one-way ANOVA was used to evaluate the original data set, i.e. including the extreme outliers, statistical significance may not even have been reported.

Although the data is not presented, since it contravenes the proposed statistical strategy, a p-value of 0.045 was reported for a one-way ANOVA on the original data set, including the extreme outliers. The global difference is still reported by the more stringent test, even though assumptions may have been violated. The p-value is still significant beyond the 0.05 significance level, but is higher than the Kruskal-Wallis p-value of 0.017. Since no statistically significant differences were reported from the blood L/P data set, the differences between dose groups can only be discussed in terms of a trend, rather than true differences supported by statistical data.

Table 5.34 Graphic and tabulated summary of the blood L/P ratio data analysed via a two-way ANOVA

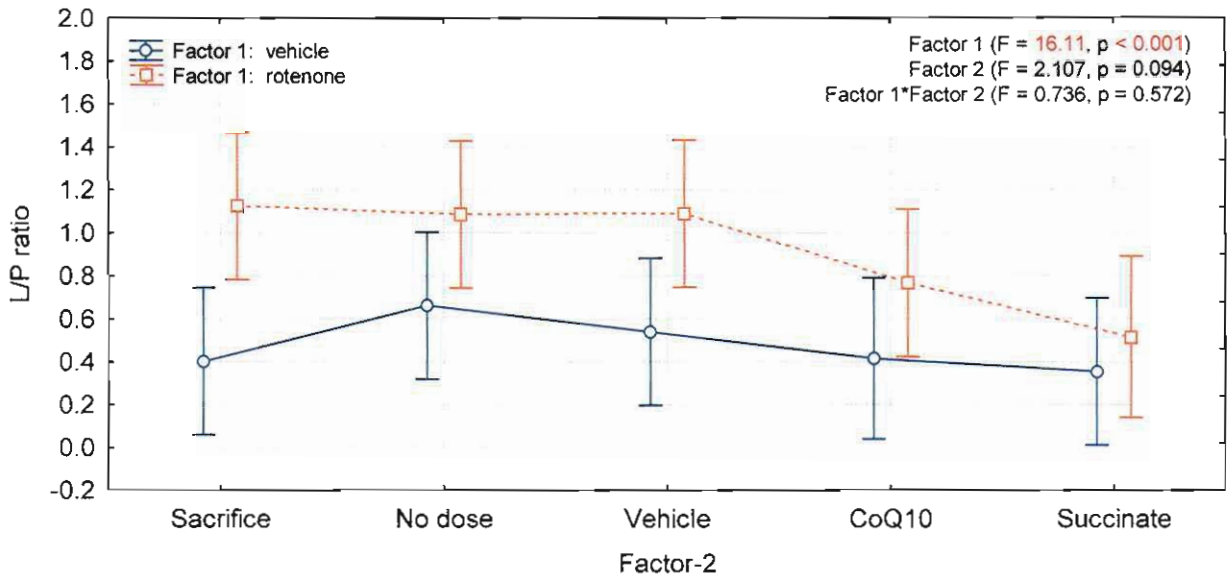
A: Data set including extreme outliers



Description		VX	VN	VV	VC	VS	RX	RN	RV	RC	RS
With extreme outliers	UCI	0.80	1.05	0.93	0.94	0.75	1.52	1.48	1.48	1.16	1.20
	mean	0.40	0.66	0.54	0.54	0.36	1.13	1.09	1.09	0.77	0.81
	LCI	0.01	0.27	0.15	0.15	-0.03	0.73	0.70	0.70	0.38	0.42

Table 5.34 Continued...

B: Data set excluding extreme outliers



Description		VX	VN	VV	VC	VS	RX	RN	RV	RC	RS
Without extreme outliers	UCI	0.75	1.01	0.88	0.79	0.70	1.47	1.43	1.43	1.11	0.89
	mean	0.40	0.66	0.54	0.42	0.36	1.13	1.09	1.09	0.77	0.52
	LCI	0.06	0.32	0.20	0.04	0.02	0.78	0.74	0.75	0.43	0.14

The plot legends for each graph are indicated in the top left corners of the respective graphs, while the two-way ANOVA F-statistics (F) and p-values (p) for Factor-1, Factor-2 and Factor-1*Factor-2 are located in the top right corner, with the statistically significant values indicated in red. The vertical whiskers at each mean data point represent 95% confidence intervals for the respective data sets. The mean values in green text, located in the data point summary tables below the graphs, indicate those that were adjusted due to the exclusion of extreme outliers. < = less than, LCI = lower 95% confidence interval data point, L/P = ratio of lactate to pyruvate, UCI = upper 95% confidence interval data point. Rats were treated with NN = no dose regimen, VX = vehicle and sacrificed, VN = vehicle and no dose, VV = vehicle and vehicle, VC = vehicle and CoQ_{10}, VS = vehicle and succinate, RX = rotenone and sacrificed, RN = rotenone and no dose, RV = rotenone and vehicle, RC = rotenone and CoQ_{10}, RS = rotenone and succinate.

Factor-1 and Factor-2 dose regimens were analysed via a two-way ANOVA and presented via graphic summary in Table 5.34. The F-statistics and p-values generated from the factorial analysis revealed statistically significant contributions from Factor-1 when extreme outliers were included and excluded from the data set. Factor-2 and the interaction between Factor-1 and Factor-2 were not determined to be statistically significant. It can also be observed from the graphic displays in Table 5.34 that the exclusion of VC-6 and RS-5 as extreme outliers resulted in a slight increase in the F-statistic for Factor-2. This can be confirmed by the visible tail mergence of the plots due to the exclusion of RS-5. In addition, the exclusion of the extreme outliers resulted in a decrease in the 95% confidence intervals from 0.79 to 0.69.

It is evident from both graphic summaries that the rotenone Factor-1 plots were consistently higher than the vehicle Factor-1 plots. The statistically significant Factor-1 F-statistics and p-values confirms that rotenone contribute to raised L/P ratios. However, the impact of vehicle on the ratios should not be disregarded. By referring back to

Table 5.25, it was evident that the median data points and IQRs for the vehicle Factor-1 dose groups were mostly lower than the environmental controls NN, once again illustrating that sunflower oil may have influenced the response of rats. The fact that rats that received no dose on days 15 and 16 presented with slightly higher L/P ratios, further supports the notion that the vehicle may be beneficial and aid in reducing L/P ratios in blood. However, as discussed previously, these groups did not differ significantly from each other, rendering these differences as mere trends. The box-whisker plots from Table 5.25 also indicate raised L/P ratios for the Factor-1 rotenone dose groups RX, RN and RV when compared to the environmental controls NN. The L/P ratios for RC and RS are very similar to that of NN.

As mentioned previously, dose groups that received vehicle as a Factor-1 dose presented with lowered L/P ratios when compared to the environmental controls NN. If sunflower oil is assumed to induce these beneficial effects, it should be taken into consideration when interpreting the data generated from rats that received rotenone, since the inhibitor was dosed in the presence of the sunflower oil vehicle. Therefore, the observed ratios in each of the rotenone-induced complex I deficient dose groups may indeed be under-estimates due to the counter effects of sunflower oil. If a vehicle with no beneficial effects were used, it may be that higher L/P ratios would have been recorded.

It is of interest to note that when rats received either CoQ_{10} or succinate, improved L/P ratios were observed. This is the case in both the vehicle and rotenone Factor-1 treated rat groups. Dose groups VC and VS, as well as RC and RS harboured the lowest L/P ratios in their respective Factor-1 dose groups. As mentioned previously, the contributions of Factor-2 doses improved when the extreme outliers were excluded, but not to the point that a statistically significant contribution was recorded. Nonetheless, the trend in response to the CoQ_{10} and succinate doses indeed suggests alleviation in L/P ratios. The most noted improvements can of course be observed in the induced deficiency dose groups RC and RS. The L/P ratios did not decrease to quite as low as the vehicle counterparts VC and VS, but they did diminish to levels similar to and, in some cases, lower than rats in the environmental control group NN. This is a remarkable recovery, especially since rats only received therapeutically beneficial regimens for a period of two days. The blood lactate concentrations listed in Table D.1 of the rotenone-treated rats, indicated improved lactate levels for the groups that received CoQ_{10} and succinate on days 15 and 16. The median lactate concentrations for RX and RN both exceeded 500 $\mu mol.L^{-1}$, whereas the median concentrations for RC and RS were approximately

300 $\mu mol.L^{-1}$. The lactate concentrations for RV cannot be ignored with a mean and median of 394 $\mu mol.L^{-1}$ and 298 $\mu mol.L^{-1}$, respectively. This strongly supports previous statements that the sunflower oil may too contribute to improving redox status in rats.

It was unfortunate that no statistically significant differences were reported by the multiple comparison data. Moreover, the two-way ANOVA results did not indicate that Factor-2 doses significantly improved L/P ratios. The factorial ANOVA results indicated that any differences between groups are largely due to vehicle and rotenone Factor-1 contributions. Therefore, the arguments surrounding beneficial effects of the various Factor-2 doses are purely speculative and should be portrayed as trends, not as true differences.

5.3.5 ATP/ADP ratios in blood

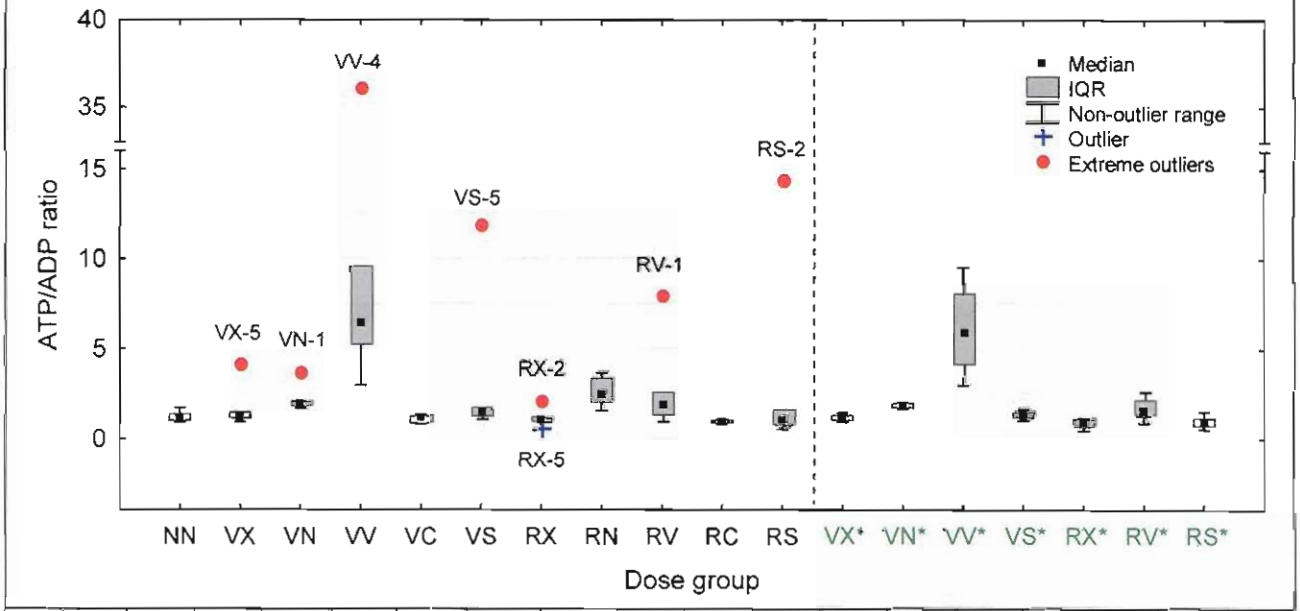
The concentrations of ATP and ADP were determined from blood that was collected on the days that rats were sacrificed. Data was captured in Excel® spreadsheets, followed by ratio determination and statistical evaluation utilising the STATISTICA™ programme. Table 5.35 presents the ATP/ADP ratios generated from blood. In addition, all data points and descriptive statistics according to dose group are presented. Prior to evaluating the box-whisker representations, it should be noted that four data points are missing from the overall set of data, namely, VX-6, VN-4, VV-2 and RX-1. It was not possible to determine the adenylate concentrations from these blood samples since insufficient prep volumes were available to perform both ATP and ADP repeat assays.

The box-whisker plots for the blood ATP/ADP data indicate the presence of seven extreme outliers, more than has been observed in any of the previously analysed data sets. However, it should also be noted that the IQRs for all the groups containing extreme outliers are very narrow, which in turn results in very stringent conditions for the outlier analysis. Nevertheless, since the core data points of these data sets are positioned in close proximity to each other, it can be expected that the central tendency statistics would be relatively accurate reflections of the blood ATP/ADP ratios. In addition to the seven extreme outliers, a single outlier was determined to be present in dose group RX. Since the outlier RX-5 does not extend into the extreme outlier range, it will not be excluded for future statistical analyses and will therefore not be discussed further.

The first extreme outlier, VX-5, is situated at an ATP/ADP ratio of 4.08, with the next ratio being at 1.50 for rat VX-3. Since VX-5 is more than double that of its closest ratio and that dose group VX has an IQR of 0.32, it is not unexpected that it is to be regarded an extreme outlier. In addition, dose group VX contains one missing data point, VX-6. Therefore, upon exclusion of VX-5, the group consists of four data points only, which is the minimal sample size, considered for further statistical evaluation. The exclusion of VX-5 results in a mean ATP/ADP ratio decrease from 1.80 to 1.22, and a SD diminishing from 1.29 to 0.22. The non-parametric statistics remained very stable with the median decreasing from 1.24 to 1.21, and the IQR decreasing only slightly from 0.32 to 0.30.

Table 5.35 Box-whisker representation and descriptive statistics of the blood ATP/ADP ratio data generated from the main study

A: Box-whisker plots and data points according to rat groups



Rat	NN	VX	VN	VV	VC	VS	RX	RN	RV	RC	RS	VX*	VN*	VV*	VS*	RX*	RV*	RS*
1	1.02	1.18	•3.62	9.57	1.30	1.36	—	2.09	•7.87	0.92	1.56	1.18	EXCL	9.57	1.36	—	EXCL	1.56
2	1.76	1.24	1.97	—	1.38	1.23	•2.03	3.38	1.30	0.98	•14.4	1.24	1.97	—	1.23	EXCL	1.30	EXCL
3	1.30	1.50	2.09	5.24	1.23	1.05	1.07	2.89	2.56	0.86	0.56	1.50	2.09	5.24	1.05	1.07	2.56	0.56
4	0.94	0.97	—	•36.0	0.89	1.52	1.19	2.08	2.12	1.08	0.77	0.97	—	EXCL	1.52	1.19	2.12	0.77
5	1.03	•4.08	1.86	3.01	1.21	•11.8	+0.49	3.71	1.60	0.98	0.93	EXCL	1.86	3.01	EXCL	0.49	1.60	0.93
6	1.39	—	1.72	6.45	0.84	1.70	0.94	1.60	0.92	1.11	1.21	—	1.72	6.45	1.70	0.94	0.92	1.21

B: Descriptive statistics

Dose group	Sample size	Mean	SD	Median	Min	Max	Range	Lower quartile	Upper quartile	IQR
NN	6	1.24	0.31	1.16	0.94	1.76	0.81	1.02	1.39	0.38
VX	5	1.80	1.29	1.24	0.97	4.08	3.12	1.18	1.50	0.32
VX*	4	1.22	0.22	1.21	0.97	1.50	0.54	1.07	1.37	0.30
VN	5	2.25	0.78	1.97	1.72	3.62	1.90	1.86	2.09	0.23
VN*	4	1.91	0.16	1.92	1.72	2.09	0.38	1.79	2.03	0.24
VV	5	12.1	13.6	6.45	3.01	36.0	33.0	5.24	9.57	4.34
VV*	4	6.07	2.74	5.84	3.01	9.57	6.56	4.12	8.01	3.89
VC	6	1.14	0.22	1.22	0.84	1.38	0.54	0.89	1.30	0.41

Table 5.35 Continued...

Dose group	Sample size	Mean	SD	Median	Min	Max	Range	Lower quartile	Upper quartile	IQR
VS	6	3.11	4.27	1.44	1.05	11.8	10.8	1.23	1.70	0.47
VS*	5	1.37	0.25	1.36	1.05	1.70	0.65	1.23	1.52	0.29
RX	5	1.14	0.56	1.07	0.49	2.03	1.54	0.94	1.19	0.25
RX*	4	0.92	0.31	1.00	0.49	1.19	0.70	0.71	1.13	0.42
RN	6	2.63	0.83	2.49	1.60	3.71	2.11	2.08	3.38	1.30
RV	6	2.73	2.58	1.86	0.92	7.87	6.94	1.30	2.56	1.26
RV*	5	1.70	0.65	1.60	0.92	2.56	1.63	1.30	2.12	0.82
RC	6	0.99	0.09	0.98	0.86	1.11	0.25	0.92	1.08	0.16
RS	6	3.23	5.46	1.07	0.56	14.4	13.8	0.77	1.56	0.79
RS*	5	1.01	0.39	0.93	0.56	1.56	1.00	0.77	1.21	0.44

Rat codes for outliers and extreme outliers are located above or below the respective blue crosses (+) and red dots (•), which correspond to data point values listed in the table directly below the graph. The vertical dashed line in the box-whisker graphic representation separates original dose group box-whiskers from those that have had the extreme outliers excluded, which are also indicated by the asterisk (*) following the dose group code. Data sets with excluded data points are designated in green text. A scale break was implemented on the Y-axis between a ratio of 15 and 35. Rats were treated with NN = no dose regimen, VX = vehicle and sacrificed, VN = vehicle and no dose, VV = vehicle and vehicle, VC = vehicle and CoQ_{10}, VS = vehicle and succinate, RX = rotenone and sacrificed, RN = rotenone and no dose, RV = rotenone and vehicle, RC = rotenone and CoQ_{10}, RS = rotenone and succinate. '---' = missing data point, ATP/ADP = ratio of adenosine triphosphate to adenosine diphosphate, EXCL = excluded data point, IQR = inter-quartile range, Min = minimum data point value, Max = maximum data point value, SD = standard deviation.

Dose group VN also comprised of a missing data point as well as an extreme outlier. Rat VN-1 presented with an ATP/ADP ratio of 3.62. In view of the complete blood ATP/ADP data set, this ratio does not appear to be extreme in nature. However, since dose group VN displays the narrowest of all the IQRs at 0.23, highly stringent conditions of determining outliers and extreme outliers exists for this group. Upon exclusion of VN-1, the mean decreased from 2.25 to 1.91, while the SD decreased from 0.78 to 0.16. The median decreased a mere 0.05 units from 1.97 to 1.92, and the IQR increased from 0.23 to 0.24. The latter mentioned adjustment to the IQR may be surprising since it would be expected that the exclusion of an extreme outlier would result in a narrowing of the IQR, rather than an increase. However, since dose group VN comprises of only five data points due to the missing data for rat VN-4, the exclusion of VN-1 results in the minimum sample size of four. Consequently, the calculation of the IQR is adjusted to include the lowest and highest ranked remaining data points to determine the upper and lower quartile statistics. For a group of four data points the upper quartile is determined by calculating the average between the maximum statistic and the closest ranked data point. In the case of dose group VN*, the maximum statistic is 2.09 and the next ranked data point is that of 1.97 for VN-2. Therefore, the upper quartile is calculated to be 2.03. Similarly, the lower quartile is determined by calculating the average of the minimum statistic, 1.72, and the closest ranked data point, in this case 1.87 for VN-5. The lower quartile is therefore calculated to be 1.79. Finally, the IQR is calculated by determining the range between the upper and lower quartile, which is the previously mentioned 0.24.

It is no surprise that rat VV-4 harboured a blood ATP/ADP ratio that was regarded as an extreme outlier. With an ATP/ADP ratio of 36.0, VV-4 is located well above all the other ratios in the complete set of data. It should be noted that dose group VV also presented with a sample size of five data points due to a missing data point for VV-2. Therefore, the exclusion of VV-4 as an extreme outlier results in a final four data points remaining in dose group VV, which can be regarded as being the minimal acceptable sample size. It can also be deduced from the box-whisker plot and the IQR of 4.34 that dose group VV presented with the most variation when compared to all the groups. The dose group also consists of ATP/ADP ratios that are mostly higher than the remaining 10 dose groups. If sunflower oil vehicle were to improve ATP/ADP ratios, it would be expected that VX would display similar improvements, or that all groups that received vehicle Factor-1 doses would present with higher ratios than the environmental controls NN. However, this is not the case with the majority of dose groups presenting with mean ATP/ADP ratios between 1.0 and 3.5. The exclusion of VV-4 results in the parametric mean decreasing from 12.06 to 6.07, and a large SD decrease from 13.6 to 2.74. The median lowered from 6.45 to 5.84, and the IQR from 4.34 to 3.89. Once again it is evident that the median and IQR descriptive statistics are more reliable indicators that do not fluctuate as severely as the mean and SD due to the presence and removal of extreme outliers.

Dose group VS presented with a mean blood ATP/ADP ratio of 3.11. The extreme outlier, VS-5, harboured a ratio of 11.8, while the next highest ratio was at 1.70 for rat VS-6. An exclusion of the 11.8 data point from the VS data set results in a considerable mean ratio decrease to 1.37 from the previously mentioned 3.11. As predicted, the SD markedly diminishes from 4.27 to 0.25. The median and IQR adjusted far less from 1.44 to 1.36 and from 0.47 to 0.29 respectively.

Dose group RX, the final group to consist of a missing data point also presented with the presence of an extreme outlier, RX-2. The aforementioned rat harboured a blood ATP/ADP ratio of 2.03 that was less than 1.00 ratio unit larger than the closest ranked data point. However, the extremely narrow IQR of 0.25 meant that the upper outlier boundary was situated at an ATP/ADP ratio of 1.94, resulting in the classification of RX-2 as an extreme outlier. Upon exclusion of RX-2, the mean and SD decreased from 1.14 to 0.92 and from 0.56 to 0.31 respectively. The median adjusted slightly from 1.07 to 1.00, while the IQR increased from 0.25 to 0.42. As with the exclusion of the extreme outlier from dose group VN, the exclusion of RX-2 from RX resulted in an increase in the IQR statistic. Similarly, the reasoning for this occurrence is due to the missing data point and

exclusion of an extreme outlier that results in an adjusted final sample size of four rats. Consequently, the upper and lower quartiles are determined by calculating the averages between the third and fourth ranked data points as well as the averages between the first and second ranked data points respectively. Since RX* presented with outlier RX-5, that appeared to be lower than the remaining three data points, it resulted in a considerably decreased lower quartile statistic and consequently increased IQR. The sixth extreme outlier, RV-1, presented with an ATP/ADP ratio of 7.87 that was positioned 5.31 ratio units above the next ranked data point of 2.56 for rat RV-3. An exclusion of RV-1 resulted in a mean decrease from 2.73 to 1.70, and a SD adjustment from 2.58 to 0.65. The median and IQR decreased from 1.86 to 1.60 and from 1.26 to 0.82 respectively.

Finally, dose group RS consisted of five data points and an extreme outlier. Rat RS-2 harboured an ATP/ADP ratio of 14.4, whereas the mean ratio for the dose group was 3.23. The closest ranked data point was for rat RS-1 that harboured an ATP/ADP ratio of 1.56. Therefore, it is no surprise that RS-1 was classified as an extreme outlier when compared to the remaining five data points in its group. The exclusion of RS-2 resulted in a notable mean decrease to 1.01 from the previously mentioned ATP/ADP ratio of 3.23, while the SD diminished to 0.39 from 5.46. In contrast, the median decreased only slightly from 1.07 to 0.93 and the IQR from 0.79 to 0.44.

Via a visual inspection of the blood ATP/ADP data presented in Table 5.35.A, the most characteristic figure emerging from the graph is the box-whisker plot for dose group VV. The remaining data distributions, indicated by the box-whisker plots, appear to deviate only slightly from each other. Therefore, it may be expected that the striking differences between dose group VV and the remaining groups would result in statistically significant comparisons. This can be verified by referring to the ANOVA and multiple comparison p-values generated from the blood ATP/ADP data set, as presented in Table 5.36. Investigation of the ANOVA p-values, generated prior to and after the exclusion of extreme outliers, indicate that highly significant differences existed among dose groups of the blood ATP/ADP data set.

The characteristic data distribution observed from the box-whisker representations in Table 5.35.A is extrapolated to the multiple comparison grid in Table 5.36.A, where dose group VV is illustrated to differ statistically significantly from all dose groups upon exclusion of the extreme outliers. In addition, all comparisons with VV were also determined to be of biological significance. Prior to the exclusion of the seven extreme

outliers, VV differed significantly from only three of the remaining 10 dose groups. The marked increase in the number of statistically significant differences from three to 10, upon the exclusion of extreme outliers, can be accounted for by the considerable decrease in the overall variation of the data. Since a number of seven data points were determined to be present within the extreme outlier ranges, their exclusion resulted in a significantly large decrease in overall variation, which in turn resulted in an ATP/ADP data set with more defined central tendencies. Furthermore, the exclusion resulted in the minimisation of overlapping data distributions.

Table 5.36 Multiple comparison statistics of the blood ATP/ADP ratio data generated from the rat main study

A: Non-parametric (original data set) and parametric (excluding extreme outliers) p-values

Dose group	NN	VX	VN	VV	VC	VS	RX	RN	RV	RC	RS
NN		1.000	1.000	0.146	1.000	1.000	1.000	1.000	1.000	1.000	1.000
		1.000	0.984	< 0.001	1.000	1.000	1.000	0.150	0.998	1.000	1.000
VX	1.000		1.000	0.943	1.000	1.000	1.000	1.000	1.000	1.000	1.000
	1.000		0.981	< 0.001	1.000	1.000	1.000	0.382	0.999	1.000	1.000
VN	1.000	1.000		1.000	1.000	1.000	1.000	1.000	1.000	0.208	1.000
	0.984	0.981		< 0.001	0.959	0.997	0.827	0.975	1.000	0.881	0.892
VV	0.146	0.943	1.000		0.037	1.000	0.048	1.000	1.000	0.003	0.083
	< 0.001	< 0.001	< 0.001		< 0.001	< 0.001	< 0.001	< 0.001	< 0.001	< 0.001	< 0.001
VC	1.000	1.000	1.000	0.037		1.000	1.000	0.415	1.000	1.000	1.000
	1.000	1.000	0.959	< 0.001		1.000	1.000	0.094	0.991	1.000	1.000
VS	1.000	1.000	1.000	1.000	1.000		1.000	1.000	1.000	1.000	1.000
	1.000	1.000	0.997	< 0.001	1.000		0.999	0.383	1.000	1.000	1.000
RX	1.000	1.000	1.000	0.048	1.000	1.000		0.478	1.000	1.000	1.000
	1.000	1.000	0.827	< 0.001	1.000	0.999		0.146	0.956	1.000	1.000
RN	1.000	1.000	1.000	1.000	0.415	1.000	0.478		1.000	0.051	0.826
	0.150	0.382	0.975	< 0.001	0.094	0.383	0.146		0.783	0.044	0.097
RV	1.000	1.000	1.000	1.000	1.000	1.000	1.000	1.000		0.902	1.000
	0.998	0.999	1.000	< 0.001	0.991	1.000	0.956	0.783		0.951	0.957
RC	1.000	1.000	0.208	0.003	1.000	1.000	1.000	0.051	0.902		1.000
	1.000	1.000	0.881	< 0.001	1.000	1.000	1.000	0.044	0.951		1.000
RS	1.000	1.000	1.000	0.083	1.000	1.000	1.000	0.826	1.000	1.000	
	1.000	1.000	0.892	< 0.001	1.000	1.000	1.000	0.097	0.957	1.000	

B: ANOVA p-values

Kruskal-Wallis p-value < 0.001	One-way ANOVA p-value < 0.001

C: Statistical and biological significance

Comparison		Statistical significance (p)		Biological significance (d)	
		Including EOs	Excluding EOs	Including EOs	Excluding EOs
NN	VV	0.146	< 0.001	N/A	5.874
VX	VV	0.943	< 0.001	N/A	5.898
VN	VV	1.000	< 0.001	N/A	5.059
VV	VC	0.037	< 0.001	0.803	5.995
VV	VS	1.000	< 0.001	N/A	5.716
VV	RX	0.048	< 0.001	0.803	6.263
VV	RN	1.000	< 0.001	N/A	4.183
VV	RV	1.000	< 0.001	N/A	5.314
VV	RC	0.003	< 0.001	0.814	6.178

Table 5.36 Continued...

Comparison		Statistical significance (p)		Biological significance (d)	
		Including EOs	Excluding EOs	Including EOs	Excluding EOs
VV	RS	0.083	< 0.001	N/A	6.153
RN	RC	0.051	0.044	N/A	1.994

A: All comparison statistics are indicated as p-values. The upper p-value is the non-parametric multiple comparison test statistic, generated from the original set of data. The lower p-value was generated via the parametric Tukey *unequal number HSD* (Honestly Significant Difference) test, after the exclusion of extreme outliers. P-values indicated in red are statistically significant at the pre-determined significance level of 0.05. P-values in black text represent those that are not statistically significant, but have complementary p-values that are statistically significant. The remainder of p-values are listed in grey. The comparisons surrounded by the **bold** black line are those that were determined to be statistically significant by both the non-parametric and parametric multiple comparison procedures. The turquoise shaded blocks represent statistically significant comparisons that were also determined to be of biological significance. B: P-values for the non-parametric Kruskal-Wallis ANOVA and parametric one-way ANOVA are listed, with significant p-values, less than the 0.05 significance level, indicated in red. C: List of comparisons determined to be statistically significant with corresponding biological significance. A d-value greater than or equal to 0.8 signifies biological significance, indicated in red. Rats were treated with NN = no dose regimen, VX = vehicle and sacrificed, VN = vehicle and no dose, VV = vehicle and vehicle, VC = vehicle and CoQ_{10}, VS = vehicle and succinate, RX = rotenone and sacrificed, RN = rotenone and no dose, RV = rotenone and vehicle, RC = rotenone and CoQ_{10}, RS = rotenone and succinate. < = less than, ANOVA = analysis of variance, ATP/ADP = ratio of adenosine triphosphate to adenosine diphosphate, EOs = extreme outliers, N/A = not applicable.

As mentioned previously, dose group VV presented with blood ATP/ADP ratios that were unexpectedly higher than the majority of other data points. It is difficult to explain as to why this group would harbour markedly higher ratios. The group consisted of five data points only, due to the missing ATP/ADP ratio for rat VV-2. In addition, one of the five data points was markedly elevated and consequently excluded as an extreme outlier. Upon exclusion, the mean ratio for VV decreased by approximately half from 12.06 to 6.07, as discussed previously. However, even with the extreme outlier excluded, dose group VV still presented with the highest mean and median ratios as well as the largest IQR. With an IQR of 3.89 for dose group VV*, the next closest IQR was approximately a third at 1.30, for dose group RN. The wide IQR itself is suggestive of the fact that a difference indeed exists between VV* and the remaining groups of the main study. By referring to Table F.1 of Appendix F, a list of adenylate concentrations generated from blood can be viewed. The table indicates, with the exclusion of the extreme outlier VV-4, that neither abnormally high, nor low, ATP and ADP concentrations were recorded for dose group VV. It cannot be conclusively explained as to where the aberrantly elevated central tendency statistics arose from, except that ATP/ADP ratios of dose group VV were simply distributed within a wide range.

Rats of dose group VV, even though they simply received a vehicle dose for 16 consecutive days, responded aberrantly resulting in unpredicted blood ATP/ADP ratios. The reliability of ratios generated from VV is certainly questionable. It is doubtful that a 16-day vehicle dose would result in such a marked increase in blood ATP/ADP ratios, especially since all other groups that received vehicle consistently presented with lowered ratios. Nonetheless, the data was further analysed with the inclusion of dose group VV,

with interpretation of results performed by taking the aberrant nature of VV into consideration.

Table 5.36 illustrated that dose group VV differed significantly from three dose groups both prior to and after the exclusion of the extreme outliers. These groups included VC, RX and RC. Upon exclusion of the extreme outliers, VV was determined to differ significantly from all groups in the main study. The uncharacteristic ATP/ADP ratios of VV resulted in the striking appearance of statistically significant p-values in the multiple comparison grid. The unfortunate outcome of an occurrence is that it is not possible for reliable inference to be made when dose group VV is involved in the comparison. From the graphic representation in Table 5.35 and the multiple comparison grid in Table 5.36, it is evident that the data suggests that dose group VV presented with the highest of ATP/ADP ratios. However, it cannot be motivated from the dose regimen point of view that a 16-day supplementation of sunflower oil would result in observed elevation of ATP/ADP ratios. Moreover, there is no support from the other vehicle-dosed groups for the improvement in ATP/ADP ratios.

Apart from comparisons from VV, p-values in Table 5.36 indicate that an additional dose group comparison was determined to be statistically significant upon the exclusion of the extreme outliers. The Tukey *unequal number HSD* p-value of 0.044 indicates that dose group RN differed statistically significantly from RC. The comparison was also determined to be of biological significance with a d-value of 1.994. Since RN presented with a mean ATP/ADP ratio of 2.63, while RC had a mean ratio of 0.99, the data suggests that the two-day recovery from rotenone dosing was more beneficial to rats than receiving CoQ_{10} as a Factor-2 dose. It can be argued that the vehicle may have contributed to decreasing ATP/ADP ratios. However, if this were to be the case, it would be expected that dose group NN would harbour higher ratios than rats that received vehicle. This is because the environmental control rats of NN received no dose at all. This was not the case with NN presenting with mean and median ATP/ADP ratios that were in similar ranges to the remainder of the groups. Nonetheless, since it has been displayed in previous data sets that sunflower oil has indeed contributed to response patterns in rats, the argument that it affected rat response may not be inaccurate. The significant difference between RN and RC does of course also suggest that CoQ_{10} did not improve ATP/ADP status in rats. This is supported by the observation that dose group VC presented with no statistically significant improvements when compared to other groups of the study.

The blood ATP/ADP data was in addition analysed via a factorial ANOVA in order to evaluate significant contributions from the various dose factors utilised. The impact of aberrant ATP/ADP ratios for dose group VV was taken into consideration when interpreting the F-statistics and p-values for Factor-1, Factor-2 and the interaction. Graphic summaries of the two-way ANOVA, with the inclusion and exclusion of extreme outliers, are presented in Table 5.37.

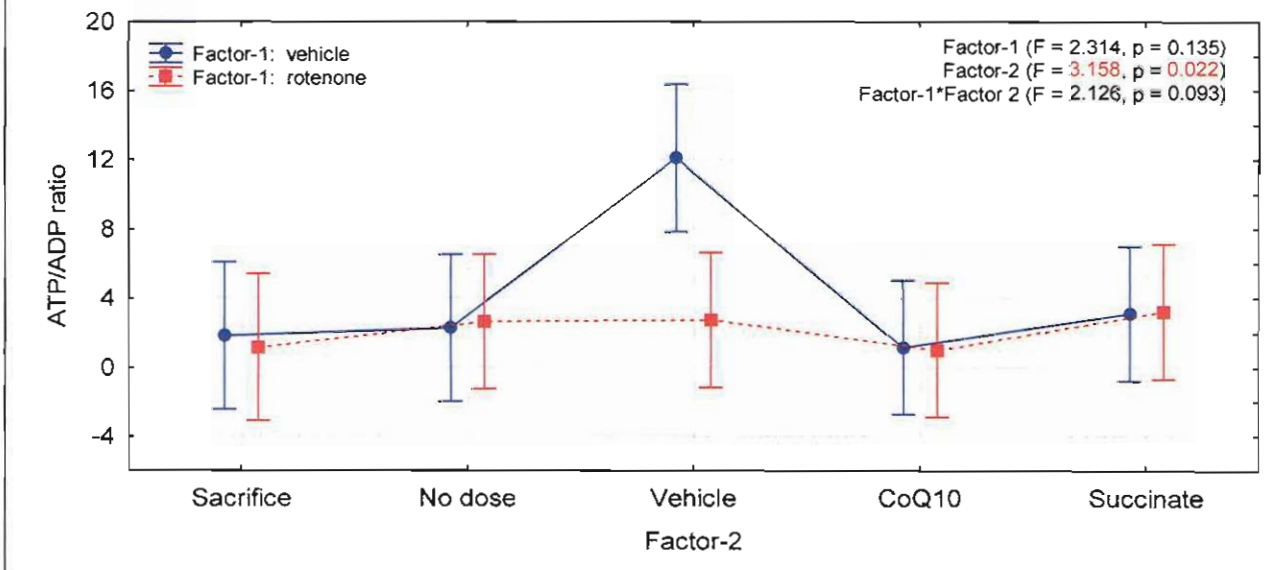
Since seven extreme outliers were present in the overall blood ATP/ADP data set, it may be expected that F-statistics of the two-way ANOVA would vary considerably prior to and after extreme outlier exclusion. This was indeed the case with marked increases in F-statistics being observed. Moreover, the statistical significance of dose factors differed considerably with highly significant p-values being reported for Factor-1, Factor-2 and the interaction effect, as opposed to statistical significance reported for Factor-2 only when the extreme outliers were not excluded. A visibly distinctive reduction in 95% confidence intervals can also be observed from the graphic representations in Table 5.37.

Table 5.37.A illustrates that Factor-2 dose regimens influenced most on the blood ATP/ADP response profiles. However, the graphic summary evidently depicts a predominant peak in the vehicle Factor-1 plot for dose group VV. The statistics suggest that the difference in ratios between the vehicle and rotenone Factor-1 plots depends mostly on Factor-2 dose regimens. This can be explained graphically by observing that the plots appear to remain constant throughout the Factor-2 treatments, except when a vehicle Factor-2 regimen was dosed. An alternative explanation is that similar ATP/ADP ratios were attained throughout the study, with rats in dose group VV presenting extraordinary ATP/ADP ratios.

Upon exclusion of the extreme outliers, a similar trend in response was still portrayed, except that the displacement between VV and the remainder of the groups decreased by approximately half. In addition, an interaction effect was reported, shifting the interpretation of results. A statistically significant interaction effect suggests that both Factor-1 and Factor-2 dose regimens together affected response profiles in rats.

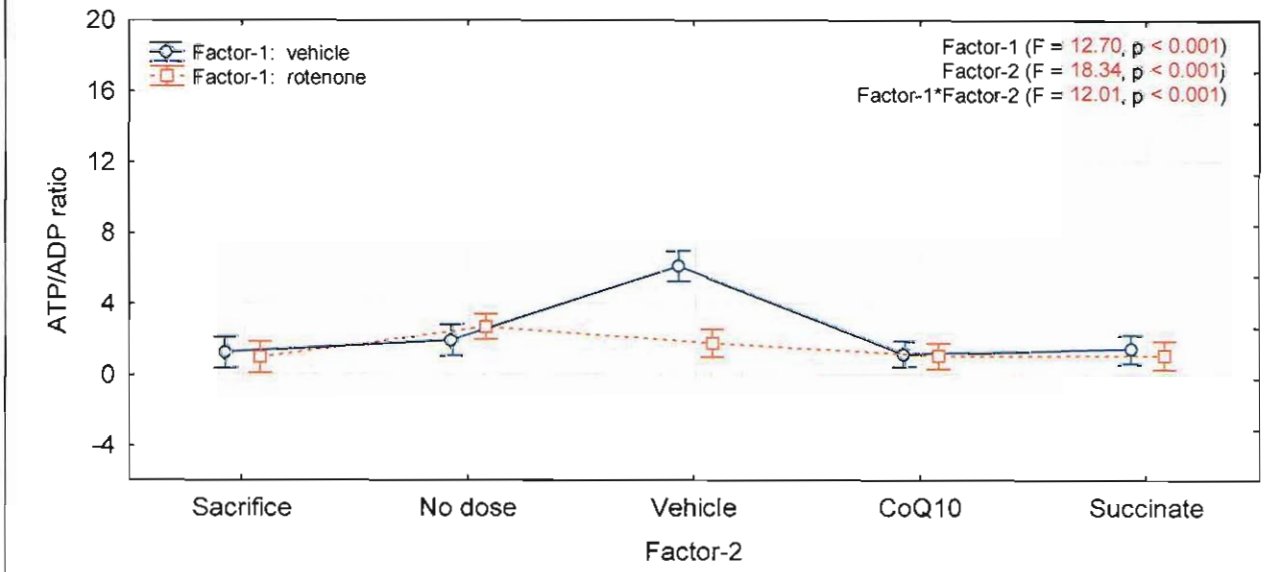
Table 5.37 Graphic and tabulated summary of the blood ATP/ADP ratio data analysed via a two-way ANOVA

A: Data set including extreme outliers



Description		VX	VN	VV	VC	VS	RX	RN	RV	RC	RS
With extreme outliers	UCI	6.05	6.51	16.3	5.02	7.00	5.40	6.51	6.61	4.87	7.11
	mean	1.80	2.25	12.1	1.14	3.11	1.14	2.63	2.73	0.99	3.23
	LCI	-2.46	-2.00	7.80	-2.74	-0.77	-3.11	-1.26	-1.16	-2.89	-0.65

B: Data set excluding extreme outliers



Description		VX	VN	VV	VC	VS	RX	RN	RV	RC	RS
Without extreme outliers	UCI	2.10	2.79	6.94	1.86	2.16	1.80	3.34	2.48	1.70	1.79
	mean	1.22	1.91	6.07	1.14	1.37	0.92	2.63	1.70	0.99	1.01
	LCI	0.35	1.03	5.19	0.42	0.59	0.04	1.91	0.92	0.27	0.22

The plot legends for each graph are indicated in the top left corners of the respective graphs, while the two-way ANOVA F-statistics (F) and p-values (p) for Factor-1, Factor-2 and Factor-1*Factor-2 are located in the top right corner, with the statistically significant values indicated in red. The vertical whiskers at each mean data point represent 95% confidence intervals for the respective data sets. The mean values in green text, located in the data point summary tables below the graphs, indicate those that were adjusted due to the exclusion of extreme outliers. < = less than, ATP/ADP = ratio of adenosine triphosphate to adenosine diphosphate, LCI = lower 95% confidence interval data point, UCI = upper 95% confidence interval data point. Rats were treated with NN = no dose regimen, VX = vehicle and sacrificed, VN = vehicle and no dose, VV = vehicle and vehicle, VC = vehicle and CoQ_{10}, VS = vehicle and succinate, RX = rotenone and sacrificed, RN = rotenone and no dose, RV = rotenone and vehicle, RC = rotenone and CoQ_{10}, RS = rotenone and succinate.

The graphic representation in Table 5.37.B evidently illustrates that the most significant of differences between plots occurs when dose group VV is encountered. An elevated mean for dose group VV resulted in an increase in the divergence of the Factor-1 plots, a typical occurrence when interaction effects are reported by a factorial ANOVA. It can also be argued that the intersection of Factor-1 plots between the sacrifice and no dose Factor-2 treatments contributed to the significance of the interaction F-statistic and p-value. However, in view of the distributions of the vehicle and rotenone Factor-1 plots in Table 5.37.B, it is argued that the interaction effect may have been induced by the overwhelming impact of dose group VV. Since the mean data points for nine of the 10 dose groups in the graph are positioned within an extremely narrow range of less than 2.0 ratio units, it can be argued that very little variation in response to the dose regimens was observed. The uncharacteristic elevation in ATP/ADP ratios for dose group VV is suggestive of a significant Factor-2 contribution, as reported by the two-way ANOVA prior to the exclusion of the extreme outliers, presented in Table 5.37.A. Therefore, this result is an appraisal of the proposed statistical strategy that was established predominantly on the basis of reporting complete sets of data in parallel with those modified via the exclusion of extreme outliers.

5.3.6 NAD/NADH ratios in blood

Blood was collected and appropriately prepared upon sacrificing the rats. The pyridine concentrations were determined spectrophotometrically and the data captured in Excel® spreadsheets, followed by a statistical evaluation in STATISTICA™. Table 5.38 depicts the distribution of data points according to rat dose group as well as a table of descriptive statistics. It should be noted that there are seven missing data points in the complete blood NAD/NADH data set. These samples could not be assayed successfully due to the requirement of high sample volumes that did not allow for the appropriate optimisation and repeat analyses. Furthermore, it should be noted that three data points were missing in dose group RV. Such a scenario severely compromises the accuracy of statistical evaluations describing the central tendency as well as multiple comparisons performed with dose group RV. Therefore, caution should be taken as to the interpretation of statistics relating to this dose group.

The box-whisker representations in Table 5.38.A reveal the presence of two extreme outliers and three outliers. In addition to presenting with a missing data point, dose group VS also comprised of an extreme outlier and an outlier. Data points in dose group VS

presented with a narrow IQR of 0.09, hence increasing the stringency for the determination of outliers and extreme outliers. Consequently, although rat VS-1 was only 0.13 ratio units from the next ranked data point, VS-2, it was still classified as an outlier. The extreme outlier of VS-4 harboured an NAD/NADH ratio of 0.89. The exclusion of VS-4 from dose group VS resulted in a mean ratio decrease from 0.39 to 0.26, and a SD decrease from 0.29 to 0.09. The median decreased similarly from 0.29 to 0.28, while the IQR increased from 0.09 to 0.12. The increased IQR arising from the exclusion of VS-4 can be accounted for partly by the fact that dose group VS presented with a missing data point. The exclusion of an extreme outlier from a dose group that already only comprised of five data points due to a missing data point, results in the final count of only four data points for the group. The IQR is therefore calculated via the incorporation of the lowest and highest ranked data points. Moreover, since dose group VS consisted of an outlier data point, the IQR for the group is increased accordingly. The second extreme outlier was determined to be present in dose group RS. Rat RS-2 harboured a blood NAD/NADH ratio of 4.51, which appeared to be extreme with the closest data point being at a ratio of 0.61. In addition, a missing data point for rat RS-5 was also present in dose group RS. The exclusion of the extreme outlier RS-2 resulted in a large mean ratio decrease from 1.11 to 0.25, and a SD diminishing from 1.92 to 0.26. The median decreased from 0.29 to 0.17, while the IQR adjusted to 0.39 from a ratio of 0.55.

Table 5.38 Box-whisker representation and descriptive statistics of the blood NAD/NADH ratio data generated from the main study

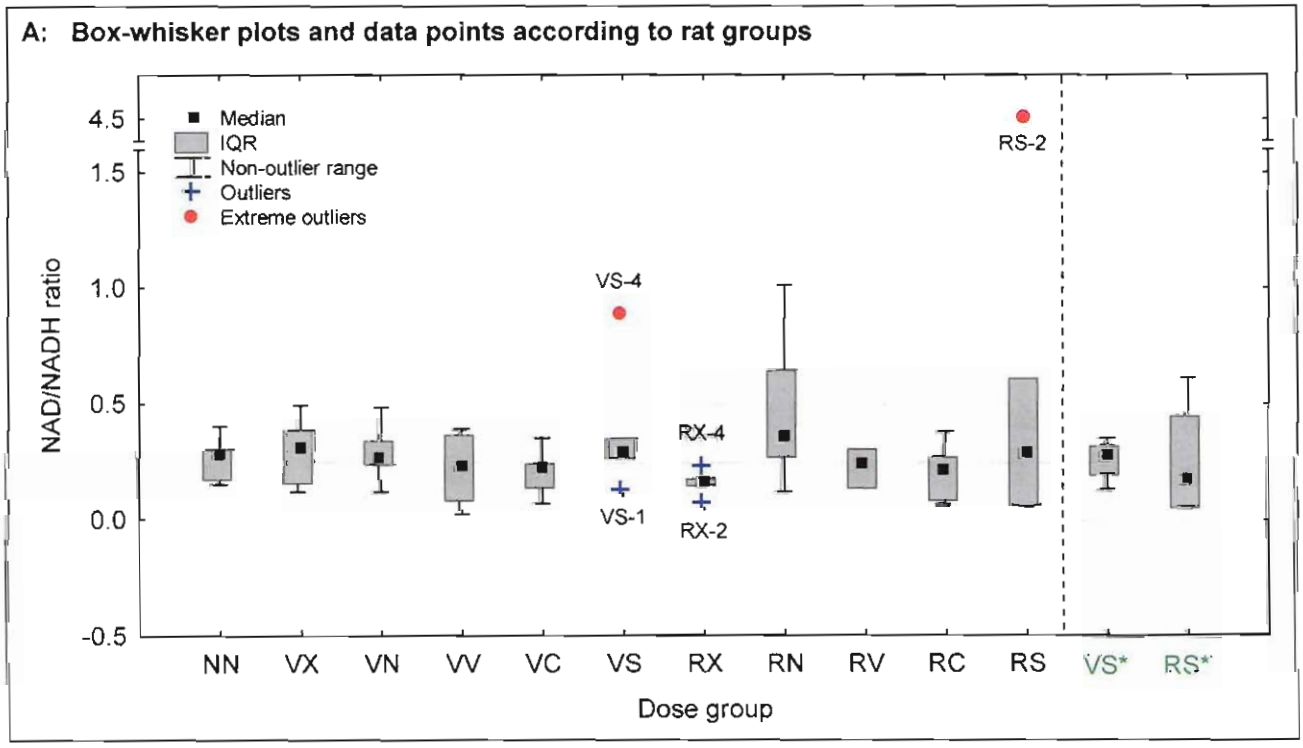


Table 5.38 Continued...

Rat	NN	VX	VN	VV	VC	VS	RX	RN	RV	RC	RS	VS*	RS*
1	0.17	0.12	0.26	0.08	0.22	+ 0.13	0.15	0.30	0.25	0.07	0.61	0.13	0.61
2	—	0.28	0.34	0.02	0.07	0.26	+ 0.08	0.64	0.31	0.23	• 4.51	0.26	EXCL
3	0.40	0.16	0.24	0.13	0.24	0.29	0.16	0.42	—	0.09	0.06	0.29	0.06
4	0.15	0.34	0.48	0.36	0.35	• 0.89	+ 0.24	0.12	—	0.21	0.06	EXCL	0.06
5	0.30	0.39	0.28	0.33	0.23	—	0.18	1.01	0.14	0.27	—	---	---
6	0.28	0.49	0.12	0.39	0.14	0.35	—	0.27	—	0.38	0.29	0.35	0.29

B: Descriptive statistics

Dose group	Sample size	Mean	SD	Median	Min	Max	Range	Lower quartile	Upper quartile	IQR
NN	5	0.26	0.10	0.28	0.15	0.40	0.25	0.17	0.30	0.13
VX	6	0.30	0.14	0.31	0.12	0.49	0.37	0.16	0.39	0.23
VN	6	0.29	0.12	0.27	0.12	0.48	0.37	0.24	0.34	0.10
VV	6	0.22	0.16	0.23	0.02	0.39	0.37	0.08	0.36	0.28
VC	6	0.21	0.10	0.23	0.07	0.35	0.28	0.14	0.24	0.10
VS	5	0.39	0.29	0.29	0.13	0.89	0.76	0.26	0.35	0.09
VS*	4	0.26	0.09	0.28	0.13	0.35	0.22	0.20	0.32	0.12
RX	5	0.16	0.06	0.16	0.08	0.24	0.16	0.15	0.18	0.03
RN	6	0.46	0.32	0.36	0.12	1.01	0.89	0.27	0.64	0.37
RV	3	0.23	0.09	0.25	0.14	0.31	0.17	0.14	0.31	0.17
RC	6	0.21	0.12	0.22	0.07	0.38	0.31	0.09	0.27	0.19
RS	5	1.11	1.92	0.29	0.06	4.51	4.46	0.06	0.61	0.55
RS*	4	0.25	0.26	0.17	0.06	0.61	0.56	0.06	0.45	0.39

Rat codes for outliers and extreme outliers are located above or below the respective blue crosses (+) and red dots (•), which correspond to data point values listed in the table directly below the graph. The vertical dashed line in the box-whisker graphic representation separates original dose group box-whiskers from those that have had the extreme outliers excluded, which are also indicated by the asterisk (*) following the dose group code. Data sets with excluded data points are designated in green text. A scale break was implemented on the Y-axis between a ratio of 1.5 and 4.5. Rats were treated with NN = no dose regimen, VX = vehicle and sacrificed, VN = vehicle and no dose, VV = vehicle and vehicle, VC = vehicle and CoQ_{10}, VS = vehicle and succinate, RX = rotenone and sacrificed, RN = rotenone and no dose, RV = rotenone and vehicle, RC = rotenone and CoQ_{10}, RS = rotenone and succinate. '—' = missing data point, EXCL = excluded data point, IQR = inter-quartile range, Min = minimum data point value, Max = maximum data point value, NAD/NADH = ratio of oxidised to reduced nicotinamide adenine dinucleotide, SD = standard deviation.

The remaining two outliers were determined to be present in dose group RX. This rat group also presented with a missing data point for rat RX-6. Dose group RX had the narrowest IQR of all dose groups, resulting in increased stringency in determining outliers and extreme outliers. Therefore, even though the outliers, RX-2 and RX-4, were closely gathered together with the remaining three data points of the group, they were still classified as outliers. Exclusion of these data points would result in minor adjustments to the central tendency statistics and minimise variation. Nonetheless, RX-2, RX-4 and the previously discussed VS-1 were not classified as extreme outliers and thus not excluded. Blood NAD/NADH ratios were evaluated utilising the appropriate ANOVA and multiple comparison procedures. Table 5.39 presents the p-values generated from the ANOVA and multiple comparison tests. Section A of the table illustrates that no statistically significant differences existed between any of the blood NAD/NADH ratios generated. The non-parametric Kruskal-Wallis and parametric one-way ANOVA tests both indicated p-values that were not statistically significant and well above the 0.05 significance level.

Table 5.39 Multiple comparison statistics of the blood NAD/NADH ratio data generated from the rat main study

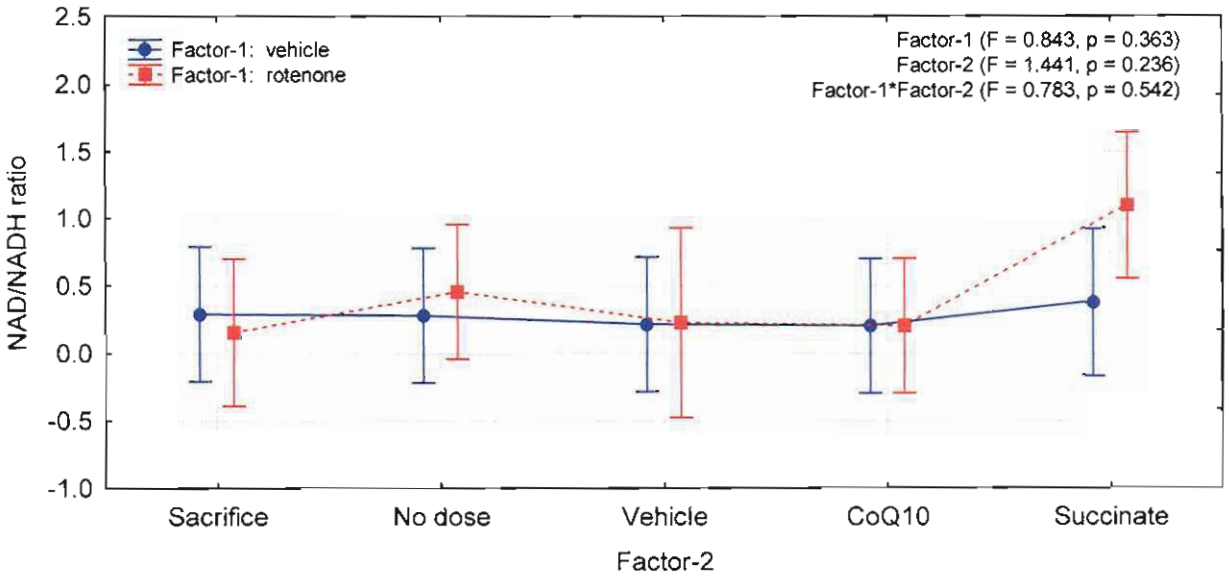
A: Non-parametric (original data set) and parametric (excluding extreme outliers) p-values											
Dose group	NN	VX	VN	VV	VC	VS	RX	RN	RV	RC	RS
NN		1.000	1.000	1.000	1.000	1.000	1.000	1.000	1.000	1.000	1.000
		1.000	1.000	1.000	1.000	1.000	0.995	0.700	1.000	1.000	1.000
VX	1.000		1.000	1.000	1.000	1.000	1.000	1.000	1.000	1.000	1.000
	1.000		1.000	0.999	0.997	1.000	0.962	0.805	1.000	0.997	1.000
VN	1.000	1.000		1.000	1.000	1.000	1.000	1.000	1.000	1.000	1.000
	1.000	1.000		1.000	0.999	1.000	0.977	0.745	1.000	0.999	1.000
VV	1.000	1.000	1.000		1.000	1.000	1.000	1.000	1.000	1.000	1.000
	1.000	0.999	1.000		1.000	1.000	1.000	0.303	1.000	1.000	1.000
VC	1.000	1.000	1.000	1.000		1.000	1.000	1.000	1.000	1.000	1.000
	1.000	0.997	0.999	1.000		1.000	1.000	0.240	1.000	1.000	1.000
VS	1.000	1.000	1.000	1.000	1.000		1.000	1.000	1.000	1.000	1.000
	1.000	1.000	1.000	1.000	1.000		0.999	0.807	1.000	1.000	1.000
RX	1.000	1.000	1.000	1.000	1.000	1.000		1.000	1.000	1.000	1.000
	0.995	0.962	0.977	1.000	1.000	0.999		0.153	1.000	1.000	0.999
RN	1.000	1.000	1.000	1.000	1.000	1.000	1.000		1.000	1.000	1.000
	0.700	0.805	0.745	0.303	0.240	0.807	0.153		0.818	0.244	0.779
RV	1.000	1.000	1.000	1.000	1.000	1.000	1.000	1.000		1.000	1.000
	1.000	1.000	1.000	1.000	1.000	1.000	1.000	0.818		1.000	1.000
RC	1.000	1.000	1.000	1.000	1.000	1.000	1.000	1.000	1.000		1.000
	1.000	0.997	0.999	1.000	1.000	1.000	1.000	0.244	1.000		1.000
RS	1.000	1.000	1.000	1.000	1.000	1.000	1.000	1.000	1.000	1.000	
	1.000	1.000	1.000	1.000	1.000	1.000	0.999	0.779	1.000	1.000	
B: ANOVA p-values											
Kruskal-Wallis p-value = 0.527						One-way ANOVA p-value = 0.258					

A: All comparison statistics are indicated as p-values. The upper p-value is the non-parametric multiple comparison test statistic, generated from the original set of data. The lower p-value was generated via the parametric Tukey *unequal number HSD* (Honestly Significant Difference) test, after the exclusion of extreme outliers. B: P-values for the non-parametric Kruskal-Wallis ANOVA and parametric one-way ANOVA are listed. Rats were treated with NN = no dose regimen, VX = vehicle and sacrificed, VN = vehicle and no dose, VV = vehicle and vehicle, VC = vehicle and CoQ_{10}, VS = vehicle and succinate, RX = rotenone and sacrificed, RN = rotenone and no dose, RV = rotenone and vehicle, RC = rotenone and CoQ_{10}, RS = rotenone and succinate. ANOVA = analysis of variance, NAD/NADH = ratio of oxidised to reduced nicotinamide adenine dinucleotide.

Rats that were dosed with a rotenone Factor-1 dose certainly appeared and behaved in a manner that strongly suggested that the rotenone dose adversely affected them. However, even by comparing blood NAD/NADH ratios in dose groups VX and RX, it is apparent that no statistically significant difference can be reported. The fact that dose group VX harboured a mean NAD/NADH ratio of 0.30, while RX presented with a mean of 0.16 may suggest that complex I inhibition could be monitored via this assay in blood. However, the argument is not supported by the multiple comparison data and would certainly require that a more concrete result be generated before any conclusions can accurately be made. The blood NAD/NADH ratios were subsequently analysed via a two-way ANOVA to determine the impact of dose Factor-1 and Factor-2. Due to the presence of extreme outliers VS-4 and RS-2, the data was analysed comparatively via the inclusion and exclusion of extreme outliers, as presented in Table 5.40.

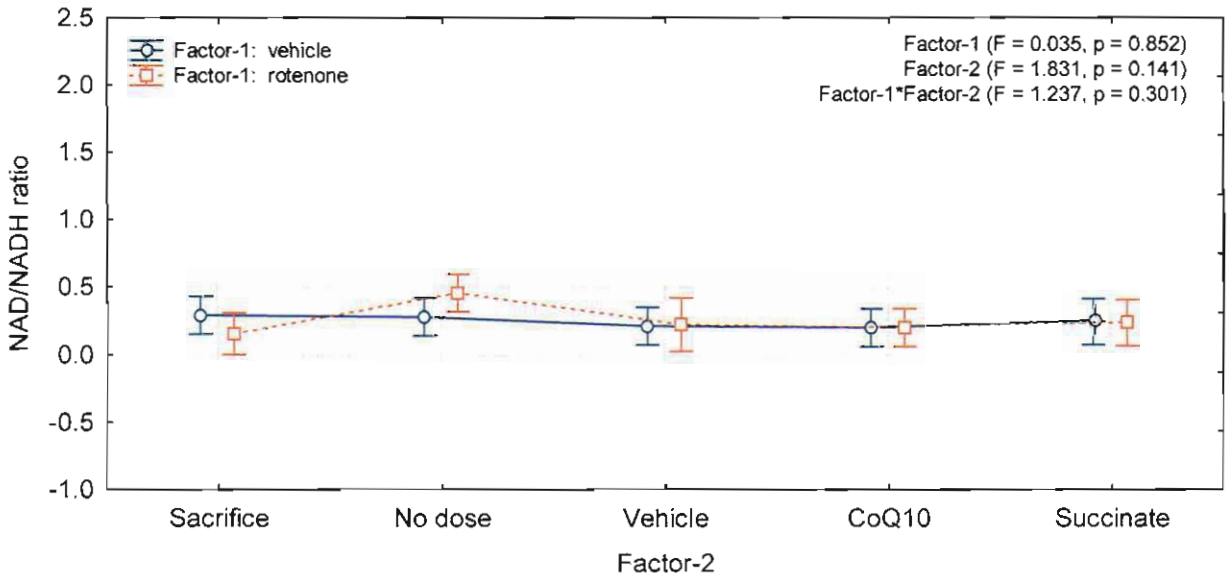
Table 5.40 Graphic and tabulated summary of the blood NAD/NADH ratio data analysed via a two-way ANOVA

A: Data set including extreme outliers



Description		VX	VN	VV	VC	VS	RX	RN	RV	RC	RS
With extreme outliers	UCI	0.79	0.78	0.72	0.70	0.93	0.70	0.96	0.93	0.70	1.65
	mean	0.30	0.29	0.22	0.21	0.39	0.16	0.46	0.23	0.21	1.11
	LCI	-0.20	-0.21	-0.28	-0.29	-0.16	-0.38	-0.04	-0.47	-0.29	0.56

B: Data set excluding extreme outliers



Description		VX	VN	VV	VC	VS	RX	RN	RV	RC	RS
Without extreme outliers	UCI	0.43	0.42	0.36	0.35	0.43	0.31	0.60	0.43	0.35	0.42
	mean	0.30	0.29	0.22	0.21	0.26	0.16	0.46	0.23	0.21	0.25
	LCI	0.16	0.15	0.08	0.07	0.09	0.01	0.32	0.03	0.07	0.08

The plot legends for each graph are indicated in the top left corners of the respective graphs, while the two-way ANOVA F-statistics (F) and p-values (p) for Factor-1, Factor-2 and Factor-1*Factor-2 are located in the top right corner. The vertical whiskers at each mean data point represent 95% confidence intervals for the respective data sets. The mean values in green text, located in the data point summary tables below the graphs, indicate those that were adjusted due to the exclusion of extreme outliers. LCI = lower 95% confidence interval data point, NAD/NADH = ratio of oxidised to reduced nicotinamide adenine dinucleotide, UCI = upper 95% confidence interval data point. Rats were treated with NN = no dose regimen, VX = vehicle and sacrificed, VN = vehicle and no dose, VV = vehicle and vehicle, VC = vehicle and CoQ_{10}, VS = vehicle and succinate, RX = rotenone and sacrificed, RN = rotenone and no dose, RV = rotenone and vehicle, RC = rotenone and CoQ_{10}, RS = rotenone and succinate.

Prior to and after the exclusion of extreme outliers, the two-way ANOVA rendered non-significant p-values for both Factor-1 and Factor-2 dose regimens. In addition, a statistically significant interaction effect was not determined to be present. The graphic representations in Table 5.40 illustrate that vehicle and rotenone Factor-1 plots consistently presented with similar mean data points, especially when the extreme outliers were excluded, depicted in Table 5.40.B. Moreover, since the environmental controls harboured a mean blood NAD/NADH ratio of 0.26, it is apparent that these ratios were hardly altered by any of the dose regimens.

The results generated by the factorial ANOVA further strengthens the argument that the NAD/NADH assay, performed on blood, was not informative in the context of this study and did not infer a true reflection of the overall bioenergetic status in rats. The fact that NAD/NADH ratios remained consistent in all rat groups is suggestive of the assay not being appropriate in evaluation of Complex I deficiency and the benefits of therapeutic regimens.

5.3.7 Blood profile of the rat main study

Several data sets were generated from the rat main study. In an attempt to determine a globalised response pattern in rats, the data sets presented in previous sections were grouped according to the different systems or organs. This enabled the construction of a biochemical profile of response for each of the systems or organs investigated. The profile data are presented by means of two-dimensional bar graphs, a median percentage grid indicating percentages in reference to the environmental control dose group NN, as well as a symbol summary of the factorial ANOVA p-values. Each of the profile summaries also included rat weight data as a reference to the physical response observed in rats.

Median percentages in the bar graphs are presented with an arbitrarily selected limit at 200%, since it was considered that inference regarding a response extending beyond this percentage would not be additionally informative. Dose groups harbouring biochemical traits extending to percentages greater than 200% of the environmental controls were argued to be the product of inaccurate sampling and data generation, or as a result of imprecise statistical interpretation due to the small sample size of each dose group, namely six. The small sample size could be argued to result in vulnerable central tendency statistics and percentages that may fluctuate easily. The former argument is

addressed by utilising median as opposed to mean central tendency statistics, while the latter argument is compensated for by the denotation of statistical significance. Median percentages of data that were determined to differ statistically and biologically significantly from the environmental controls **NN** were listed via a grid block colour-coding scheme. This allowed for a more informative and decisive elucidation of the profile data, preventing the misinterpretation of exaggerated median percentages.

The corresponding median percentages were listed directly below the bar graphs in a median percentage grid. Beneficial responses were registered as positive median percentages, i.e. greater than zero, with deviations larger than 10% indicated in blue text. A harmful response was indicated as a negative median percentage, i.e. less than zero. The greater the harmful affect, the further the median percentage deviated from zero, which was indicated in red text if the deviation extended below -10%. Percentages that deviated less than 10% from the environmental controls NN were typed in grey text. Consequently, the profile bar graphs indicate median percentages extending above and below the zero percent (0%) value on the Y-scale, which is indicated by **NN**. Therefore, all median percentages extending above the **NN** reference scale represent beneficial responses, while the negative median percentages, below **NN**, represent harmful effects incurred by the dose regimens. The advantages of representing the median percentages in the aforementioned format enabled the distinctive categorisation of data into beneficial and harmful responses, all of which were indicated in either blue or red text respectively. The bar graphs evidently portray positive and negative effects of the dose regimens with bars extending above and below the 0% scale respectively. In addition, by glancing over the grid of colour coded median percentages, it is possible to evaluate the global biochemical status of a system or organ according to dose group. Rat groups that benefited from the dose regimen would present with more median percentages listed in blue text, whereas groups that were harmfully affected would present with most percentages in red.

It should be noted that the median percentage deviations in response to the dose regimens were interpreted as 'assumed' benefits and harmful effects. The reason for this lack of certainty is that, even though median percentage deviations from the environmental controls NN could be assigned as beneficial or harmful based on the general logic, not all data could be confidently classified without taking into account the complexity of homeostatic events in a biological organism and model, as utilised in this study. The up- and down-regulation of several compensatory mechanisms within the rat

model in response to the dose regimens was an inevitable occurrence that would most certainly influence multiple biochemical and physiological parameters. The designations of beneficial and harmful effects were implemented for the purpose of simplicity to enable the reader to graphically visualise the responsive deviations in relation to an environmental control group of rats, namely dose group **NN**. A summary of the beneficial and harmful effects assumed for this study, according to the category of data evaluated, are listed in Table 5.41.

Table 5.41 Data categorisation according to assumed beneficial and harmful effects in relation to the environmental control rat group NN

Category	Assumed beneficial effects	Assumed harmful effects
Rat weights	consistent or increased weight gain	decreased weight gain or weight loss
[1] Hydroperoxides	**decreased** hydroperoxide recording	**increased** hydroperoxide recording
Complex I	increased activity	decreased activity
AC	increased capacity	decreased capacity
GSH/GSSG	increased ratio	decreased ratio
[1] L/P	**decreased** ratio	**increased** ratio
ATP/ADP	increased ratio	decreased ratio
NAD/NADH	increased ratio	decreased ratio

Assumed beneficial and harmful deviations from the environmental controls NN are indicated in blue and red text respectively. [1] = decrease in hydroperoxide and L/P ratio data recordings indicate beneficial effects, as opposed to the remaining categories where decreases suggest harmful effects, AC = antioxidant capacity, ATP/ADP = ratio of adenosine triphosphate to adenosine diphosphate, GSH/GSSG = ratio of reduced to oxidised glutathione, L/P = ratio of lactate to pyruvate, NAD/NADH = ratio of oxidised to reduced nicotinamide adenine dinucleotide.

Two assay categories are to be noted from Table 5.41, indicated by superscript ([1]). Beneficial effects for the hydroperoxide and L/P data sets are reflected in decreased recordings for these assays. Therefore, in order to present the data on a scale indicating beneficial and harmful effects more effectively, the median percentages were interpreted via an inverse adaptation. For example, if the hydroperoxide median percentage for a dose group was 15% higher than the environmental controls NN, it meant that a 15% higher hydroperoxide concentration was present in the sample. Therefore, the dose group was interpreted to be affected harmfully, and thus presented with a -15% median percentage, below the **NN** reference scale of the bar graph. In addition, the percentage was indicated in red text in the median percentage grid. Similarly if a dose group presented with a median hydroperoxide statistic that was 85% of the environmental controls NN, it was interpreted to have benefited from the dose regimen and was scored with a blue 15% in the median percentage grid and a corresponding bar extending above **NN** on the bar graph. The same interpretation of data was performed for the L/P ratio median percentages since a decreased L/P ratio indicated a beneficial response to a dose

regimen. Decreases and increases in median percentages of the remaining data sets infer harmful and beneficial effects respectively. Therefore, the data could be interpreted directly onto the bar graph scale and for the median percentage grid.

Alongside the median percentage grid, a summary of the factorial ANOVA results is presented indicating significant (s) and non-significant (n) contributions from dose Factor-1, Factor-2 and the interaction between the two factors. In addition, if extreme outliers were present in the respective data sets, the significance symbols for factors were indicated for each of the data sets including and excluding the extreme outliers. The inclusion of the factorial ANOVA results is warranted since it complements the median percentage data and enables the reader to evaluate the respective biochemical profile further in terms of the impact of the Factor-1 and Factor-2 dose regimens, without having to refer to previous sections. Furthermore, it allows for a quick assessment of the impact that extreme outliers had on a data set.

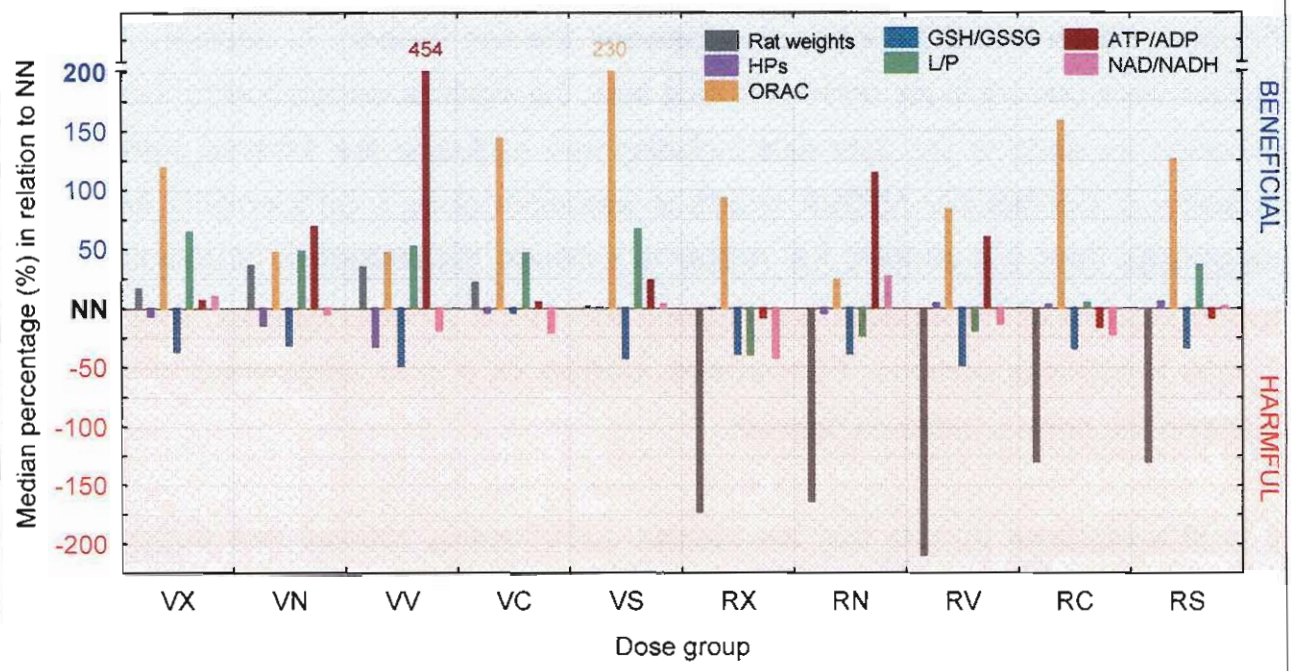
It is of importance to note that the median colour-coding scheme was designed in an attempt to evaluate profile data sets in terms of 'global' benefits and harmful effects. The rationale of such a simplistic evaluation may certainly be argued as inappropriate and scientifically invalid. Indeed, a statistically significant improvement in one biochemical parameter is not analogous with an equivalent percentage benefit recorded for that of a separate biochemical parameter. For example, a 30% improvement in the L/P ratio determined for a specific dose group is not necessarily as beneficial as a 30% increase in the antioxidant capacity, or *vice versa*. The weight or impact of each biochemical parameter on the overall status of the tissue or system type under investigation is required in order to enable speculation on equivalent benefits and harmful effects of the various data sets. However, such data is not available and it would require an intense and intricate methodology to validate these aspects appropriately. Moreover, the interspecies variation as well as tissue specificity of response profiles would certainly contribute to the aforementioned intricacies. In order to compensate partly for these discrepancies, parameter grid blocks were shaded in either green or yellow to signify the statistical and biological significance of any deviations from the environmental controls NN, prior to and after the exclusion of extreme outliers.

The blood profile was compiled from data generated via all of the biochemical assays utilised in the study. Therefore, a profile of six analysis data sets could be established to characterise the global biochemical status in blood. The blood data profile is presented in

Table 5.42 according to dose group, median percentages in relation to the environmental controls NN, as well as a summary of the factorial ANOVA p-values.

Table 5.42 Blood profile of response generated from the rat main study indicating the beneficial and harmful effects of dose regimens

A: Graphic representation



B: Median percentage (%) grid and factorial ANOVA summary

Data set	Dose group										Factorial ANOVA		
	VX	VN	VV	VC	VS	RX	RN	RV	RC	RS	F1	F2	F1*F2
Rat weights	16.9	36.4	35.1	22.1	1.30	-173	-164	-209	-130	-130	s/s	n/n	s/s
HPs	-6.81	-14.8	-32.7	-4.19	-0.63	-1.07	-4.58	3.65	2.64	5.25	s/s	s/s	n/s
AC	119	47.3	47.3	144	230	93.2	24.0	83.8	159	126	n	s	n
GSH/GSSG	-37.0	-31.7	-49.5	-4.25	-42.9	-39.2	-38.9	-49.0	-34.5	-33.7	n/n	s/s	s/s
L/P	64.1	47.9	51.8	46.1	66.3	-39.5	-23.6	-19.3	4.50	35.9	s/s	n/n	n/n
ATP/ADP	6.66	69.0	454	4.87	23.6	-8.07	114	59.6	-16.0	-8.21	n/s	s/s	n/s
NAD/NADH	9.65	-5.20	-19.0	-20.8	2.81	-42.4	26.8	-13.0	-22.4	1.68	n/n	n/n	n/n

A: Percentage bars denote either beneficial or harmful effects induced by the dose regimens. Each bar is colour coded to represent the various data sets, as indicated by the graphic key in the top right corner of the graph. The 0% line on the Y-axis is labelled **NN**, since all median percentages were calculated to deviate from the environmental controls NN. The bold 200% on the median percentage scale indicates the start of a scale break. Median percentages extending beyond the 200% boundary are indicated directly above and in text colours corresponding to the assay bars. B: The percentage data points are listed in correspondence with the bar heights. Median percentages that deviate by more than 10% from the environmental controls NN are indicated in blue and red text for beneficial and harmful deviations respectively. Percentages in grey text represent deviations less than 10%. Grid blocks shaded in green represent comparisons from the original set of data that were presented in previous sections to differ statistically and biologically significantly from the environmental controls NN. Comparisons determined to differ significantly after the exclusion of extreme outliers are indicated by yellow shading. Statistically significant (s) and non-significant (n) contributions of Factor-1 (F1) and Factor-2 (F2) dose regimens as well as the interaction (F1*F2) are indicated alongside the median percentage grid. Two symbols are indicated if extreme outliers were determined to be present in the respective data set, with the first symbol representing significance prior to exclusion, followed by the second symbol representing significance after exclusion of extreme outliers. Rats were treated with NN = no dose regimen, VX = vehicle and sacrificed, VN = vehicle and no dose, VV = vehicle and vehicle, VC = vehicle and CoQ_{10}, VS = vehicle and succinate, RX = rotenone and sacrificed, RN = rotenone and no dose, RV = rotenone and vehicle, RC = rotenone and CoQ_{10}, RS = rotenone and succinate. AC = antioxidant capacity, ATP/ADP = ratio of adenosine triphosphate to adenosine diphosphate, HPs = hydroperoxides, GSH/GSSG = ratio of reduced to oxidised glutathione, L/P = ratio of lactate to pyruvate, NAD/NADH = ratio of oxidised to reduced nicotinamide adenine dinucleotide.

Data presented in Table 5.42 demonstrate that rotenone-treated rats lost considerable amounts of weight when compared to the environmental controls NN. Table 5.42.B illustrates that the median loss in weight observed for rats that received rotenone Factor-1 dose regimens was statistically significant. However, it should be noted that the statistical significance was only determined after the exclusion of extreme outliers, indicated by the yellow shading of grid blocks for rat groups RX, RN, RV, RC and RS. It can also be suggested that the rats that received a vehicle Factor-1 dose gained more weight than NN, with VN and VV gaining the most weight at 36.4% and 35.1% respectively. This may be expected because 1 mL of sunflower oil containing approximately 1,000 milligram (mg) of total fat was ingested on a daily basis when the sunflower oil vehicle was administered. However, these weight gains were not determined to be of statistical significance.

It should also be recalled that rat group VX was dosed with the sunflower oil vehicle for a period of 14 days only. Since NN weights were recorded for a period of 16 days, the 16.9% weight gain for VX is regarded to be an underestimated median percentage. When referred to Section 5.2.2.3, the median weight gain after 14 days of dosing for rat group VX of the main study was 45.0 g, whereas it was 31.5 g for dose group NN. After 16 days, dose group NN had gained an additional 7 g in median weight to 38.5 g, thereby minimising the percentage weight gain for VX. By determining the median percentage weight gain after 14 days, it can be observed that VX had actually gained 43% more weight than NN at that point, confirming a substantial weight gain.

Dose group VS presented with a 1.3% weight gain over **NN**, which was substantially lower than VX, VN and VC. However, as determined in Section 5.2.2.3, none of the vehicle Factor-1 dosed rats differed statistically significantly from each other. Nevertheless, it can be argued that the trend appears to be that the sunflower oil induced weight gain in rats, even though the data is not statistically significant. In contrast, rats that were dosed rotenone from days 1 to 14 lost considerable weight. As with VX, dose group RX was only dosed for a period of 14 days, therefore the percentage deviation of -173% is slightly under-estimated due to the fact that weight gain for **NN** was recorded for 16 days. As discussed previously in this paragraph, dose group NN increased in weight from 31.5 g to 38.5 g over days 15 to 17. Rat group RX lost a total median weight of 28.0 g. Therefore, at the 14 day point RX had in fact lost 189% more weight than NN. Factorial ANOVA results indicate that Factor-1 dose regimens contributed statistically significantly to the weight loss as would be expected since it was evident that rotenone had a marked effect on the rats. It was discussed in Section 5.2.2.1 that the statistically significant interaction

effect was in all likelihood induced by the overwhelming effect of Factor-1. The adverse effects of the complex I inhibitor on the total body weight response observed in rats should constantly be taken into consideration whilst evaluating the various biochemical profiles. It was therefore decided that the median weight percentages be included in all profile bar graphs and median percentage tables.

Table 5.42.B indicates that the hydroperoxide content of the rats in the main study were altered significantly only when rats received the sunflower oil vehicle for a period of 16 days. That is, dose group VV was the only rat group that presented with a statistically significant increase in hydroperoxide levels, which resulted in a decrease of -32.7% of that of the environmental controls NN, in the VV group. Hydroperoxide concentrations in dose group VN were also affected adversely by the sunflower oil, although not to a statistically significant degree. The apparently harmful effects of sunflower oil may be attributed to the high polyunsaturated fat content, which has been reported to increase susceptibility to lipid peroxidation (Mataix *et al.*, 1998) and induce oxidative stress (Turpeinen *et al.*, 1998). These attributes of sunflower oil strengthen the credibility of the increased hydroperoxide levels reported for dose group VV. The remainder of the dose groups, including those that received rotenone Factor-1 doses, presented with hydroperoxide levels that deviated less than 10% from dose group NN. As discussed in Section 5.3.1.2, it was unexpected that rats that received such high doses of rotenone should present with unaltered hydroperoxide recordings, even though complex I inhibition was determined to be present. The rat pilot study indicated a directly corresponding increase in hydroperoxide levels when rats were dosed 3, 6 and 9 $mg.kg^{-1}.day^{-1}$, as discussed in Section 5.3.1.1. This was followed by the unexpected and inversely corresponding decrease in hydroperoxide levels when high doses of 12 and 15 $mg.kg^{-1}.day^{-1}$ were dosed. Thus, it was hypothesised that rotenone may have contributed to the scavenging of radicals, supported by the fact that the inhibitor itself was determined to harbour an antioxidant capacity equivalent to the vitamin E standard Trolox, as presented in Section 5.3.2.1. The recovered hydroperoxide levels were additionally attributed to the up-regulation of antioxidant and metabolic mechanisms as the concentration of rotenone dose regimens increased. It should also be noted that a statistically significant Factor-1 was reported by the factorial ANOVA, prior to and after the exclusion of the extreme outliers. This is suggestive of the fact that rotenone and sunflower oil induced conflicting effects in the rats, which have indeed been made apparent thus far from arguments raised in this paragraph.

The factorial ANOVA also reported statistically significant Factor-2 contributions, as well as an interaction effect when the extreme outliers were excluded. In view of the blood hydroperoxide median percentages, it can be observed that the influence of Factor-2 dose regimens can primarily be accounted for by the percentage fluctuations among the absence of Complex I deficiency dose groups. Therefore, the factorial ANOVA results may suggest that CoQ_{10} and succinate contributed to improved hydroperoxide levels in rats that received a vehicle Factor-1 dose, opposed to that observed for rat groups VX, VN and VV. This is supported further by the fact that VC and VS differed statistically significantly from VV, as presented in Section 5.3.1.2. The interaction, as argued in the aforementioned section, can primarily be accounted for by two aspects. Firstly, the dual influence of rotenone and the therapeutic regimens in decreasing hydroperoxide levels, and secondly to the contrasting effects of the Factor-1 regimens, namely vehicle and rotenone.

Since the 200% mark was the limit at which median percentages were evaluated, a scale break was implemented at this percentage on the bar graph in Table 5.42.A. Two median percentages extended above the 200% boundary, indicated in coloured text corresponding to the assay type. Dose group VV harboured a median ATP/ADP percentage that was 454% higher than the environmental controls NN. As presented in Section 5.3.5, dose group VV presented with a median ATP/ADP ratio of 6.45. However, the group did contain a rat that had an ATP/ADP ratio of 36.0 that was evidently far higher than all the other ratios in the overall blood ATP/ADP data set. Data point VV-4 was determined to be an extreme outlier and certainly contributed to an elevated median ATP/ADP ratio for dose group VV. Upon exclusion of VV-4, the median ratio for VV decreased to 5.84 from the previously mentioned ATP/ADP ratio of 6.45. Nonetheless, since dose group NN harboured a median ATP/ADP ratio of 1.16, the exclusion of the extreme outlier would result in a decrease in the median percentage deviation from 454% to 402%. The latter mentioned percentage is still well beyond the 200% boundary. It should also be mentioned that, prior to the exclusion of the extreme outlier, the mean ATP/ADP ratio statistic for dose group VV was an elevated 12.06, which almost halved to 6.07 when VV-4 was excluded. The mean ATP/ADP ratio for dose group NN was 1.24, slightly higher than the previously mentioned median ratio of 1.16. If mean percentages were calculated, dose group VV would present with an ATP/ADP ratio that would be an unrealistic 872% greater than the environmental controls NN, evidently over-exaggerated by the presence of the extreme outlier. Only after the exclusion of the extreme outlier would dose group VV present with a more realistic ATP/ADP ratio of approximately 400%

greater than NN. The decision to make use of median rather than mean percentages to evaluate system and organ profiles is therefore supported.

Dose group VS presented with median plasma antioxidant capacity levels of 230%, which was also indicated to exceed the 200% median boundary. As presented in Section 5.3.2, no outliers or extreme outliers were determined to be present in the plasma antioxidant capacity data set. Therefore, the elevated median antioxidant capacity for VS could not be accounted for by the presence of an extreme outlier. It can be observed from Table 5.42 that the antioxidant capacity recordings for all groups were higher than the environmental controls NN, suggesting that the vehicle may have contributed to the improved antioxidant capacities. Moreover, all these groups harboured median antioxidant capacity recordings that were more than 20% greater than NN. Since rat groups that received the vehicle Factor-1 dose harboured antioxidant capacity levels that were similar to groups that received rotenone, it can also be suggested that rotenone did not appear to have an effect on plasma antioxidant capacity in rats. This notion was confirmed by the factorial ANOVA statistics, where the contribution from Factor-1 was not determined to be statistically significant. However, based on findings in the blood hydroperoxide data generated for the rat pilot study, it may too be speculated that rotenone contributed to the increased antioxidant capacities. It was indeed determined that complex I inhibition was attained via the oral dosage of rotenone, which resulted in increased hydroperoxide formation up to 9 $mg.kg^{-1}.day^{-1}$ dose concentrations. Since hydroperoxide recordings were observed to be equivalent to that of the environmental control dose groups when rats were dosed at the highest concentration of 15 $mg.kg^{-1}.day^{-1}$ rotenone, it was postulated that rotenone contributed to this phenomena by improving antioxidant capacity, either by directly scavenging ROS or indirectly by up-regulating biologically relevant antioxidant mechanisms. As discussed in Section 5.3.2, CoQ_{10} and succinate contributed to improved antioxidant capacity levels in rats, which are supported by the factorial ANOVA statistics that indicated a statistically significant contribution of Factor-2 dose regimens. Rat groups VC and VS as well as RC and RS harboured the highest median percentage antioxidant capacities. Table 5.42.B also indicates that dose groups VC, VS and RC differed statistically significantly from the environmental controls NN, while RS did not. However, dose group VX, which presented with a median percentage of 119%, lower than the 126% for RS, also differed significantly from NN. By referring to Section 5.3.2, where antioxidant capacity data was presented for blood, it can be observed that the distribution of data points in dose group VX were more narrowly clustered within an IQR of 824 μM TE, as opposed to the IQR of 1591 μM TE for RS. It

was suspected that the increased variance observed for dose group RS resulted in the non-significant p-value when compared to NN, as generated by the Tukey *equal number HSD* multiple comparison procedure.

In addition to antioxidant capacity median percentages, the bar graph in Table 5.42.A indicates towering columns for ATP/ADP ratios in blood. Excluding the previously discussed VV rat group, it can be observed that dose groups VN, VS, RN and RV also presented with median ATP/ADP ratios that improved by more than 10% from the environmental controls NN. Dose groups VN and RN improved the most with ATP/ADP ratios that were 69.0% and 114% respectively. However, the grid indicates that only dose group VV, which was argued in Section 5.3.5 to present with the aberrantly high median percentage of 454%, differed statistically significantly from NN. Therefore, dose groups VN and RN, even though they presented with considerably improved median percentages, failed to differ from the environmental controls with statistical significance. This example is suggestive of the fact that it is certainly of value to interpret the median percentages in conjunction with statistical significance. The lack of statistical significance among the dose groups, when compared to NN, presented in Table 5.42.B does not support the usage of either CoQ_{10} or succinate in improving blood ATP/ADP status in rats. However, it should also be noted from the factorial ANOVA symbols that Factor-2 dose regimens contributed statistically significantly whether extreme outliers were excluded or not. In addition, upon exclusion of the extreme outliers, a statistically significant interaction effect was reported. Therefore, the factorial ANOVA statistics suggest that the Factor-2 dose regimens did indeed influence the ATP production in blood. However, it was suspected that the elevated median percentage for dose group VV might well have induced these significant statistics. Since rotenone did not appear to affect ATP/ADP ratios adversely, it was therefore not possible to evaluate any form of contribution from either CoQ_{10} or succinate effectively in the presence of a Complex I deficiency. Moreover, rat groups that received vehicle Factor-1 doses did not illustrate preferential responses to the therapeutic regimens either.

Glutathione status of blood in rats was mostly adversely affected by the various dose regimens. All rat groups presented with median percentages less than that of the environmental controls NN. Dose group VC, which presented with a blood GSH/GSSG ratio of -4.2%, was the only dose group that did not have a glutathione ratio that was more than 10% less than NN. This is suggestive of the fact that sunflower oil vehicle may have affected glutathione ratios adversely. As with the blood hydroperoxide data, it was

speculated that the decreased GSH/GSSG ratios resulted from the reported oxidative stress (Turpeinen *et al.*, 1998) and susceptibility to lipid peroxidation (Mataix *et al.*, 1998) induced by the polyunsaturated fat contents of sunflower oil. Upon exclusion of the extreme outliers from the blood GSH/GSSG data set, dose groups VV, VS, RX and RV differed statistically significantly from NN, while the remainder of the groups did not. Since the factorial ANOVA statistics reported a statistically significant interaction effect, whether the extreme outliers were excluded or not, it was speculated that a suppressed recovery in GSH/GSSG ratios was present in rats that were dosed with a rotenone Factor-1 dose. The argument can be further supported by the fact that dose group VC, that received a CoQ_{10} Factor-2 dose after 14 days of vehicle, consisted of rats that harboured alleviated glutathione ratios, similar to that of dose group NN. In contrast, rat group RC did not present with improved GSH/GSSG ratios. Therefore it may be hypothesised that rotenone interacted with Factor-2 dose regimens by preventing recovery, or at least partial recovery, in blood GSH/GSSG ratios.

Rats that were dosed with a vehicle Factor-1 dose presented with improved L/P ratios. Dose groups VX, VN, VV, VC and VS consisted of rats that harboured improved L/P ratios that were between 46% and 67%. Even though the L/P ratios for VX and VS were improved by 64.1% and 66.3% respectively, over the environmental controls NN, these differences were not determined to be of statistical significance. Once again, the advantages of indicating statistical significance in conjunction with median percentages are evident. The greater than 60% improvements in the median blood L/P ratios of VX and VS would have the reader believe that these differences were significant. However, this is not supported due to the lack of statistically significant differences when compared to the environmental controls NN. In view of the L/P data presented here, the rotenone-dosed rats appeared to be adversely affected by the inhibition of complex I. Rat groups RX, RN and RV harboured raised L/P ratios and hence negative median percentages that were all more than 10% lower than NN. However, the Complex I deficiency rats that received therapeutic regimens on days 15 and 16, namely RC and RS, appeared to have recovered to L/P ratios that were 4.50 and 35.9% improved over the environmental controls NN. However, it was unfortunate that the recovery could not be confirmed statistically from the multiple comparison data, as discussed in Section 5.3.4. Furthermore, the factorial ANOVA statistics suggested that only Factor-1 dose regimens contributed statistically significantly to the L/P ratios in blood.

The NAD/NADH ratios obtained from blood were not informative enough to conclude that improvements or harmful effects of the dose regimens were attained. In addition, no statistically significant contributions from either of the dose factors were determined to be present. Results obtained from rat group RX do however suggest that rotenone did indeed inhibit complex I and adversely affect the NAD/NADH ratios in rats. The aforementioned group presented with a median NAD/NADH ratio that was approximately 42.4% lower than the environmental controls NN, a result that would be expected if complex I was inhibited. However, since none of the dose groups differed statistically significantly from NN, it could not be confidently stated that any of the dose regimens influenced NAD/NADH ratios in blood, even though median percentages of the data may suggest it.

As discussed previously in this section, antioxidant capacity data of the blood profile indicated that all dose groups benefited by more than 20% from the dose regimens. This is in contrast to the blood GSH/GSSG data where all ratios were lowered, and hence interpreted as adversely affected. Factorial ANOVA statistics generated from both data sets indicated that Factor-1 dose regimens did not contribute statistically significantly, suggesting that rotenone did not additionally influence these biochemical markers. Therefore, it was deduced from the factorial ANOVA statistics that deviations from the environmental controls NN were attributed predominantly to the effects of sunflower oil. Since both assays give insight into the redox status of a sample, it may have been expected that, if improved antioxidant capacities were determined in rats via the ORAC assay, a similarly improved outcome would be attained for glutathione ratios. However, this was not determined to be the case. The glutathione assay reflects the redox status from the point of view of glutathione alone. It does not account for the additional multitude of antioxidant mechanisms that exist, which too contribute to the *in vivo* management of oxidative stress. Glutathione functions not only itself as a scavenger of free radicals, but also provides reducing capacity for various enzymatic antioxidant reactions, and is also involved in the detoxification process of xenobiotics (Pastore *et al.*, 2003). Therefore, decreased GSH/GSSG ratios indicate that this scavenging component of the total antioxidant capacity, namely that which reflects the antioxidant mechanisms influencing GSH and GSSG concentrations, has been affected adversely.

The ORAC protocol (Ou *et al.*, 2001) utilised for this study measures, as the name states, the capacity of a sample to quench peroxyl radicals generated by the AAPH reagent directly. Therefore, the assay reflects all components in the sample that directly scavenge

peroxyl radicals, which includes ascorbate, bilirubin (Frei *et al.*, 1988) and several others (Gutteridge, 1995). As noted by Ou *et al.* (2001), the ORAC assay is aqueous-based and therefore does not account for antioxidant capacity contributed by lipophilic compounds. The protocol was later adapted to enable quantification of lipophilic antioxidant capacity, which was reported to account for approximately 30% of the total antioxidant capacity of plasma (Prior *et al.*, 2003). The latter protocol was unfortunately not utilised in this investigation, hence the resulting antioxidant capacity data represented antioxidant capacities of the hydrophilic component of plasma. Another aspect to be taken into account is that the glutathione concentrations were determined from whole blood sample collections and therefore represented both intra- and extracellular glutathione concentrations. In contrast, the ORAC protocol is based on the analysis of plasma samples, and thus does not reflect intracellular antioxidant capacity at the time of collection. Furthermore, these assays do not directly reflect the enzymatic-based antioxidant activities, which include, amongst others, dismutases, peroxidases and catalase. Therefore, both analysis types estimate only selected facets of the total antioxidant capacity of a sample. In fact, there is no all-inclusive assay to evaluate antioxidant capacity in its totality. It is therefore scientifically advised to implement more than one redox-evaluating assay in study protocols, as performed in this investigation. Nonetheless, data from the blood biochemical profile suggests that the glutathione antioxidant component was depleted due to the oxidative effects of sunflower oil, while the plasma hydrophilic antioxidant capacity improved.

As mentioned previously in this section, the purpose of generating a profile of biochemical parameters was to gain additional insight into the global effect that the various dose regimens would have on the different tissue types. In view of the blood profiles generated for dose groups that received vehicle Factor-1 doses, namely VX, VN, VV, VC and VS, it can be observed that 13 median percentages were indicated in blue text, eight in red and the remaining nine in grey. The majority of the blue text is suggestive of the blood profile benefiting more than it was harmed by the sunflower oil Factor-1 dose regimens. Upon evaluation of the colour-coding scheme amongst the absence of Complex I deficiency rat groups in Table 5.42.B, it can be observed that 10 of the 13 blue median percentages can be accounted for by the antioxidant capacity and L/P data sets. This indicates that sunflower oil mostly improved biochemical status on a blood level, with the most significant impact on L/P and antioxidant capacity. However, it can be observed that the other oxidative marker data, generated via the d-ROMs and GSH/GSSG protocols, suggested harmful effects induced by the vehicle. These are in concordance with

previous reports (Turpeinen *et al.*, 1998) that the high polyunsaturated fat content of sunflower oil resulted in increased oxidative stress. The fact that L/P ratios and antioxidant capacity levels were improved amongst these rats indicates that these blood defence systems were possibly up-regulated to overcome the oxidative stress induced by the vehicle.

The rotenone Factor-1 groups, namely RX, RN, RV, RC and RS presented with a blood profile that had nine median percentages indicated in blue, 12 in red and the remaining nine in grey. It may be speculated that the majority of red percentages are suggestive of a compromised blood profile when rats received the rotenone complex I inhibitor, which was a result that was expected. However, based on the proposed antioxidant contributions of rotenone itself, it can certainly be argued that the profile could have portrayed a far worse scenario, especially if the hydroperoxide data was to present with raised hydroperoxide concentrations. Prior to initiation of the study, it was expected that increased rotenone concentrations would undoubtedly increase hydroperoxide levels in direct correlation. This was proven not to be the case beyond the 9 $mg.kg^{-1}.day^{-1}$ rotenone dose concentration in the pilot study, which was subsequently supported by data generated in the main study. If hydroperoxide concentrations were reported to be elevated in the complex I deficient rats, the overall red appearance of median percentages would have increased markedly, implicitly portraying the harmful effects of rotenone.

5.3.7.1 Impact of coenzyme Q10 and succinate on the rat blood profile

If the effects of CoQ_{10} and succinate on a blood level were to be evaluated in rats not harbouring a Complex I deficiency, namely dose groups VC and VS, it can be argued that CoQ_{10} was, overall, more beneficial than succinate. Hydroperoxide levels from both VC and VS remained consistent with the environmental controls NN. Based on the ORAC-generated data, antioxidant capacities improved statistically significantly, for both dose groups. However, the GSH/GSSG ratios for dose group VS decreased statistically significantly to a negative median percentage of -42.9%, as opposed to VC that presented with a GSH/GSSG ratio that was -4.2% of NN. Dose groups VX, VN and VV presented with diminished GSH/GSSG ratios of -37.0%, -31.7% and -49.5% respectively. Therefore, since VS harboured a median GSH/GSSG ratio similar to the aforementioned groups, it can be argued that the CoQ_{10} Factor-2 dose was more beneficial than succinate, resulting in a recovery of the glutathione status to approximately normal ratios. Furthermore, since it was previously demonstrated in Section 5.3.3 that blood GSH/GSSG ratios for VC and

VS differed statistically significantly upon the exclusion of extreme outliers, it can be concluded that CoQ_{10} was indeed more beneficial than succinate in alleviating blood GSH/GSSG ratios. Lactate/pyruvate ratios appeared equally favourable for dose groups VC and VS, while fluctuations of approximately 20% in ATP/ADP and NAD/NADH ratios were observed. Data generated from the aforementioned parameters indicated that dose groups VC and VS did not differ significantly from each other. Therefore, since the GSH/GSSG median percentage ratio was the only distinctive discrepancy between dose groups VC and VS, it can be argued that CoQ_{10} was more beneficial to the absence of Complex I deficiency rats than succinate, thereby improving the biochemical status in blood.

Rat groups receiving CoQ_{10} and succinate in the presence of Complex I deficiency, namely RC and RS, on the whole presented with isolated benefits in biochemical status on a blood level. Hydroperoxide levels deviated only slightly from the environmental controls NN with median percentages of 2.6% and 5.3% for RC and RS respectively. The median percentage antioxidant capacities for RC and RS, calculated to be 159% and 126% respectively, demonstrated not only greater than 100% improvements in antioxidant capacity but also that the improvements exceeded those of the other rotenone-treated rats, suggesting favourable response to the therapeutic regimens. However, only the 159% increase of RC was determined to differ statistically significantly from NN, although this was after the exclusion of extreme outliers. Comparative decreases in glutathione status were observed in RC and RS at -34.5% and -33.7% respectively, indicating that the therapeutic regimens did not benefit the rats in terms of GSH/GSSG ratios determined from whole blood. Dose group RS presented with a 35.9% improvement in the L/P ratio, whereas RC remained similar at 4.50% of the environmental controls NN. However, it should be noted that the remaining rotenone dose groups RX, RN and RV all presented with negatively affected L/P ratios of -39.5%, -23.6% and -19.3% respectively. Once again, the beneficial effects of therapeutic regimens are illustrated, with a more favourable response to succinate being demonstrated by the rats. In view of the ATP/ADP ratios recorded in dose groups RC and RS, a slight decrease in ATP production of -16.0% and -8.21% is demonstrated respectively. Neither of the ATP/ADP ratios for these groups differed statistically significantly from NN. Finally, it was illustrated that dose group RS harboured an NAD/NADH ratio similar to that of the environmental controls NN at 1.68%, whilst RC had an NAD/NADH ratio that was approximately 25% less than RS at -22.4%. Once again though, neither dose groups RC nor RS differed by statistically significant degrees from NN. Therefore, it can be observed and argued from the blood data

generated from rats harbouring an induced Complex I deficiency that both CoQ_{10} and succinate indeed proved to be beneficial to certain of the biochemical parameters. However, even though CoQ_{10} improved antioxidant capacity to a statistically significant degree, it cannot be concluded with confidence as to which of the therapeutic regimens benefited the complex I deficient rats the most. Succinate and CoQ_{10} were of benefit to different components of the blood profile, but were also proven ineffective to others.

5.4 RAT HEART MUSCLE DATA

The heart organs were collected upon sacrificing the rats in both the rat pilot and main studies, followed by weighing and the appropriate preparation of heart muscle for the various assays included in the study. In the rat pilot study, two sets of data were generated, namely the organ weight and complex I activities. These two data sets proved to be informative and were hence included for analysis in the rat main study. The aforementioned study also resulted in the generation of antioxidant capacity data, L/P ratio and ATP/ADP ratio data sets. Raw data generated from heart muscle during the rat pilot and main studies are presented in Appendix Chapters B, C, E and F. Glutathione and pyridine data could not be determined due to unsuccessful data generation.

The lack of success in determining GSH/GSSG ratios can be accounted for by autoxidation of the prepared samples. Glutathione redox status could also not be determined in brain and skeletal muscle for the same reason. The stability of glutathione isolates was compromised considerably by the period of time that elapsed between the collection date and date of assay. Since the rat main study consisted of 66 rats that were dosed for 14 to 16 days, followed by sacrificing and tissue preparation, it was not possible to simultaneously perform sample collection and analysis. Consequently, rat group dosing was initiated in a staggered schedule resulting in a dose and sacrificing period spanning approximately 30 days. Therefore, the initial dose groups were sacrificed several days before the final groups resulting in samples that were prepared from the former rat groups being stored for longer periods of time. Moreover, since the assays were performed according to tissue types, an extended time period elapsed before the last tissue group was analysed. The instability of glutathione, even at the storage temperature of -80°C, resulted in autoxidation and consequent exclusion of rat brain tissue, heart and skeletal muscle data sets.

Ratios of NAD to NADH are presented for blood, skeletal muscle and liver tissue. The assay could not be accurately optimised for heart muscle and brain, primarily due to the restrictions in the availability of tissue of these two organs. Since the assay for the determination of pyridine concentrations required large volumes of sample preparations per reaction, the sample became limited. It is expected that an alternative technology, such as gas or liquid chromatography, requiring smaller sample volumes would benefit similar studies in the future, which are aimed at analysing several biochemical parameters from a single tissue group.

5.4.1 Heart organ weights

Upon sacrificing the rats, the heart was removed and blood extracted from it via the use of a needle and syringe. To follow, the heart was rinsed momentarily in phosphate buffered saline (PBS) buffer and gently depressed on tissue paper to remove excess blood and buffer. The organ weights were promptly recorded and the tissue immediately stored appropriately for tissue preparation. The organ weights, as opposed to relative organ weights, which would be the organ weight divided by body weight, were evaluated for statistical variation. The reason for this decision was based on the argument that the ratio of relative organ weight is influenced by two factors, namely the organ weight and overall body weight. Since rats receiving rotenone lost considerable amounts of weight as the concentrations increased, the body weight component varied a significantly large amount.

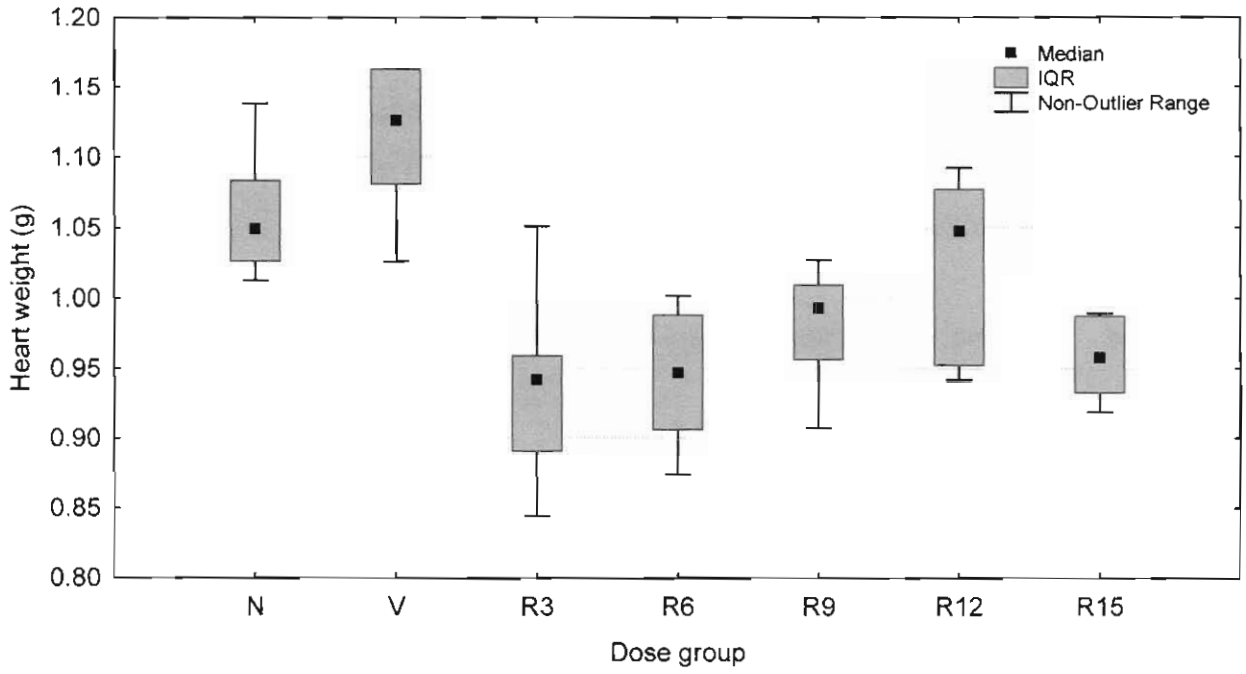
The variation range for organ weights is less than for body weights, which therefore results in the relative organ weight ratio being far more vulnerable to fluctuations, dependent on body weight. Furthermore, from a mathematical point of view, unless proportional growth in organ and body weights was observed for each rat, an exponential increase in the ratio of organ weight over body weight would be determined. In order to enable a simplified interpretation of the final organ weight data, it was therefore decided to evaluate the actual weight of organs on condition that the initial body weights did not differ significantly from each other. Although the data is not presented, it was determined that initial rat weights, that is, on day 1 of the dosage period, did not differ statistically significantly from each other within both the pilot and main studies. It was assumed that since total body weight between all rat groups did not differ statistically significantly at the start of the dosage period, the initial organ weights too would not differ significantly. Therefore, any statistically significant differences reported between organ weights would be the consequence of dose regimens received, independent of alterations to body weight. This methodology was also used when brain and liver weights were evaluated.

5.4.1.1 Rat pilot study heart weights

Heart weights in the pilot study were recorded in Excel® format and evaluated statistically via the use of STATISTICA™. The distribution of heart weights according to dose group is presented graphically in Table 5.43, along with a table of descriptive statistics. The box-whisker plots in Table 5.43.A indicate that no outliers or extreme outliers were determined to be present in the heart weight data set.

Table 5.43 Box-whisker representation and descriptive statistics of the rat heart weight data generated from the pilot study

A: Box-whisker plots and data points according to rat groups



Rat	N	V	R3	R6	R9	R12	R15
1	1.03	1.03	1.05	1.00	0.91	1.03	0.97
2	1.08	1.16	0.89	0.99	0.96	1.08	0.99
3	1.14	1.16	0.96	0.96	0.98	1.07	0.93
4	1.06	1.14	---	0.87	1.00	1.09	0.92
5	1.01	1.12	0.94	0.93	1.03	0.95	0.94
6	1.03	1.08	0.84	0.91	1.01	0.94	0.99

B: Descriptive statistics

Dose group	Sample size	Mean	SD	Median	Min	Max	Range	Lower quartile	Upper quartile	IQR
N	6	1.06	0.05	1.05	1.01	1.14	0.13	1.03	1.08	0.06
V	6	1.11	0.05	1.13	1.03	1.16	0.14	1.08	1.16	0.08
R3	5	0.94	0.08	0.94	0.84	1.05	0.21	0.89	0.96	0.07
R6	6	0.94	0.05	0.95	0.87	1.00	0.13	0.91	0.99	0.08
R9	6	0.98	0.04	0.99	0.91	1.03	0.12	0.96	1.01	0.05
R12	6	1.03	0.07	1.05	0.94	1.09	0.15	0.95	1.08	0.12
R15	6	0.96	0.03	0.96	0.92	0.99	0.07	0.93	0.99	0.05

Rats were treated with N = no dose, V = vehicle, R3 = rotenone 3 $mg.kg^{-1}.day^{-1}$, R6 = rotenone 6 $mg.kg^{-1}.day^{-1}$, R9 = rotenone 9 $mg.kg^{-1}.day^{-1}$, R12 = rotenone 12 $mg.kg^{-1}.day^{-1}$, R15 = rotenone 15 $mg.kg^{-1}.day^{-1}$. '---' = missing data point due to death of rat R3-4, g = grams, IQR = inter-quartile range, Min = minimum data point value, Max = maximum data point value, SD = standard deviation.

It appears that all rats that received a rotenone dose, even if it was only 3 $mg.kg^{-1}.day^{-1}$, presented with a decrease in heart weight. However, since the median for dose group R12 was similar to that of the control groups N and V, it can be argued that rotenone did not consistently affect heart weights throughout. Nonetheless, the majority of rats that received rotenone presented with adversely affected heart weights. It also appears that a trend was present in that an increase in the organ weight was recorded as the dose concentration increased from 3 to 12 $mg.kg^{-1}.day^{-1}$, followed by a decrease when 15 $mg.kg^{-1}.day^{-1}$ was received.

It should also be noted that dose group V presented with a slightly heavier heart than the environmental controls N. The significance of the aforementioned differences was evaluated statistically via the one-way ANOVA and Tukey *unequal number HSD* multiple comparison test. The p-values generated from these statistical tests are presented in Table 5.44, along with a table of biologically significant d-values calculated for the comparisons that proved to be of statistical significance.

Table 5.44 Multiple comparison statistics of heart weight data generated from the rat pilot study

A: Parametric Tukey *unequal number HSD* p-values

Dose group	N	V	R3	R6	R9	R12	R15
N		0.577	0.014	0.010	0.169	0.926	0.030
V	0.577		< 0.001	< 0.001	0.002	0.092	< 0.001
R3	0.014	< 0.001		1.000	0.848	0.145	0.997
R6	0.010	< 0.001	1.000		0.886	0.135	0.999
R9	0.169	0.002	0.848	0.886		0.759	0.986
R12	0.926	0.092	0.145	0.135	0.759		0.298
R15	0.030	< 0.001	0.997	0.999	0.986	0.298	

B: ANOVA p-values

One-way ANOVA p-value < 0.001

C: Statistical and biological significance

Comparison		Statistical significance (p)	Biological significance (d)
N	R3	0.014	2.256
N	R6	0.010	2.256
N	R15	0.030	1.880
V	R3	< 0.001	3.196
V	R6	< 0.001	3.196
V	R9	0.002	2.444
V	R15	< 0.001	2.820

A: All comparison statistics are indicated as p-values, generated via the Tukey *unequal number HSD* (Honestly Significant Difference) multiple comparison procedure. P-values indicated in red are statistically significant at the pre-determined significance level of 0.05. The remainder of p-values are listed in grey. The turquoise shaded blocks represent statistically significant comparisons that were also determined to be of biological significance. B: The p-value for the one-way ANOVA is listed, with significant p-values, less than the 0.05 significance level, indicated in red. C: List of comparisons determined to be statistically significant with corresponding biological significance. A d-value greater than or equal to 0.8 signifies biological significance, indicated in red. Rats were treated N = no dose, V = vehicle, R3 = rotenone 3 $mg.kg^{-1}.day^{-1}$, R6 = rotenone 6 $mg.kg^{-1}.day^{-1}$, R9 = rotenone 9 $mg.kg^{-1}.day^{-1}$, R12 = rotenone 12 $mg.kg^{-1}.day^{-1}$, R15 = rotenone 15 $mg.kg^{-1}.day^{-1}$. < = less than, ANOVA = analysis of variance.

It is apparent from the multiple comparison grid in Table 5.44.A that the rotenone dose concentrations significantly affected heart weight in rats. Dose groups R3, R6 and R15 differed statistically significantly from the environmental controls N. In addition, when compared to the vehicle control group V the same three dose groups, with the inclusion of R9, differed statistically significantly. Moreover, all of the aforementioned statistically significant differences were determined to differ with biological significance from N and V respectively. Dose group R12 did not differ significantly from any of the other dose groups. It is of importance to note that none of the rotenone-treated rat groups, namely R3 to R15, differed statistically significantly from each other, suggesting that increases in rotenone dose concentrations did not result in additionally significant alterations to heart weight.

The increase in heart weight observed for rat group V was not determined to be statistically significant when compared to the environmental controls N. Therefore, it cannot be stated confidently that the sunflower oil vehicle resulted in increased cardiac weight. However, since the IQRs for N and V did not overlap with each other and occupied distinctively separate weight ranges, as indicated in Table 5.43.A, it can certainly be argued that sunflower oil influenced heart weight, even over the short dosage period of only 14 days. It is expected that the inclusion of a larger sample size in future investigations would enable clarification of this discrepancy. If the vehicle were to affect heart weight, the effect of the sunflower oil vehicle should be taken into consideration when evaluating the effects of the rotenone dose concentrations. Therefore, the decrease in heart weight observed for rats receiving rotenone is slightly compensated for by the effects of sunflower oil, suggesting that the weight loss may in fact be underestimated.

It was not expected that organ weights would be affected by the rotenone dose concentrations over a mere 14-day dose period. However, it is apparent from the heart weight data that this was not the case. It is hypothesised that the decreased heart weights may have resulted from compromised growth and possibly apoptosis induced by high levels of oxidative stress conferred by the inhibition of complex I. As presented in Section 5.4.2, complex I activities in heart muscle were certainly lowered in rats that received rotenone. Therefore, it can be expected that a compromised state in oxidative phosphorylation, accompanied by increased free radical formation, would be present, which in turn resulted in an impaired growth and functioning of the heart. Further discussions regarding the effects of the vehicle and rotenone are discussed in the following section where heart weights generated from the main study are evaluated. In

summary, according to data presented in this section, it can be argued that the compromised cellular state was already achieved by dosing the rats with a 3 $mg.kg^{-1}.day^{-1}$ dose of rotenone for 14 days.

5.4.1.2 Rat main study heart weights

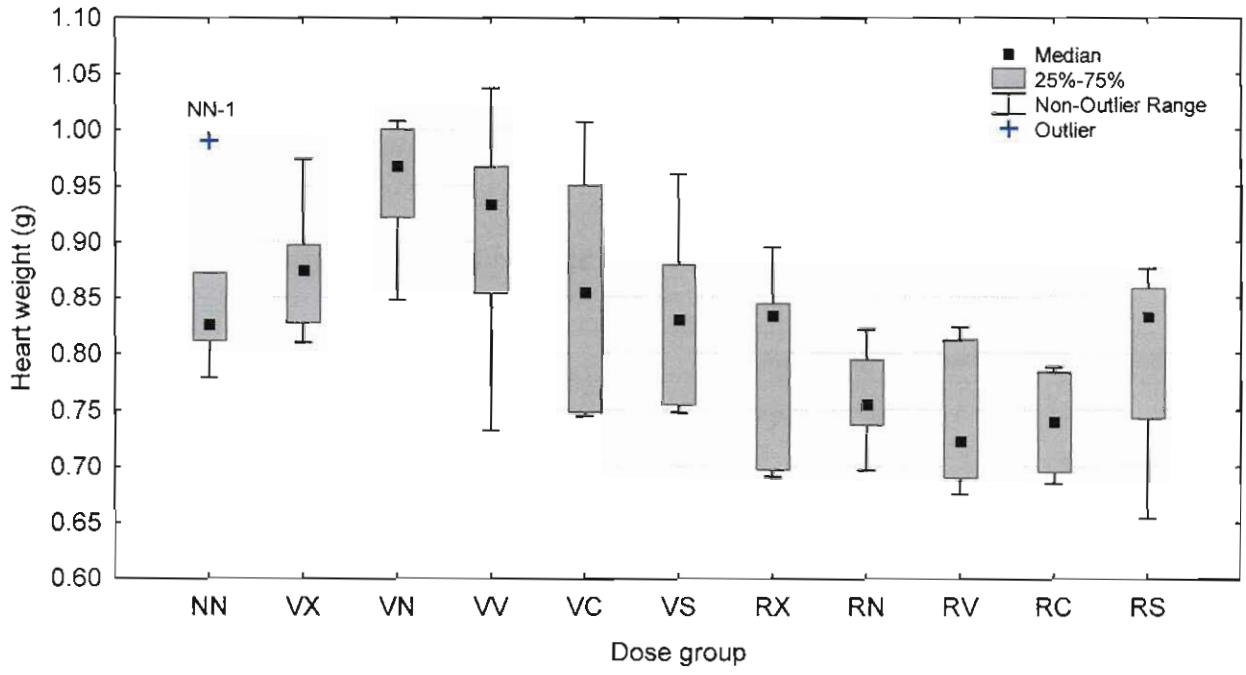
Heart weight data generated from the pilot study indicated that it would certainly be of use to evaluate the final weights of these organs in the main study. Hearts were collected and prepared in the same manner as performed in the pilot study. The distribution of heart weights as well as the descriptive statistics generated from the main study is presented in Table 5.45. The table indicates that a single outlier was determined to be present in the rat main study heart weight data set. Rat NN-1 had a final heart weight of 0.99 g, which was 0.12 g higher than the next ranked data point of 0.87 g for rat NN-3. The upper outlier boundary was calculated at 1.05 g, hence preventing the NN-1 data point of 0.06 g from being regarded an extreme outlier. Since NN-1 was relatively close to the upper outlier boundary, it would be expected that the heart weight for this rat would inflate the central tendency statistics slightly. However, since it was not determined to be an extreme outlier, it will not be excluded and will therefore contribute to the overall variation of the main study heart weight data set.

As presented in Section 5.4.1.1, it is apparent once again that rotenone indeed compromised heart weights. In general, all groups that received vehicle Factor-1 dose regimens presented with higher heart weights when compared to rats that received rotenone from days 1 to 14. This is further supported, as presented later in this section, by the factorial ANOVA results that gave rise to a statistically significant Factor-1 contribution. When compared to the environmental controls NN, it may also be argued that the sunflower oil vehicle contributed to elevated heart weights. As discussed for the rat pilot study, presented in Section 5.4.1.1, it was also demonstrated that the sunflower oil vehicle alone induced an increase in heart weights over that of the environmental control rat group. This may be argued to be the result of organ hypertrophy. Since it has been reported that an increased intake of polyunsaturated fats results in increased oxidative stress (Turpeinen *et al.*, 1998), increased susceptibility to lipid peroxidation (Mataix *et al.*, 1998) as well as DNA damage (Quiles *et al.*, 2004) and apoptosis (Cury-Boaventura *et al.*, 2005), it can be speculated that cardiac hypertrophy may have been induced to compensate for these effects. However, as presented in Table 5.46, it can be observed that none of the rat groups that received a vehicle Factor-1 dose differed

statistically significantly from the environmental controls NN. Therefore, it cannot be confidently stated that sunflower oil indeed induced a significant difference in heart weights.

Table 5.45 Box-whisker representation and descriptive statistics of the heart weight data generated from the main study

A: Box-whisker plots and data points according to rat groups



Rat	NN	VX	VN	VV	VC	VS	RX	RN	RV	RC	RS
1	+ 0.99	0.97	0.95	0.97	0.95	0.81	0.84	0.75	0.81	0.78	0.86
2	0.82	0.83	0.85	0.91	0.75	0.85	0.70	0.82	0.71	0.78	0.74
3	0.87	0.88	1.01	0.85	1.01	0.88	0.83	0.70	0.69	0.79	0.86
4	0.83	0.87	0.92	0.95	0.75	0.76	0.69	0.79	0.74	0.70	0.88
5	0.78	0.81	1.00	1.04	0.81	0.96	0.90	0.74	0.68	0.69	0.81
6	0.81	0.90	0.99	0.73	0.90	0.75	0.84	0.76	0.82	0.69	0.65

B: Descriptive statistics

Dose group	Sample size	Mean	SD	Median	Min	Max	Range	Lower quartile	Upper quartile	IQR
NN	6	0.85	0.07	0.83	0.78	0.99	0.21	0.81	0.87	0.06
VX	6	0.88	0.06	0.87	0.81	0.97	0.16	0.83	0.90	0.07
VN	6	0.95	0.06	0.97	0.85	1.01	0.16	0.92	1.00	0.08
VV	6	0.91	0.11	0.93	0.73	1.04	0.30	0.85	0.97	0.11
VC	6	0.86	0.11	0.85	0.75	1.01	0.26	0.75	0.95	0.20
VS	6	0.83	0.08	0.83	0.75	0.96	0.21	0.76	0.88	0.12
RX	6	0.80	0.08	0.83	0.69	0.90	0.20	0.70	0.84	0.15
RN	6	0.76	0.04	0.75	0.70	0.82	0.12	0.74	0.79	0.06
RV	6	0.74	0.06	0.72	0.68	0.82	0.15	0.69	0.81	0.12
RC	6	0.74	0.05	0.74	0.69	0.79	0.10	0.69	0.78	0.09
RS	6	0.80	0.09	0.83	0.65	0.88	0.22	0.74	0.86	0.11

Rat codes for the outliers are located above or below the blue crosses (+), which correspond to data point values listed in the table directly below the graph. Rats were treated with NN = no dose regimen, VX = vehicle and sacrificed, VN = vehicle and no dose, VV = vehicle and vehicle, VC = vehicle and CoQ_{10}, VS = vehicle and succinate, RX = rotenone and sacrificed, RN = rotenone and no dose, RV = rotenone and vehicle, RC = rotenone and CoQ_{10}, RS = rotenone and succinate. g = grams, IQR = inter-quartile range, Min = minimum data point value, Max = maximum data point value, SD = standard deviation.

In view of the rat groups that received CoQ_{10} and succinate as Factor-2 doses, it may be suggested that certain of the rats benefited. Amongst the rat groups that received a vehicle Factor-1 dose regimen, dose groups VC and VS presented with the lowest of median heart weights, reflecting a slight recovery in weight to that of the environmental controls NN. However, the data distributions for the aforementioned groups overlap in very similar ranges. Heart weights from the complex I deficient rats, namely RX, RN, RV, RC and RS, indicate that succinate was more beneficial in the recovery of heart weight. In an attempt to validate these speculations, the heart weight data was evaluated via ANOVA and multiple comparison test procedures. The generated p-values are presented in Table 5.46, along with d-values representing biological significance.

Table 5.46 Multiple comparison statistics of heart weight data generated from the rat main study

A: Tukey *equal number HSD* p-values

Dose group	NN	VX	VN	VV	VC	VS	RX	RN	RV	RC	RS
NN		1.000	0.464	0.961	1.000	1.000	0.983	0.616	0.341	0.311	0.984
VX	1.000		0.826	1.000	1.000	0.997	0.808	0.264	0.108	0.095	0.811
VN	0.464	0.826		0.996	0.595	0.244	0.040	0.003	< 0.001	< 0.001	0.040
VV	0.961	1.000	0.996		0.988	0.826	0.333	0.049	0.015	0.013	0.336
VC	1.000	1.000	0.595	0.988		1.000	0.952	0.484	0.240	0.216	0.953
VS	1.000	0.997	0.244	0.826	1.000		0.999	0.847	0.590	0.553	0.999
RX	0.983	0.808	0.040	0.333	0.952	0.999		0.998	0.964	0.953	1.000
RN	0.616	0.264	0.003	0.049	0.484	0.847	0.998		1.000	1.000	0.998
RV	0.341	0.108	< 0.001	0.015	0.240	0.590	0.964	1.000		1.000	0.963
RC	0.311	0.095	< 0.001	0.013	0.216	0.553	0.953	1.000	1.000		0.952
RS	0.984	0.811	0.040	0.336	0.953	0.999	1.000	0.998	0.963	0.952	

B: ANOVA p-values

One-way ANOVA p-value < 0.001

C: Statistical and biological significance

Comparison		Statistical significance (p)	Biological significance (d)
VN	RX	0.040	1.950
VN	RN	0.003	2.469
VN	RV	< 0.001	2.729
VN	RC	< 0.001	2.729
VN	RS	0.040	1.950
VV	RN	0.049	1.950
VV	RV	0.015	2.209
VV	RC	0.013	2.209

A: All comparison statistics are indicated as p-values, generated via the Tukey *equal number HSD* (Honestly Significant Difference) multiple comparison procedure. P-values indicated in red are statistically significant at the pre-determined significance level of 0.05. The remainder of p-values are listed in grey. The turquoise shaded blocks represent statistically significant comparisons that were also determined to be of biological significance. B: P-value for the one-way ANOVA is listed, with significant p-values, less than the 0.05 significance level, indicated in red. C: List of comparisons determined to be statistically significant with corresponding biological significance. A d-value greater than or equal to 0.8 signifies biological significance, indicated in red. Rats were treated with NN = no dose regimen, VX = vehicle and sacrificed, VN = vehicle and no dose, VV = vehicle and vehicle, VC = vehicle and CoQ_{10}, VS = vehicle and succinate, RX = rotenone and sacrificed, RN = rotenone and no dose, RV = rotenone and vehicle, RC = rotenone and CoQ_{10}, RS = rotenone and succinate. < = less than, ANOVA = analysis of variance.

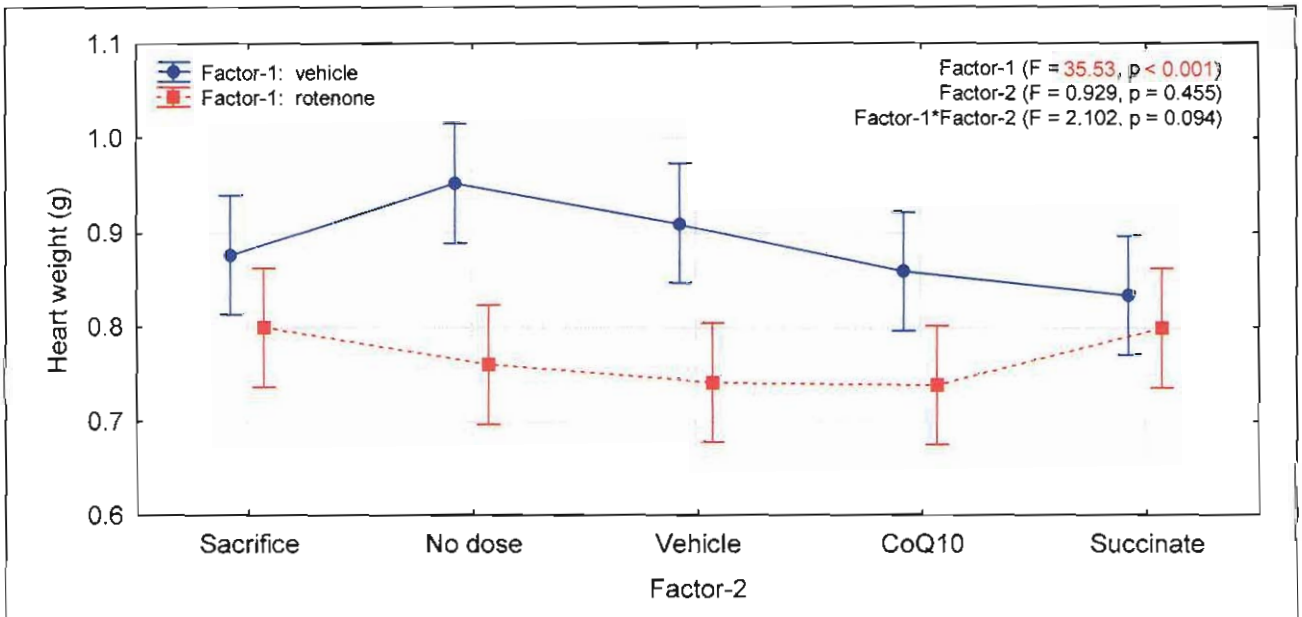
The multiple comparison grid reveals that all rats that received rotenone Factor-1 doses differed statistically significantly from dose group VN. In addition, dose groups RN, RV and RC also differed significantly from VV. Table 5.46.C provides d-values that indicates that the statistically significant comparisons also differed with biological significance. Dose groups VN and VV appeared to have harboured the highest of heart weights, suggesting that rats in these dose groups suffered most from cardiac hypertrophy. However, as mentioned previously in this section, none of the vehicle-treated rat groups differed statistically significantly from each other. In addition, since none of the rotenone-treated rat groups differed statistically significantly from each other, it cannot be concluded confidently that either of the therapeutic regimens helped recover rat heart weights. All that can be concluded from the statistically significant comparisons is that the vehicle and rotenone may have resulted in contrasting effects with regards to heart weight. As with rat groups from the pilot study, presented in Section 5.4.1.1, rats that received rotenone presented with decreased heart weights, most probably due to compromised heart growth and oxidative stress-induced apoptosis. Rat main study heart weight data were subsequently evaluated via a two-way ANOVA in order to verify Factor-1 and Factor-2 dose contributions. A summary of the two-way ANOVA results is presented in Table 5.47.

As discussed previously in this section, it was apparent that rotenone and vehicle dose regimens contributed the most to the generation of the observed heart weight data. In support of the arguments, the factorial ANOVA yielded a statistically significant contribution from the Factor-1 dose regimens. As indicated in the top right corner of the graph in Table 5.47, Factor-2 doses and the interaction between Factor-1 and Factor-2 regimens did not result in statistically significant p-values. It is also evident from the graphic representation that the vehicle and rotenone Factor-1 plots do not intersect and are continuously separate from each other. In addition, the statistically significant Factor-1 statistics, generated via the two-way ANOVA, support heart weight data from the pilot study that also indicated a statistically significant influence of rotenone on the heart. The results generated from the factorial ANOVA strengthen results of the previous section where rotenone proved to prevent heart growth in the pilot study.

It can be speculated that the inhibition of complex I by rotenone and the consequent induction of oxidative stress, among other complications, resulted in a compromised biochemical profile that in turn initiated an apoptotic cascade of events in the heart. Indeed rotenone has been reported to play a key role in inhibiting complex I and in turn inducing apoptosis (Chauvin *et al.*, 2001). Moreover, rotenone has also been reported to

induce disturbances in mitotic spindle formation and hence result in mitotic arrest (Barham and Brinkley, 1976a and b; Diaz-Corrales *et al.*, 2005). Therefore, taking into account all of the aforementioned cellular interactions of rotenone, it can certainly be argued that inhibited bioenergetics and mitotic events as well as the induction of apoptosis are all factors that may have contributed to decreased heart weights. An alternative and simplified explanation may be that since rats receiving rotenone continuously lost considerable amounts of body weight, the generally lowered heart weights in these rats may very well be accounted for by the overall inhibition of rat growth.

Table 5.47 Graphic and tabulated summary of the heart weight data analysed via a two-way ANOVA



Data points	VX	VN	VV	VC	VS	RX	RN	RV	RC	RS
UCI	0.94	1.02	0.97	0.92	0.90	0.86	0.82	0.80	0.80	0.86
mean	0.88	0.95	0.91	0.86	0.83	0.80	0.76	0.74	0.74	0.80
LCI	0.81	0.89	0.85	0.80	0.77	0.74	0.70	0.68	0.68	0.74

The plot legend for the graph is indicated in the top left corner, while the two-way ANOVA F-statistics (F) and p-values (p) for Factor-1, Factor-2 and Factor-1*Factor-2 are located in the top right corner, with the statistically significant values indicated in red. The vertical whiskers at each mean data point represent 95% confidence intervals for the respective data sets. Rats were treated with NN = no dose regimen, VX = vehicle and sacrificed, VN = vehicle and no dose, VV = vehicle and vehicle, VC = vehicle and CoQ_{10}, VS = vehicle and succinate, RX = rotenone and sacrificed, RN = rotenone and no dose, RV = rotenone and vehicle, RC = rotenone and CoQ_{10}, RS = rotenone and succinate. < = less than, g = grams, LCI = lower 95% confidence interval data point, UCI = upper 95% confidence interval data point.

The increase in heart weights recorded for the majority of rats that received vehicle Factor-1 doses was previously speculated to be the result of cardiac hypertrophy. Based on literature, as mentioned previously in this section, it was hypothesised that the high polyunsaturated content of sunflower oil resulted in cardiomyocyte susceptibility to oxidative stress, accompanied by apoptotic events. In turn, cells of the heart attempt to overcome the biochemically and mechanically stressed conditions by adopting a hypertrophic cellular state, which is characterised by an increase in the mass and volume

of cardiomyocytes as a result of qualitative and quantitative alterations in the expression profile of these cells (Wang *et al.*, 1998). Rats receiving rotenone in the presence of vehicle not only suffer the consequences induced by polyunsaturated fats, but also by the inhibition of complex I, resulting in markedly excessive superoxide formation and increased apoptotic activation (Tada-Oikawa *et al.*, 2003). The compounded harmful effects of rotenone are postulated to override all compensatory mechanisms that cardiomyocytes have to offer, resulting in overall dominance of cell death and hence decreased heart weights.

As discussed previously in this section, beneficial effects of CoQ_{10} and succinate were not determined to be statistically significant. This was supported by the factorial ANOVA statistics that reported a lack of statistical significance for Factor-2 dose regimens. This is not a surprising result since the heart is not known to be an effective tissue regenerative organ, like the liver for example. If recovery were to take place, it would be expected over a far longer period of time.

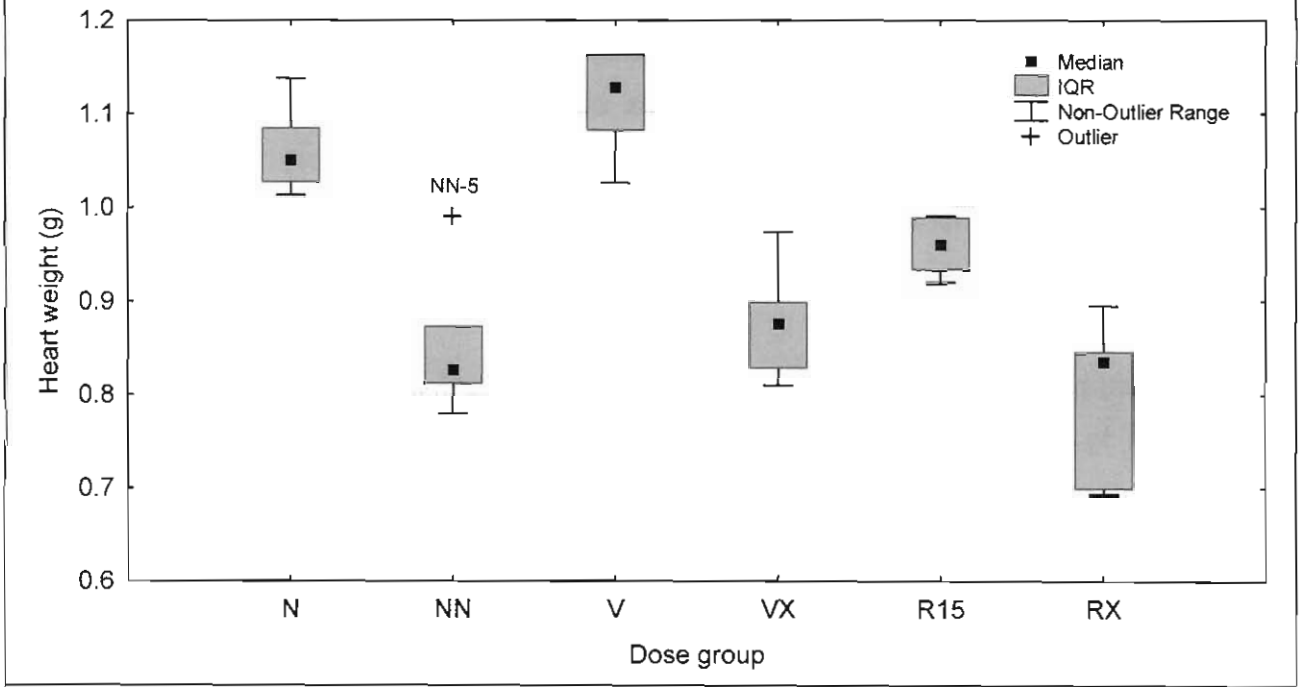
5.4.1.3 Comparative analysis of heart weight data generated from the rat pilot and main studies

In order to determine if consistency in response was recorded between the rat pilot and main studies, comparable dose groups were evaluated statistically. The comparable groups included the environmental control dose groups N and NN, the groups that received vehicle for 14 days, namely V and VX of the pilot and main studies respectively, as well rat groups that received rotenone dose concentrations for 14 days, R15 and RX. Results from the comparison are presented in Table 5.48, which includes box-whisker representations, descriptive statistics and multiple comparison p-values. The descriptive statistics presented in Table 5.48.B were obtained from Table 5.43 and Table 5.45, and is listed for ease of reference.

As can be observed from the box-whisker representations, it is apparent that all groups from the main study harboured lowered heart weights when compared to equivalent rat groups of the pilot study. Moreover, all of the comparable dose groups differed statistically significantly from each other, namely N from NN, V from VX, and R15 from RX.

Table 5.48 Summary of comparative dose groups of the rat pilot and main study heart weight data

A: Box-whisker plots and data points according to rat groups



B: Descriptive statistics (from Table 5.43 and Table 5.45)

Dose group	Sample size	Mean	SD	Median	Min	Max	Range	Lower quartile	Upper quartile	IQR
N	6	1.06	0.05	1.05	1.01	1.14	0.13	1.03	1.08	0.06
NN	6	0.85	0.07	0.83	0.78	0.99	0.21	0.81	0.87	0.06
V	6	1.11	0.05	1.13	1.03	1.16	0.14	1.08	1.16	0.08
VX	6	0.88	0.06	0.87	0.81	0.97	0.16	0.83	0.90	0.07
R15	6	0.96	0.03	0.96	0.92	0.99	0.07	0.93	0.99	0.05
RX	6	0.80	0.08	0.83	0.69	0.90	0.20	0.70	0.84	0.15

C: Tukey *equal number HSD* p-values

Dose group	N	NN	V	VX	R15	RX
N		< 0.001	0.633	< 0.001	0.063	< 0.001
NN	< 0.001		< 0.001	0.977	0.049	0.674
V	0.633	< 0.001		< 0.001	0.001	< 0.001
VX	< 0.001	0.977	< 0.001		0.216	0.262
R15	0.063	0.049	0.001	0.216		0.001
RX	< 0.001	0.674	< 0.001	0.262	0.001	

Rat codes for outliers are located above or below the respective blue crosses (+). All comparison statistics are indicated as p-values generated via the Tukey *equal number HSD* (Honestly Significant Difference) multiple comparison procedure. The p-values indicated in red are statistically significant at a significance level of 0.05, while all other p-values are in grey. Rats were treated with N = no dose regimen (pilot study), NN = no dose regimen (main study), V = vehicle (pilot study), VX = vehicle (main study), R15 = rotenone 15 $mg.kg^{-1}.day^{-1}$ (pilot study), RX = rotenone 15 $mg.kg^{-1}.day^{-1}$ (main study). < = less than, g = gram, IQR = inter-quartile range, Min = minimum data point value, Max = maximum data point value, SD = standard deviation.

It is not evident as to why the differences existed between the aforementioned dose groups. Environmental conditions, dosage and organ collection protocols remained unchanged between the studies. It was originally suspected that calibration of the measuring scale may have been altered during the time period that elapsed between the two studies. However, if this were to be the case, discrepancies in organ weights would

be recorded for brain and liver data too. As presented in subsequent sections, this was not determined to be the case, resulting in heart weight data being the exception. The fact that all main study heart weights presented in lower ranges may suggest that some or other environmental conditions may have influenced heart growth. Nonetheless, heart weight data generated from the rat pilot and main studies were evaluated in reference to the respective controls, as presented previously in this section and in Section 5.4.1.1.

5.4.2 Complex I activity in heart muscle

Enriched mitochondrial samples were prepared from heart muscle that was collected upon sacrificing of the rats. The assays were performed spectrophotometrically and the data captured for statistical evaluation in STATISTICA™. Heart muscle complex I activities in terms of UCS are presented for the rat pilot and main studies in subsequent sections.

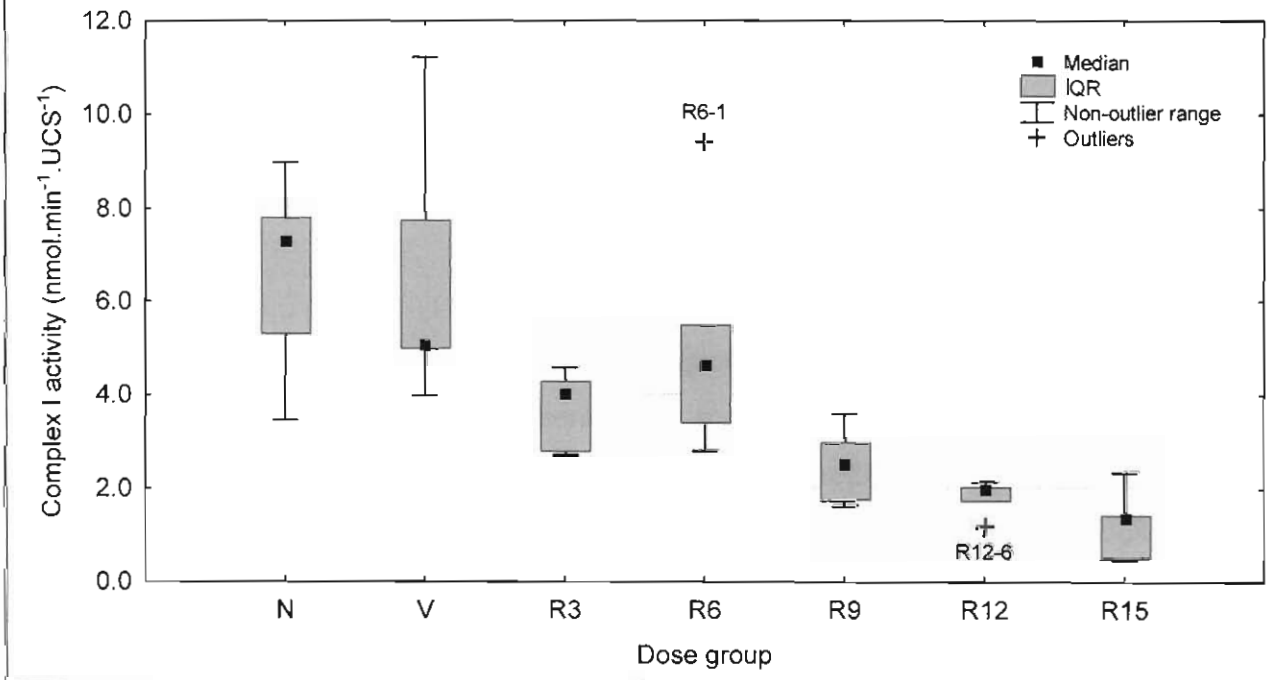
5.4.2.1 Pilot study complex I activity in heart muscle

Complex I activity was assayed in heart muscle following the determination of citrate synthase and protein concentrations in the same mitochondrial sample. The raw data generated from the three assays were captured in Excel® spreadsheets and finally evaluated statistically in STATISTICA™. The complex I activities, box-whisker plots and descriptive statistics generated from heart muscle in the pilot study are presented in Table 5.49.

A proportional decrease in the activities of complex I as the concentration of rotenone increased is evident in the box-whisker representation of Table 5.49.A. The group of rats that received 15 $mg.kg^{-1}.day^{-1}$ rotenone had a mean enzyme activity of 1.22 nanomole per minute per unit citrate synthase ($nmol.min^{-1}.UCS^{-1}$), whereas dose group V presented with a mean of 6.33 $nmol.min^{-1}.UCS^{-1}$, approximately five times higher. It can also be determined from the descriptive statistics that the median complex I activity for dose group N was higher than that determined for rat group V. However, the distribution of data within each group appears to be in very similar activity ranges.

Table 5.49 Box-whisker representation and descriptive statistics of the complex I data generated from heart muscle during the rat pilot study

A: Box-whisker plots and data points according to rat groups



Rat	N	V	R3	R6	R9	R12	R15
1	8.98	4.98	2.69	+ 9.41	1.73	2.12	1.34
2	3.45	3.97	4.25	3.38	3.59	1.70	1.38
3	7.78	5.05	3.99	2.79	2.94	1.91	2.33
4	7.68	5.04	—	5.47	2.48	1.99	1.30
5	6.85	11.21	2.77	4.13	1.61	1.95	0.49
6	5.30	7.71	4.58	5.08	2.52	+ 1.14	0.46

B: Descriptive statistics

Dose group	Sample size	Mean	SD	Median	Min	Max	Range	Lower quartile	Upper quartile	IQR
N	6	6.67	1.99	7.27	3.45	8.98	5.53	5.30	7.78	2.48
V	6	6.33	2.70	5.05	3.97	11.2	7.24	4.98	7.71	2.74
R3	5	3.66	0.87	3.99	2.69	4.58	1.89	2.77	4.25	1.48
R6	6	5.04	2.36	4.61	2.79	9.41	6.62	3.38	5.47	2.09
R9	6	2.48	0.74	2.50	1.61	3.59	1.98	1.73	2.94	1.20
R12	6	1.80	0.35	1.93	1.14	2.12	0.97	1.70	1.99	0.29
R15	6	1.22	0.69	1.32	0.46	2.33	1.87	0.49	1.38	0.89

Rat codes for outliers are located above or below the respective blue crosses (+), which correspond to data point values listed in the table directly below the graph. Rats were treated with N = no dose, V = vehicle, R3 = rotenone 3 $mg.kg^{-1}.day^{-1}$, R6 = rotenone 6 $mg.kg^{-1}.day^{-1}$, R9 = rotenone 9 $mg.kg^{-1}.day^{-1}$, R12 = rotenone 12 $mg.kg^{-1}.day^{-1}$, R15 = rotenone 15 $mg.kg^{-1}.day^{-1}$. '—' = missing data point due to death of rat R3-4, IQR = inter-quartile range, Min = minimum data point value, Max = maximum data point value, $nmol.min^{-1}.UCS^{-1}$ = nanomole per minute per unit citrate synthase activity, SD = standard deviation.

Dose groups R3 and R6 demonstrated inhibition of complex I, but not in a manner that was expected, since the median and distribution of data for R6 extended higher than that of R3. A possible explanation for this would be that the 3 $mg.kg^{-1}.day^{-1}$ dose concentration difference between R3 and R6 was not enough to inhibit complex I more than that observed in R3. It should be noted that R6 harboured an outlier within its data set, inflating the central tendency of the group. If R6-1 was excluded from the R6 group,

the mean and medians would have decreased to 4.17 and 4.13 nmol.min^{-1}.UCS^{-1} respectively. These statistics are very similar to the mean and median for R3, which are 3.66 and 3.99 respectively. The small difference between the groups, if R6-1 is excluded, supports the previously mentioned proposal that 3 mg.kg^{-1}.day^{-1} rotenone at the low concentration range of 3 and 6 mg.kg^{-1}.day^{-1} has little effect on the inhibition of complex I. In addition, as discussed later in this section, no statistically significant differences were determined to exist between groups N through to R6.

Table 5.49.A illustrates the presence of two outliers in groups R6 and R12. Rat R6-1 had an enzyme activity of 9.41 nmol.min^{-1}.UCS^{-1}, while the next highest activity in R6 was 5.47 nmol.min^{-1}.UCS^{-1}, for R6-4. The lowest recording in this group was 2.79 nmol.min^{-1}.UCS^{-1}, indicating that the range of data from the lowest to second highest data point of R6-4 is 3.32 nmol.min^{-1}.UCS^{-1}. The range from R6-4 to R6-1 is 3.94 nmol.min^{-1}.UCS^{-1}. If R6-1 were to be excluded as an extreme outlier, then it would have to have a complex I activity greater than 11.47 nmol.min^{-1}.UCS^{-1}, a value that is by definition three times the IQR above or below the upper and lower quartile data points respectively.

The second outlier, observed in R12, is far closer to the core group of data points in its data set and is regarded as an outlier only due to the fact that the IQR values are extremely clustered together within 0.29 nmol.min^{-1}.UCS^{-1}. However, R12-6 was only classified as an outlier and was therefore not excluded. Moreover, if it were to be excluded, it is expected that a notable difference would be made to the descriptive statistics due to the fact that the remaining five data points in R12 are narrowly clustered. However, since R6-1 and R12-6 are only outliers and not extreme outliers, they will not be excluded from the heart muscle complex I activity data set for future multiple comparison analyses. The Tukey *unequal number HSD* and d-values of biological significance are listed in Table 5.50.

A highly significant p-value of < 0.001 for the ANOVA is not a surprising result as there were clear differences observed upon comparison of the box-whisker plots and descriptive statistics presented in Table 5.43. The multiple comparison grid illustrates that dose groups R9, R12 and R15 differ significantly on a statistical and biological level from N and V, which themselves do not differ significantly from each other.

Table 5.50 Multiple comparison statistics of heart muscle complex I activity data generated from the rat pilot study

A: Parametric Tukey *unequal number HSD* p-values							
Dose group	**N**	**V**	**R3**	**R6**	**R9**	**R12**	**R15**
N		1.000	0.087	0.616	0.002	< 0.001	< 0.001
V	1.000		0.172	0.825	0.005	< 0.001	< 0.001
R3	0.087	0.172		0.835	0.916	0.575	0.260
R6	0.616	0.825	0.835		0.133	0.027	0.005
R9	0.002	0.005	0.916	0.133		0.991	0.838
R12	< 0.001	< 0.001	0.575	0.027	0.991		0.996
R15	< 0.001	< 0.001	0.260	0.005	0.838	0.996	

B: ANOVA p-values
One-way ANOVA p-value < 0.001

C: Statistical and biological significance			
Comparison		**Statistical significance (p)**	**Biological significance (d)**
N	R9	0.002	2.536
N	R12	< 0.001	2.945
N	R15	< 0.001	3.298
V	R9	0.005	2.328
V	R12	0.001	2.737
V	R15	< 0.001	3.089
R6	R12	0.027	1.959
R6	R15	0.005	2.312

A: All comparison statistics are indicated as p-values generated via the Tukey *unequal number HSD* (Honestly Significant Difference) multiple comparison procedure. P-values indicated in red are statistically significant at the pre-determined significance level of 0.05. The remainder of p-values are listed in grey. The turquoise shaded blocks represent statistically significant comparisons that were also determined to be of biological significance. B: The p-value for the one-way ANOVA is listed, with significant p-values, less than the 0.05 significance level, indicated in red. C: List of comparisons determined to be statistically significant with corresponding biological significance. A d-value greater than or equal to 0.8 signifies biological significance, indicated in red. Rats were treated N = no dose, V = vehicle, R3 = rotenone 3 $mg.kg^{-1}.day^{-1}$, R6 = rotenone 6 $mg.kg^{-1}.day^{-1}$, R9 = rotenone 9 $mg.kg^{-1}.day^{-1}$, R12 = rotenone 12 $mg.kg^{-1}.day^{-1}$, R15 = rotenone 15 $mg.kg^{-1}.day^{-1}$. < = less than, ANOVA = analysis of variance.

R12 and R15 also vary significantly from R6. However, as mentioned previously the presence of the outlier R6-1 resulted in inflated means and standard deviations in the group. This increased variance may well be the reason for the observed statistically significant differences with groups R12 and R15. Exclusion of R6-1 may almost certainly result in the suppression of significance. It is of value to note that even with the presence of R6-1 there was no statistically significant difference between R3 and R6. This supports the aforementioned notion that rat heart muscle is more sensitive to rotenone concentrations at only the higher concentration ranges greater than 6 $mg.kg^{-1}.day^{-1}$. Moreover, the argument is even further strengthened by the absence of statistically significant differences between any of the controls and low concentration dose groups up to and including R6.

5.4.2.2 Main study complex I activity generated from heart muscle

Heart muscle was collected and mitochondria isolated as described in Section 4.4.3.1 of Chapter Four. Complex I activities of the various groups were determined along with citrate synthase and protein concentrations before the data was collected into Excel® spreadsheets and further analysed in STATISTICA™. Table 5.51 presents the box-whisker representations and descriptive statistics of complex I data generated from heart muscle during the rat main study.

The data presented in Table 5.51 illustrates the presence of three outliers and one extreme outlier. It should be noted that the outliers and extreme outlier arose from three different dose groups where the data is well clustered within narrow IQRs. Therefore, it would appear that the labelling of VN-1, RN-3 and VC-4 as outliers and VC-2 as an extreme outlier is rather harsh considering that they are not too distant from the core data points that make up the IQR. However, criteria for outlier analysis are clear and any data points that extend beyond the non-outlier range are regarded as outliers and extreme outliers depending on the distance from the IQR.

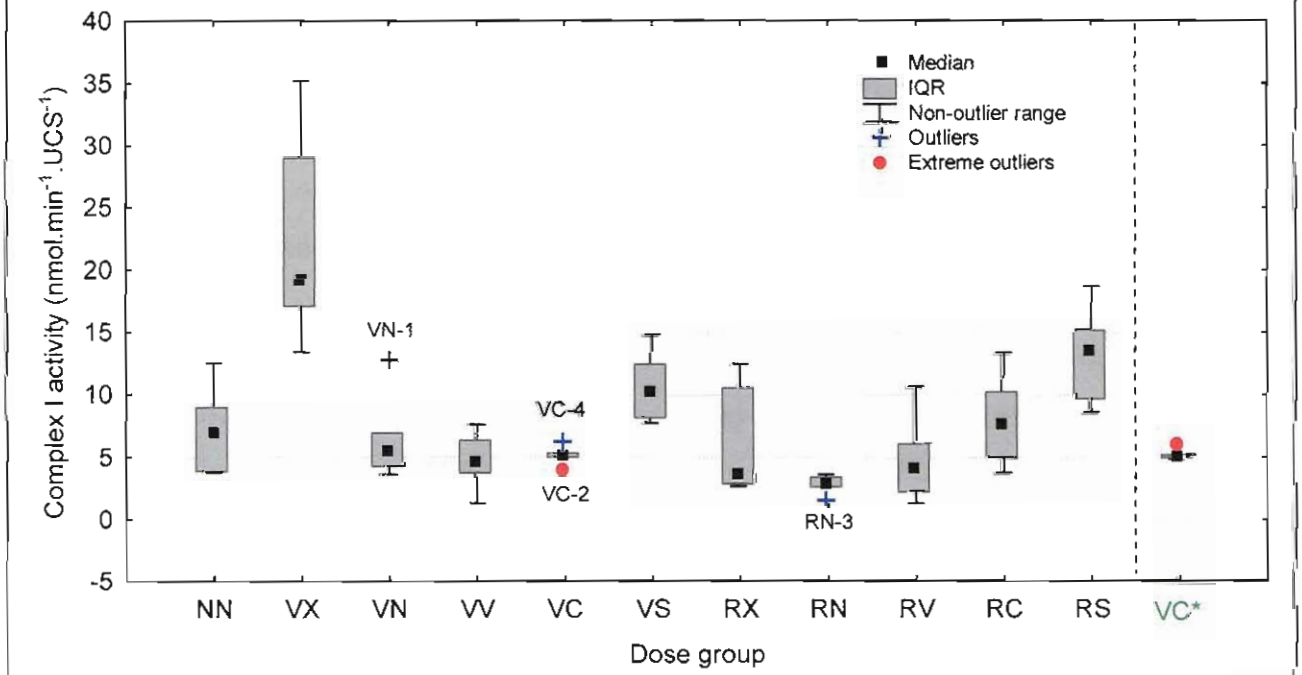
The advantages of well-clustered data are of course significant too, and that is that even if the extreme outlier VC-2 is excluded from the VC data set, very little differences are observed in the descriptive statistics. The mean complex I activity for VC changed from 5.12 to 5.36 nmol.min^{-1}.UCS^{-1}, while the median increased from 5.16 to 5.23 nmol.min^{-1}.UCS^{-1}. The most noteworthy of changes usually observed when excluding outliers and extreme outliers is that of variance and SD. However, in this scenario, due to the extremely narrow IQR of 0.32 nmol.min^{-1}.UCS^{-1}, the exclusion of VC-2 as an extreme outlier resulted in only a slight decrease in SD from 0.72 to 0.46 nmol.min^{-1}.UCS^{-1}. Although descriptive statistics were not determined in data sets where outliers would have been excluded, it is certain that minor alterations would have been made to dose groups VN, VC and RN, primarily due to the narrow IQRs. However, as mentioned previously, only extreme outliers were excluded from data sets and outliers were retained.

It is apparent from Table 5.51 that very little variation between the dose groups exists, with the exception of VX that displays the highest complex I activity as well as the largest of the IQRs. It is however expected that the other rat groups that received vehicle Factor-1 regimens, as well as the environmental controls NN, would harbour complex I activities in

a similar distribution to that of VX. All six groups received compounds that should not compromise the activities of complex I in any way. This can partly be confirmed by the results presented in Section 5.4.2.1 where dose groups N and V of the pilot study had very similar mean complex I activities of 6.67 and 6.33 nmol.min^{-1}.UCS^{-1}, respectively. However, by referring to the mean activities of NN and VX of the main study, presented in Table 5.51, it is apparent that an excessively high mean activity of 22.2 nmol.min^{-1}.UCS^{-1} was recorded for VX, whereas the mean complex I activity for NN of 7.18 nmol.min^{-1}.UCS^{-1} was similar to those obtained in the pilot study. The markedly high complex I activity for VX is unexpected and complicated interpretation of dose group comparisons within the main study.

Table 5.51 Box-whisker representation and descriptive statistics of the complex I data generated from heart muscle during the rat main study

A: Box-whisker plots and data points according to rat groups



Rat	NN	VX	VN	VV	VC	VS	RX	RN	RV	RC	RS	VC*
1	7.77	35.2	+ 12.7	5.02	5.10	12.5	10.6	3.69	1.29	10.2	15.2	5.10
2	12.5	18.0	5.10	4.25	• 3.92	10.9	12.4	3.48	6.10	8.3	18.7	EXCL
3	6.14	29.0	4.27	6.35	5.33	7.77	3.36	+ 1.52	5.92	13.3	12.7	5.33
4	3.80	13.4	5.97	1.33	+ 6.15	9.71	2.94	2.71	2.45	7.10	14.5	6.15
5	3.89	20.4	3.65	7.59	5.23	8.23	4.15	3.05	2.28	4.96	9.7	5.23
6	8.98	17.1	6.93	3.78	5.00	14.8	2.74	2.92	10.6	3.75	8.6	5.00

B: Descriptive statistics

Dose group	Sample size	Mean	SD	Median	Min	Max	Range	Lower quartile	Upper quartile	IQR
NN	6	7.18	3.33	6.96	3.80	12.5	8.73	3.89	8.98	5.09
VX	6	22.2	8.23	19.2	13.4	35.2	21.8	17.1	29.0	11.9
VN	6	6.43	3.27	5.54	3.65	12.7	9.01	4.27	6.93	2.66
VV	6	4.72	2.17	4.64	1.33	7.59	6.27	3.78	6.35	2.58

Table 5.51 Continued...

VC	6	5.12	0.72	5.16	3.92	6.15	2.23	5.00	5.33	0.32
VC*	5	5.36	0.46	5.23	5.00	6.15	1.15	5.10	5.33	0.22
VS	6	10.7	2.67	10.3	7.77	14.8	7.01	8.23	12.5	4.25
RX	6	6.04	4.31	3.75	2.74	12.4	9.69	2.94	10.6	7.66
RN	6	2.89	0.76	2.99	1.52	3.69	2.16	2.71	3.48	0.77
RV	6	4.78	3.49	4.19	1.29	10.6	9.32	2.28	6.10	3.82
RC	6	7.95	3.52	7.70	3.75	13.3	9.59	4.96	10.2	5.29
RS	6	13.2	3.73	13.6	8.56	18.7	10.1	9.72	15.2	5.48

Rat codes for outliers and extreme outliers are located above or below the respective blue crosses (+) and red dots (•), which correspond to data point values listed in the table directly below the graph. The vertical dashed line in the box-whisker graphic representation separates original dose group box-whiskers from those that have had the extreme outliers excluded, which are also indicated by the asterisk (*) following the dose group code. Data sets with excluded data points are designated in green text. Rats were treated with NN = no dose regimen, VX = vehicle and sacrificed, VN = vehicle and no dose, VV = vehicle and vehicle, VC = vehicle and CoQ_{10}, VS = vehicle and succinate, RX = rotenone and sacrificed, RN = rotenone and no dose, RV = rotenone and vehicle, RC = rotenone and CoQ_{10}, RS = rotenone and succinate. EXCL = excluded data point, IQR = inter-quartile range, Min = minimum data point value, Max = maximum data point value, $nmol.min^{-1}.UCS^{-1}$ = nanomole per minute per unit citrate synthase activity, SD = standard deviation.

The range statistic for VX indicated that another notable difference between this group and the remainder of the groups included in the main study exists. A range distribution of 21.8 $nmol.min^{-1}.UCS^{-1}$ compared to the next highest range of 10.4 $nmol.min^{-1}.UCS^{-1}$, for dose group RS, was indicative of a major difference. In addition, all of the data points in VX were demonstrated to be higher than all the other data points generated from the vehicle Factor-1 treated rat groups as well as the environmental controls. The heart muscle complex I data for groups of the main study can be further investigated in Table B.5 of Appendix B. The most notable differences that can be observed between VX and the remainder of the dose groups in the main study are those listed in the complex I activity (CIA) column. This column lists the raw complex I activities in $\mu mol.min^{-1}$, that is, the enzyme activity of the mitochondrial isolate prior to expressing it in terms of protein and UCS. The calculation is outlined in Equation 4.2 of Chapter Four. The CIA column indicates that VX had complex I activities far higher than the other 10 groups, which directly affected the expression of complex I activities in terms of protein ($\mu mol.min^{-1}.\mu g^{-1}$), listed in the $CIA.prot^{-1}$ column. The mean activity of 248.6 $\mu mol.min^{-1}.\mu g^{-1}$ for dose group VX is more than triple the activity of any of the other groups. When referring to the protein column, which lists the mitochondrial isolate protein concentrations, no overall lower isolate concentrations can be detected, even though the mean concentration for VX was the lowest of the groups. The mean protein concentration (P_{CON}) is lowered to 0.99 μg due to the low data point for VX-6, which is at 0.21 μg. However, the VX-6 data point is not a completely aberrant result as the complex I activity in the CIA column is, correspondingly, the lowest in its group. Moreover, the final complex I activity in terms of UCS for VX-6, in the complex I activity per unit citrate synthase ($CIA.UCS^{-1}$) column, is not the data point that contributes the most to the overall raised complex I activity of the

group. This fact confirms that it is indeed the raw complex I activities, listed in the CIA column, for VX that resulted in the final elevated CIA.UCS^{-1} data points.

Nevertheless, with the acceptance of an abnormally high complex I activity mean for dose group VX, a multiple comparison evaluation of the data was performed. The p-values for statistical significance and d-values for biological significance are listed in Table 5.52. Since an extreme outlier was observed to be present in the data, parametric and non-parametric p-values are presented.

Table 5.52 Multiple comparison statistics of heart muscle complex I data generated from the rat main study

A: Non-parametric (original data set) and parametric (excluding extreme outliers) p-values

Dose group	NN	VX	VN	VV	VC	VS	RX	RN	RV	RC	RS
NN		0.557	1.000	1.000	1.000	1.000	1.000	1.000	1.000	1.000	1.000
		< 0.001	1.000	0.989	1.000	0.889	1.000	0.693	0.990	1.000	0.216
VX	0.557		0.214	0.019	0.067	1.000	0.032	< 0.001	0.007	1.000	1.000
	< 0.001		< 0.001	< 0.001	< 0.001	< 0.001	< 0.001	< 0.001	< 0.001	< 0.001	0.007
VN	1.000	0.214		1.000	1.000	1.000	1.000	1.000	1.000	1.000	1.000
	1.000	< 0.001		0.999	1.000	0.710	1.000	0.877	1.000	1.000	0.104
VV	1.000	0.019	1.000		1.000	1.000	1.000	1.000	1.000	1.000	0.258
	0.989	< 0.001	0.999		1.000	0.237	1.000	0.999	1.000	0.927	0.013
VC	1.000	0.067	1.000	1.000		1.000	1.000	1.000	1.000	1.000	0.720
	1.000	< 0.001	1.000	1.000		0.528	1.000	0.994	1.000	0.992	0.068
VS	1.000	1.000	1.000	1.000	1.000		1.000	0.024	0.690	1.000	1.000
	0.889	< 0.001	0.710	0.237	0.528		0.593	0.034	0.249	0.977	0.984
RX	1.000	0.032	1.000	1.000	1.000	1.000		1.000	1.000	1.000	0.391
	1.000	< 0.001	1.000	1.000	1.000	0.593		0.939	1.000	0.999	0.068
RN	1.000	< 0.001	1.000	1.000	1.000	0.024	1.000		1.000	0.661	0.002
	0.693	< 0.001	0.877	0.999	0.994	0.034	0.939		0.999	0.462	0.001
RV	1.000	0.007	1.000	1.000	1.000	0.690	1.000	1.000		1.000	0.119
	0.990	< 0.001	1.000	1.000	1.000	0.249	1.000	0.999		0.935	0.014
RC	1.000	1.000	1.000	1.000	1.000	1.000	1.000	0.661	1.000		1.000
	1.000	< 0.001	1.000	0.927	0.992	0.977	0.999	0.462	0.935		0.398
RS	1.000	1.000	1.000	0.258	0.720	1.000	0.391	0.002	0.119	1.000	
	0.216	0.007	0.104	0.013	0.068	0.984	0.068	0.001	0.014	0.398	

B: ANOVA p-values

Kruskal-Wallis p-value < 0.001	One-way ANOVA p-value < 0.001

C: Statistical and biological significance

Comparison		Statistical significance (p)		Biological significance (d)	
		Including EOs	Excluding EOs	Including EOs	Excluding EOs
NN	VX	0.557	< 0.001	N/A	3.910
VX	VN	0.214	< 0.001	N/A	4.105
VX	VV	0.019	< 0.001	2.123	4.551
VX	VC	0.067	< 0.001	N/A	4.384
VX	VS	1.000	< 0.001	N/A	3.003
VX	RX	0.032	< 0.001	1.962	4.207
VX	RN	< 0.001	< 0.001	2.345	5.027
VX	RV	0.007	< 0.001	2.115	4.535
VX	RC	1.000	< 0.001	N/A	3.709

Table 5.52 Continued...

Comparison		Statistical significance (p)		Biological significance (d)	
		Including EOs	Excluding EOs	Including EOs	Excluding EOs
VX	RS	1.000	0.007	N/A	2.337
VV	RS	0.258	0.013	N/A	2.214
RN	RS	0.002	0.001	2.769	2.691
RV	RS	0.119	0.014	N/A	2.198

A: All comparison statistics are indicated as p-values. The upper p-value is the non-parametric multiple comparison test statistic, generated from the original set of data. The lower p-value was generated via the parametric Tukey *unequal number HSD* (Honestly Significant Difference) test, after the exclusion of extreme outliers. P-values indicated in red are statistically significant at the pre-determined significance level of 0.05. P-values in black text represent those that are not statistically significant, but have complementary p-values that are statistically significant. The remainder of p-values are listed in grey. The comparisons surrounded by the bold black line are those that were determined to be statistically significant by both the non-parametric and parametric multiple comparison procedures. The turquoise shaded blocks represent statistically significant comparisons that were also determined to be of biological significance. B: P-values for the non-parametric Kruskal-Wallis ANOVA and parametric one-way ANOVA are listed, with significant p-values, less than the 0.05 significance level, indicated in red. C: List of comparisons determined to be statistically significant with corresponding biological significance. A d-value greater than or equal to 0.8 signifies biological significance, indicated in red. Rats were treated with NN = no dose regimen, VX = vehicle and sacrificed, VN = vehicle and no dose, VV = vehicle and vehicle, VC = vehicle and CoQ_{10}, VS = vehicle and succinate, RX = rotenone and sacrificed, RN = rotenone and no dose, RV = rotenone and vehicle, RC = rotenone and CoQ_{10}, RS = rotenone and succinate. < = less than, ANOVA = analysis of variance, EOs = extreme outliers, N/A = not applicable.

Before discussing the data in Table 5.52, it should be mentioned that the complex I data was analysed to verify that inhibition was indeed obtained by dosing with rotenone, as well as to measure the rehabilitation of activity over the last two days when rats received either of the Factor-2 regimens. It is not anticipated that the activities of complex I would improve to noticeable amounts since rotenone is expected to bind to the enzyme irreversibly. It is expected however that deficient complex I enzymes and consequently mitochondria would be replenished over the Factor-2 dose period, a process that may possibly be enhanced by CoQ_{10} and succinate. The primary purpose of the study was to evaluate the overall cellular relief gained from the therapeutic compounds by analysing several biochemical parameters, not to evaluate the complex I recovery. The multiple comparison data will therefore be discussed in the aforementioned context.

The multiple comparison grid reveals both the expected statistically and biologically significant differences between VX and all the other dose groups. Prior to the exclusion of VC-2 as an extreme outlier, the non-parametric multiple comparison procedure revealed that VX differed significantly from only VV, RX, RN and RV. When VC-2 was excluded, the parametric Tukey *unequal number HSD* resulted in all 10 groups differing statistically significantly from VX. Furthermore, each of the 10 dose groups differed biologically significantly from VX, as listed in Table 5.52.C.

An additional four comparisons were determined to differ significantly by either the parametric or non-parametric multiple comparison procedures. Two of the four differed statistically prior to and after the extreme outlier VC-2 was excluded from the data set.

These were the RN-VS and RN-RS comparisons. Since the former is a comparison between two dose groups that differed considerably in terms of dose regimens received, little deduction should be inferred from the significant p-value results, except that it is, to a certain extent, expected to differ significantly. It is therefore also expected that all of the vehicle Factor-1 treated groups, including dose group NN, should differ from the rotenone-treated rats. This is certainly expected to be the case when heart complex I activities for VX were compared to RX. This was indeed demonstrated in Section 5.4.2.1, where dose groups V and R15 of the pilot study differed significantly. Since VX is the group that presented with a markedly elevated complex I activity, it most certainly differed statistically significantly from RX, but so did it from all the other groups of the main study. Therefore, definitive scientific inference with regard to VX cannot be made. Since exactly the same protocols for dosing and assaying of complex I were adhered to in both the pilot and main studies, it may be inferred that the aforementioned groups would indeed differ significantly in the main study. Moreover, the rat body weight data presented in Section 5.2 confirmed that rotenone-treated rats in both the pilot and main study lost weight similarly.

The box-whisker plots in Table 5.51.A illustrated that improvement in heart muscle complex I activities from RN to RV to RC and finally to RS, in that order, were observed. This suggests that the dosing with CoQ_{10} and succinate stimulated mitochondrial proliferation or replenishment, more so than for the groups that received no dose or the vehicle. The argument is supported, in part, by the statistically significant p-value reported for the RN and RS comparison. Furthermore, these two groups were determined to differ with biological significance. The rotenone-treated rats responded significantly better to receiving succinate over receiving a no dose Factor-2 regimen. When the extreme outlier VC-2 was excluded and the parametric Tukey *unequal number HSD* test performed, it was also determined that rats in RS responded significantly better than those in RV. Based on the p-values in Table 5.52.A, it is apparent that succinate was indeed beneficial to rats harbouring a rotenone-induced Complex I deficiency. However, even though RC rats displayed improved complex I activities than rats in RN and RV, the differences in activities were not statistically significant. Regardless, the improved response trends should be noted.

The final statistically significant comparison was between RS and VV. It can be suggested for the data that succinate dosed to an induced complex I deficient group of rats improved the activities of complex I to better than even the VV dose group, in fact to values better

than the environmental controls **NN** and all the vehicle Factor-1 treated rats. It cannot be stated, without doubt though, that a higher complex I activity would be attained after dosing a deficient rat with succinate for two days than for a rat without a deficiency. It may be suggested that the stimulated mitochondrial replenishment in RS rats was enhanced even further due to succinate dosing. The fuelling of complex II via the use of succinate may have relieved the overall stress on the respiratory chain and stimulated improved efficiency in electron transfer through complex II. This would in turn result in improved oxidative phosphorylation and mitochondrial activities, accompanied by up-regulation of mitochondrial transcripts.

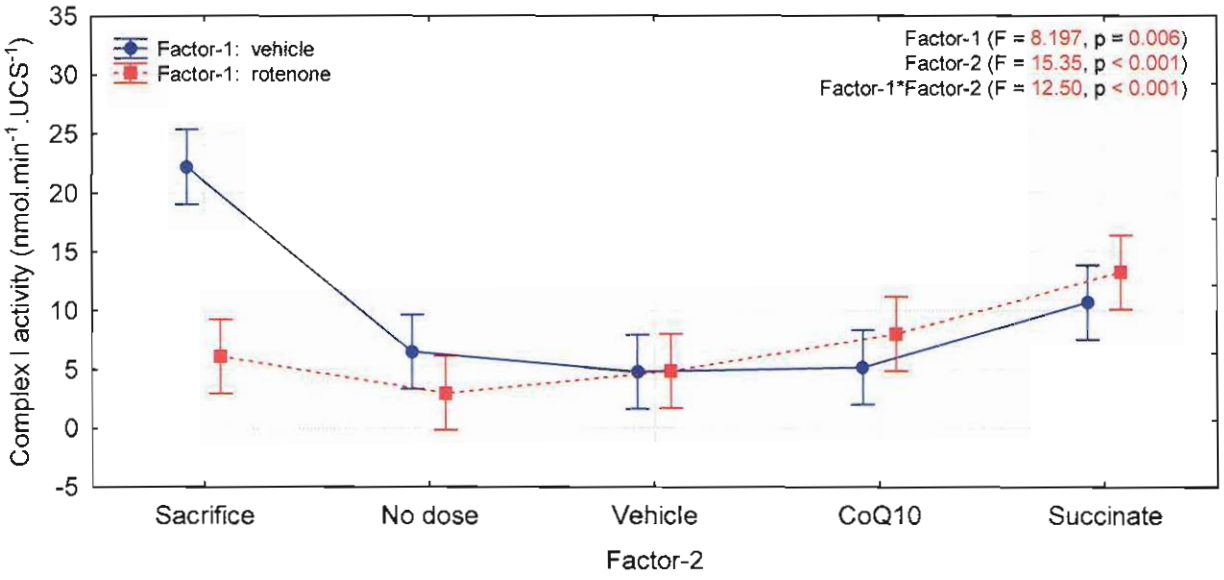
The rat main study complex I activity data for heart muscle was further analysed via a two-way ANOVA to evaluate the contributions of Factor-1 and Factor-2 regimens. Table 5.53 presents graphic representations of the factorial ANOVA, with extreme outliers included and excluded from the heart muscle complex I data set.

The two graphic representations in Table 5.53 illustrate that a visual difference between the data sets including and excluding the extreme outlier VC-2 is minimal. By referring to the data point tables directly below each of the graphs, the mean data points for dose group VC indicate a mere 0.24 $nmol.min^{-1}.UCS^{-1}$ increase after VC-2 was excluded. As discussed previously in this section, this very small change is due to the fact the other five data points in VC are clustered within a very narrow IQR. This minor adjustment to the data similarly had slight effects on the F-statistics and p-values generated for the two-way ANOVA. Whether the extreme outlier was excluded or not, the p-values for Factor-1 and Factor-2, as well as the interaction effect, were all significant at the 0.05 significance level. These statistics are indicated in the top right hand corner of the respective graphic representations. Since there is a significant interaction effect in both cases, the main effects will not be discussed.

Table 5.53 also reveals highly significant interaction effects between dose Factor-1 and Factor-2. This supports the previous arguments in this section of increased complex I activities in rats that were first dosed with rotenone. The recovery of complex I activity over the last two days to higher than expected for vehicle, CoQ_{10} and succinate treated rat groups is indicated by the two-way ANOVA to result from an interaction effect between the rotenone and the respective second dose factors. The overall compromised rotenone-treated rat organism appears to have rapidly recovered in terms of complex I activity over the last two days, with some form of contribution from the inhibitor itself.

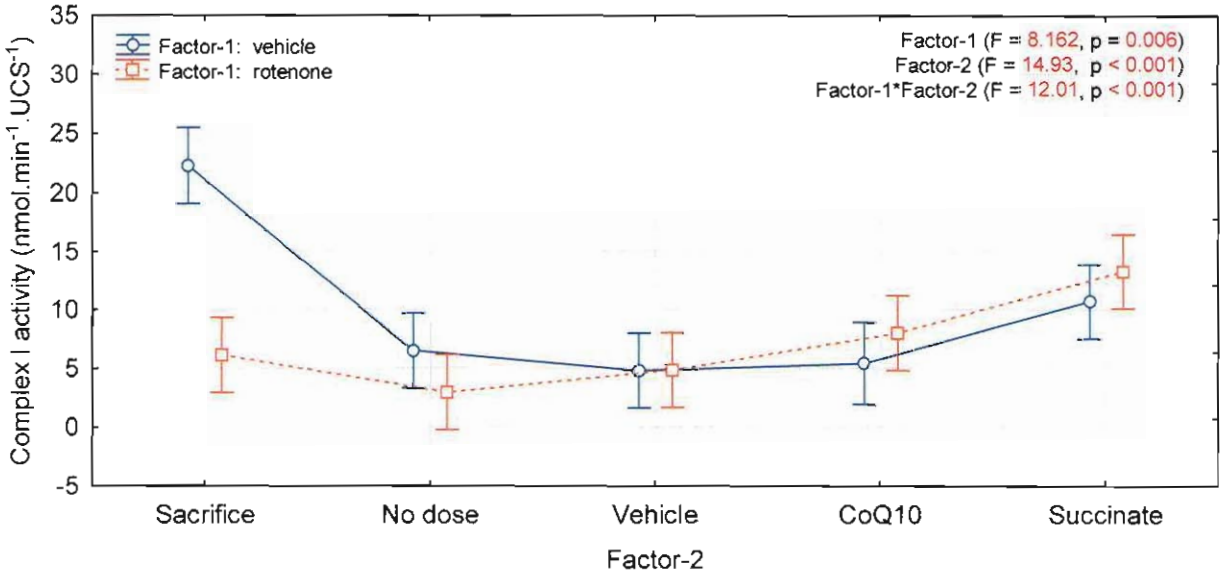
Table 5.53 Graphic and tabulated summary of heart muscle complex I data analysed via a two-way ANOVA

A: Data set including extreme outliers



Description		VX	VN	VV	VC	VS	RX	RN	RV	RC	RS
With extreme outliers	UCI	25.4	9.59	7.88	8.28	13.8	9.19	6.05	7.93	11.1	16.4
	mean	22.2	6.43	4.72	5.12	10.7	6.04	2.89	4.78	7.95	13.2
	LCI	19.0	3.27	1.56	1.96	7.50	2.88	-0.26	1.62	4.79	10.1

B: Data set excluding extreme outliers



Description		VX	VN	VV	VC	VS	RX	RN	RV	RC	RS
Without extreme outliers	UCI	25.4	9.62	7.91	8.86	13.8	9.22	6.08	7.96	11.1	16.4
	mean	22.2	6.43	4.72	5.36	10.7	6.04	2.89	4.78	7.95	13.2
	LCI	19.0	3.24	1.53	1.87	7.47	2.85	-0.29	1.59	4.76	10.0

The plot legends for each graph are indicated in the top left corners of the respective graphs, while the two-way ANOVA F-statistics (F) and p-values (p) for Factor-1, Factor-2 and Factor-1*Factor-2 are located in the top right corner, with the statistically significant values indicated in red. The vertical whiskers at each mean data point represent 95% confidence intervals for the respective data sets. The mean values in green text, located in the data point summary tables below the graphs, indicate those that were adjusted due to the exclusion of extreme outliers. Rats were treated with NN = no dose regimen, VX = vehicle and sacrificed, VN = vehicle and no dose, VV = vehicle and vehicle, VC = vehicle and CoQ_{10}, VS = vehicle and succinate, RX = rotenone and sacrificed, RN = rotenone and no dose, RV = rotenone and vehicle, RC = rotenone and CoQ_{10}, RS = rotenone and succinate. < = less than, LCI = lower 95% confidence interval data point, $nmol.min^{-1}.UCS^{-1}$ = nanomole per minute per unit citrate synthase activity, UCI = upper 95% confidence interval data point.

If the two-way ANOVA is considered to be accurate, then a mechanism by which rotenone aids the mitochondrial replenishment process may be hypothesised. Furthermore, the fact that rotenone appeared to have improved serum hydroperoxide levels, indicated in Section 5.3.1, and itself illustrated to harbour an antioxidant capacity, discussed in Section 5.3.2.1, indicates that it may have contributed to a recovery from oxidative stress. In brief, rotenone is a coenzyme Q analogue, as presented in Section 2.2.3.1 of Chapter Two, which binds to complex I in a similar manner as that of CoQ_{10}. Therefore, the structural similarities between CoQ_{10} and rotenone do not exclude the possibility that, as with CoQ_{10}, rotenone may contribute beneficially to respiratory chain stabilisation and scavenging of radicals. This characteristic, although paradoxical, may therefore be argued to play a role in or contribute to the hypothesised proliferation of mitochondria.

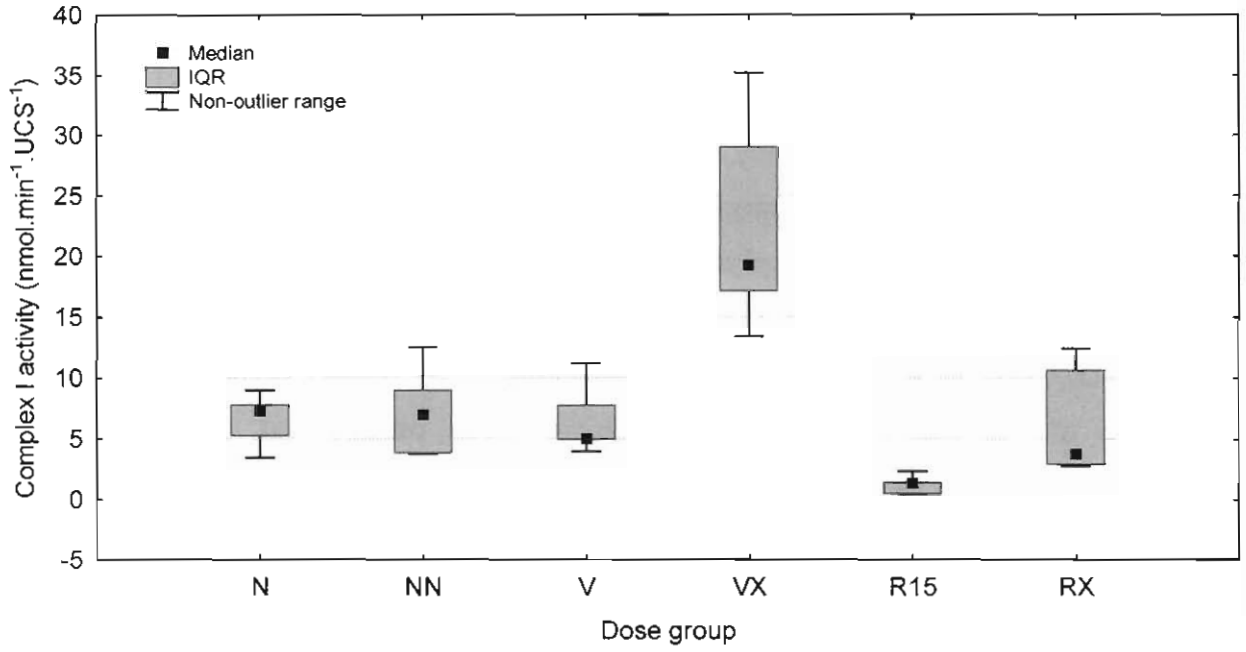
5.4.2.3 Comparative analysis of heart muscle complex I data generated from the rat pilot and main studies

Data comparison of the rat pilot and main studies was performed to statistically evaluate the differences between dose groups that may be paralleled. The dose groups included in the analysis were N, V and R15 of the pilot study and NN, VX and RX from the main study. Table 5.54 summarises the pilot and main study comparisons graphically and in tables of descriptive statistics as well as a multiple comparison grid. The descriptive statistics presented in Table 5.54.B were obtained from Table 5.49 and Table 5.51, and is listed here for ease of reference.

The box-whisker representations of the data once again illustrate the large difference between VX and the remainder of the groups, especially with regards to the distribution of data and increased complex I activity. The differences are confirmed by the statistically significant p-values in Table 5.54.C where VX differs significantly from all the other groups. It is worthwhile to note that no statistically significant differences exist between dose groups N and NN, or between R15 and RX. These groups were treated in exactly the same manner in both studies. Dose group NN differed from N only in the two extra days that it received the no dose Factor-2 treatment, which essentially makes no difference, and was therefore accepted for this investigation to be paralleled with N.

Table 5.54 Summary of comparative dose groups of the rat pilot and main study heart muscle complex I data

A: Box-whisker plots and data points according to rat groups



B: Descriptive statistics (from Table 5.49 and Table 5.51)

Dose group	Sample size	Mean	SD	Median	Min	Max	Range	Lower quartile	Upper quartile	IQR
N	6	6.67	1.99	7.27	3.45	8.98	5.53	5.30	7.78	2.48
NN	6	7.18	3.33	6.96	3.80	12.5	8.73	3.89	8.98	5.09
V	6	6.33	2.70	5.05	3.97	11.2	7.24	4.98	7.71	2.74
VX	6	22.2	8.23	19.2	13.4	35.2	21.8	17.1	29.0	11.9
R15	6	1.22	0.69	1.32	0.46	2.33	1.87	0.49	1.38	0.89
RX	6	6.04	4.31	3.75	2.74	12.4	9.69	2.94	10.6	7.66

C: Tukey *equal number HSD* p-values

Dose group	N	NN	V	VX	R15	RX
N		1.000	1.000	< 0.001	0.261	1.000
NN	1.000		0.999	< 0.001	0.181	0.997
V	1.000	0.999		< 0.001	0.327	1.000
VX	< 0.001	< 0.001	< 0.001		< 0.001	< 0.001
R15	0.261	0.181	0.327	< 0.001		0.390
RX	1.000	0.997	1.000	< 0.001	0.390	

All comparison statistics are indicated as p-values generated via the Tukey *equal number HSD* (Honestly Significant Difference) multiple comparison procedure. The p-values indicated in red are statistically significant at a significance level of 0.05, while all other p-values are in grey. Rats were treated with N = no dose regimen (pilot study), NN = no dose regimen (main study), V = vehicle (pilot study), VX = vehicle (main study), R15 = rotenone 15 mg.kg^{-1}.day^{-1} (pilot study), RX = rotenone 15 mg.kg^{-1}.day^{-1} (main study). < = less than, IQR = inter-quartile range, Min = minimum data point value, Max = maximum data point value, SD = standard deviation.

The multiple comparison grid also indicates, with the exception of VX, that there were no statistically significant differences between the rotenone-treated rat groups, namely R15 and RX, and any of the control groups N, NN and V. However, by referring to Table 5.50 of the rat pilot study, the comparison between R15 and both N and V were statistically significant at the 0.05 significance level. Since the ANOVA and Tukey multiple comparison tests are influenced by variances within and between dose groups as well as

the number of groups being compared, it is understandable that the p-values and consequently significant comparisons differ. However, for this set of data, the multiple comparison procedure was performed only to confirm the consistency in experimentation between dose groups of the pilot study that could be paralleled with groups in the main study. Nonetheless, it is evident from the mean and median statistics in Table 5.54 that both R15 and RX had the lowest complex I activities of all the other groups included in this analysis set, which is indicative of a rotenone-induced Complex I deficiency.

In summary, the vast differences observed between VX and any of the other groups investigated in both the pilot and main studies cannot be explained logically. The pilot study indicated no statistically significant differences between V and N, the anticipated result. However, this was evidently not the case in the main study. It can be argued that the complex I assay is very difficult to perform due to its relatively low reaction velocity and interfering NADH oxidation that should be accounted for. Consistency in results, when performing dilutions of a mitochondrial preparation, was difficult to attain. Moreover, the final complex I activity is expressed in terms of citrate synthase activity, which is also itself expressed in terms of protein. Therefore, it is the mergence of three different assay results in a particular manner to achieve the final complex I activity of a sample. These two factors undoubtedly complicate determination of final complex I activities.

5.4.3 Antioxidant capacity in heart muscle

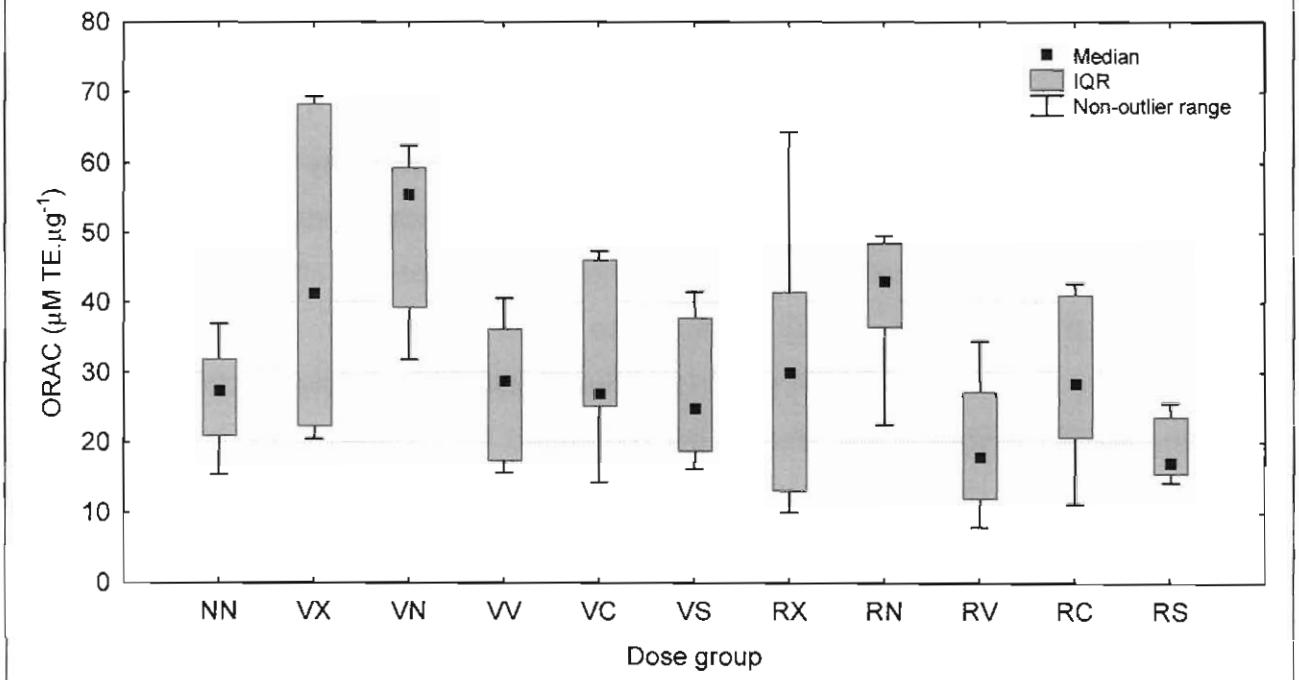
Heart muscle was appropriately homogenised and prepared via protocols presented in Sections 4.4.2 and 4.4.5 of Chapter Four, respectively. The ORAC assay was performed and resulting data evaluated statistically. It should be noted that the antioxidant capacity data for heart muscle and the remaining organs is presented in terms of micromolar Trolox equivalents per microgram ($\mu M\ TE.\mu g^{-1}$) protein, since tissue samples were homogenised and protein concentrations determined. Box-whisker plots and descriptive statistics of the heart muscle antioxidant capacity data set are presented in Table 5.55. No outliers or extreme outliers were determined to be present in any of the dose groups investigated.

It would appear from the first three box-whisker plots in Table 5.55.A that the vehicle improved the antioxidant capacity. However, the capacities for dose groups VV, VC and VS were comparatively similar to the environmental controls NN. Moreover, the antioxidant capacity data for two of the rotenone-treated rat groups were even lower than

NN. This data is suggestive of a different response pattern to that in blood plasma, as presented in Section 5.3.2.

Table 5.55 Box-whisker representation and descriptive statistics of the heart muscle antioxidant capacity data generated from the main study

A: Box-whisker plots and data points according to rat groups



Rat	NN	VX	VN	VV	VC	VS	RX	RN	RV	RC	RS
1	29.8	20.5	62.4	15.7	26.0	37.7	19.4	49.6	18.9	42.7	16.8
2	24.8	59.4	59.2	17.3	47.3	18.7	41.3	36.4	34.4	40.9	25.6
3	31.8	68.2	31.8	36.1	46.0	16.2	40.2	22.5	27.1	25.6	14.1
4	37.0	69.4	39.3	40.6	27.7	29.1	64.4	42.0	11.9	11.2	17.0
5	20.9	22.3	54.6	32.3	14.3	20.4	10.1	43.8	16.6	20.6	23.4
6	15.5	23.0	56.2	25.0	25.2	41.5	13.0	48.5	7.98	30.8	15.4

B: Descriptive statistics

Dose group	Sample size	Mean	SD	Median	Min	Max	Range	Lower quartile	Upper quartile	IQR
NN	6	26.6	7.80	27.3	15.5	37.0	21.5	20.9	31.8	10.9
VX	6	43.8	24.2	41.2	20.5	69.4	48.9	22.3	68.2	45.8
VN	6	50.6	12.2	55.4	31.8	62.4	30.6	39.3	59.2	20.0
VV	6	27.8	10.2	28.7	15.7	40.6	24.9	17.3	36.1	18.8
VC	6	31.1	13.0	26.8	14.3	47.3	33.0	25.2	46.0	20.8
VS	6	27.3	10.6	24.8	16.2	41.5	25.3	18.7	37.7	19.0
RX	6	31.4	21.0	29.8	10.1	64.4	54.3	13.0	41.3	28.3
RN	6	40.4	10.0	42.9	22.5	49.6	27.1	36.4	48.5	12.1
RV	6	19.5	9.79	17.7	7.98	34.4	26.5	11.9	27.1	15.2
RC	6	28.6	12.1	28.2	11.2	42.7	31.5	20.6	40.9	20.3
RS	6	18.7	4.64	16.9	14.1	25.6	11.4	15.4	23.4	8.04

Rats were treated with NN = no dose regimen, VX = vehicle and sacrificed, VN = vehicle and no dose, VV = vehicle and vehicle, VC = vehicle and CoQ_{10}, VS = vehicle and succinate, RX = rotenone and sacrificed, RN = rotenone and no dose, RV = rotenone and vehicle, RC = rotenone and CoQ_{10}, RS = rotenone and succinate. IQR = inter-quartile range, µM TE.μg^{-1} = micromolar Trolox equivalents per microgram protein, Min = minimum data point value, Max = maximum data point value, SD = standard deviation.

The graphic representation of the heart muscle antioxidant capacity data illustrates that a similar trend in response can be observed between the vehicle and rotenone Factor-1 treated rat groups. The sacrificed and no dose treatment groups harboured the highest antioxidant capacities whether the rats received vehicle or rotenone from day 1 to 14, followed by lowered antioxidant capacities for vehicle, CoQ_{10} and succinate treatments.

The trend of decreased antioxidant capacity for rats that received CoQ_{10} and succinate, whether a Complex I deficiency was induced or not, was not expected. The fact that the second dose factor vehicle is included in this apparently compromised antioxidant capacity, suggests that it is merely a lack of response to the second dose factors rather than an adversely affected antioxidant capacity. The statistical and biological significance of differences between groups was calculated, as presented in Table 5.56.

Table 5.56 Multiple comparison statistics of heart muscle antioxidant capacity data generated from the rat main study

A: Tukey *equal number HSD* p-values

Dose group	NN	VX	VN	VV	VC	VS	RX	RN	RV	RC	RS
NN		0.503	0.097	1.000	1.000	1.000	1.000	0.784	0.997	1.000	0.994
VX	0.503		0.998	0.609	0.857	0.559	0.874	1.000	0.086	0.677	0.068
VN	0.097	0.998		0.139	0.317	0.118	0.339	0.963	0.008	0.173	0.006
VV	1.000	0.609	0.139		1.000	1.000	1.000	0.864	0.991	1.000	0.982
VC	1.000	0.857	0.317	1.000		1.000	1.000	0.979	0.914	1.000	0.878
VS	1.000	0.559	0.118	1.000	1.000		1.000	0.829	0.995	1.000	0.989
RX	1.000	0.874	0.339	1.000	1.000	1.000		0.983	0.900	1.000	0.860
RN	0.784	1.000	0.963	0.864	0.979	0.829	0.983		0.224	0.905	0.184
RV	0.997	0.086	0.008	0.991	0.914	0.995	0.900	0.224		0.982	1.000
RC	1.000	0.677	0.173	1.000	1.000	1.000	1.000	0.905	0.982		0.969
RS	0.994	0.068	0.006	0.982	0.878	0.989	0.860	0.184	1.000	0.969	

B: ANOVA p-values

One-way ANOVA p-value = 0.003

C: Statistical and biological significance

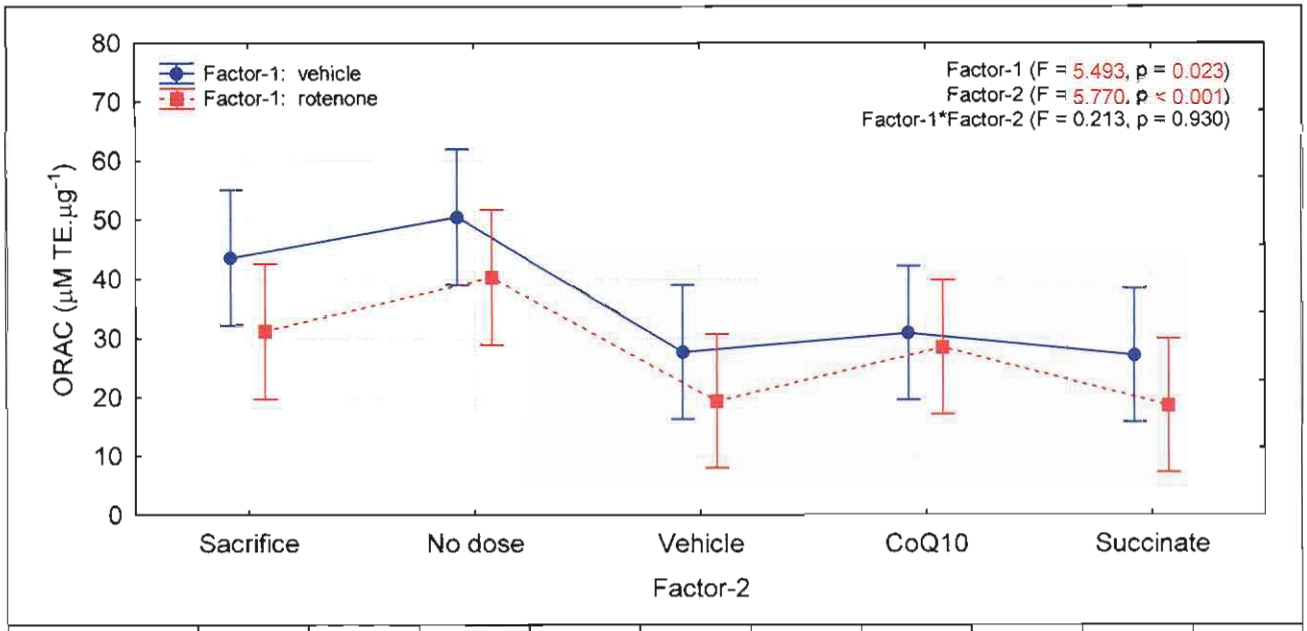
Comparison		Statistical significance (p)	Biological significance (d)
VN	RV	0.008	2.318
VN	RS	0.006	2.375

A: All comparison statistics are indicated as p-values generated via the Tukey *equal number HSD* (Honestly Significant Difference) multiple comparison procedure. P-values indicated in red are statistically significant at the pre-determined significance level of 0.05. The remainder of p-values are listed in grey. The turquoise shaded blocks represent statistically significant comparisons that were also determined to be of biological significance. B: P-value for the one-way ANOVA is listed, with significant p-values, less than the 0.05 significance level, indicated in red. C: List of comparisons determined to be statistically significant with corresponding biological significance. A d-value greater than or equal to 0.8 signifies biological significance, indicated in red. Rats were treated with NN = no dose regimen, VX = vehicle and sacrificed, VN = vehicle and no dose, VV = vehicle and vehicle, VC = vehicle and CoQ_{10}, VS = vehicle and succinate, RX = rotenone and sacrificed, RN = rotenone and no dose, RV = rotenone and vehicle, RC = rotenone and CoQ_{10}, RS = rotenone and succinate. ANOVA = analysis of variance.

The Tukey *equal number HSD* multiple comparison procedure reported the presence of two statistically significant differences. Furthermore, these differences were also determined to differ on a biological level with d-values greater than 2.3, as presented in Table 5.56.C. The significant differences were reported to be between dose groups VN and RV and between VN and RS. In both cases the antioxidant capacity of the rotenone-treated rats was lower than VN. Dose group VN harboured the highest mean and median antioxidant capacity of all rat groups. However, data points in VN do overlap with the distribution of data in several other dose groups, indicating similar antioxidant capacities among the groups. This is supported by the fact that no statistically significantly differences were determined to be present among any of the groups that received vehicle or rotenone Factor-1 treatments. Dose groups RV and RS are the only two groups that can visually be confirmed to harbour lower antioxidant capacities than the environmental controls NN. The antioxidant capacity for RC was higher than both RV and RS, suggesting a slight improvement in response to CoQ_{10}. The higher antioxidant capacity for dose group RN is unexpected, especially if it is postulated that the vehicle is associated with improved antioxidant capacities. Nonetheless, RN does not differ significantly from any of the other rotenone-treated rat groups, as indicated in the multiple comparison grid of Table 5.56.

The heart muscle antioxidant capacity data was analysed via a two-way ANOVA to verify the contributions from dose factors 1 and 2. Table 5.57 presents a graphic summary of the two-way ANOVA results accompanied by F-statistics and p-values for Factor-1 and Factor-2, as well as the interaction between these factors. The graphic representation confirms the trend similarity in antioxidant capacity of heart muscle between the vehicle and rotenone Factor-1 groups. The vehicle and rotenone Factor-1 plots do not intersect each other at any point, which is confirmed by the low F-statistic and p-value greater than 0.05 for the interaction effect. The statistical summary in the top right corner of the graph confirms the statistically significant main effect contributions from both factors 1 and 2. Although the F-statistics are very similar to each other at 5.493 and 5.770 for Factor-1 and Factor-2 respectively, the p-values differ considerably. Factor-2 was determined to make a highly significant contribution with a p-value of < 0.001, while Factor-1 had a significant p-value between the 0.05 and 0.01 significance levels. Nevertheless, both factors were statistically significant and their effects should be discussed.

Table 5.57 Graphic and tabulated summary of the heart muscle antioxidant capacity data analysed via a two-way ANOVA



Data points	VX	VN	VV	VC	VS	RX	RN	RV	RC	RS
UCI	55.2	61.9	39.2	42.4	38.6	42.7	51.8	30.8	40.0	30.1
mean	43.8	50.6	27.8	31.1	27.3	31.4	40.4	19.5	28.6	18,7
LCI	32.4	39.2	16.5	19.7	15.9	20.0	29.1	8.10	17.3	7.35

The plot legend is indicated in the top left corner of the graph, while the two-way ANOVA F-statistics (F) and p-values (p) for Factor-1, Factor-2 and Factor-1*Factor-2 are located in the top right corner, with the statistically significant values indicated in red. The vertical whiskers at each mean data point represent 95% confidence intervals for the respective data sets. Rats were treated with NN = no dose regimen, VX = vehicle and sacrificed, VN = vehicle and no dose, VV = vehicle and vehicle, VC = vehicle and CoQ_{10}, VS = vehicle and succinate, RX = rotenone and sacrificed, RN = rotenone and no dose, RV = rotenone and vehicle, RC = rotenone and CoQ_{10}, RS = rotenone and succinate. < = less than, LCI = lower 95% confidence interval data point, µM TE.μg^{-1} = micromolar Trolox equivalents per microgram protein, UCI = upper 95% confidence interval data point.

The two-way ANOVA results verify that a difference in antioxidant capacities can be accounted for, in part, by the Factor-1 rotenone dose. Table 5.57 illustrates that the vehicle Factor-1 plot consistently remained above the rotenone Factor-1 plot, no matter which treatment the rats received. Since the rats that received vehicle from days 1 to 14 all harboured, on average, higher antioxidant capacities than the environmental controls NN, it may be suggested that the vehicle contributed to the antioxidant capacity in heart muscle. This can be confirmed by referring to the descriptive statistics presented in Table 5.55. Moreover, the rotenone-induced complex I deficient rats harboured either similar or slightly lowered antioxidant capacities than NN. Therefore, the statistical significance for Factor-1 can be accounted for by the counteracting effects of both vehicle and rotenone.

The contribution from sunflower oil is, as mentioned in previous sections, an unexpected result and not ideal for the experimental goals of this study. The ideal vehicle should not result in a divergence in the biochemical parameters from the environmental controls. However, it is noteworthy to report on the beneficial effects of sunflower oil.

The highly significant main effect for dose Factor-2 suggests that the final two-day dose regimens indeed made a difference to the antioxidant capacities in rats. Since the two plots in Table 5.57 remain remarkably parallel and similar throughout, it can be deduced that the various differences may be derived from the Factor-2 treatments. The two-way ANOVA graphic representation does not validate that CoQ_{10} or succinate was of benefit to rats, as both the vehicle and rotenone Factor-1 plots are lowest at the CoQ_{10} and succinate data points. It is doubtful that these regimens would adversely alter the capacity of heart muscle to scavenge ROS.

The graph in Table 5.57 illustrates that rat groups that physically received dose regimens for a full 16-days all appear to harbour lower antioxidant capacities. The data is suggestive of the fact that the groups that received a no dose Factor-2 regimen recovered to antioxidant capacities greater than those that were sacrificed on day 15. However, the groups that were physically dosed and received vehicle, CoQ_{10} or succinate, regardless of which dose Factor-1 they received, all harboured antioxidant capacities that were even lower than rats that were sacrificed on day 15. This may imply that the dosage procedure itself could have affected or possibly imposed discomfort on the rats. It was discussed in Section 5.1.3 that minimal distress was observed in the rats throughout the dosage procedure, except when rotenone was dosed. The latter groups of rats progressively resisted the rotenone dose, complicating the dose intubation procedure. It was not foreseeable that oesophageal intubation itself would diminish antioxidant capacity in heart muscle. However, the procedure is invasive to the rodents and may acutely distress rats to a point that biochemical homeostasis may be altered. If the differences between these groups could be accounted for by oesophageal intubation with certainty, it was unexpected that the ORAC assay would be sensitive enough to detect such subtle differences.

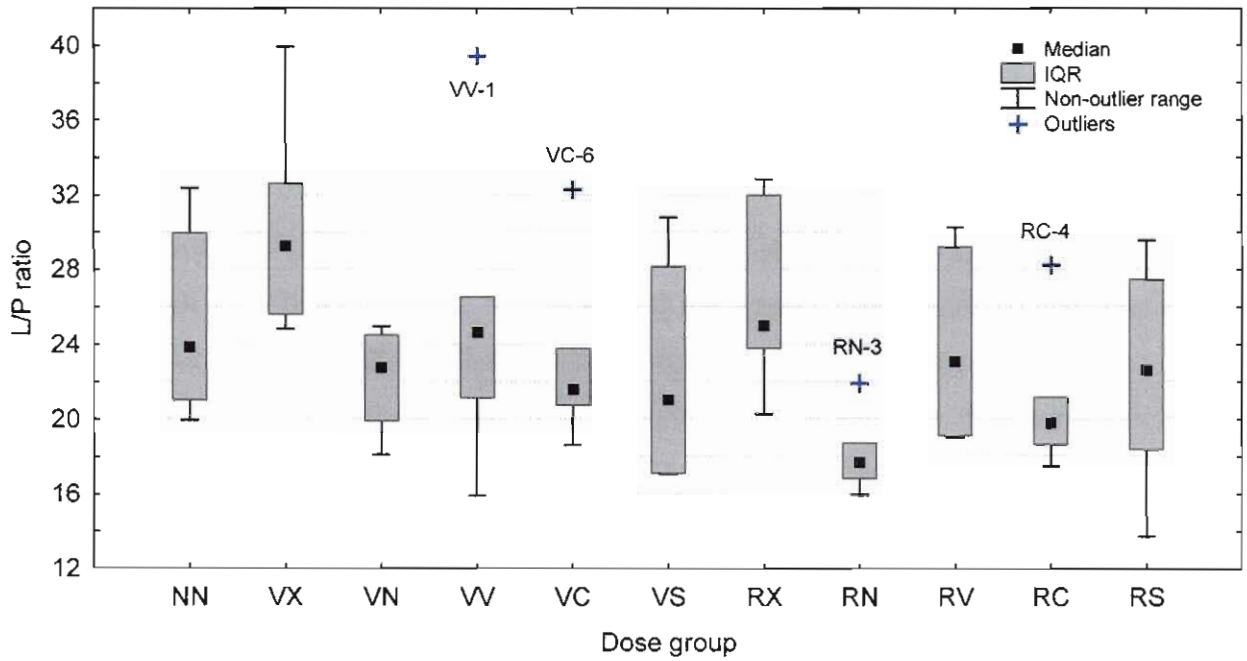
5.4.4 Lactate/pyruvate ratios in heart muscle

Heart muscle was isolated from rats in the different dose groups and the tissue prepared appropriately for analysis of the lactate and pyruvate concentrations. The ratio of lactate to pyruvate was determined for each sample and the data evaluated statistically to verify the contributions of the various dose regimens. The L/P ratios according to dose group are presented in Table 5.58. The data indicates the presence of four outliers, but no

extreme outliers. Therefore, a simplified statistical evaluation of the data was performed with no need for a parallel of analyses where extreme outliers were excluded.

Table 5.58 Box-whisker representation and descriptive statistics of the heart muscle L/P data generated from the main study

A: Box-whisker plots and data points according to rat groups



Rat	NN	VX	VN	VV	VC	VS	RX	RN	RV	RC	RS
1	26.2	39.9	22.9	+ 39.5	22.4	18.4	23.8	18.7	30.3	17.5	27.5
2	32.4	29.6	22.7	24.2	23.8	28.1	20.3	17.5	25.6	20.3	26.3
3	30.0	24.8	24.5	26.5	20.8	30.8	25.6	+ 21.9	29.2	21.1	19.0
4	20.0	25.6	18.1	21.1	20.8	23.6	24.4	16.8	19.1	+ 28.2	13.7
5	21.0	32.6	25.0	25.1	18.6	17.1	32.9	17.8	20.6	19.3	29.6
6	21.5	28.9	19.9	15.9	+ 32.3	17.1	32.0	16.0	19.0	18.6	18.4

B: Descriptive statistics

Dose group	Sample size	Mean	SD	Median	Min	Max	Range	Lower quartile	Upper quartile	IQR
NN	6	25.2	5.17	23.9	20.0	32.4	12.4	21.0	30.0	8.92
VX	6	30.3	5.53	29.3	24.8	39.9	15.1	25.6	32.6	7.02
VN	6	22.2	2.66	22.8	18.1	25.0	6.8	19.9	24.5	4.57
VV	6	25.4	7.86	24.7	15.9	39.5	23.6	21.1	26.5	5.37
VC	6	23.1	4.84	21.6	18.6	32.3	13.7	20.8	23.8	3.02
VS	6	22.5	5.96	21.0	17.1	30.8	13.8	17.1	28.1	11.0
RX	6	26.5	4.94	25.0	20.3	32.9	12.6	23.8	32.0	8.20
RN	6	18.1	2.09	17.7	16.0	21.9	5.98	16.8	18.7	1.88
RV	6	24.0	5.09	23.1	19.0	30.3	11.3	19.1	29.2	10.1
RC	6	20.9	3.84	19.8	17.5	28.2	10.7	18.6	21.1	2.50
RS	6	22.4	6.25	22.6	13.7	29.6	15.8	18.4	27.5	9.09

Rat codes for the outliers are located above or below the blue crosses (+), which correspond to data point values listed in the table directly below the graph. Rats were treated with NN = no dose regimen, VX = vehicle and sacrificed, VN = vehicle and no dose, VV = vehicle and vehicle, VC = vehicle and CoQ_{10}, VS = vehicle and succinate, RX = rotenone and sacrificed, RN = rotenone and no dose, RV = rotenone and vehicle, RC = rotenone and CoQ_{10}, RS = rotenone and succinate. IQR = inter-quartile range, L/P = ratio of lactate to pyruvate, Min = minimum data point value, Max = maximum data point value, SD = standard deviation.

The box-whisker plots in Table 5.58.A do not appear to illustrate any pertinent trend in response to the various dose regimens. Several of the dose groups harboured L/P ratios that were very similar to that of the environmental controls NN. Dose groups VX, RN and RC are the only groups that may be argued to have altered ratios. Dose group VX harboured six L/P ratios that were all greater than the median data point of NN. A similar scenario is true for dose group RN that consists of six data points that are all lower than the median of NN. Moreover, the only data point in RN to overlap with the distribution of data in NN is that of the outlier RN-3. Dose group RC also displays six data points below the median of NN, but too has data points that overlap with the distribution of NN.

The outliers were determined to be present in dose groups VV, VC, RN and RC. All four outliers were ratios that were higher than the other five data points in their respective dose groups. Observation of the graphic representation of the data indicates that the outliers are not extreme with regards to the complete data set. Outlier VV-1 harboured an L/P ratio of 39.5, which was higher than rat VV-3 by a ratio of 13.0, the closest ranked data point. However, it was equalled by an L/P ratio of 39.9 for a rat in dose group VX. The remaining three outliers were comfortably located within ranges of several other dose groups.

The exclusion of the aforementioned outliers would result in a decrease, although minimal, in the central tendency statistics and consequently may alter the ANOVA statistics due to the decreased variation. However, the proposed statistical strategy allows for exclusion of extreme outliers only. Therefore, the aforementioned outliers were not excluded and the heart muscle L/P data set was consequently further evaluated via a parametric one-way ANOVA and Tukey *equal number HSD* multiple comparison procedure. The p-values and d-values for biological significance of statistically significant comparisons are listed in Table 5.59. The multiple comparison grid reveals the presence of one statistically significant comparison, as indicated by the p-value of 0.007 for the comparison between dose groups RN and VX. The presence of the statistically significant comparison supported the statistically significant ANOVA p-value of 0.027. The significant difference between VX and RN was also determined to be biologically significant with a d-value of 2.195.

Table 5.59 Multiple comparison statistics of heart muscle L/P data generated from the rat main study

A: Tukey *equal number HSD* p-values											
Dose group	NN	VX	VN	VV	VC	VS	RX	RN	RV	RC	RS
NN		0.828	0.995	1.000	1.000	0.998	1.000	0.406	1.000	0.930	0.997
VX	0.828		0.223	0.863	0.389	0.279	0.971	0.007	0.576	0.084	0.258
VN	0.995	0.223		0.991	1.000	1.000	0.931	0.953	1.000	1.000	1.000
VV	1.000	0.863	0.991		0.999	0.996	1.000	0.362	1.000	0.906	0.995
VC	1.000	0.389	1.000	0.999		1.000	0.987	0.842	1.000	1.000	1.000
VS	0.998	0.279	1.000	0.996	1.000		0.960	0.921	1.000	1.000	1.000
RX	1.000	0.971	0.931	1.000	0.987	0.960		0.183	0.999	0.722	0.951
RN	0.406	0.007	0.953	0.362	0.842	0.921	0.183		0.676	0.998	0.933
RV	1.000	0.576	1.000	1.000	1.000	1.000	0.999	0.676		0.993	1.000
RC	0.930	0.084	1.000	0.906	1.000	1.000	0.722	0.998	0.993		1.000
RS	0.997	0.258	1.000	0.995	1.000	1.000	0.951	0.933	1.000	1.000	

B: ANOVA p-values
One-way ANOVA p-value = 0.027

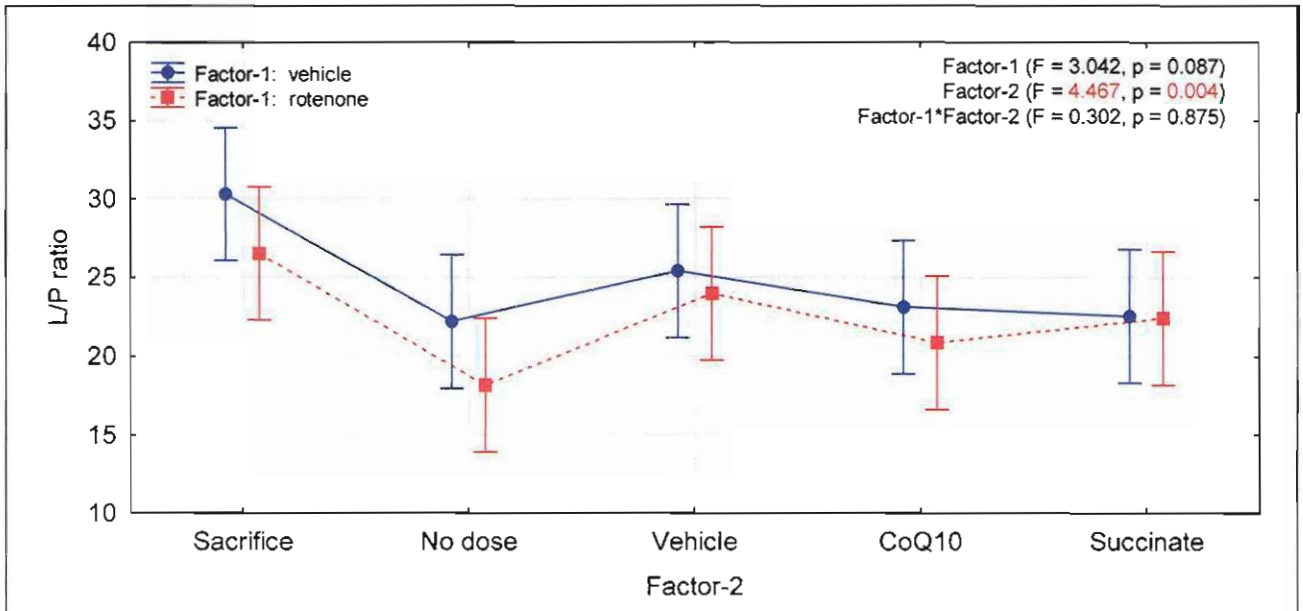
C: Statistical and biological significance			
Comparison		Statistical significance (p)	Biological significance (d)
VX	RN	0.007	2.195

A: All comparison statistics are indicated as p-values generated via the Tukey *equal number HSD* (Honestly Significant Difference) multiple comparison procedure. P-values indicated in red are statistically significant at the pre-determined significance level of 0.05. The remainder of p-values are listed in grey. The turquoise shaded blocks represent statistically significant comparisons that were also determined to be of biological significance. B: P-value for the one-way ANOVA is listed, with significant p-values, less than the 0.05 significance level, indicated in red. C: List of comparisons determined to be statistically significant with corresponding biological significance. A d-value greater than or equal to 0.8 signifies biological significance, indicated in red. Rats were treated with NN = no dose regimen, VX = vehicle and sacrificed, VN = vehicle and no dose, VV = vehicle and vehicle, VC = vehicle and CoQ_{10}, VS = vehicle and succinate, RX = rotenone and sacrificed, RN = rotenone and no dose, RV = rotenone and vehicle, RC = rotenone and CoQ_{10}, RS = rotenone and succinate. ANOVA = analysis of variance.

It was discussed previously that these two dose groups along with RC could be argued to display different data distributions when compared to NN as well as to the remaining dose groups. It was also mentioned that VX had six higher ratios than the NN median, while RN harboured six ratios less than the median of NN. It is therefore not completely unexpected that dose groups VX and RN would differ significantly from each other. If any statistically significant differences were to be present in the heart muscle L/P data set, from a visual inspection of the box-whisker plots in Table 5.58, it would be expected that these two groups would certainly be of the first to be considered. This statistically significant comparison does not reveal any relevant answer except that a difference between the two groups exists. The RN group was dosed rotenone for 14 days, followed by a two-day recovery before sacrificing. Dose group VX received sunflower oil vehicle for 14 days before being sacrificed. Thus, too many variables are present in this comparison to enable an accurate measurement of a single effect.

It is of value to note that no additional statistically significant differences existed between other groups that included comparisons between dose groups VX, RN and RC. The arguable differences in their data distributions are not supported by the Tukey *equal number HSD* multiple comparison procedure. Regardless of this, it is not too clear as to why the aforementioned dose groups displayed data distributions that appear slightly aberrant to the rest of the groups. To attain further insight into rat responses, the heart muscle L/P data was analysed via a two-way ANOVA in order to elucidate the roles of the different dose factors in the response of rats. The statistical data generated from the factorial ANOVA is presented in Table 5.60 via graphic summary and factor statistics. The mean and 95% confidence interval data points, as indicated in the graph, are also listed in table directly below.

Table 5.60 Graphic and tabulated summary of the heart muscle L/P data analysed via a two-way ANOVA



Data points	VX	VN	VV	VC	VS	RX	RN	RV	RC	RS
UCI	34.5	26.4	29.6	27.3	26.8	30.7	22.4	28.2	25.1	26.6
mean	30.3	22.2	25.4	23.1	22.5	26.5	18.1	24.0	20.9	22.4
LCI	26.0	17.9	21.2	18.9	18.3	22.2	13.9	19.7	16.6	18.2

The plot legend is indicated in the top left corner of the graph, while the two-way ANOVA F-statistics (F) and p-values (p) for Factor-1, Factor-2 and Factor-1*Factor-2 are located in the top right corner, with the statistically significant values indicated in red. The vertical whiskers at each mean data point represent 95% confidence intervals for the respective data sets. Rats were treated with NN = no dose regimen, VX = vehicle and sacrificed, VN = vehicle and no dose, VV = vehicle and vehicle, VC = vehicle and CoQ_{10}, VS = vehicle and succinate, RX = rotenone and sacrificed, RN = rotenone and no dose, RV = rotenone and vehicle, RC = rotenone and CoQ_{10}, RS = rotenone and succinate. LCI = lower 95% confidence interval data point, L/P = ratio of lactate to pyruvate, UCI = upper 95% confidence interval data point.

The vehicle and rotenone plots display very similar trends in response to the Factor-2 doses. This correlates well with the F-statistics and p-values indicated in the top right corner of the graph that confirm a statistically significant contribution from Factor-2 doses. A p-value of 0.004, beyond the 0.01 significance level, indicates a highly significant impact

on the L/P ratio response in rats. It should also be noted that even though the Factor-1 statistics are not indicated to be significant, the p-value of 0.087 is very near to being statistically significant at the 0.05 significance level. Moreover, the F-statistics for Factor-1 and Factor-2 are not very different at 3.042 and 4.467 respectively.

It is unexpected that the rotenone plot continuously remains below the vehicle plot. It was previously demonstrated in Section 5.4.2.2 that a Complex I deficiency was indeed induced in heart muscle of rats that received rotenone. It would be expected that the L/P ratio in this tissue would be affected adversely by the inhibition of complex I, especially since the effect of Factor-1 doses was determined to be statistically significant in the blood L/P data set, as discussed in Section 5.3.4. The differences between the rotenone and vehicle plots are visibly detectible, but it is also clear that the 95% confidence intervals overlap considerably throughout. This is the most likely reason that a statistically significant Factor-1 p-value was not reported by the two-way ANOVA.

Both the rotenone and vehicle plots appear to suggest that the rats receiving doses on days 15 and 16 display lowered L/P ratios than those that were sacrificed on day 15, namely VX and RX. It also suggests that rats that received a vehicle Factor-2 dose had higher L/P ratios than those that received no dose. In addition, the rats that were dosed CoQ_{10} and succinate Factor-2 doses harboured slightly lower L/P ratios than those that received the vehicle. It is suspected that the statistical significance for Factor-2 arises due to the discrepancies between the sacrificed and no dose treatments. It may be argued that the receiving of a dose itself could be a contributing factor to the increased L/P ratios when compared to the rats that received no dose Factor-2 regimens. As presented in Section 5.4.3, antioxidant capacity data generated from heart muscle revealed a similar scenario. The antioxidant capacity in the groups that were physically dosed appeared to be compromised when compared to the rats that received a no dose Factor-2 regimen. The two data sets support each other and strengthen the argument that the dosage procedure may indeed affect the heart.

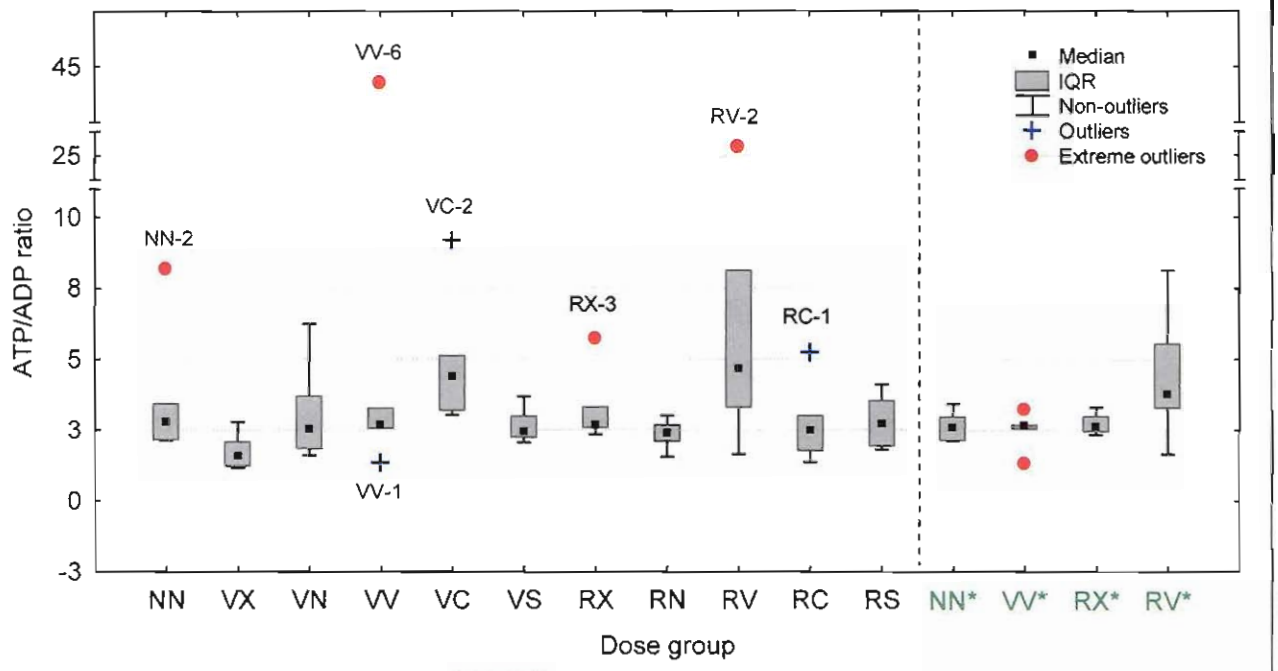
5.4.5 ATP/ADP ratios in heart muscle

Heart muscle was collected on the days that rats were sacrificed. The tissue was homogenised and samples deproteinised according to protocols discussed in Sections 4.4.2 and 4.4.8 of Chapter Four. Adenylate concentrations were determined spectrophotometrically and the data analysed via statistical applications to verify

significance of the variation in response profiles. Heart muscle ATP/ADP ratio data is presented in Table 5.61 along with a table of descriptive statistics. The box-whisker representations of heart muscle ATP/ADP ratios depicts the presence of six extreme outliers, of which two were present in dose group VV* after an initial extreme outlier was excluded from the original VV data set. Consequently, the latter two mentioned extreme outliers are not discussed further. In addition, three outliers were also determined to be present in dose groups VV, VC and RC.

Table 5.61 Box-whisker representation and descriptive statistics of the heart muscle ATP/ADP ratio data generated from the main study

A: Box-whisker plots and data points according to rat groups



Rat	NN	VX	VN	VV	VC	VS	RX	RN	RV	RC	RS	NN*	VV*	RX*	RV*
1	2.59	2.77	1.59	+ 1.34	5.11	2.45	2.34	3.00	3.29	+ 5.24	2.40	2.59	1.34	2.34	3.29
2	• 8.16	1.22	2.67	2.55	+ 9.15	2.98	2.67	2.35	• 25.4	2.94	4.11	EXCL	2.55	2.67	EXCL
3	2.96	1.16	2.36	3.26	3.02	3.68	• 5.74	2.67	1.64	2.01	1.80	2.96	3.26	EXCL	1.64
4	3.42	1.71	1.84	2.67	3.80	2.06	2.59	2.43	3.80	1.36	3.53	3.42	2.67	2.59	3.80
5	2.13	1.46	3.68	2.67	4.98	2.24	---	1.55	5.55	2.99	1.93	2.13	2.67	---	5.55
6	2.15	2.06	6.24	• 44.5	3.19	2.41	3.30	2.10	8.11	1.77	3.02	2.15	EXCL	3.30	8.11

B: Descriptive statistics

Dose group	Sample size	Mean	SD	Median	Min	Max	Range	Lower quartile	Upper quartile	IQR
NN	6	3.57	2.30	2.77	2.13	8.16	6.04	2.15	3.42	1.27
NN*	5	2.65	0.55	2.59	2.13	3.42	1.29	2.15	2.96	0.81
VX	6	1.73	0.61	1.58	1.16	2.77	1.61	1.22	2.06	0.85
VN	6	3.06	1.72	2.52	1.59	6.24	4.65	1.84	3.68	1.84
VV	6	9.49	17.1	2.67	1.34	44.5	43.1	2.55	3.26	0.71
VV*	5	2.50	0.70	2.67	1.34	3.26	1.92	2.55	2.67	0.12
VC	6	4.88	2.27	4.39	3.02	9.15	6.13	3.19	5.11	1.92
VS	6	2.64	0.60	2.43	2.06	3.68	1.62	2.24	2.98	0.73

Table 5.61 Continued...

Dose group	Sample size	Mean	SD	Median	Min	Max	Range	Lower quartile	Upper quartile	IQR
RX	5	3.33	1.39	2.67	2.34	5.74	3.39	2.59	3.30	0.71
RX*	4	2.72	0.41	2.63	2.34	3.30	0.96	2.47	2.98	0.52
RN	6	2.35	0.50	2.39	1.55	3.00	1.45	2.10	2.67	0.57
RV	6	7.96	8.82	4.68	1.64	25.4	23.6	3.29	8.11	4.82
RV*	5	4.48	2.47	3.80	1.64	8.11	6.48	3.29	5.55	2.26
RC	6	2.72	1.39	2.47	1.36	5.24	3.87	1.77	2.99	1.22
RS	6	2.80	0.92	2.71	1.80	4.11	2.31	1.93	3.53	1.59

Rat codes for outliers and extreme outliers are located above or below the respective blue crosses (+) and red dots (•), which correspond to data point values listed in the table directly below the graph. The vertical dashed line in the box-whisker graphic representation separates original dose group box-whiskers from those that have had the extreme outliers excluded, which are also indicated by the asterisk (*) following the dose group code. Data sets with excluded data points are designated in green text. A scale-break was implemented between ratios of 10 and 25 as well as between 25 and 45. Rats were treated with NN = no dose regimen, VX = vehicle and sacrificed, VN = vehicle and no dose, VV = vehicle and vehicle, VC = vehicle and CoQ_{10}, VS = vehicle and succinate, RX = rotenone and sacrificed, RN = rotenone and no dose, RV = rotenone and vehicle, RC = rotenone and CoQ_{10}, RS = rotenone and succinate. '—' = missing data point, ATP/ADP = ratio of adenosine triphosphate to adenosine diphosphate, EXCL = excluded data point, IQR = inter-quartile range, Min = minimum data point value, Max = maximum data point value, SD = standard deviation.

The environmental controls NN harboured an extreme outlier, namely NN-2, which presented with an ATP/ADP ratio of 8.16. Since the mean ATP/ADP ratio for NN was at 3.57, and since the remainder of the five data points were within a range of 1.29, rat NN-2 harboured a ratio that was distinctly separate from the rest, as indicated in Table 5.61.A. An exclusion of this data point resulted in a mean decrease in ratio to 2.65 and a SD decrease from 2.30 to 0.55. The median decreased only slightly from 2.77 to 2.59, while the IQR was adjusted from 1.27 to 0.81. A second extreme outlier, present in dose group VV, was abnormally elevated with an ATP/ADP ratio of 44.5. The exclusion of VV-6 resulted in a marked decrease in the mean for VV from 9.49 to 2.50. The SD diminished to 0.70 from 17.14, while the IQR decreased from 0.71 to 0.12. Finally, the median for VV* remained constant at an ATP/ADP ratio of 2.67 due to the presence of two central data points presenting with identical 2.67 ratios.

Dose group RX originally harboured five data points due to the fact that insufficient sample preparation was available to perform repeat analysis for rat RX-5. In addition to the missing data point, RX was determined to harbour an extreme outlier, RX-3. Even though RX-3 does not appear to be positioned at an aberrantly high ATP/ADP ratio, it is evident that a narrow IQR of 0.71 was determined for dose group RX. Consequently, the upper outlier boundary was situated at an ATP/ADP ratio of 5.43, which resulted in the 5.74 ratio for RX-3 being classified as an extreme outlier. The exclusion of RX-3 from data set RX results in a mean decrease from 3.33 to 2.72, and a SD decrease from 1.39 to 0.41. The median decreased only slightly from 2.67 to 2.63, while the IQR decreased from 0.71 to 0.52.

Rat RV-2 harboured an ATP/ADP ratio of 25.4, which was determined to be an extreme outlier within data set RV. Being the highest ratio in the RV dose group, RV-2 also appeared to be elevated when compared to the overall heart muscle ATP/ADP data set. An exclusion of RV-2 resulted in a marked mean decrease from 7.96 to 4.48, and a SD decrease from 8.82 to 2.47. The median for the rat group decreased from 4.68 to 3.80, while the IQR decreased considerably from 4.82 to 2.26.

Upon a visual inspection of the box-whisker plots in Table 5.61.A, it appears that a similar distribution of data was determined for all groups of the rat main study. With the inclusion of extreme outliers, the median fluctuation of heart muscle ATP/ADP ratios ranged between 1.73 and 4.88. Furthermore, even though the IQRs were not widely distributed, the distributions of data for most groups overlapped within similar ranges. It would therefore not be expected that many statistically significant differences would exist when dose groups were compared to each other. This can be confirmed by the fact that only three statistically significant p-values were reported by multiple comparison procedures, as presented in Table 5.62.

When the ATP/ADP ratios from dose groups VX and VC were compared to each other, both the non-parametric and parametric multiple comparison procedures resulted in statistically significant p-values. In addition, both comparisons were determined to be of biological significance with d-values of 1.388 and 2.383, prior to and after the exclusion of extreme outliers, respectively. Although the tests for statistical and biological significance are mutually exclusive evaluations of the data, it is of interest to note that the increase in biological significance upon the exclusion of extreme outliers corresponds well with the increase in statistical significance where p-values decreased from 0.010 to 0.006 for the inclusion and exclusion of the extreme outliers respectively. Dose group VX harboured a mean ATP/ADP ratio of 1.73, as opposed to the mean of 4.88 for VC. The data therefore suggests that an additional two days of dosing with CoQ_{10} significantly improved ATP/ADP ratios in heart muscle. Moreover, since VC presented with a higher ATP/ADP ratio than VN, VV* and VS, it may be argued that CoQ_{10} was more beneficial to rats that received a vehicle Factor-1 regimen. However, as indicated in Table 5.62, these differences were not supported on a statistical level. Nonetheless, the trend in data is suggestive of improved heart muscle ATP/ADP ratios in rats that received CoQ_{10}. In contrast, this is not supported by similarly increased ATP/ADP ratios in the rat groups that harboured the rotenone-induced Complex I deficiency. The only rat group, harbouring a Complex I

deficiency, which indicates that heart muscle ATP/ADP ratios may have been improved is RV. The remainder of the rat groups that received rotenone Factor-1 doses presented with similar ATP/ADP ratios. On the other hand, statistically significant differences were not determined to be present among any of the rotenone-treated rat groups.

Table 5.62 Multiple comparison statistics of heart muscle ATP/ADP ratio data generated from the rat main study

A: Non-parametric (original data set) and parametric (excluding extreme outliers) p-values

Dose group	NN	VX	VN	VV	VC	VS	RX	RN	RV	RC	RS
NN		1.000	1.000	1.000	1.000	1.000	1.000	1.000	1.000	1.000	1.000
		0.989	1.000	1.000	0.247	1.000	1.000	1.000	0.524	1.000	1.000
VX	1.000		1.000	1.000	0.010	1.000	1.000	1.000	0.043	1.000	1.000
	0.989		0.803	0.997	0.006	0.981	0.992	0.999	0.062	0.966	0.943
VN	1.000	1.000		1.000	1.000	1.000	1.000	1.000	1.000	1.000	1.000
	1.000	0.803		1.000	0.404	1.000	1.000	0.997	0.832	1.000	1.000
VV	1.000	1.000	1.000		1.000	1.000	1.000	1.000	1.000	1.000	1.000
	1.000	0.997	1.000		0.172	1.000	1.000	1.000	0.407	1.000	1.000
VC	1.000	0.010	1.000	1.000		1.000	1.000	0.543	1.000	1.000	1.000
	0.247	0.006	0.404	0.172		0.142	0.449	0.059	1.000	0.178	0.219
VS	1.000	1.000	1.000	1.000	1.000		1.000	1.000	1.000	1.000	1.000
	1.000	0.981	1.000	1.000	0.142		1.000	1.000	0.513	1.000	1.000
RX	1.000	1.000	1.000	1.000	1.000	1.000		1.000	1.000	1.000	1.000
	1.000	0.992	1.000	1.000	0.449	1.000		1.000	0.729	1.000	1.000
RN	1.000	1.000	1.000	1.000	0.543	1.000	1.000		1.000	1.000	1.000
	1.000	0.999	0.997	1.000	0.059	1.000	1.000		0.304	1.000	1.000
RV	1.000	0.043	1.000	1.000	1.000	1.000	1.000	1.000		1.000	1.000
	0.524	0.062	0.832	0.407	1.000	0.513	0.729	0.304		0.578	0.642
RC	1.000	1.000	1.000	1.000	1.000	1.000	1.000	1.000	1.000		1.000
	1.000	0.966	1.000	1.000	0.178	1.000	1.000	1.000	0.578		1.000
RS	1.000	1.000	1.000	1.000	1.000	1.000	1.000	1.000	1.000	1.000	
	1.000	0.943	1.000	1.000	0.219	1.000	1.000	1.000	0.642	1.000	

B: ANOVA p-values

Kruskal-Wallis p-value = 0.025	One-way ANOVA p-value = 0.009

C: Statistical and biological significance

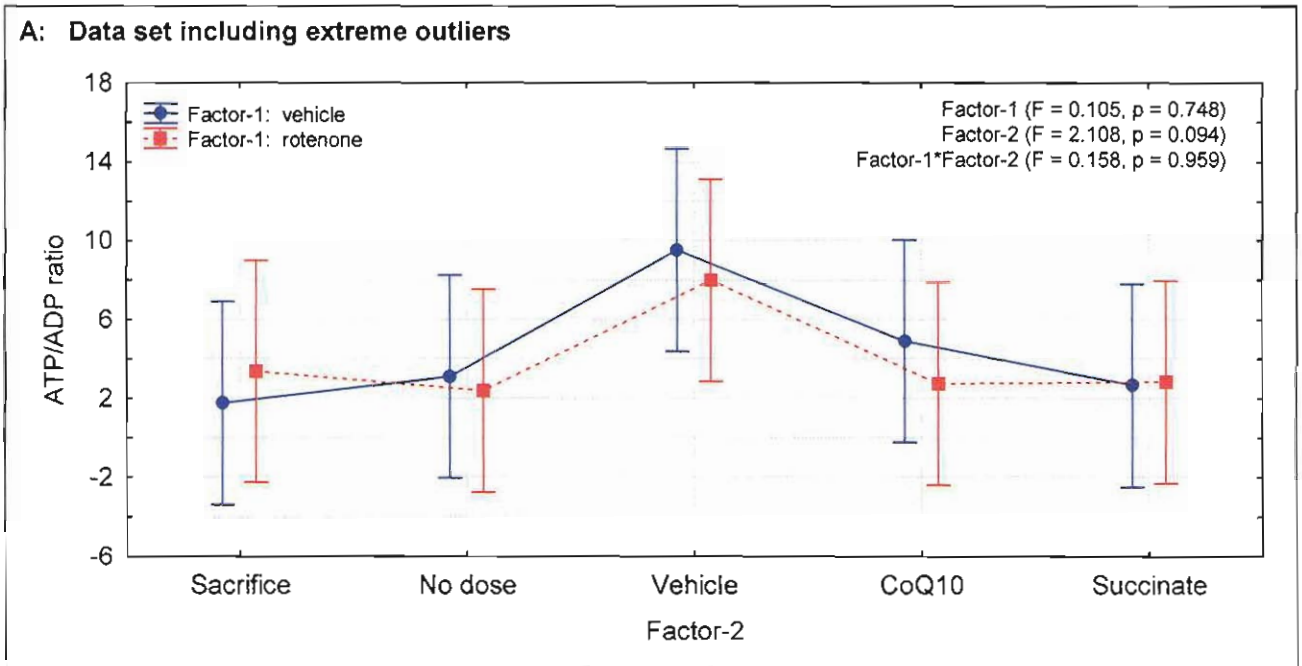
Comparison		Statistical significance (p)		Biological significance (d)	
		Including EOs	Excluding EOs	Including EOs	Excluding EOs
VX	VC	0.010	0.006	1.388	2.383
VX	RV	0.043	0.062	0.706	N/A

A: All comparison statistics are indicated as p-values. The upper p-value is the non-parametric multiple comparison test statistic, generated from the original set of data. The lower p-value was generated via the parametric Tukey *unequal number HSD* (Honestly Significant Difference) test, after the exclusion of extreme outliers. P-values indicated in red are statistically significant at the pre-determined significance level of 0.05. P-values in black text represent those that are not statistically significant, but have complementary p-values that are statistically significant. The remainder of p-values are listed in grey. The comparisons surrounded by the **bold** black line are those that were determined to be statistically significant by both the non-parametric and parametric multiple comparison procedures. The turquoise shaded blocks represent statistically significant comparisons that were also determined to be of biological significance. B: P-values for the non-parametric Kruskal-Wallis ANOVA and parametric one-way ANOVA are listed, with significant p-values, less than the 0.05 significance level, indicated in red. C: List of comparisons determined to be statistically significant with corresponding biological significance. A d-value greater than or equal to 0.8 signifies biological significance, indicated in red. Rats were treated with NN = no dose regimen, VX = vehicle and sacrificed, VN = vehicle and no dose, VV = vehicle and vehicle, VC = vehicle and CoQ_{10}, VS = vehicle and succinate, RX = rotenone and sacrificed, RN = rotenone and no dose, RV = rotenone and vehicle, RC = rotenone and CoQ_{10}, RS = rotenone and succinate. ANOVA = analysis of variance, EOs = extreme outliers, N/A = not applicable.

The multiple comparison grid presented in Table 5.62.A also indicates that, prior to the exclusion of extreme outliers, the ATP/ADP ratios for groups VX and RV differed significantly on a statistical level. Since these dose groups received dose regimens that do not allow for the inference of single effects, the statistical significance will not be discussed. As indicated in Table 5.61, dose group RV harboured an extreme outlier that was positioned well above the remaining five data points in RV. Therefore, an elevated mean and variance for RV resulted in the statistically supported difference, when compared to VX. The statistical significance was eradicated upon the exclusion of all extreme outliers, suggesting that the variation among the groups, and within RV itself, contributed largely to the generation of the aforementioned statistically significant p-value. Moreover, the argument is supported by the fact that VX did not differ from RV with biological significance, as indicated by the the d-value of 0.062 in Table 5.62.C. In order to evaluate the contributions of Factor-1 and Factor-2 dose regimens in the generation of the heart muscle ATP/ADP data, a factorial ANOVA approach was used. Since extreme outliers were determined to be present in the data set, the two-way ANOVA was performed via the inclusion and exclusion of extreme outliers. Results of the factorial ANOVAs are presented in Table 5.63, along with corresponding F-statistics and p-values. A listing of 95% confidence intervals and mean data points are also presented.

Table 5.63 Graphic and tabulated summary of the heart muscle ATP/ADP ratio data analysed via a two-way ANOVA

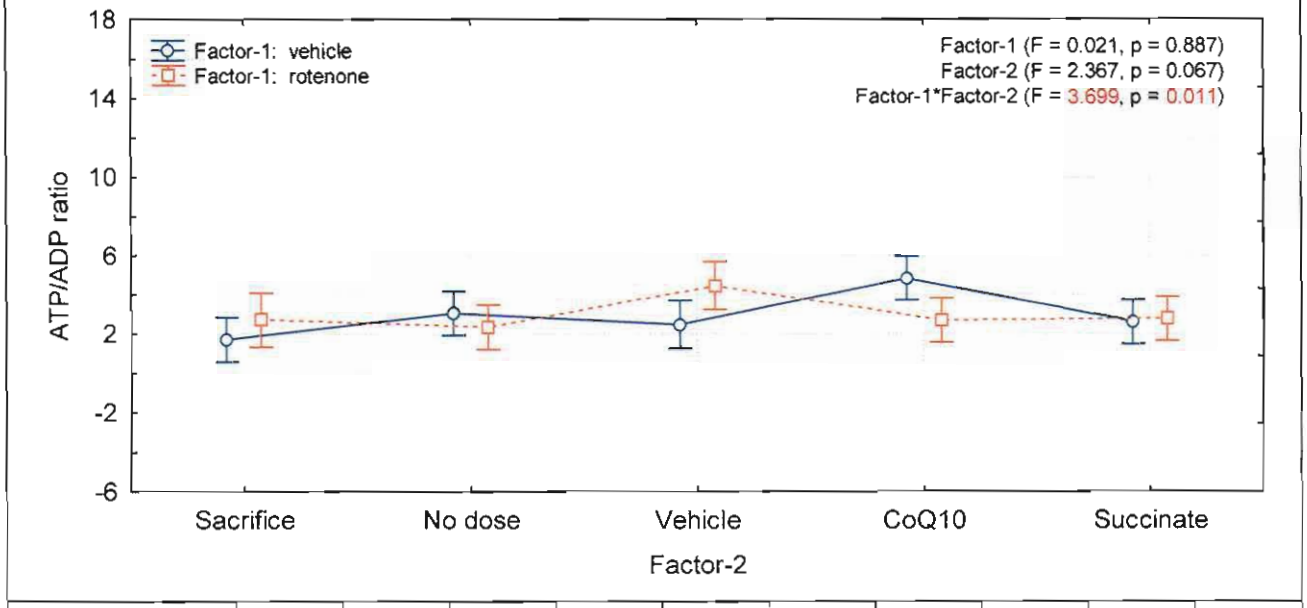
A: Data set including extreme outliers



Description		VX	VN	VV	VC	VS	RX	RN	RV	RC	RS
With extreme outliers	UCI	6.87	8.21	14.6	10.0	7.78	8.96	7.49	13.1	7.86	7.94
	mean	1.73	3.06	9.49	4.88	2.64	3.33	2.35	7.96	2.72	2.80
	LCI	-3.41	-2.08	4.35	-0.27	-2.51	-2.31	-2.79	2.82	-2.43	-2.35

Table 5.63 Continued...

B: Data set excluding extreme outliers



Description		VX	VN	VV	VC	VS	RX	RN	RV	RC	RS
Without extreme outliers	UCI	2.85	4.19	3.73	6.00	3.76	4.10	3.47	5.71	3.84	3.92
	mean	1.73	3.06	2.50	4.88	2.64	2.72	2.35	4.48	2.72	2.80
	LCI	0.61	1.94	1.27	3.75	1.51	1.35	1.22	3.25	1.59	1.67

The plot legends for each graph are indicated in the top left corners of the respective graphs, while the two-way ANOVA F-statistics (F) and p-values (p) for Factor-1, Factor-2 and Factor-1*Factor-2 are located in the top right corner, with the statistically significant values indicated in red. The vertical whiskers at each mean data point represent 95% confidence intervals for the respective data sets. The mean values in green text, located in the data point summary tables below the graphs, indicate those that were adjusted due to the exclusion of extreme outliers. Rats were treated with NN = no dose regimen, VX = vehicle and sacrificed, VN = vehicle and no dose, VV = vehicle and vehicle, VC = vehicle and CoQ_{10}, VS = vehicle and succinate, RX = rotenone and sacrificed, RN = rotenone and no dose, RV = rotenone and vehicle, RC = rotenone and CoQ_{10}, RS = rotenone and succinate. ATP/ADP = ratio of adenosine triphosphate to adenosine diphosphate, LCI = lower 95% confidence interval data point, UCI = upper 95% confidence interval data point.

Prior to the exclusion of outliers, the two-way ANOVA yielded no statistically significant contributions from either of the dose factors, nor did it indicate the presence of an interaction effect. The vehicle and rotenone Factor-1 plots in Table 5.63.A presented remarkably similar trends, with mean increases at the vehicle Factor-2 level. However, as discussed previously in this section and in referral to Table 5.61, it is evident that the elevated means for dose groups VV and RV are accounted for by the presence of extreme outliers in each of these groups. Therefore, although it may appear that a trend is present, which is suggestive of improved ATP/ADP ratios for rats that received vehicle Factor-2 dose regimens, this is certainly not a true reflection of the data when viewed in light of the influence of highly elevated extreme outlier ratios.

Upon exclusion of the extreme outliers, a statistically significant interaction effect with a p-value of 0.011 was determined from the two-way ANOVA. The Factor-1 vehicle and rotenone plots presented with similar means. In addition, the plots intersected on more than one occasion, indicative of an interaction effect pattern. The F-statistics and p-values

in the top right corner of the graphic summary in Table 5.63.B are suggestive of the fact that rotenone did not further compromise ATP/ADP ratios in heart muscle, but rather that it interacted with Factor-2 dose regimens. The same holds true for the vehicle Factor-1 dose. The fact that vehicle and rotenone Factor-1 plots do not visibly diverge by large amounts corresponds well with the data generated from the multiple comparison procedures, where few statistically significant differences were determined to exist between dose groups.

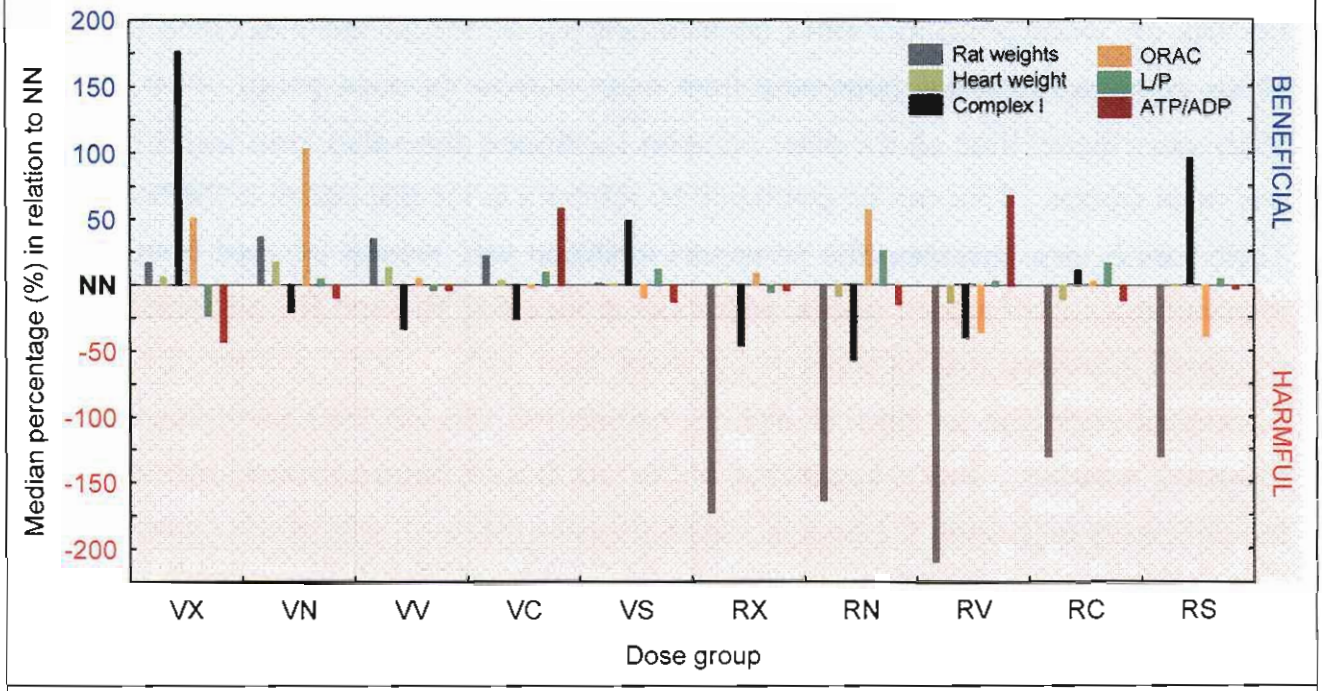
5.4.6 Heart muscle profile of the rat main study

The heart profile was established from data generated via the various biochemical assays incorporated in the study. Rat weight and heart weight data were also included in the heart profile, as presented in Table 5.64. A corresponding list of median percentages in relation to the environmental control dose group NN is presented in Section B of the table. Rat weights are not discussed since the median percentage deviations were addressed previously in the blood profile of Section 5.3.7.

As presented in Table 5.64, heart weights did not deviate by a large degree from the environmental control rat group NN. Dose groups VN and VV presented with median heart weights that were 17.1% and 13.0% higher than NN respectively. These increases were suggested to be the result of organ hypertrophy induced by the oxidative stress incurred via the high dosage of polyunsaturated fat contents (Turpeinen *et al.*, 1998) inherent in sunflower oil, as discussed in Section 5.4.1.2. However, this speculation was not supported due to the fact that heart weights for VN and VV did not differ statistically significantly from NN, as indicated in Table 5.64.B. Furthermore, the aforementioned heart weights were not determined to differ by a statistically significant degree from the remaining vehicle Factor-1 dose groups, namely VX, VC and VS, as confirmed in Section 5.4.1.2. It is also apparent that dose groups RV and RC presented with the lowest median heart weights, which were -12.5% and -10.4% lower than NN. Although the two dose groups did not differ statistically significantly from the environmental controls, it was hypothesised that rotenone inhibited growth by means of apoptotic induction processes (Chauvin *et al.*, 2001) and mitotic arrest (Barham and Brinkley, 1976a and 1976b). These arguments gained credibility due to the fact that a statistically significant Factor-1 was generated by the two-way ANOVA. This result is strongly suggestive of rotenone indeed adversely affecting heart weight, be it directly or indirectly.

Table 5.64 Heart muscle profile of response generated from the rat main study indicating the beneficial and harmful effects of dose regimens

A: Graphic representation



B: Median percentage (%) grid and factorial ANOVA summary

Data set	Dose group										Factorial ANOVA		
	VX	VN	VV	VC	VS	RX	RN	RV	RC	RS	F1	F2	F1*F2
Rat weights	16.9	36.4	35.1	22.1	1.30	-173	-164	-209	-130	-130	s/s	n/n	s/s
Heart weight	5.86	17.1	13.0	3.38	0.48	0.90	-8.62	-12.5	-10.4	0.78	s	n	n
Complex I	176	-20.4	-33.3	-25.8	48.5	-46.0	-57.1	-39.8	10.7	95.4	s/s	s/s	s/s
AC	51.0	103	4.91	-1.73	-9.34	8.98	57.0	-35.1	3.24	-38.2	s	s	n
L/P	-22.6	4.55	-3.32	9.57	11.9	-4.76	26.0	3.29	17.1	5.13	n	s	n
ATP/ADP	-42.9	-9.35	-3.70	58.3	-12.4	-3.93	-13.9	68.5	-10.9	-2.47	n/n	n/n	n/s

A: Percentage bars denote either beneficial or harmful effects induced by the dose regimens. Each bar is colour coded to represent the various data sets, as indicated by the graphic key in the top right corner of the graph. The 0% line on the Y-axis is labelled **NN**, since all median percentages were calculated to deviate from the environmental controls NN. B: The percentage data points are listed in correspondence with the bar heights. Median percentages that deviate by more than 10% from the environmental controls NN are indicated in blue and red text for beneficial and harmful deviations respectively. Percentages in grey text represent deviations less than 10%. Comparisons determined to differ significantly after the exclusion of extreme outliers are indicated by yellow shading. Statistically significant (s) and non-significant (n) contributions of Factor-1 (F1) and Factor-2 (F2) dose regimens as well as the interaction (F1*F2) between these factors are indicated alongside the median percentage grid. Two symbols are indicated if extreme outliers were determined to be present in the respective data set, with the first symbol representing significance status prior to exclusion, followed by the second symbol representing significance status after exclusion of extreme outliers. AC = antioxidant capacity, L/P = ratio of lactate to pyruvate, ATP/ADP = ratio of adenosine triphosphate to adenosine diphosphate. Rats were treated with NN = no dose regimen, VX = vehicle and sacrificed, VN = vehicle and no dose, VV = vehicle and vehicle, VC = vehicle and CoQ_{10}, VS = vehicle and succinate, RX = rotenone and sacrificed, RN = rotenone and no dose, RV = rotenone and vehicle, RC = rotenone and CoQ_{10}, RS = rotenone and succinate.

Lowered complex I activities were observed in heart muscle of dose groups VN, VV and VC. Similarly, as presented in Section 5.4.2.1, the median complex I activity for dose group V of the rat pilot study was also reported to be lower than that of dose group N, the environmental controls for that study. The median percentages in Table 5.64.B also indicate that dose group VN, VV and VC deviated by more than 20% from the environmental controls NN. However, these dose groups did not differ statistically

significantly from NN. Therefore, the decreased median complex I activities were not supported on a statistical level and should therefore not be definitively interpreted as complex I deficient. The only dose group determined to differ statistically significantly from NN was VX, which presented with a considerably higher median complex I activity. In fact, all six complex I activities generated from heart muscle for dose group VX of the main study were higher than all the other complex I activities generated from both the rat pilot and main studies. This can be confirmed by referring to the discussion in Section 5.4.2.2. Table 5.64.B also indicates that complex I inhibition was indeed attained from rats that received rotenone Factor-1 doses, with dose groups RX, RN and RV all presenting with complex I activities that decreased by more than 35%. Dose groups that received therapeutic regimens on days 15 and 16, namely RC and RS, harboured improved final complex I activities. This is suggestive of the fact that rat heart complex I recovered from the deficiency only when therapeutic regimens were received, with greater improvements when succinate was dosed.

The antioxidant capacity data generated from heart muscle indicated that a vehicle Factor-1 dose may have improved antioxidant status in dose groups VX and VN, which harboured the highest antioxidant capacities that increased by 51.0% and 103% respectively. However, these benefits were not determined to be of statistical significance. The remaining vehicle Factor-1 dosed rat groups, namely VV, VC and VS, deviated by less than 10% from the environmental controls NN and therefore did not present with improved antioxidant capacity recordings. With regards to the groups that received rotenone Factor-1 doses, it was observed that the antioxidant capacities were affected adversely. The exception was dose group RN, which presented with an antioxidant capacity that increased by 57.0%, suggesting that receiving a no dose Factor-2 regimen benefited the rat heart antioxidant capacity more than any of the other Factor-2 treatments. The fact that dose group RX presented with a similar median antioxidant capacity to that of NN could be argued to be the result of a counter-balancing effect of the vehicle and rotenone. Heart muscle from dose group RX indeed suffered from an induced Complex I deficiency, which would be expected to further induce ROS formation and hence reduce antioxidant capacity. It should also be noted that the dosage of the sunflower oil vehicle alone would result in increased polyunsaturated fat content in the membranes and hence increase hydroperoxide levels (Mataix *et al.*, 1998). The recovery in antioxidant capacities may thus have resulted from the induction of antioxidant mechanisms, most likely by the increased vitamin E intake inherent in sunflower oil.

Median percentages of heart muscle L/P data across all groups did not deviate by more than 30%, indicating that heart muscle L/P ratios were certainly more resistant to fluctuation when compared to other parameters that were measured in the study. However, none of the L/P ratios for the various dose groups differed statistically significantly from the environmental controls NN, as presented in Table 5.64. It may be argued that the sunflower oil vehicle decreased L/P ratios in heart muscle of rats due to the fact that dose group VX presented with the most affected ratio that was -22.6% lower than the environmental controls NN. However, the L/P ratio for VV was calculated to be only -3.32% lower than NN, which was initially expected to be equivalent to, or lower than VX, since these rats received vehicle for 16 days. Nonetheless, neither VX nor VV differed by a statistically significant degree from NN, nor did they differ significantly from each other, as presented in Section 5.4.4. It was surprising that L/P ratios of heart muscle in rats that received a rotenone Factor-1 dose did not present adversely, especially dose group RX that did not receive a Factor-2 dose to aid recovery. The resistance of heart muscle to fluctuation in L/P ratios, even in the presence of a Complex I deficiency, can be attributed to a postulated adaptability to oxidative stress and respiratory chain inhibition. The fact that a statistically significant Factor-2 contribution was reported by the two-way ANOVA suggests that the slight differences in L/P ratios can be accounted primarily for by the regimens received on days 15 and 16.

Adenylate concentrations generated from heart muscle indicated that the vehicle proved to be harmful in this regard. Dose group VX presented with a median percentage decrease in ratio that was calculated to be -42.9% of the environmental controls NN. However, as with the L/P data from heart muscle discussed in the previous paragraph, dose group VV did not correspondingly present with an adverse response. In addition, the similarity is extended to encompass the lack of statistically significant differences when each of the groups was compared to NN. Since VN harboured equivalent ATP/ADP ratios to NN, it can be speculated that these rats recovered from the no dose Factor-2 regimen. However, this notion is unlikely due to the fact that dose group VV also harboured an equivalent ratio. The 58.3% improvement in the ATP/ADP ratio for VC suggests that CoQ_{10} markedly improved ATP production. This recovery was not observed when succinate was dosed following 14 days of vehicle, since rat group VS harboured a median ATP/ADP ratio of -12.4%. Among the rotenone-treated rats, significant fluctuations in ATP/ADP ratios were not observed. The fact that dose group RX did not present with a diminished ATP/ADP ratio indicates once again that adaptive mechanisms in heart muscle

may have intervened and aided stabilisation of heart muscle biochemical status, even in the presence of a Complex I deficiency.

In view of the overall status of heart muscle in rats that received a vehicle Factor-1 dose, a definitive evaluation as to the global beneficial or harmful effects cannot be stated with confidence. Excluding rat weight data, a total of eight median percentages (indicated in blue), signifying greater than 10% improvements, and six median percentages (in red) representing greater than 10% harmful effects, were reported. The only statistically significant difference was reported when complex I activity for rat group VX was determined to be significantly greater than the environmental controls NN. Unfortunately, this increase was regarded as aberrant, as discussed in Section 5.4.2.2, and could not be relied upon as a conclusive result. The lack of statistically significant differences reported amongst the rats that received a sunflower oil Factor-1 dose regimen is indicative of the fact that heart muscle biochemistry was resistant to changes that may have been induced by the high polyunsaturated fat contents of sunflower oil.

Rats that harboured a rotenone-induced Complex I deficiency also appeared to present with a heart muscle profile that was not affected by extreme median percentages. On the whole, the tissue can be argued to be affected adversely based on the fact that nine median percentages were determined to be lower than NN by more than 10% (indicated in red), as opposed to the six that improved by more than 10% (indicated in blue). However, it should be noted that the median percentage data was classified according to assumed beneficial and harmful effects, as indicated in Table 5.41. It was evident from their physical deterioration and increased weight loss that the rats were affected by the rotenone dosage regimens. Furthermore, Complex I deficiency was indeed induced in heart muscle of rats, as presented in Section 5.4.2.2. As mentioned previously, it could be argued that heart muscle harboured adaptive abilities and a resistance that appeared to overcome the inhibitory effects of rotenone and maintain a stable biochemical profile. Furthermore, it is suggested that the proposed antioxidant effects of rotenone played an important role in the reduction of oxidative stress factors.

5.4.6.1 Impact of coenzyme Q10 and succinate on rat heart muscle

If the beneficial effects of CoQ_{10} and succinate were to be evaluated in rats that received vehicle as a Factor-1 dose, it can be observed that two contrasting biochemical responses were reported. The first is the improved complex I activity reported for rat group VS as

opposed to the rats receiving CoQ_{10} as a Factor-2 dose. Dose group VS presented with a median complex I activity that was 48.5% greater than the environmental control group NN, while dose group VC harboured a final complex I activity with a median percentage of -25.8% when compared to NN. This comparison indicates that succinate was indeed more beneficial to rat heart muscle in terms of complex I activity. In fact, as presented in Section 5.4.2.2, the median complex I activity for dose group VC was approximately half of that reported for VS. However, the groups were not reported to differ statistically significantly from each other. It can be speculated that this difference may be due to the water vehicle used for succinate. As discussed in Section 4.3.2 of Chapter Four, succinate was diluted in Milli-Q® water, in contrast to rotenone and CoQ_{10}, which were dosed via the use of a sunflower oil vehicle. The previously reported oxidative stress that may be induced by sunflower oil (Mataix *et al.*, 1998) may have accounted for the reduced complex I activity recorded for dose group VC. If the median complex I activity for dose group VC were to be compared to that of VV, it would appear that CoQ_{10} did not benefit the rats at all.

The second contrasting response amongst the vehicle Factor-1 dosed rats was determined from the ATP/ADP data set, where dose group VC presented with a markedly improved ratio of 58.3%, as opposed to the -12.4% of dose group VS. It therefore appears that, in the absence of Complex I deficiency, CoQ_{10} was far more beneficial to heart muscle ATP/ADP ratios when compared to succinate. Although, multiple comparison data, as presented in Section 5.4.5, demonstrated that the dose groups did not differ statistically significantly from each other. It cannot therefore be argued with confidence that CoQ_{10} was indeed more beneficial to rat heart ATP/ADP ratios. As discussed in Section 5.3.7 of the blood profile, it was observed that the therapeutic regimens aided different components of the biochemical status in rats. Therefore, in rats receiving a vehicle Factor-1 dose, data suggests that succinate improved complex I activity, while CoQ_{10} improved ATP/ADP ratios in heart muscle.

Amongst the rotenone-induced complex I deficient rats that received Factor-2 therapeutic regimens, it was again determined that succinate improved complex I activity more so than CoQ_{10}. Rat group RS harboured a final complex I activity that was 95.4% higher than the environmental controls NN, while dose group RC improved to 10.7%. However, both improvements are to be noted since rats receiving no dose or vehicle on days 15 and 16, namely dose groups RN and RV, presented with no improvements in complex I activities. Therefore, both therapeutic regimens benefited rat heart muscle in the recovery from the

induced Complex I deficiency, with succinate improving the recovery to a greater extent. Furthermore, the improvements in complex I activity for dose group RS were determined to be of statistical significance when compared to dose groups RN and RV, as presented in Section 5.4.2.2.

In contrast, upon evaluation of the heart antioxidant capacity data of dose groups RC and RS, it was demonstrated that CoQ_{10} was the superior treatment. The antioxidant capacity for rat group RC was very similar to that of environmental controls NN, in opposition to RS where an antioxidant capacity of -38.2% was calculated. This could be explained by the inherent antioxidant capacity of CoQ_{10} that may have contributed to the maintenance of sub-lethal oxidative stress levels or as a stimulant to the recovery of the Complex I deficiency. The remainder of data sets presented with median percentage variations from NN that were not strikingly different and will therefore not be discussed. It was apparent from the data presented for rat groups RC and RS that CoQ_{10} and succinate were beneficial to the recovery of biochemical status in heart muscle. However, as with dose groups VC and VS, the dose regimens improved different components of the biochemical profile, with CoQ_{10} proving to be more beneficial to the antioxidant capacity and succinate to complex I activity in heart muscle.

5.5 RAT BRAIN DATA

Whole brain was collected from rats and data sets generated accordingly. Brain weights, complex I activities, antioxidant capacity and L/P ratio data are presented and discussed in subsequent sections. Raw data generated from brain tissue during the rat pilot and main studies are presented in Appendix Chapters B, C, and E. Glutathione redox status, NAD/NADH ratios and ATP/ADP ratios are not presented due to unsuccessful generation of data. As discussed in Section 5.3, glutathione concentrations could not be determined due to autoxidation of the sample preparations. The assay for pyridine concentrations required optimisation with high volumes of sample preparations, as discussed also in Section 5.3. For the same reasoning, adenylate values could not be determined. Consequently, limitations in brain tissue mass did not allow for successful optimisation of the two aforementioned assays.

5.5.1 Brain organ weights

Whole brains were carefully removed upon sacrificing the rats and weighed immediately before preparation for the various analyses. Even though, it was expected that biochemical aspects of the brain would be adversely affected by the inhibition of complex I, including apoptosis of neuronal cells, it was not expected that it would be altered to the extent that measurements in weight would vary for each of the dose regimens. This was indeed observed to be the case, as presented in subsequent sections.

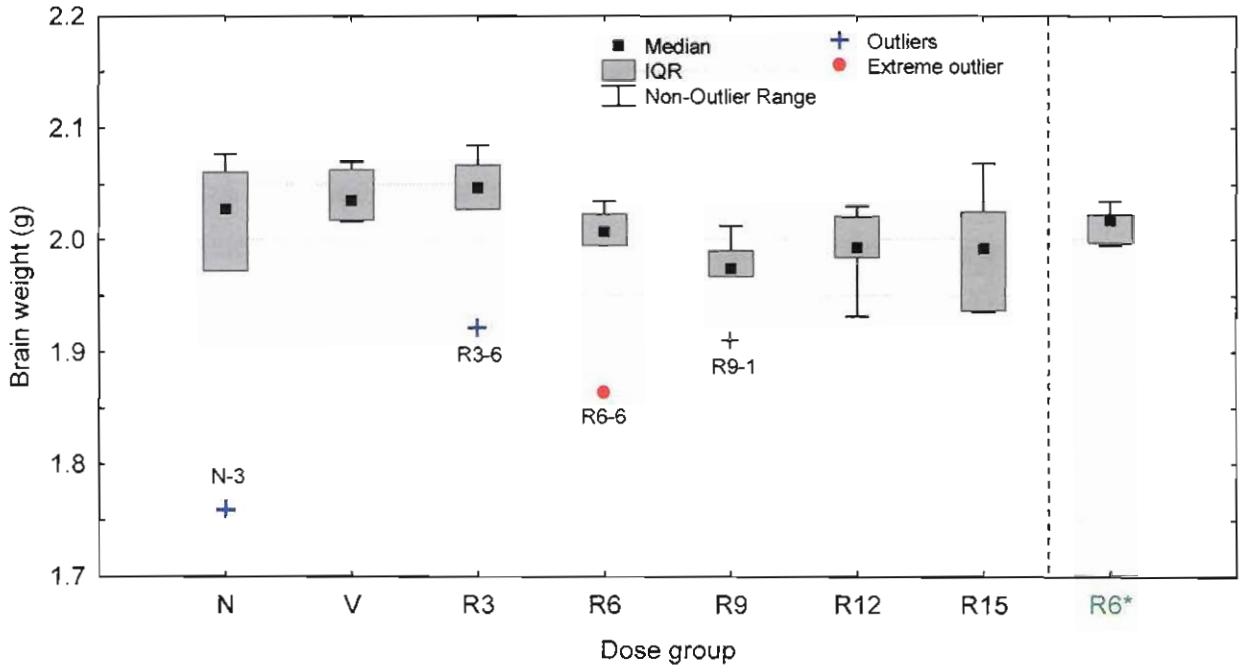
5.5.1.1 Rat pilot study brain weights

Rat brain weight recordings were captured in Excel® spreadsheets and exported to STATISTICA™ for statistical evaluation. The distribution of brain weight data recorded during the pilot study is presented graphically in Table 5.65. The graphic representation is accompanied by a complete list of weight recordings as well as a table of descriptive statistics.

It is apparent from Table 5.65.A that three outliers and one extreme outlier were determined to be present in the brain weight data set. Since only extreme outliers were excluded from data sets, it is not required that the outliers be discussed. However, since outlier N-3 appeared to be positioned far from the IQR for dose group N, it was decided that the impact that N-3 had on the group should be discussed. Rat N-3 presented with a brain weight of 1.76 g that was positioned a mere 0.06 g above the lower outlier boundary at 1.7 g. Therefore, the N-3 data point was extremely close to being regarded as an extreme outlier. Furthermore, by looking at the box-whisker plots in Table 5.65.A, it can certainly be observed that the positioning of N-3 is the lowest brain weight recording in the complete pilot study data set. Nonetheless, as with data points R3-6 and R9-1, N-3 is not positioned in the extreme outlier range and will not be excluded. In contrast, R6-6 was excluded from dose group R6 and the brain weight data set. The exclusion of this data point results in a mean increase from 1.99 to 2.01 g, while the SD decreased from 0.06 to 0.02 g. The median for dose group N increased from 2.01 to 2.02 g and the IQR remained unchanged at 0.03 g. The narrow variable ranges for brain weights are evident from the descriptive statistics.

Table 5.65 Box-whisker representation and descriptive statistics of the rat brain weight data generated from the pilot study

A: Box-whisker plots and data points according to rat groups



Rat	N	V	R3	R6	R9	R12	R15	R6*
1	2.08	2.02	2.07	2.02	+ 1.91	2.03	1.98	2.02
2	2.05	2.02	2.05	2.03	1.97	2.02	2.07	2.03
3	+ 1.76	2.05	2.08	2.02	1.99	1.98	2.00	2.02
4	2.06	2.06	—	2.00	2.01	1.99	1.94	2.00
5	1.97	2.07	2.03	1.99	1.98	1.99	1.94	1.99
6	2.00	2.02	+ 1.92	• 1.86	1.97	1.93	2.02	EXCL

B: Descriptive statistics

Dose group	Sample size	Mean	SD	Median	Min	Max	Range	Lower quartile	Upper quartile	IQR
N	6	1.99	0.12	2.03	1.76	2.08	0.32	1.97	2.06	0.09
V	6	2.04	0.02	2.04	2.02	2.07	0.05	2.02	2.06	0.04
R3	5	2.03	0.06	2.05	1.92	2.08	0.16	2.03	2.07	0.04
R6	6	1.99	0.06	2.01	1.86	2.03	0.17	1.99	2.02	0.03
R6*	5	2.01	0.02	2.02	1.99	2.03	0.04	2.00	2.02	0.03
R9	6	1.97	0.03	1.97	1.91	2.01	0.10	1.97	1.99	0.02
R12	6	1.99	0.03	1.99	1.93	2.03	0.10	1.98	2.02	0.04
R15	6	1.99	0.05	1.99	1.94	2.07	0.13	1.94	2.02	0.09

Rat codes for outliers and extreme outliers are located above or below the respective blue crosses (+) and red dots (•), which correspond to data point values listed in the table directly below the graph. The vertical dashed line in the box-whisker graphic representation separates original dose group box-whiskers from those that have had the extreme outliers excluded, which are also indicated by the asterisk (*) following the dose group code. Data sets with excluded data points are designated in green text. Rats were treated with N = no dose, V = vehicle, R3 = rotenone 3 $mg.kg^{-1}.day^{-1}$, R6 = rotenone 6 $mg.kg^{-1}.day^{-1}$, R9 = rotenone 9 $mg.kg^{-1}.day^{-1}$, R12 = rotenone 12 $mg.kg^{-1}.day^{-1}$, R15 = rotenone 15 $mg.kg^{-1}.day^{-1}$. '—' = missing data point due to death of rat R3-4, EXCL = excluded data point, g = grams, IQR = inter-quartile range, Min = minimum data point value, Max = maximum data point value, SD = standard deviation.

By investigating the box-whisker representations in Table 5.65.A, it is apparent that all rat brain weights were similar. Irrespective of the rotenone dose concentrations received, brain weight data distributions overlapped for all dose groups. This data is therefore suggestive of the fact that no alterations could be determined at the level of brain weights.

The data set was subsequently analysed via ANOVA and multiple comparison test statistics. Since an extreme outlier was present in the pilot study brain weight data, non-parametric and parametric statistical analyses were performed on the original data set as well as on the data set that had had the extreme outlier excluded, respectively. P-values for the ANOVA and multiple comparison data are presented in Table 5.66.

Table 5.66 Multiple comparison statistics of brain weight data generated from the rat pilot study

A: Non-parametric (original data set) and parametric (excluding extreme outliers) p-values							
Dose group	**N**	**V**	**R3**	**R6**	**R9**	**R12**	**R15**
N		1.000	1.000	1.000	1.000	1.000	1.000
		0.726	0.917	0.992	0.999	1.000	1.000
V	1.000		1.000	1.000	0.126	1.000	1.000
	0.726		1.000	0.992	0.433	0.803	0.798
R3	1.000	1.000		1.000	0.320	1.000	1.000
	0.917	1.000		1.000	0.712	0.952	0.950
R6	1.000	1.000	1.000		1.000	1.000	1.000
	0.992	0.992	1.000		0.915	0.997	0.997
R9	1.000	0.126	0.320	1.000		1.000	1.000
	0.999	0.433	0.712	0.915		0.996	0.996
R12	1.000	1.000	1.000	1.000	1.000		1.000
	1.000	0.803	0.952	0.997	0.996		1.000
R15	1.000	1.000	1.000	1.000	1.000	1.000	
	1.000	0.798	0.950	0.997	0.996	1.000	
B: ANOVA p-values							
Kruskal-Wallis p-value = 0.099				One-way ANOVA p-value = 0.441			

A: All comparison statistics are indicated as p-values. The upper p-value is the non-parametric multiple comparison test statistic, generated from the original set of data. The lower p-value was generated via the parametric Tukey *unequal number HSD* (Honestly Significant Difference) test, after the exclusion of extreme outliers. P-values in grey, indicate that no significant differences exist. B: P-values for the non-parametric Kruskal-Wallis ANOVA and parametric one-way ANOVA are listed. Rats were treated with N = no dose, V = vehicle, R3 = rotenone 3 $mg.kg^{-1}.day^{-1}$, R6 = rotenone 6 $mg.kg^{-1}.day^{-1}$, R9 = rotenone 9 $mg.kg^{-1}.day^{-1}$, R12 = rotenone 12 $mg.kg^{-1}.day^{-1}$, R15 = rotenone 15 $mg.kg^{-1}.day^{-1}$. ANOVA = analysis of variance.

The overall grey appearance of the multiple comparison grid reveals that none of the dose groups differed statistically significantly from each other. These p-values are supported by those generated from the Kruskal-Wallis and one-way ANOVA, which too were greater than 0.05, the predetermined level of significance. Therefore, rotenone, even at concentrations of 15 $mg.kg^{-1}.day^{-1}$, did not affect rat brain weight. As mentioned previously in this section, it was not expected that weight changes of the brain would be encountered, as supported by the data generated from the rat pilot study. Consequently, rat brain weights were not required for analysis in the rat main study.

5.5.2 Complex I activity in brain

The enriched mitochondrial preparations were prepared on the same day that rats were sacrificed and whole brain collected. The complex I assays for brain were determined

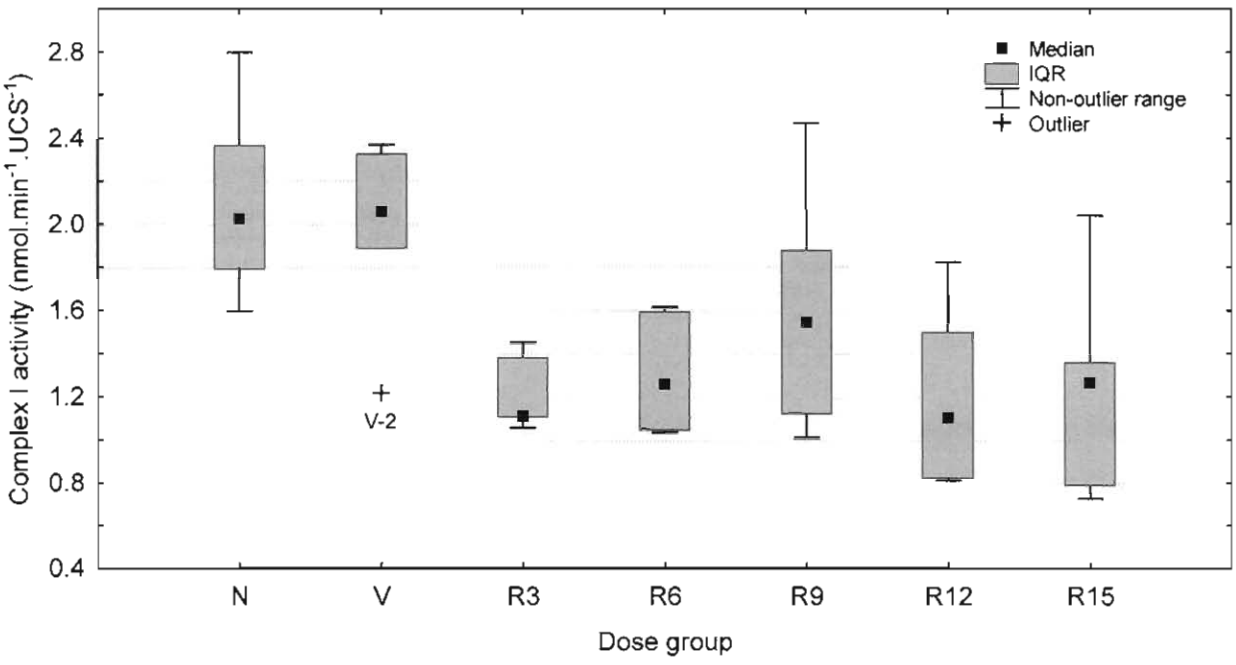
spectrophotometrically and the data evaluated with citrate synthase activities and protein concentrations of the isolated mitochondrial samples. Finally, the complex I data was expressed in terms of UCS and evaluated in STATISTICA™. Rat pilot and main study complex I data generated from whole brain is presented in Sections 5.5.2.1 and 5.5.2.2.

5.5.2.1 Pilot study complex I activity in brain tissue

Brain tissue mitochondria were isolated and the complex I activities determined via the protocol described in Section 4.4.3.4 of Chapter Four. The data was analysed in Excel® format and statistically evaluated in STATISTICA™. Table 5.67 contains graphic presentations, rat data points and descriptive statistics generated from the brain tissue mitochondrial isolates during the pilot study.

Table 5.67 Box-whisker representation and descriptive statistics of the complex I data generated from brain tissue during the rat pilot study

A: Box-whisker plots and data points according to rat groups



Rat	N	V	R3	R6	R9	R12	R15
1	2.80	2.37	1.45	1.33	1.88	1.82	1.24
2	1.60	+ 1.21	1.12	1.59	1.35	1.24	0.79
3	2.12	2.32	1.38	1.20	1.74	0.83	1.36
4	1.80	1.89	—	1.04	1.13	0.97	0.72
5	2.36	2.09	1.11	1.61	2.47	1.50	2.04
6	1.93	2.03	1.06	1.05	1.01	0.81	1.29

B: Descriptive statistics

Dose group	Sample size	Mean	SD	Median	Min	Max	Range	Lower quartile	Upper quartile	IQR
N	6	2.10	0.43	2.03	1.60	2.80	1.20	1.80	2.36	0.57

Table 5.67 Continued...

Dose group	Sample size	Mean	SD	Median	Min	Max	Range	Lower quartile	Upper quartile	IQR
V	6	1.99	0.42	2.06	1.21	2.37	1.15	1.89	2.32	0.43
R3	5	1.22	0.18	1.12	1.06	1.45	0.39	1.11	1.38	0.27
R6	6	1.30	0.26	1.26	1.04	1.61	0.57	1.05	1.59	0.54
R9	6	1.60	0.55	1.55	1.01	2.47	1.46	1.13	1.88	0.75
R12	6	1.20	0.40	1.11	0.81	1.82	1.01	0.83	1.50	0.67
R15	6	1.24	0.47	1.27	0.72	2.04	1.31	0.79	1.36	0.56

Rat codes for outliers are located above or below the respective blue crosses (+), which correspond to data point values listed in the table directly below the graph. Rats were treated with N = no dose, V = vehicle, R3 = rotenone 3 $mg.kg^{-1}.day^{-1}$, R6 = rotenone 6 $mg.kg^{-1}.day^{-1}$, R9 = rotenone 9 $mg.kg^{-1}.day^{-1}$, R12 = rotenone 12 $mg.kg^{-1}.day^{-1}$, R15 = rotenone 15 $mg.kg^{-1}.day^{-1}$. '—' = missing data point due to death of rat R3-4, IQR = inter-quartile range, Min = minimum data point value, Max = maximum data point value, $nmol.min^{-1}.UCS^{-1}$ = nanomole per minute per unit citrate synthase activity, SD = standard deviation.

The box-whisker plots in Table 5.67.A indicate that all the rat groups that received rotenone displayed decreased complex I activities. However, there was no distinctive trend correlating to the dose concentrations, as was observed for rat heart muscle in Section 5.4.2.1. The fact that the mean complex I activity for R15 was 1.24 $nmol.min^{-1}.UCS^{-1}$ and 1.22 $nmol.min^{-1}.UCS^{-1}$ for R3, suggests that complex I inhibition in brain may have reached its effective maximum at 3 $mg.kg^{-1}.day^{-1}$ rotenone concentration level. If this was the case, it is of importance to note that, in rat groups R6 to R15, there may be a time period where excessively high rotenone amounts would be present and transported in the circulatory system of rats. This may explain the subdued and sedated behaviour observed in the rats, previously discussed in Section 5.1.3.

An alternative explanation could be that a threshold is required to be attained before further inhibition of the enzyme will occur. In Section 5.4.2.1, where complex I data for heart muscle were presented, it was observed that this organ required a minimum of 6 $mg.kg^{-1}.day^{-1}$ dose of rotenone before a significant level of complex I inhibition could be attained. In contrast, brain complex I activity in dose groups R3 and R6 were determined to differ statistically significantly from the environmental control dose group N, as presented in Table 5.68. It can be observed from the multiple comparison grid in Section A of the table that dose group N also differed significantly from groups R12 and R15.

Table 5.68 Multiple comparison statistics of brain tissue complex I activity data generated from the rat pilot study

A: Parametric Tukey *unequal number HSD* p-values							
Dose group	**N**	**V**	**R3**	**R6**	**R9**	**R12**	**R15**
N		0.999	0.027	0.028	0.354	0.009	0.014
V	0.999		0.077	0.087	0.652	0.030	0.048
R3	0.027	0.077		1.000	0.779	1.000	1.000
R6	0.028	0.087	1.000		0.875	0.999	1.000
R9	0.354	0.652	0.779	0.875		0.623	0.743
R12	0.009	0.030	1.000	0.999	0.623		1.000
R15	0.014	0.048	1.000	1.000	0.743	1.000	

B: ANOVA p-values
One-way ANOVA p-value < 0.001

C: Statistical and biological significance			
Comparison		**Statistical significance (p)**	**Biological significance (d)**
N	R3	0.027	2.142
N	R6	0.028	1.949
N	R12	0.009	2.214
N	R15	0.014	2.101
V	R12	0.030	1.933
V	R15	0.048	1.819

A: All comparison statistics are indicated as p-values generated via the Tukey *unequal number HSD* (Honestly Significant Difference) multiple comparison procedure. P-values indicated in red are statistically significant at the pre-determined significance level of 0.05. The remainder of p-values are listed in grey. The turquoise shaded blocks represent statistically significant comparisons that were also determined to be of biological significance. B: The p-value for the one-way ANOVA is listed, with significant p-values, less than the 0.05 significance level, indicated in red. C: List of comparisons determined to be statistically significant with corresponding biological significance. A d-value greater than or equal to 0.8 signifies biological significance, indicated in red. Rats were treated N = no dose, V = vehicle, R3 = rotenone 3 $mg.kg^{-1}.day^{-1}$, R6 = rotenone 6 $mg.kg^{-1}.day^{-1}$, R9 = rotenone 9 $mg.kg^{-1}.day^{-1}$, R12 = rotenone 12 $mg.kg^{-1}.day^{-1}$, R15 = rotenone 15 $mg.kg^{-1}.day^{-1}$. < = less than, ANOVA = analysis of variance.

Two important aspects should be mentioned though. The first is that R9 was not demonstrated to differ significantly from N along with all the other groups that received rotenone. By referring to the box-whisker plots and range statistic in Table 5.67 respectively, it is evident that the most amount of variation within a dose group was recorded in R9. This fact is supported by wider standard deviation and IQR values. Although no outliers are detected in this dose group, the increased distribution in data when compared to the other groups certainly contributed to the loss in detection of a statistically significant comparison between N and R9. The second important factor to note is the presence of an outlier in dose group V. The V-2 outlier not only contributes to the variance in V, but also results in a lowering of the mean and median statistics. The exclusion of V-2 would result in an increase in the mean from 1.99 to 2.14 $nmol.min^{-1}.UCS^{-1}$ and a decrease in the range from 1.15 to 0.48 $nmol.min^{-1}.UCS^{-1}$. These alterations in statistics would most certainly result in statistically significant differences between V and all of the rotenone-treated groups. However, since only extreme outliers were excluded, the aforementioned arguments are merely a topic of speculation.

5.5.2.2 Main study complex I activity in brain tissue

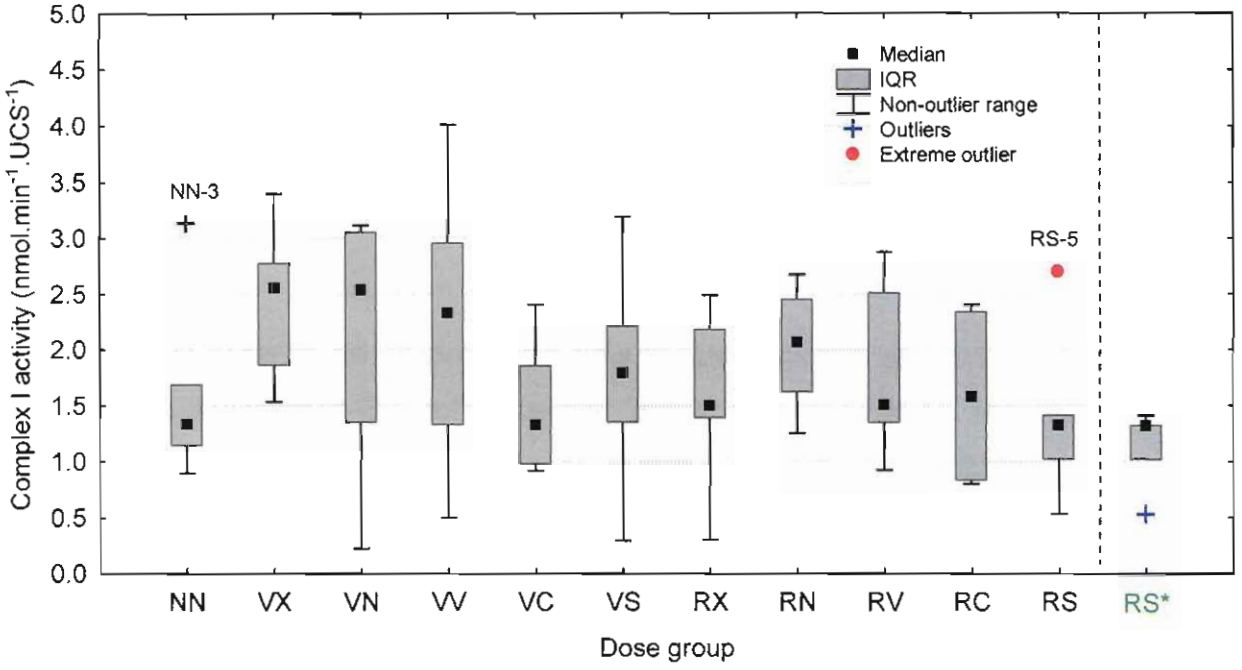
Upon sacrificing of the rats, whole brain was collected and mitochondria prepared appropriately. Protein concentration and citrate synthase activities of the mitochondrial preparations were determined prior to assaying the activities of complex I in the various dose group samples. Box-whisker representations of the data as well as descriptive statistics are indicated in Table 5.69.

Only one outlier and one extreme outlier was observed to be present in the complete complex I data set generated from brain tissue. The RS-5 extreme outlier was at 2.70 $nmol.min^{-1}.UCS^{-1}$, while the other five data points in the group ranged from 0.53 to 1.41 $nmol.min^{-1}.UCS^{-1}$. The IQR for dose group RS, which was 0.39 $nmol.min^{-1}.UCS^{-1}$, was the narrowest of all the dose groups, hence the increased probability of detecting outliers and extreme outliers in the RS set of data. The exclusion of RS-5 resulted in a decrease in the group mean from 1.39 to 1.12 $nmol.min^{-1}.UCS^{-1}$, while the median remained unchanged at 1.33 $nmol.min^{-1}.UCS^{-1}$. The SD halved from 0.72 to 0.36 $nmol.min^{-1}.UCS^{-1}$ and the IQR decreased only slightly from 0.39 to 0.30 $nmol.min^{-1}.UCS^{-1}$.

The adjustments in descriptive statistics due to the exclusion of the extreme outlier once again exemplify the robustness of median and IQR non-parametric statistics versus the parametric counterparts, i.e. the mean and SD. The exclusion of RS-5 from RS resulted in the appearance of an additional outlier, observed below the RS* box-whisker plot presented in Table 5.69.A. This outlier will not be discussed since it only appeared upon the second round of outlier analysis. The NN-3 outlier, which had a complex I activity of 3.13 $nmol.min^{-1}.UCS^{-1}$, was very close to being regarded an extreme outlier since it fell barely within the outlier range. If NN-3 was greater than 3.3 $nmol.min^{-1}.UCS^{-1}$ then it would have fallen beyond the outlier range and within the extreme outlier range. Consequently, NN-3 would be excluded from the data set. However, this was not the case and NN-3 therefore remained a data point within dose group NN.

Table 5.69 Box-whisker representation and descriptive statistics of the complex I data generated from brain tissue during the rat main study

A: Box-whisker plots and data points according to rat groups



Rat	NN	VX	VN	VV	VC	VS	RX	RN	RV	RC	RS	RS*
1	0.90	3.40	3.12	2.96	2.40	0.29	2.49	1.90	1.64	0.84	1.33	1.33
2	1.23	1.53	2.81	1.33	1.09	1.39	1.39	2.68	2.51	0.80	0.53	0.53
3	+ 3.13	1.86	1.35	2.46	1.86	3.19	1.47	1.25	2.88	2.23	1.33	1.33
4	1.68	2.73	0.22	0.50	1.58	1.36	2.18	1.62	1.35	2.40	1.41	1.41
5	1.44	2.77	3.05	4.01	0.99	2.21	0.30	2.45	1.37	2.34	• 2.70	EXCL
6	1.14	2.39	2.27	2.19	0.92	2.19	1.53	2.23	0.92	0.94	1.02	1.02

B: Descriptive statistics

Dose group	Sample size	Mean	SD	Median	Min	Max	Range	Lower quartile	Upper quartile	IQR
NN	6	1.59	0.80	1.34	0.90	3.13	2.23	1.14	1.68	0.54
VX	6	2.45	0.67	2.56	1.53	3.40	1.87	1.86	2.77	0.91
VN	6	2.14	1.14	2.54	0.22	3.12	2.89	1.35	3.05	1.70
VV	6	2.24	1.23	2.33	0.50	4.01	3.51	1.33	2.96	1.62
VC	6	1.47	0.59	1.33	0.92	2.40	1.49	0.99	1.86	0.87
VS	6	1.77	0.99	1.79	0.29	3.19	2.90	1.36	2.21	0.85
RX	6	1.56	0.76	1.50	0.30	2.49	2.19	1.39	2.18	0.78
RN	6	2.02	0.53	2.06	1.25	2.68	1.42	1.62	2.45	0.83
RV	6	1.78	0.75	1.51	0.92	2.88	1.95	1.35	2.51	1.16
RC	6	1.59	0.81	1.58	0.80	2.40	1.60	0.84	2.34	1.50
RS	6	1.39	0.72	1.33	0.53	2.70	2.17	1.02	1.41	0.39
RS*	5	1.12	0.36	1.33	0.53	1.41	0.88	1.02	1.33	0.30

Rat codes for outliers and extreme outliers are located above or below the respective blue crosses (+) and red dots (•), which correspond to data point values listed in the table directly below the graph. The vertical dashed line in the box-whisker graphic representation separates original dose group box-whiskers from those that have had the extreme outliers excluded, which are also indicated by the asterisk (*) following the dose group code. Data sets with excluded data points are designated in green text. Rats were treated with NN = no dose regimen, VX = vehicle and sacrificed, VN = vehicle and no dose, VV = vehicle and vehicle, VC = vehicle and CoQ_{10}, VS = vehicle and succinate, RX = rotenone and sacrificed, RN = rotenone and no dose, RV = rotenone and vehicle, RC = rotenone and CoQ_{10}, RS = rotenone and succinate. EXCL = excluded data point, IQR = inter-quartile range, Min = minimum data point value, Max = maximum data point value, $nmol.min^{-1}.UCS^{-1}$ = nanomole per minute per unit citrate synthase activity, SD = standard deviation.

By viewing the box-whisker plots in Table 5.69.A, it can be observed that no distinctive trend or response to the therapeutic regimens of CoQ_{10} or succinate were present. As with the heart muscle data set for complex I activity, presented in Section 5.4.2.1, a notable recovery in dose groups that received rotenone from days 1 to 14 can be identified. It is of concern that dose group **NN** is in a lower range than all the other dose groups that did not harbour the rotenone-induced Complex I deficiency. This was not the case in the pilot study complex I data for the same tissue, discussed in Section 5.5.2.1.

Brain tissue complex I data generated from the rat main study was further analysed via ANOVA and multiple comparison procedures. Table 5.70 lists the p-values generated via parametric and non-parametric multiple comparison procedures along the complementing ANOVA results.

Table 5.70 Multiple comparison statistics of brain tissue complex I activity data generated from the rat main study

A: Non-parametric (original data set) and parametric (excluding extreme outliers) p-values											
Dose group	**NN**	**VX**	**VN**	**VV**	**VC**	**VS**	**RX**	**RN**	**RV**	**RC**	**RS**
NN		1.000	1.000	1.000	1.000	1.000	1.000	1.000	1.000	1.000	1.000
		0.775	0.985	0.951	1.000	1.000	1.000	0.998	1.000	1.000	0.998
VX	1.000		1.000	1.000	1.000	1.000	1.000	1.000	1.000	1.000	1.000
	0.775		1.000	1.000	0.622	0.939	0.742	0.998	0.944	0.780	0.314
VN	1.000	1.000		1.000	1.000	1.000	1.000	1.000	1.000	1.000	1.000
	0.985	1.000		1.000	0.945	0.999	0.979	1.000	1.000	0.986	0.695
VV	1.000	1.000	1.000		1.000	1.000	1.000	1.000	1.000	1.000	1.000
	0.951	1.000	1.000		0.871	0.996	0.936	1.000	0.996	0.953	0.561
VC	1.000	1.000	1.000	1.000		1.000	1.000	1.000	1.000	1.000	1.000
	1.000	0.622	0.945	0.871		1.000	1.000	0.985	1.000	1.000	1.000
VS	1.000	1.000	1.000	1.000	1.000		1.000	1.000	1.000	1.000	1.000
	1.000	0.939	0.999	0.996	1.000		1.000	1.000	1.000	1.000	0.975
RX	1.000	1.000	1.000	1.000	1.000	1.000		1.000	1.000	1.000	1.000
	1.000	0.742	0.979	0.936	1.000	1.000		0.996	1.000	1.000	0.999
RN	1.000	1.000	1.000	1.000	1.000	1.000	1.000		1.000	1.000	1.000
	0.998	0.998	1.000	1.000	0.985	1.000	0.996		1.000	0.998	0.822
RV	1.000	1.000	1.000	1.000	1.000	1.000	1.000	1.000		1.000	1.000
	1.000	0.944	1.000	0.996	1.000	1.000	1.000	1.000		1.000	0.973
RC	1.000	1.000	1.000	1.000	1.000	1.000	1.000	1.000	1.000		1.000
	1.000	0.780	0.986	0.953	1.000	1.000	1.000	0.998	1.000		0.998
RS	1.000	1.000	1.000	1.000	1.000	1.000	1.000	1.000	1.000	1.000	
	0.998	0.314	0.695	0.561	1.000	0.975	0.999	0.822	0.973	0.998	
B: ANOVA p-values											
Kruskal-Wallis p-value = 0.395						One-way ANOVA p-value = 0.290					

A: All comparison statistics are indicated as p-values. The upper p-value is the non-parametric multiple comparison test statistic, generated from the original set of data. The lower p-value was generated via the parametric Tukey *unequal number HSD* (Honestly Significant Difference) test, after the exclusion of extreme outliers. P-values in grey, indicate that no significant differences exist. B: P-values for the non-parametric Kruskal-Wallis ANOVA and parametric one-way ANOVA are listed. Rats were dosed NN = no dose and no dose, VX = vehicle and sacrificed, VN = vehicle and no dose, VV = vehicle and vehicle, VC = vehicle and CoQ_{10}, VS = vehicle and succinate, RX = rotenone and sacrificed, RN = rotenone and no dose, RV = rotenone and vehicle, RC = rotenone and CoQ_{10}, RS = rotenone and succinate. ANOVA = analysis of variance.

Data presented in Table 5.70 indicate that there were no statistically significant differences between any of the dose groups of the main study when comparing complex I data from brain tissue. These results suggest that complex I from brain tissue was not significantly affected by any of the compounds that were dosed to the rats. It was expected that dose groups VX and RX would at least differ significantly. This was not the case though, which suggests that in the scope of the main study as a whole, the complex I activity of rats that received 15 $mg.kg^{-1}.day^{-1}$ rotenone for 14 days could not be statistically distinguished from those that received vehicle or even no dose at all. As presented in the pilot study data of Section 5.5.2.1, the high rotenone concentration dose groups, R12 and R15, were demonstrated to differ significantly from the control groups VX and N.

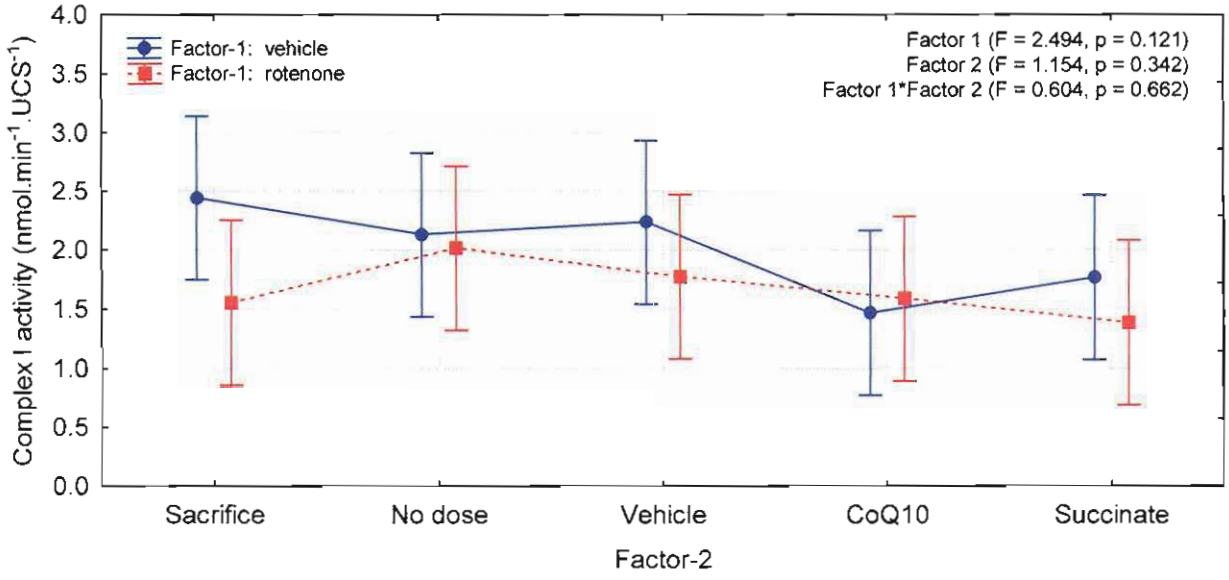
Furthermore, data presented in Section 5.5.2.3 confirmed that the environmental groups N and NN did not differ from each other, nor did the experimental control groups V and VX and finally nor did R15 and RX. Since no statistically significant differences existed between the paralleled groups from the pilot and main studies, it may have been expected that RX would differ significantly from VX in the main study. However, the Tukey *equal number HSD* test is based on evaluating mean differences between groups that are compared, taking global variance among the groups into consideration.

As a general indicator of the overall variance in the pilot and main studies, an average SD and IQR was calculated for both of the sub-studies. The average SD for the pilot study was 0.39 $nmol.min^{-1}.UCS^{-1}$ and 0.82 $nmol.min^{-1}.UCS^{-1}$ for the main study. The average IQR for pilot and main studies were 0.54 and 1.01 $nmol.min^{-1}.UCS^{-1}$ respectively. These general interpretations of global variation between the studies evidently indicate that approximately double the variation was observed in the main study when referring to both the average SD and IQR statistics. The increased distribution of complex I data points in the main study, as opposed to the pilot study, resulted in a decreased sensitivity in the multiple comparison procedures. An alternative view is that the increased variation within the dose groups has lead to an increased stringency in the multiple comparison procedures, making it more difficult to detect a statistically significant difference among all of the comparisons.

The contributions of dose Factor-1 and Factor-2 were analysed via a two-way ANOVA. Since the extreme outlier RS-5 was determined to be present in the data, a two-way ANOVA was performed on both the data set including and excluding RS-5. Results of the factor analysis are presented in Table 5.71.

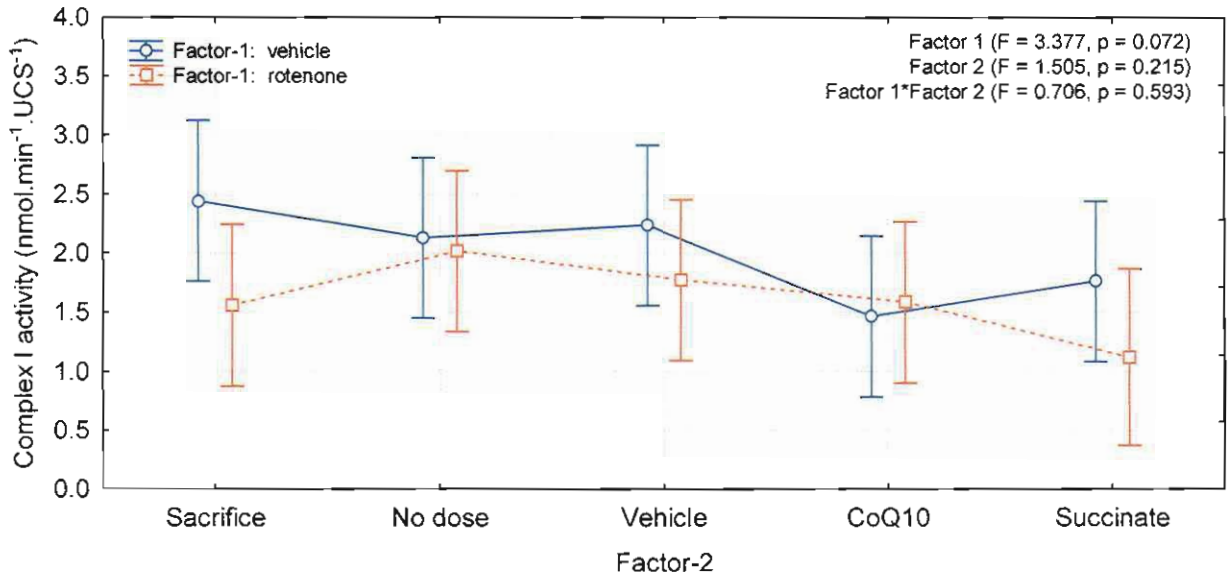
Table 5.71 Graphic and tabulated summary of the brain tissue complex I data analysed via a two-way ANOVA

A: Data set including extreme outliers



Description		VX	VN	VV	VC	VS	RX	RN	RV	RC	RS
With extreme outliers	UCI	3.14	2.83	2.94	2.17	2.47	2.26	2.72	2.47	2.29	2.08
	mean	2.45	2.14	2.24	1.47	1.77	1.56	2.02	1.78	1.59	1.39
	LCI	1.75	1.44	1.55	0.78	1.08	0.86	1.33	1.08	0.90	0.69

B: Data set excluding extreme outliers



Description		VX	VN	VV	VC	VS	RX	RN	RV	RC	RS
Without extreme outliers	UCI	3.13	2.82	2.92	2.15	2.45	2.24	2.70	2.46	2.27	1.87
	mean	2.45	2.14	2.24	1.47	1.77	1.56	2.02	1.78	1.59	1.12
	LCI	1.77	1.45	1.56	0.79	1.09	0.88	1.34	1.10	0.91	0.38

The plot legends for each graph are indicated in the top left corners of the respective graphs, while the two-way ANOVA F-statistics (F) and p-values (p) for Factor-1, Factor-2 and Factor-1*Factor-2 are located in the top right corner. The vertical whiskers at each mean data point represent 95% confidence intervals for the respective data sets. The mean values in green text, located in the data point summary tables below the graphs, indicate those that were adjusted due to the exclusion of extreme outliers. Rats were treated with NN = no dose regimen, VX = vehicle and sacrificed, VN = vehicle and no dose, VV = vehicle and vehicle, VC = vehicle and CoQ_{10}, VS = vehicle and succinate, RX = rotenone and sacrificed, RN = rotenone and no dose, RV = rotenone and vehicle, RC = rotenone and CoQ_{10}, RS = rotenone and succinate. LCI = lower 95% confidence interval data point, $nmol.min^{-1}.UCS^{-1}$ = nanomole per minute per unit citrate synthase activity, UCI = upper 95% confidence interval data point.

The two graphic representations in Table 5.71 are very similar. The exclusion of RS-5 resulted in a 0.27 $nmol.min^{-1}.UCS^{-1}$ decrease in the mean complex I activity for dose group RS. This slight decrease in the mean can be visualised on the graphs by referring to the final succinate data points for the rotenone Factor-1 plots. In addition, the corresponding tables containing the data points for all plots indicate the decrease in the 95% confidence intervals as well as the adjusted mean for RS, indicated in green in Table 5.71.B. The 95% confidence interval lengths decreased only slightly from 1.39 to 1.36 $nmol.min^{-1}.UCS^{-1}$ when the extreme outlier was excluded.

The exclusion of RS-5 resulted in no changes to the F-statistics and p-values for Factor-1 and Factor-2 as well as the interaction, in terms of significance. However, the F-statistics, indicated in the top right hand corner of the respective graphs, do reveal that, with the exclusion of RS-5, an increase in the contributions of Factor-1 and Factor-2. These increases are accompanied by an increase in the F-statistic for the interaction effect. Even though neither of the factors made significant contributions at the 0.05 significance level, it should be noted that the highest contribution came from Factor-1 in both data sets. This indicates to a certain extent that the vehicle or rotenone dose factors contributed most to the response in complex I brain tissue. The contributions from Factor-2 dose regimens are however not irrelevant, since their F-statistics and p-values are similar to those for Factor-1. The F-statistics and p-values for the interaction effects prior to and after the exclusion of the extreme outlier remain the least significant of the results, even though the Factor-1 plots do intersect each other, whether RS-5 is included or excluded from the data.

The graphic summaries of the two-way ANOVA results are suggestive of the fact that neither CoQ_{10} nor succinate improved complex I activities in the brain tissue of rotenone-treated rats. In heart muscle of the same study, the data in Section 5.4.2.2 was suggestive of the fact that the aforementioned therapeutic compounds, in conjunction with rotenone, improved complex I activities. It was hypothesised that a process of mitochondrial replenishment over the final two days was positively stimulated by the supplementation of CoQ_{10} and succinate. This appears not to be the case in brain tissue though, as complex I activities displayed an apparent lack of response to the regimens. This dissimilarity in response to dose compounds observed between heart muscle and brain tissue is not unexpected, since it is a known fact that energy demands and biochemical profiles vary for tissue to tissue. Brain tissue may have required longer dose

periods of Factor-2 before displaying any differences in response. Alternatively, the rate of mitochondrial replenishment may well just be higher in heart muscle than for brain tissue. Both organs require a high-energy demand, but a clear discrepancy in the responsiveness to rotenone as well as other dose factors has been demonstrated here. As discussed in Section 5.5.2.1, complex I data of the pilot study illustrated that a considerable difference in the inhibition percentages between the organs were recorded. Section 5.4.2.2 illustrated that heart muscle complex I activities responded to each of the rotenone dose concentrations in a near linear fashion, whereas Section 5.5.2.1 for whole brain illustrated complex I inhibition, but with no dose concentration and complex I inhibition trend *per se*. The variation in response to dose regimens between the different tissues was often encountered can be confirmed in Section 5.8 where all data sets from both the rat pilot and main studies are presented collectively.

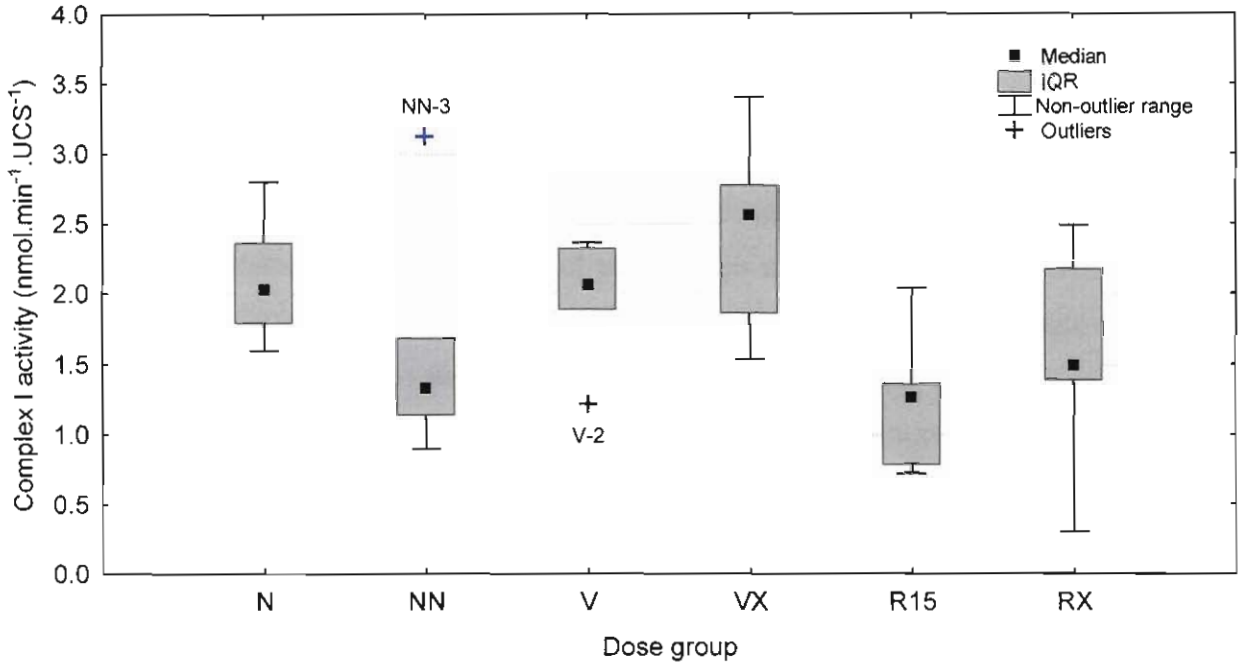
5.5.2.3 Comparative analysis of brain tissue complex I data generated from the rat pilot and main studies

Table 5.72 presents the brain tissue complex I data of paralleled dose groups from the pilot and main study in the form of box-whisker plots and in a table of descriptive statistics. A multiple comparison grid of p-values to test the significance of differences in complex I activities is also included. The descriptive statistics presented in Table 5.72.B were presented previously in Table 5.67 and Table 5.69, and is displayed here for ease of reference.

Outliers indicated in the box-whisker representation are not discussed since they have already been presented in Sections 5.5.2.1 and 5.5.2.2. The box-whisker representations of the data sets reveal that complex I activities between the pilot and main studies were relatively consistent. As mentioned in the previous section, the lowered complex I activities in dose group NN were of concern. Data in Table 5.72.C is however suggestive of the fact that brain complex I activities of dose groups N and NN, of the pilot and main studies respectively, did not differ statistically significantly. In addition, when NN was compared to dose groups V and VX, no significant differences were determined on a statistical level. These statistics not only diminish the concern that complex I activities in dose group NN were aberrant to the main study, but also support the consistency in experimentation between the pilot and main study.

Table 5.72 Summary of comparative dose groups of the rat pilot and main study brain tissue complex I data

A: Box-whisker plots and data points according to rat groups



B: Descriptive statistics (from Table 5.67 and Table 5.69)

Dose group	Sample size	Mean	SD	Median	Min	Max	Range	Lower quartile	Upper quartile	IQR
N	6	2.10	0.43	2.03	1.60	2.80	1.20	1.80	2.36	0.57
NN	6	1.59	0.80	1.34	0.90	3.13	2.23	1.14	1.68	0.54
V	6	1.99	0.42	2.06	1.21	2.37	1.15	1.89	2.32	0.43
VX	6	2.45	0.67	2.56	1.53	3.40	1.87	1.86	2.77	0.91
R15	6	1.24	0.47	1.27	0.72	2.04	1.31	0.79	1.36	0.56
RX	6	1.56	0.76	1.50	0.30	2.49	2.19	1.39	2.18	0.78

C: Tukey *equal number HSD* p-values

Dose group	N	NN	V	VX	R15	RX
N		0.696	0.999	0.920	0.179	0.650
NN	0.696		0.867	0.177	0.922	1.000
V	0.999	0.867		0.779	0.313	0.832
VX	0.920	0.177	0.779		0.021	0.154
R15	0.179	0.922	0.313	0.021		0.943
RX	0.650	1.000	0.832	0.154	0.943	

All comparison statistics are indicated as p-values generated via the Tukey *equal number HSD* (Honestly Significant Difference) multiple comparison procedure. The p-values indicated in red are statistically significant at a significance level of 0.05, while all other p-values are in grey. Rats were treated with N = no dose regimen (pilot study), NN = no dose regimen (main study), V = vehicle (pilot study), VX = vehicle (main study), R15 = rotenone 15 $mg.kg^{-1}.day^{-1}$ (pilot study), RX = rotenone 15 $mg.kg^{-1}.day^{-1}$ (main study). IQR = inter-quartile range, Min = minimum data point value, Max = maximum data point value, $nmol.min^{-1}.UCS^{-1}$ = nanomole per minute per unit citrate synthase activity, SD = standard deviation.

The only statistically significant difference that was determined by the Tukey *equal number HSD* multiple comparison procedure was between R15 of the pilot study and VX. This difference is expected to be significant since the former dose group harboured the rotenone-induced deficiency, whilst the latter did not. However, it would be expected that both R15 and RX would in addition differ significantly from dose groups V, N and NN, as

these groups did not receive any compound that would compromise the activity of complex I. In spite of this, the statistical evaluation of the selected groups from the pilot and main studies, as presented in Table 5.72, was performed solely to evaluate the consistency in results obtained between the two sub-studies. Statistical analysis of dose group comparisons within the pilot and main studies is to be analysed in each of the sub-study sections, independent from each other.

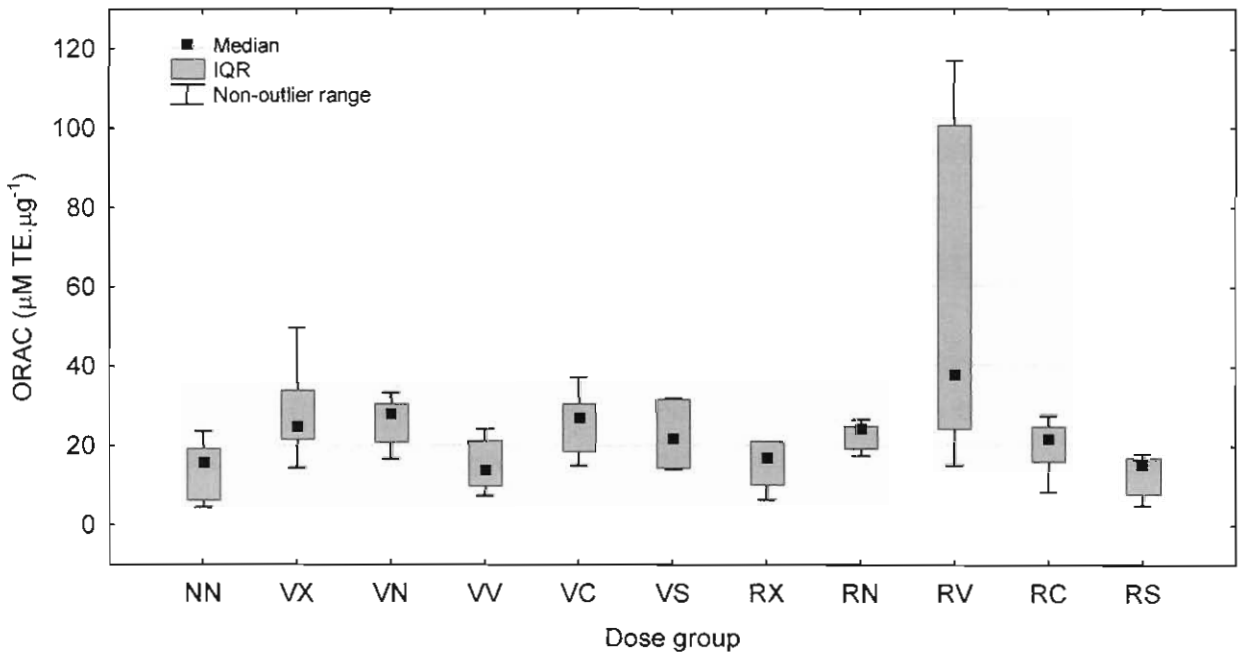
5.5.3 Antioxidant capacity in brain tissue

Whole brain was collected and macerated in total before a sub-section was utilised for homogenisation and appropriate preparation for the ORAC assay. The assay was performed utilising the FL 600 Microplate Fluorescence Reader [Bio-Tek Instruments], after which the data was captured in Excel® format and statistically evaluated utilising the STATISTICA™ programme. The distribution of antioxidant capacity data generated from brain according to rat dose group is presented in Table 5.73 along with a table of descriptive statistics. No outliers or extreme outliers were determined to be present in the data set.

It is evident from the box-whisker presentation that very little variation in antioxidant capacity existed amongst the dose groups, except for the aberrant looking data distribution for dose group RV. The RV data set consists of two extremely high antioxidant capacity data points in excess of 100 μM TE.μg^{-1}. Unfortunately, these are not regarded as outliers based on the outlier analysis protocol selected for this study. As described in Section 4.5.1 of Chapter Four, outliers and extreme outliers were determined based on the distribution of the IQR. As six rats were utilised for each of the rat groups, the IQR consists of the four innermost data points, of rank 2 to 5. Therefore, since the fifth ranked data point in RV, for rat RV-6, was at 100 μM TE.μg^{-1}, the IQR upper boundary extends well above the remaining three data points that make up this IQR. This can be verified by referring to the six listed data points for RV tabulated directly below the box-whisker plots in Table 5.73.A. The fourth ranked data point, for RV-5, is positioned at 50.7 μM TE.μg^{-1}. The antioxidant capacity values for all rats were determined by performing the assays in duplicate. If the duplicate values varied by more than 10% from each other, the assay was repeated for that sample. It can therefore be concluded with certainty that the results are an accurate reflection of the antioxidant capacity of that sample.

Table 5.73 Box-whisker representation and descriptive statistics of the brain tissue antioxidant capacity data generated from the main study

A: Box-whisker plots and data points according to rat groups



Rat	NN	VX	VN	VV	VC	VS	RX	RN	RV	RC	RS
1	12.6	21.5	33.3	9.76	30.4	31.8	21.1	23.6	24.1	27.6	15.4
2	4.47	25.5	30.4	24.3	27.5	19.6	21.1	26.7	15.0	23.9	5.0
3	19.1	33.8	30.1	17.4	37.3	14.3	13.6	17.4	24.7	15.8	16.5
4	6.09	49.7	20.8	21.1	18.4	23.9	19.9	24.8	117	8.39	18.0
5	23.6	24.0	25.7	9.85	14.9	31.6	6.37	24.7	50.7	19.1	15.2
6	18.5	14.3	16.7	7.36	26.3	14.0	10.1	19.2	100	24.7	7.6

B: Descriptive statistics

Dose group	Sample size	Mean	SD	Median	Min	Max	Range	Lower quartile	Upper quartile	IQR
NN	6	14.0	7.66	15.5	4.47	23.6	19.1	6.09	19.1	13.0
VX	6	28.1	12.3	24.7	14.3	49.7	35.4	21.5	33.8	12.3
VN	6	26.2	6.38	27.9	16.7	33.3	16.7	20.8	30.4	9.57
VV	6	15.0	6.95	13.6	7.36	24.3	16.9	9.76	21.1	11.4
VC	6	25.8	8.11	26.9	14.9	37.3	22.4	18.4	30.4	12.0
VS	6	22.5	7.99	21.7	14.0	31.8	17.8	14.3	31.6	17.3
RX	6	15.4	6.30	16.8	6.37	21.1	14.7	10.1	21.1	11.0
RN	6	22.7	3.61	24.2	17.4	26.7	9.22	19.2	24.8	5.64
RV	6	55.3	43.4	37.7	15.0	117	102	24.1	100	76.2
RC	6	19.9	7.03	21.5	8.39	27.6	19.2	15.8	24.7	8.83
RS	6	13.0	5.31	15.3	5.04	18.0	13.0	7.56	16.5	8.98

Rats were treated with NN = no dose regimen, VX = vehicle and sacrificed, VN = vehicle and no dose, VV = vehicle and vehicle, VC = vehicle and CoQ_{10}, VS = vehicle and succinate, RX = rotenone and sacrificed, RN = rotenone and no dose, RV = rotenone and vehicle, RC = rotenone and CoQ_{10}, RS = rotenone and succinate. IQR = inter-quartile range, $\mu M\ TE.\mu g^{-1}$ = micromolar Trolox equivalents per microgram protein, Min = minimum data point value, Max = maximum data point value, SD = standard deviation.

Since each group is made up of the small sample size of six rats only, the procedure adopted for the determination of outliers and extreme outliers can be regarded as limiting. Since four of the six data points in each of the rat group data sets constitute the IQR, the method allows for the determination of only one outlier, or extreme outlier, above or below

the IQR. Therefore if a data set happened to truly harbour two extreme outliers that were both situated above or below the IQR, as may very well be the case with dose group RV, neither or only one may be labelled for exclusion. This is because the second and fifth ranked data points form the upper and lower boundary points of the IQR. Consequently, the first or sixth ranked data points in the complete data set would not appear to be aberrant when compared to the boundary data points of the IQR. In dose group RV, the data points for RV-4 and RV-6 do appear to be extreme when compared to not only the remaining four data points in that group but also to the complete data set encompassing all 11 groups. Moreover, by referring to Table 5.73.B, it is evident that the SD for RV is more than three and half times larger than any of the other groups in the study. Nonetheless, the test for outliers and extreme outliers proved to be effective in previous sections, and will continue to do so in subsequent data sets. The adopted statistical strategy was designed to evaluate the data as accurately as possible and to ensure reliable interpretation of the data. Unfortunately, the model is not the "best fit" for the data set at hand, but a deviation from the statistical strategy was not an option specified in the design. Therefore, the apparently aberrant data points in RV will not be excluded and will remain as part of the data set under discussion. Therefore, the complete data set was further analysed via Tukey *equal number HSD* multiple comparison procedure. The p-values generated from the multiple comparison procedure are listed in Table 5.74, followed by the inclusion of a one-way ANOVA p-value and biologically significant d-values.

As would be expected, dose group RV differed from most of the other groups. The only dose group not to differ significantly from RV is dose group VX, which had mean and median values of 28.1 and 24.7 μM TE.μg^{-1} respectively. The mean and median values for RV were 55.3 and 37.7 μM TE.μg^{-1} respectively. These statistics are expected to be considerably different from each other as the distribution of data in RV is extremely wide. The median would therefore be accepted as the more reliable of the two statistics, as it is far more robust than its parametric counterpart, the mean. Consequently, by comparing the medians of RV and VX, even though dose group RV presented with a wide data distribution, it was evident that the difference between RV and VX was not as marked as it was thought initially.

Table 5.74 Multiple comparison statistics of brain tissue antioxidant capacity data generated from the rat main study

A: Tukey *equal number HSD* p-values

Dose group	NN	VX	VN	VV	VC	VS	RX	RN	RV	RC	RS
NN		0.858	0.940	1.000	0.951	0.996	1.000	0.994	< 0.001	1.000	1.000
VX	0.858		1.000	0.902	1.000	1.000	0.918	1.000	0.082	0.996	0.794
VN	0.940	1.000		0.964	1.000	1.000	0.972	1.000	0.046	1.000	0.900
VV	1.000	0.902	0.964		0.972	0.998	1.000	0.998	0.001	1.000	1.000
VC	0.951	1.000	1.000	0.972		1.000	0.978	1.000	0.041	1.000	0.916
VS	0.996	1.000	1.000	0.998	1.000		0.999	1.000	0.014	1.000	0.989
RX	1.000	0.918	0.972	1.000	0.978	0.999		0.999	0.001	1.000	1.000
RN	0.994	1.000	1.000	0.998	1.000	1.000	0.999		0.015	1.000	0.986
RV	< 0.001	0.082	0.046	0.001	0.041	0.014	0.001	0.015		0.006	< 0.001
RC	1.000	0.996	1.000	1.000	1.000	1.000	1.000	1.000	0.006		0.999
RS	1.000	0.794	0.900	1.000	0.916	0.989	1.000	0.986	< 0.001	0.999	

B: ANOVA p-values

One-way ANOVA p-value < 0.001

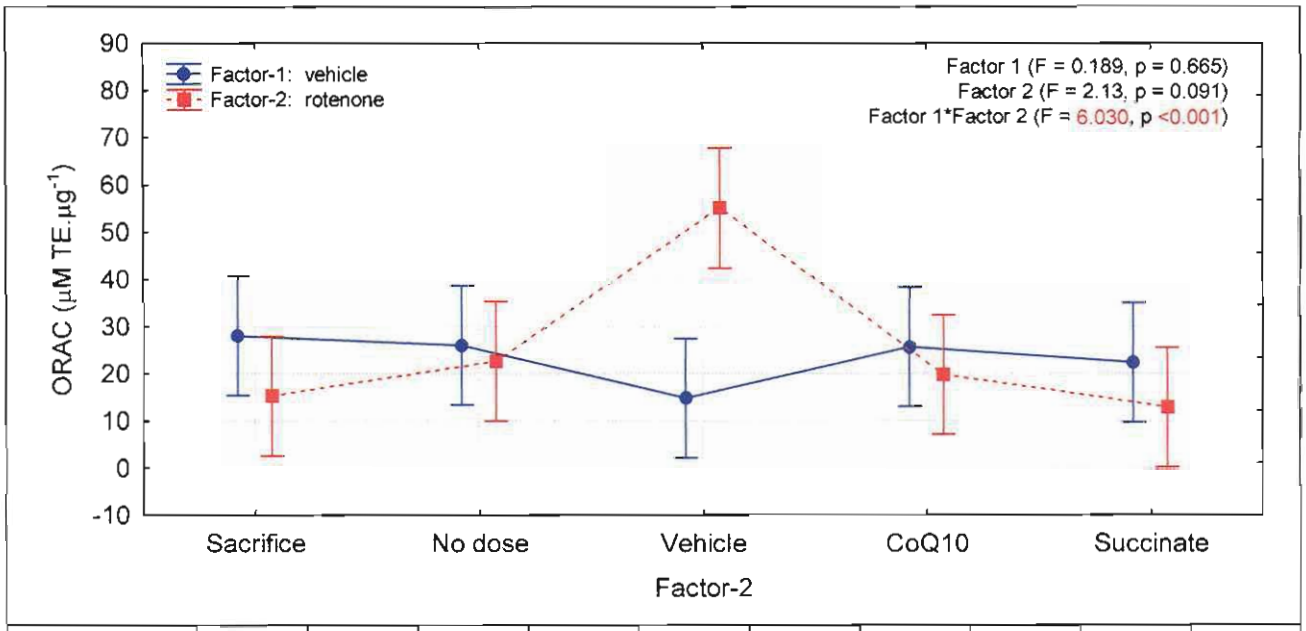
C: Statistical and biological significance

Comparison		Statistical significance (p)	Biological significance (d)
NN	RV	< 0.001	2.771
VN	RV	0.046	1.957
VV	RV	0.001	2.710
VC	RV	0.041	1.981
VS	RV	0.014	2.202
RX	RV	0.001	2.683
RN	RV	0.015	2.187
RC	RV	0.006	2.378
RS	RV	< 0.001	2.845

A: All comparison statistics are indicated as p-values, generated via the Tukey *equal number HSD* (Honestly Significant Difference) multiple comparison procedure. P-values indicated in red are statistically significant at the pre-determined significance level of 0.05. The remainder of p-values are listed in grey. The turquoise shaded blocks represent statistically significant comparisons that were also determined to be of biological significance. B: P-value for the one-way ANOVA is listed, with significant p-values, less than the 0.05 significance level, indicated in red. C: List of comparisons determined to be statistically significant with corresponding biological significance. A d-value greater than or equal to 0.8 signifies biological significance, indicated in red. Rats were treated with NN = no dose regimen, VX = vehicle and sacrificed, VN = vehicle and no dose, VV = vehicle and vehicle, VC = vehicle and CoQ_{10}, VS = vehicle and succinate, RX = rotenone and sacrificed, RN = rotenone and no dose, RV = rotenone and vehicle, RC = rotenone and CoQ_{10}, RS = rotenone and succinate. < = less than, ANOVA = analysis of variance.

As mentioned previously and with the exclusion of dose group RV, there is little fluctuation in antioxidant capacity between all of the brain tissue data sets. It may be suggested that some subtle differences do exist in the shadow of RV and will therefore be mentioned briefly. However, before entering into discussion regarding these slight differences, it is of use to analyse the data further via a factorial ANOVA, as presented in Table 5.75.

Table 5.75 Graphic and tabulated summary of the brain tissue antioxidant capacity data analysed via a two-way ANOVA



Data points	VX	VN	VV	VC	VS	RX	RN	RV	RC	RS
UCI	40.8	38.8	27.6	38.5	35.2	28.0	35.4	68.0	32.6	25.6
mean	28.1	26.2	15.0	25.8	22.5	15.4	22.7	55.3	19.9	13.0
LCI	15.5	13.5	2.31	13.2	9.86	2.71	10.1	42.7	7.26	0.31

The plot legend is indicated in the top left corner of the graph, while the two-way ANOVA F-statistics (F) and p-values (p) for Factor-1, Factor-2 and Factor-1*Factor-2 are located in the top right corner, with the statistically significant values indicated in red. The vertical whiskers at each mean data point represent 95% confidence intervals for the respective data sets. Rats were treated with NN = no dose regimen, VX = vehicle and sacrificed, VN = vehicle and no dose, VV = vehicle and vehicle, VC = vehicle and CoQ_{10}, VS = vehicle and succinate, RX = rotenone and sacrificed, RN = rotenone and no dose, RV = rotenone and vehicle, RC = rotenone and CoQ_{10}, RS = rotenone and succinate. < = less than, LCI = lower 95% confidence interval data point, µM TE.μg^{-1} = micromolar Trolox equivalents per microgram protein, UCI = upper 95% confidence interval data point.

The F-statistics and p-values for the two-way ANOVA indicate that the interaction between Factor-1 and Factor-2 is statistically significant. The graphic representation in Table 5.75 confirms that the graphs intersect and that a difference indeed exists. It should also be noted that the interaction statistics are exaggerated by the extremely high mean antioxidant capacity for dose group RV. If either RV-4 or RV-6 were to be excluded from the data set, the rotenone Factor-1 plot would deviate far less at the vehicle dose Factor-2 mean data point, thereby minimising the displacement between the two plots. In so doing, the interaction F-statistic would diminish along with the consequent decrease in statistical significance. Therefore, the statistical significance of the interaction may be interpreted as an exaggerated effect resulting from the elevated data points in dose group RV.

Nonetheless, with the exclusion of dose group RV, four of the five mean data points for the rotenone Factor-1 plot are lower than the vehicle data points. By referring to the graphic summary of the two-way ANOVA results as well as to data presented in Table 5.75, it becomes apparent that the dose groups that received vehicle Factor-1 regimens, on average, harbour slightly higher antioxidant capacities than NN. In contrast,

the rat groups that harboured the rotenone-induced Complex I deficiency, with the exclusion of RV, had approximately similar antioxidant capacities to NN. Even though the differences may be very subtle, the antioxidant capacity data again suggests that the sunflower oil vehicle improved antioxidant capacity. However, it would be expected that a main effect from Factor-1 would be reported by the two-way ANOVA. Once again, the repercussions of an exaggerated RV data set may well have prevented the effect of Factor-1 to be statistically significant.

Nevertheless, the variation in brain antioxidant capacity data is limited and no statistically significant differences exist between groups, except when comparisons are made with RV. This can be confirmed by referring to Table 5.74. It is apparent that brain tissue was not very sensitive to the dose regimens used in this study. The fluctuations in antioxidant capacity were extremely subtle and global statistical significance was reported by the one-way and two-way ANOVA due to the exaggerated effects of RV on the complete data set.

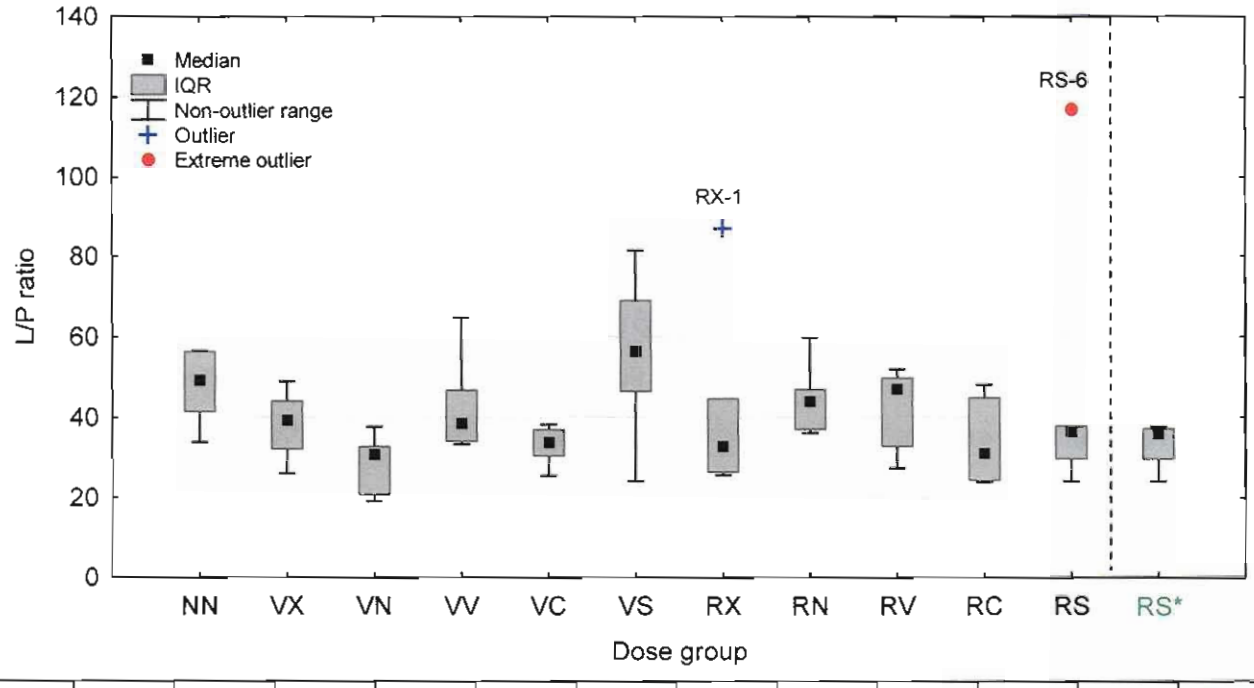
5.5.4 Lactate/pyruvate ratios in brain tissue

Whole brain was removed from the rats and macerated by hand. A sub-section was subsequently prepared according to the appropriate protocols. The concentrations of lactate and pyruvate were determined and the ratio of lactate to pyruvate calculated. The data was subsequently analysed in STATISTICA™ and interpreted accordingly. The distribution of brain L/P ratio data is presented in Table 5.76. The table also contains each of the six data points per dose group and complementing descriptive statistics.

The presence of one outlier and a single extreme outlier can be observed from the box-whisker plots in Table 5.76.A. The RX-1 outlier harboured an L/P ratio of 87.2, which is almost double the ratio obtained for next highest ratio in the group, namely rat RX-2 with a ratio of 44.6. The upper boundary of the outlier range for dose group RX is at a ratio of 99.2. Therefore, being positioned at a ratio of 12.0 below the upper outlier boundary, RX-1 is relatively close to being classified as an extreme outlier.

Table 5.76 Box-whisker representation and descriptive statistics of the brain tissue L/P data generated from the main study

A: Box-whisker plots and data points according to rat groups



Rat	NN	VX	VN	VV	VC	VS	RX	RN	RV	RC	RS	RS*
1	41.5	42.1	19.1	34.1	38.2	46.6	+ 87.2	59.8	52.0	23.8	37.1	37.1
2	33.8	49.0	37.7	33.3	36.9	24.1	44.6	41.3	45.6	48.1	37.7	37.7
3	56.5	44.0	30.5	46.8	25.4	46.7	36.3	46.9	48.4	35.7	24.0	24.0
4	54.0	36.5	20.8	39.3	30.4	66.2	25.6	46.7	49.7	24.3	29.6	29.6
5	44.4	32.2	30.9	37.8	32.9	68.9	29.4	37.1	32.8	26.2	36.0	36.0
6	56.3	26.1	32.6	64.8	34.6	81.5	26.4	36.1	27.4	44.8	• 117	EXCL

B: Descriptive statistics

Dose group	Sample size	Mean	SD	Median	Min	Max	Range	Lower quartile	Upper quartile	IQR
NN	6	47.8	9.30	49.2	33.8	56.5	22.7	41.5	56.3	14.8
VX	6	38.3	8.40	39.3	26.1	49.0	22.9	32.2	44.0	11.9
VN	6	28.6	7.21	30.7	19.1	37.7	18.6	20.8	32.6	11.9
VV	6	42.7	11.9	38.5	33.3	64.8	31.5	34.1	46.8	12.7
VC	6	33.1	4.68	33.7	25.4	38.2	12.8	30.4	36.9	6.50
VS	6	55.7	20.5	56.5	24.1	81.5	57.3	46.6	68.9	22.3
RX	6	41.6	23.5	32.8	25.6	87.2	61.6	26.4	44.6	18.2
RN	6	44.7	8.72	44.0	36.1	59.8	23.7	37.1	46.9	9.85
RV	6	42.6	10.1	47.0	27.4	52.0	24.6	32.8	49.7	16.9
RC	6	33.8	10.8	30.9	23.8	48.1	24.3	24.3	44.8	20.5
RS	6	46.9	34.7	36.5	24.0	117	92.9	29.6	37.7	8.11
RS*	5	32.9	5.91	36.0	24.0	37.7	13.7	29.6	37.1	7.48

Rat codes for outliers and extreme outliers are located above or below the respective blue crosses (+) and red dots (•), which correspond to data point values listed in the table directly below the graph. The vertical dashed line in the box-whisker graphic representation separates original dose group box-whiskers from those that have had the extreme outliers excluded, which are also indicated by the asterisk (*) following the dose group code. Data sets with excluded data points are designated in green text. Rats were treated with NN = no dose regimen, VX = vehicle and sacrificed, VN = vehicle and no dose, VV = vehicle and vehicle, VC = vehicle and CoQ_{10}, VS = vehicle and succinate, RX = rotenone and sacrificed, RN = rotenone and no dose, RV = rotenone and vehicle, RC = rotenone and CoQ_{10}, RS = rotenone and succinate. EXCL = excluded data point, IQR = inter-quartile range, L/P = ratio of lactate to pyruvate, Min = minimum data point value, Max = maximum data point value, SD = standard deviation.

The extreme outlier in dose group RS presented with an L/P ratio of 117, evidently extreme in nature when compared to the remaining rats in the group. By referring to Table E.3 in Appendix E, it can be determined that the pyruvate concentration of 5.002 $\mu mol.L^{-1}$ for rat RS-6 is the likely reason why the ratio is abnormally elevated. The remaining pyruvate concentrations in RS were all greater than 17 $\mu mol.L^{-1}$, with a mean statistic of 18.15 $\mu mol.L^{-1}$. The exclusion of RS-6 from dose group RS results in considerable decreases in mean and SD statistics from ratios of 46.9 to 32.9 and from 34.7 to 5.91, respectively. The non-parametric based median and IQR statistics were more stable, decreasing from a ratio of 36.5 to 36.0 and from 8.11 to 7.48 respectively. It is apparent from the box-whisker plots for RS and RS* that the exclusion of the extreme outlier resulted in very slight differences to the non-parametric statistics.

The box-whisker plots do not depict characteristic differences between the various dose groups. As with the blood L/P data, it may appear that the sunflower oil may have contributed to lowering the L/P ratios in rats. With the exclusion of dose group VS, all dose groups harboured lower or slightly lower L/P ratios. Even dose groups that received a rotenone Factor-1 dose appeared to present with a similar trend. Although the differences are very subtle in most cases, the notion that sunflower oil may be beneficial in reducing L/P ratios in brain tissue should not be disregarded. The distribution of data for dose group VS appears to be wider than for all the other groups which is verified by the IQR statistic to be the highest of all the groups at 22.3. Table E.3 of Appendix E indicates that VS-2 harboured an elevated pyruvate concentration of 25.4 $\mu mol.L^{-1}$, which in turn resulted in a lowered L/P ratio. In addition, the L/P ratio for rat VS-6 was relatively higher than the remaining ratios in the dose group, which is due to an arguably lower pyruvate concentration of 8.0 $\mu mol.L^{-1}$. Therefore, the lengthy box-whisker for VS is due to a general wide distribution of the data points within the VS data set and cannot be confidently accounted for by specific lactate and pyruvate concentration anomalies.

According to the box-whisker plots, all dose groups appear to harbour L/P ratios that range slightly above or below that of 40. Dose group VS and possibly VN may be exclusions to this apparent stability between all dose groups. Nonetheless, the lack of response to dose regimens in brain tissue may only be confirmed after multiple comparison and factorial analyses of the complete data set has been presented. Table 5.77 lists the parametric and non-parametric multiple comparison p-values along with ANOVA results and biological significance of statistically significant comparisons.

Table 5.77 Multiple comparison statistics of brain tissue L/P data generated from the rat main study

A: Non-parametric and parametric p-values

Dose group	NN	VX	VN	VV	VC	VS	RX	RN	RV	RC	RS
NN		1.000	0.235	1.000	1.000	1.000	1.000	1.000	1.000	1.000	1.000
		0.962	0.240	1.000	0.618	0.989	0.998	1.000	1.000	0.686	0.716
VX	1.000		1.000	1.000	1.000	1.000	1.000	1.000	1.000	1.000	1.000
	0.962		0.954	1.000	1.000	0.375	1.000	0.998	1.000	1.000	1.000
VN	0.235	1.000		1.000	1.000	0.145	1.000	0.607	1.000	1.000	1.000
	0.240	0.954		0.675	1.000	0.016	0.771	0.488	0.677	1.000	1.000
VV	1.000	1.000	1.000		1.000	1.000	1.000	1.000	1.000	1.000	1.000
	1.000	1.000	0.675		0.958	0.767	1.000	1.000	1.000	0.976	0.974
VC	1.000	1.000	1.000	1.000		1.000	1.000	1.000	1.000	1.000	1.000
	0.618	1.000	1.000	0.958		0.085	0.982	0.869	0.959	1.000	1.000
VS	1.000	1.000	0.145	1.000	1.000		1.000	1.000	1.000	1.000	1.000
	0.989	0.375	0.016	0.767	0.085		0.671	0.901	0.766	0.108	0.150
RX	1.000	1.000	1.000	1.000	1.000	1.000		1.000	1.000	1.000	1.000
	0.998	1.000	0.771	1.000	0.982	0.671		1.000	1.000	0.991	0.989
RN	1.000	1.000	0.607	1.000	1.000	1.000	1.000		1.000	1.000	1.000
	1.000	0.998	0.488	1.000	0.869	0.901	1.000		1.000	0.910	0.913
RV	1.000	1.000	1.000	1.000	1.000	1.000	1.000	1.000		1.000	1.000
	1.000	1.000	0.677	1.000	0.959	0.766	1.000	1.000		0.976	0.974
RC	1.000	1.000	1.000	1.000	1.000	1.000	1.000	1.000	1.000		1.000
	0.686	1.000	1.000	0.976	1.000	0.108	0.991	0.910	0.976		1.000
RS	1.000	1.000	1.000	1.000	1.000	1.000	1.000	1.000	1.000	1.000	
	0.716	1.000	1.000	0.974	1.000	0.150	0.989	0.913	0.974	1.000	

B: ANOVA p-values

Kruskal-Wallis p-value = 0.042	One-way ANOVA p-value = 0.022

C: Statistical and biological significance

Comparison		Statistical significance (p)		Biological significance (d)	
		Including EOs	Excluding EOs	Including EOs	Excluding EOs
VN	VS	0.145	0.016	N/A	2.179

A: All comparison statistics are indicated as p-values. The upper p-value is the non-parametric multiple comparison test statistic, generated from the original set of data. The lower p-value was generated via the parametric Tukey *unequal number HSD* (Honestly Significant Difference) test, after the exclusion of extreme outliers. P-values indicated in red are statistically significant at the pre-determined significance level of 0.05. P-values in black text represent those that are not statistically significant, but have complementary p-values that are statistically significant. The remainder of p-values are listed in grey. The turquoise shaded blocks represent statistically significant comparisons that were also determined to be of biological significance. B: P-values for the non-parametric Kruskal-Wallis ANOVA and parametric one-way ANOVA are listed, with significant p-values, less than the 0.05 significance level, indicated in red. C: List of comparisons determined to be statistically significant with corresponding biological significance. A d-value greater than or equal to 0.8 signifies biological significance, indicated in red. Rats were treated with NN = no dose regimen, VX = vehicle and sacrificed, VN = vehicle and no dose, VV = vehicle and vehicle, VC = vehicle and CoQ_{10}, VS = vehicle and succinate, RX = rotenone and sacrificed, RN = rotenone and no dose, RV = rotenone and vehicle, RC = rotenone and CoQ_{10}, RS = rotenone and succinate. ANOVA = analysis of variance, EOs = extreme outliers, N/A = not applicable.

The parametric and non-parametric ANOVA results indicate statistically significant differences among the 11 dose groups. However, the non-parametric Kruskal-Wallis test is once again not complemented by statistically significant comparisons, as revealed by the upper p-values in the multiple comparison grid. This situation has been encountered in previous data sets of the study and cannot be conclusively explained. The Kruskal-Wallis ANOVA detects a global difference, but the complementing multiple comparison procedure was not able to pinpoint exactly where the difference exists. The accumulation of slight differences between dose groups appears to have resulted in a

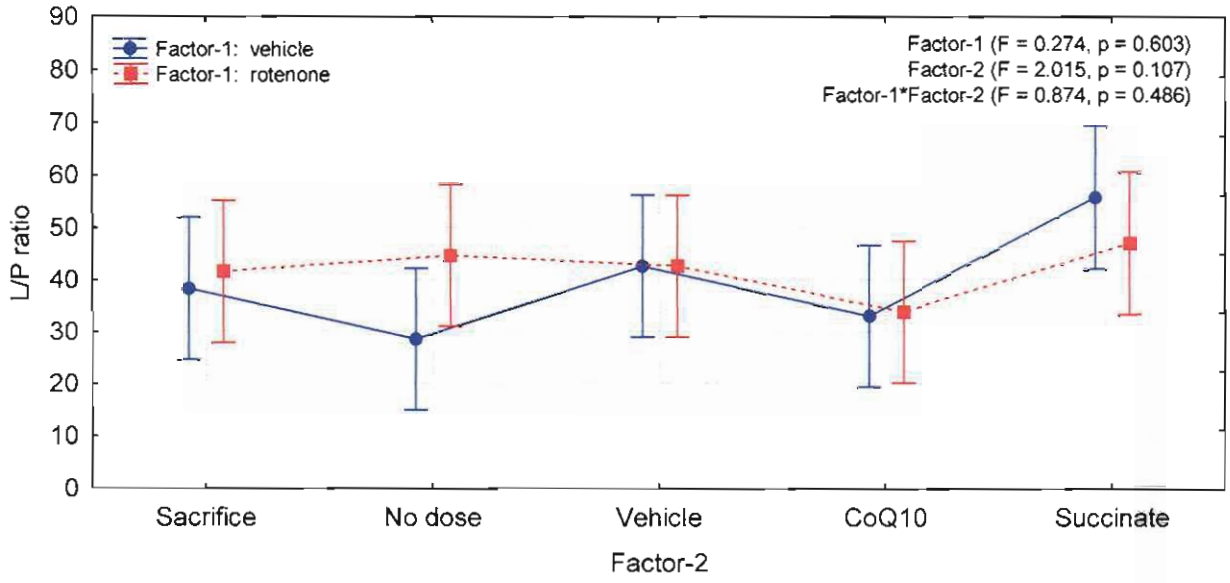
statistically significant p-value. The Kruskal-Wallis ANOVA p-value of 0.042 for this data set is only just significant at the 0.05 significance level. Regardless, the p-value is significant and should be taken into consideration.

The exclusion of the extreme outlier RS-6 from the data set resulted in the Tukey *unequal number HSD* multiple comparison procedure determining a single comparison to be statistically significant. The difference between VN and VS was, in addition, calculated to differ significantly on a biological level with a d-value of 2.179. Dose group VN had a mean L/P ratio of 28.6, while the mean ratio for VS was 55.7. As discussed previously, the variation within dose group VS was greater than for any other group. Since the Tukey multiple comparison procedures are parametric based and therefore take variance within groups into account, it can certainly be argued that the variation within VS played a dominant role in the generation of the statistically significant p-value of 0.016. Nevertheless, the data is suggestive of the fact that a rat dosed with a succinate Factor-2 dose would be affected adversely and present with an increased L/P ratio. If this were to be the case, it would be expected that dose group RS would also have an increased L/P ratio when compared to the other rotenone-treated rat groups. By referring to the box-whisker plots in Table 5.76, it is apparent that this is not the case with RS harbouring very similar L/P ratios to RX, RV and RC. Moreover, dose group RN harboured ratios that were mostly higher than RS. The fact that RS did not harbour raised L/P ratios, even though a Complex I deficiency was induced via the dosage of rotenone, does not support the notion that succinate may adversely affect the rats. A two-way ANOVA was performed on the brain L/P data to investigate the contributions of Factor-1 and Factor-2 doses to rat response. Since the data set contained an extreme outlier, it was required that the factorial analysis be performed with the inclusion and exclusion of RS-6. Graphic summaries of the two-way ANOVA results are depicted in Table 5.78.

The exclusion of the extreme outlier resulted in an increase in the interaction F-statistic from 0.874 to 3.451, which in turn resulted in the p-value decreasing from 0.486 to 0.015, beyond the 0.05 significance level. The exclusion of RS-6 graphically resulted in a further divergence of the vehicle and rotenone Factor-1 plots at the succinate Factor-2 data points. Factor-1 and Factor-2 doses alone were not determined to make statistically significant contributions to the L/P ratios in brain tissue. Finally, the 95% confidence intervals decreased from 27.2 to 20.8 with the exclusion of RS-6.

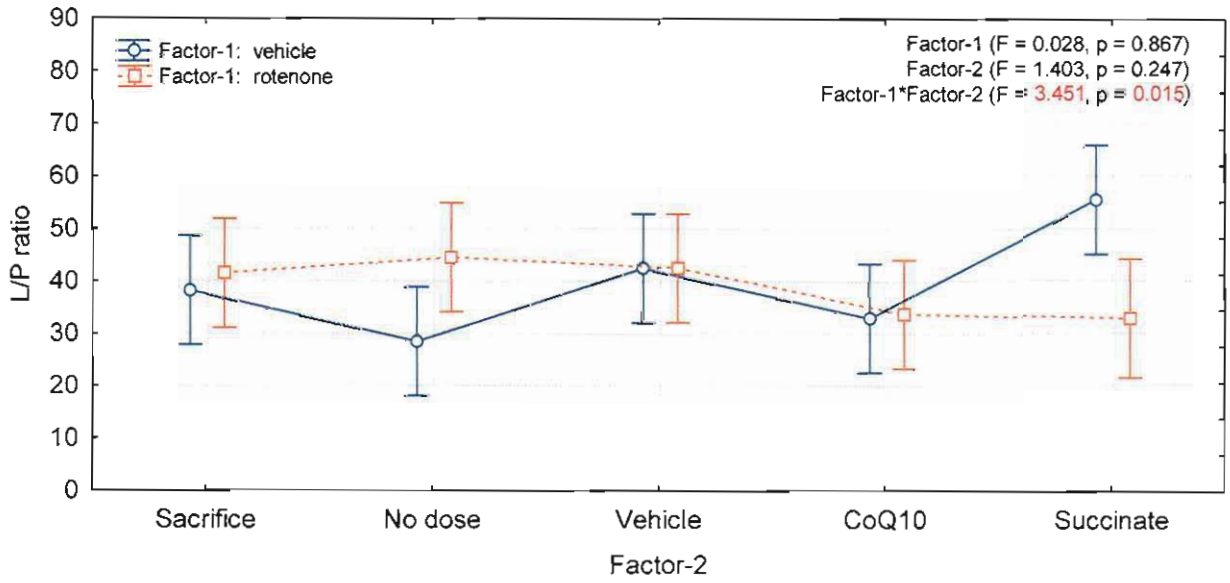
Table 5.78 Graphic and tabulated summary of the brain tissue L/P ratio data analysed via a two-way ANOVA

A: Data set including extreme outliers



Description		VX	VN	VV	VC	VS	RX	RN	RV	RC	RS
With extreme outliers	UCI	51.9	42.2	56.3	46.7	69.3	55.2	58.3	56.3	47.4	60.5
	mean	38.3	28.6	42.7	33.1	55.7	41.6	44.7	42.6	33.8	46.9
	LCI	24.7	15.0	29.1	19.5	42.1	27.9	31.1	29.0	20.2	33.3

B: Data set excluding extreme outliers



Description		VX	VN	VV	VC	VS	RX	RN	RV	RC	RS
Without extreme outliers	UCI	48.7	39.0	53.1	43.5	66.1	52.0	55.1	53.1	44.2	44.3
	mean	38.3	28.6	42.7	33.1	55.7	41.6	44.7	42.6	33.8	32.9
	LCI	27.9	18.2	32.3	22.7	45.2	31.1	34.3	32.2	23.4	21.5

The plot legends for each graph are indicated in the top left corners of the respective graphs, while the two-way ANOVA F-statistics (F) and p-values (p) for Factor-1, Factor-2 and Factor-1*Factor-2 are located in the top right corner, with the statistically significant values indicated in red. The vertical whiskers at each mean data point represent 95% confidence intervals for the respective data sets. The mean values in green text, located in the data point summary tables below the graphs, indicate those that were adjusted due to the exclusion of extreme outliers. Rats were treated with NN = no dose regimen, VX = vehicle and sacrificed, VN = vehicle and no dose, VV = vehicle and vehicle, VC = vehicle and CoQ_{10}, VS = vehicle and succinate, RX = rotenone and sacrificed, RN = rotenone and no dose, RV = rotenone and vehicle, RC = rotenone and CoQ_{10}, RS = rotenone and succinate. ATP/ADP = ratio of adenosine triphosphate to adenosine diphosphate, LCI = lower 95% confidence interval data point, UCI = upper 95% confidence interval data point.

Both of the graphical representations in Table 5.78 are suggestive of rotenone not having an impact on L/P ratios in brain tissue. The rotenone plot may remain slightly above the vehicle plot until the succinate Factor-2 dose is reached, but the differences between the mean data points is minimal. Moreover, the 95% confidence interval whiskers continuously overlap with each other. This argument is supported by Factor-1 not resulting in a statistically significant p-value. It can be recalled from the complex I data for brain tissue, presented in Section 5.5.2.2, that very little variation and inhibition of complex I was attained from the rats of the main study. This correlates well with the L/P ratios presented here, since it would not be expected that raised L/P ratios would accompany relatively unaltered complex I activities.

The statistically significant p-value for the interaction is confirmed by the crossing over of the vehicle and rotenone plots, indicating divergence in response patterns. The significant interaction effect observed when the extreme outlier was excluded can be accounted for primarily by the increased fluctuation in response amongst the dose groups that received a vehicle Factor-1 dose. The rotenone Factor-1 plot in Table 5.78.B illustrates subtle differences in the means, as opposed to the vehicle Factor-1 plot that deviates considerably more. The most noted difference is, as mentioned previously, the elevated L/P ratio for dose group VS, which makes the most distinctive contribution to the overall variation and difference between the vehicle and rotenone plots. It was argued previously that it was unexpected that succinate would contribute to raised L/P ratios. The increased variation within the VS dose group may be considered to be a factor. Dose group VS is comprised of six data points that overlap consistently with L/P ratios in several other dose groups. However, no extreme outliers or even outliers were determined to be present in the group. Since the rotenone plot remained relatively stable throughout and did not fluctuate in response to Factor-2 doses, it may be that succinate was dosed in too low a concentration or for too short a period for it to induce an altered response. The interaction F-statistic and p-value of the two-way ANOVA is indicative of the fact that Factor-1 and Factor-2 doses interacted in some way or another to result in the observed responses in rats. Therefore, it could be argued that the Factor-2 doses had to be dosed in combination with a vehicle Factor-1 dose for altered responses to be observed. Alternatively, the rotenone could be argued to diminish or soften fluctuations in response. Definitive reasoning for the increased L/P ratio observed for VS cannot be determined. Even though it may appear graphically from Table 5.76 that certain rats in VS responded in an aberrant manner, the fact that data points in VS overlap with data distributions of

several other dose groups, in conjunction with the lack of statistically significant differences determined by the multiple comparison procedures, indicates that a definitive difference cannot be concluded.

5.5.5 Brain tissue profile of the rat main study

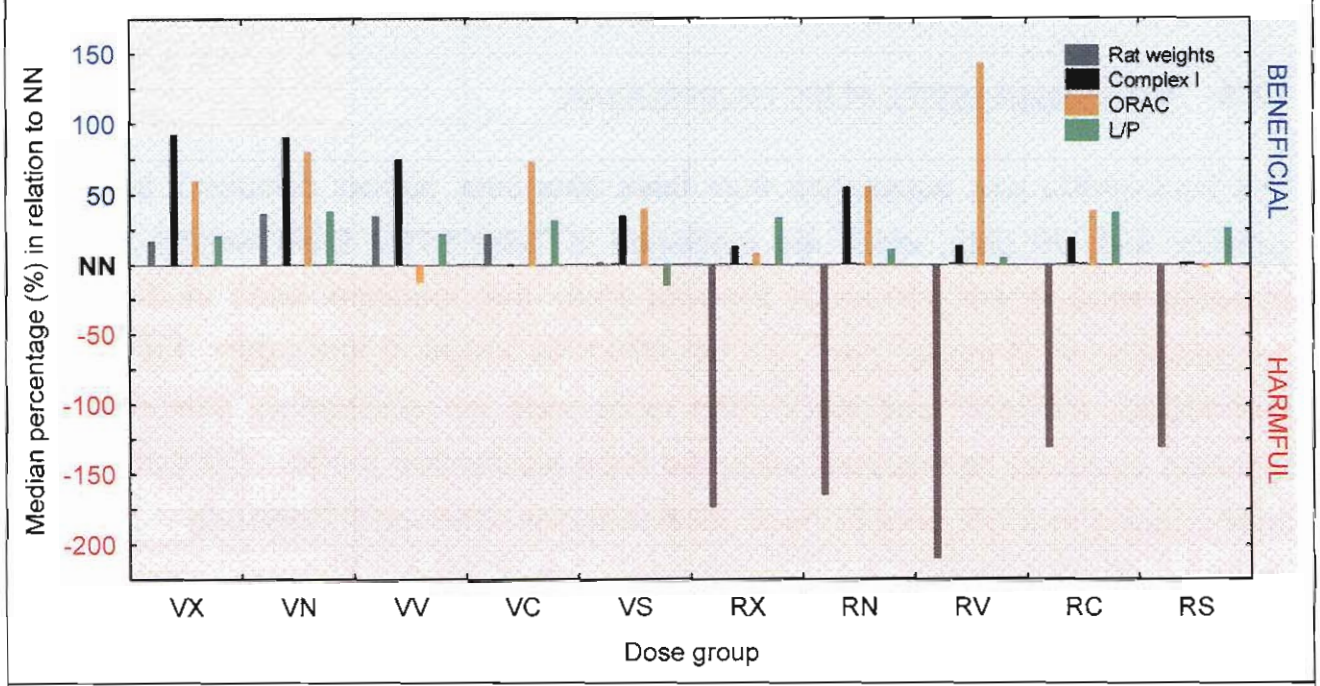
The brain profile was established from three data sets, namely complex I, antioxidant capacity and L/P data, which are presented in Table 5.79. Brain weights were not recorded since it was proven in the pilot study that rotenone, even at the highest concentration of 15 $mg.kg^{-1}.day^{-1}$, did not affect the weight of this organ. Furthermore, GSH/GSSG, ATP/ADP and NAD/NADH ratios were not successfully determined and therefore could not be analysed within the brain biochemical profile. Rat body weights were included as a reference to the physical response observed in these rats.

Before evaluating the biochemical profile in brain, it should be noted that the analyses were performed on brain that was macerated manually, as a whole, prior to tissue preparation. Therefore, the data presented here is a reflection of the biochemical status encompassing the brain as a whole. It is of importance to note this since the majority of publications regarding neurological functioning and the use of rotenone in the induction of Complex I deficiency are focused largely on brain sub-structures, for example the substantia nigra and its role in Parkinson's disorder. However, it has been demonstrated that rotenone does bind complex I uniformly throughout the brain (Betarbet *et al.*, 2000), supporting the proposed strategy to evaluate biochemical parameters in whole brain.

As presented in Section 5.5.2.1, brain complex I activity reported for the environmental control dose group NN was lower than expected. Moreover, the brain complex I activity was also illustrated to be lower than that of N, the environmental control group of the rat pilot study. The difference in activity between the environmental controls of the pilot and main studies were of concern, but were on the other hand not determined to differ from each other by a statistically significant degree. Nevertheless, the decreased complex I activity of NN could not be ignored, nor could this fact not be taken into account when analysing the data of the other dose groups. Consequently, the majority of dose groups presented with median percentages that appeared beneficial over that of NN. Regardless, the median percentages could be investigated in relation to each other, taking into account the under-estimated complex I activity of NN.

Table 5.79 Brain tissue profile of response generated from the rat main study indicating the beneficial and harmful effects of the dose regimens

A: Graphic representation



B: Median percentage (%) grid and factorial ANOVA summary

Data set	Dose group										Factorial ANOVA		
	VX	VN	VV	VC	VS	RX	RN	RV	RC	RS	F1	F2	F1*F2
Rat weights	16.9	36.4	35.1	22.1	1.30	-173	-164	-209	-130	-130	s/s	n/n	s/s
Complex I	91.7	90.2	74.2	-0.20	34.2	12.4	54.6	12.8	18.6	-0.71	n/n	n/n	n/n
AC	59.4	79.8	-12.2	73.3	40.0	8.12	55.7	143	38.4	-1.56	n	n	s
L/P	20.1	37.7	21.7	31.5	-14.7	33.3	10.6	4.54	37.2	25.8	n/n	n/n	n/s

A: Percentage bars denote either beneficial or harmful effects induced by the dose regimens. Each bar is colour coded to represent the various data sets, as indicated by the graphic key in the top right corner of the graph. The 0% line on the Y-axis is labelled **NN**, since all median percentages were calculated to deviate from the environmental controls NN. B: The percentage data points are listed in correspondence with the bar heights. Median percentages that deviate by more than 10% from the environmental controls NN are indicated in blue and red text for beneficial and harmful deviations respectively. Percentages in grey text represent deviations less than 10%. Grid blocks shaded in green represent comparisons from the original set of data that were presented in previous sections to differ statistically and biologically significantly from the environmental controls NN. Comparisons determined to differ significantly after the exclusion of extreme outliers are indicated by yellow shading. Statistically significant (s) and non-significant (n) contributions of Factor-1 (F1) and Factor-2 (F2) dose regimens as well as the interaction (F1*F2) are indicated alongside the median percentage grid. Two symbols are indicated if extreme outliers were determined to be present in the respective data set, with the first symbol representing significance status prior to exclusion, followed by the second symbol representing significance status after exclusion of extreme outliers. Rats were treated with NN = no dose regimen, VX = vehicle and sacrificed, VN = vehicle and no dose, VV = vehicle and vehicle, VC = vehicle and CoQ_{10}, VS = vehicle and succinate, RX = rotenone and sacrificed, RN = rotenone and no dose, RV = rotenone and vehicle, RC = rotenone and CoQ_{10}, RS = rotenone and succinate. AC = antioxidant capacity, L/P = ratio of lactate to pyruvate.

Amongst the rat groups that received a vehicle Factor-1 dose, it was apparent that dose groups VC and VS harboured the lowest complex I activities. These were unexpected results considering that therapeutic regimens CoQ_{10} and succinate were received as Factor-2 doses. Furthermore, the same scenario was observed amongst the rats that harboured the rotenone-induced Complex I deficiency. Dose groups RC and RS presented with brain complex I activities that were analogous to RX and RV, and hence did not appear to benefit from CoQ_{10} and succinate. The only rat group that may be argued to have recovered was that of RN, suggesting that no dose Factor-2 regimen was

more beneficial to brain complex I activities than any of the other Factor-2 dose regimens. It can also be observed from the median percentages presented in Table 5.79.B that complex I inhibition was indeed attained via the administration of rotenone, with dose groups RX, RN and RV all harbouring brain complex I activities lower than the vehicle counterparts VX, VN and VV. Unfortunately, this was not supported by the factorial ANOVA, which reported a non-significant Factor-1.

The brain antioxidant capacity median percentages for dose groups not harbouring a Complex I deficiency, except for VV, appeared to be consistently higher than the environmental controls NN. This may be indicative of the fact that the vitamin E content of sunflower oil may have contributed to the improvements in antioxidant capacity determined from rat whole brain. Alternatively, since it is known that sunflower oil may well be involved in increasing oxidative stress, it could also be argued that the increased antioxidant capacity may be the result of induced antioxidant and compensatory mechanisms. Dose group VV presented with a median percentage of -12.2%, while the remainder of the vehicle Factor-1 groups all harboured antioxidant capacities that were improved by 40.0% or more. The lowered brain antioxidant capacity reported for VV does not corroborate the antioxidant capacity data generated from dose groups VX, VN, VC and VS. However, this single lowered median antioxidant capacity for VN should not steer away from the fact that sunflower oil may well have contributed to improving antioxidant capacity in brain. Furthermore, although it was indicated in Table 5.79.B that none of the vehicle Factor-1 dosed groups differed statistically significantly from NN, it could not be ignored that four of the five dose groups presented with markedly improved brain antioxidant capacities. Therefore, it cannot definitively be stated that the final two days of vehicle further resulted in decreased antioxidant capacity in brain. The rotenone-treated rats too presented with improved brain antioxidant capacity on the whole. The only two groups that did not present beneficially were RX and RS. Rat group RX was evidently affected adversely by the rotenone regimen and, since these rats were sacrificed on day 15 directly after 14 daily doses of rotenone, these rats did not have an opportunity to be relieved of, and recover, from the inhibitory effects of rotenone, as was the case for RN, RV, RC and RS. Even though antioxidant effects may have been contributed by rotenone and possibly the vehicle itself, accompanied by the induction of compensatory antioxidant mechanisms, these were in all likelihood largely depleted in dose group RX, resulting in an antioxidant capacity lower than three of the four rotenone-treated rat groups. It should however be noted that the antioxidant capacity for RX was still equivalent to that of the environmental control dose group NN. Since dose group RS also

presented with a lowered antioxidant capacity, it can be argued that succinate did not aid in the recovery of brain antioxidant capacity. The only dose group to differ statistically significantly from the environmental controls NN was RV, which harboured a final brain antioxidant capacity that was calculated to have a median percentage that was 143% greater than NN itself. However, this dose group was additionally argued in Section 5.5.3 to consist of two data points that were exceedingly elevated, but could not be excluded as extreme outliers due to the small sample size of six data points per dose group. The brain antioxidant capacity for this dose group was consequently analysed with caution since it was demonstrated in the aforementioned section to differ statistically significantly from nine of the 10 other dose groups included in the study.

The L/P ratios generated from brain tissue appeared not to be affected adversely by any of the dose regimens received. Among the dose groups receiving vehicle as a Factor-1 dose, it was observed that dose group VS presented with an L/P ratio that was lowered to a median percentage of -14.7%. However, it should be noted from Table 5.79.B that the other biochemical parameters for dose group VS also presented with lower median percentages when compared to VX, VN, VV and VC. Moreover, VS was the only dose group that did not gain more than 10% body weight over the environmental controls NN. This group appeared to have been affected more adversely, which has become more evident upon evaluation of the brain biochemical profile. The remainder of the vehicle Factor-1 dosed rats presented with L/P ratios that improved to median percentages that were in excess of 20%. As with the heart muscle L/P data presented in Section 5.5.4, the data presented here for brain illustrated that, even though the rotenone-treated rats received the high dose concentration of 15 $mg.kg^{-1}.day^{-1}$, the L/P ratios were not affected to the extreme median percentages that were initially expected. In fact, all of the rotenone-treated rats, except for RV, harboured final brain L/P ratios that were more than 10% greater than NN. It should also be mentioned again that these rats presented predominantly with a Complex I deficiency in whole brain, especially when compared to all rat groups that received vehicle Factor-1 dose regimens. As discussed in several previous sections, the compensatory mechanisms induced by oxidative stress and complex I inhibition certainly played a considerable role in response profiles and several of the biochemical parameters. Moreover, the possibility that sunflower oil and rotenone contributed to the improvement of various biochemical aspects of the cell cannot be excluded.

By analysing the colour code scheme of median percentages in Table 5.79.B, it can be observed that brain tissue presented mostly with improved percentages. However, as discussed previously in this section, the brain complex I activities may be interpreted as over-estimates due to the fact that the environmental control dose group **NN** presented with an extraordinarily lowered median activity. Therefore, it can be argued that all dose groups that received a rotenone Factor-1 dose, namely RX, RN, RV, RC and RS, may well have presented with complex I activities that were less than zero and, in all likelihood, with negative percentages in red. If this were to be the case, the median percentages for the rotenone-dosed rats would have reflected a far more red-like appearance. The only exception may have been dose group **RN**, which harboured an increased complex I activity of 54.6%. Apart from the complex I data, it can also be concluded that antioxidant capacity and L/P ratios generated from whole brain were not affected as adversely as would be expected by the rotenone-induced Complex I deficiency. The rotenone-treated rats presented with brain antioxidant capacities that were either equivalent to or higher than that generated from the environmental controls **NN**. The same was true for L/P data, indicating that these parameters in brain were not affected adversely by rotenone. This can be confirmed by referring to the factorial ANOVA results as well as the median percentages for rat groups receiving vehicle Factor-1 dose regimens in both the antioxidant capacity and L/P data sets. The two-way ANOVA statistics in both data sets resulted in a non-significant Factor-1. This is indicative of the fact that it is not possible to distinguish the rotenone-treated rats definitively from those that received vehicle as Factor-1 dose.

5.5.5.1 Impact of coenzyme Q10 and succinate on rat brain

In rats receiving vehicle Factor-1 dose regimens, it was once again demonstrated that CoQ_{10} and succinate contributed to different aspects of the biochemical profile. Dose group **VC** presented with a lowered complex I activity when compared to **VX**, **VN**, **VV** and **VS**. Furthermore, although dose group **VS** presented with a brain complex I activity that was higher than that of **VC**, it still presented with a complex I activity that was lower than **VX**, **VN** and **VV**. Therefore, it was apparent that neither of the therapeutic dose regimens improved complex I activities in brain. However, even though brain complex I activities were surprisingly lowered, it was observed that the antioxidant capacity for dose groups **VC** and **VS** were considerably improved to 73.3% and 40.0% respectively. As discussed from Section 4.3.2 of Chapter Four, succinate was transported in a Milli-Q® water vehicle, as opposed to CoQ_{10} that utilised sunflower oil. Therefore, the slightly higher antioxidant

capacity for VC can be argued to result from the added antioxidant capacity contributed by the vitamin E content of the sunflower oil vehicle as well as CoQ_{10} itself, a well known antioxidant. These facts could certainly be argued to have had significant impacts on response patterns, as indicated here for brain antioxidant capacity. However, since the factorial ANOVA reported only a statistically significant interaction effect, it cannot be argued with confidence that CoQ_{10} and succinate were central to the improved antioxidant capacities in brain. It appears more likely that the sunflower oil may have contributed the most, with four of the five vehicle Factor-1 treated rat groups harbouring antioxidant capacities greater than 40.0% when compared to the environmental controls NN. The beneficial effects of CoQ_{10} are supported further by the fact that dose group VC presented with a median L/P ratio that was 31.5% higher than NN, as opposed to VS that harboured an L/P ratio that was lower than NN. However, as with the antioxidant capacity data, a non-significant Factor-2 was reported, not supporting the notion that Factor-2 dose regimens contributed significantly to improving L/P ratios. Regardless, it could be argued from the brain biochemical profile data, presented for rats receiving a vehicle Factor-1 dose, that CoQ_{10} was more beneficial to the rats than succinate.

Among the rats harbouring a Complex I deficiency induced by rotenone, it can also be argued that CoQ_{10} was more beneficial in improving the biochemical profile of rat brain. Complex I activities were similarly lowered and did not present with improvements when either of the therapeutic dose regimens were administered. Antioxidant capacities were improved when CoQ_{10} was dosed as a Factor-2 regimen, whereas no apparent improvement was recorded in rats that received succinate. Dose group RC harboured a final antioxidant capacity that was 38.4% higher than NN, whereas the median percentages for RS were calculated to be equivalent to NN. Brain L/P ratios improved by 37.2% and 25.8% for RC and RS respectively, indicating that both CoQ_{10} and succinate improved brain L/P ratios equivalently. However, as discussed previously in this section, neither a statistically significant Factor-1 nor Factor-2 was reported by the two-way ANOVA, it cannot be concluded confidently that either of the therapeutic regimens were indeed beneficial and improved biochemical status in brain.

5.6 RAT SKELETAL MUSCLE DATA

Skeletal muscle was collected from the anterior aspect of the proximal lower limbs of rats on all occasions when the rats were sacrificed. The muscle was subsequently homogenised and prepared appropriately for all of the assays to be performed. In the rat pilot study, complex I activity data was collected. In the rat main study, data was successfully generated for all the analyses included in the study, except for glutathione redox status. As discussed in Section 5.4, samples that were prepared for glutathione quantification underwent autoxidation and hence did not result in successful data generation. Raw data generated from skeletal muscle during the rat pilot and main studies are presented in Appendix Chapters B, C, E, F and G.

5.6.1 Complex I activity in skeletal muscle

The complex I activity in skeletal muscle was generated in both the rat pilot and main studies. Upon sacrificing the rats and collection of muscle, the mitochondria were isolated and stored at -80°C until the samples were assayed for complex I activity. Complex I data generated in the pilot and main studies are presented in Sections 5.6.1.1 and 5.6.1.2, respectively.

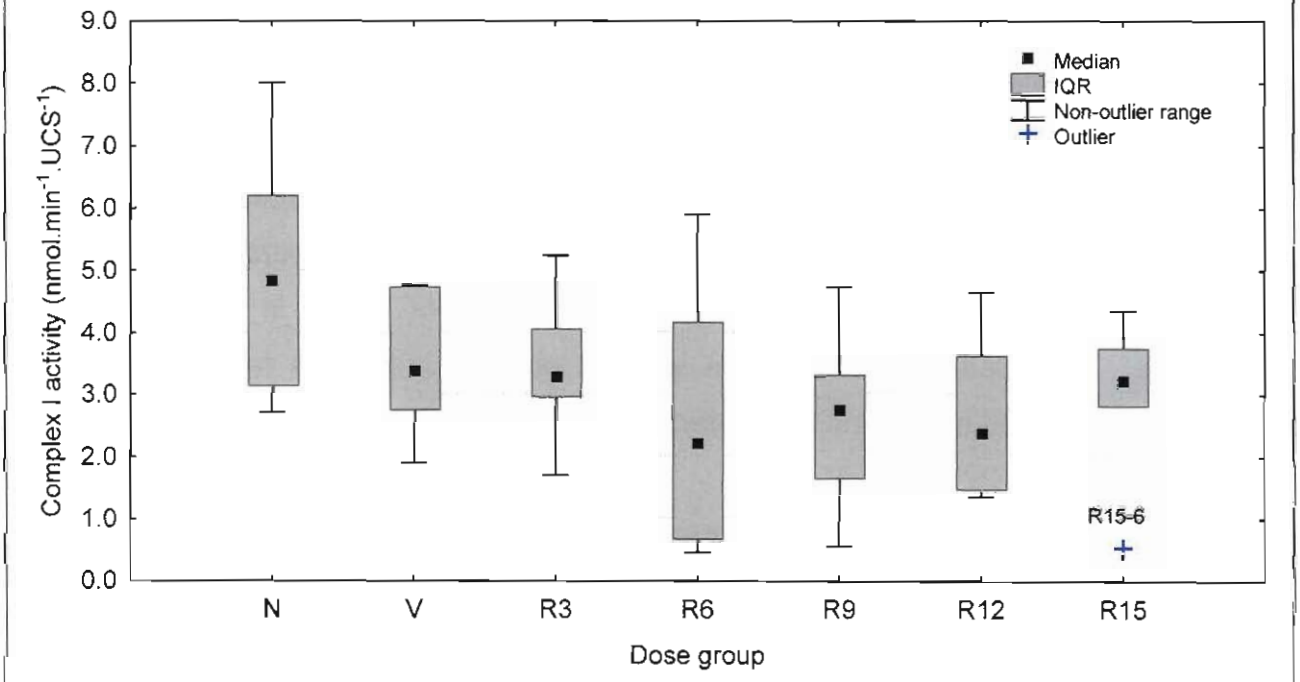
5.6.1.1 Pilot study complex I activity in skeletal muscle

It was of interest to determine the activity of complex I in skeletal muscle since the deficiency is often determined in skeletal muscle of patients. However, results generated from the analyses revealed poor inhibition by rotenone, as indicated in Table 5.80 by the box-whisker representations and table of descriptive statistics.

The data in Table 5.80 indicates that complex I activity generated from skeletal muscle did not vary considerably. In addition, there are very similar distributions of data points in the different groups with the parametric SD statistics ranging from a mere 1.11 to 2.11 $nmol.min^{-1}.UCS^{-1}$. However, it can be argued, by observing the box-whisker representations in Table 5.80.A, that a downward trend in the rat groups that received rotenone was determined.

Table 5.80 Box-whisker representation and descriptive statistics of the complex I data generated from skeletal muscle during the rat pilot study

A: Box-whisker plots and data points according to rat groups



Rat	N	V	R3	R6	R9	R12	R15
1	4.73	4.74	5.24	2.52	4.74	3.59	3.28
2	2.71	1.90	2.94	1.87	0.57	1.91	2.78
3	8.01	4.71	4.03	0.46	3.28	4.65	4.36
4	6.19	3.36	—	4.15	1.63	1.45	3.71
5	4.93	2.74	1.71	0.65	2.72	2.79	3.11
6	3.13	3.35	3.26	5.91	2.72	1.36	+ 0.49

B: Descriptive statistics

Dose group	Sample size	Mean	SD	Median	Min	Max	Range	Lower quartile	Upper quartile	IQR
N	6	4.95	1.96	4.83	2.71	8.01	5.30	3.13	6.19	3.06
V	6	3.47	1.11	3.36	1.90	4.74	2.84	2.74	4.71	1.97
R3	5	3.44	1.31	3.26	1.71	5.24	3.54	2.94	4.03	1.09
R6	6	2.59	2.11	2.19	0.46	5.91	5.45	0.65	4.15	3.50
R9	6	2.61	1.43	2.72	0.57	4.74	4.18	1.63	3.28	1.65
R12	6	2.62	1.31	2.35	1.36	4.65	3.29	1.45	3.59	2.14
R15	6	2.95	1.32	3.19	0.49	4.36	3.86	2.78	3.71	0.93

Rat codes for outliers are located above or below the respective blue crosses (+), which correspond to data point values listed in the table directly below the graph. Rats were treated with N = no dose, V = vehicle, R3 = rotenone 3 $mg.kg^{-1}.day^{-1}$, R6 = rotenone 6 $mg.kg^{-1}.day^{-1}$, R9 = rotenone 9 $mg.kg^{-1}.day^{-1}$, R12 = rotenone 12 $mg.kg^{-1}.day^{-1}$, R15 = rotenone 15 $mg.kg^{-1}.day^{-1}$. '—' = missing data point due to death of rat R3-4, IQR = inter-quartile range, Min = minimum data point value, Max = maximum data point value, $nmol.min^{-1}.UCS^{-1}$ = nanomole per minute per unit citrate synthase activity, SD = standard deviation.

One outlier, that of R15-6, was observed to be present in the complete data set of complex I activity in skeletal muscle. If this outlier were to be excluded from the R15 group, then the mean activity would increase from 2.95 to 3.45 $nmol.min^{-1}.UCS^{-1}$, which is very much the same activity as for the experimental controls V at 3.47 $nmol.min^{-1}.UCS^{-1}$. Therefore, even at the highest concentration of rotenone, inhibition of complex I could not

be attained in skeletal muscle. Table 5.81 presents the multiple comparison data for complex I activity in skeletal muscle.

Table 5.81 Multiple comparison statistics of the skeletal muscle complex I activity data generated from the rat pilot study

A: Parametric Tukey *equal number HSD* p-values							
Dose group	**N**	**V**	**R3**	**R6**	**R9**	**R12**	**R15**
N		0.649	0.718	0.148	0.154	0.159	0.308
V	0.649		1.000	0.956	0.960	0.963	0.997
R3	0.718	1.000		0.976	0.979	0.980	0.999
R6	0.148	0.956	0.976		1.000	1.000	1.000
R9	0.154	0.960	0.979	1.000		1.000	1.000
R12	0.159	0.963	0.980	1.000	1.000		1.000
R15	0.308	0.997	0.999	1.000	1.000	1.000	
B: ANOVA p-values							
One-way ANOVA p-value = 0.133							

A: All comparison statistics are indicated as p-values generated via the Tukey *unequal number HSD* (Honestly Significant Difference) multiple comparison procedure. P-values in grey, indicate that no significant differences exist. B: The p-value for the one-way ANOVA is listed. Rats were treated N = no dose, V = vehicle, R3 = rotenone 3 $mg.kg^{-1}.day^{-1}$, R6 = rotenone 6 $mg.kg^{-1}.day^{-1}$, R9 = rotenone 9 $mg.kg^{-1}.day^{-1}$, R12 = rotenone 12 $mg.kg^{-1}.day^{-1}$, R15 = rotenone 15 $mg.kg^{-1}.day^{-1}$. ANOVA = analysis of variance.

The p-values in Table 5.81 confirm that there are no statistically significant differences between any of the dose groups included in the pilot study, which is also confirmed by the one-way ANOVA p-value of 0.133. This was unexpected, especially since complex I was demonstrated to be inhibited by rotenone to statistically significant levels in all of the other tissues investigated in the study. It may be argued that higher concentrations of rotenone were required when dosing rats in order to obtain significant inhibition of complex I in skeletal muscle. However, as mentioned above, significant inhibition of the enzyme was observed in the other three evaluated tissues. Moreover, the mean activity of complex I in the R15 group for heart muscle was approximately 20% of the control groups N and V. It would be a risk to include higher rotenone concentrations when heart muscle functioning was already considerably compromised. The pilot study was not aimed at correlating toxicity levels with rotenone dose concentrations in Sprague Dawley rats, it was to establish an overall Complex I deficiency profile. Therefore, dosing rats with rotenone concentrations that severely affected the survival of rats would have not been ideal for the overall study and main study that followed. It is possible that the 14-day dose period was not long enough to realise an induction of Complex I deficiency in skeletal muscle. However, as discussed in Section 5.1.3, rat behaviour patterns and resistance to receiving rotenone, especially the higher concentrations, became increasingly difficult to manage. The above-mentioned facts do not support the notion of increasing the rotenone dose concentration to achieve significant inhibition in skeletal muscle. It was apparent that

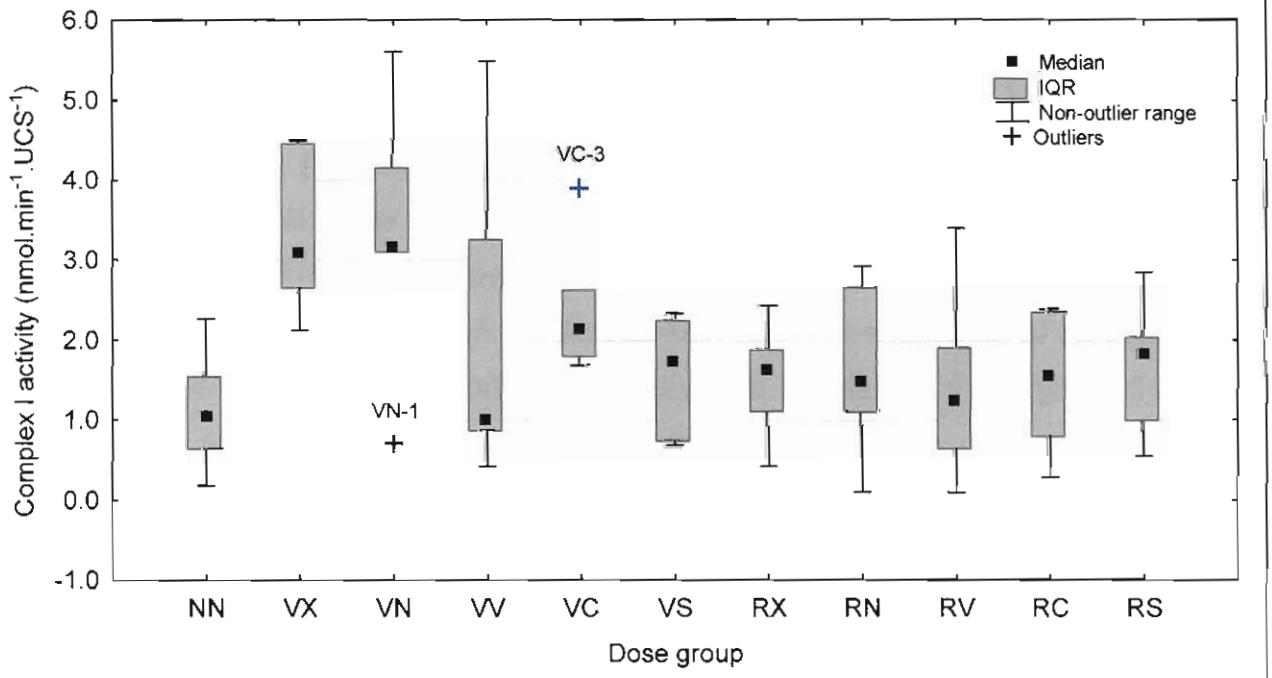
skeletal muscle was not as responsive to the enzyme inhibitor as previously hoped, even though the remaining three tissue types presented with significant inhibition.

5.6.1.2 Main study complex I activity in skeletal muscle

The activities of complex I in skeletal muscle were assayed in conjunction with mitochondrial isolate protein concentrations and citrate synthase activities. The data was captured in Microsoft Excel® and exported to STATISTICA™ for statistical evaluation. The distribution of complex I data along with descriptive statistics for skeletal muscle generated from the rat main study are presented in Table 5.82.

Table 5.82 Box-whisker representation and descriptive statistics of the complex I data generated from skeletal muscle during the rat main study

A: Box-whisker plots and data points according to rat groups



Rat	NN	VX	VN	VV	VC	VS	RX	RN	RV	RC	RS
1	0.64	4.50	0.69	3.26	1.80	0.68	1.88	2.66	3.40	2.40	2.85
2	1.54	2.12	3.16	5.48	1.92	1.76	0.42	1.44	0.65	1.85	1.76
3	0.75	2.65	4.15	0.42	3.91	2.25	1.41	2.92	0.09	0.28	2.04
4	0.18	3.08	3.10	0.87	1.69	0.75	1.11	1.56	1.71	1.29	0.54
5	2.27	4.46	3.16	0.91	2.63	1.72	1.86	1.10	0.79	0.81	1.00
6	1.33	3.10	5.60	1.12	2.37	2.34	2.43	0.10	1.91	2.36	1.91

B: Descriptive statistics

Dose group	Sample size	Mean	SD	Median	Min	Max	Range	Lower quartile	Upper quartile	IQR
NN	6	1.12	0.75	1.04	0.18	2.27	2.09	0.64	1.54	0.90
VX	6	3.32	0.97	3.09	2.12	4.50	2.38	2.65	4.46	1.80
VN	6	3.31	1.61	3.16	0.69	5.60	4.91	3.10	4.15	1.05
VV	6	2.01	1.97	1.01	0.42	5.48	5.06	0.87	3.26	2.38
VC	6	2.39	0.83	2.15	1.69	3.91	2.22	1.80	2.63	0.82

Table 5.82 Continued...

Dose group	Sample size	Mean	SD	Median	Min	Max	Range	Lower quartile	Upper quartile	IQR
VS	6	1.58	0.72	1.74	0.68	2.34	1.66	0.75	2.25	1.51
RX	6	1.52	0.70	1.64	0.42	2.43	2.02	1.11	1.88	0.77
RN	6	1.63	1.04	1.50	0.10	2.92	2.82	1.10	2.66	1.56
RV	6	1.43	1.18	1.25	0.09	3.40	3.30	0.65	1.91	1.26
RC	6	1.50	0.86	1.57	0.28	2.40	2.12	0.81	2.36	1.55
RS	6	1.68	0.81	1.83	0.54	2.85	2.30	1.00	2.04	1.03

Rat codes for outliers are located above or below the respective blue crosses (+), which correspond to data point values listed in the table directly below the graph. Rats were treated with NN = no dose regimen, VX = vehicle and sacrificed, VN = vehicle and no dose, VV = vehicle and vehicle, VC = vehicle and CoQ_{10}, VS = vehicle and succinate, RX = rotenone and sacrificed, RN = rotenone and no dose, RV = rotenone and vehicle, RC = rotenone and CoQ_{10}, RS = rotenone and succinate. IQR = inter-quartile range, Min = minimum data point value, Max = maximum data point value, $nmol.min^{-1}.UCS^{-1}$ = nanomole per minute per unit citrate synthase activity, SD = standard deviation.

Table 5.82.A indicates the presence of two outliers, but no extreme outliers. The first of the outliers, VN-1 has a complex I activity of 0.69 $nmol.min^{-1}.UCS^{-1}$ and is comfortably positioned within the outlier boundary at 0 $nmol.min^{-1}.UCS^{-1}$. The calculated outlier boundary is in fact at -0.05 $nmol.min^{-1}.UCS^{-1}$, but since negative complex I activities would not be considered for inclusion in analyses, the boundary was assigned to be at 0 $nmol.min^{-1}.UCS^{-1}$. A similar scenario is true for outlier VC-3, as its data point is positioned at 3.91 $nmol.min^{-1}.UCS^{-1}$, which is within the outlier boundary of 5.09 $nmol.min^{-1}.UCS^{-1}$. Neither of the two aforementioned outliers was positioned near to the outlier boundaries in their respective data sets. Therefore, whether they were to be excluded or not from the data set, minor adjustments would be made to the descriptive statistics. Nevertheless, since they are not extreme outliers they will not be excluded.

The box-whisker representations of the data in Table 5.82.A are suggestive of an even distribution of complex I activities across all dose groups except for VX and VN. The complex I activities for these two groups are considerably higher than the remaining nine dose groups. It is expected that the other groups not harbouring a Complex I deficiency, namely VV, VC and VS as well as the environmental controls NN would also be in a similar range.

The skeletal muscle complex I data was further analysed via ANOVA and multiple comparison procedures, as presented in Table 5.83. The biological significance of statistically significant comparisons in the main study is also presented. Since no extreme outliers were determined to be present in the complex I skeletal muscle data set, a parametric one-way ANOVA and Tukey *equal number HSD* evaluation was performed on the data.

Table 5.83 Multiple comparison statistics of the skeletal muscle complex I data generated from the rat main study

A: Tukey *equal number HSD* p-values

Dose group	NN	VX	VN	VV	VC	VS	RX	RN	RV	RC	RS
NN		0.041	0.042	0.946	0.664	1.000	1.000	0.999	1.000	1.000	0.998
VX	0.041		1.000	0.620	0.928	0.223	0.182	0.256	0.133	0.168	0.297
VN	0.042	1.000		0.626	0.931	0.227	0.186	0.261	0.136	0.172	0.303
VV	0.946	0.620	0.626		1.000	1.000	0.999	1.000	0.998	0.999	1.000
VC	0.664	0.928	0.931	1.000		0.973	0.954	0.982	0.913	0.945	0.989
VS	1.000	0.223	0.227	1.000	0.973		1.000	1.000	1.000	1.000	1.000
RX	1.000	0.182	0.186	0.999	0.954	1.000		1.000	1.000	1.000	1.000
RN	0.999	0.256	0.261	1.000	0.982	1.000	1.000		1.000	1.000	1.000
RV	1.000	0.133	0.136	0.998	0.913	1.000	1.000	1.000		1.000	1.000
RC	1.000	0.168	0.172	0.999	0.945	1.000	1.000	1.000	1.000		1.000
RS	0.998	0.297	0.303	1.000	0.989	1.000	1.000	1.000	1.000	1.000	

B: ANOVA p-values

One-way ANOVA p-value = 0.009

C: Statistical and biological significance

Comparison		Statistical significance (p)	Biological significance (d)
NN	VX	0.041	1.984
NN	VN	0.042	1.975

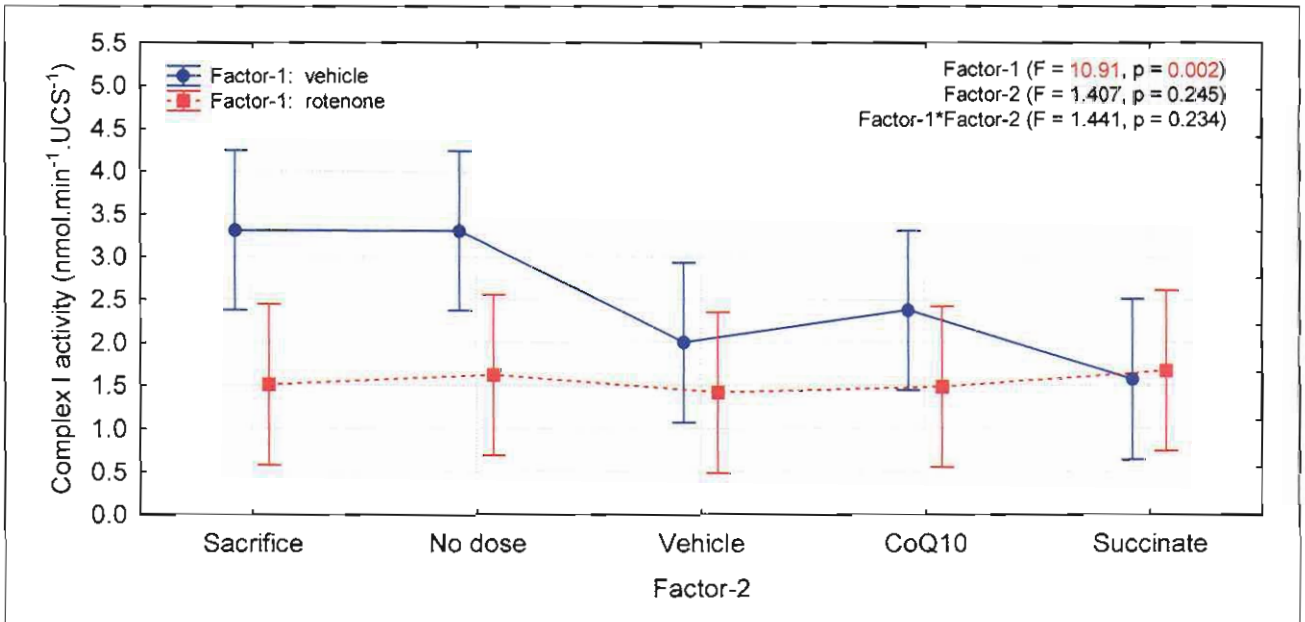
A: All comparison statistics are indicated as p-values generated via the Tukey *equal number HSD* (Honestly Significant Difference) multiple comparison procedure. P-values indicated in red are statistically significant at the pre-determined significance level of 0.05. The remainder of p-values are listed in grey. The turquoise shaded blocks represent statistically significant comparisons that were also determined to be of biological significance. B: P-value for the one-way ANOVA is listed, with significant p-values, less than the 0.05 significance level, indicated in red. C: List of comparisons determined to be statistically significant with corresponding biological significance. A d-value greater than or equal to 0.8 signifies biological significance, indicated in red. Rats were treated with NN = no dose regimen, VX = vehicle and sacrificed, VN = vehicle and no dose, VV = vehicle and vehicle, VC = vehicle and CoQ_{10}, VS = vehicle and succinate, RX = rotenone and sacrificed, RN = rotenone and no dose, RV = rotenone and vehicle, RC = rotenone and CoQ_{10}, RS = rotenone and succinate. ANOVA = analysis of variance.

Table 5.83 indicates significant p-values for the comparisons between NN and VX as well as with VN. These differences were also calculated to differ significantly on a biological level, as presented in Table 5.83.C. Dose group NN did not however differ statistically significantly from the remaining dose groups that received a vehicle Factor-1 regimen, namely VV, VC and VS. This suggests that the NN complex I activity in skeletal muscle was not completely aberrant to the full complement of skeletal muscle complex I data. The previous speculations that NN rats were affected adversely as based on data presented in previous sections should not be relied upon too heavily since it has not been supported statistically.

The multiple comparison grid in Table 5.83.A also illustrates that no statistically significant differences exist between any of the rat groups that received a rotenone Factor-1 regimen. This result is not unexpected as it was determined in the pilot study and Section 5.6.1.1 that skeletal muscle was not a very responsive tissue to the inhibitory effects of rotenone.

Therefore, a lack of significant response to dose regimens encountered in the main study would be expected. Rats in the main study once again displayed poor complex I inhibition to rotenone, confirmed by the box-whisker presentations in Table 5.82.A as well as by the lack of statistical significance demonstrated in Table 5.83. However, by referring to the means and medians in Table 5.82.C, it may be suggested that a mild trend of deficiency was obtained by dosing with rotenone, even though rats received secondary treatments after the first 14 days of rotenone dosing. The same scenario was true for the skeletal muscle response to rotenone. In both studies, a suggested inhibition of complex I was attained, but could not be confirmed to be statistically significant. Possible reasons for the lack of response were speculated in Section 5.6.1.1, but a definitive answer could not be reached. As indicated by the statistical strategy in Section 4.5 of Chapter Four, dose Factor-1 and Factor-2 were evaluated via a two-way ANOVA. A summary of the factorial analysis for skeletal muscle complex I data is presented graphically in Table 5.84. Since no extreme outliers were determined to be present in the data set, a single interpretation of the data was required with the complete set of data points included.

Table 5.84 Graphic and tabulated summary of the skeletal muscle complex I data analysed via a two-way ANOVA



Data points	VX	VN	VV	VC	VS	RX	RN	RV	RC	RS
UCI	4.25	4.25	2.94	3.32	2.52	2.45	2.56	2.36	2.43	2.62
mean	3.32	3.31	2.01	2.39	1.58	1.52	1.63	1.43	1.50	1.68
LCI	2.38	2.38	1.08	1.45	0.65	0.59	0.70	0.49	0.56	0.75

The plot legend is indicated in the top left corner of the graph, while the two-way ANOVA F-statistics (F) and p-values (p) for Factor-1, Factor-2 and Factor-1*Factor-2 are located in the top right corner, with the statistically significant values indicated in red. The vertical whiskers at each mean data point represent 95% confidence intervals for the respective data sets. Rats were treated with NN = no dose regimen, VX = vehicle and sacrificed, VN = vehicle and no dose, VV = vehicle and vehicle, VC = vehicle and CoQ_{10}, VS = vehicle and succinate, RX = rotenone and sacrificed, RN = rotenone and no dose, RV = rotenone and vehicle, RC = rotenone and CoQ_{10}, RS = rotenone and succinate. LCI = lower 95% confidence interval data point, $nmol.min^{-1}.UCS^{-1}$ = nanomole per minute per unit citrate synthase activity, UCI = upper 95% confidence interval data point.

Table 5.84 illustrates that the there is a dominating main effect in the skeletal muscle complex I data set. The F-statistic for Factor-1 is far greater than that for Factor-2 as well as the interaction effect, indicated in the top right corner of the graph. Therefore, it may be hypothesised that the main contribution to the complex I activities comes from the rats either being dosed with vehicle or rotenone over the first 14 days. This fact supports the previously discussed aspect that, although minimal statistically significant comparisons were demonstrated to be present in both the pilot and main studies, inhibition of complex I could indeed be observed in dose groups that received rotenone.

Therefore, the two-way ANOVA statistically supports the notion that differences in skeletal muscle complex I activities between dose groups stems primarily from dose Factor-1, which is either vehicle or rotenone. The data presented here is therefore also indicative of a lack of response to Factor-2 regimens. However, as discussed in 5.6.1.1, skeletal muscle complex I data appears not to be affected adversely by rotenone, even though Complex I deficiency was indeed induced in the remaining three tissues investigated.

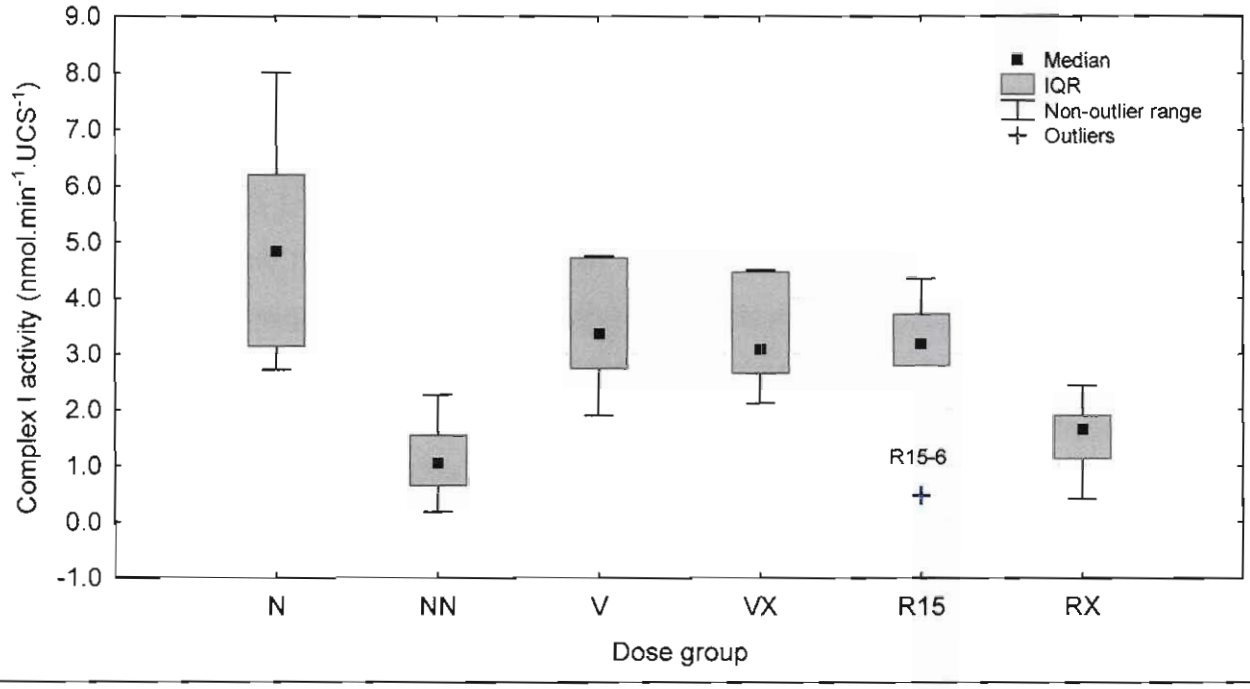
5.6.1.3 Comparative analysis of skeletal muscle complex I data generated from the rat pilot and main studies

Skeletal muscle complex I data from the pilot and main studies was compared where applicable. A summary of the comparisons is presented in Table 5.85, with the descriptive statistics presented in Section B of the table, obtained from Table 5.80 and Table 5.82. The descriptive statistics are listed here for ease of reference. Furthermore, the outlier in dose group R15 was discussed previously and will not be addressed again.

The previously mentioned discrepancies that were observed in the box-whisker plots of Table 5.80.A have again been identified here in Table 5.85.A. A marked difference can be observed between dose groups N of the pilot study and NN of the main study, where the NN distribution of data is well below that of N. This discernable difference is also demonstrated in Table 5.85.C to be statistically significant, not only to N, but also to V and VX. The fact that NN complex I activities differ so much from their pilot study parallel group N cannot be explained with certainty. Rats from both groups were housed individually in their respective cages for similar periods of 14 and 16 days. These rats were not handled in any way for the full period and both groups had free access to food and water.

Table 5.85 Summary of comparative dose groups of the rat pilot and main study skeletal muscle complex I data

A: Box-whisker plots and data points according to rat groups



B: Descriptive statistics (from Table 5.80 and Table 5.82)

Dose group	Sample size	Mean	SD	Median	Min	Max	Range	Lower quartile	Upper quartile	IQR
N	6	4.95	1.96	4.83	2.71	8.01	5.30	3.13	6.19	3.06
NN	6	1.12	0.75	1.04	0.18	2.27	2.09	0.64	1.54	0.90
V	6	3.47	1.11	3.36	1.90	4.74	2.84	2.74	4.71	1.97
VX	6	3.32	0.97	3.09	2.12	4.50	2.38	2.65	4.46	1.80
R15	6	2.95	1.32	3.19	0.49	4.36	3.86	2.78	3.71	0.93
RX	6	1.52	0.70	1.64	0.42	2.43	2.02	1.11	1.88	0.77

C: Tukey *equal number HSD* p-values

Dose group	N	NN	V	VX	R15	RX
N		< 0.001	0.305	0.213	0.076	< 0.001
NN	< 0.001		0.024	0.040	0.124	0.992
V	0.305	0.024		1.000	0.976	0.088
VX	0.213	0.040	1.000		0.995	0.137
R15	0.076	0.124	0.976	0.995		0.341
RX	< 0.001	0.992	0.088	0.137	0.341	

All comparison statistics are indicated as p-values generated via the Tukey *equal number HSD* (Honestly Significant Difference) multiple comparison procedure. The p-values indicated in red are statistically significant at a significance level of 0.05, while all other p-values are in grey. Rats were treated with N = no dose regimen (pilot study), NN = no dose regimen (main study), V = vehicle (pilot study), VX = vehicle (main study), R15 = rotenone 15 mg.kg^{-1}.day^{-1} (pilot study), RX = rotenone 15 mg.kg^{-1}.day^{-1} (main study). < = less than, IQR = inter-quartile range, Min = minimum data point value, Max = maximum data point value, nmol.min^{-1}.UCS^{-1} = nanomole per minute per unit citrate synthase activity, SD = standard deviation.

In Section 5.2.2.3, where rat weight data from days 1 to 15 was compared between the pilot and main study, indicated that no statistically significant difference in weight gain was observed between dose groups N and NN. However, by referring to the mean weight gains it was evident that NN did not gain as much weight as N and most of the dose groups that were treated with vehicle for the first 14 days. NN gained a mean weight of

33.7 g, while N and all the groups that received vehicle from day 1 to 14, except VS, gained a mean weight greater than 43.5 g. In addition, it was observed in Sections 5.4.2.2 and 5.5.2.2 that the complex I activities in heart muscle and brain tissue for dose group NN were consistently low, but were only determined to differ significantly in skeletal muscle, as presented here.

The final statistically significant difference indicated in Table 5.85 is between RX and N. The significance of this comparison is only to be mentioned and not discussed here since the purpose of the statistical analysis is to verify consistency in experimental procedures and data gathering. The aim was to determine if similar complex I activities existed between paralleled dose groups, namely between N and NN, between V and VX, and finally between R15 and RX. As discussed previously, N differed from NN, but the other two comparisons displayed the desired consistency.

5.6.2 Antioxidant capacity in skeletal muscle

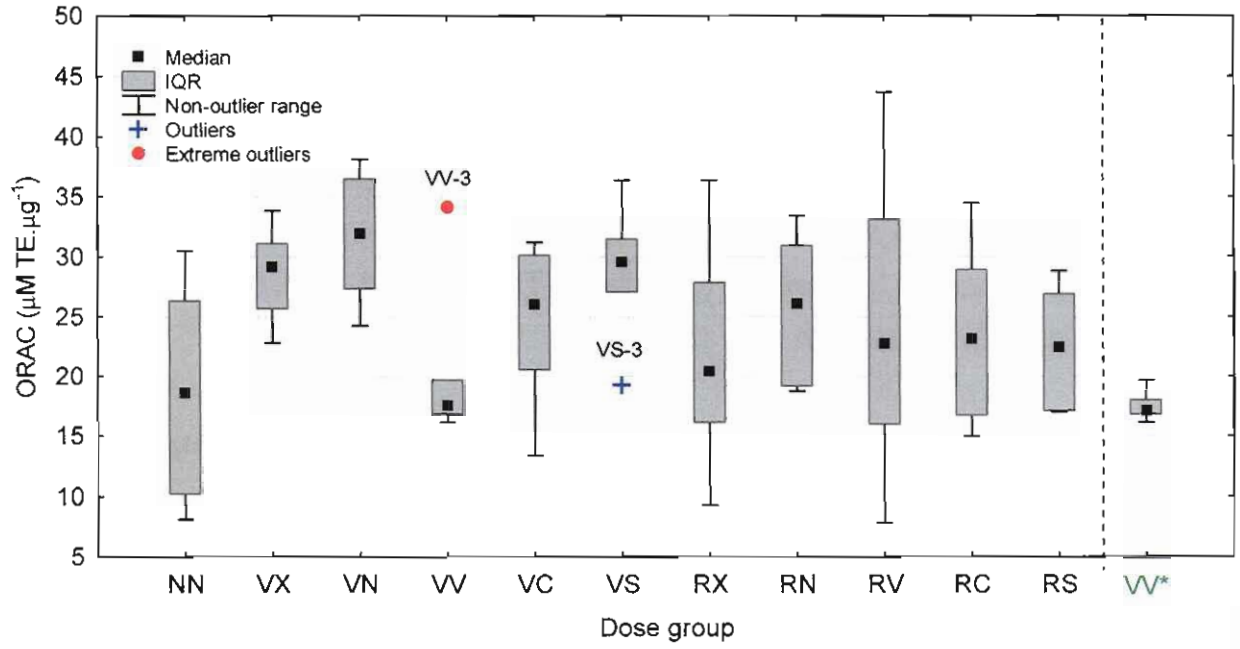
Skeletal muscle was collected and prepared appropriately for the analysis of antioxidant capacity. The generated data was collected in Excel® format followed by statistical evaluations of the distribution of data. Basic statistics of the antioxidant capacity data generated from skeletal muscle are presented in Table 5.86. The box-whisker plots reveal the presence of one extreme outlier in dose group VV and one outlier in VS. Since extreme outliers were excluded from all data sets, the skeletal muscle antioxidant capacity data was therefore analysed via the inclusion and exclusion of VV-3, the extreme outlier.

The exclusion of VV-3 from the VV dose group resulted in a mean decrease from 20.3 to 17.6 μM TE.μg^{-1}. The SD markedly decreased from 6.89 to 1.36 μM TE.μg^{-1}. The non-parametric median remained stable at approximately 17.0 μM TE.μg^{-1}, while the IQR decreased from 2.82 to 1.22 μM TE.μg^{-1}. This profile of descriptive statistic adjustments, due to the exclusion of an extreme outlier typifies a data set that has the remaining data points well clustered within a narrow range, which is certainly the case with VV, as presented by the box-whisker plots in Table 5.86.A. The exclusion of VV-3 resulted in dose group VV having the lowest mean and median antioxidant capacity. However, although the central tendency statistics of VV are of the lowest, the overall data distribution for the group is encompassed within the range of the environmental controls NN. Table 5.86.A illustrates that three of the NN data points are lower than any of the

points in VV. Therefore, it is not accurate to assume that the dose regimen received by VV compromised antioxidant capacities.

Table 5.86 Box-whisker representation and descriptive statistics of the skeletal muscle data generated from the main study

A: Box-whisker plots and data points according to rat groups



Rat	NN	VX	VN	VV	VC	VS	RX	RN	RV	RC	RS	VV*
1	8.13	22.8	38.1	19.7	31.2	36.4	27.9	25.2	16.0	20.2	21.7	19.7
2	13.9	30.7	31.9	16.8	30.1	29.9	36.4	19.2	33.1	26.2	17.1	16.8
3	23.3	31.1	24.3	• 34.2	27.6	+ 19.3	16.2	18.7	27.8	15.0	23.3	EXCL
4	30.5	25.7	36.5	17.1	20.6	27.1	24.2	33.4	43.7	16.8	26.9	17.1
5	10.3	33.9	27.4	16.1	13.4	29.3	16.7	26.9	17.7	34.5	28.8	16.1
6	26.3	27.7	32.0	18.1	24.5	31.5	9.30	31.0	7.86	28.9	17.0	18.1

B: Descriptive statistics

Dose group	Sample size	Mean	SD	Median	Min	Max	Range	Lower quartile	Upper quartile	IQR
NN	6	18.7	9.22	18.6	8.13	30.5	22.4	10.3	26.3	16.1
VX	6	28.6	4.01	29.2	22.8	33.9	11.0	25.7	31.1	5.40
VN	6	31.7	5.26	32.0	24.3	38.1	13.9	27.4	36.5	9.16
VV	6	20.3	6.89	17.6	16.1	34.2	18.1	16.8	19.7	2.82
VV*	5	17.6	1.36	17.1	16.1	19.7	3.5	16.8	18.1	1.22
VC	6	24.6	6.71	26.1	13.4	31.2	17.8	20.6	30.1	9.54
VS	6	28.9	5.64	29.6	19.3	36.4	17.1	27.1	31.5	4.40
RX	6	21.8	9.69	20.5	9.30	36.4	27.1	16.2	27.9	11.7
RN	6	25.8	5.99	26.1	18.7	33.4	14.7	19.2	31.0	11.8
RV	6	24.4	13.0	22.8	7.86	43.7	35.8	16.0	33.1	17.1
RC	6	23.6	7.57	23.2	15.0	34.5	19.5	16.8	28.9	12.2
RS	6	22.5	4.89	22.5	17.0	28.8	11.8	17.1	26.9	9.79

Rat codes for outliers and extreme outliers are located above or below the respective blue crosses (+) and red dots (•), which correspond to data point values listed in the table directly below the graph. The vertical dashed line in the box-whisker graphic representation separates original dose group box-whiskers from those that have had the extreme outliers excluded, which are also indicated by the asterisk (*) following the dose group code. Data sets with excluded data points are designated in green text. Rats were treated with NN = no dose regimen, VX = vehicle and sacrificed, VN = vehicle and no dose, VV = vehicle and vehicle, VC = vehicle and CoQ_{10}, VS = vehicle and succinate, RX = rotenone and sacrificed, RN = rotenone and no dose, RV = rotenone and vehicle, RC = rotenone and CoQ_{10}, RS = rotenone and succinate. EXCL = excluded data point, IQR = inter-quartile range, $\mu M\ TE.\mu g^{-1}$ = micromolar Trolox equivalents per microgram protein, Min = minimum data point value, Max = maximum data point value, SD = standard deviation.

Based on the distribution of data in the vehicle Factor-1 treated groups, it is apparent that CoQ_{10} and succinate did not improve the antioxidant capacity in skeletal muscle. However, the overall trend in antioxidant capacities observed for skeletal muscle suggests that antioxidant capacity was indeed compromised by complex I inhibition, with a mild recovery observed in the groups that were treated for an additional two days. Dose group RX evidently experienced a diminished antioxidant capacity when compared to its vehicle control VX. The remaining rotenone-treated groups harboured antioxidant capacities that recovered to levels lower or slightly lower than VX. The statistical significance of all the dose group comparisons was determined via non-parametric and parametric protocols, due to the presence of the extreme outlier. The ANOVA and multiple comparison p-values are listed in Table 5.87.

Table 5.87 Multiple comparison statistics of the skeletal muscle antioxidant capacity data generated from the rat main study

A: Non-parametric (original data set) and parametric (excluding extreme outliers) p-values											
Dose group	NN	VX	VN	VV	VC	VS	RX	RN	RV	RC	RS
NN		1.000	0.297	1.000	1.000	1.000	1.000	1.000	1.000	1.000	1.000
		0.430	0.109	1.000	0.950	0.390	1.000	0.855	0.961	0.986	0.998
VX	1.000		1.000	1.000	1.000	1.000	1.000	1.000	1.000	1.000	1.000
	0.430		1.000	0.400	0.996	1.000	0.868	1.000	0.995	0.981	0.929
VN	0.297	1.000		0.557	1.000	1.000	1.000	1.000	1.000	1.000	1.000
	0.109	1.000		0.113	0.843	1.000	0.429	0.944	0.818	0.710	0.537
VV	1.000	1.000	0.557		1.000	1.000	1.000	1.000	1.000	1.000	1.000
	1.000	0.400	0.113		0.912	0.365	0.998	0.801	0.927	0.967	0.993
VC	1.000	1.000	1.000	1.000		1.000	1.000	1.000	1.000	1.000	1.000
	0.950	0.996	0.843	0.912		0.994	1.000	1.000	1.000	1.000	1.000
VS	1.000	1.000	1.000	1.000	1.000		1.000	1.000	1.000	1.000	1.000
	0.390	1.000	1.000	0.365	0.994		0.839	1.000	0.991	0.972	0.908
RX	1.000	1.000	1.000	1.000	1.000	1.000		1.000	1.000	1.000	1.000
	1.000	0.868	0.429	0.998	1.000	0.839		0.997	1.000	1.000	1.000
RN	1.000	1.000	1.000	1.000	1.000	1.000	1.000		1.000	1.000	1.000
	0.855	1.000	0.944	0.801	1.000	1.000	0.997		1.000	1.000	0.999
RV	1.000	1.000	1.000	1.000	1.000	1.000	1.000	1.000		1.000	1.000
	0.961	0.995	0.818	0.927	1.000	0.991	1.000	1.000		1.000	1.000
RC	1.000	1.000	1.000	1.000	1.000	1.000	1.000	1.000	1.000		1.000
	0.986	0.981	0.710	0.967	1.000	0.972	1.000	1.000	1.000		1.000
RS	1.000	1.000	1.000	1.000	1.000	1.000	1.000	1.000	1.000	1.000	
	0.998	0.929	0.537	0.993	1.000	0.908	1.000	0.999	1.000	1.000	
B: ANOVA p-values											
Kruskal-Wallis p-value = 0.120						One-way ANOVA p-value = 0.059					

A: All comparison statistics are indicated as p-values. The upper p-value is the non-parametric multiple comparison test statistic, generated from the original set of data. The lower p-value was generated via the parametric Tukey *unequal number HSD* (Honestly Significant Difference) test, after the exclusion of extreme outliers. P-values in grey, indicate that no significant differences exist. B: P-values for the non-parametric Kruskal-Wallis ANOVA and parametric one-way ANOVA are listed. Rats were dosed NN = no dose and no dose, VX = vehicle and sacrificed, VN = vehicle and no dose, VV = vehicle and vehicle, VC = vehicle and CoQ_{10}, VS = vehicle and succinate, RX = rotenone and sacrificed, RN = rotenone and no dose, RV = rotenone and vehicle, RC = rotenone and CoQ_{10}, RS = rotenone and succinate. ANOVA = analysis of variance.

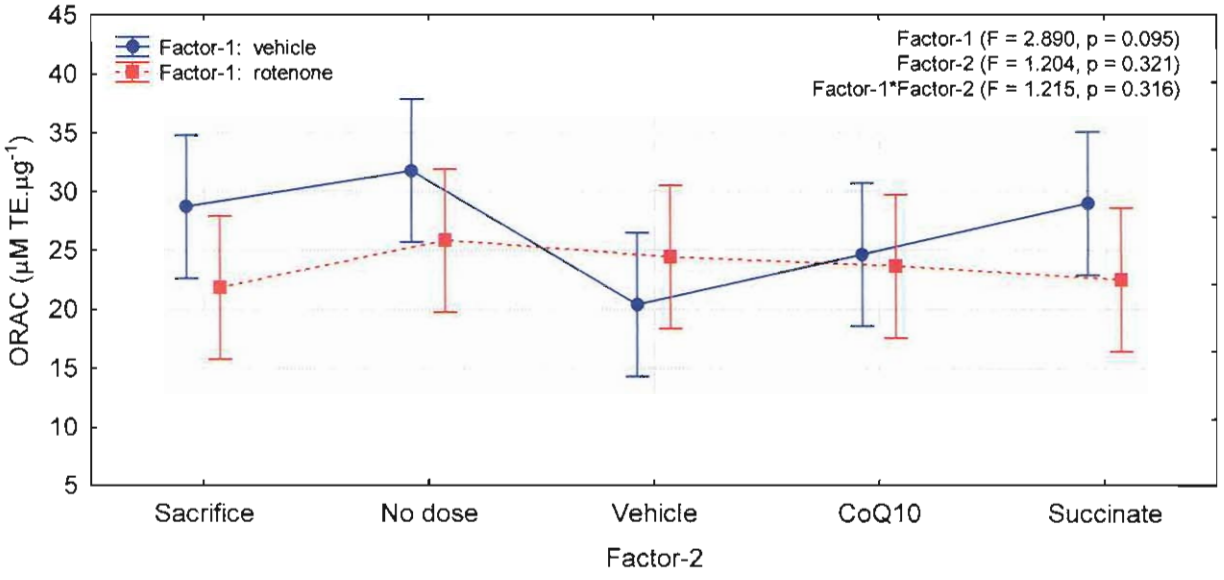
The data in Table 5.87 illustrate that no statistically significant differences existed between any of the dose groups that were compared. The Kruskal-Wallis and one-way ANOVA results, indicated in Section B of the table, supported this. It is worthy to note that, whether the extreme outlier was included or excluded from the complete data set, the statistical procedures still indicated that no differences existed between the groups. Therefore, the data presented here suggests that even though the raw data and descriptive statistics in Table 5.86 suggested differences between groups, these differences were too subtle for the multiple comparison procedures to find statistically significant changes in antioxidant capacities. The contributions from the dose Factor-1 and Factor-2 regimens were investigated via a two-way factorial ANOVA. Since the skeletal muscle antioxidant capacity data set presented with a single extreme outlier, the data set was analysed via the inclusion and exclusion of VV-3. Summary graphs of the two-way ANOVA are presented in Table 5.88.

The factorial ANOVA results verify the multiple comparison statistics presented in Table 5.87 that no statistically significant differences exist between the groups. The data sets in the presence or absence of VV-3 indicate no statistically significant contributions from either of the dose factors. In addition, no interaction effect was reported. The rotenone plots in both graphs remained consistently stable no matter which Factor-2 dose the rats received. The vehicle Factor-1 plots in both Sections A and B of Table 5.88 presented with a decrease in antioxidant capacities when a vehicle Factor-2 dose was received. The decrease is of course milder when the extreme outlier was excluded from the data set, which is confirmed by the decrease in the interaction F-statistic. The lowered interaction F-statistic is due to the decrease in deviation of the vehicle Factor-1 plot upon exclusion of VV-3, which in turn resulted in a more parallel-like configuration in the graphic representation, as indicated in Table 5.88.B.

The fact that the statistical evaluations presented here indicated that no significant differences existed between the dose groups or any of the dose regimens, suggests strongly that skeletal muscle is a poor responder, in terms of antioxidant capacity, to the different dose regimens. In addition, the scenario was supported by the data presented in Sections 5.6.1.1 and 5.6.1.2 where skeletal muscle complex I data illustrated few statistically significant differences in the pilot and main studies respectively. Thus far, it is becoming evident that skeletal muscle data may not be as informative to response profiles as the other organs investigated in the study.

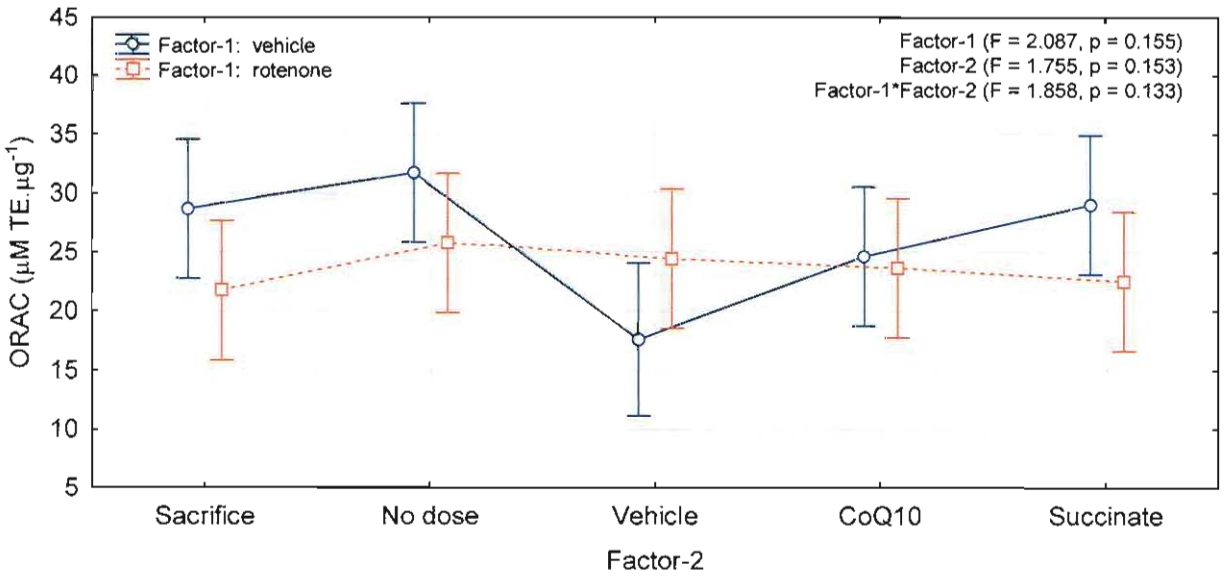
Table 5.88 Graphic and tabulated summary of the skeletal muscle antioxidant capacity data analysed via a two-way ANOVA

A: Data set including extreme outliers



Description		VX	VN	VV	VC	VS	RX	RN	RV	RC	RS
With extreme outliers	UCI	34.7	37.8	26.4	30.7	35.0	27.8	31.8	30.4	29.7	28.5
	mean	28.7	31.7	20.3	24.6	28.9	21.8	25.8	24.4	23.6	22.5
	LCI	22.6	25.6	14.3	18.5	22.9	15.7	19.7	18.3	17.5	16.4

B: Data set excluding extreme outliers



Description		VX	VN	VV	VC	VS	RX	RN	RV	RC	RS
Without extreme outliers	UCI	34.5	37.6	24.0	30.5	34.8	27.6	31.6	30.2	29.5	28.3
	mean	28.7	31.7	17.6	24.6	28.9	21.8	25.8	24.4	23.6	22.5
	LCI	22.8	25.8	11.1	18.7	23.1	15.9	19.9	18.5	17.7	16.6

The plot legends for each graph are indicated in the top left corners of the respective graphs, while the two-way ANOVA F-statistics (F) and p-values (p) for Factor-1, Factor-2 and Factor-1*Factor-2 are located in the top right corner, with the statistically significant values indicated in red. The vertical whiskers at each mean data point represent 95% confidence intervals for the respective data sets. The mean values in green text, located in the data point summary tables below the graphs, indicate those that were adjusted due to the exclusion of extreme outliers. Rats were treated with NN = no dose regimen, VX = vehicle and sacrificed, VN = vehicle and no dose, VV = vehicle and vehicle, VC = vehicle and CoQ_{10}, VS = vehicle and succinate, RX = rotenone and sacrificed, RN = rotenone and no dose, RV = rotenone and vehicle, RC = rotenone and CoQ_{10}, RS = rotenone and succinate. LCI = lower 95% confidence interval data point, µM TE μg^{-1} = micromolar Trolox equivalents per microgram protein, UCI = upper 95% confidence interval data point.

As presented in Section 4.3.1 of Chapter Four, rats were housed individually in cages with limited roaming area. Since rats are social animals, it is likely that the restricted environment influenced the naturally active habits of socialising and roaming. Therefore, it may be argued that the inability to roam freely and consequent lack of physical activity may have influenced the biochemical profiles in skeletal muscle. In turn, it could be argued that the muscles were not required to endure times of metabolic stress. In contrast, the other organs investigated are constantly active and undergoing stresses to maintain and restore cellular functions, especially while the rats are being dosed various regimens like rotenone. An investigation of rat behaviour *per se* in response to the dose regimens was not within the scope of the project. It may have been of interest to evaluate physical activities, like exercise tolerance, balance and exploration capabilities in response to the various dose compounds, particularly rotenone.

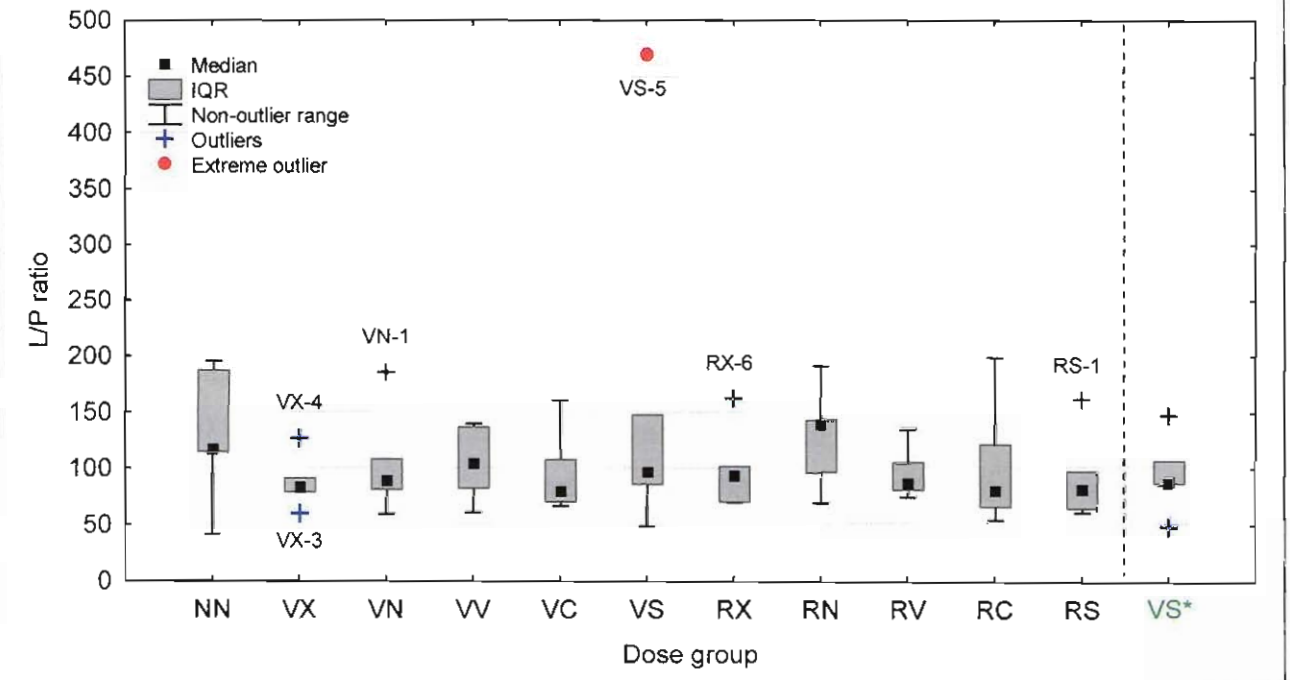
5.6.3 Lactate/pyruvate ratios in skeletal muscle

Lactate and pyruvate concentrations were determined in skeletal muscle isolated from rats. The muscle was prepared on the day that rats were sacrificed according to the protocol described in Section 4.4.7 of Chapter Four. Data were captured in Excel® format and statistically evaluated utilising the STATISTICA™ programme. Box-whisker representations and descriptive statistics of the skeletal muscle L/P ratio data are presented in Table 5.89.

The box-whisker representations of skeletal muscle L/P data indicate the presence of one extreme outlier and seven outliers. Two of the outliers in the graphic display, indicated above and below the IQR box plot for VS*, are not labelled since they were classified as outliers only after the extreme outlier VS-5 was excluded. Each of the remaining five outliers appears to be positioned in a range very similar to the global distribution of data points for the L/P skeletal muscle data set. This could be accounted for by the apparent overall lack in variation observed in the box-whisker plots presented in Table 5.89. It is therefore not foreseen that exclusions of these outliers would alter the statistical evaluations of the data to a large extent. Nonetheless, since the proposed statistical strategy was to exclude extreme outliers only, further discussion regarding the outliers will not be required.

Table 5.89 Box-whisker representation and descriptive statistics of the skeletal muscle L/P ratio data generated from the rat main study

A: Box-whisker plots and data points according to rat groups



Rat	NN	VX	VN	VV	VC	VS	RX	RN	RV	RC	RS	VS*
1	115	79.7	+ 185	117	72.2	86.6	90.8	69.2	74.2	199	+ 161	86.6
2	195	90.7	81.6	60.5	107	85.6	70.1	139	135	52.8	74.6	85.6
3	186	+ 58.9	93.9	81.9	66.0	105	69.5	95.5	104	77.9	95.9	105
4	116	+ 126	59.1	136	69.8	147	101	191	85.2	64.8	62.9	147
5	41.4	78.4	108	139	85.8	• 468	94.6	142	79.7	79.8	83.6	EXCL
6	116	85.2	80.6	89.9	160	48.2	+ 162	138	84.7	120	59.1	48.2

B: Descriptive statistics

Dose group	Sample size	Mean	SD	Median	Min	Max	Range	Lower quartile	Upper quartile	IQR
NN	6	128	56.2	116	41.4	195	153	115	186	71.8
VX	6	86.5	22.3	82.4	58.9	126	67.4	78.34	90.7	12.3
VN	6	101	44.1	87.7	59.1	185	126	80.6	108	27.2
VV	6	104	31.8	104	60.5	139	79.0	81.9	136	54.2
VC	6	93.6	36.1	79.0	66.0	160	94.4	69.8	107	37.4
VS	6	157	156	95.9	48.2	468	420	85.6	147	61.7
VS*	5	94.6	36.0	86.6	48.2	147	99.1	85.6	105	19.6
RX	6	98.0	33.9	92.7	69.5	162	92.5	70.1	101	31.0
RN	6	129	42.3	139	69.2	191	122	95.5	142	46.8
RV	6	93.8	22.4	85.0	74.2	135	60.4	79.7	104	24.4
RC	6	99.0	54.0	78.8	52.8	199	146	64.8	120	55.4
RS	6	89.6	37.7	79.1	59.1	161	102	62.9	95.9	32.9

Rat codes for outliers and extreme outliers are located above or below the respective blue crosses (+) and red dots (•), which correspond to data point values listed in the table directly below the graph. The vertical dashed line in the box-whisker graphic representation separates original dose group box-whiskers from those that have had the extreme outliers excluded, which are also indicated by the asterisk (*) following the dose group code. Data sets with excluded data points are designated in green text. Rats were treated with NN = no dose regimen, VX = vehicle and sacrificed, VN = vehicle and no dose, VV = vehicle and vehicle, VC = vehicle and CoQ_{10}, VS = vehicle and succinate, RX = rotenone and sacrificed, RN = rotenone and no dose, RV = rotenone and vehicle, RC = rotenone and CoQ_{10}, RS = rotenone and succinate. EXCL = excluded data point, IQR = inter-quartile range, L/P = ratio of lactate to pyruvate, Min = minimum data point value, Max = maximum data point value, SD = standard deviation.

The exclusion of the extreme outlier VS-5 resulted in a mean ratio decrease from 157 to 94.6, while the median ratio decreased from 95.9 to 86.6. The SD diminished considerably from 156 to 36.0, whilst the IQR decreased from 61.7 to 19.6. The lactate and pyruvate concentrations for skeletal muscle, listed in Table E.4 in Appendix E, indicate that the elevated ratio for VS-5 is due to a low pyruvate concentration of 3.616 $\mu mol.L^{-1}$. The mean pyruvate concentration for VS was 16.20 $\mu mol.L^{-1}$. The lactate concentration of 1,692 $\mu mol.L^{-1}$ for VS-5 is consistent with the mean for VS, which was calculated to be 1,546 $\mu mol.L^{-1}$. It could be argued that the pyruvate assay should have been repeated for rat VS-5 since it did harbour the lowest of the pyruvate concentrations that resulted in an uncharacteristically elevated L/P ratio of 468. However, it is of value to note that outlier analysis enabled the rapid detection of this extreme outlier and its subsequent exclusion to improve interpretation of this data set. The ANOVA p-values and multiple comparison data for this skeletal muscle data set are presented in Table 5.90.

Table 5.90 Multiple comparison statistics of the skeletal muscle L/P ratio data generated from the rat main study

A: Non-parametric (original data set) and parametric (excluding extreme outliers) p-values											
Dose group	NN	VX	VN	VV	VC	VS	RX	RN	RV	RC	RS
NN		1.000	1.000	1.000	1.000	1.000	1.000	1.000	1.000	1.000	1.000
		0.754	0.982	0.992	0.905	0.955	0.959	1.000	0.908	0.968	0.829
VX	1.000		1.000	1.000	1.000	1.000	1.000	1.000	1.000	1.000	1.000
	0.754		1.000	0.999	1.000	1.000	1.000	0.726	1.000	1.000	1.000
VN	1.000	1.000		1.000	1.000	1.000	1.000	1.000	1.000	1.000	1.000
	0.982	1.000		1.000	1.000	1.000	1.000	0.976	1.000	1.000	1.000
VV	1.000	1.000	1.000		1.000	1.000	1.000	1.000	1.000	1.000	1.000
	0.992	0.999	1.000		1.000	1.000	1.000	0.989	1.000	1.000	1.000
VC	1.000	1.000	1.000	1.000		1.000	1.000	1.000	1.000	1.000	1.000
	0.905	1.000	1.000	1.000		1.000	1.000	0.887	1.000	1.000	1.000
VS	1.000	1.000	1.000	1.000	1.000		1.000	1.000	1.000	1.000	1.000
	0.955	1.000	1.000	1.000	1.000		1.000	0.945	1.000	1.000	1.000
RX	1.000	1.000	1.000	1.000	1.000	1.000		1.000	1.000	1.000	1.000
	0.959	1.000	1.000	1.000	1.000	1.000		0.949	1.000	1.000	1.000
RN	1.000	1.000	1.000	1.000	1.000	1.000	1.000		1.000	1.000	1.000
	1.000	0.726	0.976	0.989	0.887	0.945	0.949		0.890	0.959	0.804
RV	1.000	1.000	1.000	1.000	1.000	1.000	1.000	1.000		1.000	1.000
	0.908	1.000	1.000	1.000	1.000	1.000	1.000	0.890		1.000	1.000
RC	1.000	1.000	1.000	1.000	1.000	1.000	1.000	1.000	1.000		1.000
	0.968	1.000	1.000	1.000	1.000	1.000	1.000	0.959	1.000		1.000
RS	1.000	1.000	1.000	1.000	1.000	1.000	1.000	1.000	1.000	1.000	
	0.829	1.000	1.000	1.000	1.000	1.000	1.000	0.804	1.000	1.000	
B: ANOVA p-values											
Kruskal-Wallis p-value = 0.638						One-way ANOVA p-value = 0.638					

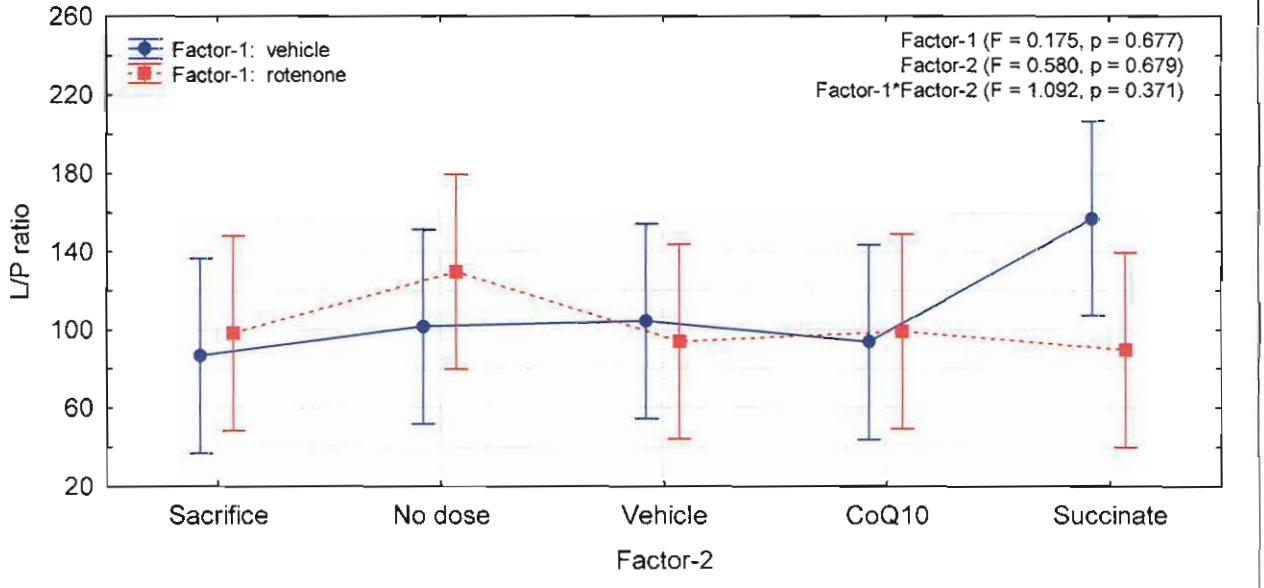
A: All comparison statistics are indicated as p-values. The upper p-value is the non-parametric multiple comparison test statistic, generated from the original set of data. The lower p-value was generated via the parametric Tukey *unequal number HSD* (Honestly Significant Difference) test, after the exclusion of extreme outliers. P-values in grey, indicate that no significant differences exist. B: P-values for the non-parametric Kruskal-Wallis ANOVA and parametric one-way ANOVA are listed. Rats were dosed NN = no dose and no dose, VX = vehicle and sacrificed, VN = vehicle and no dose, VV = vehicle and vehicle, VC = vehicle and CoQ_{10}, VS = vehicle and succinate, RX = rotenone and sacrificed, RN = rotenone and no dose, RV = rotenone and vehicle, RC = rotenone and CoQ_{10}, RS = rotenone and succinate. ANOVA = analysis of variance.

The Kruskal-Wallis ANOVA as well as the one-way ANOVA coincidently resulted in the generation of p-values of 0.638, well above the 0.05 significance level. These statistics were supported by the multiple comparison procedures that too presented with no statistically significant differences between dose groups, whether the extreme outlier was excluded or not. These results are not unexpected, as the box-whisker plots in Table 5.89 appear to depict a consistent overlapping of data between ratios of approximately 50 and 200 units. The data was subsequently further analysed via a two-way ANOVA in order to verify if statistically significant contributions could be assigned to Factor-1 and Factor-2 dose regimens. The two-way ANOVA results are illustrated in Table 5.91.

Once again, the exclusion of the extreme outlier made little difference to the F-statistics and p-values. Both data sets presented with no statistically significant contributions from Factor-1 and Factor-2 doses. The exclusion of VS-5 resulted in a marked lowering of the mean data point for the vehicle plot for the Factor-2 succinate dose. Consequently, the differences between the vehicle and rotenone Factor-1 plots were softened considerably, eliminating the possibility that an interaction effect may be present. This is confirmed by a decrease in the F-statistic for the interaction, from 1.092 to 0.483.

Table 5.91 Graphic and tabulated summary of the skeletal muscle L/P ratio data analysed via a two-way ANOVA

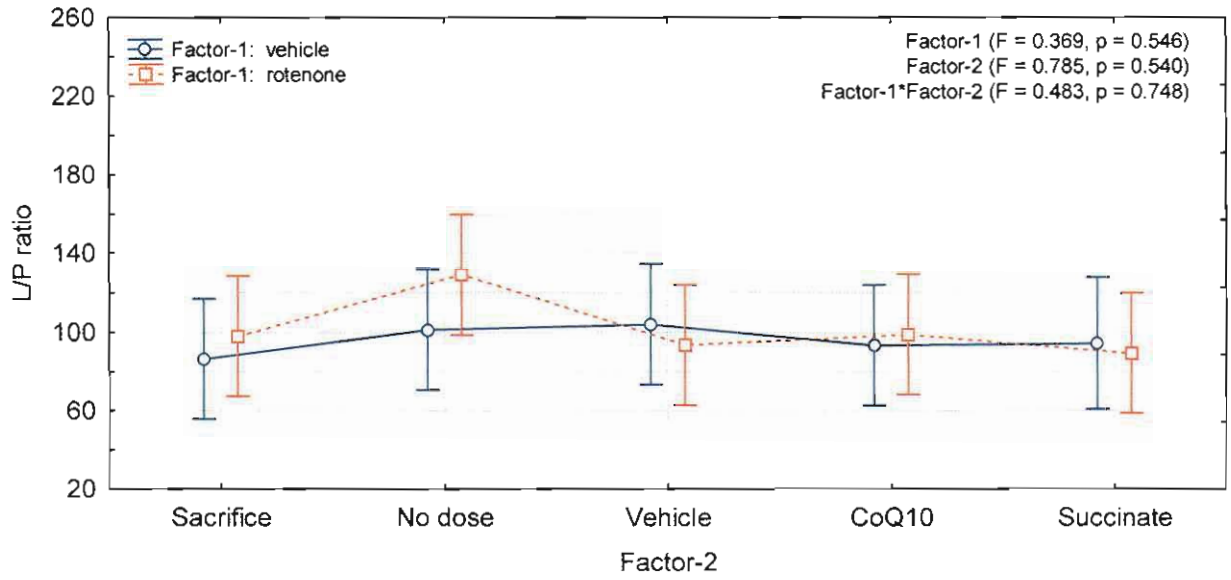
A: Data set including extreme outliers



Description		VX	VN	VV	VC	VS	RX	RN	RV	RC	RS
With extreme outliers	UCI	136	151	154	143	207	148	179	143	149	139
	mean	86.5	101	104	93.6	157	98.0	129	93.8	99.1	89.6
	LCI	36.8	51.6	54.4	43.8	107	48.3	79.5	44.0	49.3	39.8

Table 5.91 Continued...

B: Data set excluding extreme outliers



Description		VX	VN	VV	VC	VS	RX	RN	RV	RC	RS
Without extreme outliers	UCI	117	132	135	124	128	129	160	124	130	120
	mean	86.5	101	104	93.6	94.6	98.0	129	93.8	99.1	89.6
	LCI	56.0	70.9	73.7	63.1	61.2	67.5	98.7	63.2	68.5	59.1

The plot legends for each graph are indicated in the top left corners of the respective graphs, while the two-way ANOVA F-statistics (F) and p-values (p) for Factor-1, Factor-2 and Factor-1*Factor-2 are located in the top right corner, with the statistically significant values indicated in red. The vertical whiskers at each mean data point represent 95% confidence intervals for the respective data sets. The mean recordings in green text, located in the data point summary tables below the graphs, indicate those that have changed due to the removal of extreme outliers. UCI = upper 95% confidence interval data point, LCI = lower 95% confidence interval data point. Rats were treated with NN = no dose regimen, VX = vehicle and sacrificed, VN = vehicle and no dose, VV = vehicle and vehicle, VC = vehicle and CoQ_{10}, VS = vehicle and succinate, RX = rotenone and sacrificed, RN = rotenone and no dose, RV = rotenone and vehicle, RC = rotenone and CoQ_{10}, RS = rotenone and succinate.

The diminished interaction F-statistic results in increased Factor-1 and Factor-2 F-statistics. The Factor-1 F-statistic increased from 0.175 to 0.369. Similarly, the Factor-2 F-statistic increased from 0.580 to 0.785. As expected, the 95% confidence interval also decreased considerably due to the exclusion of VS-5. Prior to exclusion, the confidence interval was 99.5 in length, while it decreased to 61.0 after the extreme outlier was excluded. This is a notable decrease considering that it results from the exclusion of only a single data point from the complete data set. Regardless of this, the overall uniformity in data spreads across the various dose groups resulted in no dose group differences of statistical significance. The data presented here correlates well with previous skeletal muscle data sets that too displayed little variation among dose groups.

5.6.4 ATP/ADP ratios in skeletal muscle

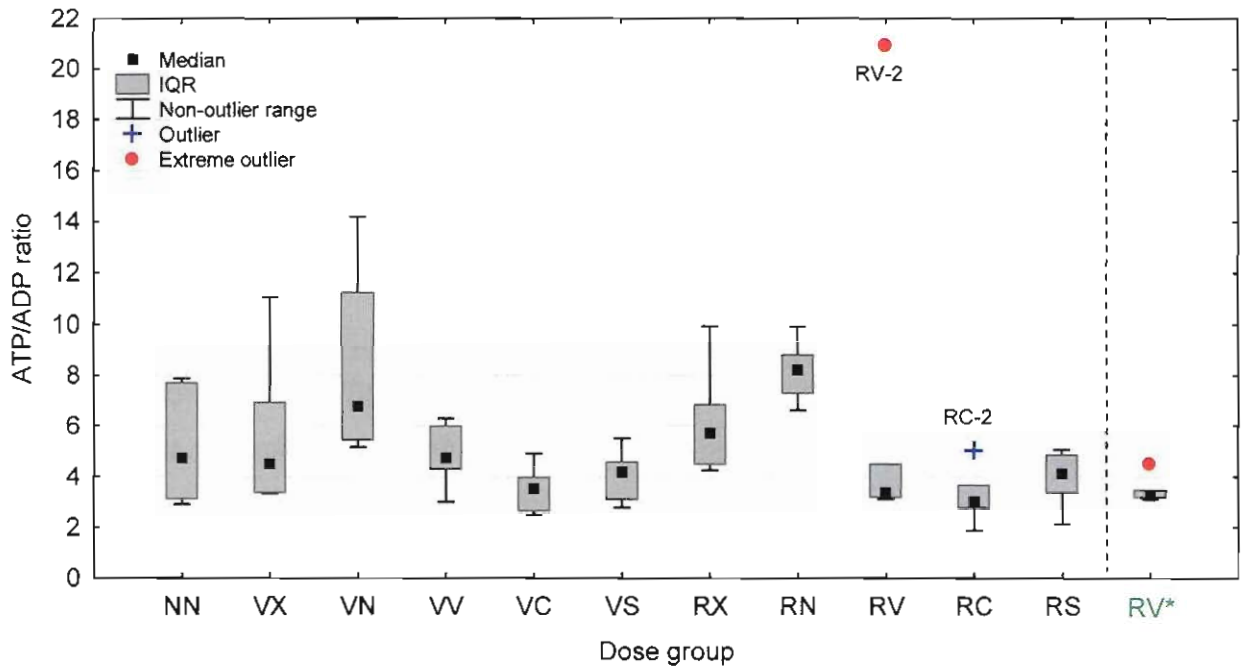
Skeletal muscle was collected and appropriately prepared via homogenisation and deproteinisation. The data was captured in Excel® format where ratios of ATP to ADP were determined. Subsequently, the data was exported to STATISTICA™ for a statistical

evaluation. The distribution of data is graphically summarised by means of box-whisker plots in Table 5.92. The table also contains a list of all data points as well as descriptive statistics.

Dose group RV is the only group to present with an extreme outlier. Rat RV-2 harboured an ATP/ADP ratio of 20.9, which was the highest of all the skeletal muscle ATP/ADP data points. The extreme nature of the RV-2 is evident when observing the distribution of data in Table 5.92.A. The exclusion of RV-2 from dose group RV resulted in a mean decrease in ratio of 2.91 from 6.42 to 3.51. The SD diminished considerably from 7.13 to 0.57. The non-parametric median decreased from a ratio of 3.37 to 3.27, while the IQR decreased from 1.31 to 0.28. As a result of the exclusion, an additional extreme outlier was determined to be present in dose group RV*, which will consequently not be discussed.

Table 5.92 Box-whisker representation and descriptive statistics of the skeletal muscle ATP/ADP ratio data generated from the main study

A: Box-whisker plots and data points according to rat groups



Rat	NN	VX	VN	VV	VC	VS	RX	RN	RV	RC	RS	RV*
1	7.70	4.73	7.14	4.45	2.48	2.78	5.24	8.80	3.27	3.17	2.13	3.27
2	2.91	3.34	5.16	4.99	2.67	3.11	6.83	8.35	• 20.9	+ 5.02	4.85	EXCL
3	3.14	3.38	6.39	5.98	3.79	5.50	4.50	8.08	3.20	2.88	5.06	3.20
4	7.87	11.1	5.44	3.00	3.98	4.25	9.94	7.30	3.47	3.66	3.38	3.47
5	4.12	6.92	11.2	4.30	3.24	4.10	6.14	6.61	4.50	1.89	3.38	4.50
6	5.34	4.24	14.2	6.29	4.91	4.57	4.25	9.91	3.12	2.79	4.84	3.12

B: Descriptive statistics

Dose group	Sample size	Mean	SD	Median	Min	Max	Range	Lower quartile	Upper quartile	IQR
NN	6	5.18	2.19	4.73	2.91	7.87	4.96	3.14	7.70	4.56

Table 5.92 Continued...

Dose group	Sample size	Mean	SD	Median	Min	Max	Range	Lower quartile	Upper quartile	IQR
VX	6	5.61	2.97	4.49	3.34	11.1	7.72	3.38	6.92	3.54
VN	6	8.25	3.64	6.76	5.16	14.2	9.02	5.44	11.2	5.79
VV	6	4.83	1.20	4.72	3.00	6.29	3.29	4.30	5.98	1.67
VC	6	3.51	0.91	3.51	2.48	4.91	2.43	2.67	3.98	1.31
VS	6	4.05	0.99	4.17	2.78	5.50	2.73	3.11	4.57	1.46
RX	6	6.15	2.10	5.69	4.25	9.94	5.69	4.50	6.83	2.33
RN	6	8.17	1.15	8.21	6.61	9.91	3.30	7.30	8.80	1.50
RV	6	6.42	7.13	3.37	3.12	20.9	17.8	3.20	4.50	1.31
RV*	5	3.51	0.57	3.27	3.12	4.50	1.38	3.20	3.47	0.28
RC	6	3.24	1.05	3.03	1.89	5.02	3.13	2.79	3.66	0.88
RS	6	3.94	1.17	4.11	2.13	5.06	2.93	3.38	4.85	1.47

Rat codes for outliers and extreme outliers are located above or below the respective blue crosses (+) and red dots (•), which correspond to data point values listed in the table directly below the graph. The vertical dashed line in the box-whisker graphic representation separates original dose group box-whiskers from those that have had the extreme outliers excluded, which are also indicated by the asterisk (*) following the dose group code. Data sets with excluded data points are designated in green text. Rats were treated with NN = no dose regimen, VX = vehicle and sacrificed, VN = vehicle and no dose, VV = vehicle and vehicle, VC = vehicle and CoQ_{10}, VS = vehicle and succinate, RX = rotenone and sacrificed, RN = rotenone and no dose, RV = rotenone and vehicle, RC = rotenone and CoQ_{10}, RS = rotenone and succinate. ATP/ADP = ratio of adenosine triphosphate to adenosine diphosphate, EXCL = excluded data point, IQR = inter-quartile range, Min = minimum data point value, Max = maximum data point value, SD = standard deviation.

In addition to extreme outlier RV-2, an outlier was revealed in dose group RC. The outlier, RC-2, presented with an ATP/ADP ratio of 5.02, which was comfortably positioned within the upper outlier boundary at a ratio of 6.03. If RC-2 were to be excluded, the central tendency statistics would be altered slightly with mean and median ATP/ADP ratios lowering. Dose group RC already presents with the lowest mean and median ratio of all dose groups. Therefore, the exclusion of RC-2 would further displace RC from the remainder of the dose groups. However, since RC-2 is not positioned in the extreme outlier range, it will not be excluded.

Upon a visual inspection of the box-whisker plots in Table 5.92, it can be observed that the highest median ratios were recorded for dose groups VN and RN. Both rat groups received no dose on days 15 and 16. Interpretation of the data therefore suggests that the vehicle and possibly the dosage procedure appeared to have affected skeletal muscle ATP/ADP ratios in rats. The significance of variation in skeletal muscle ATP/ADP ratios were investigated via ANOVA and multiple comparison procedures, as presented in Table 5.93. Non-parametric and parametric protocols were utilised to analyse the skeletal muscle ATP/ADP ratio data set via the inclusion and exclusion of extreme outliers respectively.

Table 5.93 Multiple comparison statistics of the skeletal muscle ATP/ADP ratio data generated from the rat main study

A: Non-parametric (original data set) and parametric (excluding extreme outliers) p-values

Dose group	NN	VX	VN	VV	VC	VS	RX	RN	RV	RC	RS
NN		1.000	1.000	1.000	1.000	1.000	1.000	1.000	1.000	1.000	1.000
		1.000	0.179	1.000	0.903	0.993	0.998	0.208	0.944	0.785	0.986
VX	1.000		1.000	1.000	1.000	1.000	1.000	1.000	1.000	1.000	1.000
	1.000		0.373	1.000	0.698	0.935	1.000	0.418	0.799	0.530	0.902
VN	1.000	1.000		1.000	0.075	0.557	1.000	1.000	0.924	0.028	0.690
	0.179	0.373		0.088	0.003	0.013	0.695	1.000	0.009	0.001	0.009
VV	1.000	1.000	1.000		1.000	1.000	1.000	1.000	1.000	1.000	1.000
	1.000	1.000	0.088		0.979	1.000	0.979	0.104	0.989	0.925	0.999
VC	1.000	1.000	0.075	1.000		1.000	0.963	0.020	1.000	1.000	1.000
	0.903	0.698	0.003	0.979		1.000	0.376	0.004	1.000	1.000	1.000
VS	1.000	1.000	0.557	1.000	1.000		1.000	0.185	1.000	1.000	1.000
	0.993	0.935	0.013	1.000	1.000		0.701	0.016	1.000	1.000	1.000
RX	1.000	1.000	1.000	1.000	0.963	1.000		1.000	1.000	0.447	1.000
	0.998	1.000	0.695	0.979	0.376	0.701		0.741	0.511	0.241	0.634
RN	1.000	1.000	1.000	1.000	0.020	0.185	1.000		0.326	0.007	0.235
	0.208	0.418	1.000	0.104	0.004	0.016	0.741		0.011	0.002	0.012
RV	1.000	1.000	0.924	1.000	1.000	1.000	1.000	0.326		1.000	1.000
	0.944	0.799	0.009	0.989	1.000	1.000	0.511	0.011		1.000	1.000
RC	1.000	1.000	0.028	1.000	1.000	1.000	0.447	0.007	1.000		1.000
	0.785	0.530	0.001	0.925	1.000	1.000	0.241	0.002	1.000		1.000
RS	1.000	1.000	0.690	1.000	1.000	1.000	1.000	0.235	1.000	1.000	
	0.986	0.902	0.009	0.999	1.000	1.000	0.634	0.012	1.000	1.000	

B: ANOVA p-values

Kruskal-Wallis p-value < 0.001	One-way ANOVA p-value < 0.001

C: Statistical and biological significance

Comparison		Statistical significance (p)		Biological significance (d)	
		Including EOs	Excluding EOs	Including EOs	Excluding EOs
VN	VC	0.075	0.003	N/A	2.508
VN	VS	0.557	0.013	N/A	2.222
VN	RV	0.924	0.009	N/A	2.508
VN	RC	0.028	0.001	1.376	2.651
VN	RS	0.690	0.009	N/A	2.280
VC	RN	0.020	0.004	4.052	2.466
VS	RN	0.185	0.016	N/A	2.180
RN	RV	0.326	0.011	N/A	2.466
RN	RC	0.007	0.002	4.287	2.609
RN	RS	0.235	0.012	N/A	2.238

A: All comparison statistics are indicated as p-values. The upper p-value is the non-parametric multiple comparison test statistic, generated from the original set of data. The lower p-value was generated via the parametric Tukey *unequal number HSD* (Honestly Significant Difference) test, after the exclusion of extreme outliers. P-values indicated in red are statistically significant at the pre-determined significance level of 0.05. P-values in black text represent those that are not statistically significant, but have complementary p-values that are statistically significant. The remainder of p-values are listed in grey. The comparisons surrounded by the **bold** black line are those that were determined to be statistically significant by both the non-parametric and parametric multiple comparison procedures. The turquoise shaded blocks represent statistically significant comparisons that were also determined to be of biological significance. B: P-values for the non-parametric Kruskal-Wallis ANOVA and parametric one-way ANOVA are listed, with significant p-values, less than the 0.05 significance level, indicated in red. C: List of comparisons determined to be statistically significant with corresponding biological significance. A d-value greater than or equal to 0.8 signifies biological significance, indicated in red. Rats were treated with NN = no dose regimen, VX = vehicle and sacrificed, VN = vehicle and no dose, VV = vehicle and vehicle, VC = vehicle and CoQ_{10}, VS = vehicle and succinate, RX = rotenone and sacrificed, RN = rotenone and no dose, RV = rotenone and vehicle, RC = rotenone and CoQ_{10}, RS = rotenone and succinate. < = less than, ANOVA = analysis of variance, EOs = extreme outliers, N/A = not applicable.

The multiple comparison grid reveals that three comparisons were determined to be statistically significant prior to and after the exclusion of the extreme outlier. In addition, these comparisons were also determined to differ biologically significantly from each other. The first of these was a comparison between dose groups VC and RN. Since these two groups cannot be paralleled based on their dose regimens, the comparison will not be discussed further. The next two comparisons that were determined to be significant prior to and after the exclusion of the extreme outlier involved dose group RC when compared to VN and RN. The former comparison does not allow for an evaluation of the effects of a single dose regimen, while the comparison of RC with RN is more informative. As mentioned previously in this section, rat groups VN and RN presented with the highest skeletal muscle ATP/ADP ratios. The fact that RN differed significantly from RC, whether the extreme outlier was excluded or not, strongly suggests that rat skeletal muscle responded more positively to a no dose regimen than to CoQ_{10}. Furthermore, when the extreme outlier was excluded, RN differed statistically significantly from dose groups RV and RS, thereby indicating that the two-day recovery was more beneficial to skeletal muscle ATP/ADP ratios than any of the other Factor-2 dose regimens.

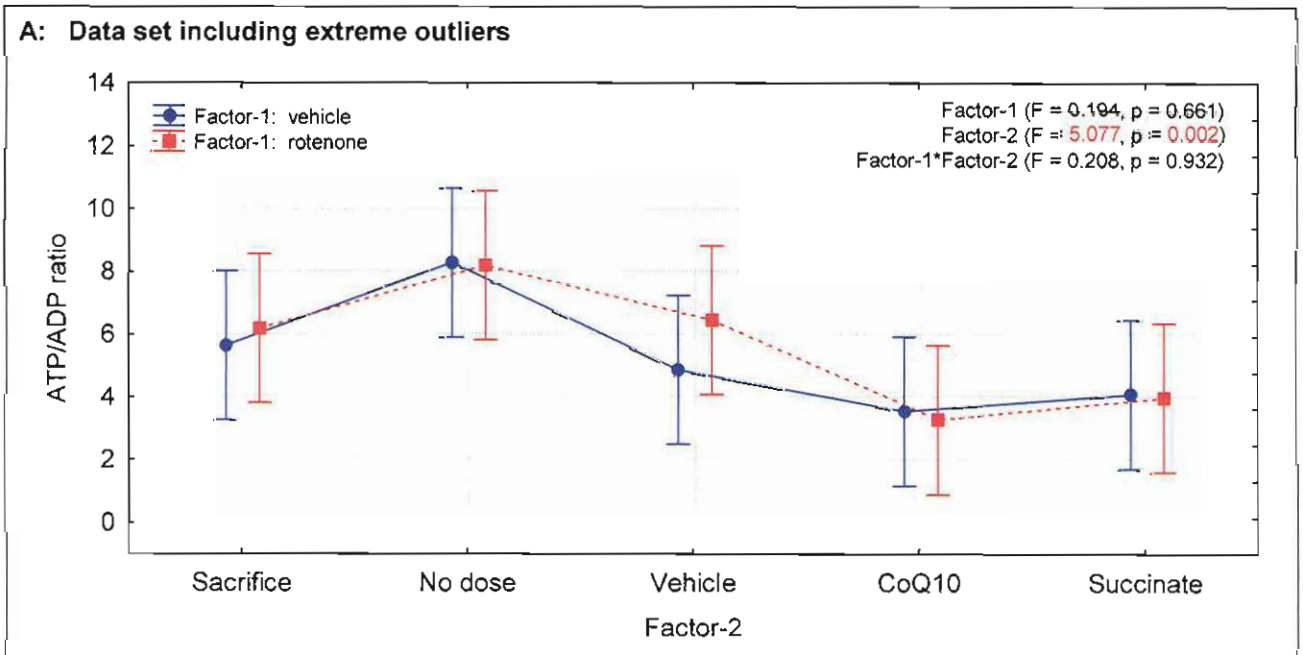
Dose group VN differed significantly from VC and VS, but also from RV, RC and RS. The latter comparisons with VN are not informative due to the combination of dose regimens being compared. Both dose groups VC and VS harboured lower ATP/ADP ratios when compared to VN. Since VN differed significantly from VC and VS, the data is suggestive of the fact that ATP/ADP ratios in skeletal muscle improved when a no dose Factor-2 regimen was received by rats, more so than when rats were dosed with CoQ_{10} or succinate. A similar scenario was discussed in the previous paragraph regarding the elevated ATP/ADP ratios in dose group RN. The statistical significance reported for comparisons with VN and RN is strongly suggestive of the no dose Factor-2 regimen being more beneficial to ATP/ADP ratios in skeletal muscle of rats.

The data and statistics thus far indicate that, no matter which Factor-1 dose was received by rats, the alleviation from receiving a no dose Factor-2 regimen improved skeletal muscle ATP/ADP ratios. It is difficult to comprehend that skeletal muscle would benefit more from receiving no dose than receiving therapeutic regimens such as CoQ_{10} and succinate. It should also be noted that, even though this trend seems to be apparent, none of the experimental dose groups differed statistically significantly from the environmental controls NN, or from dose group VX that received only vehicle for 14 days.

Therefore, the data may be suggestive of an increase or decrease in ATP/ADP levels among the groups reflecting a generalised distribution of data, affected only slightly by the administration of dose regimens. In order to evaluate the data further, a factorial ANOVA protocol was utilised. Graphic representations of the results are depicted in Table 5.94. Upon exclusion of the extreme outlier RV-2, the statistical significance of dose factors remained unaltered. The F-statistic for Factor-2 increased from 5.077 to 13.31, which in turn resulted in a marked decrease in the p-value beyond the sixth decimal place, as indicated in Table 5.94.B. Regardless of this, prior to the exclusion of the extreme outlier, the p-value for Factor-2 was already significant at 0.002. The Factor-1 plots consistently present with mean data points that increase or decrease correspondingly. This suggests that ATP/ADP ratios in skeletal muscle were not affected by the rotenone Factor-1 dose regimen when compared to rat groups that received vehicle. The lack of significance indicated for Factor-1 by the two-way ANOVA supports the notion that rotenone did not contribute to the response. Furthermore, since the environmental controls **NN** presented with a mean ratio of 5.18, it can be observed from the Factor-1 plots that, if the mean for **NN** were to be plotted, it would be positioned approximately central to fluctuations for the remaining dose regimens. Therefore, it can also not be stated that Factor-1 doses influenced ATP/ADP ratios in skeletal muscle.

Table 5.94 Graphic and tabulated summary of the skeletal muscle ATP/ADP ratio data analysed via a two-way ANOVA

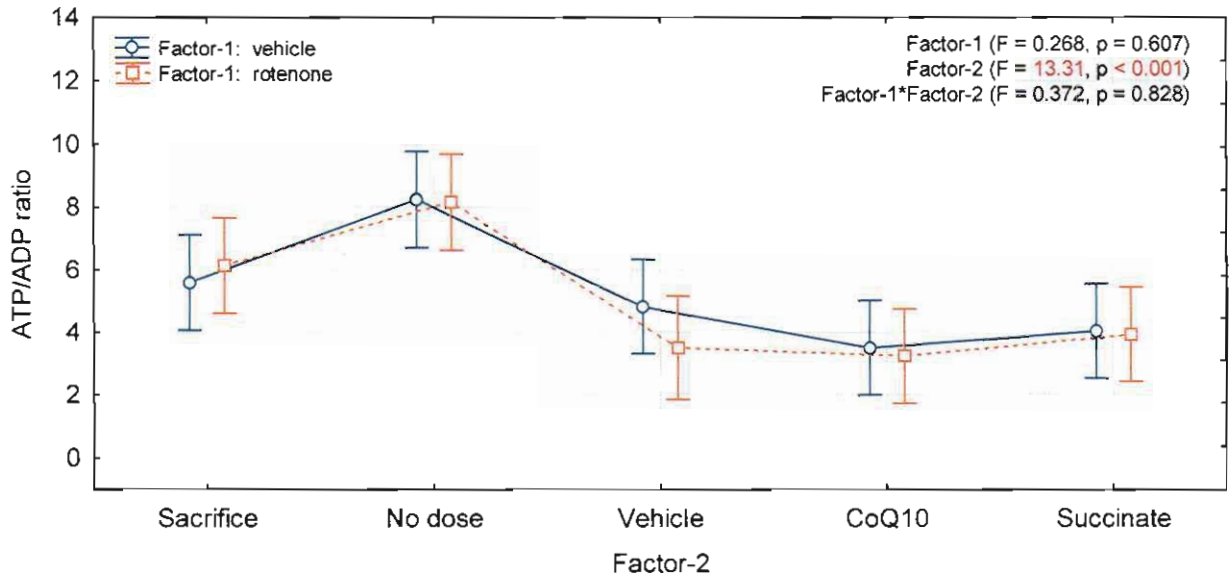
A: Data set including extreme outliers



Description		VX	VN	VV	VC	VS	RX	RN	RV	RC	RS
With extreme outliers	UCI	7.99	10.6	7.22	5.89	6.43	8.53	10.6	8.80	5.62	6.32
	Mean	5.61	8.25	4.83	3.51	4.05	6.15	8.17	6.42	3.24	3.94
	LCI	3.23	5.87	2.45	1.13	1.67	3.77	5.79	4.03	0.85	1.56

Table 5.94 Continued...

B: Data set excluding extreme outliers



Description		VX	VN	VV	VC	VS	RX	RN	RV	RC	RS
Without extreme outliers	UCI	7.14	9.78	6.36	5.03	5.57	7.67	9.70	5.18	4.76	5.46
	mean	5.61	8.25	4.83	3.51	4.05	6.15	8.17	3.51	3.24	3.94
	LCI	4.09	6.73	3.31	1.99	2.53	4.63	6.65	1.84	1.71	2.42

The plot legends for each graph are indicated in the top left corners of the respective graphs, while the two-way ANOVA F-statistics (F) and p-values (p) for Factor-1, Factor-2 and Factor-1*Factor-2 are located in the top right corner, with the statistically significant values indicated in red. The vertical whiskers at each mean data point represent 95% confidence intervals for the respective data sets. The mean values in green text, located in the data point summary tables below the graphs, indicate those that were adjusted due to the exclusion of extreme outliers. Rats were treated with NN = no dose regimen, VX = vehicle and sacrificed, VN = vehicle and no dose, VV = vehicle and vehicle, VC = vehicle and CoQ_{10}, VS = vehicle and succinate, RX = rotenone and sacrificed, RN = rotenone and no dose, RV = rotenone and vehicle, RC = rotenone and CoQ_{10}, RS = rotenone and succinate. < = less than, ATP/ADP = ratio of adenosine triphosphate to adenosine diphosphate, LCI = lower 95% confidence interval data point, UCI = upper 95% confidence interval data point.

A statistically significant Factor-2 contribution to skeletal muscle ATP/ADP ratios suggests that variation in response can be attributed largely to dose regimens received on days 15 and 16. The distribution of Factor-1 plots in Table 5.94 suggests that rats that received vehicle, CoQ_{10} and succinate on days 15 and 16 harboured the lowest ATP/ADP ratios. In contrast, rats that were sacrificed on day 15, namely VX and RX, or that received no dose on days 15 and 16, namely VN and RN, harboured the highest ATP/ADP ratios. As mentioned previously, it is not conceivable that CoQ_{10} or succinate would affect skeletal muscle adversely, even though the data may suggest it. It could be argued that the dosage procedure may have induced additional stress. As reported in Section 5.1.3, rats mostly appeared to receive the oesophageal intubation procedure favourably. Occasionally, certain rats displayed resistance, primarily in groups that were dosed with rotenone. Rats that received rotenone doses in order to induce the Complex I deficiency progressively became more difficult to dose due to the discomfort caused by rotenone. On certain occasions, rats had to be dosed more forcefully and via a tighter grip in order to ensure that successful oesophageal intubation could be achieved. Therefore, on the few

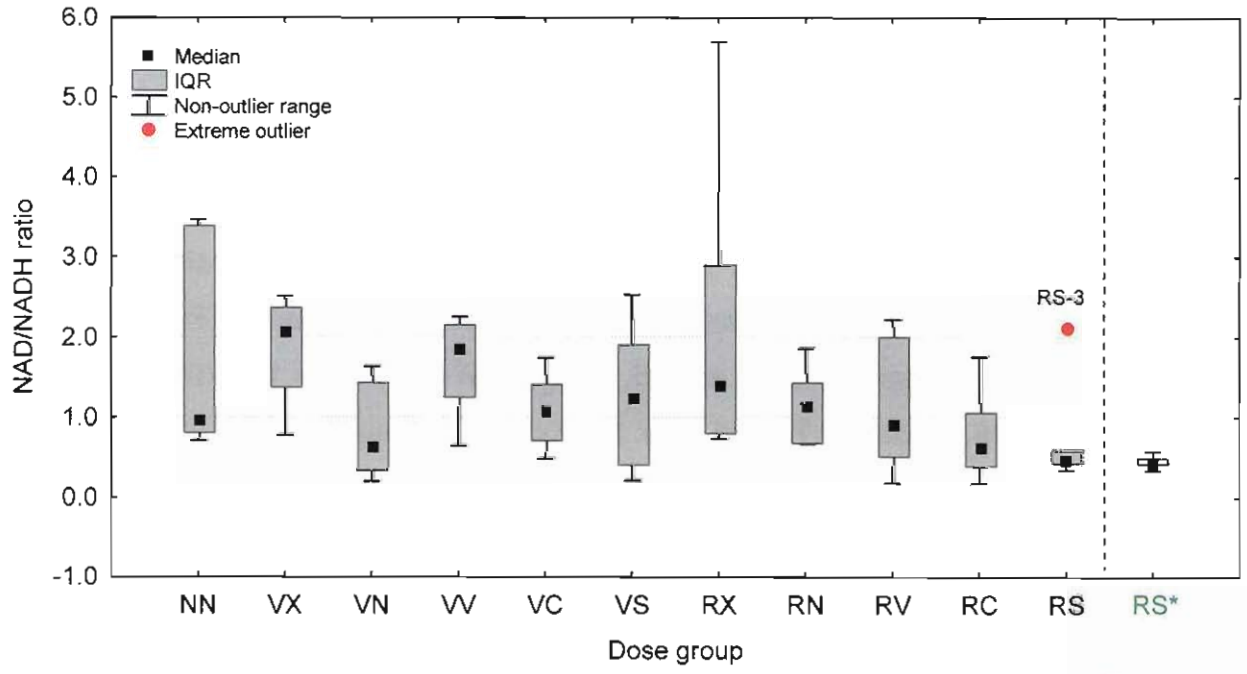
occurrences that such struggles were encountered, it may well be that a physical stress was induced, altering the biochemical status in skeletal muscle. However, it cannot be confirmed with confidence that this stress would have a direct impact on ATP/ADP ratios in skeletal muscle. Moreover, the fact that physical resistance to dose intubation was not encountered with every rat results in the argument that the dosage procedure harmfully induced lowered ATP/ADP ratios as purely speculative, even if the data is suggestive of the argument.

5.6.5 NAD/NADH ratios in skeletal muscle

Rat skeletal muscle was collected and homogenised appropriately. Upon splitting of the sample and appropriate preparation for analysis, the levels of NADH were determined spectrophotometrically. The ratios were calculated in Excel® format and the data evaluated in STATISTICA™. Skeletal muscle NAD/NADH ratios for the main study are presented in Table 5.95, along with a corresponding table of descriptive statistics.

Table 5.95 Box-whisker representation and descriptive statistics of the skeletal muscle NAD/NADH ratio data generated from the main study

A: Box-whisker plots and data points according to rat groups



Rat	NN	VX	VN	VV	VC	VS	RX	RN	RV	RC	RS	RS*
1	3.47	2.32	1.42	2.05	1.74	2.53	1.55	0.67	0.51	1.76	0.34	0.34
2	3.38	2.36	0.52	1.62	0.48	1.42	1.20	1.86	0.18	0.39	0.58	0.58
3	0.86	1.78	0.71	2.14	1.07	1.03	0.79	1.11	0.75	0.41	• 2.10	EXCL
4	0.71	0.78	1.63	1.24	1.40	0.21	0.73	0.66	1.99	0.18	0.43	0.43
5	1.05	2.52	0.20	2.25	1.06	1.90	5.70	1.14	1.04	1.05	0.49	0.49
6	0.80	1.37	0.34	0.64	0.70	0.40	2.89	1.42	2.22	0.80	0.43	0.43

Table 5.95 Continued...

B: Descriptive statistics										
Dose group	Sample size	Mean	SD	Median	Min	Max	Range	Lower quartile	Upper quartile	IQR
NN	6	1.71	1.33	0.95	0.71	3.47	2.76	0.80	3.38	2.57
VX	6	1.85	0.68	2.05	0.78	2.52	1.74	1.37	2.36	0.99
VN	6	0.80	0.59	0.61	0.20	1.63	1.43	0.34	1.42	1.09
VV	6	1.66	0.62	1.84	0.64	2.25	1.60	1.24	2.14	0.90
VC	6	1.08	0.46	1.07	0.48	1.74	1.26	0.70	1.40	0.70
VS	6	1.25	0.89	1.23	0.21	2.53	2.32	0.40	1.90	1.50
RX	6	2.14	1.91	1.38	0.73	5.70	4.97	0.79	2.89	2.10
RN	6	1.14	0.46	1.13	0.66	1.86	1.20	0.67	1.42	0.75
RV	6	1.11	0.82	0.89	0.18	2.22	2.04	0.51	1.99	1.49
RC	6	0.76	0.58	0.61	0.18	1.76	1.58	0.39	1.05	0.67
RS	6	0.73	0.68	0.46	0.34	2.10	1.76	0.43	0.58	0.16
RS*	5	0.45	0.09	0.43	0.34	0.58	0.24	0.43	0.49	0.07

Rat codes for outliers and extreme outliers are located above or below the respective blue crosses (+) and red dots (•), which correspond to data point values listed in the table directly below the graph. The vertical dashed line in the box-whisker graphic representation separates original dose group box-whiskers from those that have had the extreme outliers excluded, which are also indicated by the asterisk (*) following the dose group code. Data sets with excluded data points are designated in green text. Rats were treated with NN = no dose regimen, VX = vehicle and sacrificed, VN = vehicle and no dose, VV = vehicle and vehicle, VC = vehicle and CoQ_{10}, VS = vehicle and succinate, RX = rotenone and sacrificed, RN = rotenone and no dose, RV = rotenone and vehicle, RC = rotenone and CoQ_{10}, RS = rotenone and succinate. EXCL = excluded data point, IQR = inter-quartile range, Min = minimum data point value, Max = maximum data point value, NAD/NADH = ratio of oxidised to reduced nicotinamide adenine dinucleotide, SD = standard deviation.

The data indicates that one extreme outlier was present in dose group RS. Rat RS-3 harboured a skeletal muscle NAD/NADH ratio of 2.10, which was more than three and half times greater than the next ranked data point of RS-2 that had a ratio of 0.58. Since the core data points of RS were well clustered within a narrow IQR of 0.16, the criteria for outlier analysis were highly stringent with the upper outlier boundary being positioned at a ratio of 1.06. The exclusion of RS-3 resulted in a mean decrease from 0.73 to 0.45, and a SD decrease from 0.68 to 0.09. The median decreased from only 0.46 to 0.43, while the IQR adjusted from 0.16 to 0.07.

It can be observed from the box-whisker plots presented in Table 5.95.A that distinctive variations in NAD/NADH ratios do not exist, based on the fact that data distributions for all dose groups overlapped considerably with the environmental controls NN. It may be argued that dose group RS is the only group that appears to differ from NN. In order to evaluate the statistical significance of differences between the dose groups, ANOVA and multiple comparison procedures were utilised. Results of these tests are presented in Table 5.96.

Table 5.96 Multiple comparison statistics of the skeletal muscle NAD/NADH ratio data generated from the rat main study

A: Non-parametric (original data set) and parametric (excluding extreme outliers) p-values											
Dose group	**NN**	**VX**	**VN**	**VV**	**VC**	**VS**	**RX**	**RN**	**RV**	**RC**	**RS**
NN		1.000	1.000	1.000	1.000	1.000	1.000	1.000	1.000	1.000	1.000
		1.000	0.810	1.000	0.978	0.998	0.999	0.990	0.986	0.767	0.517
VX	1.000		0.924	1.000	1.000	1.000	1.000	1.000	1.000	0.607	0.311
	1.000		0.643	1.000	0.917	0.984	1.000	0.953	0.938	0.591	0.358
VN	1.000	0.924		1.000	1.000	1.000	1.000	1.000	1.000	1.000	1.000
	0.810	0.643		0.859	1.000	0.999	0.291	1.000	1.000	1.000	1.000
VV	1.000	1.000	1.000		1.000	1.000	1.000	1.000	1.000	1.000	0.924
	1.000	1.000	0.859		0.988	0.999	0.997	0.995	0.993	0.822	0.579
VC	1.000	1.000	1.000	1.000		1.000	1.000	1.000	1.000	1.000	1.000
	0.978	0.917	1.000	0.988		1.000	0.619	1.000	1.000	1.000	0.990
VS	1.000	1.000	1.000	1.000	1.000		1.000	1.000	1.000	1.000	1.000
	0.998	0.984	0.999	0.999	1.000		0.822	1.000	1.000	0.997	0.946
RX	1.000	1.000	1.000	1.000	1.000	1.000		1.000	1.000	1.000	1.000
	0.999	1.000	0.291	0.997	0.619	0.822		0.704	0.666	0.253	0.134
RN	1.000	1.000	1.000	1.000	1.000	1.000	1.000		1.000	1.000	1.000
	0.990	0.953	1.000	0.995	1.000	1.000	0.704		1.000	1.000	0.979
RV	1.000	1.000	1.000	1.000	1.000	1.000	1.000	1.000		1.000	1.000
	0.986	0.938	1.000	0.993	1.000	1.000	0.666	1.000		1.000	0.985
RC	1.000	0.607	1.000	1.000	1.000	1.000	1.000	1.000	1.000		1.000
	0.767	0.591	1.000	0.822	1.000	0.997	0.253	1.000	1.000		1.000
RS	1.000	0.311	1.000	0.924	1.000	1.000	1.000	1.000	1.000	1.000	
	0.517	0.358	1.000	0.579	0.990	0.946	0.134	0.979	0.985	1.000	
B: ANOVA p-values											
Kruskal-Wallis p-value = 0.079						One-way ANOVA p-value = 0.069					

A: All comparison statistics are indicated as p-values. The upper p-value is the non-parametric multiple comparison test statistic, generated from the original set of data. The lower p-value was generated via the parametric Tukey *unequal number HSD* (Honestly Significant Difference) test, after the exclusion of extreme outliers. P-values in grey, indicate that no significant differences exist. B: P-values for the non-parametric Kruskal-Wallis ANOVA and parametric one-way ANOVA are listed. Rats were dosed NN = no dose and no dose, VX = vehicle and sacrificed, VN = vehicle and no dose, VV = vehicle and vehicle, VC = vehicle and CoQ_{10}, VS = vehicle and succinate, RX = rotenone and sacrificed, RN = rotenone and no dose, RV = rotenone and vehicle, RC = rotenone and CoQ_{10}, RS = rotenone and succinate. ANOVA = analysis of variance.

P-values in Table 5.96 reveal that no statistically significant differences in skeletal muscle NAD/NADH ratios occurred between any of the dose groups of the rat main study. The Kruskal-Wallis and one-way ANOVA p-values were both greater than the 0.05 significance level, indicating that the presence of the extreme outlier did not significantly influence the global variation within the data set. These statistics are well complemented by the multiple comparison p-values that also indicated none of the NAD/NADH ratios from the 11 dose groups to differ significantly from each other, prior to and after the exclusion of the extreme outlier RS-3. The previously mentioned comment that only dose group RS may differ from the environmental controls NN is not statistically supported. The grey appearance of the multiple comparison grid correlates well with the overlapping box-whisker plots representing the NAD/NADH data generated from skeletal muscle.

Finally, a factorial ANOVA was performed on the NAD/NADH ratio data in order to investigate the contributions of the various dose factors. The presence of an extreme outlier necessitated that the data be analysed via the inclusion and exclusion of the aforementioned data point. Table 5.97 depicts graphic summaries of the two-way ANOVA with corresponding F-statistics and p-values. The 95% confidence interval and mean data points are listed in addition to the graphic representations.

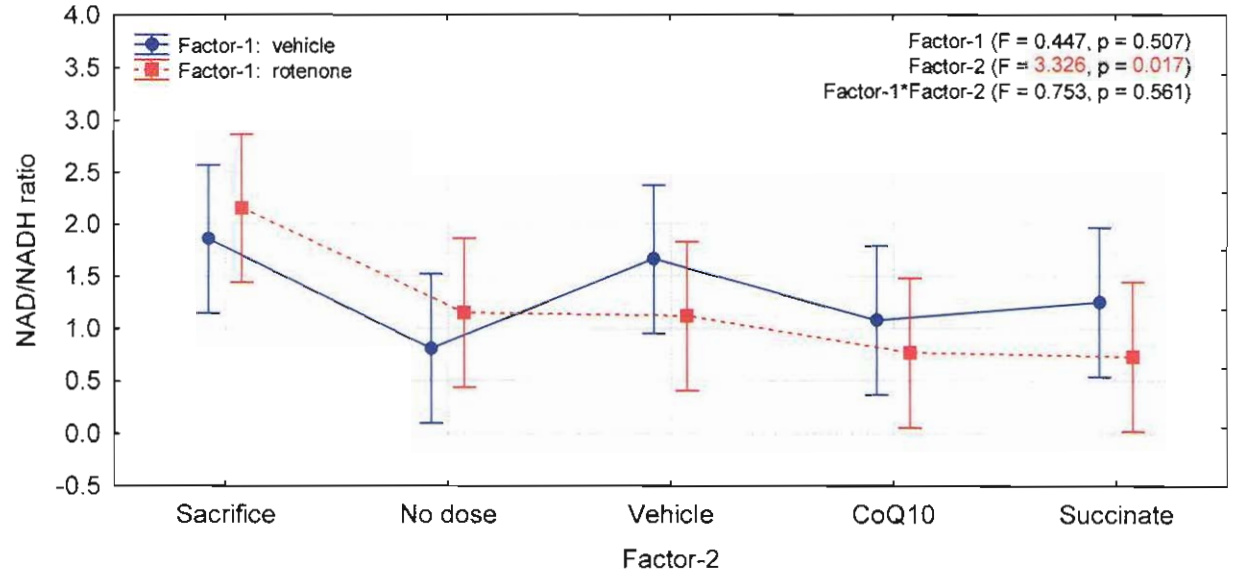
Sections A and B of Table 5.97 illustrate that Factor-1 vehicle and rotenone plots similarly display overall decreasing trends in mean NAD/NADH ratios. Whether the extreme outlier was included or not, it was determined by the two-way ANOVA that Factor-2 dose regimens contributed statistically significantly to the NAD/NADH ratios in skeletal muscle. Upon exclusion of RS-3, the Factor-1 and interaction F-statistics increased slightly, but neither to a statistically significant level. The fact that the two-way ANOVA reported no statistical significance for Factor-1 indicates that responses in rats were very similar, regardless of whether they received a vehicle or rotenone Factor-1 dose.

The statistically significant p-values for Factor-2 are indicative of the fact that any variations observed between dose groups can be predominantly accounted for by dose regimens received on days 15 and 16. Therefore, the decreased mean NAD/NADH ratio observed for dose group RS, when compared to RX primarily, can be argued to be accounted for by the Factor-2 treatment of succinate. It can be argued that succinate contributed to the respiratory chain by supplying electrons via complex II and in turn decreasing the stress load on the already deficient complex I. Therefore, mitochondria did not require that complex I enzymes function optimally, resulting in the increased levels in NADH and consequently lowered NAD/NADH ratios.

The primary goal of the utilisation of succinate for a therapeutic benefit was to drive complex I circumvention and alleviate stress on the enzyme. It may therefore be deduced from the data presented here that complex I was indeed circumvented. However, since dose group RC also presented with a lowered NAD/NADH ratio, it is apparent that CoQ_{10} may have also alleviated stress load from complex I.

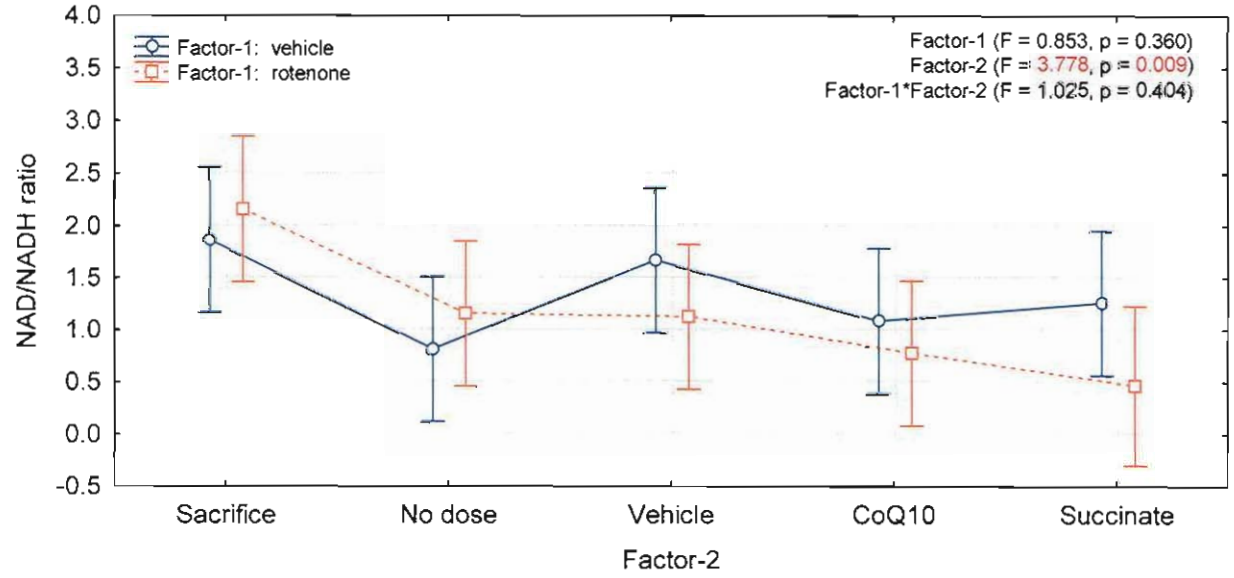
Table 5.97 Graphic and tabulated summary of the skeletal muscle NAD/NADH ratio data analysed via a two-way ANOVA

A: Data set including extreme outliers



Description		VX	VN	VV	VC	VS	RX	RN	RV	RC	RS
With extreme outliers	UCI	2.57	1.51	2.37	1.79	1.96	2.86	1.85	1.82	1.47	1.44
	mean	1.85	0.80	1.66	1.08	1.25	2.14	1.14	1.11	0.76	0.73
	LCI	1.14	0.09	0.95	0.36	0.54	1.43	0.43	0.40	0.05	0.02

B: Data set excluding extreme outliers



Description		VX	VN	VV	VC	VS	RX	RN	RV	RC	RS
Without extreme outliers	UCI	2.55	1.50	2.36	1.77	1.95	2.84	1.84	1.81	1.46	1.22
	mean	1.85	0.80	1.66	1.08	1.25	2.14	1.14	1.11	0.76	0.45
	LCI	1.16	0.11	0.96	0.38	0.55	1.45	0.45	0.42	0.07	-0.31

The plot legends for each graph are indicated in the top left corners of the respective graphs, while the two-way ANOVA F-statistics (F) and p-values (p) for Factor-1, Factor-2 and Factor-1*Factor-2 are located in the top right corner, with the statistically significant values indicated in red. The vertical whiskers at each mean data point represent 95% confidence intervals for the respective data sets. The mean values in green text, located in the data point summary tables below the graphs, indicate those that were adjusted due to the exclusion of extreme outliers. Rats were treated with NN = no dose regimen, VX = vehicle and sacrificed, VN = vehicle and no dose, VV = vehicle and vehicle, VC = vehicle and CoQ_{10}, VS = vehicle and succinate, RX = rotenone and sacrificed, RN = rotenone and no dose, RV = rotenone and vehicle, RC = rotenone and CoQ_{10}, RS = rotenone and succinate. LCI = lower 95% confidence interval data point, NAD/NADH = ratio of oxidised to reduced nicotinamide adenine dinucleotide, UCI = upper 95% confidence interval data point.

The graphic representations in Table 5.97 illustrate that CoQ_{10} and succinate did not improve ratios of NAD to NADH in skeletal muscle. The lowered ratios in dose groups RC and RS is suggestive of the therapeutic regimens not alleviating redox status, in terms of the ratio of NAD and NADH. The same argument holds true for rat groups that received vehicle Factor-1 doses and present with NAD/NADH ratios that do not fluctuate by statistically significant amounts from each other.

5.6.6 Skeletal muscle profile of the rat main study

The skeletal muscle profile was evaluated via the inclusion of five biochemical data sets, namely complex I, antioxidant capacity, L/P, ATP/ADP and the NAD/NADH data set. The fluctuations in median percentages of the various data sets in relation to the environmental control dose group NN are presented graphically and in grid format in Table 5.98.

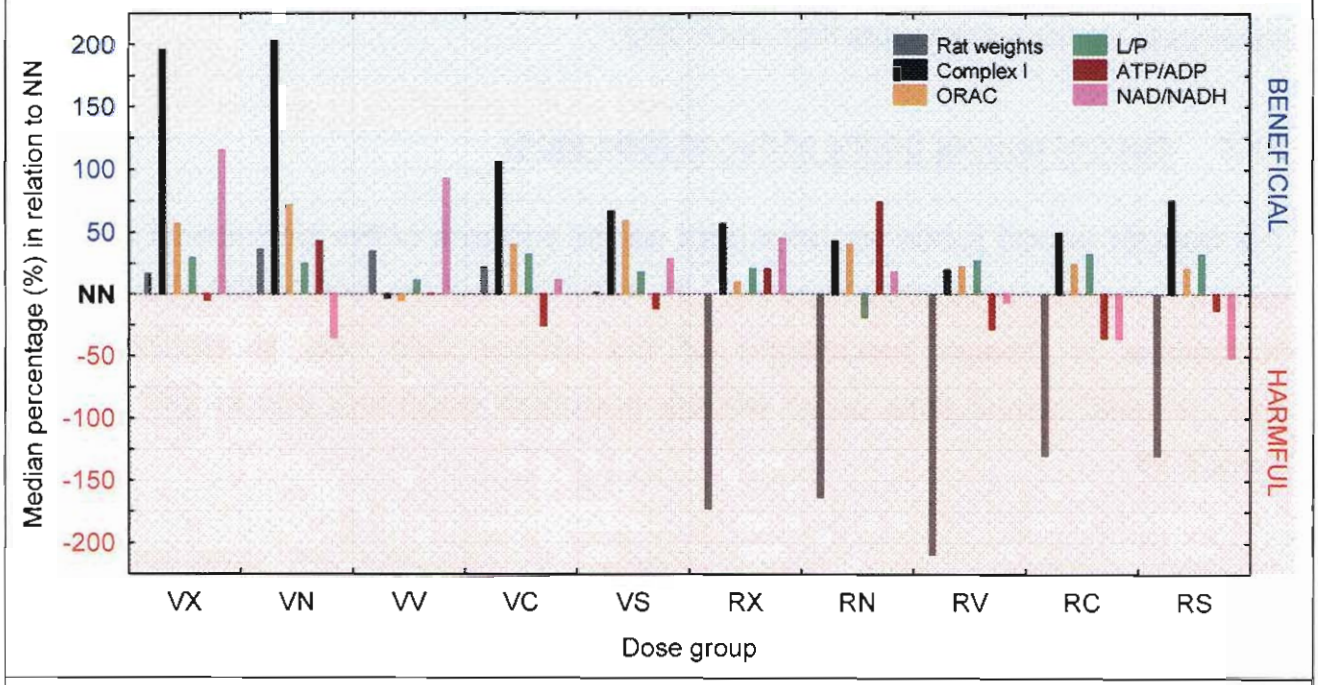
Complex I activities generated from skeletal muscle presented with increased variation amongst the rat groups that received vehicle Factor-1 dose regimens than in rats that received rotenone. Rat groups VX and VN presented with increased complex I activities that were 196% and 203% higher than the environmental control dose group NN. Moreover, these two dose groups differed statistically significantly from NN, indicating that the vehicle improved activity of the respiratory chain enzyme. The argument is strengthened by the fact that dose groups VC and VS also presented with increased complex I activities that improved by more than 65%. However, the notion that sunflower oil improved complex I activity is disputed, due to the unaltered complex I activity for dose group VV, which deviated by a mere -3.09%.

The rotenone-treated rats all presented with increased median percentage complex I activities, in relation to dose group NN, suggesting that rotenone did not inhibit complex I in skeletal muscle. This is supported by data presented in Section 5.6.1.1, where skeletal muscle complex I activities in the pilot study were not determined to differ statistically significantly from each other. However, by carefully evaluating the median percentages of the rotenone-treated rats in comparison to the vehicle Factor-1 treated rats, it can be argued that rotenone may well have appeared to induce a Complex I deficiency. The statistically significant Factor-1 reported by the two-way ANOVA strengthens the argument. Nonetheless, as presented in Table 5.98.B, none of the rotenone-treated rats

were determined to present with a statistically significant Complex I deficiency when compared to NN, as was the case in the rat pilot study, presented in Section 5.6.1.1.

Table 5.98 Skeletal muscle profile of response generated from the rat main study indicating the beneficial and harmful effects of the dose regimens

A: Graphic representation



B: Median percentage (%) grid and factorial ANOVA summary

Data set	Dose group										Factorial ANOVA		
	VX	VN	VV	VC	VS	RX	RN	RV	RC	RS	F1	F2	F1*F2
Rat weights	16.9	36.4	35.1	22.1	1.30	-173	-164	-209	-130	-130	s/s	n/n	s/s
Complex I	196	203	-3.09	106	66.9	56.9	43.4	20.0	49.9	75.2	s	n	n
AC	57.0	71.9	-5.41	40.2	59.3	10.0	40.3	22.5	24.6	20.9	n/n	n/n	n/n
L/P	29.1	24.5	10.9	32.0	17.5	20.2	-19.3	26.9	32.2	31.9	n/n	n/n	n/n
ATP/ADP	-5.12	43.1	-0.24	-25.7	-11.7	20.4	73.8	-28.7	-36.0	-13.0	n/n	s/s	n/n
NAD/NADH	115	-35.6	92.6	11.7	28.5	44.5	17.9	-6.64	-36.5	-51.7	n/n	s/s	n/n

A: Percentage bars denote either beneficial or harmful effects induced by the dose regimens. Each bar is colour coded to represent the various data sets, as indicated by the graphic key in the top right corner of the graph. The 0% line on the Y-axis is labelled **NN**, since all median percentages were calculated to deviate from the environmental controls NN. B: The percentage data points are listed in correspondence with the bar heights. Median percentages that deviate by more than 10% from the environmental controls NN are indicated in blue and red text for beneficial and harmful deviations respectively. Percentages in grey text represent deviations less than 10%. Grid blocks shaded in green represent comparisons from the original set of data that were presented in previous sections to differ statistically and biologically significantly from the environmental controls NN. Comparisons determined to differ significantly after the exclusion of extreme outliers are indicated by yellow shading. Statistically significant (s) and non-significant (n) contributions of Factor-1 (F1) and Factor-2 (F2) dose regimens as well as the interaction (F1*F2) are indicated alongside the median percentage grid. Two symbols are indicated if extreme outliers were determined to be present in the respective data set, with the first symbol value representing significance status prior to exclusion, followed by the second symbol representing significance status after exclusion of extreme outliers. Rats were treated with NN = no dose regimen, VX = vehicle and sacrificed, VN = vehicle and no dose, VV = vehicle and vehicle, VC = vehicle and CoQ_{10}, VS = vehicle and succinate, RX = rotenone and sacrificed, RN = rotenone and no dose, RV = rotenone and vehicle, RC = rotenone and CoQ_{10}, RS = rotenone and succinate. AC = antioxidant capacity, ATP/ADP = ratio of adenosine triphosphate to adenosine diphosphate, L/P = ratio of lactate to pyruvate, NAD/NADH = ratio of oxidised to reduced nicotinamide adenine dinucleotide.

As discussed in Section 5.6.1.2, the main study environmental control dose group NN harboured a lowered complex I activity that differed statistically significantly from N, the environmental control dose group of the rat pilot study. As presented for the brain profile

data in Section 5.5.5, the complex I activity for dose group NN was also discussed and observed to be lower than all the other dose groups in the data set. Fortunately, the enzyme activities for comparative dose groups of the rat pilot and main studies, namely V and VX as well as R15 and RX, did not differ statistically significantly. This confirmed that NN might have presented with a lowered skeletal muscle complex I activity. Therefore, it may also be that the median complex I activities presented in Table 5.98.B are over-estimated and hence mostly portrayed to be beneficial responses to the dose regimens. Nevertheless, as discussed previously in this paragraph, the differences were not determined to be of statistical significance. Consequently, the impact of rotenone and Factor-2 dose regimens did not result in significant deviations of skeletal muscle complex I activity.

Antioxidant capacity in skeletal muscle was reported in all dose groups to be improved by more than 10% over the environmental controls NN, except for dose group VV. This is indicative of the fact that the vitamin E content of the sunflower oil vehicle contributed to improving antioxidant capacity. This notion is further supported by the factorial ANOVA that resulted in non-significant Factor-1 and Factor-2 statistics. The non-significant Factor-1 statistic in addition confirms that rotenone did not additionally influence antioxidant capacity, even though it induced a Complex I deficiency. However, it can be argued that rotenone may have compromised the antioxidant capacity in skeletal muscle. With the exception of dose group VV, the median percentages for VX, VN, VC and VS ranged between 40.2% and 71.9%, whereas the median percentages for the rotenone-treated rats ranged between 10.0% and 40.3%.

As with the antioxidant capacity data, the L/P ratios for skeletal muscle did not vary considerably from each other. Furthermore, non-significant Factor-1 and Factor-2 statistics were reported by the factorial ANOVA. The fact that Factor-1 was not significant is suggestive of rotenone not contributing to variation in the L/P ratios of skeletal muscle. Rat group RN was the only group that presented with a lowered median percentage L/P ratio in skeletal muscle when compared to the environmental controls NN. Rat group RN did however not differ statistically significantly from any of the dose groups. In overview, it was observed that L/P ratios improved by more than 10% in all dose groups, with the previously mentioned exception of RN. The improved L/P ratios in skeletal muscle were therefore argued to be due to the contribution of the sunflower oil vehicle, even though this argument is not supported statistically. This notion is however not supported by multiple comparison data, presented in Section 5.6.3, as well as the factorial ANOVA statistics that

reported no statistically significant differences nor statistically significant Factor-1 and Factor-2 statistics, respectively.

The ATP/ADP ratios generated from skeletal muscle presented with a considerable degree of variation. Dose groups VX and VV harboured ATP/ADP ratios that were equivalent to the environmental controls NN. Dose group VN presented with a considerably improved ratio of 43.1%, suggesting that the no dose recovery on days 15 and 16 was more beneficial to rat skeletal muscle ATP/ADP ratios. Dose group VC and VS harboured final ATP/ADP ratios that were both more than 10% lower than NN. This is suggestive of the fact that the therapeutic regimens CoQ_{10} and succinate may have harmfully reduced skeletal muscle ATP/ADP ratios. However, upon evaluation of the rotenone-treated rats, it can be observed that dose groups RV, RC and RS similarly harboured skeletal muscle ATP/ADP ratios that were lowered by more than 10% of NN. Therefore, it could also be argued that CoQ_{10} and succinate was not able to relieve or improve skeletal muscle ATP/ADP ratios. Rat groups that received vehicle Factor-1 doses indicated that vehicle itself did not alter ATP/ADP ratios in skeletal muscle, except when the Factor-2 dose regimen was changed. Furthermore, the factorial ANOVA resulted in a statistically significant Factor-2 contribution, thus supporting the aforementioned notion. As with the vehicle Factor-1 treated rats, the rats also portrayed that a no dose recovery on days 15 and 16 was more beneficial to skeletal muscle ATP/ADP ratios when compared to other Factor-2 dose regimens.

The skeletal muscle pyridine data indicated that the sunflower oil vehicle might have contributed to lowering NADH levels and hence increasing NAD/NADH ratios. Dose groups VX, VV, VC and VS all presented with increased NAD/NADH ratios, as opposed to dose group VN that harboured a skeletal muscle NAD/NADH ratio that was calculated to be -35.6% lower than the environmental control dose group median. Among the rotenone-treated rat groups, RX and RN presented with raised skeletal muscle NAD/NADH ratios, an unexpected result. A deficiency in complex I should in theory result in increased NADH concentrations, since decreased amounts of the reduced form would be oxidised by complex I. Dose group RV presented with an unchanged skeletal muscle NAD/NADH ratio, while dose groups RC and RS both harboured decreased final ratios. The fact that the factorial ANOVA reported a statistically significant Factor-2 contribution, it can be agreed that the ratios were varied primarily due to the dose regimens received on days 15 and 16. However, as reported in Section 5.6.5, it was observed that none of the dose groups differed statistically significantly from each other. Therefore, although

variation may be observed between certain dose groups, it cannot be argued with confidence that dose regimens improved or harmfully affected NAD/NADH ratios in skeletal muscle. It may seem apparent though that the sunflower oil vehicle had an influence on the NAD/NADH ratios. These ratios can also be altered by the influence of other enzymes, like pyruvate dehydrogenase for example. This enzyme functions to import pyruvate into the mitochondria and plays a major role in the control of pyridine concentrations. Therefore, the influence of sunflower oil and its constituents on other enzymes and mechanisms in the control of the NAD/NADH ratio cannot be excluded.

In overview of the global effects of the dose regimens on the skeletal muscle biochemical profiles, it may be argued that skeletal muscle benefited far more than it was harmed. The rat groups that received a vehicle Factor-1 dose presented with 18 median percentages that improved (indicated in blue), while only three represented harmful effects (coloured in red). The rotenone-treated rats also presented with 18 median percentages coloured in blue and hence indicated beneficial effects, but also with five indicating parameters that were affected harmfully, as coloured in red. It could therefore be argued that rotenone did not influence the biochemical profile in skeletal muscle to a greater degree than the sunflower oil vehicle. As discussed previously in this section, the complex I activities of skeletal muscle may have appeared to be elevated to some extent due to the fact that the environmental control dose group presented with a speculated decreased complex I activity. Therefore, it may certainly be argued that additional rat groups could have portrayed a less overwhelming blue appearance, as currently displayed by the median percentage grid of Table 5.98.B. Nonetheless, the skeletal muscle data is indicative of a limited variation in biochemical parameters, supported by a lack of statistically significant differences when compared to the environmental control dose group NN.

5.6.6.1 Impact of coenzyme Q10 and succinate on rat skeletal muscle

The effects of CoQ_{10} and succinate were evaluated in skeletal muscle among the rats harbouring either a rotenone-induced Complex I deficiency or not. Rat groups VC and VS, which received sunflower oil vehicle as a Factor-1 dose regimen, presented with similar response profiles. Since dose group VC harboured a median percentage complex I activity of 106% as opposed to the 66.9% of VS, it can be argued that CoQ_{10} may have contributed to the improvement of complex I activity, more so than succinate. It can also be speculated that CoQ_{10} was more beneficial to improving skeletal muscle L/P

ratios, since VC presented with a 32.0% improved L/P ratio that was almost double that of the 17.5% of VS. Succinate appeared to be more beneficial in improving antioxidant capacity, ATP/ADP and NAD/NADH ratios in rats receiving a rotenone Factor-1 dose. However, the differences were subtle on most occasions and not supported by statistical significance. Therefore, it has been illustrated once again that CoQ_{10} and succinate appear to improve different components of the biochemical profile and to varying degrees. The lack of statistical significance between the comparisons observed within the skeletal muscle profile allows for only speculations as to the benefits of these therapeutic regimens.

In view of the rat groups harbouring the rotenone-induced Complex I deficiency, CoQ_{10} and succinate once again illustrated a similar pattern of response. It could be argued that succinate aided more in the recovery of complex I activity due to the fact that RS presented with a median percentage that was 75.2% improved, in contrast to the 49.9% improvement recorded for RC. The antioxidant capacity and L/P ratios in skeletal muscle were recorded to have improved equivalently by more than 20%, whether CoQ_{10} or succinate were administered as a Factor-2 dose. As discussed in the previous section, ATP/ADP ratios of skeletal muscle did not appear to have benefited from either of the therapeutic regimens. However, rat group RS did harbour a final skeletal muscle ATP/ADP ratio that was not as severely affected as that of RC, suggesting that succinate may have been more beneficial. The fact that RV presented with an ATP/ADP ratio that was almost as low as RC and that succinate was transported in a Milli-Q® water vehicle, it could be speculated that the sunflower oil vehicle Factor-2 dose may have contributed to the compromised recovery in skeletal muscle ATP/ADP ratios. Concerning the NAD/NADH ratios, although the difference is not significant, CoQ_{10} could be argued to be more beneficial to skeletal muscle status in rotenone-treated rats. In summary, due to the lack of statistically significant differences reported between dose groups, it was noted that the skeletal muscle biochemical profile was not influenced to a large degree by the various dose regimens implemented in this study. Skeletal muscle appeared to be more resistant to fluctuations in the biochemical parameters and hence did not allow for concrete deductions regarding the benefits and harmful effects of dose regimens. Nonetheless, based on the data presented in this section, it could be argued that the CoQ_{10} and succinate induced varying response profiles in rat skeletal muscle.

5.7 RAT LIVER DATA

The liver organs were removed from rats upon sacrificing and evaluated for organ weight, followed by the appropriate preparation for the various assays to be performed. The data generated from the assays were collected in Excel® spreadsheets and exported to STATISTICA™ for statistical analysis. Raw data generated from liver tissue during the rat pilot and main studies are presented in Appendix Chapters B to G.

5.7.1 Liver weights

Upon sacrificing the rats, liver organs were removed and weights determined. As with heart and brain weight data, liver weights were recorded during the rat pilot study to verify whether adverse effects were encountered by the various rotenone dose concentrations. In addition, recording and evaluating liver weights in the pilot study verified whether it would be of use to do so in the rat main study. As discussed in subsequent sections, rats receiving the higher concentrations of rotenone appeared to present with decreased liver weights.

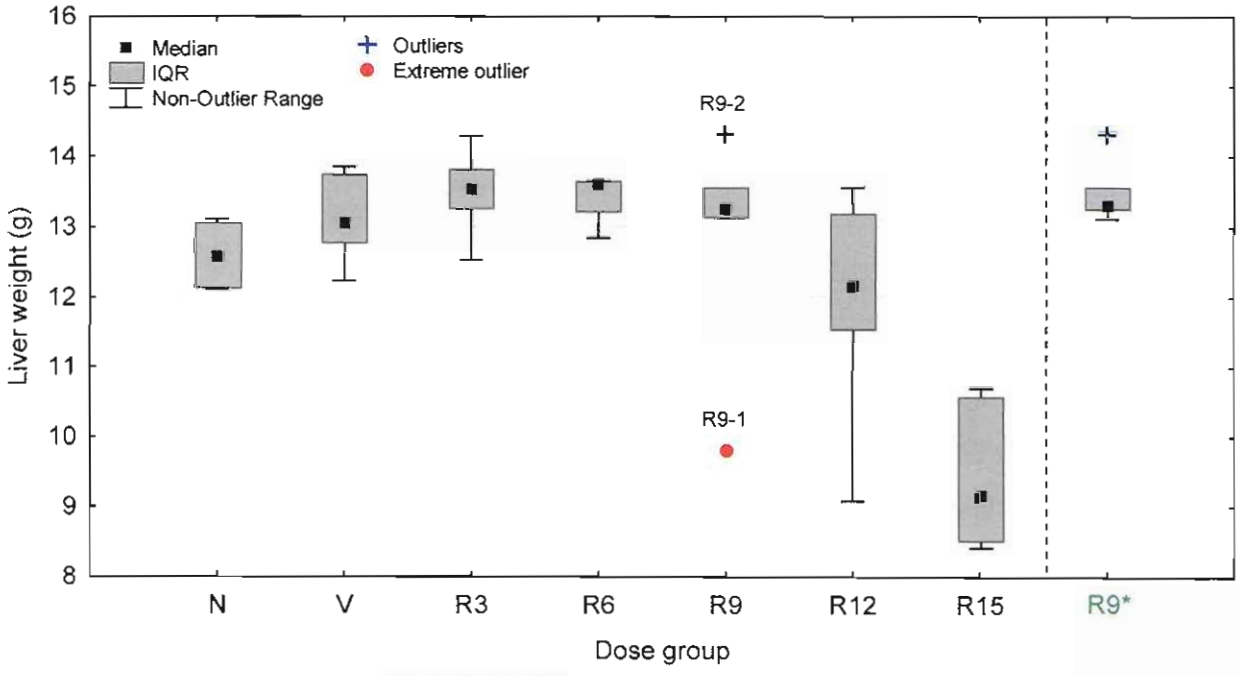
5.7.1.1 Rat pilot study liver weights

Liver weights were recorded and captured in Excel® format. The data was subsequently exported to STATISTICA™ for statistical evaluation. Table 5.99 presents a box-whisker representation of the data, a complete listing of data points as well as a table of descriptive statistics.

Before discussing the liver weight data generated from the pilot study, it should be noted that an additional data point was recorded as missing. The liver weight for rat R6-4 was not recorded due to accidental tissue preparation prior to recording of the total weight of the organ. Table 5.99.A illustrates that two outliers and one extreme outlier were determined to be present in the pilot study liver weight data. Of the two outliers, one was classified only after the exclusion of the extreme outlier from dose group R9, and will therefore not be discussed. The second outlier, R9-2, presented with the highest liver weight amongst all of the pilot study rat groups, namely 14.3 g. However, since the four data points that constitute the IQR are narrowly clustered and not too distant from the outlier R9-2, it would not be expected that the inclusion or exclusion of the outlier would markedly alter the central tendency statistics for R9. Regardless, R9-2 is not positioned within the extreme outlier range and will therefore not be excluded.

Table 5.99 Box-whisker representation and descriptive statistics of the rat liver weight data generated from the pilot study

A: Box-whisker plots and data points according to rat groups



Rat	N	V	R3	R6	R9	R12	R15	R9*
1	12.1	12.9	14.3	13.6	• 9.77	13.2	9.23	EXCL
2	13.1	12.2	13.5	13.7	+ 14.3	12.0	9.04	14.3
3	12.2	13.9	13.3	13.2	13.1	13.6	10.7	13.1
4	12.9	13.2	—	—	13.5	11.5	8.39	13.5
5	13.1	13.7	13.8	12.8	13.3	9.08	8.50	13.3
6	12.1	12.8	12.5	13.6	13.2	12.3	10.5	13.2

B: Descriptive statistics

Dose group	Sample size	Mean	SD	Median	Min	Max	Range	Lower quartile	Upper quartile	IQR
N	6	12.6	0.48	12.6	12.1	13.1	0.99	12.1	13.1	0.91
V	6	13.1	0.61	13.0	12.2	13.9	1.61	12.8	13.7	0.96
R3	5	13.5	0.65	13.5	12.5	14.3	1.75	13.3	13.8	0.55
R6	5	13.4	0.35	13.6	12.8	13.7	0.80	13.2	13.6	0.43
R9	6	12.9	1.58	13.3	9.77	14.3	4.54	13.1	13.5	0.41
R9*	5	13.5	0.48	13.3	13.1	14.3	1.19	13.2	13.5	0.30
R12	6	11.9	1.59	12.2	9.08	13.6	4.48	11.5	13.2	1.65
R15	6	9.39	0.99	9.13	8.39	10.7	2.27	8.5	10.5	2.04

Rat codes for outliers and extreme outliers are located above or below the respective blue crosses (+) and red dots (•), which correspond to data point values listed in the table directly below the graph. The vertical dashed line in the box-whisker graphic representation separates original dose group box-whiskers from those that have had the extreme outliers excluded, which are also indicated by the asterisk (*) following the dose group code. Data sets with excluded data points are designated in green text. Rats were treated with N = no dose, V = vehicle, R3 = rotenone 3 $mg.kg^{-1}.day^{-1}$, R6 = rotenone 6 $mg.kg^{-1}.day^{-1}$, R9 = rotenone 9 $mg.kg^{-1}.day^{-1}$, R12 = rotenone 12 $mg.kg^{-1}.day^{-1}$, R15 = rotenone 15 $mg.kg^{-1}.day^{-1}$. '---' = missing data points, g = gram, IQR = inter-quartile range, Min = minimum data point value, Max = maximum data point value, SD = standard deviation.

The extreme outlier R9-1 in dose group R9 presented with a liver weight of 9.77 g, which was certainly lower than the remaining five data points in the dose group. However, it was not completely aberrant since rats in dose group R15 all presented with liver weights in a

similar range. It is of importance to note that rat R9-1 was also the only rat in the R9 group that lost body weight over its 14-day dose period, as presented in Section 5.2.1. Therefore, it can be understood that the loss in body weight would be accompanied by a decreased liver weight. The exclusion of R9-1 resulted in a mean liver weight increase from 12.9 to 13.5 g and an SD decrease from 1.58 to 0.48 g. The median remained consistent at 13.3 g, while the IQR decreased from 0.41 to 0.30 g. The exclusion of the extreme outlier therefore certainly had an impact on the descriptive statistics for dose group R9.

The box-whisker representations reveal a trend in liver weights in response to the rotenone dose concentrations. Since the liver weights for V appeared to be slightly higher than that for the environmental controls N, it may be suggested that the sunflower oil vehicle contributed to the slight increase in liver weight. As presented in Section 5.4.1.1, heart weights also increased when rats received vehicle dose regimens. In addition, rat groups R3, R6 and R9 also presented with slightly increased liver weights. However, it should be observed that as the rotenone dose concentrations increased to 12 and 15 $mg.kg^{-1}.day^{-1}$, rats tended to present with lowered liver organ weights. In particular, rat group R15 revealed liver weight data points that were all almost exclusively lower than those attained for rats from the other six dose groups. The significance of the aforementioned changes in response to dose regimens was determined via the ANOVA and multiple comparison test procedures. Statistical p-values and biological d-values are presented in Table 5.100.

The multiple comparison grid in Table 5.100 reveals that the only group to differ statistically significantly from other groups was that of R15. Prior to the exclusion of the extreme outlier, dose group R15 differed statistically significantly from R3, R6 and R9. However, after the exclusion of R9-1, R15 differed statistically significantly from all dose groups included in the pilot study. Upon testing for biological significance of the statistically significant comparisons, it became evident that the differences were indeed also of biological significance. Therefore, the highest rotenone dose concentrations of 15 $mg.kg^{-1}.day^{-1}$ received by dose group R15 resulted in a marked decrease in liver weight, strongly supported by both statistical and biological significance.

Table 5.100 Multiple comparison statistics of the liver organ weight data generated from the rat pilot study

A: Non-parametric (original data set) and parametric (excluding extreme outliers) p-values

Dose group	N	V	R3	R6	R9	R12	R15
N		1.000	1.000	1.000	1.000	1.000	1.000
		0.942	0.668	0.772	0.653	0.831	< 0.001
V	1.000		1.000	1.000	1.000	1.000	0.050
	0.942		0.993	0.999	0.991	0.245	< 0.001
R3	1.000	1.000		1.000	1.000	0.901	0.006
	0.668	0.993		1.000	1.000	0.097	< 0.001
R6	1.000	1.000	1.000		1.000	1.000	0.009
	0.772	0.999	1.000		1.000	0.140	< 0.001
R9	1.000	1.000	1.000	1.000		1.000	0.028
	0.653	0.991	1.000	1.000		0.093	< 0.001
R12	1.000	1.000	0.901	1.000	1.000		1.000
	0.831	0.245	0.097	0.140	0.093		< 0.001
R15	1.000	0.050	0.006	0.009	0.028	1.000	
	< 0.001	< 0.001	< 0.001	< 0.001	< 0.001	< 0.001	

B: ANOVA p-values

Kruskal-Wallis p-value = 0.002	One-way ANOVA p-value < 0.001

C: Statistical and biological significance

Comparison		Statistical significance (p)		Biological significance (d)	
		Including EOs	Excluding EOs	Including EOs	Excluding EOs
N	R15	1.000	< 0.001	N/A	3.737
V	R15	0.050	< 0.001	N/A	4.330
R3	R15	0.006	< 0.001	4.131	4.761
R6	R15	0.009	< 0.001	4.030	4.645
R9	R15	0.028	< 0.001	3.515	4.773
R12	R15	1.000	< 0.001	N/A	2.968

A: All comparison statistics are indicated as p-values. The upper p-value is the non-parametric multiple comparison test statistic, generated from the original set of data. The lower p-value was generated via the parametric Tukey *unequal number HSD* (Honestly Significant Difference) test, after the exclusion of extreme outliers. P-values indicated in red are statistically significant at the pre-determined significance level of 0.05. P-values in black text represent those that are not statistically significant, but have complementary p-values that are statistically significant. The remainder of p-values are listed in grey. The comparisons surrounded by the **bold** black line are those that were determined to be statistically significant by both the non-parametric and parametric multiple comparison procedures. The turquoise shaded blocks represent statistically significant comparisons that were also determined to be of biological significance. B: P-values for the non-parametric Kruskal-Wallis ANOVA and parametric one-way ANOVA are listed, with significant p-values, less than the 0.05 significance level, indicated in red. C: List of comparisons determined to be statistically significant with corresponding biological significance. A d-value greater than or equal to 0.8 signifies biological significance, indicated in red. Rats were treated with N = no dose, V = vehicle, R3 = rotenone 3 $mg.kg^{-1}.day^{-1}$, R6 = rotenone 6 $mg.kg^{-1}.day^{-1}$, R9 = rotenone 9 $mg.kg^{-1}.day^{-1}$, R12 = rotenone 12 $mg.kg^{-1}.day^{-1}$, R15 = rotenone 15 $mg.kg^{-1}.day^{-1}$. < = less than, ANOVA = analysis of variance, EOs = extreme outliers, N/A = not applicable.

It appears that rotenone too had a similar impact on liver growth, as described for heart weight in Section 5.4.1.1, whereby it was proposed that rotenone inhibited complex I electron transfer, induced apoptosis and prevented mitotic events. In contrast to heart weights, the decreased liver weights were only encountered at the higher rotenone dose concentrations of 12 and 15 $mg.kg^{-1}.day^{-1}$. The raised threshold for inhibited liver growth may be explained by the fact that the liver harbours the highest concentration of cytochrome P450 enzymes that metabolise rotenone into its non-toxic metabolites. Therefore, it would be required that a high concentration of rotenone be administered to rats in order to outweigh the counteracting effects of cytochrome P450 biotransformation.

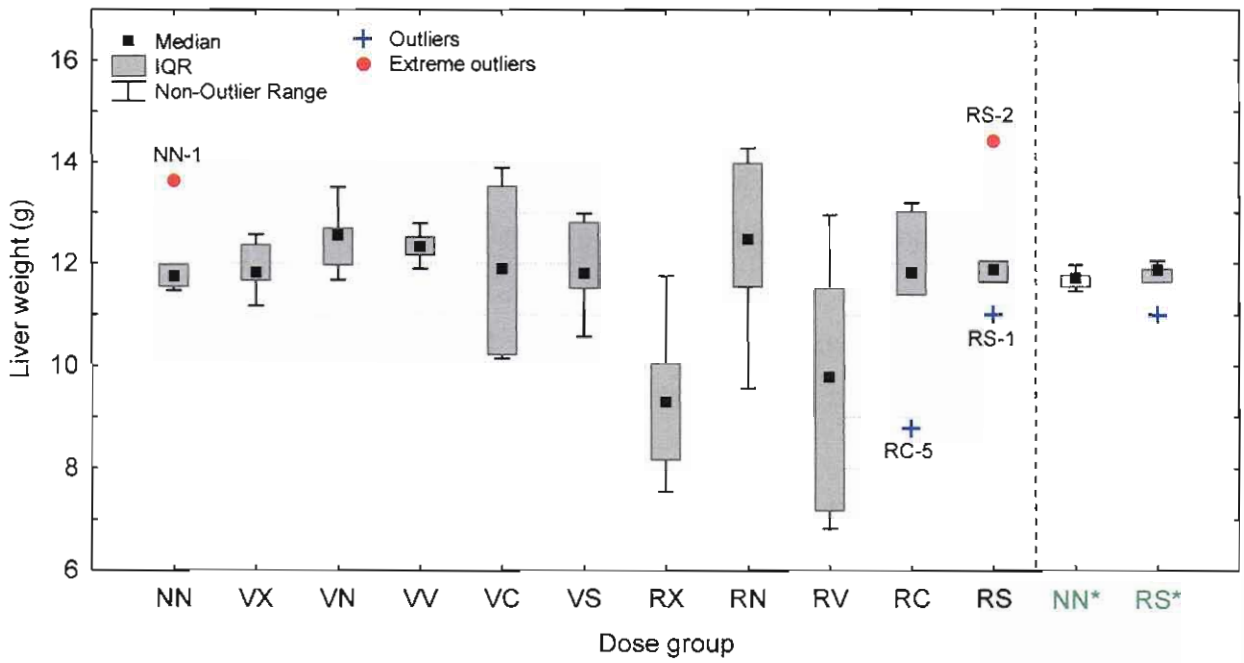
The significant impact of rotenone on liver weights observed from the rat pilot study resulted in the requirement that liver weights be recorded and statistically evaluated during the rat main study.

5.7.1.2 Rat main study liver weights

Liver weights of the rat main study were recorded upon sacrificing the rats and subsequently analysed for variations in response to dose regimens via the use of statistical test procedures. The distribution of liver weights recorded during the main study is presented in Table 5.101, along with a list of all the data points and a table of descriptive statistics.

Table 5.101 Box-whisker representation and descriptive statistics of the liver weight data generated from the main study

A: Box-whisker plots and data points according to rat groups



Rat	NN	VX	VN	VV	VC	VS	RX	RN	RV	RC	RS	NN*	RS*
1	• 13.7	12.4	12.4	12.2	13.9	11.5	11.8	14.0	8.47	11.5	+ 11.0	EXCL	11.0
2	11.5	12.6	12.0	12.3	10.2	11.9	8.17	12.5	11.5	13.2	• 14.4	11.5	EXCL
3	11.7	11.7	13.5	11.9	13.5	12.8	10.1	14.3	11.1	12.2	11.9	11.7	11.9
4	11.8	11.7	11.7	12.4	11.1	11.8	7.54	11.5	7.17	11.4	11.6	11.8	11.6
5	12.0	11.2	12.7	12.8	10.1	13.0	9.58	12.4	6.82	+ 8.79	11.9	12.0	11.9
6	11.6	11.9	12.7	12.5	12.7	10.6	9.02	9.57	13.0	13.0	12.1	11.6	12.1

B: Descriptive statistics

Dose group	Sample size	Mean	SD	Median	Min	Max	Range	Lower quartile	Upper quartile	IQR
NN	6	12.0	0.82	11.8	11.5	13.7	2.18	11.6	12.0	0.43
NN*	5	11.7	0.20	11.7	11.5	12.0	0.51	11.6	11.8	0.23
VX	6	11.9	0.51	11.8	11.2	12.6	1.40	11.7	12.4	0.69

Table 5.101 Continued...

Dose group	Sample size	Mean	SD	Median	Min	Max	Range	Lower quartile	Upper quartile	IQR
VN	6	12.5	0.64	12.6	11.7	13.5	1.83	12.0	12.7	0.72
VV	6	12.3	0.31	12.3	11.9	12.8	0.89	12.2	12.5	0.35
VC	6	11.9	1.66	11.9	10.2	13.9	3.74	10.2	13.5	3.29
VS	6	11.9	0.88	11.8	10.6	13.0	2.41	11.5	12.8	1.28
RX	6	9.36	1.49	9.31	7.55	11.8	4.21	8.18	10.1	1.88
RN	6	12.4	1.72	12.5	9.57	14.3	4.71	11.5	14.0	2.43
RV	6	9.68	2.53	9.79	6.83	13.0	6.14	7.18	11.5	4.35
RC	6	11.7	1.60	11.8	8.80	13.2	4.39	11.4	13.0	1.63
RS	6	12.2	1.17	11.9	11.0	14.4	3.41	11.7	12.0	0.40
RS*	5	11.7	0.40	11.9	11.0	12.1	1.02	11.7	11.9	0.24

Rat codes for outliers and extreme outliers are located above or below the respective blue crosses (+) and red dots (•), which correspond to data point values listed in the table directly below the graph. The vertical dashed line in the box-whisker graphic representation separates original dose group box-whiskers from those that have had the extreme outliers excluded, which are also indicated by the asterisk (*) following the dose group code. Data sets with excluded data points are designated in green text. Rats were treated with NN = no dose regimen, VX = vehicle and sacrificed, VN = vehicle and no dose, VV = vehicle and vehicle, VC = vehicle and CoQ_{10}, VS = vehicle and succinate, RX = rotenone and sacrificed, RN = rotenone and no dose, RV = rotenone and vehicle, RC = rotenone and CoQ_{10}, RS = rotenone and succinate. EXCL = excluded data point, g = gram, IQR = inter-quartile range, Min = minimum data point value, Max = maximum data point value, SD = standard deviation.

The box-whisker representation of the rat main study liver weight data revealed the presence of two outliers and two extreme outliers. The outliers will not be discussed in-depth since only extreme outliers were excluded from data sets. It should be noted though that the data point for RS-1 was not labelled for dose group RS*, the group which had an extreme outlier excluded. The second outlier, RC-5, was determined to be present in dose group RC and presented with a liver weight of 8.8 g. This data point was however distributed in a range similar to that of dose groups RX and RV, and was therefore not regarded as aberrant even though the remaining five data points in the group were positioned well above that of RC-5.

The first extreme outlier NN-1 presented with a liver weight of 13.7 g. Exclusion of NN-1 from the data set resulted in mean decrease from 12.0 to 11.7 g and an SD decrease from 0.82 to 0.20 g. The non-parametric counterparts of the median and IQR were adjusted to a lesser extent than the parametric mean and SD. The median decreased slightly from 11.8 to 11.7 g, while the IQR approximately halved from 0.43 to 0.23 g. The robustness of the non-parametric descriptive statistics is exemplified by the exclusion of NN-1. The second extreme outlier RS-2 resulted in a mean decrease from 12.2 to 11.7 g, while the SD decreased considerably from 1.17 to 0.40 g. Similarly, the non-parametric median remained unchanged at 11.9 g. The IQR for dose group RS decreased to 0.24 from 0.40 g. Therefore, exclusion of the extreme outliers certainly resulted in considerable adjustments to central tendency statistics and variation within the respective dose groups.

In view of the distribution of liver weight data points in Table 5.101.A, it can be observed that the variation in liver weights was far greater amongst the rat groups that received rotenone Factor-1 dose regimens. The consistency among dose groups VX through VS can be explained by the decreased requirement of the liver to metabolise dose regimens. In contrast, the rotenone-treated rats required not only the metabolism of rotenone itself, but also suffered biochemical consequences induced by the complex I inhibitor. In addition, it is not apparent whether CoQ_{10} or succinate improved liver organ weights in dose groups VC and VS. Although, it does appear that these therapeutic compounds did make a difference to liver weights based on the observed increase in variation. An improved evaluation of this matter was obtained upon analysing the data set via a factorial ANOVA, as presented in Table 5.103.

Liver weights recorded for rat groups RX, RN, RV, RC and RS proved to be more informative than the rat groups that received vehicle Factor-1 regimens. Dose group RX presented with considerably decreased liver weights when compared to the environmental controls NN. Rats from dose groups RN, RC and RS appeared to have recovered from the decreased liver weights induced by rotenone. This was however not the case for dose group RV, suggesting that the sunflower oil vehicle prevented liver weight restoration. Before further discussing the impact of the various dose regimens, it is required that the differences in liver weights be confirmed on statistical level. Table 5.102 presents p-values generated from the non-parametric and parametric ANOVA tests as well as multiple comparison data generated via the inclusion and exclusion of extreme outliers, respectively.

Prior to and after the exclusion of the extreme outliers, it was reported by the ANOVA tests that a difference was indeed present among the dose groups of the main study. The Kruskal-Wallis and one-way ANOVA resulted in p-values of 0.042 and < 0.001 respectively, both of which were below the predetermined significance level of 0.05. However, the complementing multiple comparison test for the non-parametric Kruskal-Wallis ANOVA did not reveal any statistically significant differences among the dose groups. This is in all likelihood accounted for by the presence of the extreme outliers. The parametric Tukey *unequal number HSD* test did however indicate that seven dose group comparisons were of statistical significance. Furthermore, the statistically significant differences were also determined to be of biological significance, as indicated by the d-values listed in Table 5.102.C.

Table 5.102 Multiple comparison statistics of the liver organ weight data generated from the rat main study

A: Non-parametric (original data set) and parametric (excluding extreme outliers) p-values											
Dose group	NN	VX	VN	VV	VC	VS	RX	RN	RV	RC	RS
NN		1.000 1.000	1.000 0.997	1.000 1.000	1.000 1.000	1.000 1.000	1.000 0.187	1.000 0.999	1.000 0.377	1.000 1.000	1.000 1.000
VX	1.000 1.000		1.000 0.999	1.000 1.000	1.000 1.000	1.000 1.000	1.000 0.054	1.000 1.000	1.000 0.147	1.000 1.000	1.000 1.000
VN	1.000 0.997	1.000 0.999		1.000 1.000	1.000 1.000	1.000 1.000	0.087 0.006	1.000 1.000	0.533 0.021	1.000 0.991	1.000 0.997
VV	1.000 1.000	1.000 1.000	1.000 1.000		1.000 1.000	1.000 1.000	0.119 0.011	1.000 1.000	0.690 0.037	1.000 0.998	1.000 1.000
VC	1.000 1.000	1.000 1.000	1.000 1.000	1.000 1.000		1.000 1.000	1.000 0.049	1.000 1.000	1.000 0.136	1.000 1.000	1.000 1.000
VS	1.000 1.000	1.000 1.000	1.000 1.000	1.000 1.000	1.000 1.000		1.000 0.052	1.000 1.000	1.000 0.141	1.000 1.000	1.000 1.000
RX	1.000 0.187	1.000 0.054	0.087 0.006	0.119 0.011	1.000 0.049	1.000 0.052		0.224 0.009	1.000 1.000	1.000 0.112	1.000 0.187
RN	1.000 0.999	1.000 1.000	1.000 1.000	1.000 1.000	1.000 1.000	1.000 1.000	0.224 0.009		1.000 0.031	1.000 0.997	1.000 0.999
RV	1.000 0.377	1.000 0.147	0.533 0.021	0.690 0.037	1.000 0.136	1.000 0.141	1.000 1.000	1.000 0.031		1.000 0.269	1.000 0.378
RC	1.000 1.000	1.000 1.000	1.000 0.991	1.000 0.998	1.000 1.000	1.000 1.000	1.000 0.112	1.000 0.997	1.000 0.269		1.000 1.000
RS	1.000 1.000	1.000 1.000	1.000 0.997	1.000 1.000	1.000 1.000	1.000 1.000	1.000 0.187	1.000 0.999	1.000 0.378	1.000 1.000	

B: ANOVA p-values	
Kruskal-Wallis p-value = 0.042	One-way ANOVA p-value < 0.001

C: Statistical and biological significance					
Comparison		Statistical significance (p)		Biological significance (d)	
		Including EOs	Excluding EOs	Including EOs	Excluding EOs
VN	RX	0.087	0.006	N/A	2.371
VN	RV	0.533	0.021	N/A	2.129
VV	RX	0.119	0.011	N/A	2.250
VV	RV	0.690	0.037	N/A	2.008
VC	RX	1.000	0.049	N/A	1.941
RX	RN	0.224	0.009	N/A	2.288
RN	RV	1.000	0.031	N/A	2.046

A: All comparison statistics are indicated as p-values. The upper p-value is the non-parametric multiple comparison test statistic, generated from the original set of data. The lower p-value was generated via the parametric Tukey *unequal number HSD* (Honestly Significant Difference) test, after the exclusion of extreme outliers. P-values indicated in red are statistically significant at the pre-determined significance level of 0.05. P-values in black text represent those that are not statistically significant, but have complementary p-values that are statistically significant. The remainder of p-values are listed in grey. The turquoise shaded blocks represent statistically significant comparisons that were also determined to be of biological significance. B: P-values for the non-parametric Kruskal-Wallis ANOVA and parametric one-way ANOVA are listed, with significant p-values, less than the 0.05 significance level, indicated in red. C: List of comparisons determined to be statistically significant with corresponding biological significance. A d-value greater than or equal to 0.8 signifies biological significance, indicated in red. Rats were dosed NN = no dose for 16 days, VX = vehicle and sacrificed, VN = vehicle and no dose, VV = vehicle and vehicle, VC = vehicle and CoQ_{10}, VS = vehicle and succinate, RX = rotenone and sacrificed, RN = rotenone and no dose, RV = rotenone and vehicle, RC = rotenone and CoQ_{10}, RS = rotenone and succinate. < = less than, ANOVA = analysis of variance, EOs = extreme outliers, N/A = not applicable.

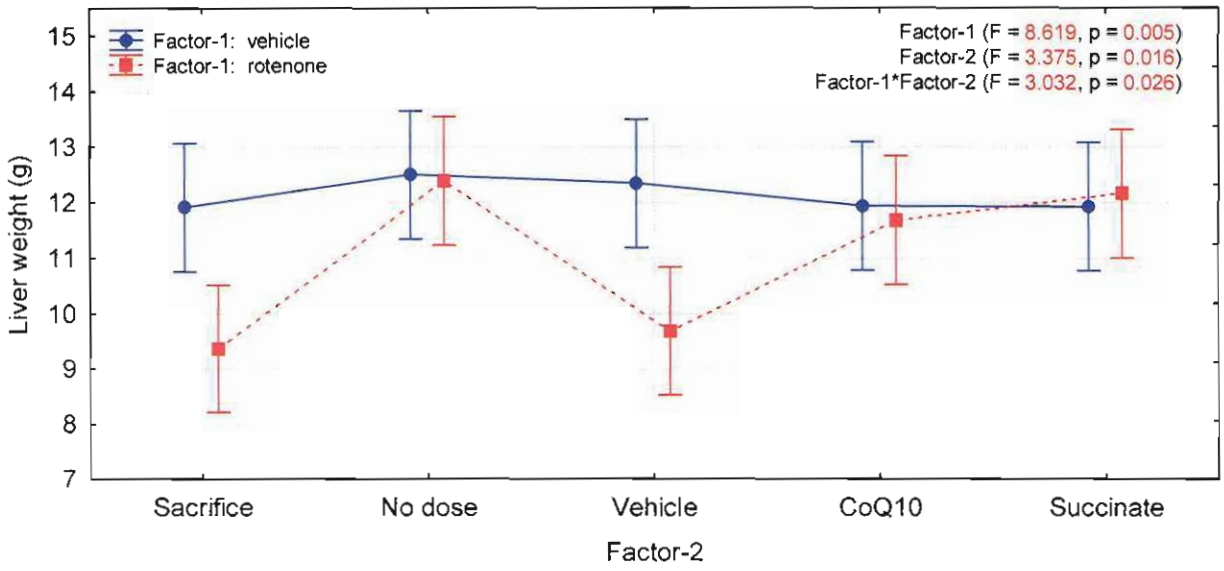
In the pilot study data set, presented in Section 5.7.1.1, liver weights of dose group R15 differed statistically significantly from the respective environmental controls N after the extreme outlier was excluded. Even though it is apparent that RX of the main study presented with five liver weights that were well below that of dose group NN, the groups

did not differ significantly from each other. It is suspected that the presence of one data point in RX that was in the range of data points in NN, namely RX-1, resulted in the lack of significance when compared to NN. Dose group RX did however also differ significantly from VN, VV, VC and RN. The comparisons with the first three dose groups are not informative to the study since too many dose factors are to be accounted for. Similarly, the statistically significant differences between dose group RV and VN as well as VV will not be discussed.

The fact that RX differed significantly from RN indicates that the recovery in liver weight over two days where rats received no dose at all was significantly beneficial. It is of importance to notice that RN also differed significantly from RV, which consisted of liver weights that may have recovered partially. As mentioned previously, the liver weights from rat groups RC and RS also recovered to levels similar to that of the environmental controls NN. The inhibited restoration of liver weights in dose group RV can be suggested to result from the sunflower oil vehicle received as a Factor-2 dose. As discussed for heart weight data in Section 5.4.1, the high polyunsaturated content of sunflower oil has been reported to be associated with increased susceptibility to lipid peroxidation (Mataix *et al.*, 1998), DNA damage (Quiles *et al.*, 2004) and apoptosis of cells (Cury-Boaventura *et al.*, 2005). Therefore, the lack of recovery observed for liver weights in rats from dose group RV can be argued to result from a further induction or maintenance of oxidative stress, originally induced largely by the complex I inhibitor rotenone. It is suspected that liver weights would recover to that of the control dose groups over a slightly longer period of time. It is therefore hypothesised that the recovery rate of the liver is simply suppressed by the sunflower oil Factor-2 vehicle dose regimen. In addition to determining which dose groups differed significantly from each other, the rat main study liver weight data was evaluated via the use of factorial ANOVA. Summary results of the two-way ANOVA are presented in Table 5.103. Since extreme outliers were determined to be present in the liver weight data set under investigation, it was required that the two-way ANOVA be performed via the inclusion and exclusion of the extreme outliers. The graphic representations in Table 5.103 indicate that only a slight difference can be accounted for by the exclusion of the extreme outlier RS-2, resulting in the loss of an intersection of the vehicle and rotenone Factor-1 plots. Regardless, an interaction effect was still reported by the two-way ANOVA. In addition, the exclusion of the extreme outlier did not result in significant alterations to the factorial ANOVA p-values. Factor-1, Factor-2 as well as the interaction between these factors all remained statistically significant, whether RS-2 was included or not in the liver weight data set.

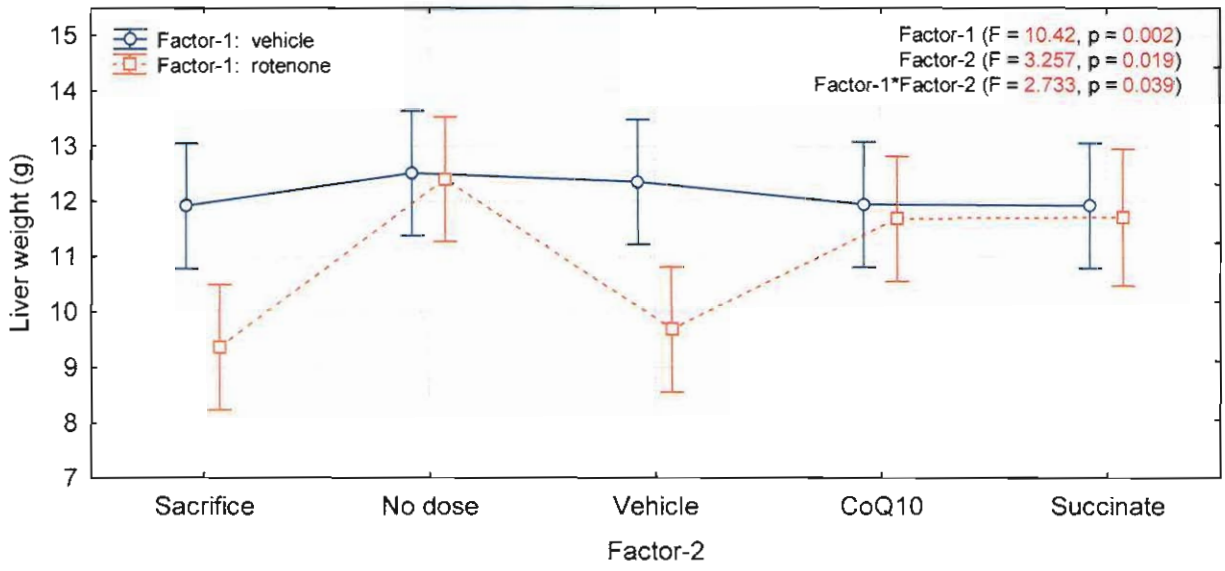
Table 5.103 Graphic and tabulated summary of the liver weight data analysed via a two-way ANOVA

A: Data set including extreme outliers



Description		VX	VN	VV	VC	VS	RX	RN	RV	RC	RS
With extreme outliers	UCI	13.1	13.7	13.5	13.1	13.1	10.5	13.5	10.8	12.8	13.3
	mean	11.9	12.5	12.3	11.9	11.9	9.36	12.4	9.68	11.7	12.2
	LCI	10.8	11.3	11.2	10.8	10.8	8.20	11.2	8.52	10.5	11.0

B: Data set excluding extreme outliers



Description		VX	VN	VV	VC	VS	RX	RN	RV	RC	RS
Without extreme outliers	UCI	13.0	13.6	13.5	13.1	13.1	10.5	13.5	10.8	12.8	12.9
	mean	11.9	12.5	12.3	11.9	11.9	9.36	12.4	9.68	11.7	11.7
	LCI	10.8	11.4	11.2	10.8	10.8	8.23	11.3	8.55	10.6	10.5

The plot legends for each graph are indicated in the top left corners of the respective graphs, while the two-way ANOVA F-statistics (F) and p-values (p) for Factor-1, Factor-2 and Factor-1*Factor-2 are located in the top right corner, with the statistically significant values indicated in red. The vertical whiskers at each mean data point represent 95% confidence intervals for the respective data sets. The mean values in green text, located in the data point summary tables below the graphs, indicate those that were adjusted due to the exclusion of extreme outliers. Rats were treated with NN = no dose regimen, VX = vehicle and sacrificed, VN = vehicle and no dose, VV = vehicle and vehicle, VC = vehicle and CoQ_{10}, VS = vehicle and succinate, RX = rotenone and sacrificed, RN = rotenone and no dose, RV = rotenone and vehicle, RC = rotenone and CoQ_{10}, RS = rotenone and succinate. g = gram, LCI = lower 95% confidence interval data point, UCI = upper 95% confidence interval data point.

Since an interaction effect was reported by the factorial ANOVA, caution should be exercised as to the interpretation of Factor-1 and Factor-2 statistics. Based on the observations from data presented in Table 5.101 and Table 5.103, it can certainly be argued that both dose factors contributed to the responses in liver weight. Rotenone undoubtedly resulted in decreased liver weight recordings. This was statistically confirmed in the rat main and pilot studies, presented previously in this section as well as in Section 5.7.1.1 respectively. This fact implicates a statistically significant Factor-1 contribution. Furthermore, as that liver weights in dose group RV did not recover to that of RN, RC and RS, strongly suggests that the sunflower oil vehicle prevented liver restoration and consequently resulted in a statistically significant Factor-2 contribution.

However, taking into account that Factor-2 regimens had no influence on rats receiving a vehicle Factor-1 dose, it has to be suggested that the interaction effect would not have been reported without the contribution of a rotenone Factor-1 dose. The observed effects amongst the complex I deficient rats are accounted for by considerable effects from both Factor-1 and Factor-2 dose regimens, hence an interaction effect was reported by the factorial ANOVA.

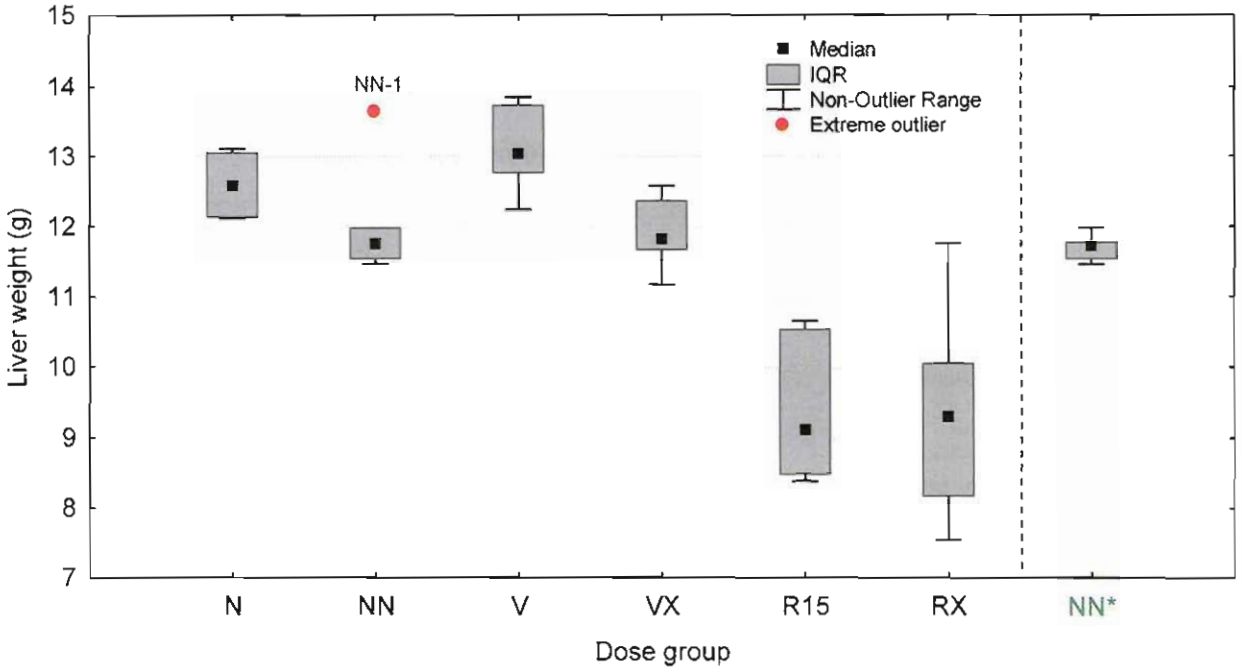
5.7.1.3 Comparative analysis of the liver weight data generated from the rat pilot and main studies

In an attempt to evaluate the consistency of experimentation between the pilot and main studies, groups with similar dosage regimens were compared. These respectively included rat groups N and NN, V and VX, as well as R15 and RX. The comparative data is presented in Table 5.104.

It can be observed from the box-whisker representations that the comparative dose groups did not visibly differ a great deal from each other. The presence of NN-1, the extreme outlier of the main study, is revealed once again along with the box-whisker NN*, where NN-1 was excluded. A replication of the descriptive statistics obtained from Table 5.99.B and Table 5.101.B for all dose groups is included in Table 5.104.B for ease of reference.

Table 5.104 Summary of comparative dose groups of the rat pilot and main study liver weight data

A: Box-whisker plots and data points according to rat groups



B: Descriptive statistics

Dose group	Sample size	Mean	SD	Median	Min	Max	Range	Lower quartile	Upper quartile	IQR
N	6	12.6	0.48	12.6	12.1	13.1	0.99	12.1	13.1	0.91
NN	6	12.0	0.82	11.8	11.5	13.7	2.18	11.6	12.0	0.43
NN*	5	11.7	0.20	11.7	11.5	12.0	0.51	11.6	11.8	0.23
V	6	13.1	0.61	13.0	12.2	13.9	1.61	12.8	13.7	0.96
VX	6	11.9	0.51	11.8	11.2	12.6	1.40	11.7	12.4	0.69
R15	6	9.39	0.99	9.13	8.39	10.7	2.27	8.50	10.5	2.04
RX	6	9.36	1.49	9.31	7.55	11.8	4.21	8.18	10.1	1.88

C: Non-parametric (original data set) and parametric (excluding extreme outliers) p-values

Dose group	N	NN	V	VX	R15	RX
N		1.000 0.551	1.000 0.893	1.000 0.710	0.014 < 0.001	0.017 < 0.001
NN	1.000 0.551		0.880 0.116	1.000 0.999	0.560 0.002	0.639 0.002
V	1.000 0.893	0.880 0.116		0.880 0.161	0.001 < 0.001	0.001 < 0.001
VX	1.000 0.710	1.000 0.999	0.880 0.161		0.560 < 0.001	0.639 < 0.001
R15	0.014 < 0.001	0.560 0.002	0.001 < 0.001	0.560 < 0.001		1.000 1.000
RX	0.017 < 0.001	0.639 0.002	0.001 < 0.001	0.639 < 0.001	1.000 1.000	

All comparison statistics are indicated as p-values. The upper p-value is the non-parametric multiple comparison test statistic, generated from the original set of data. The lower p-value was generated via the parametric Tukey *unequal number HSD* (Honestly Significant Difference) test, after the exclusion of extreme outliers. P-values indicated in red are statistically significant at the pre-determined significance level of 0.05. P-values in black text represent those that are not statistically significant, but have complementary p-values that are statistically significant. The remainder of p-values are listed in grey. The comparisons surrounded by the **bold** black line are those that were determined to be statistically significant by both the non-parametric and parametric multiple comparison procedures. Rats were treated with N = no dose regimen (pilot study), NN = no dose regimen (main study), V = vehicle (pilot study), VX = vehicle (main study), R15 = rotenone 15 $mg.kg^{-1}.day^{-1}$ (pilot study), RX = rotenone 15 $mg.kg^{-1}.day^{-1}$ (main study). < = less than, IQR = inter-quartile range, Min = minimum data point value, Max = maximum data point value, SD = standard deviation.

Most importantly, the data in Table 5.104.C reveals that none of the comparative dose groups differed statistically significantly from each other. Dose groups N and NN were determined to be similar, as were V and VX, and R15 and RX. The multiple comparison grid indicates that the rotenone-treated dose groups R15 and RX differed statistically significantly from N and V prior to the exclusion of the extreme outlier NN-1. R15 and RX did however also differ significantly from NN and VX after NN-1 was excluded, as would be expected. Since the goal of the statistical evaluation presented in Table 5.104 was to verify consistency between the pilot and main study, it was not required that any other comparisons be evaluated. Therefore, the statistically significant differences between the rotenone-treated rats and the environmental controls as well as vehicle controls will not be discussed.

5.7.2 Complex I activity in liver

Complex I activities were determined in liver tissues collected during both the rat pilot and main studies, which are presented in subsequent sections. Citrate synthase activities and protein concentrations of the mitochondrial preparations were also determined and the data merged in Excel® spreadsheets. Finally the data was exported to STATISTICA™ and evaluated on a statistical level.

5.7.2.1 Pilot study complex I activity in liver tissue

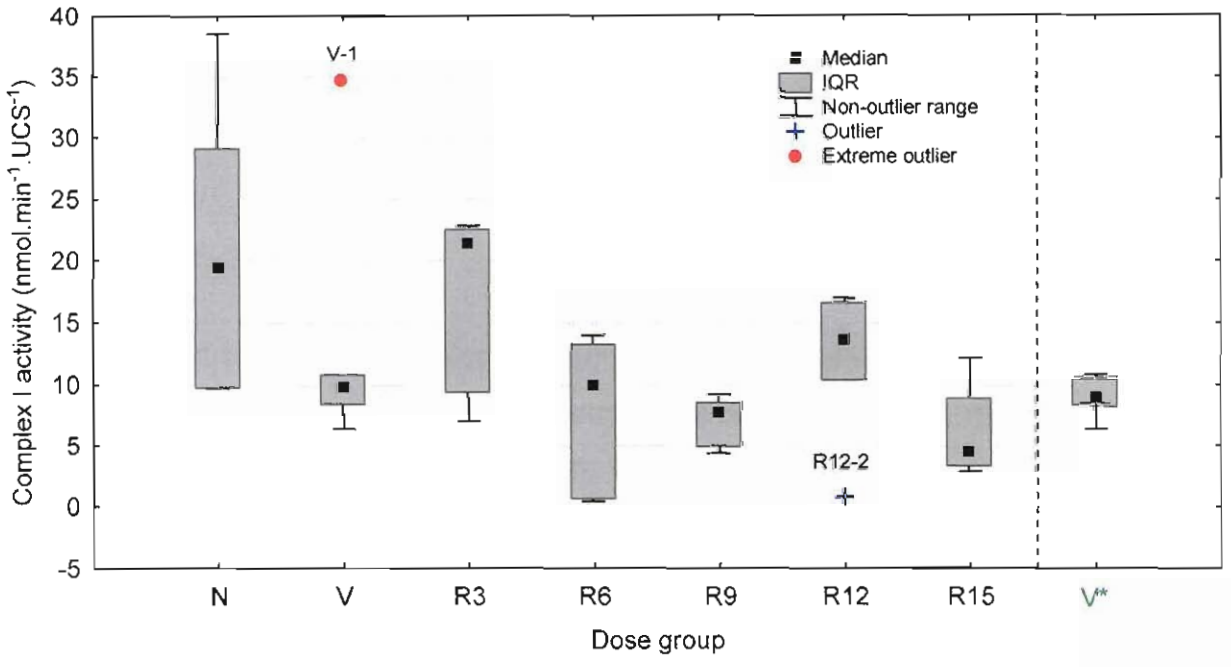
Mitochondria were isolated from liver tissue collected upon sacrificing the rats. After citrate synthase activity and protein concentration data was merged with that of the complex I data, the final complex I activities in terms of UCS were analysed statistically. Table 5.105 presents box-whisker representations and descriptive statistics of the complex I data generated from liver tissue during the rat pilot study. It appeared that there was indeed inhibition of complex I in liver in selected dose groups of the pilot study. The profile is similar to that obtained from brain tissue where it is clear that a Complex I deficiency was induced, but no apparent trend could be observed correlating dose concentration with inhibition percentages. However, it should be noted that the experimental control group V also appeared to harbour a deficiency in complex I.

In Table 5.105.A, it can be observed that all the V data points are clustered together except for V-1, which was excluded as an extreme outlier. The exclusion of V-1 resulted in minor adjustments to the mean, median and quartile statistics. The mean complex I

activity for dose group V decreased from 13.3 to 9.05 nmol.min^{-1}.UCS^{-1}, which is not a large decrease considering that V-1 was more than three times higher than any of the other data points in V. The median decreased from 9.80 to 9.00 nmol.min^{-1}.UCS^{-1}, while the IQR changed from 2.38 to 2.15 nmol.min^{-1}.UCS^{-1}.

Table 5.105 Box-whisker representation and descriptive statistics of the complex I data generated from liver tissue during the rat pilot study

A: Box-whisker plots and data points according to rat groups



Rat	N	V	R3	R6	R9	R12	R15	V*
1	38.5	• 34.7	22.5	12.3	7.20	10.4	5.71	EXCL.
2	22.8	8.44	9.44	7.73	4.40	+ 0.74	2.87	8.44
3	9.82	10.8	22.8	13.3	8.34	16.6	12.2	10.8
4	16.0	6.37	—	0.50	4.96	14.7	3.46	6.37
5	29.1	10.6	21.4	14.0	9.20	17.0	8.98	10.6
6	9.76	9.00	7.00	0.71	8.59	12.6	3.47	9.00

B: Descriptive statistics

Dose group	Sample size	Mean	SD	Median	Min	Max	Range	Lower quartile	Upper quartile	IQR
N	6	21.0	11.4	19.4	9.76	38.5	28.7	9.82	29.1	19.3
V	6	13.3	10.6	9.80	6.37	34.7	28.3	8.44	10.8	2.38
V*	5	9.05	1.81	9.00	6.37	10.8	4.46	8.44	10.6	2.15
R3	5	16.6	7.75	21.4	7.00	22.8	15.8	9.44	22.5	13.1
R6	6	8.09	6.19	10.0	0.50	14.0	13.5	0.71	13.3	12.6
R9	6	7.11	2.00	7.77	4.40	9.20	4.80	4.96	8.59	3.63
R12	6	12.0	6.05	13.6	0.74	17.0	16.2	10.4	16.6	6.17
R15	6	6.11	3.73	4.59	2.87	12.2	9.29	3.46	8.98	5.51

Rat codes for outliers and extreme outliers are located above or below the respective blue crosses (+) and red dots (•), which correspond to data point values listed in the table directly below the graph. The vertical dashed line in the box-whisker graphic representation separates original dose group box-whiskers from those that have had the extreme outliers excluded, which are also indicated by the asterisk (*) following the dose group code. Data sets with excluded data points are designated in green text. Rats were treated with N = no dose, V = vehicle, R3 = rotenone 3 mg.kg^{-1}.day^{-1}, R6 = rotenone 6 mg.kg^{-1}.day^{-1}, R9 = rotenone 9 mg.kg^{-1}.day^{-1}, R12 = rotenone 12 mg.kg^{-1}.day^{-1}, R15 = rotenone 15 mg.kg^{-1}.day^{-1}. '—' = missing data points, IQR = inter-quartile range, Min = minimum data point value, Max = maximum data point value, nmol.min^{-1}.UCS^{-1} = nanomole per minute per unit citrate synthase activity, SD = standard deviation.

An outlier was also observed in dose group R12. Since all the other points in the R12 are relatively well clustered within an IQR of 6.17 $nmol.min^{-1}.UCS^{-1}$, minimal modifications to the descriptive statistics would also be observed if this outlier were to be excluded from the data set. Nonetheless, R12-2 was not excluded, as it was not an extreme outlier. The statistical and biological significance of differences between dose groups are listed in Table 5.106.

Table 5.106 Multiple comparison statistics of the liver complex I data generated from the rat pilot study

A: Non-parametric (original data set) and parametric (excluding extreme outliers) p-values							
Dose group	**N**	**V**	**R3**	**R6**	**R9**	**R12**	**R15**
N		1.000	1.000	0.632	0.109	1.000	0.054
		0.079	0.933	0.022	0.012	0.224	0.006
V	1.000		1.000	1.000	1.000	1.000	1.000
	0.079		0.517	1.000	0.999	0.990	0.990
R3	1.000	1.000		1.000	0.725	1.000	0.426
	0.933	0.517		0.376	0.257	0.912	0.163
R6	0.632	1.000	1.000		1.000	1.000	1.000
	0.022	1.000	0.376		1.000	0.937	0.998
R9	0.109	1.000	0.725	1.000		1.000	1.000
	0.012	0.999	0.257	1.000		0.840	1.000
R12	1.000	1.000	1.000	1.000	1.000		0.851
	0.224	0.990	0.912	0.937	0.840		0.692
R15	0.054	1.000	0.426	1.000	1.000	0.851	
	0.006	0.990	0.163	0.998	1.000	0.692	

B: ANOVA p-values	
Kruskal-Wallis p-value = 0.019	One-way ANOVA p-value = 0.003

C: Statistical and biological significance					
Comparison		**Statistical significance**		**Biological significance**	
		Including EOs	**Excluding EOs**	**Including EOs**	**Excluding EOs**
N	R6	0.632	0.022	N/A	2.004
N	R9	0.109	0.012	N/A	2.155
N	R15	0.054	0.006	N/A	2.311

A: All comparison statistics are indicated as p-values. The upper p-value is the non-parametric multiple comparison test statistic, generated from the original set of data. The lower p-value was generated via the parametric Tukey *unequal number HSD* (Honestly Significant Difference) test, after the exclusion of extreme outliers. P-values indicated in red are statistically significant at the pre-determined significance level of 0.05. P-values in black text represent those that are not statistically significant, but have complementary p-values that are statistically significant. The remainder of p-values are listed in grey. The turquoise shaded blocks represent statistically significant comparisons that were also determined to be of biological significance. B: P-values for the non-parametric Kruskal-Wallis ANOVA and parametric one-way ANOVA are listed, with significant p-values, less than the 0.05 significance level, indicated in red. C: List of comparisons determined to be statistically significant with corresponding biological significance. A d-value greater than or equal to 0.8 signifies biological significance, indicated in red. Rats were treated with N = no dose, V = vehicle, R3 = rotenone 3 $mg.kg^{-1}.day^{-1}$, R6 = rotenone 6 $mg.kg^{-1}.day^{-1}$, R9 = rotenone 9 $mg.kg^{-1}.day^{-1}$, R12 = rotenone 12 $mg.kg^{-1}.day^{-1}$, R15 = rotenone 15 $mg.kg^{-1}.day^{-1}$. ANOVA = analysis of variance, EOs = extreme outliers, N/A = not applicable.

The multiple comparison grid indicates that only three of the dose groups differed significantly from each other after the extreme outlier of V-1 was excluded from the data set. No statistically significant comparisons were observed when the non-parametric multiple comparison test was performed on the original data set. However, it is of interest to note that the Kruskal-Wallis ANOVA had a significant p-value of 0.019. This result is

suggestive of a global difference in the complex I data amongst all the dose groups. It is therefore unexpected that none of the dose groups were determined to differ significantly when the non-parametric multiple comparison data was generated. This lack of concordance in complementing statistical procedures supports the adopted statistical strategy, as presented in Figure 4.3 of Chapter Four, that both the ANOVA and multiple comparison tests be performed on all data sets.

The exclusion of the extreme outlier V-2 resulted in statistically significant differences between the environmental controls N and R6, R9 and R15. Furthermore, these differences were determined to be of biological significance, as presented in Table 5.106.C. Dose group R12 would be expected to harbour a similar activity as the remainder of the rotenone-treated rats. The multiple comparison grid does however reveal that there are no statistically significant differences between any of the rotenone-dosed concentrations, supporting the concept that all the rotenone dose concentrations affected complex I activities similarly in terms of percentage inhibition and variance between the groups. It should however be viewed in the context of dose group V that presented with lowered complex I activities than the environmental controls N. However, this difference was not significant as the p-values for the V and N comparison were both greater than the pre-determined significance level of 0.05, whether the outliers were excluded or not.

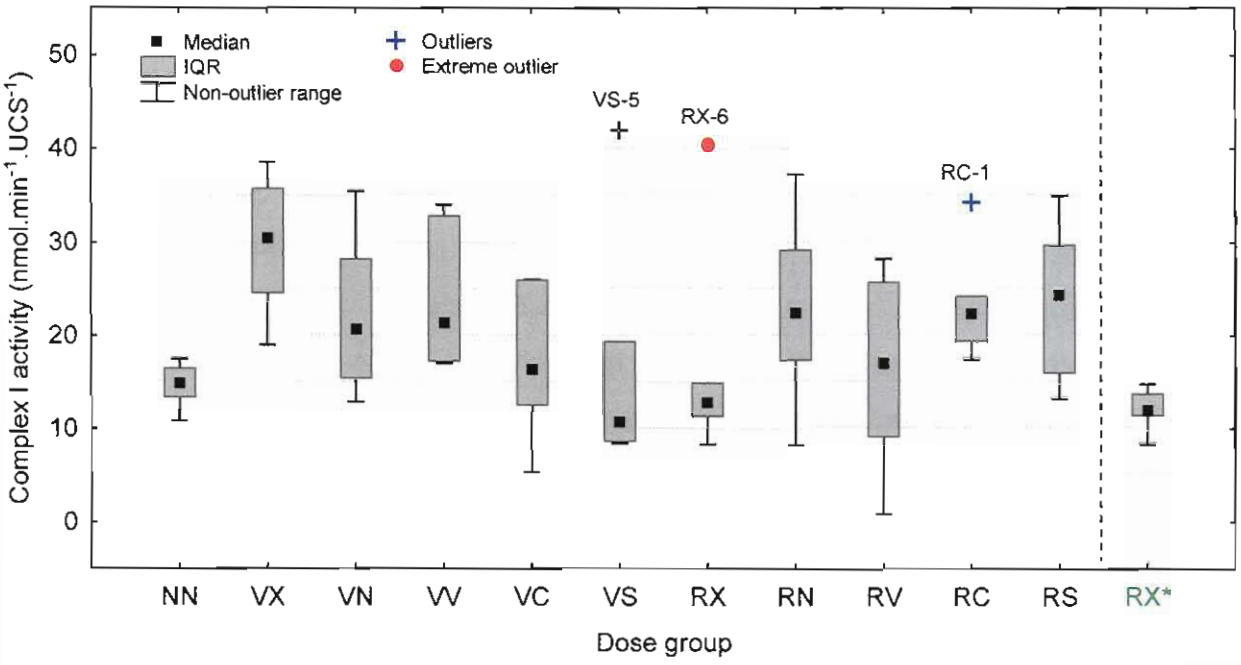
5.7.2.2 Main study complex I activity in liver tissue

Complex I data was complemented with the protein concentrations and citrate synthase activities to obtain the activities in terms of UCS. The liver tissue complex I data was evaluated in STATISTICA™. Table 5.107 presents box-whisker representations of the data as well as descriptive statistics.

Table 5.107.A illustrates the presence of two outliers and one extreme outlier. The first outlier was in dose group VS with a complex I activity of 42.0 $nmol.min^{-1}.UCS^{-1}$. This data point appears to be far from the four core data points that constitute the IQR. However, the outlier VS-5 is still positioned within the outlier range with the boundary being at 51.3 $nmol.min^{-1}.UCS^{-1}$. The closest data point to VS-5 is at 19.3 $nmol.min^{-1}.UCS^{-1}$, which is more than half the complex I activity. This large gap between the outlier and the rest of the data points in VS affects the descriptive statistics for this group, in particular the SD, which is the highest of all the other groups at 13.1 $nmol.min^{-1}.UCS^{-1}$.

Table 5.107 Box-whisker representation and descriptive statistics of the complex I data generated from liver tissue during the rat main study

A: Box-whisker plots and data points according to rat groups



Rat	NN	VX	VN	VV	VC	VS	RX	RN	RV	RC	RS	RX*
1	16.4	30.4	15.4	17.0	25.9	8.37	11.9	8.24	9.07	+ 34.3	29.7	11.9
2	17.5	35.7	28.2	32.8	17.3	19.3	14.8	29.1	25.6	21.0	13.2	14.8
3	13.3	38.6	12.9	18.8	12.5	11.6	13.6	17.3	28.3	24.2	15.9	13.6
4	14.2	30.5	20.4	34.1	5.35	9.81	8.31	24.6	17.0	23.6	26.3	8.31
5	15.3	24.5	35.5	23.9	15.3	+ 42.0	11.3	20.2	17.2	17.4	35.0	11.3
6	10.9	19.0	20.8	17.2	26.0	8.62	• 40.4	37.3	0.93	19.3	22.5	EXCL

B: Descriptive statistics

Dose group	Sample size	Mean	SD	Median	Min	Max	Range	Lower quartile	Upper quartile	IQR
NN	6	14.6	2.36	14.8	10.9	17.5	6.62	13.3	16.4	3.06
VX	6	29.8	7.18	30.4	19.0	38.6	19.6	24.5	35.7	11.2
VN	6	22.2	8.37	20.6	12.9	35.5	22.6	15.4	28.2	12.8
VV	6	23.9	7.78	21.3	17.0	34.1	17.1	17.2	32.8	15.6
VC	6	17.1	7.99	16.3	5.35	26.0	20.6	12.5	25.9	13.4
VS	6	16.6	13.1	10.7	8.37	42.0	33.6	8.62	19.3	10.7
RX	6	16.7	11.8	12.7	8.31	40.4	32.1	11.3	14.8	3.52
RX*	5	12.0	2.48	11.9	8.31	14.8	6.51	11.3	13.6	2.29
RN	6	22.8	10.0	22.4	8.24	37.3	29.1	17.3	29.1	11.8
RV	6	16.3	10.2	17.1	0.93	28.3	27.3	9.07	25.6	16.6
RC	6	23.3	5.95	22.3	17.4	34.3	16.8	19.3	24.2	4.86
RS	6	23.8	8.29	24.4	13.2	35.0	21.8	15.9	29.7	13.8

Rat codes for outliers and extreme outliers are located above or below the respective blue crosses (+) and red dots (•), which correspond to data point values listed in the table directly below the graph. The vertical dashed line in the box-whisker graphic representation separates original dose group box-whiskers from those that have had the extreme outliers excluded, which are also indicated by the asterisk (*) following the dose group code. Data sets with excluded data points are designated in green text. Rats were treated with NN = no dose regimen, VX = vehicle and sacrificed, VN = vehicle and no dose, VV = vehicle and vehicle, VC = vehicle and CoQ_{10}, VS = vehicle and succinate, RX = rotenone and sacrificed, RN = rotenone and no dose, RV = rotenone and vehicle, RC = rotenone and CoQ_{10}, RS = rotenone and succinate. EXCL = excluded data point, IQR = inter-quartile range, Min = minimum data point value, Max = maximum data point value, $nmol.min^{-1}.UCS^{-1}$ = nanomole per minute per unit citrate synthase activity, SD = standard deviation.

If the data for a dose group was well clustered or evenly distributed in a data set, as a general rule, it would be expected that the mean and median statistics would be very similar to each other. This can be exemplified by referring to the mean and median descriptive statistics columns in Table 5.107.B. The groups that indicate the biggest differences between the means and medians are those that harbour outliers or extreme outliers. Dose group VS displayed by far the largest discrepancy between the mean and median statistics at 16.6 and 10.7 nmol.min^{-1}.UCS^{-1} respectively. In the case of dose group RC, the effect of the outlier is minimal due to it being positioned just outside the non-outlier range, which has its boundary at 31.5 nmol.min^{-1}.UCS^{-1}. Since the outlier RC-1 had a complex I activity of 34.3 nmol.min^{-1}.UCS^{-1}, it falls narrowly within the outlier range. Moreover, the fact that the remaining five data points in RC are well clustered strengthens the integrity of the data set and makes it more resistant to the effects of an outlier. Nonetheless, outliers were not excluded from data sets unless they were demonstrated to be extreme, which is not the case with RS-5 and RC-1.

The effects of the extreme outlier RX-6 on dose group RX are evident too. There is a considerable discrepancy between the mean and median statistics, which are at 16.7 and 12.7 nmol.min^{-1}.UCS^{-1} respectively. The exclusion of RX-6 from the data resulted in a mean decrease from 16.7 to 12.0 nmol.min^{-1}.UCS^{-1}, as well as a SD decrease from 11.8 to 2.48 nmol.min^{-1}.UCS^{-1}. RX-6 had a complex I activity of 40.4 nmol.min^{-1}.UCS^{-1}, while the next highest data point was at 14.8 nmol.min^{-1}.UCS^{-1}. Consequently, by excluding the extreme outlier the range statistic decreased markedly from 32.1 to 6.51 nmol.min^{-1}.UCS^{-1}. The non-parametric statistics remained far more robust with the median decreasing from 12.7 to 11.9 nmol.min^{-1}.UCS^{-1} and the IQR decreasing from 3.52 to 2.29 nmol.min^{-1}.UCS^{-1}.

The box-whisker plots in Table 5.107.A reveal an extraordinary pattern of complex I activities. A consistent pattern of recovery for the dose groups RN, RV, RC and RS is evident. However, a similar pattern cannot be discerned for the environmental controls and vehicle Factor-1 treated rat groups. It appears that a downward trend in complex I activities from VX through to VS is present. The variation in liver tissue complex I activities among the rat main study dose groups are presented in Table 5.108, which contains p-values for parametric and non-parametric multiple comparison procedures as well as biological significance.

Table 5.108 Multiple comparison statistics of the liver complex I data generated from the rat main study

A: Non-parametric (original data set) and parametric (excluding extreme outliers) p-values											
Dose group	**NN**	**VX**	**VN**	**VV**	**VC**	**VS**	**RX**	**RN**	**RV**	**RC**	**RS**
NN		0.176	1.000	1.000	1.000	1.000	1.000	1.000	1.000	1.000	1.000
		0.077	0.878	0.675	1.000	1.000	1.000	0.820	1.000	0.759	0.700
VX	0.176		1.000	1.000	1.000	0.297	0.246	1.000	1.000	1.000	1.000
	0.077		0.878	0.977	0.241	0.201	0.044	0.924	0.178	0.953	0.971
VN	1.000	1.000		1.000	1.000	1.000	1.000	1.000	1.000	1.000	1.000
	0.878	0.878		1.000	0.991	0.983	0.680	1.000	0.976	1.000	1.000
VV	1.000	1.000	1.000		1.000	1.000	1.000	1.000	1.000	1.000	1.000
	0.675	0.977	1.000		0.931	0.901	0.456	1.000	0.878	1.000	1.000
VC	1.000	1.000	1.000	1.000		1.000	1.000	1.000	1.000	1.000	1.000
	1.000	0.241	0.991	0.931		1.000	0.996	0.980	1.000	0.963	0.942
VS	1.000	0.297	1.000	1.000	1.000		1.000	1.000	1.000	1.000	1.000
	1.000	0.201	0.983	0.901	1.000		0.998	0.966	1.000	0.943	0.914
RX	1.000	0.246	1.000	1.000	1.000	1.000		1.000	1.000	1.000	1.000
	1.000	0.044	0.680	0.456	0.996	0.998		0.604	0.999	0.537	0.478
RN	1.000	1.000	1.000	1.000	1.000	1.000	1.000		1.000	1.000	1.000
	0.820	0.924	1.000	1.000	0.980	0.966	0.604		0.955	1.000	1.000
RV	1.000	1.000	1.000	1.000	1.000	1.000	1.000	1.000		1.000	1.000
	1.000	0.178	0.976	0.878	1.000	1.000	0.999	0.955		0.926	0.893
RC	1.000	1.000	1.000	1.000	1.000	1.000	1.000	1.000	1.000		1.000
	0.759	0.953	1.000	1.000	0.963	0.943	0.537	1.000	0.926		1.000
RS	1.000	1.000	1.000	1.000	1.000	1.000	1.000	1.000	1.000	1.000	
	0.700	0.971	1.000	1.000	0.942	0.914	0.478	1.000	0.893	1.000	

B: ANOVA p-values	
Kruskal-Wallis p-value = 0.046	One-way ANOVA p-value = 0.023

C: Statistical and biological significance					
Comparison		**Statistical significance (p)**		**Biological significance (d)**	
		Including EOs	**Excluding EOs**	**Including EOs**	**Excluding EOs**
VX	RX	0.246	0.044	N/A	2.156

A: All comparison statistics are indicated as p-values. The upper p-value is the non-parametric multiple comparison test statistic, generated from the original set of data. The lower p-value was generated via the parametric Tukey *unequal number HSD* (Honestly Significant Difference) test, after the exclusion of extreme outliers. P-values indicated in red are statistically significant at the pre-determined significance level of 0.05. P-values in black text represent those that are not statistically significant, but have complementary p-values that are statistically significant. The remainder of p-values are listed in grey. The turquoise shaded blocks represent statistically significant comparisons that were also determined to be of biological significance. B: P-values for the non-parametric Kruskal-Wallis ANOVA and parametric one-way ANOVA are listed, with significant p-values, less than the 0.05 significance level, indicated in red. C: List of comparisons determined to be statistically significant with corresponding biological significance. A d-value greater than or equal to 0.8 signifies biological significance, indicated in red. Rats were treated with NN = no dose regimen, VX = vehicle and sacrificed, VN = vehicle and no dose, VV = vehicle and vehicle, VC = vehicle and CoQ_{10}, VS = vehicle and succinate, RX = rotenone and sacrificed, RN = rotenone and no dose, RV = rotenone and vehicle, RC = rotenone and CoQ_{10}, RS = rotenone and succinate. ANOVA = analysis of variance, EOs = extreme outliers, N/A = not applicable.

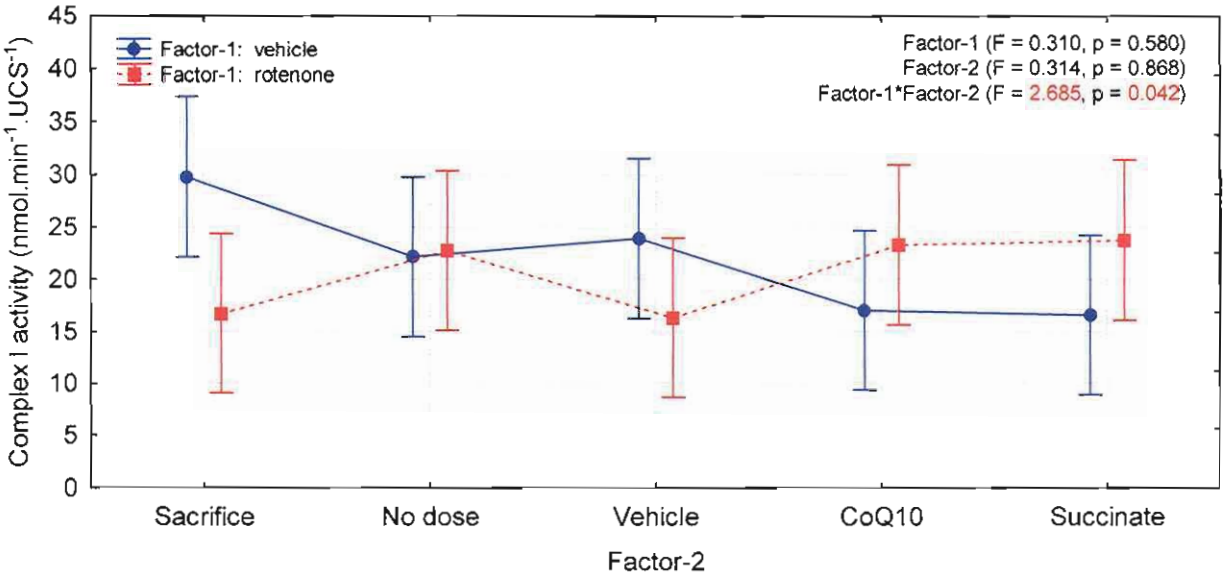
The data in Table 5.108 indicates the presence of only one statistically significant comparison, namely that between VX and RX. Moreover, this comparison was only determined to be significant upon the exclusion of the extreme outlier RX-6. Dose group VX differed statistically significantly from RX, as was expected. Dose groups VX and RX also differed with biological significance, as indicated by the d-value of 2.156 in Table 5.108.C. Dose group VX received the sunflower oil vehicle for 14 days, making it the true control for RX that received 15 $mg.kg^{-1}.day^{-1}$ rotenone, in the sunflower oil vehicle, for the same time period. However, as discussed previously in this section, VX presented

with an unusually elevated complex I activity. Nevertheless, the complex I data for this dose group was argued previously in this section to be accurate based on the fact that the majority of data points clustered within an acceptable range. The VX-RX comparison was not determined to be statistically significant before the exclusion of RX-6. In fact, the non-parametric multiple comparison test indicated that no dose groups differed statistically significantly from each other. However, the Kruskal-Wallis ANOVA did indicate a global difference in the data set with a p-value of 0.046. This inconsistency between the non-parametric ANOVA and multiple comparison procedure was also illustrated in Section 5.7.2.1, where the liver complex I data for the pilot study was presented. This scenario provides strong motivation for the use and effectiveness of the designed statistical strategy presented in Section 4.5 of Chapter Four, which states that regardless of whether the ANOVA p-value is significant or not, it will be performed in complement with a multiple comparison procedure.

The previous hypothesis that liver complex I data for dose group VX of the main study was aberrant is not supported by the p-values presented in Table 5.108. Both the parametric and non-parametric multiple comparison procedures demonstrated that no statistically significant differences existed between the groups that received vehicle Factor-1 doses, including the environmental controls NN. Although VX harboured the highest complex I activity when compared to the remaining vehicle Factor-1 treated dose groups, it was not determined to differ significantly. The rotenone-treated rats that received a no dose Factor-2 regimen illustrated, according to the box-whisker plots in Table 5.107.A, a recovery of liver complex I activity to activities very similar to, or possibly slightly higher than, the rats not treated with rotenone. This is supported by the multiple comparison data presented in Table 5.108, where no differences between the groups can be statistically validated. It is therefore evident that a rapid recovery in liver tissue, as with heart muscle and brain tissue, is observed. The contributions of Factor-1 and Factor-2 dose regimens, including and excluding extreme outliers, were evaluated via a factorial ANOVA, as presented in Table 5.109. The F-statistics and p-values listed in this table indicate an interaction effect between dose Factor-1 and Factor-2. The exclusion of extreme outlier RX-6 resulted in a more prominent interaction effect that lowered the p-value from 0.042 to 0.005.

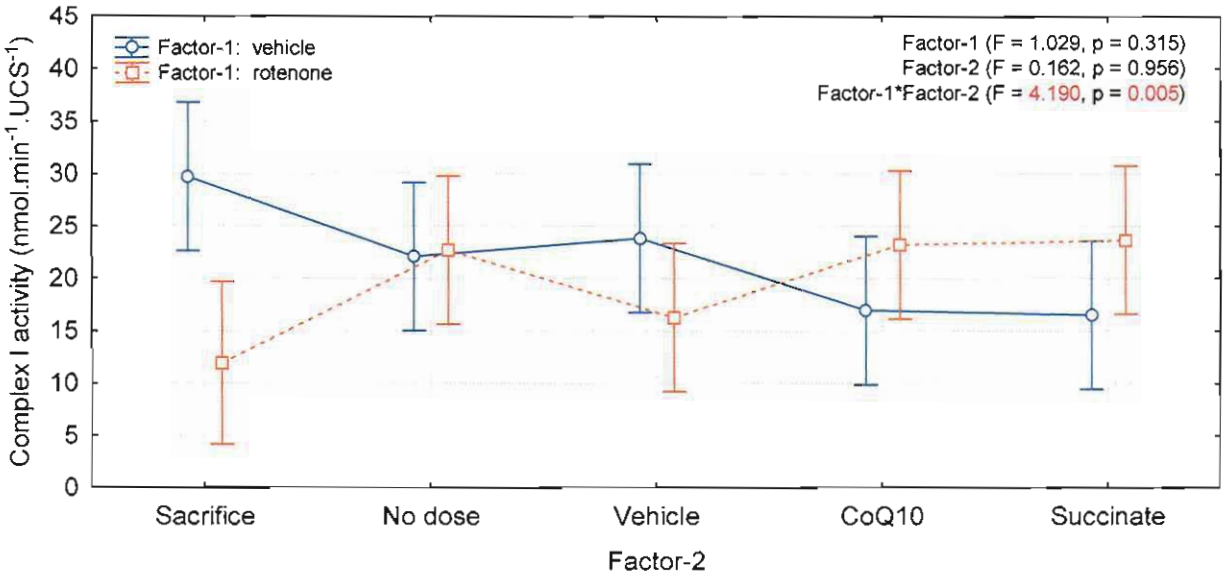
Table 5.109 Graphic and tabulated summary of the liver tissue complex I data analysed via a two-way ANOVA

A: Data set including extreme outliers



Description		VX	VN	VV	VC	VS	RX	RN	RV	RC	RS
With extreme outliers	UCI	37.4	29.8	31.6	24.7	24.2	24.4	30.4	24.0	30.9	31.4
	mean	29.8	22.2	23.9	17.1	16.6	16.7	22.8	16.3	23.3	23.8
	LCI	22.2	14.6	16.3	9.43	8.99	9.09	15.2	8.71	15.7	16.1

B: Data set excluding extreme outliers



Description		VX	VN	VV	VC	VS	RX	RN	RV	RC	RS
Without extreme outliers	UCI	36.9	29.3	31.0	24.1	23.7	19.7	29.9	23.4	30.4	30.8
	mean	29.8	22.2	23.9	17.1	16.6	12.0	22.8	16.3	23.3	23.8
	LCI	22.7	15.1	16.9	10.0	9.53	4.22	15.7	9.25	16.2	16.7

The plot legends for each graph are indicated in the top left corners of the respective graphs, while the two-way ANOVA F-statistics (F) and p-values (p) for Factor-1, Factor-2 and Factor-1*Factor-2 are located in the top right corner, with the statistically significant values indicated in red. The vertical whiskers at each mean data point represent 95% confidence intervals for the respective data sets. The mean values in green text, located in the data point summary tables below the graphs, indicate those that were adjusted due to the exclusion of extreme outliers. Rats were treated with NN = no dose regimen, VX = vehicle and sacrificed, VN = vehicle and no dose, VV = vehicle and vehicle, VC = vehicle and CoQ_{10}, VS = vehicle and succinate, RX = rotenone and sacrificed, RN = rotenone and no dose, RV = rotenone and vehicle, RC = rotenone and CoQ_{10}, RS = rotenone and succinate. LCI = lower 95% confidence interval data point, $nmol.min^{-1}.UCS^{-1}$ = nanomole per minute per unit citrate synthase activity, UCI = upper 95% confidence interval data point.

The confidence interval and mean data point tables directly below the respective graphs illustrate the change in the mean of dose group RX in green text as well as the decrease in confidence intervals due to the exclusion of the extreme outlier. As discussed previously in this section, the mean complex I activity for RX changed from 16.7 to 12.0 nmol.min^{-1}.UCS^{-1} when the extreme outlier was excluded. The exclusion of RX-6 resulted in a decrease in the confidence intervals from 15.3 to 14.2 nmol.min^{-1}.UCS^{-1}, a result expected from a data set that has had an extreme outlier excluded.

The graphic representations in Table 5.109 evidently display that the vehicle and rotenone plots intersect, which is consistent with the reported interaction effect. It can certainly be argued that CoQ_{10} and succinate contributed to the improved complex I activities amongst the rotenone-treated rats. However, this is not apparent in dose groups VC and VS, which received the vehicle Factor-1 regimen. The F-statistics for Factor-1 and Factor-2 in both Sections A and B of Table 5.109 were reported as significantly lower than that of the interaction F-statistics, confirming that there is indeed an interaction regardless of whether the extreme outlier was excluded or not. Therefore, the interaction effect may be argued to result from the improved recovery of liver complex I activities in the presence of a rotenone-induced deficiency. However, the fact that dose group RN harboured a mean liver complex I activity equivalent to that of RC and RS, makes it impossible to conclude that the therapeutic regimens were the primary compounds resulting in a recovery of complex I activities. Rather, it is speculated that the recovered complex I activities were the result of cellular recovery and mitochondrial proliferation in response to rats being relieved of their rotenone dose regimens. This is a more realistic argument since neither CoQ_{10} nor succinate were expected to directly improve complex I activities based on the facts that CoQ_{10} is prevented from interacting with complex I by rotenone binding and, secondly, since succinate is the substrate compound for complex II. This supported by the fact that dose groups VC and VS presented with the lowest mean complex I activities in liver, indicating that CoQ_{10} and succinate did not improve complex I activity. However, the notion that these regimens may contribute to the recovery cannot be excluded, since both are known to have beneficial effects on a cellular level.

5.7.2.3 Comparative analysis of the liver complex I data generated from the rat pilot and main studies

A summary of the rat main and pilot study liver complex I data is presented in Table 5.110. The descriptive statistics of the paralleled dose groups were taken from Table 5.105.B and

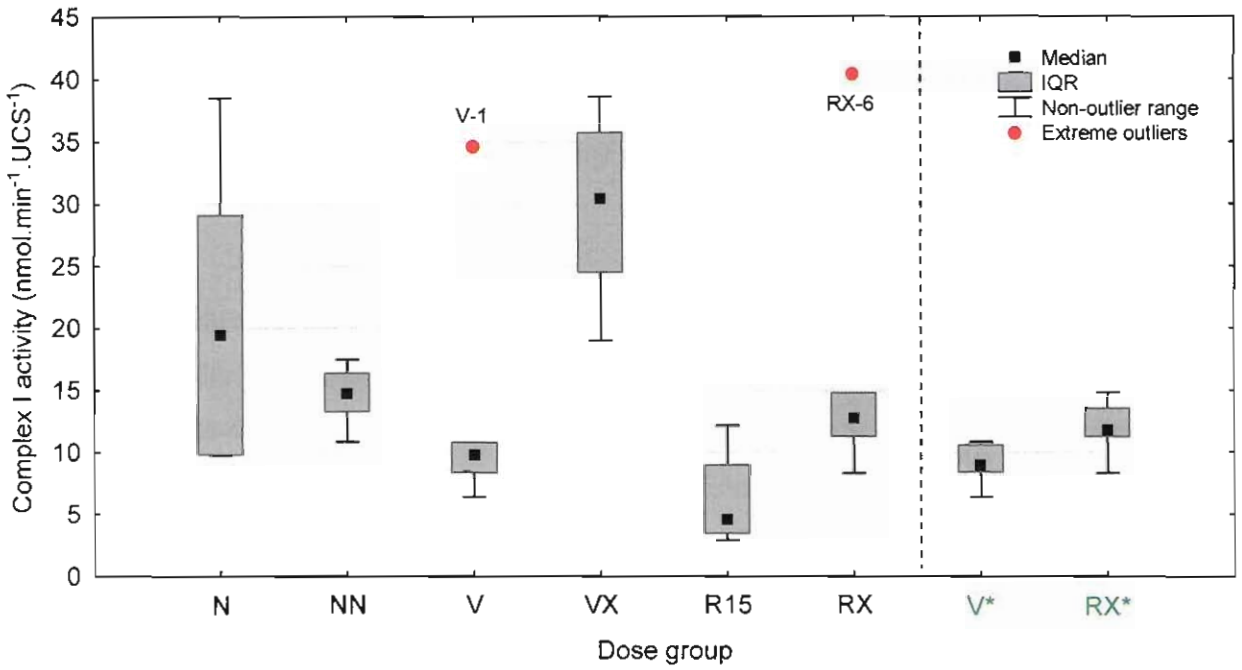
Table 5.107.B, and are listed here for ease of reference. In addition, the extreme outliers have already been discussed in the previous respective sections. However, since their presence does influence the multiple comparison data, non-parametric and parametric p-values have been included. The non-parametric multiple comparison p-values were generated from the complete data set including the extreme outliers, while the Tukey *unequal number HSD* test was performed on the data set where the extreme outliers were excluded.

It should be noted that dose groups V of the pilot study and VX of the main study differed statistically significantly after the extreme outliers were excluded. By visually inspecting the data distributions of V and VX in the context of their respective sub-studies, it can be determined that the VX complex I data may be more questionable than V. The mean and median complex I activities of 29.8 and 30.4 $nmol.min^{-1}.UCS^{-1}$ respectively for VX are higher than any of other activities in the pilot study as well as the environmental controls NN and vehicle Factor-1 treated rats in the main study. As listed in Table 5.107, the median complex I activities nearest to VX within the vehicle Factor-1 treated dose groups, namely 20.6 and 21.3 $nmol.min^{-1}.UCS^{-1}$ for VN and VV respectively, were both approximately 10 $nmol.min^{-1}.UCS^{-1}$ lower than the median for VX itself. This deviation in complex I activity supports the argument that VX data points are at least partly atypical to the main study.

It may be suggested that certain aberrant data points in VX were generated, resulting in abnormally elevated central tendency statistics. However, by referring to the distribution of data in Table 5.110.A, it is clear that four of the six data points in VX are greater than 30.0 $nmol.min^{-1}.UCS^{-1}$ and are well clustered within a range of approximately 8.00 $nmol.min^{-1}.UCS^{-1}$. The close grouping of data points provides concrete support that the central tendency statistics are accurate. Citrate synthase activities, protein concentration data and final complex I activities in terms of UCS can be referred to in Table B.8 of Appendix B. The VX dose group data in all the columns of Table C.8 are not extraordinary and are similar to that of other dose groups. Therefore, the data itself is supportive of the final liver tissue complex I activities for group VX.

Table 5.110 Summary of comparative dose groups of the rat pilot and main study liver tissue complex I data

A: Box-whisker plots and data points according to rat groups



B: Descriptive statistics (from Table 5.105.B and Table 5.107.B)

Dose group	Sample size	Mean	SD	Median	Min	Max	Range	Lower quartile	Upper quartile	IQR
N	6	21.0	11.4	19.4	9.76	38.5	28.7	9.82	29.1	19.3
NN	6	14.6	2.36	14.8	10.9	17.5	6.62	13.3	16.4	3.06
V	6	13.3	10.6	9.80	6.37	34.7	28.3	8.44	10.8	2.38
V*	5	9.05	1.81	9.00	6.37	10.8	4.46	8.44	10.6	2.15
VX	6	29.8	7.18	30.4	19.0	38.6	19.6	24.5	35.7	11.2
R15	6	6.11	3.73	4.59	2.87	12.2	9.29	3.46	8.98	5.51
RX	6	16.7	11.8	12.7	8.31	40.4	32.1	11.3	14.8	3.52
RX*	5	12.0	2.48	11.9	8.31	14.8	6.51	11.3	13.6	2.29

C: Non-parametric and parametric p-values

Dose group	N	NN	V	VX	R15	RX
N		1.000	1.000	1.000	0.100	1.000
		0.472	0.046	0.160	0.003	0.215
NN	1.000		1.000	1.000	0.239	1.000
	0.472		0.706	0.002	0.189	0.983
V	1.000	1.000		0.060	1.000	1.000
	0.046	0.706		< 0.001	0.972	0.972
VX	1.000	1.000	0.060		< 0.001	0.827
	0.160	0.002	< 0.001		< 0.001	0.001
R15	0.100	0.239	1.000	< 0.001		0.489
	0.003	0.189	0.972	< 0.001		0.654
RX	1.000	1.000	1.000	0.827	0.489	
	0.215	0.983	0.972	0.001	0.654	

All comparison statistics are indicated as p-values. The upper p-value is the non-parametric multiple comparison test statistic, generated from the original set of data. The lower p-value was generated via the parametric Tukey *unequal number HSD* (Honestly Significant Difference) test, after the exclusion of extreme outliers. P-values indicated in red are statistically significant at the pre-determined significance level of 0.05. P-values in black text represent those that are not statistically significant, but have complementary p-values that are statistically significant. The remainder of p-values are listed in grey. The comparisons surrounded by the **bold** black line are those that were determined to be statistically significant by both the non-parametric and parametric multiple comparison procedures. Rats were treated with N = no dose regimen (pilot study), NN = no dose regimen (main study), V = vehicle (pilot study), VX = vehicle (main study), R15 = rotenone 15 mg.kg^{-1}.day^{-1} (pilot study), RX = rotenone 15 mg.kg^{-1}.day^{-1} (main study). < = less than, IQR = inter-quartile range, Min = minimum data point value, Max = maximum data point value, SD = standard deviation.

Finally, the complex I assay should be discussed since it was experienced as being of the more complicated analyses to perform. Although the results are not indicated, consistent complex I activities when experimenting with dilutions of mitochondrial preparations could not be attained accurately, as opposed to the citrate synthase assay where reproducibility was far more consistent. It should also be kept in mind that the complex I activity of a sample is the delicate integration of four different assay results to obtain the final complex I activity per UCS. Gellerich *et al.* (2004) reported that several complications are to be considered, namely mitochondrial content, in homogeneity of samples, instability of enzymes during storage and preparation, temperature control and spectrophotometer variation. Therefore, it is evident that there were several contributing factors that might have complicated complex I analysis.

5.7.3 Antioxidant capacity in liver tissue

The ORAC assay was performed on liver tissue preparations in order to determine the antioxidant capacity in the various dose groups. The data was collected and analysed statistically to determine the significance of variations within the complete data set. Table 5.111 presents the liver tissue antioxidant capacity data according to dose group in terms of box-whisker plots and a table of descriptive statistics.

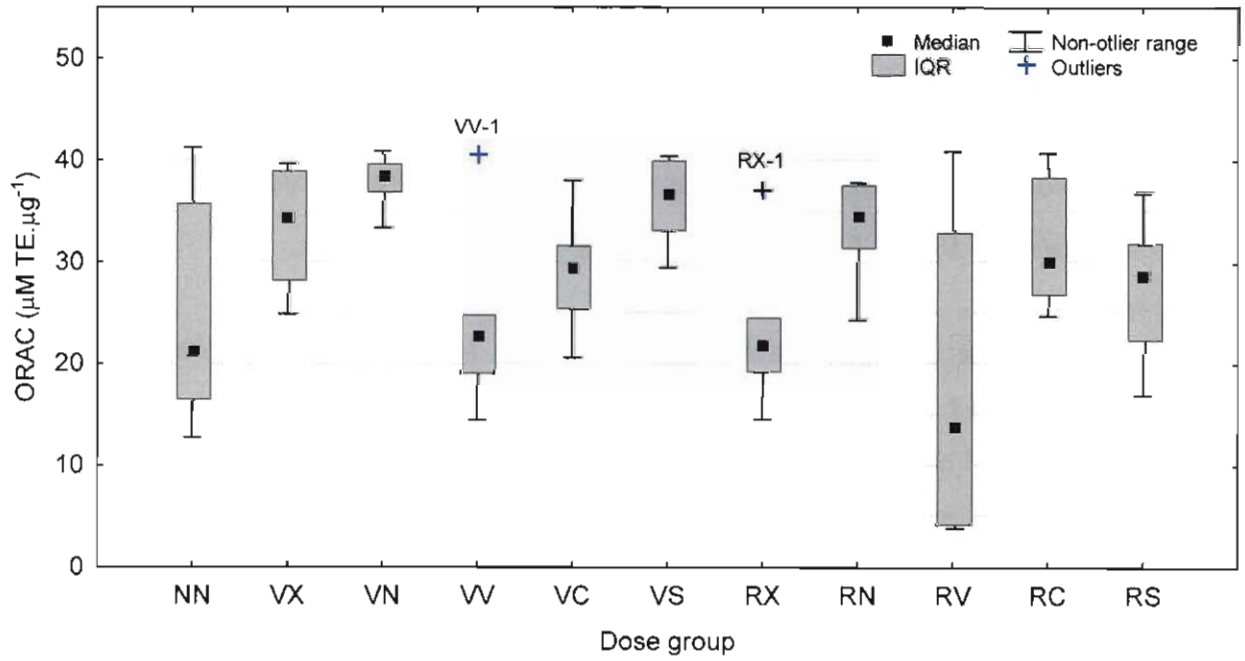
The liver antioxidant capacity data is illustrated in Table 5.111.A to present with two outliers, namely VV-1 and RX-1. Neither of the outliers is extreme with regards to the complete data set. The descriptive statistics for dose groups VV and RX indicate that the data points in each of the groups are relatively well clustered, which in turn results in stable central tendency statistics. The means and medians for VV and RX are very similar. Moreover, even though VV and RX harbour outliers in their groups, the SDs for both groups are not aberrantly high, in fact the SDs are comparable to the other dose groups. The exclusion of RV-1 and RX-1 would not result in marked changes to the respective dose group data sets. Regardless of this, the outliers were not excluded since they were not classified as extreme outliers.

It is notable that the RV dose group again presented with the greatest amount of variation within the complete data set. Three rats in dose group RV appeared to present with aberrant antioxidant capacities. These rats were RV-4, RV-5 and RV-6, all of which harboured the lowest antioxidant capacities of rats included in the study. Coincidently, it was presented in Section 5.5.3 that these same three rats harboured the highest

antioxidant capacity in brain tissue. It is odd that the same rats contributed the lowest and highest antioxidant capacities in the two respective tissues. In fact, by referring to Sections 5.3.2 and 5.4.3, where antioxidant capacities were determined from blood serum and heart muscle, it can also be observed that these same rats consistently harboured the lowest antioxidant capacities. In addition, these rats lost more weight than all the other rats in the study while they were being dosed rotenone, as illustrated in Section 5.2.2. The reasons for the adverse response in specifically these three rats cannot be explained with certainty. The dosage regimens and experimental procedures were consistently maintained throughout the study. These three rats appeared to have simply responded more adversely to the rotenone dose regimen.

Table 5.111 Box-whisker representation and descriptive statistics of the liver antioxidant capacity data generated from the main study

A: Box-whisker plots and data points according to rat groups



Rat	NN	VX	VN	VV	VC	VS	RX	RN	RV	RC	RS
1	12.8	28.2	38.9	40.4	25.4	33.0	37.0	32.7	17.6	38.2	28.3
2	20.7	33.6	36.8	14.5	38.0	40.4	23.3	31.4	32.8	30.0	22.3
3	35.7	38.8	37.8	22.9	31.3	39.9	14.6	24.3	40.9	24.7	29.1
4	21.6	35.0	39.5	22.4	27.5	29.5	24.5	37.8	9.85	26.8	31.8
5	41.2	39.6	33.4	24.7	20.6	34.8	19.2	37.5	4.15	30.0	36.8
6	16.5	24.9	40.9	19.0	31.6	38.3	20.3	36.2	3.78	40.8	16.9

B: Descriptive statistics

Dose group	Sample size	Mean	SD	Median	Min	Max	Range	Lower quartile	Upper quartile	IQR
NN	6	24.8	11.2	21.2	12.8	41.2	28.5	16.5	35.7	19.1
VX	6	33.4	5.84	34.3	24.9	39.6	14.8	28.2	38.8	10.6
VN	6	37.9	2.63	38.4	33.4	40.9	7.56	36.8	39.5	2.72
VV	6	24.0	8.83	22.6	14.5	40.4	25.9	19.0	24.7	5.74

Table 5.111 Continued...

Dose group	Sample size	Mean	SD	Median	Min	Max	Range	Lower quartile	Upper quartile	IQR
VC	6	29.1	5.99	29.4	20.6	38.0	17.4	25.4	31.6	6.18
VS	6	36.0	4.28	36.6	29.5	40.4	10.9	33.0	39.9	6.81
RX	6	23.1	7.64	21.8	14.6	37.0	22.5	19.2	24.5	5.28
RN	6	33.3	5.11	34.4	24.3	37.8	13.4	31.4	37.5	6.08
RV	6	18.2	15.5	13.7	3.78	40.9	37.1	4.15	32.8	28.6
RC	6	31.7	6.35	30.0	24.7	40.8	16.0	26.8	38.2	11.3
RS	6	27.5	7.03	28.7	16.9	36.8	19.9	22.3	31.8	9.46

Rat codes for the outliers are located above or below the blue crosses (+), which correspond to data point values listed in the table directly below the graph. Rats were treated with NN = no dose regimen, VX = vehicle and sacrificed, VN = vehicle and no dose, VV = vehicle and vehicle, VC = vehicle and CoQ_{10}, VS = vehicle and succinate, RX = rotenone and sacrificed, RN = rotenone and no dose, RV = rotenone and vehicle, RC = rotenone and CoQ_{10}, RS = rotenone and succinate. IQR = inter-quartile range, $\mu M\ TE.\mu g^{-1}$ = micromolar Trolox equivalents per microgram protein, Min = minimum data point value, Max = maximum data point value, ORAC = oxygen radical absorbance capacity, SD = standard deviation.

A trend very similar to skeletal muscle antioxidant capacity, as presented in Section 5.6.2, is observed from the box-whisker plots in Table 5.111. By comparing the antioxidant capacity data points for dose group VX and RX, it appears that the rats that received rotenone decreased in liver antioxidant capacity. The inhibition of complex I in liver, as demonstrated in Section 5.7.2.2, appears to have also affected antioxidant capacity in the same tissue. Therefore, as a reference, all antioxidant capacities relative to RX would indicate either improvements or deterioration in response. Improvements can be observed in dose groups RN, RC and RS. These reflect a recovery in capacity to levels equivalent to the dose groups that were not treated with rotenone. The decreased median antioxidant capacity in RV is primarily due the three low data points of RV-4, RV-5 and RV-6, as discussed previously.

Dose group VV displayed the lowest antioxidant capacity among the vehicle Factor-1 treated groups. However, the central tendency statistics for VV were very similar to the environmental controls NN. If the vehicle is postulated to increase the antioxidant capacity in rats, it would be expected that rats in VV would harbour of the highest antioxidant capacities. This is not the case though, except for rat VV-1 that is marked as an outlier in the box-whisker representations. This may be suggestive of rats in dose group VV being compromised in some way or another. However, this is unlikely since all dose groups were maintained in identical environments and were treated with matching protocols. The statistical significance of the differences between dose groups was determined via the Tukey *equal number HSD* multiple comparison procedure. The p-values, along with the one-way ANOVA p-value and biological significance d-values are listed in Table 5.112.

The multiple comparison grid reveals that dose group RV differed statistically significantly from VN and VS. Rat group RV also differed with biological significance from the aforementioned groups VN and VS. The latter two groups harboured the highest antioxidant capacities of all the groups, as opposed to RV that had the lowest, primarily due to the three very low data points contributed by RV-4, RV-5 and RV-6. Nonetheless, dose groups VN and VS are not groups that can be compared to RV to deduce single effects. It should also be noted that even though RV consisted of three low antioxidant capacity data points, the dose group did not differ significantly from the other rotenone-treated dose groups.

Table 5.112 Multiple comparison statistics of the liver antioxidant capacity data generated from the rat main study

A: Tukey *equal number HSD* p-values

Dose group	NN	VX	VN	VV	VC	VS	RX	RN	RV	RC	RS
NN		0.746	0.176	1.000	0.997	0.377	1.000	0.752	0.939	0.913	1.000
VX	0.746		0.996	0.639	0.997	1.000	0.517	1.000	0.064	1.000	0.973
VN	0.176	0.996		0.122	0.716	1.000	0.080	0.996	0.004	0.961	0.498
VV	1.000	0.639	0.122		0.990	0.284	1.000	0.646	0.973	0.844	0.999
VC	0.997	0.997	0.716	0.990		0.918	0.969	0.998	0.421	1.000	1.000
VS	0.377	1.000	1.000	0.284	0.918		0.201	1.000	0.014	0.998	0.768
RX	1.000	0.517	0.080	1.000	0.969	0.201		0.523	0.992	0.745	0.997
RN	0.752	1.000	0.996	0.646	0.998	1.000	0.523		0.065	1.000	0.975
RV	0.939	0.064	0.004	0.973	0.421	0.014	0.992	0.065		0.144	0.639
RC	0.913	1.000	0.961	0.844	1.000	0.998	0.745	1.000	0.144		0.998
RS	1.000	0.973	0.498	0.999	1.000	0.768	0.997	0.975	0.639	0.998	

B: ANOVA p-values

One-way ANOVA p-value = 0.002

C: Statistical and biological significance

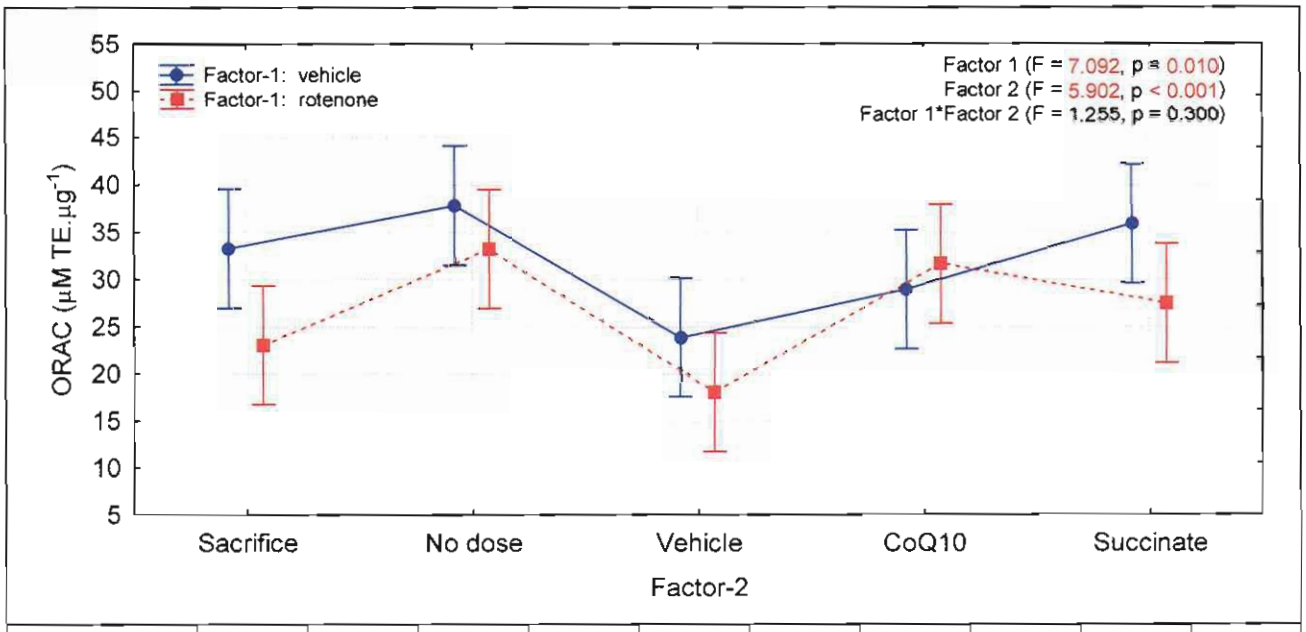
Comparison		Statistical significance (p)	Biological significance (d)
VN	RV	0.004	2.448
VS	RV	0.013	2.210

A: All comparison statistics are indicated as p-values generated via the Tukey *equal number HSD* (Honestly Significant Difference) multiple comparison procedure. P-values indicated in red are statistically significant at the pre-determined significance level of 0.05. The remainder of p-values are listed in grey. The turquoise shaded blocks represent statistically significant comparisons that were also determined to be of biological significance. B: P-value for the one-way ANOVA is listed, with significant p-values, less than the 0.05 significance level, indicated in red. C: List of comparisons determined to be statistically significant with corresponding biological significance. A d-value greater than or equal to 0.8 signifies biological significance, indicated in red. Rats were treated with NN = no dose regimen, VX = vehicle and sacrificed, VN = vehicle and no dose, VV = vehicle and vehicle, VC = vehicle and CoQ_{10}, VS = vehicle and succinate, RX = rotenone and sacrificed, RN = rotenone and no dose, RV = rotenone and vehicle, RC = rotenone and CoQ_{10}, RS = rotenone and succinate. ANOVA = analysis of variance.

Concerning previous discussions about the lowered antioxidant capacity of dose group VV, the multiple comparison p-values also indicate that the group did not differ significantly from the other dose groups that received vehicle Factor-1 regimens. The liver tissue antioxidant capacity data was finally analysed via the factorial ANOVA to elucidate

the effects of the different dose regimens. These statistical results are summarised in Table 5.113. A table listing the exact data point values of the means and 95% confidence intervals accompanies the graphic representation of the two-way ANOVA data.

Table 5.113 Graphic and tabulated summary of the liver tissue antioxidant capacity data analysed via a two-way ANOVA



Data points	VX	VN	VV	VC	VS	RX	RN	RV	RC	RS
UCI	39.6	44.2	30.3	35.4	42.3	29.4	39.6	24.5	38.0	33.8
mean	33.4	37.9	24.0	29.1	36.0	23.1	33.3	18.2	31.7	27.5
LCI	27.1	31.6	17.7	22.8	29.7	16.8	27.0	11.9	25.5	21.3

The plot legend is indicated in the top left corner of the graph, while the two-way ANOVA F-statistics (F) and p-values (p) for Factor-1, Factor-2 and Factor-1*Factor-2 are located in the top right corner, with the statistically significant values indicated in red. The vertical whiskers at each mean data point represent 95% confidence intervals for the respective data sets. Rats were treated with NN = no dose regimen, VX = vehicle and sacrificed, VN = vehicle and no dose, VV = vehicle and vehicle, VC = vehicle and CoQ_{10}, VS = vehicle and succinate, RX = rotenone and sacrificed, RN = rotenone and no dose, RV = rotenone and vehicle, RC = rotenone and CoQ_{10}, RS = rotenone and succinate. < = less than, LCI = lower 95% confidence interval data point, µM TE.μg^{-1} = micromolar Trolox equivalents per microgram protein, UCI = upper 95% confidence interval data point.

The vehicle and rotenone Factor-1 plots once again illustrate the effect of the two doses on antioxidant capacity. The lower rotenone plot suggests that the complex I inhibitor compromised antioxidant capacity, even though it was reported in Section 5.3.2.1 that rotenone itself harboured an antioxidant capacity similar to that of Trolox. In contrast, by referring to Table 5.111, it was apparent that the vehicle Factor-1 groups harboured antioxidant capacities mostly higher than those obtained for the environmental controls NN, which had a mean antioxidant capacity of 24.8 µM TE.μg^{-1}. Consequently, the contrasting effects of vehicle and rotenone resulted in the statistically significant p-value for Factor-1, indicated in the top right corner of the two-way ANOVA summary graph. It is again argued that the vitamin E content in the sunflower oil contributed to improved antioxidant capacity. However, the compromising impact of rotenone on the respiratory

chain cannot be ignored as a factor that induced the discrepancy in antioxidant capacity values observed in liver.

The Factor-2 p-value was also determined to be statistically significant, indicative of these regimens contributing to liver antioxidant capacities. As mentioned previously, it is unexpected that dose group VV had a lower antioxidant capacity than the other vehicle Factor-1 treated rats. It is clear from the graphic representation in Table 5.113 that RV also decreased to the lowest of the rotenone Factor-1 groups. The data therefore does suggest that vehicle dosing on days 15 and 16 compromised antioxidant capacities. This unlikely event is supported by the fact that rats that received no dose or either CoQ_{10} or succinate, on average harboured higher antioxidant capacities. However, it is more credible that the compromised liver antioxidant capacities in dose group RV were the result of sustained oxidative stress, induced by the rotenone Factor-1 regimen. Furthermore, the apparently lowered mean antioxidant capacity for RV is also accounted for by the lowered antioxidant capacities determined for rats RV-4, RV-5 and RV-6. However, the data is clustered far better for dose group VV, resulting in accurate central tendency statistics. Nonetheless, as discussed previously in this section, neither VV nor RV differed statistically significantly from any of the groups in their respective Factor-1 dose categories.

The graphic representation in Table 5.113 illustrates that it was not beneficial for the rats to receive either of the therapeutic compounds, CoQ_{10} or succinate. This is exemplified by the CoQ_{10} and succinate Factor-2 data points not extending above either of their respective control groups. It can be possible that the rats were not dosed long enough with the therapeutic regimens before antioxidant capacities could be improved. However, the goals of the study were to evaluate the responses of rats to a therapeutic boost dose in the presence of an induced Complex I deficiency. Therefore, in the scope of this project it is irrelevant to consider the effects of longer dose periods for the second dose factors. It is speculated that improved antioxidant capacities would be attained if longer dose periods of the therapeutic regimens were implemented.

5.7.4 Lactate/pyruvate ratios in liver tissue

The lactate and pyruvate concentrations of liver tissue preparations were determined in consistency with protocols utilised for all tissue groups investigated. Statistical evaluations of the data were performed according to the proposed statistical strategy in Section 4.5 of

Chapter Four. A graphic representation of the liver L/P data set according to dose group is presented in Table 5.114, accompanied by a list of all data points per group and a table of descriptive statistics.

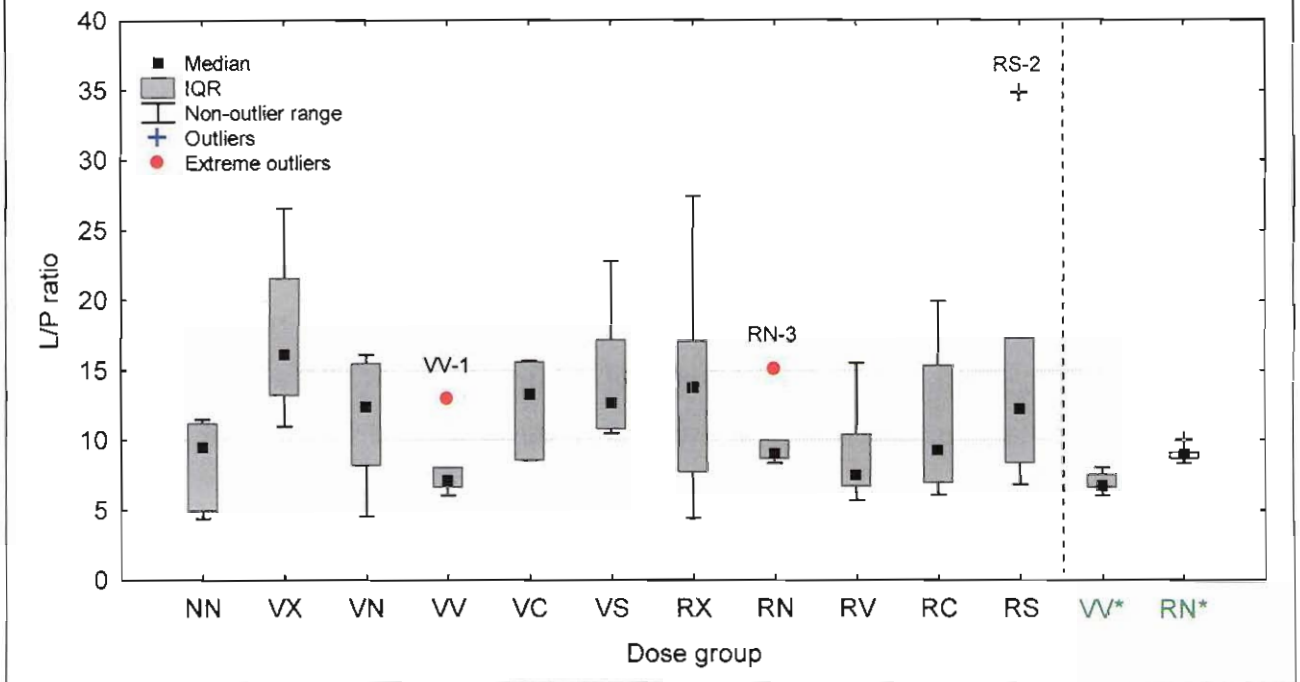
Table 5.114.A indicates the presence of two extreme outliers, one in dose group VV and the other in RN. In addition, two outliers have been determined to be present. One of these appears due to the exclusion of the extreme outlier RN-3 and was therefore not a true outlier of the original RN data set. The second outlier, RS-2, harboured an L/P ratio of 34.8. It appears to be distant from the remaining five data points in the group, with its closest rival being RS-5, which had a ratio of 17.3. However, data point RS-2 is still comfortably within the outlier range and would have to extend beyond 44.1 for it to be classified an extreme outlier.

The exclusion of extreme outlier VV-1 from dose group VV results in a slight mean decrease from 7.99 to 6.98. The SD decreased moderately from 2.55 to 0.78, an expected decrease due to the sensitivity of this parametric statistic to the presence of outliers and extreme outliers. The non-parametric counterpart statistics displayed similar alterations, with the median decreasing from 7.10 to 6.71 and IQR decreasing from 1.39 to 0.85. A comparable scenario was true for the RN data set when RN-3 was excluded. The mean ratio for RN decreased only slightly from 10.0 to 9.02, and the SD from 2.55 to 0.61. The median statistic adjusted slightly from 9.04 to 8.97 and the IQR narrowed from 1.28 to 0.42. The comparative adjustments between the parametric and non-parametric descriptive statistics are accounted for by the close grouping of the remaining five data points in both dose groups VV and RN. This can be confirmed graphically by referring to the heights of the boxes in the box-whisker plots in Table 5.114.A, as well as by the considerably narrower IQR statistics in the corresponding table of descriptive statistics.

The narrow grouping of the core data points results in central tendency statistics that are far more robust to fluctuations than when compared to a data set that has widely scattered data. In addition, a data set with a well-clustered core of data points considerably improves the reliability of the central tendency statistics. The presence of these extreme outliers consequently required that multiple comparisons of dose groups be performed via parametric and non-parametric protocols, as presented in Table 5.115.

Table 5.114 Box-whisker representation and descriptive statistics of the liver tissue L/P ratio data generated from the main study

A: Box-whisker plots and data points according to rat groups



Rat	NN	VX	VN	VV	VC	VS	RX	RN	RV	RC	RS	VV*	RN*
1	11.2	13.2	8.18	• 13.0	8.55	17.2	27.4	8.97	7.29	19.9	11.5	EXCL	8.97
2	9.34	17.3	14.8	7.49	8.58	11.2	7.74	9.11	10.4	9.87	+ 34.8	7.49	9.11
3	9.56	26.6	9.91	8.03	15.6	10.8	4.42	• 15.1	15.5	8.69	6.81	8.03	EXCL
4	4.95	15.0	15.5	6.05	15.5	22.8	13.5	8.69	6.71	6.97	8.40	6.05	8.69
5	4.40	21.5	16.1	6.71	11.2	14.2	17.1	10.0	5.69	6.06	17.3	6.71	10.0
6	11.5	11.0	4.55	6.64	15.7	10.5	13.9	8.34	7.72	15.3	13.0	6.64	8.34

B: Descriptive statistics

Dose group	Sample size	Mean	SD	Median	Min	Max	Range	Lower quartile	Upper quartile	IQR
NN	6	8.48	3.07	9.45	4.40	11.5	7.07	4.95	11.2	6.22
VX	6	17.4	5.76	16.1	11.0	26.6	15.6	13.2	21.5	8.33
VN	6	11.5	4.68	12.4	4.55	16.1	11.6	8.18	15.5	7.27
VV	6	7.99	2.55	7.10	6.05	13.0	6.95	6.64	8.03	1.39
VV*	5	6.98	0.78	6.71	6.05	8.03	1.98	6.64	7.49	0.85
VC	6	12.5	3.49	13.3	8.55	15.7	7.11	8.58	15.6	6.99
VS	6	14.4	4.84	12.7	10.5	22.8	12.3	10.8	17.2	6.34
RX	6	14.0	8.01	13.7	4.42	27.4	23.0	7.74	17.1	9.34
RN	6	10.0	2.55	9.04	8.34	15.1	6.78	8.69	10.0	1.28
RN*	5	9.02	0.61	8.97	8.34	10.0	1.64	8.69	9.11	0.42
RV	6	8.89	3.61	7.50	5.69	15.5	9.83	6.71	10.4	3.70
RC	6	11.1	5.39	9.28	6.06	19.9	13.9	6.97	15.3	8.37
RS	6	15.3	10.2	12.3	6.81	34.8	28.0	8.40	17.3	8.92

Rat codes for outliers and extreme outliers are located above or below the respective blue crosses (+) and red dots (•), which correspond to data point values listed in the table directly below the graph. The vertical dashed line in the box-whisker graphic representation separates original dose group box-whisker plots from those that have had the extreme outliers excluded, which are also indicated by the asterisk (*) following the dose group code. Data sets with excluded data points are designated in green text. Rats were treated with NN = no dose regimen, VX = vehicle and sacrificed, VN = vehicle and no dose, VV = vehicle and vehicle, VC = vehicle and CoQ_{10}, VS = vehicle and succinate, RX = rotenone and sacrificed, RN = rotenone and no dose, RV = rotenone and vehicle, RC = rotenone and CoQ_{10}, RS = rotenone and succinate. EXCL = excluded data point, IQR = inter-quartile range, L/P = ratio of lactate to pyruvate, Min = minimum data point value, Max = maximum data point value, SD = standard deviation.

Table 5.115.B indicates that an overall statistically significant variation exists between dose groups of the liver tissue L/P data set. Prior to the exclusion of the two extreme outliers, the Kruskal-Wallis ANOVA resulted in a p-value of 0.038. A statistically significant p-value of 0.043 was determined by a one-way ANOVA for the data set that had had VV-1 and RN-3 excluded. Both p-values were significant at the 0.05 significance level. However, the multiple comparison p-values, indicated in Section A of the same table, do not reveal any dose groups that differ significantly from each other.

Table 5.115 Multiple comparison statistics of the liver L/P ratio data generated from the rat main study

A: Non-parametric and parametric p-values											
Dose group	**NN**	**VX**	**VN**	**VV**	**VC**	**VS**	**RX**	**RN**	**RV**	**RC**	**RS**
NN		0.488	1.000	1.000	1.000	1.000	1.000	1.000	1.000	1.000	1.000
		0.166	0.996	1.000	0.968	0.715	0.791	1.000	1.000	0.999	0.530
VX	0.488		1.000	0.067	1.000	1.000	1.000	1.000	0.311	1.000	1.000
	0.166		0.720	0.109	0.885	0.996	0.990	0.355	0.216	0.644	1.000
VN	1.000	1.000		1.000	1.000	1.000	1.000	1.000	1.000	1.000	1.000
	0.996	0.720		0.962	1.000	0.997	0.999	1.000	0.999	1.000	0.978
VV	1.000	0.067	1.000		1.000	0.467	1.000	1.000	1.000	1.000	1.000
	1.000	0.109	0.962		0.873	0.535	0.614	1.000	1.000	0.978	0.371
VC	1.000	1.000	1.000	1.000		1.000	1.000	1.000	1.000	1.000	1.000
	0.968	0.885	1.000	0.873		1.000	1.000	0.994	0.985	1.000	0.998
VS	1.000	1.000	1.000	0.467	1.000		1.000	1.000	1.000	1.000	1.000
	0.715	0.996	0.997	0.535	1.000		1.000	0.884	0.792	0.993	1.000
RX	1.000	1.000	1.000	1.000	1.000	1.000		1.000	1.000	1.000	1.000
	0.791	0.990	0.999	0.614	1.000	1.000		0.926	0.858	0.997	1.000
RN	1.000	1.000	1.000	1.000	1.000	1.000	1.000		1.000	1.000	1.000
	1.000	0.355	1.000	1.000	0.994	0.884	0.926		1.000	1.000	0.756
RV	1.000	0.311	1.000	1.000	1.000	1.000	1.000	1.000		1.000	1.000
	1.000	0.216	0.999	1.000	0.985	0.792	0.858	1.000		1.000	0.618
RC	1.000	1.000	1.000	1.000	1.000	1.000	1.000	1.000	1.000		1.000
	0.999	0.644	1.000	0.978	1.000	0.993	0.997	1.000	1.000		0.959
RS	1.000	1.000	1.000	1.000	1.000	1.000	1.000	1.000	1.000	1.000	
	0.530	1.000	0.978	0.371	0.998	1.000	1.000	0.756	0.618	0.959	
B: ANOVA p-values											
Kruskal-Wallis p-value = 0.038						One-way ANOVA p-value = 0.043					

A: All comparison statistics are indicated as p-values. The upper p-value is the non-parametric multiple comparison test statistic, generated from the original set of data. The lower p-value was generated via the parametric Tukey *unequal number HSD* (Honestly Significant Difference) test, after the exclusion of extreme outliers. P-values in grey, indicate that no significant differences exist. B: P-values for the non-parametric Kruskal-Wallis ANOVA and parametric one-way ANOVA are listed, with significant p-values, less than the 0.05 significance level, indicated in red. Rats were dosed NN = no dose and no dose, VX = vehicle and sacrificed, VN = vehicle and no dose, VV = vehicle and vehicle, VC = vehicle and CoQ_{10}, VS = vehicle and succinate, RX = rotenone and sacrificed, RN = rotenone and no dose, RV = rotenone and vehicle, RC = rotenone and CoQ_{10}, RS = rotenone and succinate. ANOVA = analysis of variance.

The lack of correspondence between the complementing statistical procedures has been reported in previous sections and cannot be explained with certainty. The global variation among all dose groups is reported to be statistically significant, but is supported by neither the non-parametric multiple comparison procedure nor by the Tukey *unequal number HSD* test. Such statistical outputs may suggest that variations in response may indeed be

present between groups and that possible trends should be taken into consideration. Moreover, it does not completely exclude the possibility that differences exist between dose groups.

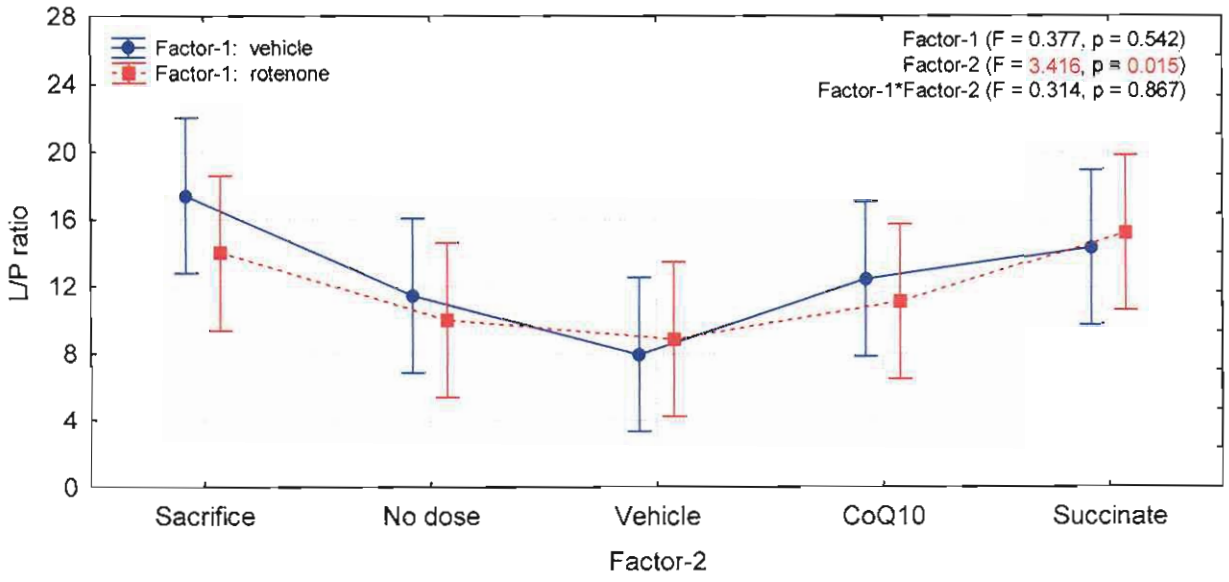
In order to investigate the possible significance of differences in response between dose groups of the liver tissue L/P data, a factorial analysis was performed, as presented in Table 5.116. As discussed previously, the narrow grouping of the core data points of dose groups VV and RN resulted in a robust and reliable set of central tendency statistics that were not very sensitive to the exclusion of their respective extreme outliers. This is further supported by the similarity in vehicle and rotenone Factor-1 plots in both Sections A and B of Table 5.116.

Visible differences between the graphic representations are not markedly evident, with very similar trends in the plots observed. Moreover, the statistical significance of the Factor-1 and Factor-2 F-statistics remained consistent whether the extreme outliers were included or not. Factorial analysis of the liver L/P data set indicated that Factor-2 dose regimens contributed most to the responses observed in liver tissue of rats. Regardless of the Factor-1 regimen received, decreased liver L/P ratios were observed in rats that received a vehicle Factor-2 dose.

It should be noted however that the mean data point for dose group RN was also as low as that for RV. The vehicle and rotenone Factor-1 plots also indicate that CoQ_{10} and succinate were not beneficial and hence did not improve L/P ratios in liver tissue. In addition, it can be observed from both Sections A and B of Table 5.116 that the 95% confidence intervals consistently overlapped, regardless of which Factor-1 and Factor-2 dose regimens the rats received.

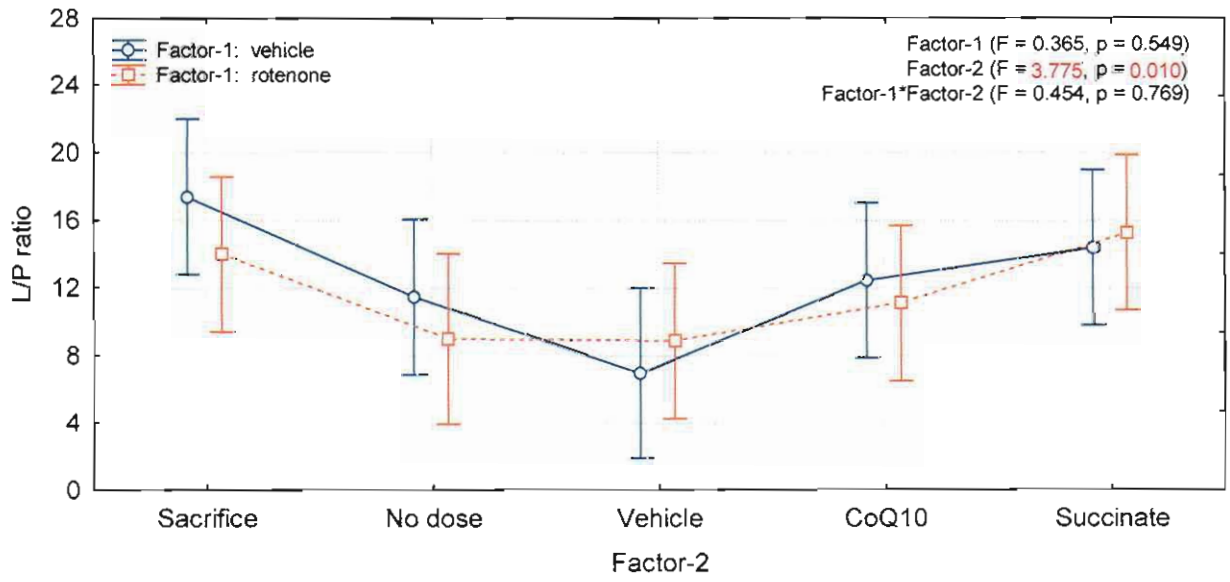
Table 5.116 Graphic and tabulated summary of the liver tissue L/P ratio data analysed via a two-way ANOVA

A: Data set including extreme outliers



Description		VX	VN	VV	VC	VS	RX	RN	RV	RC	RS
With extreme outliers	UCI	22.0	16.1	12.6	17.1	19.0	18.6	14.6	13.5	15.7	19.9
	mean	17.4	11.5	7.99	12.5	14.4	14.0	10.0	8.89	11.1	15.3
	LCI	12.8	6.91	3.39	7.89	9.83	9.43	5.44	4.29	6.54	10.7

B: Data set excluding extreme outliers



Description		VX	VN	VV	VC	VS	RX	RN	RV	RC	RS
Without extreme outliers	UCI	22.0	16.1	12.0	17.1	19.0	18.6	14.1	13.5	15.8	19.9
	mean	17.4	11.5	6.98	12.5	14.4	14.0	9.02	8.89	11.1	15.3
	LCI	12.8	6.90	1.94	7.89	9.82	9.42	3.97	4.28	6.53	10.7

The plot legends for each graph are indicated in the top left corners of the respective graphs, while the two-way ANOVA F-statistics (F) and p-values (p) for Factor-1, Factor-2 and Factor-1*Factor-2 are located in the top right corner, with the statistically significant values indicated in red. The vertical whiskers at each mean data point represent 95% confidence intervals for the respective data sets. The mean values in green text, located in the data point summary tables below the graphs, indicate those that were adjusted due to the exclusion of extreme outliers. Rats were treated with NN = no dose regimen, VX = vehicle and sacrificed, VN = vehicle and no dose, VV = vehicle and vehicle, VC = vehicle and CoQ_{10}, VS = vehicle and succinate, RX = rotenone and sacrificed, RN = rotenone and no dose, RV = rotenone and vehicle, RC = rotenone and CoQ_{10}, RS = rotenone and succinate. L/P = ratio of lactate to pyruvate, LCI = lower 95% confidence interval data point, UCI = upper 95% confidence interval data point.

The environmental controls, not depicted in the two-way ANOVA summary graphs, harboured a liver tissue L/P ratio of 8.48. Therefore, by referring to the mean data point recordings in Table 5.116, it can be observed that all the dose groups, with the exception of VV, harboured higher L/P ratios than NN. Although the differences were not determined by the multiple comparison procedures in Table 5.115 to be statistically significant, this observation should be noted. Since all the rat groups, excluding NN, received vehicle, the data may therefore suggest that sunflower oil may have contributed to increased L/P ratios in liver. A contribution from rotenone to the L/P ratios in liver tissue appears to be in the minority due to the observation that the rotenone plots in Table 5.116 tend to remain consistently similar to the vehicle plots.

5.7.5 GSH/GSSG ratios in liver tissue

Liver tissue was homogenised and prepared appropriately for the generation of glutathione data. Following the assay for glutathione levels in the prepared samples, the data was captured in Excel® and subsequently exported to STATISTICA™ for an evaluation of the different response profiles generated from the various dose groups. The data, according to dose group, are presented in Table 5.117, along with descriptive statistics.

Table 5.117 Box-whisker representation and descriptive statistics of the liver GSH/GSSG ratio data generated from the main study

A: Box-whisker plots and data points according to rat groups

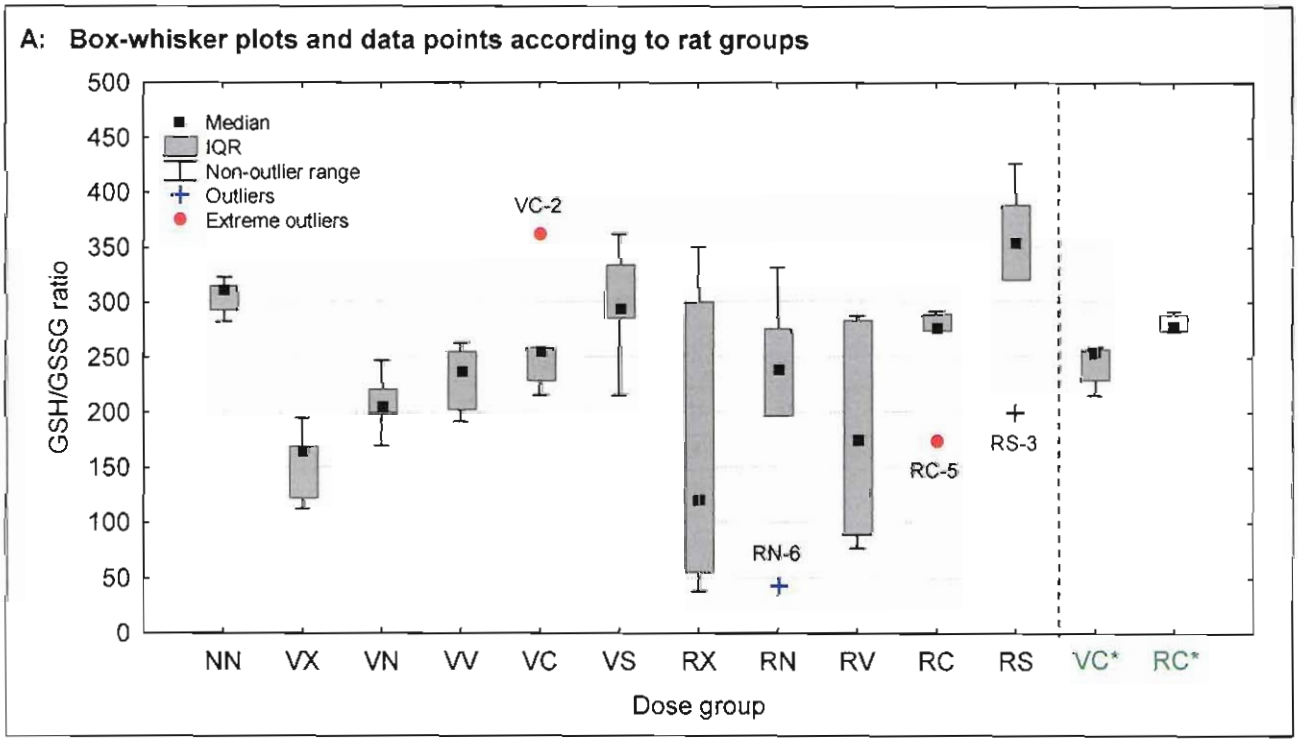


Table 5.117 Continued...

Rat	NN	VX	VN	VV	VC	VS	RX	RN	RV	RC	RS	VC*	RC*
1	312	162	170	202	228	334	147	275	77.2	274	320	228	274
2	310	167	208	192	• 361	362	38.3	240	283	289	377	EXCL	289
3	282	195	247	254	254	300	55.1	237	288	278	+ 199	254	278
4	314	122	220	231	258	216	92.7	197	89.5	292	427	258	292
5	323	169	199	263	216	285	299	332	177	• 173	330	216	EXCL
6	293	112	201	242	256	287	351	+ 42.4	171	274	388	256	274

B: Descriptive statistics

Dose group	Sample size	Mean	SD	Median	Min	Max	Range	Lower quartile	Upper quartile	IQR
NN	6	306	15.2	311	282	323	40.7	293	314	21.8
VX	6	155	31.2	165	112	195	82.4	122	169	46.8
VN	6	208	25.5	205	170	247	77.1	199	220	21.1
VV	6	231	28.6	236	192	263	71.5	202	254	52.4
VC	6	262	51.5	255	216	361	146	228	258	30.2
VC*	5	242	19.3	254	216	258	42.8	228	256	27.8
VS	6	297	49.9	294	216	362	147	285	334	48.3
RX	6	164	131	120	38.3	351	313	55.1	299	244
RN	6	220	98.3	238	42.4	332	289	197	275	78.6
RV	6	181	90.5	174	77.2	288	211	89.5	283	193
RC	6	263	44.8	276	173	292	119	274	289	15.0
RC*	5	281	8.40	278	274	292	18.2	274	289	14.3
RS	6	340	79.5	354	199	427	228	320	388	68.5

Rat codes for outliers and extreme outliers are located above or below the respective blue crosses (+) and red dots (•), which correspond to data point values listed in the table directly below the graph. The vertical dashed line in the box-whisker graphic representation separates original dose group box-whisker plots from those that have had the extreme outliers excluded, which are also indicated by the asterisk (*) following the dose group code. Data sets with excluded data points are designated in green text. Rats were treated with NN = no dose regimen, VX = vehicle and sacrificed, VN = vehicle and no dose, VV = vehicle and vehicle, VC = vehicle and CoQ_{10}, VS = vehicle and succinate, RX = rotenone and sacrificed, RN = rotenone and no dose, RV = rotenone and vehicle, RC = rotenone and CoQ_{10}, RS = rotenone and succinate. EXCL = excluded data point, GSH/GSSG = ratio of reduced to oxidised glutathione, IQR = inter-quartile range, Min = minimum data point value, Max = maximum data point value, SD = standard deviation.

Table 5.117.A illustrates that two outliers and two extreme outliers are present in the complete liver GSH/GSSG data set. Rat VC-2 presented with a ratio of 361, which is more than 100 ratio units larger than the closest ranked ratio of 258 for VC-4. The exclusion of VC-2 results in a mean decrease from 262 to 242, and the SD decrease from 51.5 to 19.3. The non-parametric median decreased only from 255 to 254. Similarly, the IQR remained more stable decreasing from 30.2 to 27.8. An evident indication as to the sensitivity of the parametric descriptive statistics to the presence of extreme outliers is again illustrated. The non-parametric median and IQR statistics remained far more constant and reliable in interpreting the central tendency of dose group VC. The second extreme outlier, RC-5, harboured a liver GSH/GSSG ratio of 173, which was also approximately 100 ratio units from the closest ranked ratio of 274 for rat RC-6. Upon exclusion of RC-5 from dose group RC, the mean increased from a ratio of 263 to 281, while the median increased only slightly from 276 to 278. The SD decreased markedly from 44.8 to 8.40, while IQR decreased from only 15.0 to 14.3. Dose group RC typically

exemplifies the robustness of non-parametric descriptive statistics to the presence of outliers, as opposed to the parametric counterparts, which have consistently illustrated their vulnerability to portraying skewed central tendency statistics.

Outlier RN-6 is very close to being classified an extreme outlier. The lower outlier boundary is positioned at 39.5. Therefore, since RN-6 harboured a GSH/GSSG ratio of 42.4, it is a mere 2.9 units from being regarded an extreme outlier. In addition, RN-6 is more than 150 ratio units from that generated for rat RN-4, the next closest ranked data point. The extreme outliers, VC-2 and RC-5, were approximately 100 ratio units from their closest ranked data points. However, since the 78.6 IQR for dose group RN is wider than for both the IQRs for VC and RC, the stringency of outlier analysis is lowered. Thus, the non-outlier and outlier ranges are more widely dispersed for data set RN. This allows more freedom for outliers and extreme outliers like RN-6, which can hence be positioned further from the lower quartile data point without being classified an extreme outlier. The fact that RN-6 is situated so close to the lower outlier boundary, exclusion would certainly result in raised mean and median GSH/GSSG ratios for dose group RN. The decreased variation would in turn also influence ANOVA and multiple comparison statistics. Nonetheless, RN-6 was not classified as an extreme outlier and will not be excluded.

Data point RS-3, the second outlier, presented with a GSH/GSSG ratio of 199, which is approximately 120 units from the closest ranked ratio of 320 for RS-1. The lower outlier boundary is positioned at 183, which is lower than RS-3 by a ratio of 16.3. Therefore, it may be expected that exclusion of RS-3 would impact on statistical interpretations. However, these effects, in addition to those predicted via the exclusion of RN-6, are purely speculative since RS-3 and RN-6 are not extreme outliers and will not be excluded.

The box-whisker representations in Table 5.117.A reflect that rat groups were mostly affected adversely by the dose regimens. As with the blood GSH/GSSG data, discussed in Section 5.3.3, it is uncertain whether rotenone further affected or improved GSH/GSSG ratios. It can be suggested from the data distributions that the rotenone-treated rats presented with increased variation in response. Among the groups that received a vehicle Factor-1 dose, it appeared that liver GSH/GSSG ratios improved as rats received different Factor-2 doses. A comparative scenario can be argued for the induced Complex I deficiency rats, where improved GSH/GSSG ratios were observed when various Factor-2 treatments were received. The statistical and biological significance of individual dose group comparisons are presented in Table 5.118.

Table 5.118 Multiple comparison statistics of the liver GSH/GSSG ratio data generated from the rat main study

A: Non-parametric and parametric p-values

Dose group	NN	VX	VN	VV	VC	VS	RX	RN	RV	RC	RS
NN		0.012	0.533	1.000	1.000	1.000	0.357	1.000	0.341	1.000	1.000
		0.010	0.300	0.681	0.913	1.000	0.021	0.504	0.067	1.000	0.998
VX	0.012		1.000	1.000	1.000	0.039	1.000	1.000	1.000	0.661	0.004
	0.010		0.948	0.662	0.590	0.019	1.000	0.820	1.000	0.118	< 0.001
VN	0.533	1.000		1.000	1.000	1.000	1.000	1.000	1.000	1.000	0.246
	0.300	0.948		1.000	0.999	0.426	0.986	1.000	1.000	0.804	0.040
VV	1.000	1.000	1.000		1.000	1.000	1.000	1.000	1.000	1.000	1.000
	0.681	0.662	1.000		1.000	0.810	0.809	1.000	0.966	0.980	0.168
VC	1.000	1.000	1.000	1.000		1.000	1.000	1.000	1.000	1.000	1.000
	0.913	0.590	0.999	1.000		0.964	0.735	1.000	0.925	0.997	0.435
VS	1.000	0.039	1.000	1.000	1.000		0.887	1.000	0.851	1.000	1.000
	1.000	0.019	0.426	0.810	0.964		0.037	0.648	0.112	1.000	0.988
RX	0.357	1.000	1.000	1.000	1.000	0.887		1.000	1.000	1.000	0.160
	0.021	1.000	0.986	0.809	0.735	0.037		0.922	1.000	0.191	0.001
RN	1.000	1.000	1.000	1.000	1.000	1.000	1.000		1.000	1.000	1.000
	0.504	0.820	1.000	1.000	1.000	0.648	0.922		0.994	0.931	0.093
RV	0.341	1.000	1.000	1.000	1.000	0.851	1.000	1.000		1.000	0.152
	0.067	1.000	1.000	0.966	0.925	0.112	1.000	0.994		0.396	0.005
RC	1.000	0.661	1.000	1.000	1.000	1.000	1.000	1.000	1.000		1.000
	1.000	0.118	0.804	0.980	0.997	1.000	0.191	0.931	0.396		0.943
RS	1.000	0.004	0.246	1.000	1.000	1.000	0.160	1.000	0.152	1.000	
	0.998	< 0.001	0.040	0.168	0.435	0.988	0.001	0.093	0.005	0.943	

B: ANOVA p-values

Kruskal-Wallis p-value < 0.001	One-way ANOVA p-value < 0.001

C: Statistical and biological significance

Comparison		Statistical significance (p)		Biological significance (d)	
		Including EOs	Excluding EOs	Including EOs	Excluding EOs
NN	VX	0.012	0.010	4.843	2.270
NN	RX	0.357	0.021	N/A	2.131
VX	VS	0.039	0.019	2.862	2.146
VX	RS	0.004	< 0.001	2.335	2.789
VN	RS	0.246	0.040	N/A	1.991
VS	RX	0.887	0.037	N/A	2.006
RX	RS	0.160	0.001	N/A	2.649
RV	RS	0.152	0.005	N/A	2.394

A: All comparison statistics are indicated as p-values. The upper p-value is the non-parametric multiple comparison test statistic, generated from the original set of data. The lower p-value was generated via the parametric Tukey *unequal number HSD* (Honestly Significant Difference) test, after the exclusion of extreme outliers. P-values indicated in red are statistically significant at the pre-determined significance level of 0.05. P-values in black text represent those that are not statistically significant, but have complementary p-values that are statistically significant. The remainder of p-values are listed in grey. The comparisons surrounded by the **bold** black line are those that were determined to be statistically significant by both the non-parametric and parametric multiple comparison procedures. The turquoise shaded blocks represent statistically significant comparisons that were also determined to be of biological significance. B: P-values for the non-parametric Kruskal-Wallis ANOVA and parametric one-way ANOVA are listed, with significant p-values, less than the 0.05 significance level, indicated in red. C: List of comparisons determined to be statistically significant with corresponding biological significance. A d-value greater than or equal to 0.8 signifies biological significance, indicated in red. Rats were treated with NN = no dose regimen, VX = vehicle and sacrificed, VN = vehicle and no dose, VV = vehicle and vehicle, VC = vehicle and CoQ_{10}, VS = vehicle and succinate, RX = rotenone and sacrificed, RN = rotenone and no dose, RV = rotenone and vehicle, RC = rotenone and CoQ_{10}, RS = rotenone and succinate. < = less than, ANOVA = analysis of variance, EOs = extreme outliers, N/A = not applicable.

Since two extreme outliers were determined to be present in the liver tissue GSH/GSSG data set, parametric and non-parametric protocols with exclusion and inclusion of extreme outliers were performed. Kruskal-Wallis and one-way ANOVA p-values were highly

statistically significant with p-values of < 0.001 for both. Prior to the exclusion of VC-2 and RC-5, three dose group comparisons were determined to differ statistically significantly from each other, all of which included comparisons with dose group VX. These comparisons were also determined to differ with biological significance, as indicated in Table 5.118.B. Furthermore, even upon exclusion of the extreme outliers, these groups were illustrated to differ significantly from each other. Dose group VX differed significantly from the environmental controls NN, as well as from dose groups VS and RS. The latter comparison will not be discussed, as it is not possible to evaluate the effect of a single dose.

The environmental controls harboured a mean GSH/GSSG ratio of 306, whereas VX had a mean of 155, approximately half of NN. This suggests that the sunflower oil vehicle significantly affects liver GSH ratios. However, if this were to be the case, it would be expected that dose group VV would present with a similar ratio, if not lower than VX. This cannot be confidently confirmed since the mean ratio for VV is 231, considerably higher than that of the 155 mean ratio for dose group VX. Nonetheless, these two groups did not differ statistically significantly from each other, whether extreme outliers were included or not. Dose group VX also differed significantly from VS, which had almost double the mean GSH/GSSG ratio of VX at 297. Since the environmental controls NN presented with a mean ratio of 306, the data suggests that succinate re-established GSH/GSSG ratios in rats that received a vehicle Factor-1 dose. This is in contrast to data presented in Section 5.3.3 where CoQ_{10} proved to restore GSH/GSSG ratios in blood.

It is apparent from the graphic representation of the liver GSH/GSSG data that succinate improved ratios regardless of whether rats received vehicle or rotenone Factor-1 dose regimens. Moreover, succinate improved liver GSH/GSSG ratios better than CoQ_{10} or any of the other Factor-2 dose regimens. However, even though dose group VS and RS displayed the highest GSH/GSSG ratios in their respective Factor-1 dose groups, it should be noted that neither VS nor RS differed statistically significantly from VC or RC respectively. Therefore, it cannot be conclusively stated that succinate was indeed more beneficial than CoQ_{10} as a Factor-2 dose. Dose groups VC and RC did not differ statistically significantly from any group in the main study, suggesting that no beneficial or harmful effects were incurred. Upon exclusion of the extreme outliers, it was revealed that RS differed statistically significantly from an additional three dose groups, namely VN, RX and RV. Moreover, these dose groups also differed with biological significance from RS. The significant difference between RS and RX, as well as between RS and RV, supports

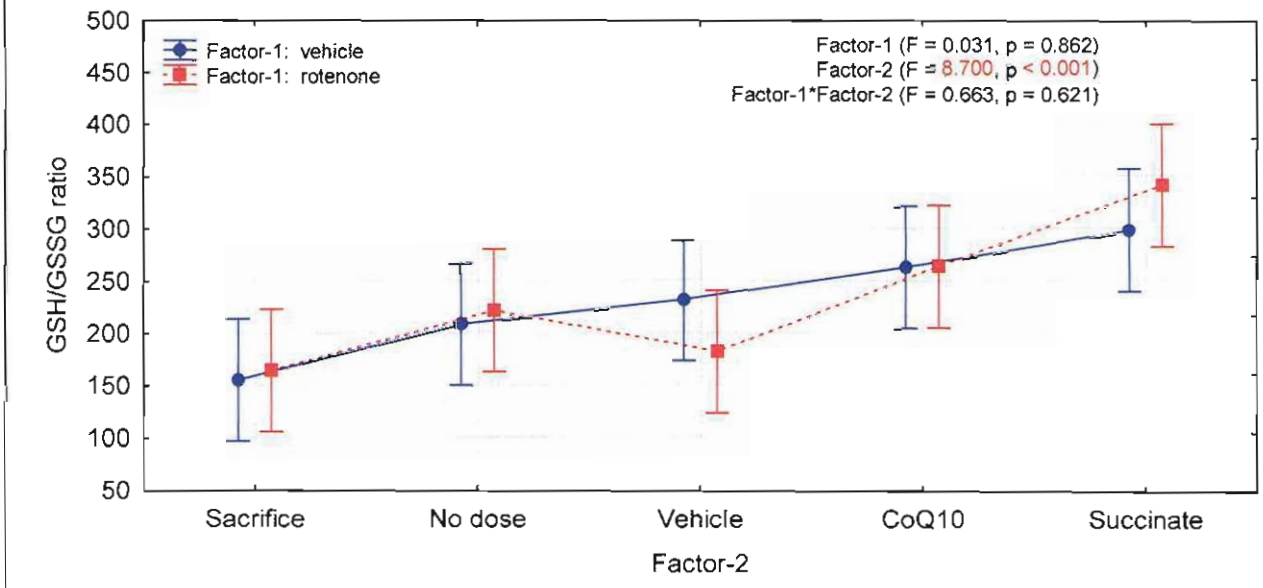
the notion further that a succinate Factor-2 dose was indeed beneficial. A comparison between RS and VN is not of value when determining single dose effects and will therefore not be discussed.

Finally, it should also be mentioned that, after the exclusion of extreme outliers, dose group RX differed statistically significantly from NN and VS. These differences were also determined to be of biological significance, as listed in Table 5.118.C. As with previously mentioned comparisons that measure more than one dosage effect, the comparison between RX and VS will not be considered for discussion. With regards to RX and NN, it should be noted that the distribution of data for RX was far more dispersed. The same is true if RX is compared to VX. However, the mean ratios for RX and VX are comparable at 164 and 155 respectively. Since RX and VX did not differ significantly from each other, it can be argued that rotenone did not influence GSH/GSSG ratios any more than the sunflower oil vehicle itself. Furthermore, since both RX and VX differed significantly from NN, even though the RX-NN comparison was significant only after extreme outliers were excluded, suggests that rats were indeed influenced adversely by the sunflower oil vehicle. Observing from the box-whisker plots in Table 5.117.A that the majority of rats receiving dosage regimens harboured lowered GSH/GSSG ratios in liver supports this. Contributions of the various Factor-1 and Factor-2 dose regimens were further evaluated via a factorial ANOVA. Summary graphs and statistical significance of Factor-1 and Factor-2 dose regimens are presented in Table 5.119. Graphic representations are presented in parallel with extreme outliers included and excluded accordingly.

Table 5.119 indicates that Factor-2 doses made highly significant contributions prior to and after extreme outlier exclusion. The F-statistics for Factor-2, when compared to Factor-1 and the interaction F-statistics, illustrates unequivocally that response in rats was determined largely by the Factor-2 dose regimens. Factor-1 F-statistics improved from 0.031 to 0.345 after the extreme outliers were excluded, while Factor-1*Factor-2 F-statistics increased from 0.663 to 0.824. The F-statistic for Factor-2 increased from 8.700 to 8.989 upon extreme outlier exclusion. This supports previous statements that rotenone did not influence GSH/GSSG ratios in rats.

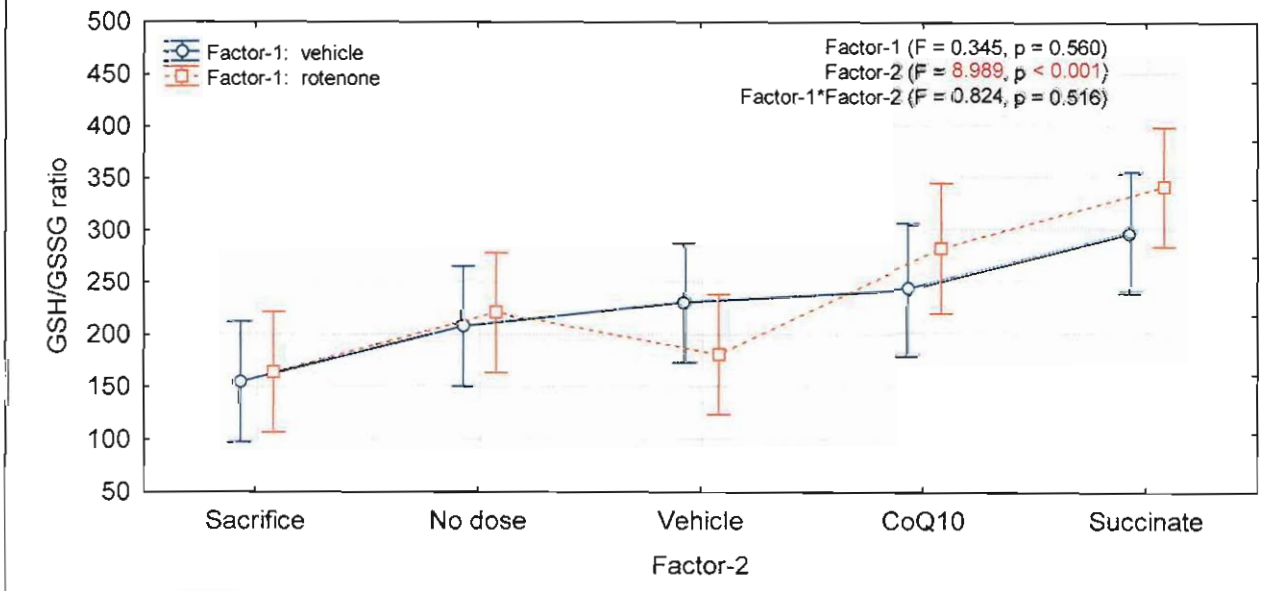
Table 5.119 Graphic and tabulated summary of the liver tissue GSH/GSSG ratio data analysed via a two-way ANOVA

A: Data set including extreme outliers



Description		VX	VN	VV	VC	VS	RX	RN	RV	RC	RS
With extreme outliers	UCI	213	266	289	321	356	222	279	239	322	399
	mean	154	208	231	262	297	164	220	181	263	340
	LCI	95.9	149	172	204	239	105	162	122	205	282

B: Data set excluding extreme outliers



Description		VX	VN	VV	VC	VS	RX	RN	RV	RC	RS
Without extreme outliers	UCI	212	265	288	305	355	221	278	238	344	397
	mean	154	208	231	242	297	164	220	181	281	340
	LCI	97.2	150	173	180	240	107	163	124	218	283

The plot legends for each graph are indicated in the top left corners of the respective graphs, while the two-way ANOVA F-statistics (F) and p-values (p) for Factor-1, Factor-2 and Factor-1*Factor-2 are located in the top right corner, with the statistically significant values indicated in red. The vertical whiskers at each mean data point represent 95% confidence intervals for the respective data sets. The mean values in green text, located in the data point summary tables below the graphs, indicate those that were adjusted due to the exclusion of extreme outliers. Rats were treated with NN = no dose regimen, VX = vehicle and sacrificed, VN = vehicle and no dose, VV = vehicle and vehicle, VC = vehicle and CoQ_{10}, VS = vehicle and succinate, RX = rotenone and sacrificed, RN = rotenone and no dose, RV = rotenone and vehicle, RC = rotenone and CoQ_{10}, RS = rotenone and succinate. < = less than, GSH/GSSG = ratio of reduced to oxidised glutathione, LCI = lower 95% confidence interval data point, UCI = upper 95% confidence interval data point.

It appears that an increasing trend in response can be detected in rats that received Factor-2 doses, with the greatest improvements observed when therapeutic CoQ_{10} and succinate were administered. As argued previously, succinate appeared to contribute most to the improvements in liver GSH/GSSG ratios, which can again be confirmed by the higher mean data points for VS and RS when compared to VC and RC respectively. However, as p-values indicated in Table 5.118.A, the differences between VC and VS as well as between RC and RS were not determined to be statistically significant. The fact that neither VC nor RC differed statistically significantly from any of the other groups in their respective Factor-1 dose categories, as opposed to VS and RS, further supports the notion that succinate was more beneficial to the recovery of liver GSH/GSSG ratios.

5.7.6 ATP/ADP ratios in liver tissue

Liver tissue was collected from rats on the days that they were sacrificed and prepared appropriately via homogenisation and deproteinisation. The concentrations of adenylates were subsequently determined via spectrophotometric analysis and the data captured in Excel® spreadsheets. Upon statistical evaluation of the data in STATISTICA™ it was determined that the ATP/ADP ratio data set for liver tissue contained four missing data points, for rats VN-2, VN-4, VN-5 and RN-3. It is unfortunate that three of the four missing data points were within one dose group, namely VN. Consequently, the VN data set is severely compromised, with the reliability of central tendency statistics and multiple comparison data questionable. Therefore, interpretation of the descriptive statistics and any dose group comparisons regarding VN should be performed with caution. The distribution of liver tissue ATP/ADP ratios is presented in Table 5.120, accompanied by a list of all data points and a table of descriptive statistics.

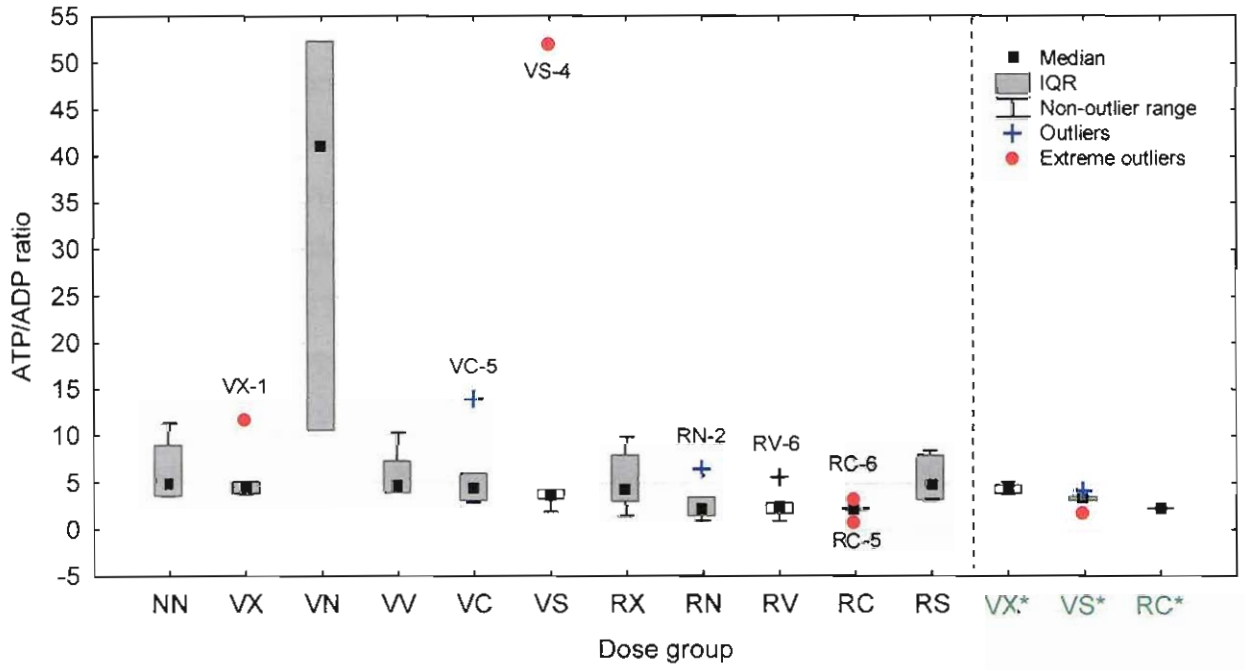
The box-whisker representations of the data indicate the presence of five extreme outliers and four outliers. However, one outlier and one extreme outlier were determined in dose group VS*, which were classified only after an extreme outlier had been excluded from the original group VS. The exclusion of the extreme outlier VS-4 resulted in a reduced IQR and the consequent detection of the additional outlier and extreme outlier, which was consequently not excluded. The previously mentioned VS-4 rat harboured an ATP/ADP ratio of 52.0, which was well above the closest ranked data point for VS-6 harbouring an ATP/ADP ratio of 4.26. As expected, upon exclusion of VS-4, the mean and SD ATP/ADP ratios for dose group VS diminished from 11.5 to 3.34 and from 19.9 to 0.87 respectively.

The median and IQR were more consistent, decreasing slightly from 3.61 to 3.56 and from 0.95 to 0.35 respectively.

Rat VX-1 presented with a liver ATP/ADP ratio of 11.7, which was determined to be an extreme outlier in dose group VX. The group consisted of an additional five data points that ranged from ratios of 3.79 to 5.10. The exclusion of VX-1 resulted in a decreased mean ATP/ADP ratio of 4.40 from 5.61, as well as a considerable decrease in SD from 3.02 to 0.56. The median for dose group VX adjusted slightly from 4.61 to 4.49, while the IQR decreased from 1.21 to 0.84.

Table 5.120 Box-whisker representation and descriptive statistics of the liver tissue ATP/ADP ratio data generated from the main study

A: Box-whisker plots and data points according to rat groups



Rat	NN	VX	VN	VV	VC	VS	RX	RN	RV	RC	RS	VX*	VS*	RC*
1	3.60	• 11.7	52.3	7.31	5.97	3.66	9.84	2.26	2.31	2.32	3.34	EXCL	3.66	2.32
2	3.58	4.49	—	4.15	3.14	3.31	5.19	+ 6.43	2.84	2.35	3.22	4.49	3.31	2.35
3	5.12	3.79	41.1	3.96	5.11	1.91	1.48	—	2.67	2.17	7.99	3.79	1.91	2.17
4	11.3	3.88	—	3.95	2.89	• 52.0	3.10	3.50	1.71	2.15	5.40	3.88	EXCL	2.15
5	4.62	4.73	—	10.3	+ 13.8	3.56	3.47	0.97	0.92	• 0.80	8.53	4.73	3.56	EXCL
6	8.96	5.10	10.6	5.17	3.65	4.26	7.98	1.56	+ 5.53	• 3.31	4.13	5.10	4.26	EXCL

B: Descriptive statistics

Dose group	Sample size	Mean	SD	Median	Min	Max	Range	Lower quartile	Upper quartile	IQR
NN	6	6.20	3.21	4.87	3.58	11.3	7.76	3.60	8.96	5.36
VX	6	5.61	3.02	4.61	3.79	11.7	7.89	3.88	5.10	1.21
VX*	5	4.40	0.56	4.49	3.79	5.10	1.31	3.88	4.73	0.84
VN	3	34.7	21.6	41.1	10.6	52.3	41.7	10.6	52.3	41.7
VV	6	5.81	2.55	4.66	3.95	10.3	6.36	3.96	7.31	3.35
VC	6	5.77	4.15	4.38	2.89	13.9	11.0	3.14	5.97	2.83

Table 5.120 Continued...

Dose group	Sample size	Mean	SD	Median	Min	Max	Range	Lower quartile	Upper quartile	IQR
VS	6	11.5	19.9	3.61	1.91	52.0	50.1	3.31	4.26	0.95
VS*	5	3.34	0.87	3.56	1.91	4.26	2.35	3.31	3.66	0.35
RX	6	5.18	3.18	4.33	1.48	9.84	8.36	3.10	7.98	4.88
RN	5	2.95	2.16	2.26	0.97	6.43	5.46	1.56	3.50	1.94
RV	6	2.66	1.57	2.49	0.92	5.53	4.61	1.71	2.84	1.13
RC	6	2.18	0.81	2.25	0.80	3.31	2.52	2.15	2.35	0.20
RC*	4	2.25	0.10	2.25	2.15	2.35	0.20	2.16	2.34	0.18
RS	6	5.43	2.33	4.76	3.22	8.53	5.31	3.34	7.99	4.65

Rat codes for outliers and extreme outliers are located above or below the respective blue crosses (+) and red dots (•), which correspond to data point values listed in the table directly below the graph. The vertical dashed line in the box-whisker graphic representation separates original dose group box-whisker plots from those that have had the extreme outliers excluded, which are also indicated by the asterisk (*) following the dose group code. Data sets with excluded data points are designated in green text. Rats were treated with NN = no dose regimen, VX = vehicle and sacrificed, VN = vehicle and no dose, VV = vehicle and vehicle, VC = vehicle and CoQ_{10}, VS = vehicle and succinate, RX = rotenone and sacrificed, RN = rotenone and no dose, RV = rotenone and vehicle, RC = rotenone and CoQ_{10}, RS = rotenone and succinate. '—' = missing data point, ATP/ADP = ratio of adenosine triphosphate to adenosine diphosphate, EXCL = excluded data point, IQR = inter-quartile range, Min = minimum data point value, Max = maximum data point value, SD = standard deviation.

Dose group RC consisted of two rats that harboured liver tissue ATP/ADP ratios that were classified as extreme outliers when compared to the remaining four data points in the group. Rats RC-5 and RC-6 harboured ATP/ADP ratios of 0.80 and 3.31 respectively. It would be expected that if a data set presented with two extreme outliers, it should have a core group of data points that are extremely well clustered. This is certainly the case with dose group RC that had an IQR of 0.20. The exclusion of RC-5 and RC-6 resulted in an ATP/ADP ratio mean increase from 2.18 to 2.25, while the SD decreased from 0.81 to 0.10. The median ratio remained constant at 2.25, while the IQR decreased only slightly from 0.20 to 0.18.

The distribution of the box-whisker plots in Table 5.120.A illustrates that relatively constant ATP/ADP ratios, ranging between 0 and 10 were generated from liver tissue samples. The exception to this distribution is dose group VN, which consisted of only three data points. As mentioned previously in this section, tentative interpretations of statistics regarding this dose group should be performed. It could be argued that if there were no missing data points in dose group VN, the outlier analyses may have classified at least one of the current data points as an extreme outlier. Since the missing data points severely compromise the accuracy of statistics related to VN, it could be argued that future analyses be performed on the remaining 10 data sets only, thereby excluding dose group VN. However, it was preferred not to deviate from the proposed statistical strategy in Section 4.5 of Chapter Four. Rather than to exclude dose group VN, it was decided that the three data points be maintained as they are still a true reflection of the variation within the complete data set. However, cautious interpretation of results was still required.

The ANOVA and multiple comparison data generated from the liver tissue ATP/ADP ratios are presented in Table 5.121. In addition, the biological significance of statistically significant dose group comparisons is included.

The multiple comparison grid in Table 5.121.A indicates, prior to the exclusion of the four extreme outliers, that dose group RV and RC differed statistically significantly from VN. As discussed previously in this section, comparisons with dose group VN were to be interpreted with caution, not relying too heavily on the accuracy of the result. Moreover, it is not possible to compare these groups to VN due to there being too many factors that complicate the measurement of a single dose effect. Nonetheless, it should be noted that even though dose groups RV and RC differed statistically significantly from VN, they did not differ biologically significantly. The lack of biological significance can be attributed primarily to the large SD reported for dose group VN. As illustrated by the equations in Table 4.2 of Chapter Four, biological significance is essentially dependent on the SD of the means that are being compared. The large SD for VN compromised the accuracy and reliability of the mean as a descriptive statistic for the central tendency, which in turn was reflected in the lack of biological significance.

Table 5.121 Multiple comparison statistics of the liver ATP/ADP ratio data generated from the rat main study

A: Non-parametric (original data set) and parametric (excluding extreme outliers) p-values

Dose group	NN	VX	VN	VV	VC	VS	RX	RN	RV	RC	RS
NN		1.000	1.000	1.000	1.000	1.000	1.000	1.000	0.942	0.230	1.000
		1.000	< 0.001	1.000	1.000	0.998	1.000	0.994	0.979	0.989	1.000
VX	1.000		1.000	1.000	1.000	1.000	1.000	1.000	1.000	0.342	1.000
	1.000		< 0.001	1.000	1.000	1.000	1.000	1.000	1.000	1.000	1.000
VN	1.000	1.000		1.000	1.000	1.000	1.000	0.094	0.034	0.008	1.000
	< 0.001	< 0.001		< 0.001	< 0.001	< 0.001	< 0.001	< 0.001	< 0.001	< 0.001	< 0.001
VV	1.000	1.000	1.000		1.000	1.000	1.000	1.000	0.790	0.188	1.000
	1.000	1.000	< 0.001		1.000	0.999	1.000	0.998	0.991	0.995	1.000
VC	1.000	1.000	1.000	1.000		1.000	1.000	1.000	1.000	1.000	1.000
	1.000	1.000	< 0.001	1.000		1.000	1.000	0.998	0.992	0.996	1.000
VS	1.000	1.000	1.000	1.000	1.000		1.000	1.000	1.000	1.000	1.000
	0.998	1.000	< 0.001	0.999	1.000		1.000	1.000	1.000	1.000	1.000
RX	1.000	1.000	1.000	1.000	1.000	1.000		1.000	1.000	1.000	1.000
	1.000	1.000	< 0.001	1.000	1.000	1.000		1.000	0.999	0.999	1.000
RN	1.000	1.000	0.094	1.000	1.000	1.000	1.000		1.000	1.000	1.000
	0.994	1.000	< 0.001	0.998	0.998	1.000	1.000		1.000	1.000	0.999
RV	0.942	1.000	0.034	0.790	1.000	1.000	1.000	1.000		1.000	1.000
	0.979	1.000	< 0.001	0.991	0.992	1.000	0.999	1.000		1.000	0.997
RC	0.230	0.342	0.008	0.188	1.000	1.000	1.000	1.000	1.000		0.603
	0.989	1.000	< 0.001	0.995	0.996	1.000	0.999	1.000	1.000		0.998
RS	1.000	1.000	1.000	1.000	1.000	1.000	1.000	1.000	1.000	0.603	
	1.000	1.000	< 0.001	1.000	1.000	1.000	1.000	0.999	0.997	0.998	

Table 5.121 Continued...

B: ANOVA p-values					
Kruskal-Wallis p-value = 0.002			One-way ANOVA p-value < 0.001		
C: Statistical and biological significance					
Comparison		**Statistical significance (p)**		**Biological significance (d)**	
		Including EOs	**Excluding EOs**	**Including EOs**	**Excluding EOs**
NN	VN	1.000	< 0.001	N/A	5.603
VX	VN	1.000	< 0.001	N/A	5.957
VN	VV	1.000	< 0.001	N/A	5.680
VN	VC	1.000	< 0.001	N/A	5.688
VN	VS	1.000	< 0.001	N/A	6.166
VN	RX	1.000	< 0.001	N/A	5.804
VN	RN	0.094	< 0.001	N/A	6.242
VN	RV	0.034	< 0.001	0.779	6.299
VN	RC	0.008	< 0.001	0.791	6.380
VN	RS	1.000	< 0.001	N/A	5.755

A: All comparison statistics are indicated as p-values. The upper p-value is the non-parametric multiple comparison test statistic, generated from the original set of data. The lower p-value was generated via the parametric Tukey *unequal number HSD* (Honestly Significant Difference) test, after the exclusion of extreme outliers. P-values indicated in red are statistically significant at the pre-determined significance level of 0.05. P-values in black text represent those that are not statistically significant, but have complementary p-values that are statistically significant. The remainder of p-values are listed in grey. The comparisons surrounded by the **bold** black line are those that were determined to be statistically significant by both the non-parametric and parametric multiple comparison procedures. The turquoise shaded blocks represent statistically significant comparisons that were also determined to be of biological significance. B: P-values for the non-parametric Kruskal-Wallis ANOVA and parametric one-way ANOVA are listed, with significant p-values, less than the 0.05 significance level, indicated in red. C: List of comparisons determined to be statistically significant with corresponding biological significance. A d-value greater than or equal to 0.8 signifies biological significance, indicated in red. Rats were treated with NN = no dose regimen, VX = vehicle and sacrificed, VN = vehicle and no dose, VV = vehicle and vehicle, VC = vehicle and CoQ_{10}, VS = vehicle and succinate, RX = rotenone and sacrificed, RN = rotenone and no dose, RV = rotenone and vehicle, RC = rotenone and CoQ_{10}, RS = rotenone and succinate. < = less than, ANOVA = analysis of variance, EOs = extreme outliers, N/A = not applicable.

Upon the exclusion of the extreme outliers, it was observed that all dose groups differed statistically significantly from dose group VN. Furthermore, all dose groups differed with biological significance from VN. The exclusion of the extreme outliers resulted in a marked decrease in variation within dose groups VX, VS and RC. This in turn resulted in a decreased overlap of data distributions with dose group VN and the consequently exaggerated profile of statistically significant differences. It is argued that, even though all groups differed significantly from VN, the reliability of these statistics should be questioned. Since dose group VN consisted of three data points only, it was initially uncertain as to whether the group should be included in the statistical analyses. Ultimately, it was decided that the three data points of VN are still representative of the total variation in ATP/ADP ratios generated from liver tissue and will therefore remain as part of the data set. However, it would be highly speculative if a data set consisting of three data points were considered to be a true reflection of the response obtained from this rat group.

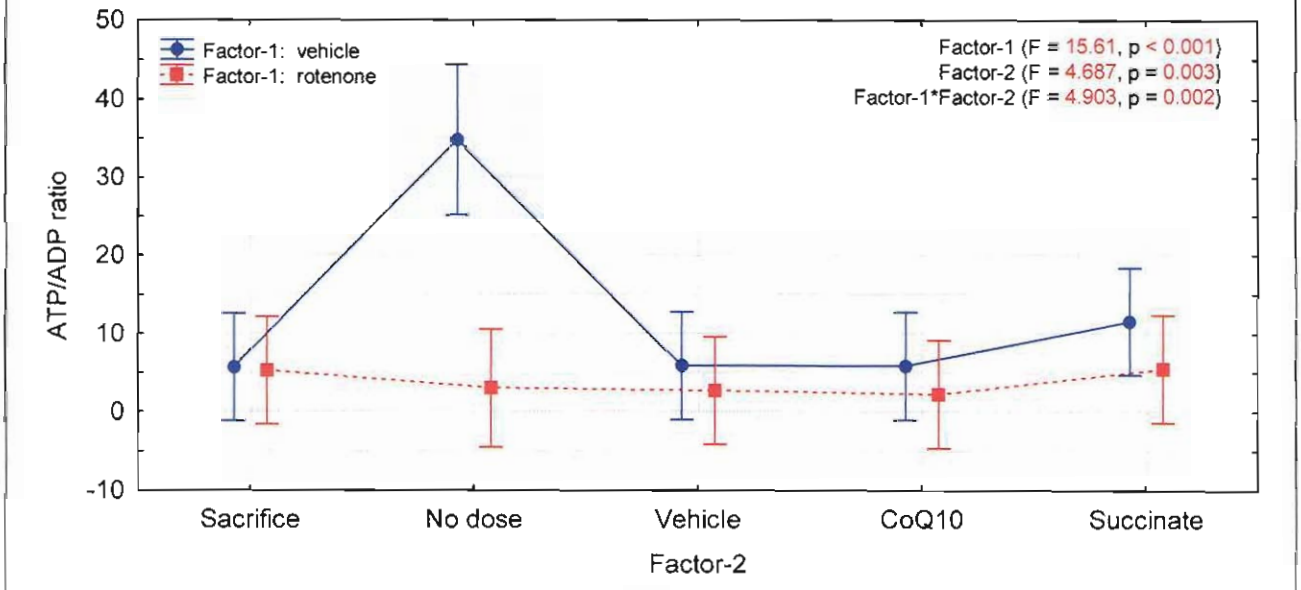
As can be observed in Table 5.120.B, dose group VN, with a sample size of three, has a median that is the second ranked value out of three data points and an IQR that is

identical to the range statistic, indicating that an IQR does in fact not exist. It is therefore not possible to determine if an outlier or extreme outlier is present. Consequently, it can be confidently argued that any statistics describing or relating to dose group VN may well be inappropriate. Therefore, even though dose group VN presented with a mean ATP/ADP ratio that was statistically significantly higher than, amongst others, dose groups VV, VC and VS, it would be unrealistic to argue that a no dose Factor-2 dose would significantly improve adenylate status over therapeutic regimens CoQ_{10} and succinate. The liver tissue ATP/ADP ratio data set was further analysed via a two-way ANOVA. The presence of extreme outliers required that the factorial ANOVA be performed on the original data set as well as with the exclusion of the extreme outliers. Graphic representations of the two-way ANOVA results are presented in Table 5.122.

The exclusion of the extreme outliers did not alter the statistical significance of the two dose factors, nor the interaction effect. Two-way ANOVA results generated from the original data, as well as from the data set that excludes extreme outliers, indicated statistically significant p-values for Factor-1, Factor-2 and the interaction of these dose regimens. The exclusion simply resulted in an increase in the F-statistics and statistical significance accordingly.

Table 5.122 Graphic and tabulated summary of the liver ATP/ADP ratio data analysed via a two-way ANOVA

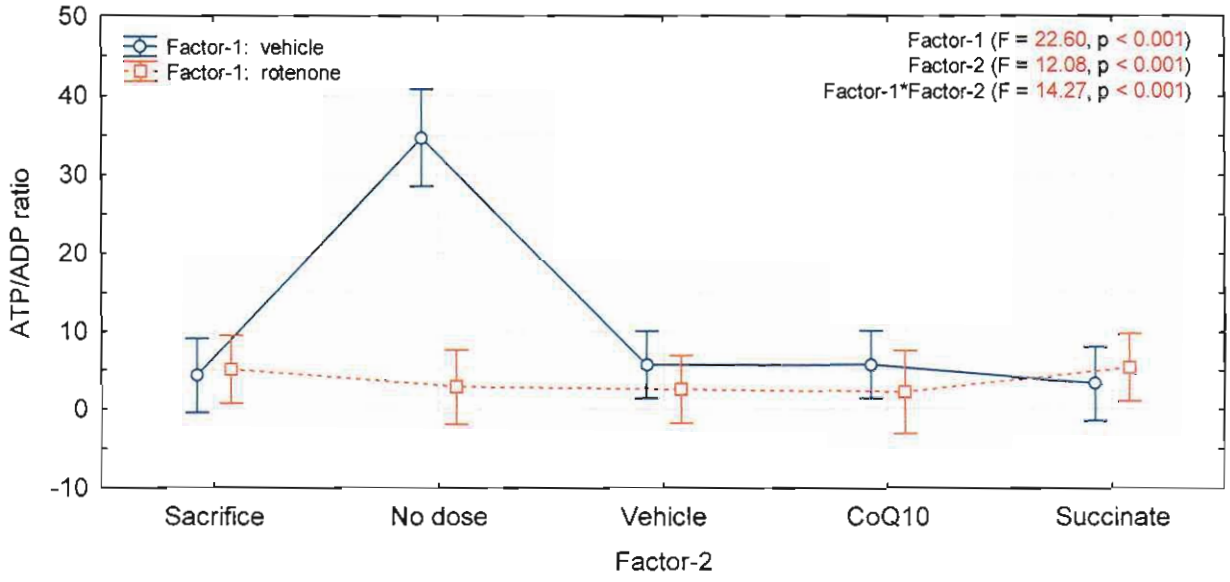
A: Data set including extreme outliers



Description		VX	VN	VV	VC	VS	RX	RN	RV	RC	RS
With extreme outliers	UCI	12.5	44.4	12.7	12.6	18.3	12.0	10.4	9.50	9.02	12.3
	mean	5.61	34.7	5.81	5.77	11.5	5.18	2.95	2.66	2.18	5.43
	LCI	-1.23	25.0	-1.03	-1.07	4.62	-1.66	-4.55	-4.18	-4.66	-1.41

Table 5.122 Continued...

B: Data set excluding extreme outliers



Description		VX	VN	VV	VC	VS	RX	RN	RV	RC	RS
Without extreme outliers	UCI	9.15	40.8	10.2	10.1	8.09	9.51	7.70	7.00	7.56	9.77
	mean	4.40	34.7	5.81	5.77	3.34	5.18	2.95	2.66	2.25	5.43
	LCI	-0.35	28.6	1.47	1.44	-1.41	0.84	-1.80	-1.67	-3.06	1.10

The plot legends for each graph are indicated in the top left corners of the respective graphs, while the two-way ANOVA F-statistics (F) and p-values (p) for Factor-1, Factor-2 and Factor-1*Factor-2 are located in the top right corner, with the statistically significant values indicated in red. The vertical whiskers at each mean data point represent 95% confidence intervals for the respective data sets. The mean values in green text, located in the data point summary tables below the graphs, indicate those that were adjusted due to the exclusion of extreme outliers. Rats were treated with NN = no dose regimen, VX = vehicle and sacrificed, VN = vehicle and no dose, VV = vehicle and vehicle, VC = vehicle and CoQ_{10}, VS = vehicle and succinate, RX = rotenone and sacrificed, RN = rotenone and no dose, RV = rotenone and vehicle, RC = rotenone and CoQ_{10}, RS = rotenone and succinate. < = less than, ATP/ADP = ratio adenosine triphosphate to adenosine diphosphate, LCI = lower 95% confidence interval data point, UCI = upper 95% confidence interval data point.

Due to the aberrant distribution of data points for dose group VN, there is a strong suspicion that the resulting two-way ANOVA statistics may have presented with an induced statistical significance. If the sharp increase in ATP/ADP ratios for dose group VN were to be excluded from the graphic representations in Table 5.122, it can be observed that the remaining dose groups presented with ATP/ADP ratios in similar ranges with overlapping confidence intervals. It could therefore be argued, with the exclusion of dose group VN, statistical significance of dose Factor-1 and Factor-2, as well as the interaction effect may not have been determined. This argument is supported by the fact that none of the dose groups, excluding VN, differed statistically significantly from each other when multiple comparison statistics were generated, as indicated in Table 5.121.A. However, the Factor-1 plots in Table 5.122.B do intersect upon exclusion of the extreme outlier from dose group VS. This suggests that an interaction effect may still be reported by the two-way ANOVA.

Regardless of the statistics generated from the factorial ANOVA, it cannot be confidently stated whether any of the Factor-2 dose regimens were of therapeutic benefit to rat ATP/ADP ratios in skeletal muscle. The elevated ratios indicated for rat group VN have been argued to arise primarily due to the impact of missing points in the dose group, which did not allow for outlier analysis and consequent exclusion of extreme outliers. Regardless of this, since it is possible to exclude only one extreme outlier on either side of the IQR, it would still be expected that dose group VN presented with an elevated mean ATP/ADP ratio.

The decision not to exclude data set VN from the statistical evaluations of the data may be questioned due to the fact that its presence impacted significantly on the statistics generated by the ANOVA and multiple comparison test procedures. Not only did dose group VN differ significantly from all the other rat groups, but it was also argued to affect the reliability of the two-way ANOVA results adversely. However, two additional points should be noted. The first is that the consideration for exclusion of dose group VN was based on the criteria that the group presented with three missing data points, not because it presented with an abnormally wide IQR. As mentioned in the previous paragraph, even if the three data points were not missing from VN, it would still be expected that the group would present with an increased mean ATP/ADP ratio in skeletal muscle. The wide IQR is not a function of the fact that three data points were missing, but rather that dose group VN itself comprised of three data points that were widely distributed. The second point stems from the fact that the factorial ANOVA utilised to investigate the data is a parametric-based algorithm. Therefore, the two-way ANOVA test is expected to be sensitive to the presence of outliers and extreme outliers as well as to the fact that the variation in liver ATP/ADP ratios for dose group VN was far greater than the remaining dose groups included in the study. However, there is no non-parametric algorithm that is the equivalent to a parametric factorial ANOVA. It is partly for this reason that it was decided to present all statistical evaluations in parallel, via the inclusion and exclusion of extreme outliers.

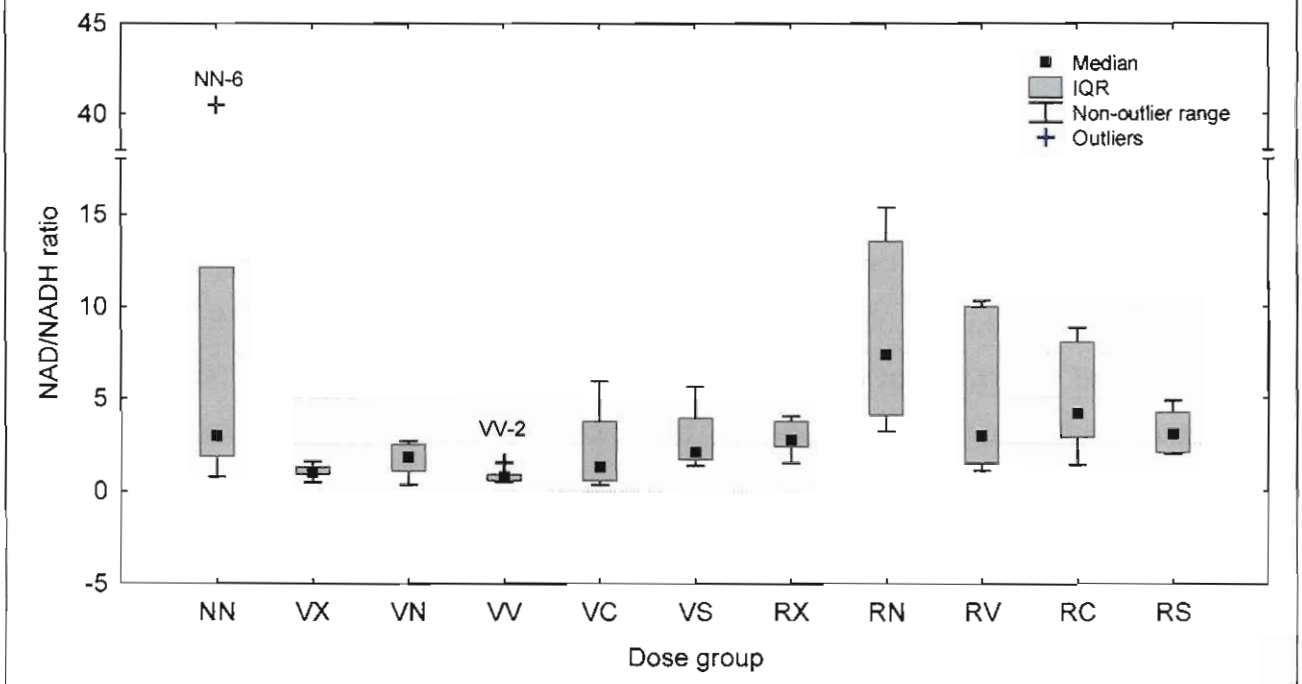
5.7.7 NAD/NADH ratios in liver tissue

Liver tissue was collected from rats and prepared appropriately for the analysis of pyridine nucleotides. Concentrations were determined spectrophotometrically and the data captured in Excel® spreadsheets. Statistical evaluation of NAD/NADH ratios from liver tissue was performed via the use of the STATISTICA™ programme. Box whisker

representations of the ratios according to dose group are presented in Table 5.123, along with a listing of all data points as well as a table of descriptive statistics.

Table 5.123 Box-whisker representation and descriptive statistics of the liver tissue NAD/NADH ratio data generated from the main study

A: Box-whisker plots and data points according to rat groups



Rat	NN	VX	VN	VV	VC	VS	RX	RN	RV	RC	RS
1	1.84	0.46	1.51	0.86	0.30	2.00	2.81	13.5	2.73	8.83	2.91
2	12.1	0.90	0.32	+ 1.54	5.90	1.35	2.62	3.20	1.48	5.33	4.21
3	3.75	0.90	2.46	0.74	1.35	3.88	3.99	4.05	1.07	2.87	2.06
4	0.76	1.27	2.07	0.55	0.54	2.13	1.48	10.1	10.3	1.38	3.24
5	2.19	1.56	1.06	0.47	1.18	1.65	3.70	4.59	9.96	8.03	1.98
6	+ 40.5	1.07	2.65	0.74	3.69	5.62	2.35	15.3	3.22	3.02	4.86

B: Descriptive statistics

Dose group	Sample size	Mean	SD	Median	Min	Max	Range	Lower quartile	Upper quartile	IQR
NN	6	10.2	15.4	2.97	0.76	40.5	39.7	1.84	12.1	10.3
VX	6	1.03	0.37	0.99	0.46	1.56	1.10	0.90	1.27	0.37
VN	6	1.68	0.89	1.79	0.32	2.65	2.32	1.06	2.46	1.41
VV	6	0.82	0.38	0.74	0.47	1.54	1.06	0.55	0.86	0.31
VC	6	2.16	2.19	1.26	0.30	5.90	5.60	0.54	3.69	3.15
VS	6	2.77	1.65	2.06	1.35	5.62	4.27	1.65	3.88	2.22
RX	6	2.83	0.92	2.72	1.48	3.99	2.51	2.35	3.70	1.35
RN	6	8.47	5.25	7.36	3.20	15.3	12.2	4.05	13.5	9.45
RV	6	4.79	4.21	2.97	1.07	10.3	9.22	1.48	9.96	8.48
RC	6	4.91	3.02	4.17	1.38	8.83	7.46	2.87	8.03	5.16
RS	6	3.21	1.15	3.08	1.98	4.86	2.88	2.06	4.21	2.15

Rat codes for the outliers are located above or below the blue crosses (+), which correspond to data point values listed in the table directly below the graph. A scale break was implemented on the Y-axis between a ratio of 15 and 40. Rats were treated with NN = no dose regimen, VX = vehicle and sacrificed, VN = vehicle and no dose, VV = vehicle and vehicle, VC = vehicle and CoQ_{10}, VS = vehicle and succinate, RX = rotenone and sacrificed, RN = rotenone and no dose, RV = rotenone and vehicle, RC = rotenone and CoQ_{10}, RS = rotenone and succinate. IQR = inter-quartile range, Min = minimum data point value, Max = maximum data point value, NAD/NADH = ratio of oxidised to reduced nicotinamide adenine dinucleotide, SD = standard deviation.

The liver tissue NAD/NADH ratio data revealed the presence of two outliers, but no extreme outliers. The first outlier, NN-6, was situated higher than all data points generated from the complete data set. Dose group NN presented with an IQR of 10.3, the widest of all the rat groups. Consequently, the upper outlier boundary is situated at a ratio of 42.9. Therefore, rat NN-6 harboured a liver NAD/NADH ratio that was positioned a mere 2.4 ratio units from being classified an extreme outlier. If NN-6 were to be excluded, it would be expected that the central tendency statistics would indeed be affected, with the mean and SD decreasing quite considerably. In contrast to NN, dose group VV presented with the narrowest of all IQRs. This group did however also present with an outlier, VV-2, which harboured an NAD/NADH ratio of 1.54. Since the IQR for dose group VV was a very narrow 0.31, it meant that the upper boundary of the non-outlier range was situated at an NAD/NADH ratio of 1.33, while the upper outlier boundary was at 1.79. If VV-2 were to be excluded, it would not be expected that major adjustments would be made to the descriptive statistics, primarily due to the close grouping of the core data points. Nonetheless, neither NN-6 nor VV-2 were excluded, as they were not determined to be positioned within the respective extreme outlier ranges.

The box-whisker plots in Table 5.123 illustrate that NAD/NADH ratios consistently overlapped between dose groups. It would therefore be expected that few, if any, statistically significant differences be reported by the ANOVA and multiple comparison statistics. This proved to be the case, as can be observed from the p-values presented in Table 5.124. Since no extreme outliers were determined to be present in the complete liver NAD/NADH data set, the data was analysed via the parametric one-way ANOVA and Tukey *equal number HSD* multiple comparison procedure.

The one-way ANOVA resulted in a non-significant p-value of 0.053. However, since the significance level was pre-determined to be at 0.05, it can be observed that the ANOVA p-value was only just beyond the significance level. Nonetheless, the p-value was not less than 0.05 and it is therefore not considered that a significant difference in variation existed among the liver tissue NAD/NADH ratios. Correspondingly, the parametric Tukey multiple comparison procedure did not indicate that any of the liver NAD/NADH ratios differed statistically significantly from each other.

Table 5.124 Multiple comparison statistics of the liver tissue NAD/NADH ratio data generated from the rat main study

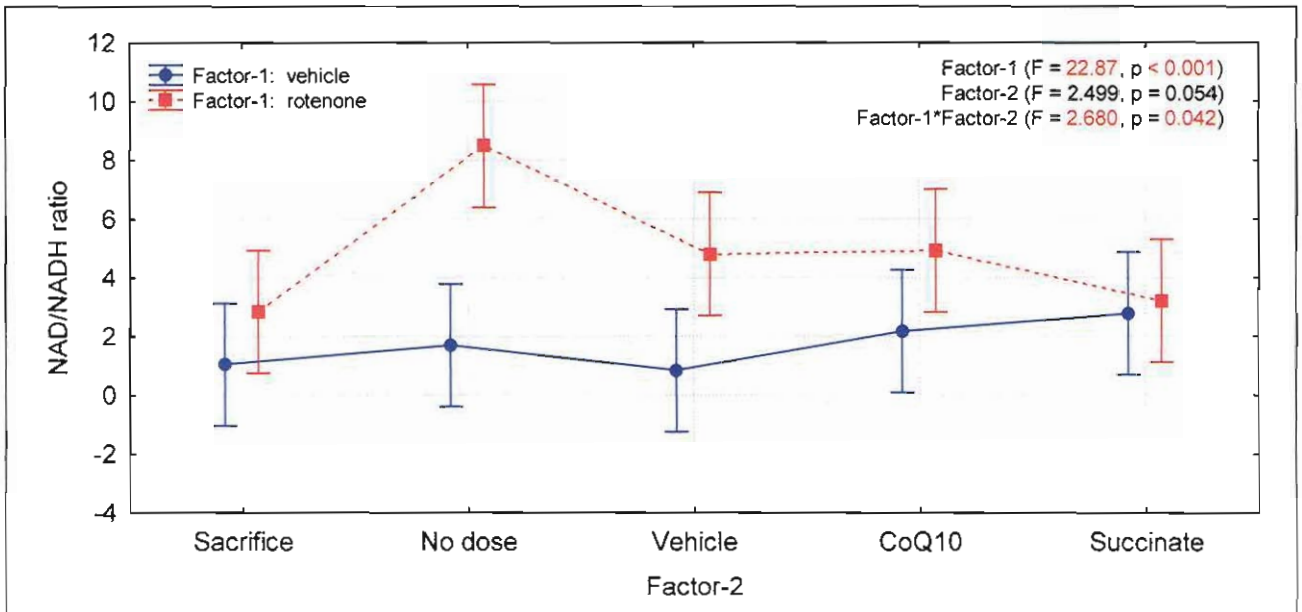
A: Parametric Tukey *equal number HSD* p-values											
Dose group	**NN**	**VX**	**VN**	**VV**	**VC**	**VS**	**RX**	**RN**	**RV**	**RC**	**RS**
NN		0.113	0.181	0.096	0.248	0.355	0.366	1.000	0.785	0.806	0.445
VX	0.113		1.000	1.000	1.000	1.000	1.000	0.351	0.974	0.968	1.000
VN	0.181	1.000		1.000	1.000	1.000	1.000	0.486	0.994	0.992	1.000
VV	0.096	1.000	1.000		1.000	1.000	1.000	0.312	0.963	0.955	0.999
VC	0.248	1.000	1.000	1.000		1.000	1.000	0.593	0.998	0.998	1.000
VS	0.355	1.000	1.000	1.000	1.000		1.000	0.725	1.000	1.000	1.000
RX	0.366	1.000	1.000	1.000	1.000	1.000		0.737	1.000	1.000	1.000
RN	1.000	0.351	0.486	0.312	0.593	0.725	0.737		0.978	0.983	0.809
RV	0.785	0.974	0.994	0.963	0.998	1.000	1.000	0.978		1.000	1.000
RC	0.806	0.968	0.992	0.955	0.998	1.000	1.000	0.983	1.000		1.000
RS	0.445	1.000	1.000	0.999	1.000	1.000	1.000	0.809	1.000	1.000	
B: ANOVA p-values											
One-way ANOVA p-value = 0.053											

A: All comparison statistics are indicated as p-values generated via the Tukey *equal number HSD* (Honestly Significant Difference) multiple comparison procedure. P-values in grey, indicate that no significant differences exist. B: P-value for the one-way ANOVA is listed. Rats were treated with NN = no dose regimen, VX = vehicle and sacrificed, VN = vehicle and no dose, VV = vehicle and vehicle, VC = vehicle and CoQ_{10}, VS = vehicle and succinate, RX = rotenone and sacrificed, RN = rotenone and no dose, RV = rotenone and vehicle, RC = rotenone and CoQ_{10}, RS = rotenone and succinate. ANOVA = analysis of variance.

The lack of variation in NAD/NADH ratios generated from liver tissue is suggestive of this analysis possibly not being informative enough to detect an improvement in redox status or even to detect the presence of a Complex I deficiency. This argument is strengthened by the fact that a congruent scenario was observed for NAD/NADH ratios in blood and skeletal muscle, as presented in Sections 5.3.6 and 5.6.5 respectively.

Multiple comparison procedure testing performed on the blood and skeletal muscle data sets also indicated that none of the dose group NAD/NADH ratios differed statistically significantly from each other. In an attempt to investigate if the various dose factors contributed significantly to rat response and NAD/NADH ratios in liver, a factorial ANOVA was performed on the data. Since no extreme outliers were determined to be present in the overall data set, it was not required that parallel two-way ANOVA results be presented. A graphic summary of the factorial ANOVA results is presented in Table 5.125, along with corresponding F-statistics and p-values. The mean and 95% confidence interval data points are also listed directly below the graph.

Table 5.125 Graphic and tabulated summary of the liver tissue NAD/NADH ratio data analysed via a two-way ANOVA



Data points	VX	VN	VV	VC	VS	RX	RN	RV	RC	RS
UCI	3.12	3.77	2.91	4.25	4.86	4.92	10.56	6.89	7.00	5.30
mean	1.03	1.68	0.82	2.16	2.77	2.83	8.47	4.79	4.91	3.21
LCI	-1.07	-0.41	-1.28	0.07	0.68	0.73	6.38	2.70	2.82	1.12

The plot legend is indicated in the top left corner of the graph, while the two-way ANOVA F-statistics (F) and p-values (p) for Factor-1, Factor-2 and Factor-1*Factor-2 are located in the top right corner, with the statistically significant values indicated in red. The vertical whiskers at each mean data point represent 95% confidence intervals for the respective data sets. Rats were treated with NN = no dose regimen, VX = vehicle and sacrificed, VN = vehicle and no dose, VV = vehicle and vehicle, VC = vehicle and CoQ_{10}, VS = vehicle and succinate, RX = rotenone and sacrificed, RN = rotenone and no dose, RV = rotenone and vehicle, RC = rotenone and CoQ_{10}, RS = rotenone and succinate. < = less than, LCI = lower 95% confidence interval data point, NAD/NADH = ratio of oxidised to reduced nicotinamide adenine dinucleotide, UCI = upper 95% confidence interval data point.

The factorial ANOVA results indicate statistical significance for dose Factor-1 and for the interaction between Factor-1 and Factor-2. The vehicle and rotenone Factor-1 plots also indicate the presence of dissimilar trends in mean NAD/NADH ratios, resulting in the statistically significant interaction effect. The fact that the rotenone plot consistently presented with mean data points greater than the vehicle Factor-1 plot suggests that the inhibitor indeed influenced NAD/NADH ratios in liver, which is supported by the statistically significant p-value of < 0.001 for Factor-1. However, since an interaction effect was also determined to be present with a statistically significant p-value of 0.042, caution should be taken as to the interpretation of the effects of the various dose factors. Although, the interaction statistic was statistically significant at the 0.05 significance level, while the Factor-1 p-value was highly significant. In addition, the F-statistic for Factor-1 was approximately 10-fold greater than the interaction F-statistic at 22.87 and 2.680 respectively. Therefore, it could be speculated that statistical significance for the interaction may have been influenced primarily due to the large divergence of mean data points at the no dose Factor-2 level. In other words, the divergence in mean data points for dose group VN and RN may have induced the statistically significant interaction effect.

Nonetheless, a statistically significant interaction was reported by the two-way ANOVA, suggesting that dose Factor-1 and Factor-2 together affected NAD/NADH ratios in liver tissue.

Since the mean liver NAD/NADH ratio for the environmental controls NN was an elevated 10.2, it can be argued that the sunflower oil vehicle reduced NAD/NADH ratios in liver. The same holds true for rat groups that received rotenone as a Factor-1 dose. Even though the mean NAD/NADH ratio data points for the rotenone-dosed rats were higher than those that received vehicle, they were still all lower than the mean for NN. Once again, as observed with several of the previously discussed data sets, evidence of the effects of sunflower oil has been realised. The fact that the rotenone vehicle appeared to alter NAD/NADH ratios in liver tissue, complicates interpretation of analysis results. It was also apparent from Table 5.125 that all mean NAD/NADH data points for rats that received rotenone Factor-1 doses were higher than the corresponding vehicle Factor-1 plots. However, it would be expected that an inhibition of complex I would result in increased NADH levels and consequently lowered NAD/NADH ratios. Nevertheless, multiple comparison statistics presented in Table 5.124.A revealed that none of the dose groups in the liver tissue NAD/NADH data set differed statistically significantly from each other. It cannot therefore be conclusively determined that rotenone improved NAD/NADH ratios.

Alternatively, since a significant interaction effect was reported by the factorial ANOVA, it could be argued that the differences in NAD/NADH ratios observed between the Factor-1 plots may be due to the interaction of rotenone with its corresponding Factor-2 treatments. Since rotenone was proven to induce Complex I deficiency in rats, it may be speculated that the alleviated NAD/NADH ratios in liver tissue could be due to a type of recovery mechanism, such as mitochondrial proliferation. The concept of mitochondrial replenishment was initially proposed when complex I activities were discussed in the aforementioned sections. Since the liver is a highly active organ with several functions and roles in metabolic homeostasis, the argument suggesting mitochondrial proliferation (Koopman *et al.*, 2005) may not be inaccurate. In light of the NAD/NADH ratio response observed for rats dosed with rotenone Factor-1 doses, it can be argued that the proliferation of mitochondria aided in recovery of liver tissue, thereby improving NAD/NADH ratios to higher than that in rats that received the vehicle Factor-1 dose regimens. The factorial ANOVA does not support the notion that Factor-2 doses contributed to the improvement in NAD/NADH ratios, but it is suggestive of the interaction. However, it should be noted once again that all rats that were dosed with a regimen still

presented with compromised NAD/NADH ratios in liver when compared to the environmental controls NN. Furthermore, the fact that no statistically significant differences existed amongst any of the dose groups, as presented in Table 5.124, does not conclusively support the aforementioned argument.

5.7.8 Liver tissue profile of the rat main study

Liver organs were collected, weighed and the complete biochemical profile generated. The median percentage deviations from the environmental control dose group NN are presented in Table 5.126 by means of a two dimensional bar graph and a median percentage grid.

Liver weights for dose groups RX and RV, which were calculated to have median percentages of -20.8% and -16.7%, were the only data sets to deviate by more than 10% from the environmental control dose group NN. It was argued in Section 5.7.1.2 that the decrease in liver weight was accounted for by the toxicity of rotenone, which was in turn argued to result from, not only complex I inhibition, but also due to the finding that rotenone had been reported in the literature to be involved in mitotic arrest (Barham and Brinkley, 1976a and 1976b). The decreased liver weights recorded for dose group RV were motivated by the fact that the sunflower oil may have prevented hepatic recovery via the continued induction of lipid peroxidation (Mataix *et al.*, 1998) and oxidative stress (Turpeinen *et al.*, 1998). The aforementioned arguments were based largely on previously reported literature and were not investigated in this study. In support of the literature that sunflower oil induced oxidative stress, it was illustrated in the blood profile of Section 5.3.7 that an increase in the hydroperoxide concentrations were observed in rats that were dosed with vehicle Factor-1 regimens.

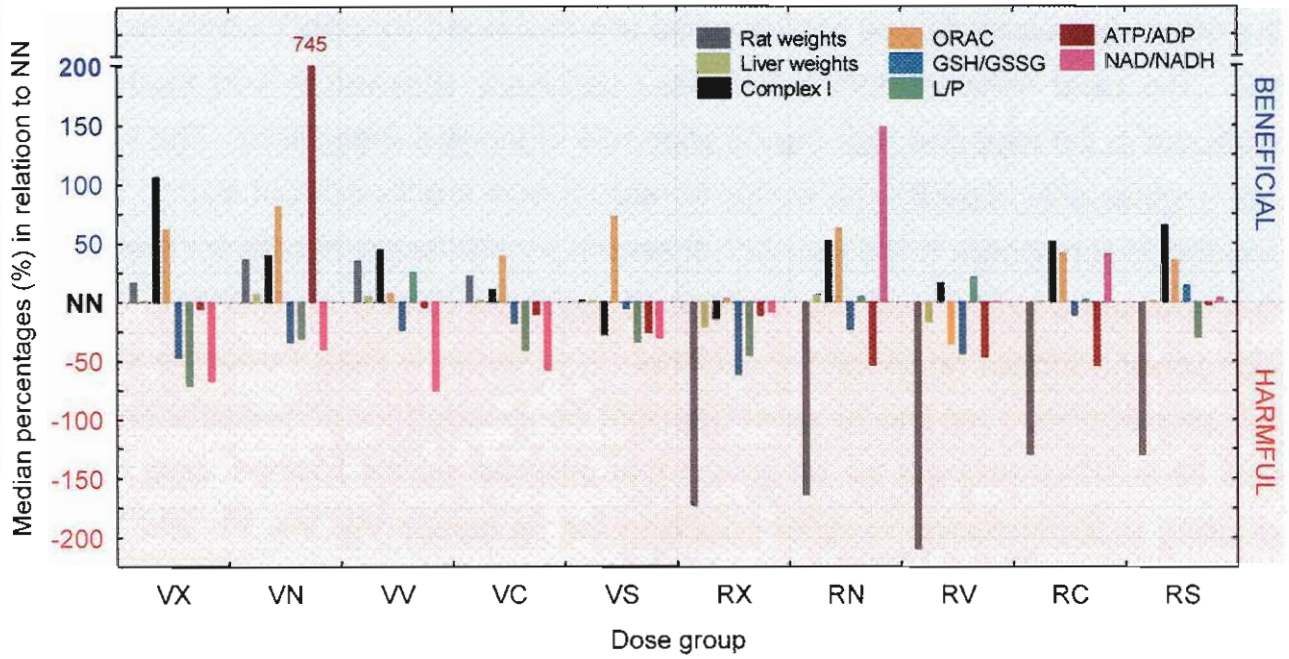
Complex I activities recorded from liver tissue and among rats that received vehicle Factor-1 doses, illustrated that activities were improved on all occasions except for dose group VS. The increased complex I activities in the vehicle treated groups are suggestive of the fact that sunflower oil induced this reaction. Furthermore, all rat groups that received rotenone and were relieved of rotenone for an additional two days, namely RN, RV, RC and RS, presented with improved complex I activities that increased to even higher levels than that of the environmental controls NN. Dose group RX, which received rotenone for 14 days and was sacrificed on day 15, presented with a deficient complex I activity. This was certainly expected and congruent with findings obtained from the rat

pilot study, as presented in Section 5.7.2.2. The factorial ANOVA reported a statistically significant interaction effect that in essence indicates that both dose factors influenced the improvement in complex I activities. Moreover, the non-significant Factor-2 also supports the notion that succinate was not the cause of a decreased complex I activity reported for VS. The rapid recovery from a Complex I deficiency observed in liver tissue can be attributed to the expected high regeneration rate of the liver organ itself. The liver has a high regeneration capacity and is able to recover from toxicity-induced injury. The rapid recovery is in response to the induction of several genetic factors at different time intervals that stimulate a biochemical and cytokine up-regulation (Chung *et al.*, 2005). Since the high polyunsaturated fat content of sunflower oil is known to induce oxidative stress and lipid peroxidation, it can also be speculated that the up-regulation of molecular factors may also be in effect amongst the rat groups that received vehicle Factor-1 dose regimens, resulting in the increased complex I activities for rat groups VX, VN, VV and VC. The lowered complex I activity recorded for VS was unexpected, but not reported to differ statistically significantly from any of the other dose groups, as presented in Section 5.7.2.2.

The antioxidant capacity recordings generated from rat liver indicate that improvements were reported for all rats except dose group RV. It was speculated that rats receiving vehicle Factor-1 dose regimens may have benefited from the vitamin E content of sunflower oil, since rat group VV was the only group that did not present with a greater than 10% improvement in liver antioxidant capacity. Furthermore, since none of the vehicle Factor-1 dosed rats differed statistically significantly from NN, the benefits of sunflower oil could not be confirmed. Dose group RX presented with a final liver antioxidant capacity that was equivalent to that of the environmental controls NN, while RN, RC and RS harboured greater than 35% improvements. The lowered antioxidant capacity for RX was speculated to result from the rotenone-induced Complex I deficiency, which did not have the luxury of a two-day recovery period, similar to the discussion regarding VX. The -35.2% median liver antioxidant capacity for rat group RV was discussed in Section 5.7.3 to be the result of three data points that were lower than any of the other data points in the complete liver antioxidant capacity data set. Dose group RV also presented with the widest IQR and distribution of data points, strengthening the argument that the previously mentioned three data points may have been aberrant and resulted in the skewed central tendency statistics. Nonetheless, the liver antioxidant capacity for RV was not determined to differ statistically significantly from any of the other rotenone-treated rats.

Table 5.126 Liver tissue profile of response generated from the rat main study indicating the beneficial and harmful effects of the dose regimens

A: Graphic representation



B: Median percentage (%) grid and factorial ANOVA summary

Data set	Dose group										Factorial ANOVA		
	VX	VN	VV	VC	VS	RX	RN	RV	RC	RS	F1	F2	F1*F2
Rat weights	16.9	36.4	35.1	22.1	1.30	-173	-164	-209	-130	-130	s/s	n/n	s/s
Liver weight	0.59	6.85	4.88	1.24	0.47	-20.8	6.15	-16.7	0.61	1.11	s/s	s/s	s/s
Complex I	106	39.5	44.2	10.3	-27.5	-13.8	51.5	15.6	50.8	65.0	n/n	n/n	s/s
AC	62.0	81.3	7.03	38.9	72.8	2.96	62.8	-35.2	41.7	35.6	s	s	n
GSH/GSSG	-47.1	-34.2	-24.0	-18.0	-5.51	-61.5	-23.4	-44.0	-11.2	13.7	n/n	s/s	n/n
L/P	-70.7	-30.9	24.9	-40.8	-34.0	-45.4	4.31	20.6	1.79	-29.7	n/n	s/s	n/n
ATP/ADP	-5.32	745	-4.24	-10.1	-25.9	-11.1	-53.5	-46.5	-53.9	-2.13	s/s	s/s	s/s
NAD/NADH	-66.8	-39.8	-75.1	-57.5	-30.5	-8.55	148	0.01	40.5	3.50	s	n	s

A: Percentage bars denote either beneficial or harmful effects induced by the dose regimens. Each bar is colour coded to represent the various data sets, as indicated by the graphic key in the top right corner of the graph. The 0% line on the Y-axis is labelled **NN**, since all median percentages were calculated to deviate from the environmental controls NN. The bold **200%** on the median percentage scale indicates the start of a scale break. Median percentages extending beyond the **200%** boundary are indicated directly above and in text colours corresponding to the assay bars. B: The percentage data points are listed in correspondence with the bar heights. Median percentages that deviate by more than 10% from the environmental controls NN are indicated in blue and red text for beneficial and harmful deviations respectively. Percentages in grey text represent deviations less than 10%. Grid blocks shaded in green represent comparisons from the original set of data that were presented in previous sections to differ statistically and biologically significantly from the environmental controls NN. Comparisons determined to differ significantly after the exclusion of extreme outliers are indicated by yellow shading. Statistically significant (s) and non-significant (n) contributions of Factor-1 (F1) and Factor-2 (F2) dose regimens as well as the interaction of these two factors (F1*F2) are indicated alongside the median percentage grid. Two symbols are indicated if extreme outliers were determined to be present in the respective data set, with the first symbol representing significance status prior to exclusion, followed by the second symbol representing significance status after exclusion of extreme outliers. AC = antioxidant capacity, ATP/ADP = ratio of adenosine triphosphate to adenosine diphosphate, GSH/GSSG = ratio of oxidised to reduced glutathione, L/P = ratio of lactate to pyruvate, NAD/NADH = ratio of oxidised to reduced nicotinamide adenine dinucleotide. Rats were dosed NN = no dose for 16 days, VX = vehicle and sacrificed, VN = vehicle and no dose, VV = vehicle and vehicle, VC = vehicle and CoQ_{10}, VS = vehicle and succinate, RX = rotenone and sacrificed, RN = rotenone and no dose, RV = rotenone and vehicle, RC = rotenone and CoQ_{10}, RS = rotenone and succinate.

Glutathione ratios indicated that sunflower oil might have been harmful to rat liver. All rat groups presented with greater than 10% lowered GSH/GSSG ratios except for VS and RS, the two groups that received succinate as a Factor-2 dose regimen. Rat group VS

harboured a final liver GSH/GSSG ratio that was equivalent to that of the environmental controls NN, while RS presented with ratios that improved to 13.7% higher than NN. The majority of negative GSH/GSSG ratios are strongly suggestive of sunflower oil playing the primary role in diminishing these ratios, as confirmed by a non-significant Factor-1 reported by the two-way ANOVA. This data is further supported by previous reports that the high polyunsaturated fat content of sunflower oil plays a role in the increase of lipid peroxidation (Mataix *et al.*, 1998) and oxidative stress (Turpeinen *et al.*, 1998). Therefore, the liver profile suggests that sunflower oil adversely affected the glutathione component of ROS management mechanisms. Furthermore, the GSH/GSSG ratios generated from VX and RX were determined to be lowered by statistically significant amounts. This indicates again that the inclusion of a Factor-2 dose regimen contributed to a relief of the biochemical profile. However, the fact that dose group VV did not harbour a final liver GSH/GSSG ratio that was adversely affected to a statistically significant degree, does support the notion that vehicle was harmful with respect to GSH/GSSG ratios. Nonetheless, it was evident that the liver GSH/GSSG ratio was adversely affected with a median percentage that was -24% of NN. The factorial ANOVA reported a non-significant Factor-1, indicating that rotenone did not further contribute by decreasing liver GSH/GSSG ratios. The statistically significant Factor-2 supports the notion that succinate aided in the recovery of liver GSH/GSSG ratios.

As with liver GSH/GSSG data, the L/P ratios generated from rat liver also indicated that the sunflower oil vehicle may have been harmful in this regard. Dose groups VX, VN, VC and VS presented with lowered L/P ratios, while VV harboured a final L/P ratio that was 24.9% higher than NN. This increased ratio was however not determined to be of statistical significance when compared to the environmental control dose group NN, nor when compared to the remainder of the rat groups that received a vehicle Factor-1 dose. Liver tissue collected from rotenone-treated rats appeared not to be as adversely affected with regards to L/P ratios. Since dose group RX presented with a median liver L/P ratio that was lower than the remaining rotenone-treated rats, it was deduced that the Factor-2 regimens were of primary importance in the response regarding L/P ratios. This is supported by the factorial ANOVA statistics that resulted in a statistically significant Factor-2. The non-significant Factor-1 indicated that rotenone did not additionally influence the liver L/P ratios. It was apparent that dose group RV displayed the most improved liver L/P ratio, while succinate improved the ratio least of all. None of the 10 dose groups was however determined by the multiple comparison statistics to differ statistically significantly from the environmental control dose group NN.

Liver ATP/ADP ratios presented with the most striking feature of a towering median percentage ratio of 745% for dose group VN. It was for this reason that a scale break was implemented for the liver data profile presentation in Table 5.126.A. Dose group VN was also the only dose group to differ statistically significantly from the environmental controls NN. However, as discussed in Section 5.7.6, dose group VN consisted of only three data points and was therefore not considered for direct statistical inference. The decision to include the VN data set in the remainder of statistical analyses was based on the fact that the data points were still a reflection of the overall variation within the complete liver ATP/ADP data set. The remainder of the liver ATP/ADP data sets revealed that rats were mostly affected adversely concerning this parameter. It could be argued that rotenone further reduced ATP production in liver tissue, which was in turn supported by a statistically significant Factor-1 contribution, as reported by the two-way ANOVA. Dose group RS harboured a final liver ATP/ADP ratio that was equivalent to the environmental controls, which thus indicated that succinate may have further stimulated a recovery of ATP/ADP ratio. Caution was taken as to the interpretation of the factorial ANOVA results since it was speculated that these might have been skewed due to the influence of the aberrant recorded data points of dose group VN. Nonetheless, a lack of statistically significant differences between dose groups, besides VN, was reported by the multiple comparison data and hence indicated that ATP/ADP ratios were not altered significantly in liver.

It was apparent that sunflower oil induced a decrease in liver NAD/NADH ratios, especially among rat groups that received a vehicle Factor-1 dose. In contrast, the liver NAD/NADH ratios presented with improvements when rats were treated with a rotenone Factor-1 dose. This was surprising since it would be expected that an inhibition of complex I would result in a backlog of NADH and hence a decrease in the NAD/NADH ratio. The contrasting effect on liver NAD/NADH ratios of the two Factor-1 dose regimens was confirmed by the statistically significant Factor-1 effect reported by the factorial ANOVA. In addition, the two-way ANOVA reported a statistically significant interaction effect, indicating that dose regimens jointly influenced NAD/NADH ratios in liver. As discussed in Section 5.6.6 of the skeletal muscle profile, it is uncertain as to the mechanism by which the contents of sunflower oil may have influenced the NAD/NADH ratios. The liver is a highly active and vital organ with the supreme ability to detoxify and regenerate after injury. Therefore, it is expected that the expression profile and regulation of the liver, in terms of maintenance and hepatocellular regeneration, is considerably different to most

other organs. It could therefore be argued that the impact of sunflower oil and recovery from oxidative stress of the liver is certainly far more complicated and regulated by several upstream and downstream molecular adjustments in response to oxidative stress. Unfortunately, such patterns cannot be explained with certainty from the data generated in this study. It is however evident that the NAD/NADH ratios were affected adversely by the contents of sunflower oil, which was counteracted by some mechanism induced by rotenone. Neither phenomena can be explained with certainty and would require further in-depth analysis into the establishment of expression profiles of the liver. Regardless, the final NAD/NADH ratios generated from liver tissue illustrated that none of the dose groups differed statistically significantly from each other. This indicated that the observed differences were not definitive.

The overall response profile observed from the colour coding system, implemented in Table 5.126.B, reveals that the liver suffered more harmful effects than beneficial. Rat groups that received vehicle Factor-1 dose regimens presented with 10 improved median percentages (coloured in blue), 16 to have decreased (indicated in red) and 9 unchanged (in grey). The rotenone-treated rats presented with 11 improved median percentages (in blue), 14 affected adversely (in red) and 10 unaltered (in grey). Complex I and antioxidant capacity data sets presented with the majority of beneficial effects, while the remainder of the biochemical profile components or data sets indicated that the liver was affected adversely. The global data view of the liver profile, as presented in Table 5.126.B, is suggestive of the fact that sunflower oil was the primary harmful dose regimen that was received by the rats. The high polyunsaturated fat content, or possibly other unknown constituents of sunflower oil, proved to have certainly induced adverse responses in the rat liver.

5.7.8.1 Impact of coenzyme Q10 and succinate on rat liver tissue

Liver weights recorded for dose groups that received a vehicle Factor-1 dose regimen, namely VX, VN, VV, VC and VS were not determined to deviate by more than 10% from that of the environmental control dose group NN. Since the complex I activities for rat groups VC and VS were lower than the remainder of the vehicle Factor-1 dosed groups, it could be stated that neither CoQ_{10} nor succinate were beneficial to complex I activities, as would be expected based on the properties of the therapeutic compounds. However, it would not be accurate to state that these regimens harmfully affected complex I activities in liver since neither of the groups differed statistically significantly from any of the other

vehicle Factor-1 dosed rats. The antioxidant capacity data for VC and VS indicated that succinate improved liver antioxidant capacity more so than CoQ_{10}. Succinate was also demonstrated to improve glutathione status in rats receiving vehicle Factor-1 doses to levels equivalent to that of the environmental controls NN. Dose groups VX, VN, VV and VC presented with negative GSH/GSSG ratios exceeding -10%, while VS harboured a final liver GSH/GSSG ratio of -5.51% of NN. Liver L/P ratios for dose groups VC and VS were demonstrated to be similarly affected with median percentages of -40.8% and -34.0% respectively. Since dose groups VX and VN harboured negative median percentages of -70.7% and -30.9%, it was concluded that neither of the therapeutic regimens improved L/P ratios in liver. Both CoQ_{10} and succinate appeared to have no beneficial effect on ATP/ADP status in liver, with succinate resulting in a greater decrease from NN than dose group VC. The liver NAD/NADH status for dose groups VC and VS presented with negatively affected ratios regardless of the therapeutic regimens utilised, indicating no beneficial impact. Dose group VS did however harbour the least affected NAD/NADH ratios and could therefore be speculated to be more beneficial than CoQ_{10} in this regard.

Liver weight data generated from the rotenone-treated rats recovered when they received CoQ_{10} and succinate Factor-2 regimens. Since dose group RN also presented with liver weights that were equivalent, and hence regained, to that of the environmental controls NN, it could not be stated with confidence that CoQ_{10} and succinate had a direct impact on the re-established liver weights. It could however be concluded that these regimens did not prevent recovery, as the vehicle Factor-2 dose did in rat group RV. Complex I activities were demonstrated to be similarly improved in both dose groups RC and RS, more so than for rat group RV. However, as with the liver weight data, dose group RN harboured a complex I activity that was equivalent to that of RC and RS, indicating that CoQ_{10} and succinate did not additionally contribute to the improved complex I activities. Antioxidant capacities for dose groups RC and RS were also improved to similar levels, but not over and above that of RN. Glutathione ratios in liver did reveal that succinate might have contributed to a further improvement in GSH/GSSG ratios, where CoQ_{10} did not. However, succinate may be argued to have prevented the recovery of liver L/P ratios in the presence of a Complex I deficiency. Dose group RS presented with a median L/P ratio of -29.7%, while RC harboured a median percentage of 1.79%, equivalent to that of the environmental controls NN. In contrast, the beneficial effects of succinate are demonstrated by the fact that liver ATP/ADP ratios recovered to that of NN, whilst dose group RC harboured a median percentage that remained lowered at -53.9%. Finally, it

can be argued that a CoQ_{10} Factor-2 dose regimen contributed more to the recovery of NAD/NADH ratios than succinate. Dose group RC harboured a median percentage NAD/NADH ratio that was 40.5% higher than NN, while RS was equivalent to NN at 3.50%. As demonstrated in this section and on several occasions in previous profile sections, both therapeutic regimens proved to be beneficial in the recovery from rotenone-induced Complex I deficiency. However, it should also be stated that CoQ_{10} and succinate had an impact on different aspects of the various biochemical profiles, which is also in congruence with previous profile data.

5.8 COLLECTIVE PRESENTATION OF RAT PILOT AND MAIN STUDIES

In an attempt to obtain a more global view of the data generated from the rat pilot and main studies, taking into account all the data sets and tissues, the data was collectively clustered and is presented in subsequent sections. The pilot study data was summarised via a graphic representation and median percentage deviations from the environmental control dose group of that study, namely N. The main study data, however, was collectively summarised by means of a grid, listing the median percentage deviations from NN. The tabulated format was selected for the main study since it was decided that it was the most effective means of evaluating the beneficial and harmful effects recorded in the study.

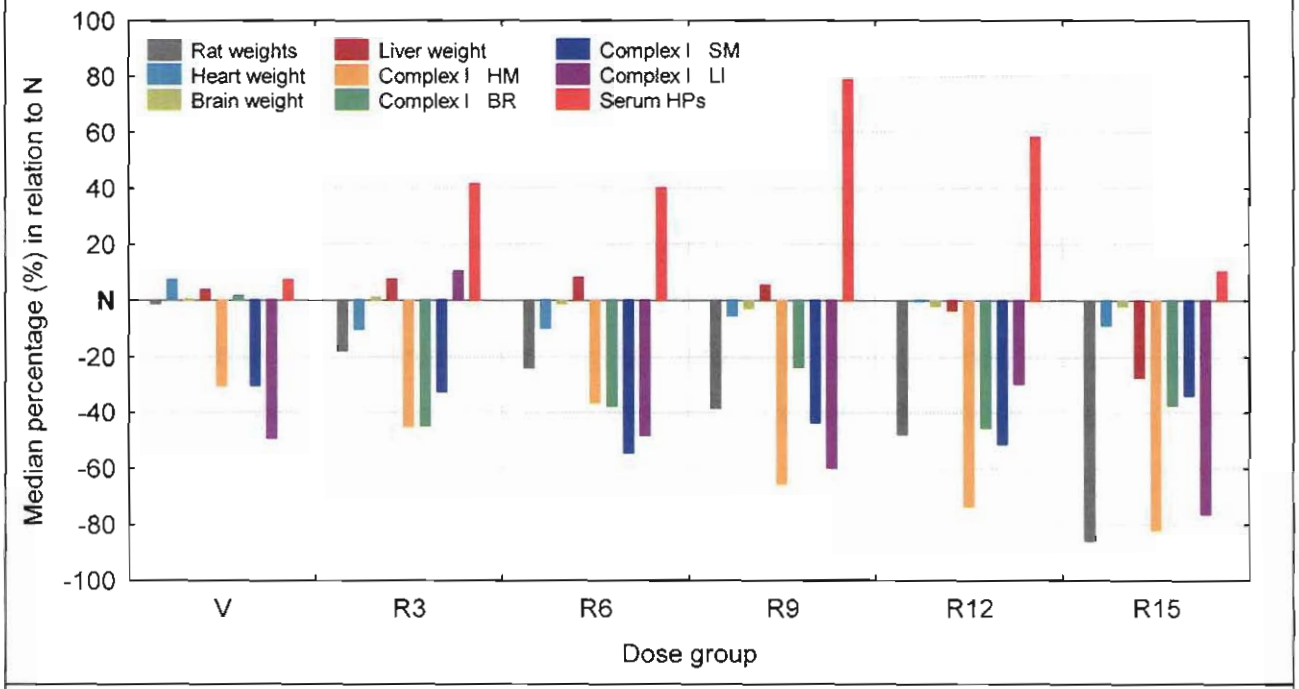
5.8.1 Rat pilot study collective summary of data

The goal of the pilot study was to determine a relationship between a rotenone dose concentration and complex I inhibition. Therefore, it was not necessary to generate a profile including all of the analysis data sets, as presented in Table 5.127. Rats from the pilot study were evaluated via daily body weight as well as organ weight recordings of whole brain, heart and liver as well as serum hydroperoxide concentrations and complex I activities. As discussed in previous sections where data from the rat pilot study was presented, the trend in responses to the increase in rotenone dose concentrations was evident with adverse responses personified by rat weight recordings and complex I activities in the various tissue types investigated. The exception to this trend was observed by the serum hydroperoxide concentrations, which presented at its highest levels when rats received 9 $mg.kg^{-1}.day^{-1}$ rotenone, followed by a decrease as dose concentrations increased to 12 and 15 $mg.kg^{-1}.day^{-1}$. Organ weight data, however, did not

present with any particular trend in response, but did indicate that the heart and liver was affected adversely. All data generated from the rat pilot study is presented in Table 5.127 by means of a bar graph and median percentage deviations from the environmental control dose group N. The grid blocks shaded in green reflect dose groups that were determined and discussed in previous sections to differ statistically and biologically significantly from the environmental controls N. Yellow shaded blocks refer to comparisons with N that were determined to differ statistically and biologically significantly only after the exclusion of extreme outliers.

Table 5.127 Graphic and tabulated representation of data generated from the rat pilot study

A: Graphic representation



B: Median percentage (%) deviations from dose group N

Data set	System	V	R3	R6	R9	R12	R15
Rat weights	All	-1.1	-17.8	-23.9	-38.3	-47.8	-85.6
Organ weight	HM	7.30	-10.2	-9.76	-5.37	-0.18	-8.70
	BR	0.37	0.93	-1.01	-2.65	-1.73	-1.77
	LI	3.66	7.50	8.12	5.37	-3.41	-27.4
Complex I activity	HM	-30.6	-45.1	-36.6	-65.6	-73.5	-81.9
	BR	1.54	-44.9	-37.7	-23.8	-45.5	-37.5
	SM	-30.6	-32.6	-54.6	-43.7	-51.4	-34.0
	LI	-49.5	10.3	-48.4	-59.9	-29.7	-76.3
Serum HPs	BL	7.31	41.4	39.8	78.5	58.1	10.3

A: Percentage bars denote the median percentage deviations in parameters from the environmental controls N. Each bar is colour coded to represent the various data sets, as indicated by the graphic key in the top left of the graph. The 0% line on the Y-axis is labelled N, since all median percentages were calculated to deviate from the environmental control dose group N. B: The percentage data points are listed in correspondence with the bar heights. Grid blocks shaded in green represent comparisons from the original set of data that were presented in previous sections to differ statistically and biologically significantly from the environmental controls N. Comparisons determined to differ significantly after the exclusion of extreme outliers are indicated by yellow shading. Rats were treated with N = no dose, V = vehicle, R3 = rotenone 3 $mg.kg^{-1}.day^{-1}$, R6 = rotenone 6 $mg.kg^{-1}.day^{-1}$, R9 = rotenone 9 $mg.kg^{-1}.day^{-1}$, R12 = rotenone 12 $mg.kg^{-1}.day^{-1}$, R15 = rotenone 15 $mg.kg^{-1}.day^{-1}$. BL = blood, BR = brain, HPs = hydroperoxides, HM = heart muscle, LI = liver, SM = skeletal muscle.

As presented in Section 5.2.1, rats lost considerable amounts of weight when dosed with rotenone. Furthermore, it was evident that the increase in weight loss was directly proportional to the concentration of rotenone that was dosed to the rats, which can be confirmed by viewing the graphic representation in Table 5.127.A. The median percentage deviations for rat body weight, listed in Section B of the same table, also indicate this adverse response. It should be noted that even when rats received the low rotenone dose concentration of 3 $mg.kg^{-1}.day^{-1}$, a median percentage decrease in weight of 17.8% was recorded. However, the difference was only determined to be statistically significant when rats received 6 $mg.kg^{-1}.day^{-1}$ rotenone and higher, as indicated by the yellow and green shading in Table 5.127.B. Based on a publication by Lapointe *et al.* (2004), it was speculated that the decreased body weights were largely the result of a decrease in digestion capacity due to the break down of stomach muscle mass.

As discussed on several occasions in this chapter, complex I inhibition was indeed obtained via the oesophageal intubation of rotenone. The median percentage deviations from dose group N of the rat pilot study are listed in Table 5.127.B. Complex I activities in heart muscle, whole brain and liver presented with statistically significant inhibition when compared to the environmental control dose group N. However, an exception to the statistical significance was determined in skeletal muscle. The argument that skeletal muscle was determined to be a poor responder tissue was confirmed in the rat main study and addressed in Section 5.6.6. The yellow shaded grid blocks for liver tissue complex I activities reflect significant differences between the respective dose groups and N only after the extreme outliers were excluded from the data set. It was unexpected, with the exception of brain tissue, that decreased complex I activities would be recorded in the vehicle-dosed rat group V. The data presented in Table 5.127.B indicates that inhibition of complex I activity by more than 30% was determined to be present in heart muscle, skeletal muscle and liver tissue when rats were dosed with the vehicle only. Previous discussions argued the effect that the dosage procedure may have on rats as well as the difficulty in the complex I assay itself. The possibility that the aforementioned circumstances may influence results to a certain degree cannot be excluded. The increased complex I activity in liver tissue for dose group R3 cannot conclusively be explained. However, the deviation of this parameter from the environmental controls N not determined to be of statistical significance.

The median percentage deviations in serum hydroperoxides amongst dose groups of the rat pilot study, as listed in Table 5.127.B, indicated that rats in dose group R9 harboured

78.5% more hydroperoxides than the environmental control dose group N. Dose groups R12 and R15 were determined to harbour 58.1% and 10.3% more hydroperoxides than N, respectively. The unexpected decrease in hydroperoxide levels beyond 9 $mg.kg^{-1}.day^{-1}$ rotenone dose concentrations was argued in Section 5.3.1.1 to be due to a possible antioxidant capacity contributed by rotenone and its metabolites. Data generated from the rat main study confirmed these findings, as presented in Section 5.3.1.2. In addition, the fact that rotenone itself was determined to harbour an antioxidant capacity equivalent to the vitamin E analogue Trolox, as presented in Section 5.3.2.1, strengthened the argument that rotenone may indeed alleviate oxidative stress in rats.

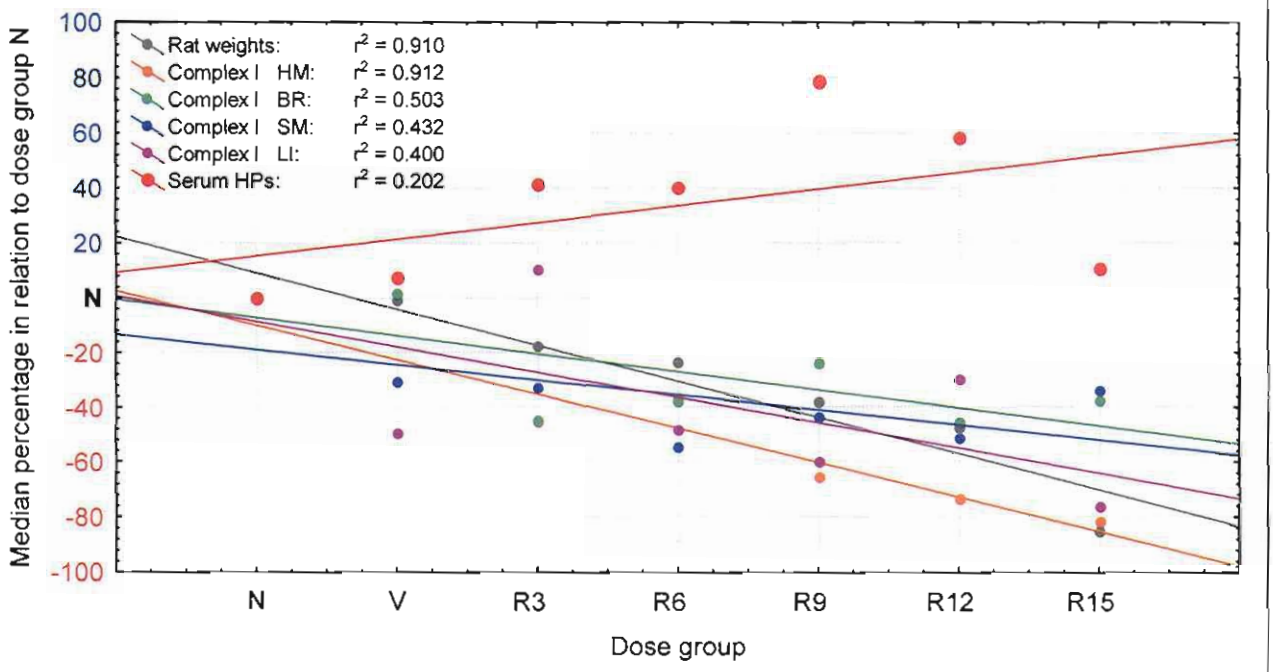
Finally, regression analysis of the rat pilot study data was performed to determine statistically significant correlations in rat responses to the increase in rotenone dose concentrations. A graphical summary and a grid of the correlation statistics are presented in Table 5.128. Statistically significant correlations are indicated in red text. It should be noted that since rat organ weight data did not present with a particular trend in response to the increasing rotenone dose concentrations, it was not included in these analyses.

As presented in Table 5.128.A, all trend lines decrease for rat weight and complex I data, in contrast to the serum hydroperoxide data, which was expected to increase as the concentration of the complex I inhibitor increased. However, as discussed previously in this section, lowered serum hydroperoxide levels were recorded in rats that received the highest dose concentrations of 12 and 15 $mg.kg^{-1}.day^{-1}$. These lowered levels for dose groups R12 and R15 results in a decrease in the linearity of the trend line and hence an r^2 value of 0.202. It was expected that the increased rotenone would result in a proportionally increased formation of hydroperoxides. The consistent increase in weight loss corresponded well with the increase in rotenone concentrations, as confirmed by the rat weight trend line that presented with an r^2 value of 0.910. The global downward trend in complex I activities for the different tissue types is evident from the graphic representation in Table 5.128. The complex I activity for heart muscle decreased steadily with an r^2 value of 0.912, whereas such consistency was not determined for the complex I activities generated from brain, skeletal muscle and liver tissue. The respective r^2 values for the latter mentioned tissue groups were 0.503, 0.432 and 0.400. The decreased association between rotenone concentrations and complex I activities for the latter mentioned tissue groups may be explained by the increased presence of NADH oxidases. Since the complex I assay is based on monitoring the oxidation of NADH in a sample, it is subject to interference from additional NADH oxidases. Results obtained from the

complex I data are suggestive of the fact that brain tissue, skeletal muscle and liver tissue preparations contained greater amounts of NADH oxidases. Therefore, it may be more useful in future experimentation to adopt an assay for complex I activity that is independent to NADH oxidation, such as one where CoQ_1 reduction may be monitored.

Table 5.128 Graphic representation and correlation statistics generated from the rat pilot study

A: Graphic representation



B: Correlation grid

Data set	Rat weights	Complex I HM	Complex I BR	Complex I SM	Complex I LI	Serum HPs
Rat weights		0.71	0.42	0.27	0.38	-0.24
Complex I HM	0.71		0.48	0.38	0.30	-0.28
Complex I BR	0.42	0.48		0.37	0.47	-0.28
Complex I SM	0.27	0.38	0.37		0.24	-0.15
Complex I LI	0.38	0.30	0.47	0.24		-0.17
Serum HPs	-0.24	-0.28	-0.28	-0.15	-0.17	

A: Percentage data points for the various assays are colour and shape coded, as indicated by the graphic key in the top left corner of the graph. The key also includes the r^2 values for each of the straight-line plots generated from the assay data points. B: Correlation statistics significant below the 0.05 significance level are indicated in red text. Rats were treated with N = no dose, V = vehicle, R3 = rotenone 3 $mg.kg^{-1}.day^{-1}$, R6 = rotenone 6 $mg.kg^{-1}.day^{-1}$, R9 = rotenone 9 $mg.kg^{-1}.day^{-1}$, R12 = rotenone 12 $mg.kg^{-1}.day^{-1}$, R15 = rotenone 15 $mg.kg^{-1}.day^{-1}$. BR = brain, HM = heart muscle, HPs = hydroperoxides, LI = liver, r^2 = square of the Pearson product moment correlation coefficient (signifying curve linearity), SM = skeletal muscle.

Statistically significant correlations were determined for 7 of the 15 data set comparisons. Rat weight loss correlated significantly with complex I activities determined from heart muscle, brain and liver tissue. The most significant correlation was determined to be between rat weight loss and complex I activity of heart muscle, which was reported with a coefficient of 0.71. As discussed in Section 5.6.6, it was apparent that skeletal muscle was an unsatisfactory tissue responder to the rotenone dose concentrations. Skeletal

muscle presented with complex I inhibition, but with poor inverse correlation to the increasing rotenone dose concentrations, as specified by the non-significant correlation coefficient of 0.27. None of the dose groups in the pilot study differed statistically significantly from each other when multiple comparisons were performed on the skeletal muscle complex I data, as presented in Table 5.83 of Section 5.6.1.2. As expected, negative correlations between the serum hydroperoxide data and remaining data sets were determined. Due to the decrease in hydroperoxide levels for dose groups R12 and R15, the slope of the trend line for this data set was diminished considerably resulting in a lack of statistically significant inverse correlations between hydroperoxide and the other pilot study data sets. Among the complex I activity data sets, the only correlations that were not significantly involved in liver tissue when correlated with heart muscle and skeletal muscle. These correlation statistics are certainly influenced by the fact that consistent dose-related increases in complex I inhibition for liver tissue and skeletal muscle could not be attained as successfully as for heart muscle. Nonetheless, a downward trend in complex I activity for all tissue types was recorded, in positive correlation with the loss in body weights.

5.8.2 Rat main study collective summary of data

In an attempt to evaluate the effects of the dose regimens over the various tissue types, the median percentage data was presented in a grid format, as illustrated in Table 5.129. As with the format used for the tissue profiles sections, the colour-coding scheme for statistical significance and median percentage deviations above and below that of the environmental control dose group NN was utilised. The table format enables the reader to evaluate the deviation in data across the different tissue types, in order to investigate tissue specific response profiles.

Rat groups that received vehicle Factor-1 dose regimens all increased in body weights when compared to the environmental controls NN. Dose group VS however was the only rat group that did not gain in excess of 10%. As expected, the rotenone-treated rats lost considerable amounts of weight, as indicated by the red median percentages that were all more than 100% lower than NN. Moreover, the latter mentioned rat groups all differed statistically significantly from the environmental control dose group.

Table 5.129 Collective summary of rat main study median percentages in relation to environmental controls

F1		Vehicle (V)									Rotenone (R)								
F2		Body weight	Organ weight	Complex I	Hydroperoxides	AC	GSH/GSSG	L/P	ATP/ADP	NAD/NADH	Body weight	Organ weight	Complex I	Hydroperoxides	AC	GSH/GSSG	L/P	ATP/ADP	NAD/NADH
Sacrifice (X)	BL	16.9	N/A	N/A	-6.81	119	-37.0	64.1	6.66	9.65	-173	N/A	N/A	-1.07	93.2	-39.2	-39.5	-8.07	-42.4
	HM		5.86	176	N/A	51.0	—	-22.6	-42.9	—		0.90	-46.0	N/A	8.98	—	-4.76	-3.93	—
	BR		N/A	91.7	N/A	59.4	—	20.1	—	—		N/A	12.4	N/A	8.12	—	33.3	—	—
	SM		N/A	196	N/A	57.0	—	29.1	-5.12	115		N/A	56.9	N/A	10.0	—	20.2	20.4	44.5
	LI		0.59	106	N/A	62.0	-47.1	-70.7	-5.32	-66.8		-20.8	-13.8	N/A	2.96	-61.5	-45.4	-11.1	-8.55
No dose (N)	BL	36.4	N/A	N/A	-14.8	47.3	-31.7	47.9	69.0	-5.20	-164	N/A	N/A	-4.58	24.0	-39.0	-23.6	114	26.8
	HM		17.1	-20.4	N/A	102	—	4.55	-9.35	—		-8.62	-57.1	N/A	57.0	—	26.0	-13.9	—
	BR		N/A	90.2	N/A	79.8	—	37.7	—	—		N/A	54.6	N/A	55.7	—	10.6	—	—
	SM		N/A	202	N/A	71.9	—	24.5	43.1	-35.6		N/A	43.4	N/A	40.3	—	-19.3	73.8	17.9
	LI		6.85	39.5	N/A	81.3	-34.2	-30.9	745	-39.8		6.15	51.5	N/A	62.8	-23.4	4.31	-53.5	148
Vehicle (V)	BL	35.1	N/A	N/A	-32.7	47.3	-49.5	51.8	454	-19.0	-209	N/A	N/A	3.65	83.8	-49.0	-19.3	59.6	-13.0
	HM		13.0	-33.3	N/A	4.91	—	-3.32	-3.70	—		-12.5	-39.8	N/A	-35.1	—	3.29	68.5	—
	BR		N/A	74.2	N/A	-12.2	—	21.7	—	—		N/A	12.8	N/A	143	—	4.54	—	—
	SM		N/A	-3.09	N/A	-5.41	—	10.9	-0.24	92.6		N/A	20.0	N/A	22.5	—	26.9	-28.7	-6.64
	LI		4.88	44.2	N/A	7.03	-24.0	24.9	-4.24	-75.1		-16.7	15.6	N/A	-35.2	-44.0	20.6	-46.5	0.08
CoQ_{10} (C)	BL	22.1	N/A	N/A	-4.19	144	-4.25	46.1	4.87	-20.8	-130	N/A	N/A	2.64	159	-34.5	4.50	-16.0	-22.4
	HM		3.38	-25.8	N/A	-1.73	—	9.57	58.3	—		-10.4	10.7	N/A	3.24	—	17.1	-10.9	—
	BR		N/A	-0.20	N/A	73.3	—	31.5	—	—		N/A	18.6	N/A	38.4	—	37.2	—	—
	SM		N/A	106	N/A	40.2	—	32.0	-25.7	11.7		N/A	49.9	N/A	24.6	—	32.2	-36.0	-36.5
	LI		1.24	10.3	N/A	38.9	-18.0	-40.8	-10.1	-57.5		0.61	50.8	N/A	41.7	-11.2	1.79	-53.9	40.5
Succinate (S)	BL	1.30	N/A	N/A	-0.63	230	-42.9	66.3	23.6	2.81	-130	N/A	N/A	5.25	126	-33.7	35.9	-8.21	1.68
	HM		0.48	48.5	N/A	-9.34	—	11.9	-12.4	—		0.78	95.4	N/A	-38.2	—	5.13	-2.47	—
	BR		N/A	34.2	N/A	40.0	—	-14.7	—	—		N/A	-0.71	N/A	-1.56	—	25.8	—	—
	SM		N/A	66.9	N/A	59.3	—	17.5	-11.7	28.5		N/A	75.2	N/A	20.9	—	31.9	-13.0	-51.7
	LI		0.47	-27.5	N/A	72.8	-5.51	-34.0	-25.9	-30.5		1.11	65.0	N/A	35.6	13.7	-29.7	-2.13	3.50

The grid is structured to reflect how each of the dose regimens affected the various tissue groups. All median percentages are presented in relation to the environmental control dose group NN. Median percentages that deviated by more than 10% from the environmental controls NN are indicated in blue and red text for beneficial and harmful deviations respectively. Percentages in grey text represent deviations less than 10%. Grid blocks shaded in green represent data that differed statistically significantly from the environmental control dose group NN. Comparisons determined to differ significantly after the exclusion of extreme outliers are indicated by yellow shading. '—' = missing data point, F1 = Factor-1 dose regimen, F2 = Factor-2 dose regimen, AC = antioxidant capacity, ATP/ADP = ratio of adenosine triphosphate to adenosine diphosphate, BL = blood, BR = brain tissue, GSH/GSSG = ratio of oxidised to reduced glutathione, HM = heart muscle, LI = liver tissue, L/P = ratio of lactate to pyruvate, N/A = parameters not applicable for the designated tissue, NAD/NADH = ratio of oxidised to reduced nicotinamide adenine dinucleotide, SM = skeletal muscle.

Heart weight for rat groups VN and VV increased by more than 10% when compared to the environmental controls NN. These two dose groups also increased the most with regards to body weight, which may partly explain the increased heart weight. However, this was not determined to be the case for the liver organs that deviated by less than 10%. Rat groups that received rotenone Factor-1 doses presented with heart and liver weights that either remained very similar to, or less than NN, even though these rats all lost large

amounts of overall body weight over the 14 days of dosing. Dose groups RX and RV presented with liver weights that were -20.8% and -16.7% of NN respectively, while the remainder of the rotenone-treated rats did not deviate by more the 10% from NN. Dose groups RV and RC were the only two groups that harboured median heart weights that were more than 10% lower than NN, at -12.5% and -10.4% respectively.

Rat groups that received a vehicle Factor-1 dose regimen indicated that all tissues presented with mostly improved complex I activities. However, it should be noted that the sunflower oil vehicle might have affected heart muscle adversely, since dose groups VN, VV and VC presented with lowered complex I activities. However, since dose group VX presented with a heart muscle complex I activity that was 176% higher than NN, it cannot be stated that sunflower oil induced a decrease in heart muscle complex I activities. The rotenone-treated rats presented with few complex I activities that were lowered. However, as discussed in Section 5.5.2.2, the complex I activity for brain tissue generated from the environmental controls was lower than expected, which arguably resulted in over-estimated median percentages for all dose groups. This in turn resulted in less median percentages for brain complex I activity that may have presented in red, even though it was apparent that the activities were recorded to be mostly lower than the rat groups that received vehicle Factor-1 doses. The fact that complex I median percentages presented mainly in blue for dose groups RC and RS, suggests that CoQ_{10} and succinate contributed to the recovery of complex I activity. However, since neither of the Factor-2 therapeutic regimens are known to act directly on complex I itself, it should be argued that these compounds may have aided overall biochemical recovery resulting in an indirect improvement of several mitochondrial parameters, including complex I activities.

Hydroperoxide levels for dose groups VX, VN, VV, VC and VS were all increased when compared to the environmental controls NN, and hence presented with negative median percentages. Dose groups VN and VV harboured the most harmfully affected hydroperoxide concentrations with median percentages of -14.8% and -32.7% respectively. This was suggestive of the high polyunsaturated fat contents of sunflower oil inducing oxidative stress. These speculations stemmed from reports by Turpeinen *et al.* (1998), Mataix *et al.* (1998) and Quiles *et al.* (2004) where it was demonstrated that a high linoleic acid intake induces oxidative stress and decreases antioxidant capacity. Since none of the rotenone-treated rats presented with increased hydroperoxide levels, even though rotenone was determined to bind and inhibit complex I, it was argued that rotenone contributed to the scavenging of ROS. The argument was strengthened by the fact that

rats in the pilot study presented with increased ROS levels when dosed rotenone up to concentrations of 9 $mg.kg^{-1}.day^{-1}$, followed by a decrease in hydroperoxide concentrations when 12 and 15 $mg.kg^{-1}.day^{-1}$ were dosed. Furthermore, experimentation illustrating the inherent antioxidant capacity of rotenone itself, as presented in Section 5.3.2.1, was argued to be a major factor contributing to improved serum hydroperoxide concentrations.

Antioxidant capacities in the various tissues of the vehicle Factor-1 treated rats were illustrated to be improved in the majority of cases, as indicated in Table 5.129. This may be accounted for by the high vitamin E content of sunflower oil, which is a well-known antioxidant. However, rats from dose group VV, which received only sunflower oil for a period of 16 days, did not convincingly illustrate that the various tissue groups benefited in terms of antioxidant capacity. Rat groups RX, RN, RV, RC and RS also presented with antioxidant capacities that were mostly improved, even though a Complex I deficiency was induced in these rats. Furthermore, it could also be argued that the two-day recovery periods, whether in the presence of therapeutic regimens or not, may have contributed to improving overall antioxidant capacity. The three decreased median percentages amongst the rotenone-treated rats is argued to be the result of a lack of recovery in antioxidant capacities. Nonetheless, these antioxidant capacities were not determined to differ by a statistically significant degree from that of the respective environmental controls NN.

Glutathione concentrations were recorded successfully from blood and liver tissue. GSH/GSSG ratios were determined from both blood and liver to be affected adversely, whether a vehicle or rotenone Factor-1 dose regimen was administered. Once again, the sunflower oil vehicle appeared to be central to response in the various rat tissues. However, in contrast to the antioxidant capacity data sets, sunflower oil proved to be harmful with regards to glutathione ratios. In this case, it was argued that the sunflower oil contents induced oxidative stress that resulted in a particular decrease in glutathione ratios, an unexpected outcome considering that ORAC-generated data presented with improved antioxidant capacities in the majority of rat groups. Glutathione therefore appeared to be an indicator or marker for the harmful effects of sunflower oil. Since the rotenone-treated rats too received the sunflower oil vehicle, GSH/GSSG ratios were also compromised. Furthermore, since the rats that received rotenone presented with blood and liver GSH/GSSG ratios that were similar to that of the rat groups that received vehicle Factor-1 doses, it was argued that rotenone might not have additionally reduced GSH/GSSG ratios. Alternatively, it could be speculated that rotenone indeed

compromised biochemical status, as would be expected by its inhibition of complex I, but balanced the formation of ROS via the use of its antioxidant capabilities. This may be further supported by the fact that a CoQ_{10} Factor-2 regimen appeared to have improved blood GSH/GSSG ratios when a vehicle Factor-1 was dosed, but not in the presence of the Complex I deficiency. This was suggestive of rotenone compromising recovery of glutathione status. Liver GSH/GSSG ratios for dose groups VC and RC were argued to have recovered equally to a minimal extent. The succinate Factor-2 regimen appeared to improve GSH/GSSG ratios in liver, but not in blood.

Rat groups that received vehicle Factor-1 dose regimens presented with L/P ratios that were mostly improved. However, there were six data sets that harboured lowered L/P ratios. Blood L/P ratios all improved by a minimum of 46% when a vehicle Factor-1 dose was received, while heart muscle L/P ratios remained mostly unaltered. Brain L/P ratios for the aforementioned rat groups all improved over that of the environmental controls NN, except for dose group VS, which presented with a median percentage that was lowered at -14.7%. Skeletal muscle L/P ratios for rats that received a vehicle Factor-1 all presented with improved L/P ratios. However, the liver L/P ratios for the same rats were mostly lowered, which is suggestive of the metabolism of sunflower oil in the liver resulting in increased L/P ratios and therefore may have been harmful. CoQ_{10} and succinate for the rotenone-treated rats indicated that the inhibition of complex I resulted in harmful affects that alleviated blood L/P ratios. However, heart muscle, brain and skeletal muscle for these same rats revealed L/P ratios that were mostly unaltered or improved, indicating that rotenone may not have compromised these biochemical markers. Liver tissue L/P ratios were decreased for dose groups RX and RS, while dose groups RN, RV and RC either remained unchanged or increased marginally.

The ATP/ADP ratios were determined successfully in all tissues except for brain. Two median percentages were recorded to exceed the 200% upper limit, namely the ATP/ADP ratios for dose groups VN and VV from liver and blood respectively. These were argued in Sections 5.7.6 and 5.3.5 to be the result of aberrantly determined data points and were not relied upon as accurate indications of ATP/ADP ratios. ATP/ADP ratios generated from the vehicle Factor-1 rat groups indicated that sunflower oil did not influence ADP phosphorylation adversely. Amongst dose groups VX, VN and VV, only one median ATP/ADP ratio was determined to be lowered from that of the environmental controls NN. However, with regards to dose groups VC and VS, five ATP/ADP ratios were recorded to be lowered by more than 10%, particularly in liver tissue. However, the highest deviation

of -25.9%, for liver tissue of dose group VS, was not determined to differ statistically significantly from NN. Therefore, it cannot be stated that either CoQ_{10} or succinate may have compromised ATP/ADP ratios in rats, but rather that these compounds did not additionally influence ATP/ADP status. Rotenone-treated rats indicated that ATP/ADP ratios may have been decreased due to the inhibition of complex I, as would be expected. However, as with the rat groups that received vehicle Factor-1 regimens, no definitive harmful affects could be concluded due to a lack of statistically significant differences. The ATP/ADP ratios for dose group RC should however be mentioned. Dose group RC was the only group that presented with lowered ATP/ADP ratios. This indicates that CoQ_{10} was indeed not beneficial to the tissue groups analysed in this study. However, since no statistically significant differences were reported, it cannot be concluded with confidence that CoQ_{10} may have additionally reduced ATP/ADP ratios.

The NAD/NADH ratios were determined successfully from blood, skeletal muscle and liver tissue collections. As with the ATP/ADP ratio data sets, none of the NAD/NADH ratios generated from the various rat groups were determined to differ by a statistically significant degree from the respective environmental control data sets. In view of the rat groups that received vehicle Factor-1 dose regimens, it could be speculated that sunflower oil may have contributed to an overall decrease in NAD/NADH ratios. However, these ratios were increased in skeletal muscle of rat groups VX, VV, VC and VS. Furthermore, it cannot be confirmed from the data presented in Table 5.129 that rotenone increased NADH concentrations, the result typically expected if complex I were to be inhibited. The NAD/NADH ratio may be influenced by several other biochemical factors, in particular the activity of the pyruvate dehydrogenase (PDH) complex, a multi-enzyme complex that imports pyruvate into the mitochondria and converts it to acetyl coenzyme A. The complex is integral to carbohydrate metabolism, creating the link between glycolysis and the Krebs cycle. By preventing pyruvate import, PDH limits the supply of acetyl coenzyme A to the Krebs cycle, where the majority of NADH required by the respiratory chain is produced. Since PDH is subject to strict regulation (Patel and Korotchkina, 2003), often affected in mitochondrial disorders (Wilichowski *et al.*, 1998) as well as by fatty acid intake (Batenburg and Olson, 1976), it may explain why the definitive interpretation of NAD/NADH ratios could not be determined.

The results generated from the rat main study are suggestive of the fact that CoQ_{10} and succinate improved different aspects of the tissue profiles. This supports the current therapeutic regimens prescribed for patients suffering from a mitochondrial cytopathy,

where a combination dose of various cofactors is received (Chinnery, 2003). There is no definitive answer as to which of the regimens are more beneficial, but it can be speculated that a combination of CoQ_{10} and succinate may be more beneficial than either of the compounds administered in isolation. The rat main study also confirmed that the 15 $mg.kg^{-1}$ daily dose of rotenone inhibited complex I activity to a satisfactory degree, in concordance with that of the rat pilot study. Furthermore, it was established that rotenone harboured an antioxidant capacity that had an impact on the biological response profile of the rat. The most noted impact of rotenone was observed in the blood profile, where hydroperoxide data presented, uncharacteristically, with unaltered concentrations when compared to the environmental control dose group NN. As presented in Section 5.3.1.1 for the rat pilot study, hydroperoxide levels increased to the highest concentrations when rats received 9 $mg.kg^{-1}.day^{-1}$ rotenone, but decreased significantly when rats were dosed with 12 and 15 $mg.kg^{-1}.day^{-1}$, a finding that has not been previously reported. The strategies and data presented here indicate the need for novel methodologies in the field of mitochondrial biology, in particular for the investigation of Complex I deficiency in an animal model.

CHAPTER SIX

CONCLUSIONS

Disorders of the mitochondrial respiratory chain have an incidence that ranges between 1 in 2,000 to 1 in 5,000 (Naviaux, 2004). The most frequent of these cytopathies result from causative alterations within the first enzyme of the respiratory chain, namely complex I. The impact of a deficiency in complex I is generally that of a failure to oxidise NADH, impairment of the Krebs cycle and an increase in the concentrations of lactate. In addition, increased production of ROS, lowered ATP generation and altered mitochondrial membrane potential are expected. Complex I deficiency is manifest primarily in phenotypes such as Leigh and Leigh-like syndromes, slowly or highly progressive encephalomyopathy, or fatal infantile lactic acidosis. In the majority of cases, these disorders present with signs of fatigue, exercise intolerance and lactic acidaemia. Therapeutic intervention strategies for mitochondrial disorders have primarily explored the use of vitamins and cofactors. However, only isolated cases of improvement have been reported with the majority representing a lack of response and hard evidence to support their use. This is largely due to the vast clinical, metabolic and genetic heterogeneity observed to be associated with these disorders. The current research program included the establishment of a complex I deficient animal model, followed by supplementation with therapeutic regimens of CoQ_{10} and succinate, in an attempt to alleviate the harmful effects of the deficiency. Metabolic consequences of the various dose regimens were evaluated in heart, skeletal muscle, brain and liver tissue. Biochemical profiles of the various tissues were determined utilising several biochemical analyses. Experimentation was performed in C57BL/6 mice and Sprague Dawley rats, with successful induction of Complex I deficiency in the latter animal model.

The rat pilot study was designed so that the rats were dosed daily with various rotenone concentrations for a period of 14 days, as presented in Section 4.1 of Chapter Four. The concentrations of rotenone ranged from 3 $mg.kg^{-1}.day^{-1}$ to 15 $mg.kg^{-1}.day^{-1}$, with the groups differing by increments of 3 $mg.kg^{-1}$ so that five different concentrations could be evaluated. In addition, a vehicle control group was included, as well as a group that received no dose for the same length of time, referred to as the environmental control dose group. Complex I data, generated from heart muscle, brain tissue, skeletal muscle and liver tissue, indicated that rotenone-induced Complex I deficiency occurred in all

tissue types and in a particularly dose-dependent manner in heart muscle. Furthermore, it was also determined that a dose-dependent weight loss was observed, along with a difficulty in the handling of the rats. Based on the adverse behaviour and the difficulty in the handling of the rats in response to the highest dose of 15 $mg.kg^{-1}.day^{-1}$, it was decided that a higher rotenone dose concentration could not be administered. Furthermore, the study design was not aimed at evaluating the toxicity of rotenone. It was also determined from the rat pilot study that rotenone may have prevented weight increase in two organs, namely the heart and liver, which was confirmed by the organ weight data generated during the rat main study. Brain weight remained unaltered by the various rotenone concentrations included in the pilot study design and was thus not evaluated in the main study. The lowered heart and liver weights were argued to be the result of rotenone interference with spindle formation and consequent mitotic arrest. As reported by Barham and Brinkley (1976a and 1976b), as well as by Diaz-Corrales *et al.* (2005), rotenone not only inhibits the respiratory chain, but also induces the aggregation of tubulin protein and hence arrests mitosis. Furthermore, experimental proof of a decrease in hepatocellular proliferation in response to even low concentrations of rotenone has previously been reported (Cunningham *et al.*, 1995).

The most striking result obtained from the pilot study was that of the hydroperoxide levels generated from blood serum. Since hydroperoxides are known to escape from cellular structures into circulation and biological fluids (Iorio, 2002), the d-ROMs assay data were a reflection of the overall hydroperoxide status of the rat organism. It was initially expected that serum hydroperoxide concentrations would increase uniformly as the daily concentrations of rotenone increased. This was indeed observed to be the case, up to a certain point. The pilot study hydroperoxide concentrations, presented in Section 5.3.1.1, increased as the concentration of rotenone increased from 0 $mg.kg^{-1}.day^{-1}$ up to, and including, 9 $mg.kg^{-1}.day^{-1}$. However, the hydroperoxide levels appeared to reduce in an incremental fashion as the rotenone concentrations were increased to 12 and 15 $mg.kg^{-1}.day^{-1}$ respectively. Serum hydroperoxide concentrations of dose group R15 were equivalent to that of the environmental control dose group NN. This occurrence took place even though a rotenone-induced Complex I deficiency was reported for these same rat groups, not to mention the notable decreases in body and organ weights. Confirmation of these results was obtained in the rat main study, presented in Section 5.3.1.2, when hydroperoxide concentrations determined from the rotenone-treated rats and environmental control rats were demonstrated to deviate by less than 10%. The unexpected hydroperoxide data generated from rat serum spurred investigation into

evaluating the speculative ROS scavenging properties of the complex I inhibitor. Rotenone was consequently investigated for its antioxidant capacity via the ORAC assay, presented in Section 5.3.2.1, revealing that the inhibitor harboured an antioxidant capacity no less than that of Trolox, the vitamin E standard used for all ORAC analyses. In support of the rat pilot study, if serum hydroperoxide levels were not determined at the various rotenone dose concentrations, it would have been concluded in the rat main study that rotenone had no influence on the formation of ROS. Furthermore, investigation into the antioxidant capacity of the compound would not have been undertaken.

Upon successfully achieving a rotenone-induced complex I deficient rat model, the rat main study was initiated, encompassing 11 dose groups, as depicted in the study design presented in Section 4.2 of Chapter Four. Five dose groups received the 15 $mg.kg^{-1}.day^{-1}$ dose of rotenone for 14 days, as performed in the rat pilot study, in an attempt to re-establish rats with Complex I deficiency. Following this, these rats received one of five treatments, which included either being sacrificed on day 15, receiving no dose regimen, vehicle, CoQ_{10} or succinate for an additional two days before being sacrificed for tissue collection and analysis. The next five rat groups received vehicle for 14 days, followed by Factor-2 treatments equivalent to the rotenone treated rats. Finally, a rat group that received no dosage regimen for a period of 14 days was included as a control and referred to as the environmental controls. Rats were handled and maintained in conditions identical to that of the pilot study. The primary goal of the rat main study was to investigate the relief of biochemical consequences of deficient complex I in the presence of two types of therapeutic regimens, namely CoQ_{10} and succinate. The effects of these regimens were evaluated exclusively and the data reported. Rat weights were once again monitored on a day-to-day basis prior to dosage. When rats were sacrificed, heart and liver weights were recorded and tissue prepared and stored appropriately for the various analyses to be performed. The rat main study incorporated several additional biochemical analyses in an attempt to generate tissue specific data sets that could be grouped and evaluated in unity and hence reflect an overall profile of response. The impact of CoQ_{10} and succinate were concluded to improve different aspects of the biochemical profiles in the various tissues, hence supporting the prescription of a combination of cofactors for individuals affected by mitochondrially related disorders.

6.1 SELECTION OF ANIMAL MODEL

In the initial pilot study that was performed in C57BL/6 mice, varied concentrations of rotenone ranging from 0 to 175 $mg.kg^{-1}$ were dosed daily for a period of 14 days. Across the complete range of rotenone concentrations, mice appeared to lose weight over a period of approximately four days, followed by weight gain and stabilisation by day seven. Complex I activities generated from mouse heart muscle and brain tissue indicated that no inhibition of the enzyme was achieved, even when high dosage concentrations of 175 $mg.kg^{-1}.day^{-1}$ were received. It was hypothesised that the lack of rotenone effectiveness was, firstly, due to the route of rotenone administration and, secondly, due to the high activity of cytochrome P450 enzymes inherent to mice. Since dosage via oesophageal intubation was utilised in the study, rotenone entered the stomach and was circulated directly through the liver via the hepatic portal system before being distributed to the rest of the rat. Consequently, since the liver is central to the metabolism of foreign compounds and hence rich in cytochrome P450 activity, the majority of rotenone was metabolised before entering circulation. The mice appeared to be physically affected, based on the loss of body weight over the first three to four days, which was however mostly regained by day seven. It is hypothesised that a several-fold metabolic up-regulation, particularly in the activity of the cytochrome P450 enzymes, was induced resulting in the breakdown of rotenone into its non-toxic metabolites.

It has previously been reported (Henderson, 1996) that the toxic effects of benzene were far more detrimental to mice than rats. Since the toxicity is attributed to the metabolites of benzene, it was speculated that mice metabolised benzene at a higher rate than rats. Nakajima *et al.* (1993) confirmed this when the cytochrome P450 enzymes, responsible for benzene metabolism, were illustrated to be more up-regulated in mouse than in rat microsomes. In fact, even the enzyme activity determined from mouse microsomes exposed to low concentrations of benzene was 1.4 times greater than in rat microsomes exposed to a high concentration of benzene (Nakajima *et al.*, 1993). The literature is therefore indicative of the fact that mice harbour increased cytochrome P450 activity. Thus, it could be argued that the up-regulation of these enzymes was far more efficient in mice and enabled them to overcome the toxic effects of rotenone.

Since C57BL/6 mice responded unfavourably, the study presented currently was performed in Sprague Dawley rats. The great variation in response between mice and rats was astounding at first, considering that these animals both descended from the

rodent lineage and are hence closely related. However, as the study progressed to completion, it became evident that even amongst the rats, which were genetically identical, a considerable degree of unexpected variation was observed. The complexities encountered when performing research in an animal model were certainly experienced in this study. The contrasting response patterns observed between mice and rats, in addition to the variation in response amongst the genetically identical rats, opens debate as to the use of animal models in research and levels of inference. In terms of the experience obtained from this study alone, it can be concluded that no inference from mice to rats can be performed, particularly concerning rotenone dose concentrations and effectiveness in complex I inhibition. The study also made it evident that deep insight, as well as several theoretical and practical considerations, were required before investigating the effects of an administered compound in an animal model.

Today, researchers in the medical sciences are required to select an animal model based on known genetic and metabolic considerations that would allow for effective extrapolation to humans. Concerning investigations that evaluate medicinal effects of compounds, prior knowledge of the cytochrome P450 enzyme family is essential (Bogaards *et al.*, 2000; Guengerich, 1997; Zuber *et al.*, 2002). Selection of an appropriate animal model has become a pertinent factor when planning studies of this nature. In essence, when evaluating a compound that is metabolised by a particular set of human cytochrome P450 enzymes, it is vital to select an animal model that expresses the same or similar enzymes. However, for this step of the planning process to be viable, the required metabolic data should already be available for the compound of interest. This is unfortunately not always the case and can only be predicted or inferred in the majority of studies. However, in this investigation, knowledge of cytochrome P450 enzymes was required not for inference to humans but for a prediction of rotenone toxicity. Since rotenone was used for the sole purpose of inducing Complex I deficiency, there was no need to find an animal model that would metabolise the inhibitor equivalently.

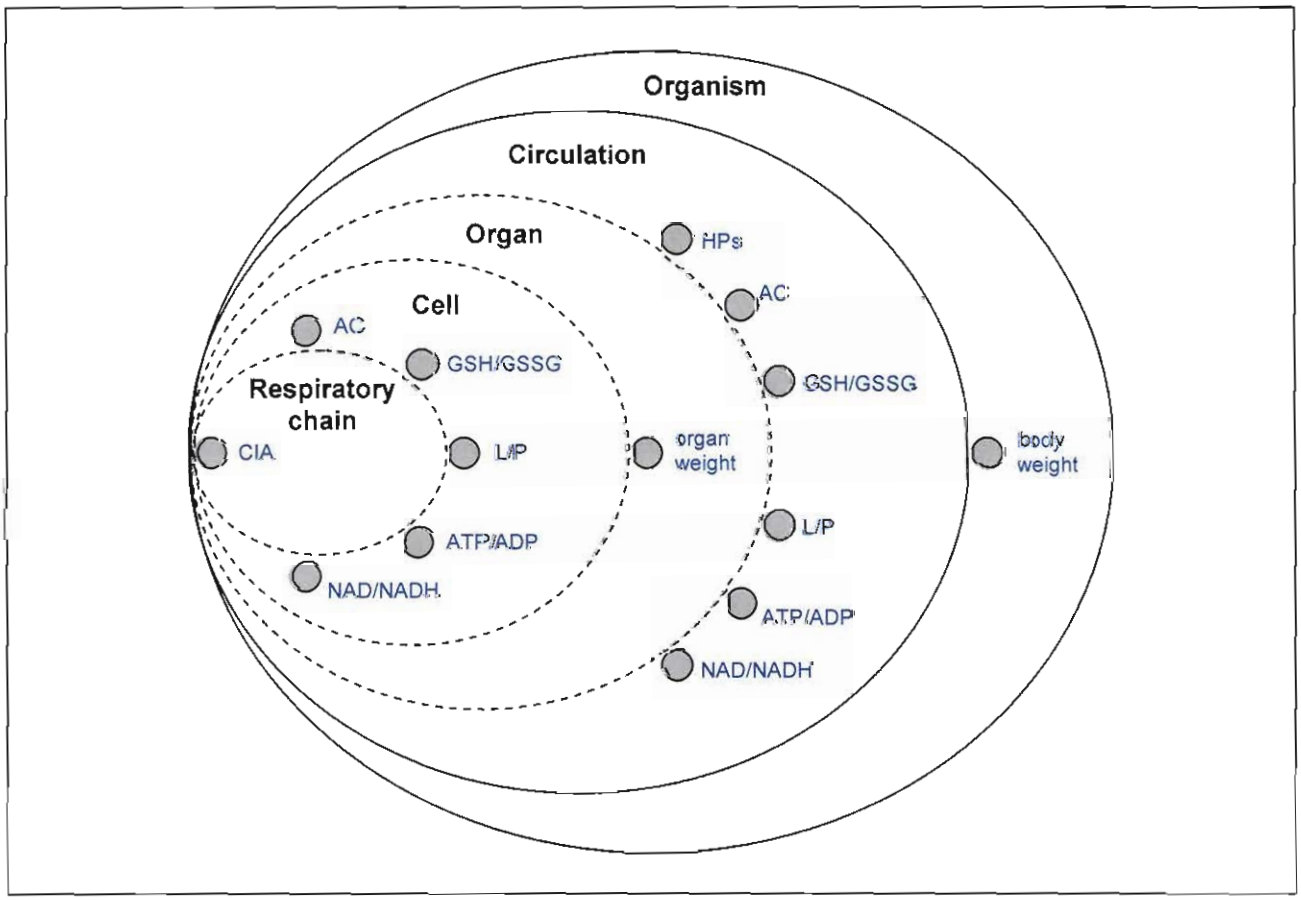
The ideal organism to be used in a study of this nature would be one that metabolises rotenone at a slow rate, enabling the compound to remain in its parent structure and hence maintain its inhibitory effects on complex I. This would allow for the dosage of lowered rotenone concentrations and hence dose volumes. As experienced in this study, rotenone had minimal inhibitory effects in the mouse model, indicating that mice rapidly metabolise rotenone. In contrast, rats undoubtedly presented with rotenone-induced complex I deficiencies in a dose related manner, confirming that the rat was the preferred

model for this study. The metabolising effects that cytochrome P450 enzymes might have had on the study were not considered prior to initiation. If knowledge of rotenone biotransformation were taken into account, the rat would certainly have been the model of choice, whilst mice would not have been included. Nonetheless, the practice of working with mice and rats and experiencing the unexpected variability was invaluable.

6.2 MODEL OF STUDY DESIGN

The considerable amounts of data presented and discussed in Chapter Five necessitated that a broader view of the data be presented, positioning the various data sets in the context of the rat organism as a whole. Therefore, a model of the study design is presented. A model of the rat main study was established taking into account each of the data sets analysed, as presented in Figure 6.1, with node structures in grey.

Figure 6.1 Model of study design for the rat main study



AC = antioxidant capacity, ATP/ADP = ratio of adenosine triphosphate to adenosine diphosphate, CIA = complex I activity, GSH/GSSG = ratio of reduced to oxidised glutathione, HPs = hydroperoxides, L/P = ratio of lactate to pyruvate, NAD/NADH = ratio of oxidised nicotinamide adenine dinucleotide to reduced nicotinamide adenine dinucleotide.

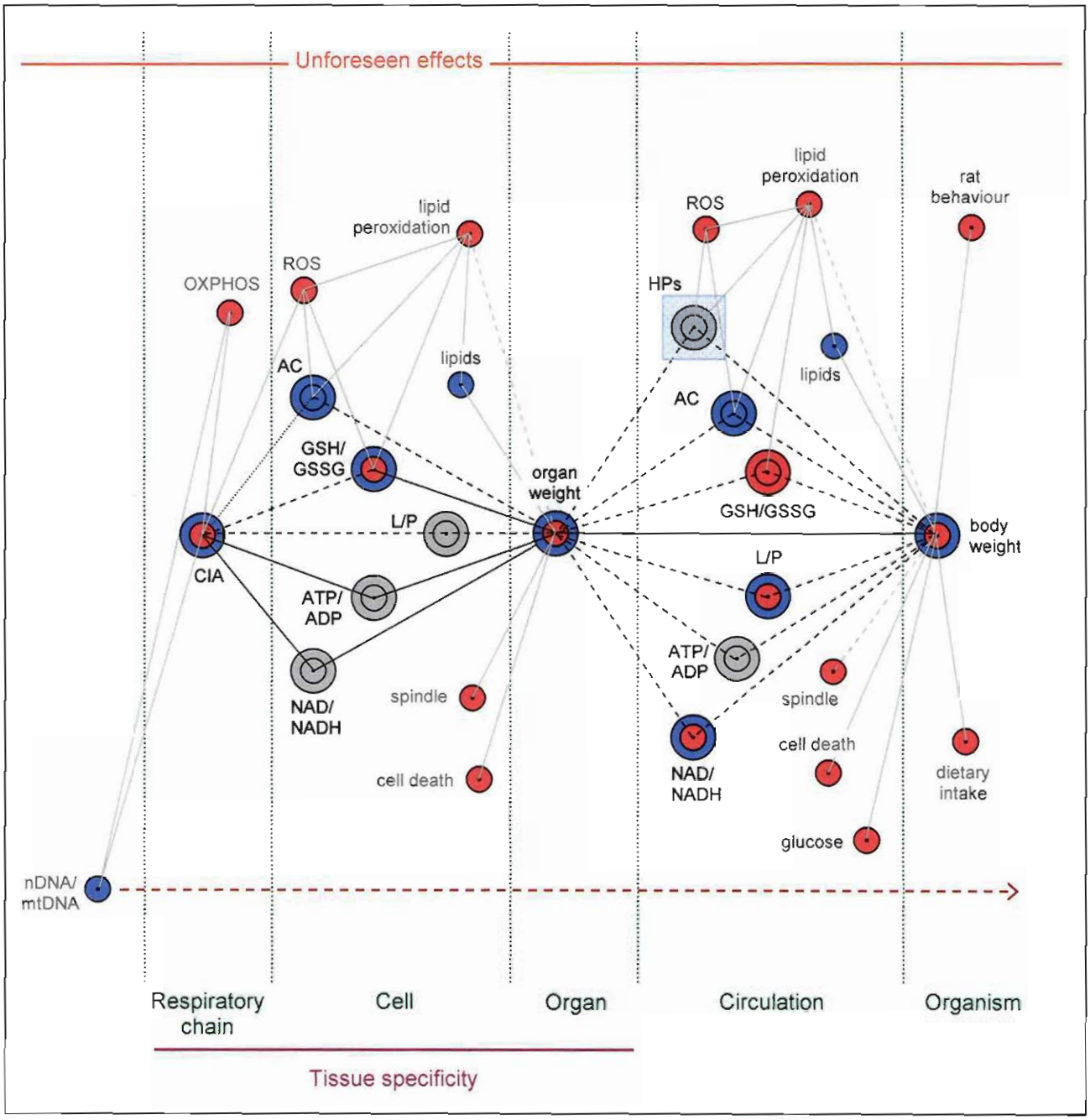
The various layers of the model refer to the different 'levels' on which the rats were investigated. The outermost layer of the model represents the rat organism as a whole, where rat body weights were recorded. The second layer from the outside represents blood-related biochemical aspects, where six biochemical parameters were investigated. The blood related data sets were separated from the organ data of the other four tissue types since several of the blood biochemical parameters were influenced by metabolite diffusion or transport from the organs into the circulatory system.

The three innermost layers of the model were indicated with dashed lines since these layers are an overall representation of all organs, cells and the respiratory chain. Alternatively, the three inner layers could be interpreted individually for each organ. On the organ level, the organ weight data sets are represented. The cellular level is composed of five biochemical assays, namely antioxidant capacity, glutathione status, L/P ratios, adenylate and NAD/NADH ratios. Finally, the inner core of the model represents the respiratory chain, and in particular, complex I, the binding site of rotenone and the focal point of the study.

6.3 MODEL OF OBSERVED EFFECTS

The model of observed effects depicts a structure that is distributed over six levels, of which the level containing the mtDNA and nDNA node was inferred. It would not be inappropriate to analyse individual data sets via the so-called 'reductionist' point of view. However, the more holistic or 'semi-reductionist' approach was employed into this analysis strategy, enabling a modular interpretation of the data, as presented in Figure 6.2, which is simply an extrapolation of the circular model presented in Figure 6.1. It should be noted that the model in Figure 6.2 reflects the response of rats in the presence of the induced Complex I deficiency, that is, all rats that received rotenone. The nodes were interconnected to form a network indicative of the rat response, enabling an overall view of the rat main study. The solid lines of the network represent a direct effect or relationship between nodes, while the dashed inter-connections indicate an indirect effect. The nodes are represented by three colours, namely grey, blue or red. The grey was indicative of a data set that deviated minimally from the environmental control dose group NN, while the blue and red represented beneficial and harmful effects, respectively.

Figure 6.2 Model representing a network of effects of therapeutic regimens in the presence of a rotenone-induced Complex I deficiency in rats



The network of nodes is distributed over six levels of analysis, which are designated in green text and divided by the green dotted vertical lines. A genome level has been included in the model summary, which is represented by a nDNA/mtDNA node. The double-layered nodes, denoted with black text and inter-connections are representative of data sets generated in the rat main study, whereas single-layered nodes indicated by grey text and lining represent inferred and speculated data. Furthermore, the inter-connecting lines are either solid or dashed signifying direct or indirect effects between nodes respectively. Red coloured nodes depict parameters and data sets that were affected adversely by dose regimens, while blue nodes indicate beneficial effects. Grey nodes are representative of no effect or unaltered parameter. The orange text and line represents unforeseen effects that take place in response to the dose regimens. The downstream effects expected to originate from mtDNA and nDNA are indicated by the brown dashed (- - -) arrow. AC = antioxidant capacity, ATP/ADP = ratio of adenosine triphosphate to adenosine diphosphate, CIA = complex I activity, GSH/GSSG = ratio of reduced to oxidised glutathione, HPs = hydroperoxides, L/P = ratio of lactate to pyruvate, mtDNA = mitochondrial DNA, NAD/NADH = ratio of oxidised to reduced nicotinamide adenine dinucleotide, nDNA = nuclear DNA, OXPHOS = oxidative phosphorylation, ROS = reactive oxygen species.

The data sets investigated in the study are represented by nodes with a core and an outer layer, whereas the nodes with no outer layer represent inferred and speculated responses. In the double-layered nodes, the core represents Factor-1, i.e. the effects of rotenone, while the outer layer represents response to the Factor-2 regimens, namely CoQ_{10} and

succinate. The joint interpretation of therapeutic regimens is justified since CoQ_{10} and succinate exclusively improved different aspects of the biochemical profiles. As will be concluded in Section 6.6, the combination dose of CoQ_{10} and succinate is advised for patients affected by the mitochondrial cytopathies. This is supportive of interpreting and presenting the data for dose groups RC and RS as a unit. It could certainly be argued though that this interpretation might be the optimal, since it cannot be stated with confidence that the combination dose of CoQ_{10} and succinate would result in similar response profiles. Furthermore, the network structure and colour designation is an interpretation by the author, based on the collection of data and an attempt to summarise the data as a whole. True clarification of this issue would be attained only if rats were dosed with the combination as a Factor-2 regimen, a dose group not included in this study. Nonetheless, for the purpose of this discussion, data sets generated from dose groups RC and RS will be summarised in unity.

In addition to the data sets investigated in the study, further effects of the dose regimens were inferred or speculated, as indicated by the core nodes lacking outer layers. Since these effects were not directly investigated in the study, it was not possible to assign quantitative benefits or harmful effects to the respective parameters accurately. These nodes therefore represent hypothesised benefits or harmful effects, based on the literature and inferred from the data generated in the rat main study. The inferred nodes are in addition labelled with grey text and inter-connected in the network with solid and dashed grey lines for direct and indirect effects respectively. Finally, the impact of unforeseen effects on the data is represented by the orange line stretching across all levels of the data summary model.

The genomic level, represented by mtDNA and nDNA, was included to precede the respiratory chain level. The impact of genome expression in response to complex I inhibition, the high lipid content of the vehicle as well as CoQ_{10} and succinate, could not be excluded. Up-regulation of complex I subunits, mitochondrial replication machinery, antioxidant mechanisms and several more genetic factors are all expected to have a major impact on the biochemical response profiles and the remaining levels of evaluation, as depicted by the brown dashed arrow for mtDNA and nDNA. The respiratory chain, cellular and organ levels are representative of an overall view of rat response taking into account heart, brain, liver and skeletal muscle. In addition, these levels are designated with a tissue specificity marking, indicating that each tissue group contributed to the overall response profile in rats.

6.3.1 Respiratory chain

As with the study model presented in Figure 6.1, a flow of effects can be assigned from the so-called 'core' of the study, namely the respiratory chain level, to the outermost level of the organism. Complex I activity was indicated with a red core node and blue outer layer, indicating that the rotenone Factor-1 dose induced a Complex I deficiency, which was improved after receiving the Factor-2 regimens of CoQ_{10} and succinate. Since CoQ_{10} and succinate were not expected to improve the induced Complex I deficiency, these compounds were speculated to relieve overall biochemical stress factors and hence indirectly aid in the overall recovery of complex I activity. In addition to the CIA node, OXPHOS was also indicated in the respiratory level of the model. The OXPHOS node was coloured in red, indicative of a decrease in oxidative phosphorylation due to the inhibited activity of complex I.

6.3.2 Cellular level

On the cellular level, the five double-layered nodes represent data that was investigated in the study, whereas five additional nodes were assigned based on speculation and inference. Antioxidant capacity was improved in all tissue groups, which was argued to be due to the scavenging contributions and inherent antioxidant capacity of rotenone, a topic discussed in Chapter Five and in Section 6.5 of this chapter. In contrast, glutathione ratios appeared decreased overall and partly recovered by CoQ_{10} and succinate administration. The blue outer layer is justified by the fact that CoQ_{10} and succinate improved glutathione status in rat groups that received vehicle Factor-1 dose regimens, that is, in dose groups VC and VS. The L/P ratios in the different tissue groups were designated a grey node, indicating that these ratios were mostly unaffected by the dose regimens. The ATP/ADP ratios were also not determined to deviate by a notable degree. However, upon evaluation of ATP/ADP ratios in liver, it could be argued that the dose regimens certainly had an impact.

Since the rats were dosed orally, the liver is the first organ to be systemically exposed to the highest concentrations of the respective regimens. Furthermore, since the parent structure of rotenone has been reported to be toxic (Caboni *et al.*, 2004), and not the metabolites, the liver is particularly susceptible to its effects. Indeed, the sunflower oil vehicle was also demonstrated to contribute to the overall response profile. However, in the context of the remaining three tissue types, dose regimens were reported to affect

ATP/ADP ratios to a minimal extent, hence the grey outer layer for the ATP/ADP node indicated in this level.

The final measurement on a cellular level was that of the NAD/NADH ratios, which was also reported in a grey node signifying no deviation of the ratios from the environmental controls **NN**. The first inferred node that was included in this level of analysis was that of lipid content, which was directly linked to a lipid peroxidation node, induced by the high polyunsaturated fat contents of the sunflower oil vehicle. The blue node for lipid content indicates increased lipid levels in cellular and mitochondrial membranes, while the red node for lipid peroxidation is indicative of increased susceptibility induced by both the increased polyunsaturated contents as well as ROS concentrations incurred via the inhibition of the respiratory chain. The third speculative node, indicated in red, represents spindle interference of rotenone, which was in turn argued to influence growth in heart and liver organs directly, as discussed in the introduction paragraphs of this chapter. Finally, apoptotic events, indicated by a red node, induced by the inhibition of the respiratory chain were speculated to contribute to a decrease in organ weights.

6.3.3 Organ level

The organ level of the model is represented by organ weight data exclusively. The inner core of the organ weight node was indicated in red since it was apparent that rotenone resulted in decreased organ weights. As mentioned in the previous paragraph, the stunted growth reported for heart and liver organs was argued to result from the interaction of rotenone with mitotic spindle formation, as well as from the induced cell death. However, no protocols to investigate mitotic arrest and the activation of cell death were included in the study design. Therefore, it cannot be decisively concluded that these occurrences directly had an impact on organ weights. The outer layer of the organ weight node was coloured in blue, since heart and liver weights were reported to deviate only marginally from that of the environmental controls **NN**, indicating recuperation in organ growth. However, it was argued that the improved organ weights were primarily due to relief from the rotenone dose regimen. This in turn resulted in a relief of the acute effects of rotenone, and hence improved dietary intakes as well as overall body weight gain.

6.3.4 Blood and circulation

In the circulation level, six blood-related data sets were generated. Serum hydroperoxide concentrations were reported to have remained unchanged from the environmental controls NN when rats were dosed with rotenone. However, serum hydroperoxide data from the rat pilot study indicated that rotenone, in high concentrations of 12 and 15 $mg.kg^{-1}.day^{-1}$, might have contributed to the scavenging of hydroperoxides. This was based on the fact that hydroperoxide concentrations peaked when rats received 9 $mg.kg^{-1}.day^{-1}$ and decreased when 12 and 15 $mg.kg^{-1}.day^{-1}$ were dosed. Furthermore, the argument was strengthened when an antioxidant capacity equivalent to Trolox was determined for rotenone, as presented in Section 5.3.2.1. Therefore, even though the hydroperoxide node was represented with a grey core and outer layer, it should be noted that the lack of deviation in hydroperoxide concentrations was the result of rotenone scavenging and not because hydroperoxides were not being produced via the inhibition of complex I and electron leak. It is for this reason that a blue screen was superimposed over the hydroperoxide node, indicating that beneficial effects were indeed incurred by a rotenone dose regimen. In agreement with the previous argument, the serum antioxidant capacity consistently portrayed an improved status, which was therefore represented by a node with a blue inner core and blue outer layer. In contrast, blood glutathione ratios were consistently reported at lower levels amongst the rotenone treated rats, suggesting that the glutathione mechanism of ROS scavenging was depleted. This may also confirm indirectly that ROS was being formed and scavenged by GSH and other previously discussed mechanisms.

The L/P ratios in blood were reported as increased when rats were dosed with rotenone and hence affected adversely, as indicated by the red core for the L/P node. However, relief was certainly observed when both CoQ_{10} and succinate were administered. Overall, the effects of rotenone and the therapeutic compounds were not concluded to have a definitive effect on ATP/ADP ratios in blood. It is for this reason that a double-layered grey node is presented for this parameter. Blood NAD/NADH ratios appeared to be influenced by the complex I inhibition of rotenone, but improved slightly when the rats were relieved from the inhibitor and dosed with both CoQ_{10} and succinate. This is indicated by the red core and blue layered node for blood NAD/NADH ratios. As on the cellular level, the three inferential nodes for ROS formation, lipid content and lipid peroxidation are represented on the blood and circulation level. The known fact that ROS are able to escape cellular structures into the circulatory system (Iorio, 2002) is motivation

for the red coloured ROS node. This node is also influenced by the increased lipid content, indicated by a blue node, as well as the consequently increased levels of lipid peroxidation, indicated in red. As mentioned previously in this section, the latter two inferential parameters were incurred due to the high polyunsaturated fat contents of the sunflower oil vehicle.

Red nodes for spindle interference, cell death and blood glucose are also represented on the circulation level. As on the cellular level, rotenone is expected to interfere with spindle formation in blood cells. However, a dashed line was indicated to link with the body weight node on the organism level. The reason for the dashed line is that a solid line would be suggestive of a direct impact on body weight. When discussing data generated on the cellular level, it was argued that the spindle interference and apoptotic events directly affected organ weight. However, blood cells do not actively undergo cell division and, therefore, will not suffer from mitotic arrest as organs do. An increase in the number of apoptotic events are expected amongst blood cells though, as indicated by the red node. The red glucose node was indicated because the inhibition of the respiratory chain may well be associated with an interference in the activity of the PDH complex, which in turn will have an impact on pyruvate levels and hence blood glucose, as discussed in Section 6.4.

6.3.5 Rat organism

The final level of evaluation in this 'semi-reductionist' form of evaluation is that of the organism level. It was evident that rotenone treated rats consistently lost weight in a dose specific manner. Furthermore, the relief from rotenone treatment, in the majority of cases, resulted in an almost instantaneous improvement in weight gain. However, weight gain over the last two days of dosing could not be confirmed to improve when CoQ_{10} and succinate regimens were dosed, since the distribution of weight gain for dose groups RN and RV overlapped markedly with that of dose group RC and RS. In addition to the rat weight node, a rat behaviour inferential node was indicated. Rat behaviour protocols were not implemented in the study, but it was apparent that the rotenone dose regimens adversely affected rat behaviour, as discussed in Section 5.1.3. The final node in the network of response represents rat dietary intake, which is also indicated in red. As reported by Lapointe *et al.* (2004), a severe loss in stomach muscle mass was incurred in the presence of rotenone dosage. This in turn resulted in drastically lowered digestion and a compacted collection of food in the stomach of rats. Therefore, it was expected that

a lowered dietary intake would be experienced by this group. Since the effect of decreased food intake and digestion was only inferred, and postulated to have a direct influence on rat weight gain, this effect was indicated by a solid grey line linked to rat weight.

6.4 IMPLICATIONS OF THE STUDY DESIGN

Based on the data generated in the study, it is argued that several biochemical and study design aspects are to be addressed in the future. The impact that the serum hydroperoxide data, generated from the rat pilot study, had on the further exploration into the properties of rotenone was truly invaluable. It may well have been concluded from the rat main study that up-regulation of endogenous antioxidant mechanisms was the only protective factor in rats that limited hydroperoxide concentrations. However, the hydroperoxide data generated from the pilot study, as well as the determined antioxidant capacity of rotenone itself, presented in Sections 5.3.1.1 and 5.3.2.1 respectively, enforced a completely shifted viewpoint of the study. An increased expression of antioxidant mechanisms was still envisaged to be in effect in rats, but was supported by the scavenging properties of rotenone. Therefore, it can certainly be argued that it would be of great value to evaluate all the biochemical parameters in future experimentation. However, since the goal of the pilot study was solely to establish a complex I deficient animal model, the study design included the evaluation of rat body and organ weights, complex I activities and serum hydroperoxide levels.

Since the serum hydroperoxide concentrations peaked when rats received rotenone concentrations of 9 $mg.kg^{-1}.day^{-1}$, it would be valuable to follow the same study design, as for the rat main study, in rats receiving this concentration of rotenone. The higher concentrations of reactive metabolites produced when rats received 9 $mg.kg^{-1}.day^{-1}$ rotenone would have a greater impact on cellular and molecular integrity. However, it should be noted that if the 9 $mg.kg^{-1}.day^{-1}$ dose concentration is to be utilised in future experimentation, that decreased inhibition of complex I activities would be induced. It could therefore be argued that a threshold point of inducing a phenotype resembling that of an accurate Complex I deficiency was reached at the 9 $mg.kg^{-1}.day^{-1}$ rotenone dose concentration. Concentrations exceeding this resulted in increased complex I inhibition, but lowered hydroperoxide levels and hence deviation from the expected biochemical consequences to be associated with a Complex I deficiency. Nonetheless, the study

design required that the highest possible inhibition of complex I be attained, precluding the use of the 9 $mg.kg^{-1}.day^{-1}$ rotenone concentration dose group in the rat main study.

The rat main study was designed to include several control rat groups, which proved to be very valuable based on the previously unanticipated impact of sunflower oil as the vehicle. Upon researching the contents and reported effects of vegetable oils high in polyunsaturated fats, which included increased susceptibility to lipid peroxidation and oxidative stress amongst others, it became evident that an alternate vehicle might have been more beneficial. The ideal vehicle should have no effect on biochemical parameters investigated in a study, rendering data equivalent to that of the environmental control rat group. An oil-based vehicle was selected since rotenone is a lipophilic compound that is insoluble in water. It is for this reason that rotenone was dosed as a suspension in oil, thus requiring that an additional dose factor be monitored.

Fortunately, a robust experimental strategy was utilised to evaluate not only the consequences of treatment with rotenone and the therapeutic compounds CoQ_{10} and succinate, but also to enable a critical evaluation of the effects of sunflower oil. The unexpected impact of the vehicle resulted in the decision to utilise dose group NN, the environmental controls, as a reference dose group from which the deviation in median percentages was calculated. Currently, the most used vehicle for rotenone is composed of a dimethylsulphoxide (DMSO) and polyethylenglycol (PEG) solution (Flemming *et al.*, 2004; Sherer *et al.*, 2002). However, the fact that DMSO and PEG may influence hydrogen bonding as well as other aspects of biochemistry, it was decided that neither of these would have been a suitable vehicle for rotenone. Furthermore, investigations utilising these combinations make use of intraperitoneal, subcutaneous or systemic administration of rotenone. The use of osmotic mini-pumps (Betarbet *et al.*, 2000) that are positioned on the back of rats is certainly an option to consider for future investigations of this nature. The mini-pumps have the advantages of releasing dose volumes at a slow and steady rate into the blood circulation, as well as limiting physical contact with the rats. However, the fact that rotenone is susceptible to photo-degradation would require that the dose be administered at a daily rate exceeding no more than a couple of hours.

An additional aspect that is to be considered in the future is using improved technologies as well as the implementation of additional forms of day-to-day monitoring of the animal model. In order to generate as complete a profile as possible for each of the organs, it would be of value to include further biochemical parameters. However, as observed in

this study, there are limitations as to the amount of tissue available from a single organ. As discussed in Sections 5.4 and 5.4.6, the optimisation and determination of pyridine concentrations required large volumes of sample. It is for this reason that NAD/NADH ratios could not be determined successfully in heart muscle and brain tissue. Therefore, an alternative strategy would be to make use of analysis types that determine metabolite concentrations from smaller volumes of tissue preparations, such as gas or liquid chromatography. This would not only enable the successful and accurate assay of certain biochemical parameters, but also aid in the expansion of data that can be generated for a tissue profile. As indicated in Sections 5.3.5, 5.4.5, 5.6.4 and 5.7.6, adenylate ratios appeared to present with unexplained inconsistencies. Similarly, future studies should include an assay with improved sensitivity for the detection of ATP and ADP.

Concerning the inclusion of further day-to-day analysis strategies, the current study made use of daily rat weight recordings, which were regarded to be of great value to the study, as increased weight loss was demonstrated to correlate directly to the daily dose concentrations of rotenone. The additional analysis types to be considered would include behavioural or exercise related investigations or, alternatively, analysis of a metabolic parameter that could be measured from blood. With regards to the former, protocols measuring rodent muscle strength, balance, exploration capabilities and exercise tolerance in response to varying degrees of complex I inhibition would certainly be important to investigate in the future. The second option of analysing blood metabolites may be limited to the volume of blood that can be collected daily from a rat. However, since technologies have evolved to analyse several metabolic parameters from a single drop of blood, the scope for increased systemic-related analyses has broadened considerably. Since simplified analysis tools that can be utilised on site are readily available, such as rapid glucose and cholesterol meters, the option should certainly be considered.

It may well be of interest to investigate both glucose and cholesterol for particular reasons. Amongst the rotenone-treated rats, it could be speculated that increased glucose levels may be encountered since a deficiency of the respiratory chain is often associated with a deficiency of PDH, the enzymatic link between glycolysis and the Krebs cycle. Moreover, the PDH complex is also under investigation amongst diabetic research groups as it is considered to be of importance to glucose homeostasis (Patel and Korotchkina, 2003). Finally, since rats received sunflower oil based vehicle, it would make sense that lipid profiles were altered as the dosage period progressed. For further investigations into

metabolite profiles, in response to the dose regimens, a drop of blood could be collected at various stages of the dosage period and analysed via chromatographic instrumentation. Nonetheless, the study design ensured that a relevant number of biochemical parameters were investigated and profiled in various tissue types. An expansion of the study design to include larger groups of rats and increase the number of biochemical analyses to be performed would undoubtedly require that a larger team of scientists be actively involved in the dosing of rats, collection of tissue and assaying of specific markers.

6.5 ROTENONE AS A COMPLEX I INHIBITOR

To date, no mitochondrial complex I knockdown or knockout animal model has been reported. It is for this reason that the most widely accepted inhibitor of complex I, namely rotenone, was utilised to induce the deficiency. However, based on the serum hydroperoxide data and antioxidant capacity of rotenone, it was argued that rotenone is not an ideal inhibitor to be utilised in a study designed to investigate redox status and the bioenergetic consequences in an animal model. Over sixty inhibitors of complex I have been reported, encompassing both those of natural and synthetic origins (Degli Esposti, 1998). However, it is uncertain as to whether enough research into the overall biological consequences of these compounds have been investigated, excluding their characteristics as complex I inhibitors. The non-specific activity of rotenone as an antioxidant was a key factor in the study that should and will be taken into consideration for future projects that require the induction of an induced Complex I deficiency.

The exact mechanism by which rotenone may have scavenged reactive oxygen metabolites was not investigated in this study. The fact that rotenone is an isoflavanoid and hence polyphenolic in structure, may explain the antioxidant capacity of the compound. In general, polyphenols act as reducing agents, hydrogen donating antioxidants and singlet oxygen scavengers (Rice-Evans *et al.*, 1996), properties that depend largely on the presence of hydroxyl groups. However, as illustrated in Figure 2.7 of Chapter Two, the parent structure of rotenone harbours no hydroxyl groups. This does not exclude the compound as an antioxidant though, since clarity on the correlation between antioxidant capacity and chemical structure has not yet been fully elucidated (Rice-Evans *et al.*, 1996). Furthermore, the possibility that the metabolites of rotenone may harbour scavenging properties cannot be excluded.

Research of this kind should preferably be performed in a genetically modified animal model that has had one of the subunits of complex I knocked out or expressed at lower levels. This would enable a more definitive investigation into the therapeutic benefits of CoQ_{10} and succinate in the presence of a true Complex I deficiency. Furthermore, background interference from rotenone and a vehicle would not be a factor complicating data interpretation. However, an animal model of this kind does not exist at present. Alternatively, future directions for the investigation of Complex I deficiency, induced by compound administration, could include the use of compounds that are expected to harbour a greater potency and specificity for complex I. This would allow for the use of lower concentrations of the inhibitor and eliminate the additional consequences that may arise beyond the inhibition of complex I. The most potent complex I inhibitors to date include the acetogenins, in particular bullatacin (Miyoshi, 2005). Other compounds to be considered should also include rhein and diphenyleneiodonium, which inhibit complex I at the site of electron entry. The use of the former mentioned compounds would facilitate an understanding of the biochemical consequences of complex I deficiencies arising from alterations in the peripheral arm of this multi-subunit enzyme. Alternatively, RNA interference methodologies to prevent the expression of complex I subunits can be utilised. The advantage of this method is that it is based on a naturally occurring regulatory mechanism in mammalian cells. Furthermore, the protocol is increasingly being utilised in similar functional investigations and hence widely accepted as the technology of choice.

The data generated from this study are indicative of the fact that rotenone should not be used as a complex I inhibitor, particularly in an animal model. Since the metabolites of rotenone do not inhibit complex I (Caboni *et al.*, 2004), the compound may well be suitable for experimentation in cell cultures where activity of the cytochrome P450 enzymes is absent or minimal. Therefore, findings from this investigation highlight the need for novel strategies to develop an animal model that more accurately portrays the phenotype of a Complex I deficiency.

6.6 COENZYME Q10 AND SUCCINATE AS THERAPEUTIC AGENTS

Success in the field of mitochondrial therapeutics is still a subject under debate. Several therapy types have been explored, encompassing supplementation with vitamins and cofactors to pharmacological agents and gene therapy. However, the minority of reports

account for improvements, whilst the majority are representative of a lack of response. Gene therapy techniques have proved to be successful *in vitro*, but failed when performed in animal models. Instead, the trend has shifted to a more global approach of improving the 'management' of patients suffering from mitochondrial disorders. This approach further includes, amongst others, improved genetic counselling methods, exercise therapy, physiotherapy as well as surgical procedures to improve the day-to-day living of patients. It has become apparent over the years that a single treatment strategy is not sufficient (Schon and DiMauro, 2003) and that a combination of carefully selected regimens is to be implemented to manage a mitochondrial disorder to the best of the clinician's ability.

The study presented here investigated the beneficial effects of CoQ_{10} and succinate. The former compound was selected because it is a known antioxidant and electron carrier in the respiratory chain. The inclusion of succinate into the strategy was to circumvent complex I and improve electron flow via complex II. Furthermore, to the knowledge of the author, the only other report that investigated therapy via the use of succinate was that of Shoffner *et al.* (1989). The report described therapeutic relief in a patient suffering from ptosis, external opthalmoplegia, slowly progressing proximal muscle weakness and most notably respiratory insufficiency. The patient was admitted due to respiratory failure requiring mechanical ventilation. When relieved from the ventilator, a regimen of CoQ_{10} and succinate was administered which resulted in a rapid improvement in lung capacity over a short period of seven days. The patient remained at home for two months without respiratory complications until she stopped taking the prescribed regimen. This resulted in a recurrence of respiratory failure and admittance for mechanical ventilation. When CoQ_{10} and succinate were re-introduced, respiration recovered within four days, confirming the benefits of the regimen. This report proved to be pertinent in the decision to investigate CoQ_{10} and succinate as therapeutic compounds for the relief of rotenone-induced Complex I deficiency.

Data determined from the rat main study indicated more often than not that CoQ_{10} and succinate improved different biochemical aspects in both the presence and absence of Complex I deficiency. Therefore, it could not be stated that either of the regimens were more beneficial. Rather, the data was supportive of the current trends in treatment strategies for patients suffering from the mitochondrial cytopathies, where clinicians preferably prescribe a selection of vitamins and cofactors to improve various deficient biochemical aspects.

In future, it would be of interest to investigate the impact of various dose concentrations of CoQ_{10} and succinate as well as combination doses of the two compounds. If various dose concentrations of CoQ_{10} and succinate were to be investigated in a similar study design that was utilised for the rat pilot study, definitive threshold benefits could be determined in the various tissue groups. Moreover, a large number of dose combinations with varying concentrations of CoQ_{10} and succinate would assist in the determination of a preferred combination dose as well as in giving insight to the interactive effects that may exist between these compounds.

6.7 FUTURE DIRECTIONS IN MITOCHONDRIAL MEDICINE

There are no definitive therapeutic intervention strategies for the treatment of mitochondrial disorders. The fact that these cytopathies have a genetic origin further complicates matters. Relieving the symptoms manifested by deficiencies of the respiratory chain is all that can currently be done. A cure for genetic disorders is, as most researchers and clinicians know, still unattainable in the medical sciences. It is expected that the field of mitochondrial biology will continue to evolve and include more sophisticated technologies and methodologies. These will include and improve on metabolomic-based technologies, in-depth pathway analysis and data evaluation via interactive networks. The identification of the complete human mitochondrial proteome (Gibson, 2005) will certainly contribute to the understanding of mitochondrial dynamics in the years to come, between different tissue types as well as between unaffected and affected tissues. Furthermore, it will be vital that an integrative approach is adopted to ensure cross-validation and coherence of data generated via the newly developed technologies.

It is envisaged that, in the future, biomedical research will expand to include strategies and devices that would enable constant monitoring of biochemical and metabolic occurrences in an affected individual. This form of monitoring would encompass the capturing of 'real-time' data that reflects instantaneous differences, as subtle as they may be, and hence enabling the evaluation of specific response profiles over any period of time. The data generated from such a technology would aid in explaining, amongst other phenomena, the vast heterogeneity in expression of the mitochondrial cytopathies. Furthermore, in order to establish the most comprehensive and all-inclusive profile of response, it is envisioned that the future of biomedicine and diagnostic strategies would undertake an integrative

approach whereby the spectrum of 'omic' data is encapsulated. The aforementioned strategy would therefore consider data generated from genomic-related technologies to that of transcriptomics, and from proteomics to regulomics, in order to enable accurate inference of the phenotypic expression of a mitochondrial cytopathy, particularly in response to therapeutic intervention strategies. This systems biology approach would further aid in elucidating the link between specific architectural features of the genome and multigenic effects to the clinical phenotype (Lehner *et al.*, 2006). Clarifying the interactions between specific combinations of genotypic alterations would facilitate understanding the effects observed at various levels in an organism.

Future medical research should consider the role of mitochondria in all affected tissues and critically evaluate the contribution of this organelle in complex polygenic disorders such as diabetes, neurodegenerative disorders and cancer. The fact that mitochondria have a crucial role in two of the most vital, yet opposing biological mechanisms of life itself, namely cellular bioenergetics and apoptosis, adds credence to the argument that the organelle may have a hand in a far greater spectrum of disorders than previously hypothesised. It has therefore been postulated (Wallace, 2005) that the focus of medical science should not only shift towards evaluation of the role of mitochondria in complex disorders, but also towards the development of therapeutic interventions that take into consideration the vitality of this organelle, the mitochondrion.

CHAPTER SEVEN

REFERENCE LIST

Abe K., Fujimura H., Nishikawa Y., Yorifuji S., Mezaki T., Hirono N., Nishitani N. and Kameyama M. Marked reduction in CSF lactate and pyruvate levels after CoQ therapy in a patient with mitochondrial myopathy, encephalomyopathy, lactic acidosis and stroke-like episodes (MELAS). *Acta Neurologica Scandinavia*, **83**, 356-359, 1991.

Alberts B., Bray D., Johnson A., Lewis J., Raff M., Roberts K. and Walter P. Essential Cell Biology. An introduction to the molecular biology of the cell. Garland Publishing, Inc. New York & London, 1997.

Anderson S., Bankier A.T., Barrell B.G., de Bruijn M.H.L., Coulson A.R., Drouin J., Aperon I.C., Nierlich D.P., Roe B.A., Sanger F., Schreir P.H., Smith A.J.H., Staden R. and Young I.G. Sequence and organisation of the human mitochondrial genome. *Nature*, **290**, 457-465, 1981.

Andreu A.L., Tanji K., Bruno C., Hadjigeorgiou G.M., Sue C.M., Jay C., Ohnishi T., Shanske S., Bonilla E. and Di Mauro S. Exercise intolerance due to a nonsense mutation in the mtDNA ND4 gene. *Annals of Neurology*, **45**, 820-823, 1999.

Andrews R.M., Kubacka I., Chinnery P.F., Lightowlers R.N., Turnbull D.M. and Howell N. Reanalysis and revision of the Cambridge reference sequence for the human mitochondrial DNA. *Nature Genetics*, **23**,147,1999.

Antoshechkin I., Bogenhagen D.F. and Mastrangelo I.A. The HMG-box mitochondrial transcription factor xl-mtTFA binds DNA as a tetramer to activate bidirectional transcription. *EMBO Journal*, **16**, 3198-3206, 1997.

Arizmendi J.M., Skehel J.M., Runswick M.J., Fearnley I.M. and Walker J.E. Complemenntary DNA sequences of two 14.5 kDa subunits of NADH:ubiquinone oxidoreductase from bovine heart mitochondria. *FEBS Letters*, **313** (1), 80-84, 1992a.

Arizmendi J.M., Runswick M.J., Skehel J.M. and Walker J.E. NADH:ubiquinone oxidoreductase from bovine heart mitochondria. A fourth nuclear encoded subunit with a homologue encoded in chloroplast genomes. *FEBS Letters*, **301** (3), 237-242, 1992b.

Asensi M., Sastre J., Pallardo V., Lloret A., Lehner M., Asuncion J.G. and Vina J. Ratio of reduced to oxidised glutathione as an indicator of oxidative stress status and DNA damage. *Methods in Enzymology*, **299**, 267-277, 1999.

Barham S.S. and Brinkley B.R. Action of rotenone and related respiratory inhibitors on mammalian cell division, 1 cell kinetics and biochemical aspects. *Cytobios*, **15**, 85-96, 1976a.

Barham S.S. and Brinkley B.R. Action of rotenone and related respiratory inhibitors on mammalian cell division, 2 ultrastructural studies. *Cytobios*, **15**, 97-109, 1976b.

Bar-Meir M., Elpeleg O.N. and Saada A. Effects of various agents on adenosine triphosphate synthesis in mitochondrial complex I deficiency. *Journal of Paediatrics*, **139**, 868-870, 2001.

Batandier C., Picard A., Tessier N. and Lunardi J. Identification of a novel T398A mutation in the ND5 subunit of the mitochondrial complex I and of three novel mtDNA polymorphisms in two patients presenting ocular symptoms. *Human Mutation*, **16** (6), 532-538, 2000.

Batenburg J.J. and Olson M.S. Regulation of pyruvate dehydrogenase by fatty acid in isolated rat liver mitochondria. *The Journal of Biological Chemistry*, **251** (5), 1364-1370, 1976.

Belogrudov G. and Hatefi Y. Catalytic sector of complex I (NADH:ubiquinone oxidoreductase): subunit stoichiometry and substrate-induced conformation changes. *Biochemistry*, **33**, 4571-4576, 1994.

Bendehan D., Desneulle C., Vanuxem D., Confort-Gouny S., Figarella-Branger D., Pellisier J.F., Kozak-Ribbens G., Pouget J., Serratrice G. and Cozzone P.J. ^{31}P NMR spectroscopy and ergometer exercise test as evidence for muscle oxidative performance improvement with coenzyme Q in mitochondrial myopathies. *Neurology*, **42**, 1203-1208, 1992.

Benit P., Chretien D., Kadhom N., De Lonlay-Debeney P., Cormier-Daire V., Cabral A., Peudenier S., Rustin P., Munnich A. and Rotig A. Large scale deletions and point mutations of the nuclear *NDUFV1* and *NDUFS1* genes in mitochondrial complex I deficiency. *American Journal of Human Genetics*, **68**, 1344-1352, 2001.

Benit P., Beugnot R., Chretien D., Giurgea I., De Lonlay-Debeney P., Issartel J.P., Corral-Debrinski M., Kerscher S., Rustin P., Rotig A. and Munnich A. Mutant NDUFV2 subunit of mitochondrial complex I causes early onset hypertrophic cardiomyopathy and encephalopathy. *Human Mutation*, **21**, 582-586, 2003.

Benit P., Slama A., Cartault F., Giurgea I., Chretien D., Lebon S., Marsac C., Munnich A., Rötig A. and Rustin P. Mutant NDUFS3 subunit of mitochondrial complex I causes Leigh syndrome. *Journal of Medical Genetics*, **41**, 14-17, 2004.

Bergmeyer, H.U. Methods of Enzymatic Analysis, 3rd Edition. VCH publishers, Suite 909, 220 East 23rd street, New York, New York, USA, 1987.

Berkow R. The Merck Manual, Sixteenth Edition. Merck Research Laboratories, Rahway, New Jersey, United State of America, 1992.

Bernsen P.L., Gabreels F.J., Ruitenbeek W. and Hamburger H.L. Treatment of complex I deficiency with riboflavin. *Journal of Neurological Sciences*, **118** (2), 181-187, 1993.

Betarbet R., Sherer T.B., MacKenzie G., Garcia-Osuna M., Panov A.V. and Greenamyre J.T. Chronic systemic pesticide exposure reproduces features of Parkinson's disease. *Nature Neuroscience*, **3** (12), 1301-1306, 2000.

Bhattacharya K., Rahmanw S. and Leonard J. Diagnosis and management of mitochondrial respiratory chain disorders. *Current Paediatrics*, **13**, 536-542, 2003.

Blakely E.L., Mitchell A.L., Fisher N., Meunier B., Nijtmans L.G., Schaefer A.M., Jackson M.J., Turnbull D.M. and Taylor R.W. A mitochondrial cytochrome b mutation causing severe respiratory chain enzyme deficiency in humans and yeast. *FEBS Journal*, **272** (14), 3583-3592, 2005.

Blumenthal D.T., Shanske S., Schochet S.S., Santorelli F.M., DiMauro S., Jaynesm M. and Bodensteiner J. Myoclonus epilepsy with ragged red fibers and multiple mtDNA deletions. *Neurology*, **50** (2), 524-525, 1998.

Bogaards J.J.P., Bertrand M., Jackson P., Oudshoorn M.J., Weavers R.J., Van Bladeren P.J. and Walther B. Determing the best animal model for human cytochrome P450 activities: a comparison of mouse, rat, rabbit, dog, micropig, monkey and man. *Xenobiotica*, **30** (12), 1131-1152, 2000.

Bogenhagen D.F., Applegate E.F. and Yoza B.K. Identification of a promoter for transcription of the heavy strand of human mtDNA: in vitro transcription and deletion mutagenesis. *Cell*, **36** (4), 1105-13, 1984.

Bolden A., Noy G.P. and Weissbach A. DNA polymerase of mitochondria is a gamma-polymerase. *Journal of Biological Chemistry*, **252** (10), 3351-3356, 1977.

Brandt U., Kerscher S., Drose S., Zwicker K. and Zickermann V. Proton pumping by NADH:ubiquinone oxidoreductase. A redox driven conformational change mechanism? *FEBS Letters*, **545**, 9-17, 2003.

Brand M.D., Affourtit C., Esteves T.C., Green K., Lamber A.J., Miwa S., Pakay J.L. and Parker N. Mitochondrial superoxide production, biological effects, and activation of uncoupling proteins. *Free Radical Biology & Medicine*, **37** (6), 755-767, 2004.

Bresolin N., Bet L., Binda A., Moggio M., Comi G., Nador F., Ferrante C., Carenzi A. and Scarlato G. Clinical and biochemical correlations in mitochondrial myopathies treated with coenzyme Q_{10}. *Neurology*, **38**, 892-899, 1990.

Brown M.D., Voljavec A.S., Lott M.T., Torroni A., Yang C-C. and Wallace D.C. Mitochondrial DNA complex I and III mutations associated with Leber's hereditary optic neuropathy. *Genetics*, **130**, 163-173, 1992.

Brown M.D., Torroni A., Reckford C.L. and Wallace D.C. Phylogenetic analysis of Leber's Hereditary Optic Neuropathy mitochondrial DNA's indicates multiple independent occurrences of the common mutations. *Human Mutation*, **6**, 311-325, 1995.

Brown M.D., Zhadanov S., Allen J.C., Hosseini S., Newman N.J., Atomanov V.V., Mikhailovskaya I.E., Sukernik R.I and Wallace D.C. Novel mtDNA mutations and oxidative phosphorylation dysfunction in Russian LHON families. *Human Genetics*, **109**, 33-39, 2001.

Budde S.M.S., Van den Heuvel L.P.W.J., Janssen A.J., Smeets R.J.P., Buskens C.A.F., DeMeirleir L., Van Coster R., Baethmann M., Voit T., Trijbels J.M.F and Smeitink J.A.M. Combined enzymatic complex I and III deficiency associated with mutations in *NDUFS4* gene. *Biochemical and Biophysical Research Communications*, **275**, 63-68, 2000.

Caboni P., Sherer T.B., Zhang N., Taylor G., Na H.M., Greenamyre T. and Casida J.E. Rotenone, deguelin, their metabolites and the rat model of Parkinson's disease. *Chemical Research in Toxicology*, **17**, 1540-1548, 2004.

Calabrese V., Lodi R., Tonon C., D'Agata V., Sapienza M., Scapagnini G., Mangiameli A., Pennisi G., Stella A.M., Butterfield D.A. Oxidative stress, mitochondrial dysfunction and cellular stress response in Friedreich's ataxia. *Journal of the Neurological Sciences*, **233**, 145-162, 2005.

Campbell M.K. Biochemistry, 2nd Edition. Saunders College Publishing, New York, New York, USA, 1995.

Campos Y., Martin M.A., Rubio J.C., Gutierrez del Olmo M.C., Cabello A. and Arenas J. Bilateral striatal necrosis and MELAS associated with a new T3308C mutation in the mitochondrial ND1 gene. *Biochemical and Biophysical Research Communications,* **238**, 323-325, 1997.

Carroll J., Shannon R. J., Fearnley I. M., Walker J. E. and Hirst J. Definition of the nuclear encoded protein composition of bovine heart mitochondrial complex I Identification of two new subunits. *Journal of Biological Chemistry*, **277**, 50311-50317, 2002.

Carroll J., Fearnley I.M., Shannon R.J., Hirst J. and Walker J.E. Analysis of the subunit composition of complex I from bovine heart mitochondria. *Molecular and Cellular Proteomics*, **2.2**, 117-126, 2003.

Chang D.D. and Clayton D.A. Precise identification of the individual promoters for transcription of each strand of human mitochondrial DNA. *Cell*, **36**, 635-643, 1984.

Chauvin C., De Oliveira F., Ronot X., Mousseau M., Leverve X. and Fontaine E. Rotenone inhibits the mitochondrial permeability transition-induced cell death in U937 and KB cells. *The Journal of Biological Chemistry*, **276** (44), 41394-41398, 2001.

Chen Y.S. and Beattie D.S. Two forms of cytochrome b in yeast mitochondria: purification, characterization, and localization in the inner mitochondrial membrane. *Biochemistry*, **20**, 7557-7565, 1981.

Chinnery P.F. and Turnbull D.M. Epidemiology and treatment of mitochondrial disorders. *American Journal of Medical Genetics (Seminars in Medical Genetics)*, **106**, 94-101, 2001.

Chinnery P.F., Brown D.T., Andrews R.M., Singh-Kler R., Riordan-Eva P., Lindley J., Applegarth D.A., Turnbull D.M. and Howell N. The mitochondrial ND6 gene is a hot spot for mutations that cause Leber's hereditary optic neuropathy. *Brain*, **124** (1), 209-218, 2001.

Chinnery P. New approaches to the treatment of mitochondrial disorders. *Reproduction BioMedicine*, **8** (1), 16-23, 2003.

Chomyn A. and Lai S.S. cDNA of the 24 kDa subunit of the bovine respiratory chain NADH dehydrogenase: high sequence conservation in mammals and tissue-specific and growth-dependent expression. *Current Genetics*, **16** (2), 117-126, 1989.

Chung H., Hong D-P., Jung J-Y., Kim H-J., Jang K-S., Sheen Y-Y., Ahn J-I., Li Y-S. and Kong G. Comprehensive analysis of differential gene expression profiles on carbon tetrachloride-induced rat liver injury and regeneration. *Toxicology and Applied Pharmacology*, **206**, 27– 42, 2005.

Clayton D.A. Nuclear gadgets in mitochondrial DNA replication and transcription. *Trends in Biochemical Sciences*, **16** (3), 107-111, 1991.

Corona P., Antozzi C., Carrara F., Díncerti L., Lamantea E., Tiranti V. and Zeviani M. A novel mtDNA mutation in the ND5 subunit of complex I in two MELAS patients. *Annals in Neurology*, **49** (1), 106-110, 2001.

Cortelli P., Montagna P., Pierangeli G., Lodi R., Barboni P., Liguori R., Carelli V., Iotti S., Zaniol P., Lugaresi E. and Barbiroli B. Clinical and brain bioenergetics improvement with idebenone in a patient with Leber's hereditary optic neuropathy: a clinical and 31P-MRS study. *Journal of Neurological Sciences*, **148** (1), 25-31, 1997.

Crimi M., Galbiati S., Moroni I., Bordoni A., Perini M.P., Lamantea E., Sciacco M., Zeviani M., Biummo I., Moggio M., Scarlato M. and Comi G.P. A missense mutation in the mitochondrial ND5 gene associated with a Leigh-MELAS overlap syndrome. *Neurology*, **60** (11), 1857-1861, 2003.

Cunningham M.L., Soliman M.S., Mostafa Z.B. and Matthews H.B. Rotenone, an anticarcinogen, inhibits cellular proliferation but not peroxisome proliferation in mouse liver. *Cancer Letters*, **95**, 93-97, 1995.

Cury-Boaventura M.F., Gorjão R., De Lima T.M., Newsholme P. and Curi R. Comparative toxicity of oleic and linoleic acid on human lymphocytes. *Life Sciences*, **78**, 1448-1456, 2005.

Davey G.P., Peuchen S. and Clark J.B. Energy thresholds in Brain mitochondria. *The Journal of Biological Chemistry*, **273** (21), 12753-12757, 1998.

Degli Esposti M., Ngo A., McMullen G.L., Ghelli A., Sparla F., Benelli B., Ratta M. and Linnane A.W. The specificity of mitochondrial complex I for ubiquinones. *Biochemical Journal*, **313**, 327-334, 1996.

Degli Esposti M. Inhibitors of NADH-ubiquinone reductase: an overview. *Biochimica et Biophysica Acta*, **1364**, 222-235, 1998.

De Vries D.D., Went L.N., Bruyn G.W., Scholte H.R., Hofstra R.M.W., Bolhuis P.A. and Van Oost B.A. Genetic and biochemical impairment of mitochondrial complex I activity of a family with Leber hereditary optic neuropathy and hereditary spastic dystonia. *American Journal of Human Genetics*, **58**, 703-711, 1996.

De Lonlay P., Valnot I., Barrientos A., Gorbatyuk M., Tzagoloff A., Taanman J., Benayoun E., Chrétien D., Kadhom N., Lombès A., De Baulny H.O., Munnich A., Rustin P. and Rötig A. A mutant mitochondrial respiratory chain assembly protein causes complex III deficiency in patients with tubulopathy, encephalopathy and liver failure. *Nature Genetics*, **29**, 57-60, 2001.

Deng P.S., Hatefi Y. and Chen S. N-arylazido-beta-alanyl-NAD+, a new NAD+ photoaffinity analogue. Synthesis and labeling of mitochondrial NADH dehydrogenase. *Biochemistry*, **29** (4), 1094-1098, 1990.

Diaz-Corrales F.J., Asanuma M., Miyazaki I., Miyoshi K. and Ogawa N. Rotenone induces aggregation of γ-tubulin protein and subsequent disorganization of the centrosome: relevance to formation of inclusion bodies and neurodegeneration. *Neuroscience*, **133**, 117-135, 2005.

DiMauro S. and Schon E.A. Mitochondrial DNA mutations in human disease. *American Journal of Medical Genetics*, **106**, 18-26, 2001.

DiMauro S., Andreu A.L., Musumeci O. and Bonilla E. Diseases of oxidative phosphorylation due to mtDNA mutations. *Seminars in Neurology*, **21** (3), 251-60, 2001.

DiMauro S. Mitochondrial diseases. *Biochimica et Biophysica Acta*, **1658,** 80-88, 2004a.

DiMauro S. Mitochondrial medicine. *Biochimica et Biophysica Acta*, **1659,** 107-114, 2004b.

Djafarzadeh R., Kerscher S., Zwicker K., Radermacher M., Lindahl M., Schagger H. and Brandt U. Biophysical and structural characterization of proton-translocating NADH-dehydrogenase (complex I) from the strictly aerobic yeast *Yarrowia lipolytica*. *Biochimica et Biophysica Acta*, **1459**, 230-238, 2000.

Dupuis A., Skehel J.M. and Walker J.E. NADH:ubiquinone oxidoreductase from bovine mitochondria. cDNA sequence of a 19 kDa cysteine-rich subunit. *Biochemical Journal*, **277** (1), 11-15, 1991a.

Dupuis A., Skehel J.M. and Walker J.E. A homologue of a nuclear-coded iron-sulfur protein subunit of bovine mitochondrial complex I is encoded in chloroplast genomes. *Biochemistry*, **30** (11), 2954-2960, 1991b.

Earley F.G.P., Patel S.D., Ragan C.I. and Attardi G. Photolabelling of a mitochondrially encoded subunit of NADH dehydrogenase with [^{3}H]dihydrorotenone. *FEBS Letters*, **219**, 108-113, 1987.

Ellis S.M. and Steyn H.S. Practical significance (effect sizes) versus or in combination with statistical significance (p-values). *Management Dynamics*, **12** (4), 51-53, 2003.

Fadic R. and Johns D.R. Clinical spectrum of mitochondrial diseases. *Seminars in Neurology*, **16** (1), 11-20, 1996.

Fauser S., Luberichs J., Besch D. and Leo-Kottler B. Sequence analysis of the complete mitochondrial genome in patients with Leber's hereditary optic neuropathy lacking the three most common pathogenic DNA mutations. *Biochemical and Biophysical Research Communications*, **295** (2), 342-347, 2002.

Fearnley I.M., Runswick M.J. and Walker J.E. A homologue of the nuclear coded 49 kD subunit of bovine mitochondrial NADH-ubiquinone reductase is coded in chloroplast DNA. *EMBO Journal*, **8** (3), 665-672, 1989.

Fearnley I.M., Finel M., Skehel J.M. and Walker J.E. NADH:ubiquinone oxidoreductase from bovine heart mitochondria. cDNA sequences of the import precursors of the nuclear-encoded 39 kDa and 42 kDa subunits. *Biochemical Journal*, **278** (3), 821-829, 1991.

Fearnley I.M., Carroll J., Shannon R.J., Runswick M.J. and Walker J.E. GRIM-19, a cell death regulator gene product, is a subunit of bovine mitochondrial NADH:ubiquinone oxidoreductase (complex I). *The Journal of Biological Chemistry*, **276** (42), 38345-38348, 2001.

Fernandez-Vizarra E., Lopez-Perez M.J. and Enriquez J.A. Isolation of biogenetically competent mitochondria from mammalian tissues and cultured cells. *Methods*, **26**, 292–297, 2002.

Finel M., Skehel J.M., Albracht S.P.J., Fearnley I.M. and Walker J.E. Resolution of NADH:ubiquinone oxidoreductase from bovine heart mitochondria into two subcomplexes, one of which contains the redox centres of the enzyme. *Biochemistry*, **31**, 11425-11434, 1992.

Finel M., Majander A.S., Tyynelä J., De Jong A.M.P., Albracht S.P.J. and Wikström M. Isolation and characterisation of subcomplexes of the mitochondrial NADH:oxidoreductase (complex I). *European Journal of Biochemistry*, **226**, 237-242, 1994.

Flemming S.M., Zhu C., Fernagat P-O., Mehta A., DiCarlo C.D., Seaman R.L. and Chesselet M-F. Behavioral and immunohistochemical effects of chronic intravenous and subcutaneous infusions of varying doses of rotenone. *Experimental Neurology*, **187**, 418– 429, 2004.

Frei B., Stocker R. and Ames B.N. Antioxidant defenses and lipid peroxidation in human blood plasma. *Proceedings of the National Academy of Sciences of the United States of America*, **85**, 9748-9752, 1988.

Friedrich T., Abelmann A., Brors B., Guénebaut V., Kintscher L., Leonard K., Rasmussen T., Scheide D., Schlitt A., Schulte U. and Weiss H. Redox components and structure of the respiratory NADH:ubiquinone oxidoreductase (complex I). *Biochimica et Biophysica Acta*, **1365**, 215-219, 1998.

Gellerich F.N., Mayr J.A., Reuter S., Sperl W. and Zierz S. The problem of interlab variation in methods for mitochondrial disease diagnosis: enzymatic measurement of respiratory chain complexes. *Mitochondrion*, **4**, 427-439, 2004.

Gibson B.W. The human mitochondrial proteome: oxidative stress, protein modifications and oxidative phosphorylation. *The International Journal of Biochemistry & Cell Biology*, **37**, 927–934, 2005.

Gills L. and Kaye E. Diagnosis and management of mitochondrial diseases. *Paediatric gastroenterology and nutrition*, **49** (1), 219, 2002

Gold R., Siebel P., Reinelt G., Schindler R., Landwehr P., Beck A. and Reichmann H. Phosphorous magnetic resonance spectroscopy in the evaluation of mitochondrial myopathies: results of a 6-month therapy study with coenzyme Q. *European Neurology*, **36**, 191-196, 1996.

Graff C., Bui T-H. and Larsson N-G. Mitochondrial diseases. *Best Practice and Research Clinical Obstetrics and Gynaecology*, **16** (5), 715-728, 2002.

Graham B.H, Waymire K.G., Cottrell B., Trounce I.A., MacGregor G.R. and Wallace D.C. A mouse model for mitochondrial myopathy and cardiomyopathy resulting from a deficiency in the heart/muscle isoform of the adenine nucleotide translocator. *Nature Genetics*, **16**, 226-234, 1997.

Grigorieff N. Three-dimensional structure of bovine NADH:Ubiquinone oxidoreductase (Complex I) at 22 Å in ice. *Journal of Biological Chemistry*, **277**, 1033-1046, 1998.

Grivennikova V.G., Maklashin E.O., Gavrikova E.V. and Vinogradov A.D. Interaction of the mitochondrial NADH-ubiquinone reductase with rotenone as related to the enzyme active/inactive transition. *Biochimica et Biophysica Acta*, **1319**, 223-232, 1997.

Guenebaut V., Schlitt A., Weiss H., Leonard K. and Friedrich T. Consistent structure between bacterial and mitochondrial NADH:ubiquinone oxidoreductase (complex I). *Journal of Molecular Biology*, **276** (1), 105-112, 1998.

Guengerich F.P. Comparisons of catalytic selectivity of cytochrome P450 subfamily enzymes from different species. *Chemico-Biological Interactions*, **106**, 161-181, 1997.

Gutteridge J.M.C. Lipid Peroxidation and Antioxidants as Biomarkers of Tissue Damage. *Clinical Chemistry*, **41** (12), 1819-1828, 1995.

Henderson R.F. Species differences in the metabolism of benzene. *Environmental Health Perspectives*, **104** (6), 1173-1175, 1996.

Hirano M., Blake D.M., Lombes A., Minetti C., Bonilla E., Hays A.P., Lovelace R.E., Butler I., Bertorini T.E., Threlkeld A.B., Mitsumoto H., Salberg L.M., Rowland L.P. and DiMauro S. Mitochondrial neurogastrointestinal encephalomyopathy (MNGIE): Clinical, biochemical, and genetic features of an autosomal recessive mitochondrial disorder. *Neurology*, **44**, 721-727, 1994.

Hixson J.E. and Clayton D.A. Initiation of transcription from each of the two human mitochondrial promoters requires unique nucleotides at the transcriptional start sites. *Proceedings of the National Academy of Sciences of the United States of America*, **82** (9), 2660-2664, 1985.

Holt I.J., Harding A.E. and Morgan-Hughes J.A. Deletions of muscle mitochondrial DNA in patients with mitochondrial myopathies. *Nature*, **331**, 717-719, 1998.

Horvath J., Horvath R., Karcagi V., Komoly S. and Johns D.R. Sequence analysis of Hungarian LHON patients not carrying the common primary mutations. *Journal of Inherited Metabolic Disorders*, **25** (4), 323-324, 2002.

Howell N., Blindoff L.A., McCullough D.A., Kubacka I. and Poulton J. Leber hereditary optic neuropathy: identification of the same mitochondrial ND1 mutation in six pedigrees. *American Journal of Human Genetics*, **49**, 939-950, 1991.

Howell N., Halvorson S., Burns J., McCullough D.A. and Paulton J. When does bilateral optic atrophy become Leber hereditary optic neuropathy? *Americal Journal of Human Genetics*, **53** (4), 959-963, 1993.

Howell N., Bogolin C., Jamieson R., Marenda D.R. and Mackey D.A. mtDNA mutations that cause optic neuropathy: How do we know? *American Journal of Human Genetics*, **62**, 196-202, 1998.

Howell N., Oostra R., Bolhuis P.A., Spruijt L., Clarke L.A., Mackey D.A., Preston G. and Herrnstadt C. Sequence analysis of the mitochondrial genomes from Dutch pedigrees with Leber hereditary optic neuropathy. *American Journal of Human Genetics*, **72**, 1460-1469, 2003.

Huoponen K., Vilkki J., Aula P., Nikoskelainen E.K. and Savontaus M-L. A new mtDNA mutation associated with Leber hereditary optic neuropathy. *American Journal of Human Genetics*, **48**, 1147-1153, 1991.

Ihara Y., Namba R., Kuroda S., Sato T. and Shirabe T. Mitochondrial encephalomyopathy (MELAS): pathological study and successful therapy with coenzyme Q10 and idebenone. *Journal of Neurological Sciences*, **90** (3), 263-271, 1989.

Inoue K., Nakada K., Ogura A., Isobe K., Goto Y.I., Nonaka I. and Hayashi J.I. Generation of mice with mitochondrial dysfunction by introducing mouse mtDNA carrying a deletion into zygotes. *Nature Genetics*, **26**, 176-181, 2000.

Iorio E.L. d-ROMs test and oxidative stress assessment. Diacron international, Grosseto, Italy, 2002.

Janssens D., Michiels C., Delaive E., Eliaers F., Drieu K. and Remacle J. Protection of hypoxia-induced ATP decrease in endothelial cells by *Ginkgo Biloba* extract and bilobalide. *Biochemical Pharmacology*, **50**, 991-999, 1995.

Janssens D., Remacle J., Drieu K. and Michiels C. Protection of mitochondrial respiration activity by bilobalide. *Biochemical Pharmacology*, **58**, 109-119, 1999.

Ježek P. and Hlavatá L. Mitochondria in homeostasis of reactive oxygen species in cell, tissues and organism. *The International Biochemistry and Cell Biology*, **37**, 2478-2503, 2005.

Johns D.R. and Berman J. Alternative, simultaneous complex I mitochondrial DNA mutations in Leber's hereditary optic neuropathy. *Biochemical and Biophysical Research Communications*, **174** (3), 1324-1330, 1991.

Johns D.R., Neufield M.J. and Park R.D. An ND-6 mitochondrial DNA mutation associated with Leber Hereditary Optic Neuropathy. *Biochemical and Biophysical Research Communications*, **187**, 1551-1557, 1992.

Jun A.S., Brown M.D. and Wallace D.C. A mitochondrial DNA mutation at nucleotide pair 14459 of the NADH dehydrogenase subunit 6 gene associated with maternally inherited Leber hereditary optic neuropathy and dystonia. *Proceedings of the National Academy of Science of the United States of America*, **91** (13), 6206-6210, 1994.

Kasahara A., Ishikawa K., Yamaoka M., Ito M., Watanabe N., Akimoto M., Sato A., Nakada K., Endo H., Suda Y., Aizawa S. and Hayashi J.I. Generation of trans-mitochondrial mice carrying homoplasmic mtDNAs with a missense mutation in a structural gene using ES cells. *Human Molecular Genetics*, **15**, 871-881, 2006.

Kasamatsu H. and Vinograd J. Replication of circular DNA in eukaryotic cells. *Annual Reviews in Biochemistry*, **43**, 695-719, 1974.

Kerscher S., Dröse S., Zwicker K., Zickermann V. and Brandt U. Yarrowia lipolytica, a yeast genetic system to study mitochondrial complex I. *Biochimica et Biophysica Acta*, **1555**, 83-91, 2002.

Kim J.Y., Hwang J.M. and Park S.S. Mitochondrial DNA C4171A/ND1 is a novel primary causative mutation of Leber's hereditary optic neuropathy with a good prognosis. *Annals of Neurology*, **51** (5), 630-634, 2002.

Kirby D.M., Salemi R., Sugiana C., Ohtake A., Parry L., Bell K.M., Kirk E.P., Boneh A., Taylor R.W., Dahl H.M., Ryan M.T. and Thorburn D.R. NDUFS6 mutations are a novel cause of lethal neonatal mitochondrial complex I deficiency. *The Journal of Clinical Investigation*, **14** (6), 837-845, 2004.

Kirkinezos I.G. and Moraes C.T. Reactive oxygen species and mitochondrial diseases. *Cell & Developmental Biology*, **12**, 449-457, 2001.

Komaki H., Akanuma J., Iwata H., Takahashi T., Mashima Y., Nonaka I. and Goto Y. A novel mtDNA C11777A mutation in Leigh syndrome. *Mitochondrion*, **2**, 293-304, 2003.

Koopman W.J.H., Verkaart S., Visch H., Van der Westhuizen F., Murphy M.P., Van den Heuvel L.W.P.J., Smeitink J.A.M. and Willems P.H.G.M. Inhibition of complex I of the electron transport chain causes $O_2^{\cdot}$ mediated mitochondrial outgrowth. *American Journal of Physiology - Cell Physiology*, **288**, 1440-1450, 2005.

Kosel S., Grasbon-Frodl E.M., Mautsch U., Egensperger R., Von Eitzen U., Frishman D., Hofmann S., Gerbitz K.D., Mehraein P. and Graeber M.B. Novel mutations of mitochondrial complex I in pathologically proven Parkinson disease. *Neurogenetics*, **1** (3), 197-204, 1998.

Krebs W., Steuber J., Gemperli A.C. and Dimroth P. Na^+ translocation by the NADH:ubiquinone oxidoreductase (complex I) from *Klebsiella pneumoniae*. *Molecular Microbiology*, **33**, 590-598, 1999.

Krishnamoorthy G. and Hinkle P.C. Studies on the electron transfer pathway, topography of iron-sulfur centers, and site of coupling in NADH-Q oxidoreductase. *The Journal of Biological Chemistry*, **263** (33), 17566-17575, 1998.

Lapointe N., St-Hilaire M., Martinoli M-G., Blanchet J., Gould P., Rouillard C. and Cicchetti F. Rotenone induces non-specific central nervous system and systemic toxicity. *The FASEB Journal*, **18**, 717-719, 2004.

Lebon S., Chol M., Benit P., Mugnier C., Chretien D., Giurgea I., Kern I., Girardin E., Hertz-Pannier L., De Lonlay P., Rötig A., Rustin P. and Munnich A. Recurrent *de novo* mitochondrial DNA mutations in respiratory chain deficiency. *Journal of Medical Genetics*, **40**, 896-899, 2003.

Lebovitz R.M., Zhang H., Vogel H., Cartwright J., Dionne L., Lu N., Huang S. and Matzuk M.M. Neurodegeneration, myocardial injury, and perinatal death in mitochondrial superoxide dismutase-deficient mice. *Proceedings of the National Academy of Sciences of the United States of America*, **93** (18), 9782-9787, 1996.

Lehner B., Crombie C., Tischler J., Fortunato A. and Fraser A.G. Sytematic mapping of genetic interactions in *Caenorhabditis elegans* identifies common modifiers of diverse signalling pathways. *Nature Genetics*, **38** (8), 896-903, 2006.

Leif H., Sled V.D., Ohnishi T., Weiss H. and Friedrich T. Isolation and characterization of the proton-translocating NADH: ubiquinone oxidoreductase from Escherichia coli. *European Journal of Biochemistry*, **230** (2), 538-548, 1995.

Leo-Kotler B., Christ-Adler M., Baumann B., Zrenner E. and Wissinger B. Leber's hereditary optic neuropathy: Clinical and molecular genetic results obtained in a family with a new point mutation at nucleotide position 14498 in the ND 6 gene. *German Journal of Ophthalmology*, **5** (4), 233-240, 1996.

Leonard J.V. and Schapira A.H.V. Mitochondrial respiratory chain disorders I: mitochondrial DNA defects. *The Lancet*, **355**, 299-306, 2000.

Lertrit P., Noer A.S., Jean-Francois M.J., Kapsa R., Dennett X., Thyagarajan D., Lethlean K., Byrne E. and Marzuki S. A new disease-related mutation for mitochondrial encephalopathy lactic acidosis and strokelike episodes (MELAS) syndrome affects the ND4 subunit of the respiratory complex I. *American Journal of Human Genetics*, **51** (3), 457-468, 1992.

Li Y., Huang T.T, Carlson E.J., Melov S., Ursell P.C., Olsen J.L., Noble L.J., Yoshimura M.P., Berger C., Chan P.H., Wallace D.C. and Epstein C.J. Dilated cardiomyopathy and neonatal lethality in mutant mice lacking manganese superoxide dismutase. *Nature Genetics*, **11**, 376-381, 1995.

Liolitsa D., Rahman S., Benton S., Carr L.J. and Hanna M.G. Is the mitochondrial complex I ND5 gene a hot-spot for MELAS causing mutations? Annals of Neurology, **53** (1), 128-132, 2003.

Loeffen J., Smeitink A., Triepels R., Smeets R., Schuelke M., Sengers R., Trijbels F., Hamel B., Mullaart R. and Van den Heuvel L. The first nuclear-encoded complex I mutation in a patient with Leigh syndrome. *American Journal of Human Genetics*, **63**, 1598-1608, 1998.

Loeffen J.L., Smeitink J.A., Trijbels J.M., Janssen A.J., Triepels R.H., Sengers R.C. and Van den Heuvel L.P. Isolated complex I deficiency in children: clinical, biochemical and genetic aspects. *Human Mutation*, **15** (2), 123-134, 2000.

Loeffen J., Elpeleg O., Smeitink J., Smeets R., Stockler-Ipsiroglu S., Mandel H., Sengers R., Trijbels F.and Van den Heuvel L. Mutations in complex I *NDUFS2* gene of patients with cardiomyopathy and encephalomyopathy. *Annals of Neurology*, **49**, 195-201, 2001.

Luft R., Ikkos D., Palmieri G., Ernster L. and Afzelius B. A case of severe hypermetabolism of nonthyroid origin with a defect in the maintenance of mitochondrial respiratory control: a correlated clinical, biochemical, and morphological study. *Journal of Clinical Investigation*, **41** (9), 1776-1804, 1962.

Luft R. The development of mitochondrial medicine. *Proceedings of the National Academy of Sciences of the United States of America*, **91**, 8731-8738, 1994.

Lust W.D., Feussner G.K., Barbehenn E.K. and Passonneau J.V. The enzymatic measurement of adenine nucleotides and p-creatine in picomole amounts. *Analytical Biochemistry*, **110**, 258-266, 1981.

Madsen C.S., Ghivizzani S.C. and Hauswirth W.W. Protein binding to a single termination-associated sequence in the mitochondrial DNA D-loop region. *Molecular and Cellular biology*, **13** (4), 2162-2171, 1993.

Majander A., Huoponen K., Savontaus M-L., Nikoskelainen E. and Wikström M. Electron transfer properties of NADH:ubiquinone oxidoreductase in the ND1/3460 and the ND4/11778 mutations of the Leber hereditary optic neuropathy (LHON). *FEBS Letters*, **292**, 289-292, 1991.

Mashima Y., Hiida Y. and Oguchi Y. Remission of Leber's hereditary optic neuropathy with idebenone. *Lancet*, **340** (8815), 368-369, 1992.

Martin M.A., Blazquez A., Gutierrez-Solana L.G., Fernandez-Moreira D., Briones P., Andreu A.L., Garesse R., Campos Y. and Arenas J. Leigh syndrome associated with mitochondrial Complex I deficiency due to a novel mutation in the NDUFS1 gene. *Archives of Neurology*, **62** (4), 659-661, 2005.

Mataix J., Quiles J.L., Huertas J.S.R., Battino M. and Manas M. Tissue specific interactions of exercise, dietary fatty acids, and vitamin E in lipid peroxidation. *Free Radical Biology & Medicine*, **24** (4), 511-521, 1998.

Matsumoto M., Haysaka S., Kadoi C., Hotta Y., Fujiki K., Fujimaki T., Takeda M., Ishida N., Endo S. and Kanai A. Secondary mutations of mitochondrial DNA in Japanese patients with Leber's hereditary optic neuropathy. *Ophthalmic Genetics*, **20** (3), 153-160, 1999.

Matthews P.M., Ford B., Dandurand R.J., Eidelman D.H., O'Connor D., Sherwin A., Karpati G., Andermann F. and Arnold D.L. Coenzyme Q_{10} with multiple vitamins is generally ineffective in treatment of mitochondrial disease. *Neurology*, **43**, 884-890, 1993.

Mayorov V., Biousse V., Newman N.J. and Brown M.D. The role of the ND5 gene in LHON: characterization of a new, heteroplasmic LHON mutation. *Annals of Neurology*, **58** (5), 807-811, 2005.

McKenzie M., Trounce I.A., Cassar C.A. and Pankart C.A. Production of homoplasmic xenomitochondrial mice. *Proceedings of the National Academy of Sciences of the United States of America*, **101**, 1685-1690, 2004.

McShane M.A., Hammans S.R., Sweeney M., Holt I.J., Beattie T.J., Brett E.M., Harding A.E. Pearson syndrome and mitochondrial encephalomyopathy in a patient with a deletion of mtDNA. *American Journal of Human Genetics*, **48** (1), 39-42, 1991.

Miyoshi H. Structure-activity relationships of some complex I inhibitors. *Biochimica et Biophysica Acta*, **1364**, 236-244, 1998.

Miyoshi H. Inhibitors of mitochondrial respiratory enzymes. *Journal Pesticide Science*, **30** (2), 120-121, 2005.

Montoya J., Christianson T., Levens D., Rabinowitz M. and Attardi G. Identification of initiation sites for heavy-strand and light-strand transcription in human mitochondrial DNA. *Proceedings of the National Academy of Sciences of the United States of America*, **79** (23), 7195-7199, 1982.

Montoya J., Gaines G.L. and Attardi G. The pattern of transcription of the human mitochondrial rRNA genes reveals two overlapping transcription units. *Cell*, **34** (1), 151-159, 1983.

Morris A.A.M., Jackson M.J., Bindoff L.A. and Turnbull D.M. The investigation of mitochondrial respiratory chain disease. *Journal of the Royal Society of Medicine*, **88**, 217-222, 1995.

Morris A.A.M. Mitochondrial respiratory chain disorders and the liver. *Liver*, **19**, 357-368, 1999.

Motulsky H. Intuitive Biostatistics. Oxford University Press, Inc., 198 Madison Avenue, New York, New York, USA, 1995.

Munnich A., Rustin P., Rötig A., Chretien D., Bonnefont J.P., Nuttin C., Cormier V., Vassault A., Parvy P., Bardet J., Charpentier C., Rabier D. and Saudabray J.M. Clinical aspects of mitochondrial disorders. *Journal of Inherited Metabolic Disorders*, **15**, 448-455, 1992.

Musumeci O., Andreu A.L., Shanske S., Bresolin N., Comi G.P., Rothstein R., Schon E.A. and DiMauro S. Intragenic inversion of mtDNA: A new type of pathogenic mutation in a patient with mitochondrial myopathy. *American Journal of Human Genetics*, **66**, 1900-1904, 2000.

Nakagawa Y., Ikegami H., Yamato E., Takekawa K., Fujisawa T., Hamada Y., Ueda H., Uchigata Y., Miki T., Kumahara Y. and Ogihara T. A new mitochondrial DNA mutation associated with non-insulin-dependent diabetes mellitus. *Biochemical and Biophysical Research Communications*, **209** (2), 664-668, 1995.

Nakajima T., Wang R., Elovaara E., Park S.S., Gelbon H.V. and Vainio H. Cytochrome P450-related differences between rats and mice in the metabolism of benzene, toluene and trichloroethylene in liver microsomes. *Biochemical Pharmocology*, **45** (5), 1079-1085, 1993.

Naviaux R.K. Developing a systematic approach to the diagnosis and classification of mitochondrial disease. *Mitochondrion*, **4**, 351-361, 2004.

Nishikawa Y., Takahashi M., Yorifuji S., Nakamura Y., Ueno S., Tarui S., Kozuka T. and Nishimura T. Long-term coenzyme Q_{10} therapy for a mitochondrial encephalomyopathy with cytochrome c oxidase deficiency: a ^{31}P NMR study. *Neurology*, **39**, 399-403, 1989.

Ogasahara S., Nishikawa Y., Yorifuji S., Soga F., Nakamura Y., Takahashi M., Hashimoto S., Kono N. and Tarui S. Treatment of Kearns-Sayre syndrome with coenzyme Q_{10}. *Neurology*, **36**, 45-53, 1986.

Ojala D., Crews S., Montoya J., Gelfand R. and Attardi G. A small polyadenylated RNA (7S RNA), containing a putative ribosome attachment site, maps near the origin of human mitochondrial DNA replication. *Journal of Molecular Biology*, **150** (2), 303-314, 1981.

Osawa S., Jukes T.H., Watanabe K. and Muto A. Recent evidence for evolution of the genetic code. *Microbiology Reviews*, **56** (1), 229-264, 1992.

Ou B., Hampsch-Woodill M. and Prior R.L. Development and Validation of an Improved Oxygen Radical Absorbance Capacity Assay Using Fluorescein as the Fluorescent Probe. *Journal of Agricultural and Food Chemistry*, **49**, 4619-4626, 2001.

Pastore, A., Federicia G., Bertinib E. and Piemonteb F. Analysis of glutathione: implication in redox and detoxification. *Clinica Chimica Acta*, **333**, 19–39, 2003.

Patel S.D., Aebersold R. and Attardi G. cDNA-derived amino acid sequence of the NADH-binding 51-kDa subunit of the bovine respiratory NADH dehydrogenase reveals striking similarities to a bacterial NAD^+-reducing hydrogenase. *Proceedings of the National Academy of Sciences of the United States of America*, **88**, 4225-4229, 1991.

Patel M.S. and Korotchkina L.G. The biochemistry of the pyruvate dehydrogenae complex. *Biochemistry and Molecular Biology Education*, **31**, 5-15, 2003.

Pearson H.A., Lobel J.S., Kocoshis S.A., Naiman J.L., Windmiller J., Lammi A.T., Hoffman R. and Marsh J.C. A new syndrome of refractory sideroblastic anemia with vacuolization of marrow precursors and exocrine pancreatic dysfunction. *The Journal of Pediatrics*, **95**, 976-984, 1979.

Peng G., Fritzsch G., Zickermann V., Schagger H., Mentele R., Lottspeich F., Bostina M., Radermacher M., Huber R., Stetter K. O. and Michel H. Isolation, characterization and electron microscopic single particle analysis of the NADH:ubiquinone oxidoreductase (complex I) from the hyperthermophilic eubacterium *Aquifex aeolicus*. *Biochemistry*, **42**, 3032-3039, 2003.

Penn A.M.W., Lee J.W.K., Thuillier P., Wagner M., Maclue K.M., Menard M.R., Hall L.D. and Kennaway N.G. MELAS syndrome with mitochondrial $tRNA^{Leu(UUR)}$ mutation: correlation of clinical state, nerve conduction, and muscle ^{31}P magnetic resonance spectroscopy during treatment with nicotinamide and riboflavin. *Neurology*, **42**, 2147-2152, 1992.

Petruzzella V., Vergari S., Puzziferri I., Boffoli D., Lamentea E., Zeviani M. and Papa S. A nonsense mutation in the *NDUFS4* gene encoding the 18 kDa (AQDQ) subunit of complex I abolishes assembly and activity of the complex in a patient with Leigh-like syndrome. *Human Molecular Genetics*, **10**, 529-535, 2001.

Pilkington S.J., Skehel J.M. and Walker J.E. The 30-kiloDalton subunit of bovine mitochondrial complex I is homologous to a protein coded in chloroplast DNA. *Biochemistry*, **30**, 1901-1908, 1991.

Pilkington S.J. and Walker J.E. Mitochondrial NADH-ubiquinone reductase: Complementary DNA sequences of import precursors of the bovine and human 24-kDa subunit. *Biochemistry*, **28**, 3257-3264, 1989.

Poole T. The UFAW Handbook on the Care and Management of Laboratory Animals, Seventh Edition. Blackwell Science Ltd, Osney Mead, Oxford, United Kingdom, 1999.

Poulton J. Duplications of mitochondrial DNA: Implications for pathogenesis. *Journal of Inherited Metabolic Disorders*, **15**, 487-498, 1992.

Poulton J., Morten K.J., Weber K., Brown G.K. and Bindoff L. Are duplications of mitochondrial DNA characteristic of Kearns-Sayre Syndrome? *Human Molecular Genetics*, **3** (6), 947-951, 1994.

Prior R.L., Hoang H., Gu L., Wu X., Bacchiocca M., Howard L. and Hampsch-Woodill M. Assays for hydrophilic and lipophilic antioxidant capacity (oxygen radical absorbance capacity (ORACFL)) of plasma and other biological and food samples. *Journal of Agricultural and Food Chemistry*, **51**, 3273-3279, 2003.

Procaccio V. and Wallace D.C. Late-onset Leigh syndrome in a patient with mitochondrial complex I NDUFS8 mutations. *Neurology*, **62** (10), 1899-1901, 2004.

Pulkes T., Liolitsa D., Nelson I.P. and Hanna M.G. Classical mitochondrial phenotypes without mtDNA mutations: the possible role of nuclear genes. *Neurology*, **61** (8), 1144-1147, 2003.

Quiles J.L., Ochoa J.J., Huertas J.R. and Mataix J. Coenzyme Q supplementation protects from age-related DNA double-strand breaks and increases lifespan in rats fed on a PUFA-rich diet. *Experimental Gerontology*, **39**, 189-194, 2004.

Rahman S., Blok R.B., Dahl H.H.M., Danks D.M., Kirby D.M., Chow C.W., Christodoulou J. and Thornburn D.R. Leigh Syndrome: Clinical features and biochemical and DNA abnormalities. *Annals in Neology*, **39**, 343-351, 1996.

Rautenbach G.S. Differential tissue response to rotenone-induced Complex I deficiency: MSc thesis, North-West University (Potchefstroom Campus), 2004.

Ravn K., Wibrand F., Hansen F.J., Horn N., Rosenberg T. and Schwartz M. An mtDNA mutation, 14453G-A, in the NADH dehydrogenase subunit 6 associated with severe MELAS syndrome. *European Journal of Human Genetics*, **9** (10), 805-809, 2001.

Reinecke F., Levanets O., Olivier Y., Louw R., Semete B., Groblers A., Hidalgo J., Olckers A. and Van der Westhuizen F.H. Metallothionein isoform 2A expression is inducible and protects against ROS-mediated cell death in rotenone-treated HeLa cells. *Biochemical Journal*, **395** (2), 405-415, 2006.

Rice-Evans C.A., Miller N.J. and Paganga G. Structure-antioxidant activity relationships of flavonoids and phenolic acids. *Free Radical Biology & Medicine*, **20** (7), 933-956, 1996.

Robinson B.H. Human Complex I deficiency: clinical spectrum and involvement of oxygen free radicals in the pathogenicity of the defect. *Biochimica et Biophysica Acta*, **1361**, 271-286, 1998.

Rötig A., Cormier V., Blanche S., Bonnefont J.P., Ledeist F., Romero N., Schmitz J., Rustin P., Fischer A., Saudubray J.M. and Munnich A. Pearson's marrow-pancreas syndrome: a multisystem mitochondrial disorder in infancy. *The Journal of Clinical Investigation,* **86,** 1601-1608, 1990.

Rötig A., Bourgeron T., Rustin P. and Munnich A. Phenotypic expression of mitochondrial genotypes in cultured skin fibroblasts and in Epstein-Barr virus – transformed lymphocytes in Pearson syndrome. *Muscle & Nerve*, **3**, 159-164, 1995.

Runswick M.J., Fearnley I.M., Skehel J.M. and Walker J.E. Presence of an acyl carrier protein in NADH:ubiquinone oxidoreductase from bovine heart mitochondria. *FEBS Letters*, **286** (1,2), 121-124, 1991.

Runswick M.J., Gennis R.B., Fearnley I.M. and Walker J.E. Mitochondrial NADH:ubiquinone reductase: complementary DNA sequence of the import precursor of the bovine 75-kDA subunit. *Biochemistry*, **28** (24), 9452-9459, 1989.

Santorelli F.M., Tanji K., Kulikova R., Shanske S., Vilarinho L., Hays A.P. and Di Mauro S. Identification of a novel mutation in the mtDNA ND5 gene associated with MELAS. *Biochemical and Biophysical Research Communications*, **238**, 326-328, 1997.

Sazanov L.A., Peak-Chew S.W., Fearnley I.M. and Walker J.E. Resolution of the membrane domain of bovine complex I into subcomplexes: implications for the structural organization of the enzyme. *Biochemistry*, **39**, 7229-7235, 2000.

Schaefer A.M., Taylor R.W., Turnbull D.M. and Chinnery P.F. The epidemiology of mitochondrial disorders - past, present and future. *Biochimica et Biophysica Acta*, **1659**, 115-120, 2004.

Scheffler I.E. A century of mitochondrial research: achievements and perspectives. *Mitochondrion*, **1**, 3-31, 2000.

Sherer T.B., Kim J-H., Betarbet R. and Greenamyre J.T. Subcutaneous rotenone exposure causes highly selective dopaminergic degeneration and α-synuclein aggregation. *Experimental Neurology*, **179**, 9-16, 2003.

Schwartz M. and Vissing J. Paternal inheritance of mitochondrial DNA. *New England Journal of Medicine*, **347** (8), 576-580, 2002.

Schon E.A. and DiMauro S. Medicinal and genetic approaches to the treatment of mitochondrial disease. *Current Medical Chemistry*, **10**, 2523-2533, 2003.

Schuelke M., Smeitink J., Mariman E., Loeffen J., Plecko B., Trijbels F., Stockler-Ipsiroglu S. and Van den Heuvel L. Mutant NDUFV1 subunit of mitochondrial complex I causes leukodystrophy and myclonic epilepsy. *Nature Genetics*, **21**(3), 260-261, 1999.

Seo B.B., Kitajima-Ihara T., Chan E.K.L., Scheffler I.E., Matsuno-Yagi A. and Yagi T. Molecular remedy of complex I defects: Rotenone-insensitive internal NADH-quinone oxidoreductase of *Saccharomyces cerevisiae* mitochondria restores the NADH oxidase activity of complex I-deficient mammalian cells. *Proceedings of the National Academy of Sciences of the United States of America*, **95**, 9167-9171, 1998.

Seo B.B., Matsuno-Yagi A. and Yagi T. Modulation of oxidative phosphorylation of human kidney 293 cells by transfection with the internal rotenone-insensitive NADH-quinone oxidoreductase (NDI1) gene of *Saccharomyces cerevisiae*. *Biochimica et Biophysica Acta*, **1412**, 56-65, 1999.

Seo B.B., Wang J., Flotte T.R., Yagi T. and Matsuno-Yagi A. Use of the NADH-quinone oxidoreductase (NDI1) gene of *Saccharomyces cerevisiae* as a possible cure for complex I defects in human cells. *The Journal of Biological Chemistry*, **274** (48), 3774-3778, 2000.

Seo B.B., Nakamaru-Ogiso E., Flotte T.R., Yagi T. and Matsuno-Yagi A. A single-subunit NADH-quinone oxidoreductase renders resistance to mammalian nerve cells against complex I inhibition. *Molecular Therapy*, **6** (3), 336-341, 2002.

Servidei S. Mitochondrial encephalomyopathies: Gene mutation. *Neuromuscular Disorders*, **14** (1), 107-116, 2004.

Shanske S. and DiMauro S. Diagnosis of the mitochondrial encephalomyopathies. *Current Opinion in Rheumatology*, **9**, 496-503, 1997.

Sheskin D. Handbook of parametric and nonparametric statistical procedures, Third Edition. Chapman and Hall/CRC, 2004.

Simon D.K. A heteroplasmic mitochondrial complex I gene mutation in adult-onset dystonia. *Neurogenetics*, **4** (4), 199-205, 2003.

Shoffner J.M., Lott M.T., Voljavec A.S., Soueidan S.A., Costigan D.A. and Wallace D.C. Spontaneous Kearns-Sayre / chronic external opthalmoplegia plus syndrome associated with a mitochondrial DNA deletion: a slip-replication model and metabolic therapy. *Proceedings of the National Academy of Science of the United States of America*, **86**, 7952-7956, 1989.

Shoffner J.M., Lott M.T., Lezza A.M.S., Seibel P., Ballinger S.W. and Wallace D.C. Myoclonic epilepsy and ragged-red fiber disease (MERRF) is associated with a mitochondrial DNA $tRNA^{Lys}$ mutation. *Cell*, **61** (6), 931-937, 1990.

Shoffner J.M. and Wallace D.C. Oxidative phosphorylation diseases and mitochondrial DNA mutations: diagnosis and treatment. *Annual Reviews in Nutrition*, **14**, 535-568, 1994.

Silver L.M. Mouse Genetics: Concepts and Applications. Oxford University Press, Inc., New York, USA, 1995.

Skehel J.M., Pilkington S.J., Runswick M.J., Fearnley I.M. and Walker J.E. NADH:ubiquinone oxidoreductase from bovine heart mitochondria: Complementary DNA sequence of the import precursor of the 10 kDa subunit of the flavoprotein fragment. *FEBS letters*, **282** (1), 135-138, 1991.

Skehel J.M., Fearnley I.M. and Walker J.E. NADH:ubiquinone oxidoreductase from bovine heart mitochondria: sequence of a novel 17.2-kDa subunit. *FEBS Letters*, **438,** 301-305, 1998.

Sligh J.E., Levy S.E., Waymire K.G., Allard P., Dillehay D.L., Nusinowitz S., Heckenlively J.R., MacGregor G.R. and Wallace D.C. Maternal germ-line transmission of mutant mtDNAs from embryonic stem cell-derived chimeric mice. *Proceedings of the National Academy of Sciences of the United States of America*, **97**, 14461-14466, 2000.

Smith P.K., Krohn R.I., Hermanson G.T., Mallia AK., Gartner F.H., Provenano M.D., Fujimoto E.K., Goeke N.M., Olson B.J. and Klenk D.C. Measurement of protein using bicinchoninic acid. *Analytical Biochemistry*, **150**, 76-85, 1985.

Smeitink J.A.M., Van den Heuvel L.W.P.J., Koopman W.J.H., Nijtmans L.G.J., Ugalde C. and Willems P.H.G.M. Cell biological consequence of mitochondrial NADH:ubiquinone oxidoreductase deficiency. *Current Neurovascular Research*, **1**, 29-40, 2004.

Solano A., Roig M., Vives-Bauza C., Hernandez-Pena J., Garcia-Arumi E., Playan A., Lopez-Perez M.J., Andreu A.L. and Montoya J. Bilateral striatal necrosis associated with a novel mutation in the mitochondrial ND6 gene. *Annals of Neurology*, **54** (4), 527-530, 2003.

Soumalainen A. and Kaukonen J. Diseases caused by nuclear genes affecting mtDNA stability. *American Journal of Medical Genetics*, **106**, 53-61, 2001.

Superti-Furga A., Schoenle E., Tuchschmid P., Caduff R., Sabato V., DeMattia D., Gitzelmann R., Steinmann B. Pearson bone marrow-pancreas syndrome with insulin-dependent diabetes, progressive renal tubulopathy, organic aciduria and elevated fetal haemoglobin caused by deletion and duplication of mitochondrial DNA. *European Journal of Pediatrics*, **152** (1) 44-50, 1993.

STATISTICA (data analysis software system), version 7. StatSoft, Inc. (2004).

Taanman J-M. The mitochondrial genome: structure, transcription, translation and replication. *Biochimica et Biophysica Acta*, **1410**, 103-123, 1999.

Tada-Oikawa S., Hiraku Y., Kawanishi M. and Kawanishi S. Mechanism for generation of hydrogen peroxide and change of mitochondrial membrane potential during rotenone-induced apoptosis. *Life Sciences*, **73**, 3277-3288, 2003.

Taylor R.W., Morris A.A., Hutchinson M. and Turnbull D.M. Leigh disease associated with a novel mitochondrial DNA ND5 mutation. *European Journal of Human Genetics*, **10** (2), 141-144, 2002.

Tietze F. Enzymic method for quantitative determination of nanogram amounts of total and oxidized glutathione: Applications to mammalian blood and other tissues. *Analytical Biochemistry*, **27**, 502-522, 1969.

Topper J.N. and Clayton D.A. Identification of transcriptional regulatory elements in human mitochondria DNA by linker substitution analysis. *Molecular and Cellular Biology*, **9** (3), 1200-1211, 1989.

Triepels R.H., Van den Heuvel L.P., Loeffen J.L., Buskens C.A., Smeets R.J., Gozalbo M.E., Budde S.M., Mariman E.C., Wijburg F.A., Barth P.G., Trijbels J.M. and Smeitink J.A. Leigh syndrome associated with a mutation in the NDUFS7 (PSST) nuclear encoded subunit of complex I. *Annals of Neurology*, **45**, 787-790, 1999.

Trounce I.A., Kim Y.L., Jun A.S. and Wallace D.C. Assessment of mitochondrial oxidative phosphorylation in patient muscle biopsies, lymphoblasts, and transmitochondrial cell lines. *Methods in Enzymology,* **264**, 484-509, 1996.

Turpeinen A.M. Basu S. and Mutanen M. A high linoleic acid diet increases oxidative stress in vivo and affects nitric oxide metabolism in humans. *Prostaglandins, Leukotrienes and Essential Fatty Acids*, **59** (3), 229-233, 1998.

Valentino M.L., Avoni P., Barboni P., Pallotti F., Rengo C., Torroni A., Bellan M., Baruzzi A., and Carelli V. Mitochondrial DNA nucleotide changes C14482G and C14482A in the ND6 gene are pathogenic for Leber's hereditary optic neuropathy. *Annals of Neurology*, **51**, 774-778, 2002.

Valentino M.L., Barboni P., Ghelli A., Bucchi L., Rengo C., Achilli A., Torroni A., Lugaresi A., Lodi R., Barbiroli B., Dotti M., Federico A., Baruzzi A. and Carelli V. The ND1 gene of complex I is a mutational hot spot for Leber's hereditary optic neuropathy. *Annals of Neurology*, **56** (5), 631-641, 2004.

Van den Heuvel L., Ruitenbeek W., Smeets R., Gelman-Kohan Z., Elpeleg O., Loeffen J., Trijbels F., Mariman E., De Bruijn D. and Smeitink J. Demonstration of a new pathogenic mutation in human complex I deficiency: a 5-bp duplication in the nuclear gene encoding the 18-kD (AQDQ) subunit. *American Journal of Human Genetics*, **62**, 262-268, 1998.

Van den Heuvel L.P., Smeitink J.A. and Rodenburg R.J.T. Biochemical examination of fibroblasts in the diagnosis and research of oxidative phosphorylation (OXPHOS) defects. *Mitochondrion*, **4,** 395-401, 2004.

Van der Westhuizen F.H., Van den Heuvel L.P., Smeets R., Veltman J.A., Pfundt R., Van Kessel A.G., Ursing B.M. and Smeitink J.A.M. Human mitochondrial complex I deficiency: investigating transcriptional responses by microarray. *Neuropediatrics*, **34**, 14-22, 2003.

Vedanarayanan V.V. Mitochondrial Disorders and Ataxia. *Seminars in Pediatric Neurology*, **10** (3), 200-209, 2003.

Videira A. Complex I from the fungus *Neurospora crassa*. *Biochimica et Biophysica Acta*, **1364**, 89-100, 1998.

Wang J., Wilhelmsson H., Graff C., Li H., Oldfors C., Rustin P., Brüning J.C., Kahn C.R., Clayton D.A., Barsh G.S., Thorén P. and Larsson N-G. Dilated cardiomyopathy and atrioventricular conduction blocks induced by heart-specific inactivation of mitochondrial DNA gene expression. *Nature Genetics*, **21**, 133-137, 1999.

Walker J.E., Arizmendi J.M., Dupius A., Fearnley I.M., Finel M., Medd S.M., Pilkington S.J., Runswick M.J. and Skehel J.M. Sequences of 20 subunits of NADH:ubiquinone oxidoreductase from bovine heart mitochondria. *Journal of Molecular Biology*, **226**, 1051-1072, 1992.

Wallace D.C., Singh G., Lott M.T., Hodge J.A., Schurr T.G., Lezza A.M.S., Elsas L.J. and Nikoskelainen E.K. Mitochondrial DNA mutation associated with Leber's Hereditary Optic Neuropathy. *Science*, **242**, 1427-1430, 1988.

Wallace D.C. A mitochondrial paradigm of metabolic degenerative diseases, aging, and cancer: A dawn for evolutionary medicine. *Annual Reviews in Genetics*, **39**, 359-407, 2005.

Wang Y., Huang S., Sah V.P., Ross J., Brown J.H., Han J. and Chien K.R. Cardiac muscle cell hypertrophy and apoptosis induced by distinct members of the p38 mitogen-activated protein kinase family. *The Journal of Biological Chemistry*, **273** (4), 2161-2168, 1998.

Wang Q., Li R., Zhao H., Peters J.L., Liu Q., Yang L., Han D., Greinwald J.H., Young W. and Guan M. Clinical and molecular characterization of a Chinese patient with a auditory neuropathy associated with mitochondrial 12S rRNA T1095C mutation. *American Journal of Medical Genetics*, **133** (1), 27-30, 2005.

Wijburg F.A., Feller N., Ruitenbeek W., Trijbels M.F., Sengers R.C.A., Scholte H.R., Przyrembel H. and Wanders R.J.A. Detection of respiratory chain dysfunction by measuring lactate and pyruvate production in cultured fibroblasts. *Journal of Inherited Metabolic Disease*, **13**, 355-358, 1990.

Wilichowski E., Korenke G.C., Ruitenbeek W., De Meirleir L., Hagendorff A., Janssen A.J.M., Lissens W. and Hanefeld F. Pyruvate dehydrogenase complex deficiency and altered respiratory chain function in a patient with Kearns-Sayre/MELAS overlap syndrome and A3243G mtDNA mutation. *Journal of Neurological Sciences*, **157**, 206-213, 1998.

Wissenger B., Besch D., Baumann B., Fauser S., Christ-Adler M., Jurklies B., Zrenner E. and Leo-Kottler B. Mutation analysis of the ND6 gene in patients with Lebers hereditary optic neuropathy. *Biochemical and Biophysical Research Communications*, **234**, 511-515, 1997.

Wredenberg A., Wibom R., Wilhelmsson H., Graff C., Wiener H.H., Burden S.J., Oldfors A., Westerblad H. and Larsson N-G. Increased mitochondrial mass in mitochondrial myopathy mice. *Proceedings of the National Academy of Sciences of the United States of America*, **99**, 15066-15071, 2002.

Yagi T., Seo B.B., Nakamaru-Ogiso E., Marella M., Barber-Singh J., Yamashita T., Kao M.C. and Matsuno-Yagi A. Can a single subunit yeast NADH dehydrogenase (Ndi1) remedy diseases caused by respiratory complex I defects? *Rejuvenation Research*, **9** (2), 191-197, 2006.

Zeviani M., Muntoni F., Savarese N., Serra G., Tiranti V., Carrara F., Mariotti C. and DiDonato S. A MERRF/MELAS overlap syndrome associated with a new point mutation in the mitochondrial DNA $tRNA^{Lys}$ gene. *European Journal of Human Genetics*, **1**, 80-87, 1993.

Zeviani M., Spinazzola A. and Carelliz V. Nuclear genes in mitochondrial disorders. *Current Opinion in Genetics & Development*, **13**, 262-270, 2003.

Zickermann V., Bostina M., Hunte C., Ruiz T., Radermacher M. and Brandt U. Functional implications from an unexpected position of the 49 kDa subunit of NADH:ubiquinone oxidoreductase. *Journal of Biological Chemistry*, **278** (31), 29072-29078, 2003.

Zerez C.R., Lee S.J. and Tanaka K.R. Spectrophotometric determination of oxidized and reduced pyridine nucleotides in erythrocytes using a single extraction procedure. *Analytical Biochemistry*, **164**, 367-373, 1987.

Zhadanov S.I., Atamanov V.V., Zhadanov N.I., Oleinikov O.V., Osipova L.P. and Schurr T.G. A novel mtDNA ND6 gene mutation associated with LHON in a Caucasian family. *Biochemical and Biophysical Research Communication*, **332**, 1115-1121, 2005.

Zuber R., Anzenbacherova E. and Anzenbacher P. Cytochrome P450 and experimental models of drug metabolism. *Journal of Cellular and Molecular Medicine*, **6** (2), 189-198, 2002.

APPENDIX A

RAT WEIGHT DATA

Rat body weights were recorded every day prior to dosing and on the final days prior to rat sacrificing and tissue collection. The daily rat weight recordings for the pilot and main studies are listed in Table A.1 and A.2 respectively. Body weight data generated from the rat pilot study, as presented in Table A.1, displays missing data for R3-4 after day 6 due to the death of the rat.

Table A.1 Daily recordings of body weight in the rat pilot study

Rat	Day														
	1	2	3	4	5	6	7	8	9	10	11	12	13	14	15
N-1	273	273	278	283	285	288	276	296	300	299	308	309	314	314	318
N-2	301	301	307	312	316	316	318	319	322	321	326	329	329	333	338
N-3	273	273	277	284	286	290	291	297	299	306	309	313	316	320	321
N-4	268	272	280	284	291	292	298	303	307	313	318	322	323	327	332
N-5	264	271	273	275	281	287	285	290	290	295	299	300	300	302	309
N-6	270	275	277	284	288	290	292	292	296	298	302	307	305	307	315
V-1	278	282	283	285	288	288	290	295	298	300	301	304	307	312	314
V-2	278	280	284	285	287	290	294	297	300	307	310	310	310	319	320
V-3	298	302	306	309	312	313	322	324	328	331	336	339	342	347	352
V-4	291	295	298	298	306	305	311	315	314	324	326	328	331	336	336
V-5	279	286	291	294	300	302	303	308	308	315	317	319	323	326	327
V-6	277	281	286	287	294	296	296	305	306	311	311	313	316	317	320
R3-1	296	299	298	307	308	309	313	309	317	319	321	317	323	327	325
R3-2	288	293	288	294	299	302	305	307	308	311	314	308	311	316	317
R3-3	287	284	289	287	290	295	295	300	298	308	309	314	314	313	321
R3-4	284	285	291	290	293	293	Died	—	—	—	—	—	—	—	—
R3-5	282	284	286	290	292	295	299	302	305	304	306	307	313	312	316
R3-6	281	284	284	288	289	292	295	299	299	303	303	305	307	305	305
R6-1	297	300	302	299	303	306	305	305	306	305	307	303	308	310	309
R6-2	293	291	298	296	301	302	301	304	307	306	307	308	309	314	318
R6-3	290	290	294	296	296	301	305	304	304	307	307	306	315	308	313
R6-4	284	285	285	286	288	286	287	286	288	292	292	295	297	292	303
R6-5	282	278	282	285	283	288	289	290	292	299	298	299	301	304	306
R6-6	280	279	281	281	286	290	291	298	297	303	304	305	305	309	312
R9-1	296	291	290	293	290	291	287	280	288	286	282	284	286	284	282
R9-2	285	283	280	278	281	271	274	275	276	278	282	287	290	287	295
R9-3	282	284	281	278	281	275	276	277	281	281	280	281	281	280	286
R9-4	283	279	279	281	284	283	283	285	284	288	290	291	300	298	298
R9-5	278	281	270	268	271	270	271	269	272	272	271	278	280	287	289
R9-6	274	273	272	271	271	270	274	275	278	279	282	286	291	296	298
R12-1	296	297	292	283	273	272	270	275	273	273	276	278	278	282	289
R12-2	292	289	286	290	282	281	274	281	275	284	285	287	293	294	292
R12-3	286	284	281	275	273	279	276	280	280	284	287	286	292	293	294
R12-4	282	279	278	275	274	275	283	275	278	283	282	284	285	290	288
R12-5	278	280	265	272	272	267	271	266	264	263	265	261	267	268	264
R12-6	275	271	261	266	268	265	274	265	265	265	270	272	271	277	279

Table A.1 Rat pilot study continued...

Rat	Day														
	1	2	3	4	5	6	7	8	9	10	11	12	13	14	15
R15-1	276	273	272	273	269	271	274	275	271	272	270	270	264	261	261
R15-2	296	292	295	298	288	290	287	289	287	285	289	291	282	272	264
R15-3	298	293	294	288	283	272	277	274	270	272	279	281	279	266	266
R15-4	279	279	279	275	275	270	267	266	263	259	258	259	252	240	235
R15-5	278	278	271	265	268	257	259	262	254	251	243	242	243	246	240
R15-6	283	281	280	280	274	271	269	262	258	267	272	267	266	270	269

'---' = missing data due to the death of rat R3-4. Rats were treated N = no dose, V = vehicle, R3 = rotenone 3 $mg.kg^{-1}.day^{-1}$, R6 = rotenone 6 $mg.kg^{-1}.day^{-1}$, R9 = rotenone 9 $mg.kg^{-1}.day^{-1}$, R12 = rotenone 12 $mg.kg^{-1}.day^{-1}$, R15 = rotenone 15 $mg.kg^{-1}.day^{-1}$.

Table A.2 lists the day-to-day rat weight recordings from day 1 to either day 15 or 17 depending on the treatments received. Dose groups VX and RX were sacrificed on day 15, hence the missing data indications (---) for the last two days. The remaining nine groups were sacrificed on day 17. Body weights for the randomly excluded rats from dose groups RX and RV are also listed and indicated in grey text at the bottom of the table.

It should be noted from Table A.2 that body weight data for three rats, namely RX-E1, RX-E2 and RV-E1 were excluded, as indicated in grey text. Data for the first two rats were excluded from dose group RX, while the latter was excluded from RV. These rats were originally assigned rat codes in their respective dose groups and were included in the study to compensate for deaths incurred by rats receiving the high rotenone dose concentrations of 15 $mg.kg^{-1}.day^{-1}$. Since the parametric test procedures, such as the one-way and factorial ANOVA used in this study, may result in compromised test statistics if an unequal number of data points in a data sets are used (Motulsky, 1995), it was decided that the three additional rats be excluded during the statistical analysis phase of the study. Moreover, as it was important to analyse the rat main study data via a factorial approach to delineate the effects of Factor-1 and Factor-2 regimens, without the risk of compromising the resulting statistics, the argument of data point exclusion and balancing the data sets was strengthened.

Therefore, the random number generator of STATISTICA™ was used and rats excluded according to the first decimal numbers. As for dose group RX, the first decimal place of two randomly generated numbers was used to exclude rats, whereas only one random number was generated for the exclusion of a rat in dose group RV. If the first decimal generated was a digit greater than the number of rats for RX and RV, the digit in the second decimal place was used. These rats were subsequently excluded for the remainder of the study and in all of the parameter data sets.

Table A.2 Daily recordings of body weight in the rat main study

Rat	Day																
	1	2	3	4	5	6	7	8	9	10	11	12	13	14	15	16	17
NN-1	278	284	286	291	293	300	303	305	307	310	314	315	317	320	323	326	331
NN-2	269	269	270	271	273	280	281	278	280	286	290	290	294	296	296	297	305
NN-3	260	265	266	268	274	279	279	282	284	289	291	293	295	295	298	300	303
NN-4	269	270	272	271	273	282	283	284	285	289	292	293	297	298	298	300	303
NN-5	265	267	268	271	271	278	279	282	283	288	290	293	295	299	299	300	306
NN-6	262	264	264	268	271	276	277	282	280	285	286	287	288	290	291	295	297
VX-1	263	266	274	276	280	283	287	291	294	301	297	301	306	311	312	—	—
VX-2	292	297	299	300	304	306	308	311	314	318	319	318	323	326	329	—	—
VX-3	287	291	293	293	298	301	303	306	305	309	310	312	314	316	319	—	—
VX-4	277	284	287	290	292	298	301	304	305	309	314	315	320	324	328	—	—
VX-5	273	279	289	286	288	291	295	300	300	301	304	309	314	316	323	—	—
VX-6	286	290	292	296	300	301	304	307	309	312	313	317	320	321	327	—	—
VN-1	279	286	290	293	300	302	309	310	313	314	316	319	323	327	330	331	333
VN-2	273	280	282	286	287	291	295	299	301	302	306	307	310	316	321	319	316
VN-3	282	286	293	298	301	306	310	314	316	320	324	325	330	338	340	340	340
VN-4	270	274	272	277	277	281	286	287	294	296	301	303	310	316	321	320	321
VN-5	290	298	297	302	305	307	312	318	320	323	324	327	333	336	339	339	340
VN-6	294	299	301	306	310	320	320	326	328	333	338	337	343	349	351	353	353
VV-1	277	280	283	289	294	297	299	306	309	308	316	324	326	326	325	323	328
VV-2	264	269	271	278	281	286	288	291	295	297	302	308	310	312	312	314	318
VV-3	268	271	273	279	283	285	289	295	299	301	306	310	314	316	316	318	324
VV-4	278	280	283	289	291	294	297	300	306	306	310	318	319	323	324	321	330
VV-5	280	283	284	290	294	300	302	306	307	311	316	320	322	322	324	327	332
VV-6	261	267	269	273	277	280	284	285	289	293	297	301	302	302	305	304	308
VC-1	270	285	287	288	296	296	306	305	308	310	320	320	324	327	332	330	337
VC-2	263	274	275	277	277	277	279	283	284	284	284	288	288	288	290	290	291
VC-3	295	305	307	310	310	311	317	317	322	325	327	331	334	335	339	338	344
VC-4	260	265	270	264	265	266	271	275	280	280	281	284	285	288	287	291	294
VC-5	261	270	270	272	278	278	286	290	296	294	295	297	300	301	305	304	306
VC-6	265	278	280	282	289	292	294	300	300	303	304	313	313	316	322	322	328
VS-1	286	287	290	297	295	299	300	304	305	305	307	309	310	313	315	314	314
VS-2	262	264	272	275	279	283	288	289	291	291	292	299	301	303	303	304	308
VS-3	268	271	274	275	280	284	288	291	291	288	293	296	301	302	303	308	310
VS-4	282	286	287	290	294	300	302	302	302	302	298	300	302	303	308	313	314
VS-5	260	265	272	274	277	285	291	294	296	292	297	299	301	307	307	310	315
VS-6	268	270	274	278	281	285	291	292	292	293	292	298	300	300	301	302	304
RX-1	287	284	277	281	281	283	279	280	275	278	285	281	281	284	278	—	—
RX-2	284	283	279	278	279	280	281	278	278	271	266	255	250	248	246	—	—
RX-3	265	267	264	263	267	269	265	267	270	271	269	268	270	270	268	—	—
RX-4	284	282	279	278	275	264	263	259	253	252	250	247	243	240	228	—	—
RX-5	284	282	277	276	274	275	268	266	265	256	250	241	233	235	231	—	—
RX-6	260	260	253	256	251	254	255	254	254	250	241	246	252	250	242	—	—
RN-1	292	291	277	268	271	278	279	277	266	267	266	258	256	254	250	251	264
RN-2	285	281	282	280	277	278	271	269	259	263	270	258	250	248	246	248	264
RN-3	270	266	262	264	260	259	256	259	251	256	254	244	243	241	238	240	251
RN-4	298	297	284	282	282	276	280	283	278	267	276	268	260	251	232	247	259
RN-5	266	268	260	262	258	260	255	242	239	243	248	241	240	240	234	231	246
RN-6	271	268	266	257	255	257	255	254	248	243	249	241	239	235	233	229	226

Table A.2 Rat main study continued...

Rat	Day																
	1	2	3	4	5	6	7	8	9	10	11	12	13	14	15	16	17
RV-1	272	268	266	254	236	248	249	241	241	243	244	246	245	249	232	228	222
RV-2	269	265	266	267	264	263	261	251	255	256	246	245	243	245	248	254	262
RV-3	269	265	262	260	259	254	255	250	242	240	246	247	247	244	241	250	252
RV-4	275	272	263	264	263	261	257	255	253	250	236	240	243	229	227	217	215
RV-5	280	276	268	269	261	260	256	251	249	245	233	235	230	225	223	215	205
RV-6	300	299	291	294	291	292	282	278	274	265	263	260	257	254	236	237	266
RC-1	261	265	258	257	251	245	246	242	241	241	241	255	250	232	238	248	252
RC-2	270	268	265	267	265	265	259	257	260	265	267	267	267	272	268	273	275
RC-3	275	271	270	267	265	260	256	256	254	252	256	255	255	254	250	255	261
RC-4	268	265	261	256	250	248	246	245	245	244	246	242	246	246	244	250	254
RC-5	266	261	259	256	255	251	245	245	247	243	237	228	234	226	224	225	217
RC-6	266	265	262	254	259	261	258	261	249	246	254	254	250	252	243	250	260
RS-1	275	272	265	265	264	265	264	260	259	259	257	256	256	256	257	262	265
RS-2	276	274	271	266	265	264	254	248	249	249	249	245	242	239	236	241	253
RS-3	282	275	273	271	271	263	259	270	269	270	268	271	270	270	267	276	277
RS-4	265	264	260	256	260	260	259	257	257	257	256	260	256	258	252	261	265
RS-5	280	273	272	271	272	269	270	260	260	260	257	255	253	249	250	259	267
RS-6	272	269	269	261	260	259	259	261	258	256	248	245	251	250	239	255	255
RX-E1	268	269	265	265	265	260	258	261	265	260	269	266	267	268	269	---	---
RX-E2	276	274	271	263	265	264	267	265	267	259	255	259	256	252	247	---	---
RV-E1	270	269	260	256	249	248	246	241	240	240	236	233	226	230	230	226	238

'—' = missing data since dose groups VX and RX were sacrificed on day 15. Rats and corresponding data points that were randomly excluded from the main study are listed at the bottom of the table in grey text and designated the codes RX-E1, RX-E2 and RV-E1 for rats from dose groups RX and RV respectively. The aforementioned rats were excluded based on the random number generator of STATISTICA™, and was applied consistently for all parameter data sets. Rats were treated with NN = no dose regimen, VX = vehicle and sacrificed, VN = vehicle and no dose, VV = vehicle and vehicle, VC = vehicle and CoQ_{10}, VS = vehicle and succinate, RX = rotenone and sacrificed, RN = rotenone and no dose, RV = rotenone and vehicle, RC = rotenone and CoQ_{10}, RS = rotenone and succinate.

APPENDIX B

COMPLEX I ACTIVITY DATA

Complex I activity for the various tissues were determined and ultimately interpreted in terms of UCS. Tables listed in Appendix B contain data generated from the mitochondrial preparations of each tissue, including protein concentrations, citrate synthase activities and complex I. The data point values are presented to a maximum of four significant numbers. Sections B.1 and B.2 present the complex I data generated from the rat pilot and main studies respectively.

The introduction paragraph to each table contains the optimised sample volumes (v) used for the respective assays. These volumes were multiplied by the protein concentrations (P_{CON}) to determine the amount of protein used in each reaction, namely for citrate synthase activity (P_{CSA}) and complex I activity (P_{CIA}). Citrate synthase activity (CSA) is divided by the corresponding P_{CSA} value to determine the activity of this enzyme in terms of its protein content ($CSA.prot^{-1}$). Similarly, the complex I activity (CIA) is divided by its corresponding P_{CIA} value to obtain complex I activity relative to the protein concentration ($CIA.prot^{-1}$). Finally, the complex I activity per unit citrate synthase ($CIA.UCS^{-1}$) was calculated by dividing the $CIA.prot^{-1}$ value by that of the $CSA.prot^{-1}$ activity.

B.1 RAT PILOT STUDY COMPLEX I DATA

Complex I data generated from the rat pilot study are presented in Tables B.1 to B.4 for heart muscle, whole brain, skeletal muscle and liver respectively. Basic statistics, namely means and standard deviations, have also been included.

Heart muscle complex I data, generated from the rat pilot study, are presented in Table B.1. Mitochondrial preparations were diluted 1:20 in a hypotonic buffer, of which 5 μL was used for the citrate synthase assay. Therefore, the $CSA.prot^{-1}$ activity of 9,866 $\mu mol.min^{-1}.\mu g^{-1}$ for mitochondrial preparation N-1 was determined by initially calculating the P_{CSA} value of 0.51 μg, which in turn was calculated by multiplying the P_{CON} of 2.03 $\mu g.\mu L^{-1}$ by 5 μL (sample volume) and dividing by the dilution factor of 20. The same preparations were used to determine complex I activities, except that 5 μL of an undiluted sample was used and the $CIA.prot^{-1}$ activity of 88.60 $\mu mol.min^{-1}.\mu g^{-1}$ calculated

in a similar manner. A final CIA.UCS^{-1} activity of 0.00898 μmol.min^{-1}.μg^{-1} was determined by dividing the CIA.prot^{-1} value by that of CSA.prot^{-1}, which was in turn multiplied by a factor of 1,000 to obtain an activity of 8.98 nmol.min^{-1}.μg^{-1}.

Table B.1 Heart muscle complex I data generated from the rat pilot study

Rat	Protein			Citrate synthase					Complex I							
				CSA.prot^{-1}					CIA.prot^{-1}					CIA.UCS^{-1}		
	P_{CON}	Mean	SD	CSA	P_{CSA}	Activity	Mean	SD	CIA	P_{CIA}	Activity	Mean	SD	Activity	Mean	SD
N-1	2.03	2.13	0.46	5,000	0.51	9,866	11,630	1,553	898.1	10.1	88.60	77.17	21.82	8.98	6.67	1.99
N-2	2.95			7,615	0.74	10,331			526.1	14.7	35.69			3.45		
N-3	2.16			5,739	0.54	10,640			892.9	10.8	82.77			7.78		
N-4	2.02			6,369	0.50	12,630			978.7	10.1	97.04			7.68		
N-5	2.12			6,681	0.53	12,600			914.9	10.6	86.27			6.85		
N-6	1.53			5,256	0.38	13,712			556.8	7.67	72.63			5.30		
V-1	2.32	2.36	0.32	8,235	0.58	14,205	13,169	3,834	819.6	11.6	70.69	75.90	11.15	4.98	6.33	2.70
V-2	2.50			11,486	0.62	18,410			912.9	12.5	73.16			3.97		
V-3	2.46			7,705	0.61	12,532			778.2	12.3	63.29			5.05		
V-4	2.78			11,144	0.70	16,024			1124	13.9	80.78			5.04		
V-5	2.26			4,808	0.56	8,523			1078	11.3	95.58			11.2		
V-6	1.82			4,250	0.46	9,318			655.7	9.12	71.88			7.71		
R3-1	2.16	2.73	0.42	11,431	0.54	21,193	17,468	4,104	614.2	10.8	56.94	61.17	5.703	2.69	3.66	0.87
R3-2	2.96			12,095	0.74	16,352			1029	14.8	69.53			4.25		
R3-3	3.08			10,581	0.77	13,748			844.6	15.4	54.87			3.99		
R3-4	---			---	---	---			---	---	---			---		
R3-5	2.42			13,521	0.60	22,371			748.6	12.1	61.93			2.77		
R3-6	3.05			10,437	0.76	13,677			955.5	15.3	62.60			4.58		
R6-1	3.18	3.06	0.54	5,716	0.79	7,196	14,186	4,132	1075	15.9	67.69	63.66	8.171	9.41	5.04	2.36
R6-2	3.26			15,165	0.81	18,634			1025	16.3	62.96			3.38		
R6-3	2.26			9,832	0.56	17,431			547.9	11.3	48.56			2.79		
R6-4	3.15			10,494	0.79	13,320			1148	15.8	72.85			5.47		
R6-5	2.68			10,657	0.67	15,919			880.3	13.4	65.75			4.13		
R6-6	3.82			12,057	0.96	12,617			1226	19.1	64.15			5.08		
R9-1	4.16	3.63	0.71	18,661	1.04	17,941	17,706	3,929	646.3	20.8	31.07	42.27	9.68	1.73	2.48	0.74
R9-2	3.96			15,527	0.99	15,693			1116	19.8	56.41			3.59		
R9-3	4.56			15,175	1.14	13,308			891.0	22.8	39.07			2.94		
R9-4	3.22			11,992	0.80	14,902			594.3	16.1	36.92			2.48		
R9-5	2.67			15,942	0.67	23,860			513.7	13.4	38.44			1.61		
R9-6	3.19			16,363	0.80	20,533			824.3	15.9	51.72			2.52		
R12-1	3.36	3.22	0.52	19,334	0.84	23,021	20,743	2,888	818.5	16.8	48.73	37.26	8.965	2.12	1.80	0.35
R12-2	3.28			16,264	0.82	19,858			554.2	16.4	33.83			1.70		
R12-3	2.78			14,675	0.69	21,140			560.3	13.9	40.36			1.91		
R12-4	3.98			22,530	0.99	22,652			896.3	19.9	45.06			1.99		
R12-5	3.44			13,212	0.86	15,351			514.7	17.2	29.90			1.95		
R12-6	2.49			13,967	0.62	22,434			319.8	12.5	25.68			1.14		
R15-1	3.92	3.85	0.51	18,153	0.98	18,542	17,048	2,677	485.0	19.6	24.77	21.15	11.80	1.34	1.22	0.69
R15-2	3.32			15,898	0.83	19,137			439.8	16.6	26.47			1.38		
R15-3	3.87			15,312	0.97	15,808			714.5	19.4	36.88			2.33		
R15-4	3.91			18,465	0.98	18,911			479.0	19.5	24.53			1.30		
R15-5	4.74			14,419	1.18	12,173			142.7	23.7	6.025			0.49		
R15-6	3.36			14,882	0.84	17,720			138.4	16.8	8.238			0.46		

'---' = missing data due to the death of rat R3-4 (also indicated in grey), CIA = complex I activity in μmol.min^{-1}, CIA.prot^{-1} = complex I activity in terms of protein in μmol.min^{-1}.μg^{-1}, CIA.UCS^{-1} = complex I activity per units citrate synthase in nmol.min^{-1}.UCS^{-1}, CSA = citrate synthase activity in μmol.min^{-1}, CSA.prot^{-1} = citrate synthase activity in terms of protein expressed in μmol.min^{-1}.μg^{-1}, P_{CIA} = amount of protein used in reaction for complex I activity, P_{CON} = protein concentration of mitochondrial isolate in μg.μL^{-1}, P_{CSA} = amount of protein used in the reaction for citrate synthase activity, SD = standard deviation. Rats were treated N = no dose, V = vehicle, R3 = rotenone 3 mg.kg^{-1}.day^{-1}, R6 = rotenone 6 mg.kg^{-1}.day^{-1}, R9 = rotenone 9 mg.kg^{-1}.day^{-1}, R12 = rotenone 12 mg.kg^{-1}.day^{-1}, R15 = rotenone 15 mg.kg^{-1}.day^{-1}.

Complex I data that was generated from the whole brain mitochondrial isolates during the rat pilot study are presented in Table B.2. As with the heart muscle preparations, 5 µL of a 1:20 dilution was used for the determination of citrate synthase activity. A 5 µL sample volume of the original mitochondrial isolation was used in the complex I activity assay.

Table B.2 Brain tissue complex I data generated from the rat pilot study

Rat	Protein			Citrate synthase					Complex I							
				CSA.prot^{-1}					CIA.prot^{-1}					CIA.UCS^{-1}		
	P_{CON}	Mean	SD	CSA	P_{CSA}	Activity	Mean	SD	CIA	P_{CIA}	Activity	Mean	SD	Activity	Mean	SD
N-1	3.89	3.69	0.51	10,613	0.97	10,922	15,550	5,352	593.7	19.4	30.55	31.13	5.272	2.80	2.10	0.43
N-2	3.07			19,574	0.77	25,519			624.4	15.3	40.71			1.60		
N-3	4.05			15,228	1.01	15,024			646.5	20.3	31.89			2.12		
N-4	4.37			18,554	1.09	16,979			666.3	21.9	30.49			1.80		
N-5	3.59			10,668	0.90	11,873			503.9	18.0	28.04			2.36		
N-6	3.19			10,345	0.80	12,981			400.0	15.9	25.10			1.93		
V-1	4.96	4.15	1.40	15,048	1.24	12,143	18,328	5,495	712.5	24.8	28.75	36.85	15.56	2.37	1.99	0.42
V-2	6.50			24,891	1.62	15,320			604.2	32.5	18.59			1.21		
V-3	2.49			17,428	0.62	28,015			810.1	12.4	65.11			2.32		
V-4	3.49			17,969	0.87	20,615			679.2	17.4	38.96			1.89		
V-5	3.82			15,574	0.95	16,328			651.6	19.1	34.10			2.09		
V-6	3.64			15,949	0.91	17,546			647.4	18.2	35.61			2.03		
R3-1	4.03	4.80	0.95	13,772	1.01	13,668	13,411	1,399	399.7	20.2	19.83	16.37	2.502	1.45	1.22	0.18
R3-2	4.44			16,337	1.11	14,728			364.9	22.2	16.45			1.12		
R3-3	6.18			19,072	1.54	12,352			526.9	30.9	17.06			1.38		
R3-4	—			—	—	—			—	—	—			—		
R3-5	5.35			15,531	1.34	11,609			345.4	26.8	12.91			1.11		
R3-6	3.99			14,658	1.00	14,700			311.2	19.9	15.61			1.06		
R6-1	5.14	5.10	1.17	17,863	1.28	13,911	15,195	2,926	475.1	25.7	18.50	19.30	2.022	1.33	1.30	0.26
R6-2	3.64			10,773	0.91	11,833			343.2	18.2	18.85			1.59		
R6-3	4.48			19,105	1.12	17,040			456.7	22.4	20.37			1.20		
R6-4	4.75			23,705	1.19	19,972			492.9	23.7	20.76			1.04		
R6-5	7.13			23,679	1.78	13,290			764.5	35.6	21.45			1.61		
R6-6	5.46			20,639	1.36	15,123			433.5	27.3	15.88			1.05		
R9-1	3.93	4.94	1.06	13,112	0.98	13,329	13,964	2,470	492.0	19.7	25.01	21.51	5.110	1.88	1.60	0.55
R9-2	3.70			15,236	0.92	16,490			410.8	18.5	22.23			1.35		
R9-3	6.07			18,341	1.52	12,077			639.6	30.4	21.06			1.74		
R9-4	5.32			16,890	1.33	12,696			380.0	26.6	14.28			1.13		
R9-5	4.49			13,041	1.12	11,615			644.1	22.5	28.69			2.47		
R9-6	6.13			26,952	1.53	17,574			545.4	30.7	17.78			1.01		
R12-1	6.43	5.39	1.13	23,237	1.61	14,461	13,663	4,044	846.8	32.1	26.35	15.67	5.716	1.82	1.20	0.40
R12-2	6.79			17,353	1.70	10,219			430.9	34.0	12.69			1.24		
R12-3	3.96			17,293	0.99	17,474			287.1	19.8	14.51			0.83		
R12-4	4.41			19,989	1.10	18,118			387.4	22.1	17.56			0.97		
R12-5	4.99			9,675	1.25	7,760			289.8	24.9	11.62			1.50		
R12-6	5.75			20,055	1.44	13,946			324.9	28.8	11.30			0.81		
R15-1	4.27	5.00	1.05	11,408	1.07	10,687	11,625	4,997	283.8	21.3	13.29	12.83	1.817	1.24	1.24	0.47
R15-2	7.02			21,489	1.75	12,246			340.9	35.1	9.71			0.79		
R15-3	5.23			12,826	1.31	9,817			348.4	26.1	13.33			1.36		
R15-4	4.35			22,886	1.09	21,058			331.6	21.7	15.26			0.72		
R15-5	4.35			7,019	1.09	6,449			286.2	21.8	13.15			2.04		
R15-6	4.80			11,393	1.20	9,491			294.1	24.0	12.25			1.29		

'—' = missing data due to the death of rat R3-4 (also indicated in grey), CIA = complex I activity in µmol.min^{-1}, CIA.prot^{-1} = complex I activity in terms of protein in µmol.min^{-1}.µg^{-1}, CIA.UCS^{-1} = complex I activity per units citrate synthase in nmol.min^{-1}.UCS^{-1}, CSA = citrate synthase activity in µmol.min^{-1}, CSA.prot^{-1} = citrate synthase activity in terms of protein expressed in µmol.min^{-1}.µg^{-1}, P_{CIA} = amount of protein used in reaction for complex I activity, P_{CON} = protein concentration of mitochondrial isolate in µg.µL^{-1}, P_{CSA} = amount of protein used in the reaction for citrate synthase activity, SD = standard deviation. Rats were treated N = no dose, V = vehicle, R3 = rotenone 3 mg.kg^{-1}.day^{-1}, R6 = rotenone 6 mg.kg^{-1}.day^{-1}, R9 = rotenone 9 mg.kg^{-1}.day^{-1}, R12 = rotenone 12 mg.kg^{-1}.day^{-1}, R15 = rotenone 15 mg.kg^{-1}.day^{-1}.

Skeletal muscle complex I activity data generated from the rat pilot study are presented in Table B.3. Since low protein concentrations were determined for the skeletal muscle homogenates, 10 µL of a 1:10 dilution was used for the optimisation of the citrate synthase assay in this tissue. Accordingly, an increased volume of 20 µL of the undiluted mitochondrial preparation was used to determine complex I activity in all samples.

Table B.3 Skeletal muscle complex I data generated from the rat pilot study

Rat	Protein			Citrate synthase					Complex I							
				CSA.prot^{-1}					CIA.prot^{-1}					CIA.UCS^{-1}		
	P_{CON}	Mean	SD	CSA	P_{CSA}	Activity	Mean	SD	CIA	P_{CIA}	Activity	Mean	SD	Activity	Mean	SD
N-1	0.43	0.61	0.25	229.9	0.43	531.9	730.5	224.3	21.8	8.64	2.52	3.43	1.44	4.735	4.952	1.962
N-2	0.41			373.4	0.41	912.5			20.3	8.18	2.48			2.714		
N-3	0.52			403.4	0.52	776.9			64.6	10.4	6.22			8.009		
N-4	1.07			441.7	1.07	414.2			54.7	21.3	2.56			6.191		
N-5	0.53			390.2	0.53	740.7			38.5	10.5	3.65			4.933		
N-6	0.70			703.2	0.70	1,007			44.1	14.0	3.16			3.134		
V-1	0.58	0.90	0.74	758.9	0.58	1,307	1,019	438.2	72.0	11.6	6.20	3.69	2.32	4.745	3.469	1.113
V-2	0.68			555.5	0.68	822.8			21.1	13.5	1.56			1.900		
V-3	0.25			345.2	0.25	1,377			32.5	5.01	6.49			4.713		
V-4	0.66			665.1	0.66	1,000			44.7	13.3	3.36			3.362		
V-5	0.85			1,155	0.85	1,357			63.3	17.0	3.72			2.739		
V-6	2.36			582.1	2.36	247.1			39.0	47.1	0.83			3.352		
R3-1	0.67	0.82	0.27	698.1	0.67	1,046	936.1	129.6	73.2	13.4	5.49	3.33	1.619	5.245	3.437	1.312
R3-2	0.88			803.7	0.88	908.3			47.3	17.7	2.67			2.942		
R3-3	0.65			716.8	0.65	1,095			57.8	13.1	4.41			4.031		
R3-4	—			—	—	—			—	—	—			—		
R3-5	0.64			517.4	0.64	806.1			17.7	12.8	1.38			1.708		
R3-6	1.27			1,051	1.27	825.6			68.5	25.5	2.69			3.256		
R6-1	0.76	0.63	0.36	261.0	0.76	344.8	929.7	566.9	13.1	15.1	0.87	2.07	2.176	2.519	2.592	2.110
R6-2	0.44			580.9	0.44	1,313			21.7	8.85	2.45			1.869		
R6-3	0.29			637.2	0.43	1,483			3.91	5.73	0.68			0.461		
R6-4	0.45			680.1	0.45	1,502			56.4	9.05	6.23			4.148		
R6-5	0.57			361.0	0.57	635.8			4.68	11.4	0.41			0.648		
R6-6	1.30			584.5	1.95	299.3			46.0	26.0	1.77			5.906		
R9-1	0.40	0.54	0.25	286.6	0.40	723.1	796.2	245.1	27.2	7.93	3.43	2.07	1.14	4.741	2.609	1.425
R9-2	0.40			243.7	0.40	606.8			2.75	8.03	0.34			0.565		
R9-3	0.91			694.3	0.91	764.7			45.6	18.2	2.51			3.282		
R9-4	0.38			408.2	0.38	1,078			13.3	7.57	1.76			1.630		
R9-5	0.81			408.2	0.81	503.5			22.2	16.2	1.37			2.720		
R9-6	0.37			408.2	0.37	1,101			22.2	7.42	2.99			2.720		
R12-1	0.57	0.44	0.09	502.1	0.57	880.3	1,184	289.9	36.0	11.4	3.16	3.09	1.715	3.587	2.624	1.308
R12-2	0.48			502.1	0.48	1,039			19.2	9.67	1.98			1.908		
R12-3	0.34			443.4	0.34	1,323			41.2	6.70	6.15			4.651		
R12-4	0.41			668.4	0.41	1,644			19.3	8.13	2.38			1.447		
R12-5	0.36			459.0	0.36	1,291			25.6	7.11	3.60			2.788		
R12-6	0.47			437.5	0.47	929.7			11.9	9.41	1.27			1.364		
R15-1	0.63	0.40	0.20	581.1	0.63	927.3	835.0	655.6	38.1	12.5	3.04	1.82	0.81	3.275	2.954	1.324
R15-2	0.66			504.8	0.66	762.1			28.1	13.2	2.12			2.782		
R15-3	0.30			238.6	0.46	522.6			13.9	6.09	2.28			4.355		
R15-4	0.17			106.8	0.26	409.5			5.29	3.48	1.52			3.711		
R15-5	0.23			104.8	0.35	300.3			4.34	4.65	0.93			3.108		
R15-6	0.42			870.6	0.42	2,088			8.54	8.34	1.02			0.491		

'—' = missing data due to the death of rat R3-4 (also indicated in grey), CIA = complex I activity in µmol.min^{-1}, CIA.prot^{-1} = complex I activity in terms of protein in µmol.min^{-1}.µg^{-1}, CIA.UCS^{-1} = complex I activity per units citrate synthase in nmol.min^{-1}.UCS^{-1}, CSA = citrate synthase activity in µmol.min^{-1}, CSA.prot^{-1} = citrate synthase activity in terms of protein expressed in µmol.min^{-1}.µg^{-1}, P_{CIA} = amount of protein used in reaction for complex I activity, P_{CON} = protein concentration of mitochondrial isolate in µg.µL^{-1}, P_{CSA} = amount of protein used in the reaction for citrate synthase activity, SD = standard deviation. Rats were treated N = no dose, V = vehicle, R3 = rotenone 3 mg.kg^{-1}.day^{-1}, R6 = rotenone 6 mg.kg^{-1}.day^{-1}, R9 = rotenone 9 mg.kg^{-1}.day^{-1}, R12 = rotenone 12 mg.kg^{-1}.day^{-1}, R15 = rotenone 15 mg.kg^{-1}.day^{-1}.

Complex I activity data of liver tissue generated from the rat pilot study is presented in Table B.4. The optimised sample volume required for the determination of citrate synthase activity was 3 µL of a 1:10 dilution of the mitochondrial preparation. Complex I was assayed successfully when 5 µL of the undiluted sample was used.

Table B.4 Liver tissue complex I data generated from the rat pilot study

Rat	Protein			Citrate synthase					Complex I							
				CSA.prot^{-1}					CIA.prot^{-1}					CIA.UCS^{-1}		
	P_{CON}	Mean	SD	CSA	P_{CSA}	Activity	Mean	SD	CIA	P_{CIA}	Activity	Mean	SD	Activity	Mean	SD
N-1	3.96	4.94	0.58	638.0	1.19	536.6	520.4	93.06	409.1	19.8	20.64	10.50	5.626	38.47	20.99	11.40
N-2	4.82			624.8	1.45	431.8			237.0	24.1	9.828			22.76		
N-3	5.36			982.5	1.61	611.5			160.7	26.8	6.002			9.815		
N-4	4.70			631.5	1.41	448.2			168.8	23.5	7.190			16.04		
N-5	5.23			700.6	1.57	446.6			339.8	26.1	13.00			29.10		
N-6	5.56			1,081	1.67	647.9			175.8	27.8	6.321			9.757		
V-1	8.13	6.64	1.40	952.9	3.25	292.9	521.7	181.9	412.7	40.7	10.15	5.962	2.590	34.65	13.31	10.58
V-2	4.90			648.2	1.47	441.3			91.22	24.5	3.727			8.444		
V-3	6.04			1,138	1.81	628.0			205.3	30.2	6.799			10.83		
V-4	7.40			1,227	2.22	553.2			130.2	37.0	3.522			6.367		
V-5	5.35			654.4	1.60	407.7			115.5	26.7	4.320			10.59		
V-6	8.01			1,940	2.40	807.0			290.8	40.1	7.260			8.996		
R3-1	5.95	6.05	1.17	692.5	1.79	387.6	471.5	110.2	260.1	29.8	8.737	7.203	2.404	22.54	16.64	7.750
R3-2	5.51			909.7	1.65	550.0			143.1	27.6	5.192			9.440		
R3-3	8.05			830.7	2.42	343.8			315.8	40.3	7.842			22.81		
R3-4	---			---	---	---			---	---	---			---		
R3-5	5.69			796.7	1.71	466.4			284.1	28.5	9.978			21.40		
R3-6	5.05			924	1.52	609.6			107.8	25.3	4.268			7.001		
R6-1	5.63	7.21	1.30	810.6	1.69	479.6	620.2	196.2	166.2	28.2	5.899	4.734	3.549	12.30	8.087	6.193
R6-2	7.11			2,072	2.13	971.4			267.0	35.6	7.508			7.730		
R6-3	8.47			1,072	2.54	421.6			236.9	42.4	5.592			13.26		
R6-4	8.64			1,414	2.59	545.8			11.80	43.2	0.273			0.501		
R6-5	7.66			1,417	2.30	616.6			331.1	38.3	8.644			14.02		
R6-6	5.77			1,189	1.73	686.4			14.14	28.9	0.490			0.714		
R9-1	8.55	6.86	1.13	1,834	2.56	715.4	617.1	161.5	220.2	42.7	5.153	4.263	1.137	7.204	7.115	2.002
R9-2	7.38			1,962	2.21	886.7			143.9	36.9	3.901			4.399		
R9-3	5.65			931.0	1.70	549.1			129.5	28.3	4.581			8.343		
R9-4	5.54			801.4	1.66	481.9			66.2	27.7	2.390			4.959		
R9-5	6.97			1,277	2.09	610.5			195.7	34.9	5.615			9.197		
R9-6	7.08			974.5	2.12	458.8			139.5	35.4	3.940			8.588		
R12-1	5.20	5.21	0.85	845.0	1.56	541.2	463.6	79.10	147.1	26.0	5.653	5.222	2.425	10.44	12.01	6.048
R12-2	5.90			1,008	1.77	569.2			12.35	29.5	0.419			0.735		
R12-3	4.20			502.0	1.26	398.4			139.0	21.0	6.619			16.61		
R12-4	4.14			468.2	1.24	377.0			114.7	20.7	5.542			14.70		
R12-5	5.76			720.7	1.73	417.4			203.8	28.8	7.083			16.97		
R12-6	6.03			865.8	1.81	478.4			181.5	30.2	6.018			12.58		
R15-1	9.05	9.40	1.73	1,749	2.72	643.9	626.9	138.4	166.6	45.3	3.680	3.510	1.535	5.714	6.111	3.729
R15-2	8.31			1,647	2.49	660.7			78.87	41.5	1.898			2.873		
R15-3	7.60			1,130	2.28	495.3			229.1	38.0	6.027			12.17		
R15-4	8.36			1,547	2.51	616.7			89.35	41.8	2.137			3.465		
R15-5	11.1			1,608	3.34	481.7			240.7	55.6	4.325			8.977		
R15-6	11.9			3,086	3.57	863.2			178.3	59.6	2.993			3.468		

'---' = missing data due to the death of rat R3-4 (also indicated in grey), CIA = complex I activity in µmol.min^{-1}, CIA.prot^{-1} = complex I activity in terms of protein in µmol.min^{-1}.µg^{-1}, CIA.UCS^{-1} = complex I activity per units citrate synthase in nmol.min^{-1}.UCS^{-1}, CSA = citrate synthase activity in µmol.min^{-1}, CSA.prot^{-1} = citrate synthase activity in terms of protein expressed in µmol.min^{-1}.µg^{-1}, P_{CIA} = amount of protein used in reaction for complex I activity, P_{CON} = protein concentration of mitochondrial isolate in µg.µL^{-1}, P_{CSA} = amount of protein used in the reaction for citrate synthase activity, SD = standard deviation. Rats were treated N = no dose, V = vehicle, R3 = rotenone 3 mg.kg^{-1}.day^{-1}, R6 = rotenone 6 mg.kg^{-1}.day^{-1}, R9 = rotenone 9 mg.kg^{-1}.day^{-1}, R12 = rotenone 12 mg.kg^{-1}.day^{-1}, R15 = rotenone 15 mg.kg^{-1}.day^{-1}.

B.2 RAT MAIN STUDY COMPLEX I DATA

Complex I data generated from the rat main study are presented in Tables B.5 to B.8 for heart muscle, whole brain, skeletal muscle and liver respectively. Means and standard deviations have also been included descriptive statistics.

Heart muscle complex I activity data generated from the rat main study are presented in Table B.5. The citrate synthase assay was optimised to use 10 μL of the mitochondrial preparation that was diluted 1:20 in a hypotonic buffer. Complex I activities were determined by using 5 μL of the original isolate.

Table B.5 Heart muscle complex I data generated from the rat main study

Rat	Protein			Citrate synthase					Complex I							
				CSA.prot^{-1}					CIA.prot^{-1}					CIA.UCS^{-1}		
	P_{CON}	Mean	SD	CSA	P_{CSA}	Activity	Mean	SD	CIA	P_{CIA}	Activity	Mean	SD	Activity	Mean	SD
NN-1	1.71	1.80	0.30	5,441	0.86	6,345	6,935	2,292	422.5	8.57	49.28	46.38	17.89	7.766	7.183	3.332
NN-2	1.53			4,705	0.77	6,139			589.2	7.66	76.88			12.52		
NN-3	1.42			3,283	0.71	4,639			201.7	7.08	28.50			6.144		
NN-4	1.94			7,330	0.97	7,576			278.4	9.68	28.78			3.798		
NN-5	2.18			12,210	1.09	11,193			474.4	10.9	43.49			3.885		
NN-6	2.04			5,834	1.02	5,718			523.8	10.2	51.33			8.978		
VX-1	1.03	0.99	0.41	3,948	0.52	7,661	12,362	5,646	1,389	5.15	269.6	248.6	74.29	35.19	22.19	8.233
VX-2	1.36			6,977	0.68	10,287			1,255	6.78	185.0			17.99		
VX-3	1.11			4,215	0.55	7,596			1,223	5.55	220.3			29.00		
VX-4	0.97			7,038	0.48	14,527			943.2	4.84	194.7			13.40		
VX-5	1.27			7,278	0.63	11,502			1,486	6.33	234.8			20.41		
VX-6	0.21			2,422	0.11	22,600			415.0	1.07	387.2			17.13		
VN-1	0.98	1.15	0.15	2,412	0.49	4,933	8,954	2,511	305.2	4.89	62.43	51.21	7.394	12.66	6.430	3.268
VN-2	1.26			6,267	0.63	9,927			319.9	6.31	50.67			5.104		
VN-3	1.10			5,319	0.55	9,713			227.2	5.48	41.49			4.271		
VN-4	1.15			4,887	0.57	8,535			291.8	5.73	50.96			5.971		
VN-5	1.39			8,729	0.70	12,543			318.3	6.96	45.74			3.646		
VN-6	1.03			4,149	0.51	8,074			287.6	5.14	55.98			6.933		
VV-1	1.70	1.40	0.33	10,547	0.85	12,407	9,611	1,757	529.1	8.50	62.24	44.74	21.72	5.017	4.720	2.174
VV-2	1.08			4,368	0.54	8,084			185.8	5.40	34.39			4.254		
VV-3	1.27			4,708	0.63	7,441			299.2	6.33	47.28			6.354		
VV-4	1.45			7,490	0.73	10,327			99.34	7.25	13.70			1.326		
VV-5	1.06			5,203	0.53	9,845			395.0	5.29	74.74			7.591		
VV-6	1.87			8,943	0.94	9,562			337.7	9.35	36.11			3.777		
VC-1	1.86	1.76	0.18	6,212	0.93	6,684	6,602	747	317.0	9.29	34.11	33.94	6.866	5.102	5.122	0.716
VC-2	1.98			6,379	0.99	6,456			250.3	9.88	25.33			3.924		
VC-3	1.63			5,414	0.82	6,632			288.3	8.16	35.32			5.326		
VC-4	1.48			5,100	0.74	6,893			313.8	7.40	42.40			6.152		
VC-5	1.81			6,917	0.91	7,624			361.5	9.07	39.84			5.226		
VC-6	1.82			4,845	0.91	5,323			242.5	9.10	26.64			5.005		
VS-1	1.65	1.62	0.21	6,228	0.82	7,562	7,444	676	777.6	8.24	94.41	78.04	13.56	12.48	10.66	2.666
VS-2	1.97			7,333	0.99	7,433			802.9	9.87	81.38			10.95		
VS-3	1.34			5,336	0.67	7,935			414.8	6.72	61.68			7.773		
VS-4	1.58			6,249	0.79	7,912			607.0	7.90	76.85			9.713		
VS-5	1.68			6,465	0.84	7,698			532.2	8.40	63.38			8.233		
VS-6	1.47			4,513	0.74	6,124			667.2	7.37	90.53			14.78		

Table B.5 Heart muscle continued...

Rat	Protein			Citrate synthase					Complex I							
				CSA.prot^{-1}					CIA.prot^{-1}					CIA.UCS^{-1}		
	P_{CON}	Mean	SD	CSA	P_{CSA}	Activity	Mean	SD	CIA	P_{CIA}	Activity	Mean	SD	Activity	Mean	SD
RX-1	1.33	1.59	0.33	7,141	0.67	10,737	9,568	2,035	756.7	6.65	113.8	57.59	40.61	10.60	6.035	4.309
RX-2	1.44			6,024	0.72	8,339			748.7	7.22	103.6			12.43		
RX-3	2.04			10,640	1.02	10,427			357.2	10.2	35.01			3.357		
RX-4	1.89			11,017	0.94	11,670			323.8	9.44	34.30			2.939		
RX-5	1.20			6,124	0.60	10,174			254.2	6.02	42.22			4.150		
RX-6	1.66			5,017	0.83	6,059			137.5	8.28	16.61			2.741		
RN-1	1.64	1.53	0.22	8,083	0.82	9,884	9,534	1,232	297.9	8.18	36.43	27.65	8.157	3.685	2.895	0.762
RN-2	1.35			6,347	0.68	9,398			220.6	6.75	32.67			3.476		
RN-3	1.88			8,614	0.94	9,153			131.2	9.41	13.94			1.523		
RN-4	1.58			9,080	0.79	11,495			246.1	7.90	31.16			2.711		
RN-5	1.39			6,682	0.70	9,602			203.9	6.96	29.30			3.052		
RN-6	1.32			5,048	0.66	7,675			147.4	6.58	22.42			2.921		
RV-1	1.25	1.47	0.29	6,097	0.63	9,726	9,577	2,322	78.60	6.27	12.54	40.59	22.12	1.289	4.775	3.490
RV-2	1.43			7,064	0.72	9,860			430.8	7.16	60.13			6.099		
RV-3	1.23			6,877	0.61	11,207			407.2	6.14	66.36			5.921		
RV-4	1.23			6,890	0.62	11,200			169.0	6.15	27.48			2.453		
RV-5	1.85			9,669	0.92	10,454			220.3	9.25	23.81			2.278		
RV-6	1.80			4,523	0.90	5,017			479.9	9.01	53.24			10.61		
RC-1	1.67	1.86	0.20	5,032	0.83	6,034	6,856	1,280	515.8	8.34	61.85	50.98	13.69	10.25	7.948	3.515
RC-2	2.18			7,510	1.09	6,894			622.4	10.9	57.13			8.288		
RC-3	1.80			4,415	0.90	4,914			589.0	8.99	65.55			13.34		
RC-4	2.05			7,205	1.02	7,041			511.9	10.2	50.03			7.105		
RC-5	1.77			7,639	0.89	8,614			378.5	8.87	42.68			4.955		
RC-6	1.72			6,584	0.86	7,640			247.0	8.62	28.66			3.751		
RS-1	2.28	2.03	0.17	4,629	1.14	4,053	5,222	1,007	703.7	11.4	61.61	66.29	9.907	15.20	13.22	3.731
RS-2	1.94			4,077	0.97	4,202			761.5	9.70	78.47			18.68		
RS-3	2.05			5,923	1.03	5,771			751.3	10.3	73.21			12.69		
RS-4	2.07			5,209	1.04	5,033			755.2	10.4	72.97			14.50		
RS-5	1.78			4,941	0.89	5,562			480.3	8.88	54.08			9.722		
RS-6	2.06			6,924	1.03	6,709			592.5	10.3	57.41			8.557		
RX-E1	1.72	N/A		7,657	0.86	8,885	N/A		1,037	8.62	120.4	N/A		13.55	N/A	
RX-E2	1.55			8,015	0.78	10,319			618.0	7.77	79.57			7.711		
RV-E1	1.60			8,673	0.80	10,820			286.3	8.02	35.72			3.301		

Rats and corresponding data points that were randomly excluded from the main study are listed at the bottom of the table in grey text and designated the codes RX-E1, RX-E2 and RV-E1 for rats from dose groups RX and RV respectively. The aforementioned rats were excluded based on the random number generator of STATISTICA™, and was applied consistently for all parameter data sets. CIA = complex I activity in $\mu mol.min^{-1}$, CIA.prot^{-1} = complex I activity in terms of protein in $\mu mol.min^{-1}.\mu g^{-1}$, CIA.UCS^{-1} = complex I activity per units citrate synthase in $nmol.min^{-1}.UCS^{-1}$, CSA = citrate synthase activity in $\mu mol.min^{-1}$, CSA.prot^{-1} = citrate synthase activity in terms of protein expressed in $\mu mol.min^{-1}.\mu g^{-1}$, P_{CIA} = amount of protein used in reaction for complex I activity, P_{CON} = protein concentration of mitochondrial isolate in $\mu g.\mu L^{-1}$, P_{CSA} = amount of protein used in the reaction for citrate synthase activity, SD = standard deviation. Rats were treated with NN = no dose regimen, VX = vehicle and sacrificed, VN = vehicle and no dose, VV = vehicle and vehicle, VC = vehicle and CoQ_{10}, VS = vehicle and succinate, RX = rotenone and sacrificed, RN = rotenone and no dose, RV = rotenone and vehicle, RC = rotenone and CoQ_{10}, RS = rotenone and succinate.

Table B.6 contains the complex I data generated from brain tissue during the rat main study. The enriched mitochondrial isolations were diluted 1:20 for the assaying of citrate synthase activity, of which an optimised volume of 5 µL was used. For complex I activity, a volume of 5 µL of the undiluted preparations was used.

Table B.6 Brain tissue complex I data generated from the rat main study

Rat	Protein			Citrate synthase					Complex I							
				CSA.prot^{-1}					CIA.prot^{-1}					CIA.UCS^{-1}		
	P_{CON}	Mean	SD	CSA	P_{CSA}	Activity	Mean	SD	CIA	P_{CIA}	Activity	Mean	SD	Activity	Mean	SD
NN-1	2.13	2.34	0.43	6,205	0.53	11,643	13,553	2434	111.4	10.7	10.45	21.96	12.32	0.897	1.587	0.800
NN-2	2.85			6,808	0.71	9,560			167.2	14.2	11.74			1.228		
NN-3	1.83			6,450	0.46	14,082			403.3	9.16	44.03			3.126		
NN-4	2.07			7,871	0.52	15,231			265.1	10.3	25.65			1.684		
NN-5	2.31			9,025	0.58	15,641			260.4	11.5	22.56			1.443		
NN-6	2.86			10,840	0.71	15,162			248.1	14.3	17.35			1.144		
VX-1	3.57	3.71	0.67	9,577	0.89	10,729	15,073	6210	651.2	17.9	36.47	34.12	6.063	3.400	2.448	0.674
VX-2	3.99			26,954	1.00	26,999			826.2	20.0	41.38			1.533		
VX-3	2.84			10,173	0.71	14,316			378.8	14.2	26.66			1.862		
VX-4	4.76			11,628	1.19	9,778			634.1	23.8	26.66			2.727		
VX-5	3.18			10,605	0.80	13,327			588.3	15.9	36.97			2.774		
VX-6	3.93			15,020	0.98	15,292			719.0	19.6	36.60			2.393		
VN-1	2.84	2.14	0.37	8,898	0.71	12,548	17,246	3978	554.4	14.2	39.09	33.73	16.35	3.115	2.137	1.145
VN-2	2.24			7,247	0.56	12,956			407.8	11.2	36.45			2.813		
VN-3	2.04			9,804	0.51	19,244			264.9	10.2	26.00			1.351		
VN-4	1.84			10,140	0.46	21,996			45.21	9.22	4.903			0.223		
VN-5	1.83			7,410	0.46	16,176			452.6	9.16	49.40			3.054		
VN-6	2.05			10,531	0.51	20,554			477.1	10.2	46.56			2.265		
VV-1	1.92	1.65	0.26	8,345	0.48	17,381	18,109	2403	493.2	9.60	51.36	40.32	20.66	2.955	2.242	1.229
VV-2	1.48			7,437	0.37	20,102			197.9	7.40	26.75			1.331		
VV-3	1.38			7,591	0.35	22,003			373.3	6.90	54.10			2.459		
VV-4	1.60			6,501	0.40	16,220			65.12	8.02	8.126			0.501		
VV-5	1.49			6,004	0.37	16,102			481.9	7.46	64.62			4.013		
VV-6	2.01			8,457	0.50	16,842			371.1	10.0	36.96			2.194		
VC-1	1.83	2.08	0.70	6,208	0.46	13,597	14,016	3965	298.6	9.13	32.70	20.33	8.536	2.405	1.472	0.586
VC-2	3.27			8,430	0.82	10,327			183.6	16.3	11.24			1.089		
VC-3	1.96			5,407	0.49	11,027			200.6	9.81	20.46			1.855		
VC-4	1.63			6,832	0.41	16,799			215.4	8.13	26.48			1.577		
VC-5	1.30			6,707	0.33	20,578			132.3	6.52	20.30			0.986		
VC-6	2.50			7,358	0.63	11,765			135.0	12.5	10.80			0.918		
VS-1	2.78	2.41	0.79	8,201	0.70	11,785	14,139	4079	47.86	13.9	3.439	27.06	21.53	0.292	1.771	0.988
VS-2	3.65			9,112	0.91	9,978			254.1	18.3	13.92			1.395		
VS-3	1.40			7,297	0.35	20,883			465.2	6.99	66.57			3.188		
VS-4	1.94			8,247	0.48	17,022			223.6	9.69	23.07			1.355		
VS-5	2.03			6,839	0.51	13,502			302.2	10.1	29.83			2.209		
VS-6	2.69			7,843	0.67	11,664			343.6	13.4	25.55			2.190		
RX-1	1.82	1.87	0.91	7,974	0.46	17,519	24,965	12813	396.6	9.10	43.57	38.64	22.10	2.487	1.560	0.757
RX-2	0.69			7,585	0.17	43,783			211.5	3.46	61.05			1.394		
RX-3	1.22			11,545	0.31	37,805			338.7	6.11	55.45			1.467		
RX-4	1.63			9,013	0.41	22,162			392.8	8.13	48.29			2.179		
RX-5	3.12			12,810	0.78	16,432			76.98	15.6	4.937			0.300		
RX-6	2.72			8,219	0.68	12,091			252.1	13.6	18.55			1.534		
RN-1	1.75	2.06	0.76	13,962	0.44	31,912	20734	9005	529.8	8.75	60.55	38.92	11.73	1.897	2.022	0.534
RN-2	2.43			8,578	0.61	14,112			459.3	12.2	37.78			2.677		
RN-3	1.05			8,368	0.26	31,842			209.8	5.26	39.91			1.253		
RN-4	1.44			7,051	0.36	19,602			228.8	7.19	31.81			1.623		
RN-5	2.97			11,328	0.74	15,248			555.4	14.9	37.38			2.452		
RN-6	2.71			7,909	0.68	11,686			353.1	13.5	26.09			2.233		
RV-1	1.63	1.39	0.69	10,371	0.41	25,411	29,991	16817	340.2	8.16	41.67	57.50	43.60	1.640	1.779	0.753
RV-2	1.49			9,121	0.37	24,458			458.1	7.46	61.42			2.511		
RV-3	0.35			4,002	0.09	46,198			230.2	1.73	132.9			2.877		
RV-4	0.78			10,577	0.19	54,579			286.1	3.88	73.83			1.353		
RV-5	2.13			9,645	0.53	18,148			264.8	10.6	24.91			1.372		
RV-6	1.96			5,452	0.49	11,151			100.7	9.78	10.30			0.924		

Table B.6 Brain tissue continued...

Rat	Protein			Citrate synthase					Complex I							
				CSA.prot^{-1}					CIA.prot^{-1}					CIA.UCS^{-1}		
	P_{CON}	Mean	SD	CSA	P_{CSA}	Activity	Mean	SD	CIA	P_{CIA}	Activity	Mean	SD	Activity	Mean	SD
RC-1	2.23	2.38	0.26	6,810	0.56	12,206	12,176	2837	114.0	11.2	10.22	19.23	11.15	0.837	1.591	0.806
RC-2	2.25			7,717	0.56	13,724			123.7	11.2	11.00			0.801		
RC-3	2.41			10,209	0.60	16,960			455.5	12.0	37.83			2.231		
RC-4	2.26			5,915	0.56	10,493			284.2	11.3	25.21			2.402		
RC-5	2.21			5,021	0.55	9,071			234.8	11.1	21.21			2.338		
RC-6	2.90			7,672	0.72	10,600			143.7	14.5	9.930			0.937		
RS-1	1.84	2.04	0.41	8,035	0.46	17,428	18,260	5053	213.0	9.22	23.10	26.72	16.56	1.325	1.388	0.722
RS-2	2.20			6,369	0.55	11,568			67.91	11.0	6.168			0.533		
RS-3	1.76			11,839	0.44	26,880			314.0	8.81	35.65			1.326		
RS-4	1.84			8,017	0.46	17,446			226.8	9.19	24.68			1.415		
RS-5	1.79			8,961	0.45	20,011			484.6	8.96	54.11			2.704		
RS-6	2.82			11,457	0.71	16,224			234.8	14.1	16.62			1.024		
RX-E1	3.04	N/A		9,412	0.76	12,376	N/A		567.1	15.2	37.29	N/A		3.013	N/A	
RX-E2	1.79			7,257	0.45	16,206			340.8	8.96	38.05			2.348		
RV-E1	1.53			7,476	0.38	19,584			291.7	7.63	38.21			1.951		

Rats and corresponding data points that were randomly excluded from the main study are listed at the bottom of the table in grey text and designated the codes RX-E1, RX-E2 and RV-E1 for rats from dose groups RX and RV respectively. The aforementioned rats were excluded based on the random number generator of STATISTICA™, and was applied consistently for all parameter data sets. CIA = complex I activity in μmol.min^{-1}, CIA.prot^{-1} = complex I activity in terms of protein in μmol.min^{-1}.μg^{-1}, CIA.UCS^{-1} = complex I activity per units citrate synthase in nmol.min^{-1}.UCS^{-1}, CSA = citrate synthase activity in μmol.min^{-1}, CSA.prot^{-1} = citrate synthase activity in terms of protein expressed in μmol.min^{-1}.μg^{-1}, P_{CIA} = amount of protein used in reaction for complex I activity, P_{CON} = protein concentration of mitochondrial isolate in μg.μL^{-1}, P_{CSA} = amount of protein used in the reaction for citrate synthase activity, SD = standard deviation. Rats were treated with NN = no dose regimen, VX = vehicle and sacrificed, VN = vehicle and no dose, VV = vehicle and vehicle, VC = vehicle and CoQ_{10}, VS = vehicle and succinate, RX = rotenone and sacrificed, RN = rotenone and no dose, RV = rotenone and vehicle, RC = rotenone and CoQ_{10}, RS = rotenone and succinate.

Complex I and related data generated from skeletal muscle during the rat main study are presented in Table B.7. The complex I assay was optimised and a volume of 20 μL used from the original isolate. Citrate synthase data was generated via the use of 10 μL of a 1:10 dilution of the mitochondrial preparations.

Table B.7 Skeletal muscle complex I data generated from the rat main study

Rat	Protein			Citrate synthase					Complex I							
				CSA.prot^{-1}					CIA.prot^{-1}					CIA.UCS^{-1}		
	P_{CON}	Mean	SD	CSA	P_{CSA}	Activity	Mean	SD	CIA	P_{CIA}	Activity	Mean	SD	Activity	Mean	SD
NN-1	1.39	1.56	0.51	2,077	1.39	1,495	1,737	263.0	26.67	27.8	0.960	2.077	1.544	0.642	1.120	0.747
NN-2	1.29			2,654	1.29	2,059			81.72	25.8	3.170			1.540		
NN-3	1.12			1,665	1.12	1,493			25.14	22.3	1.127			0.755		
NN-4	1.20			1,825	1.20	1,516			6.617	24.1	0.275			0.181		
NN-5	1.95			3,707	1.95	1,904			168.3	38.9	4.322			2.270		
NN-6	2.41			4,717	2.41	1,954			125.9	48.3	2.608			1.335		
VX-1	1.42	1.81	1.36	1,461	1.42	1,030	1,355	291.0	131.5	28.4	4.634	4.471	1.394	4.499	3.318	0.966
VX-2	1.19			1,301	1.19	1,096			55.19	23.7	2.326			2.122		
VX-3	4.58			5,723	4.58	1,249			303.8	91.7	3.314			2.654		
VX-4	1.35			2,238	1.35	1,660			137.7	27.0	5.110			3.078		
VX-5	1.05			1,420	1.05	1,358			126.5	20.9	6.053			4.457		
VX-6	1.31			2,270	1.31	1,738			140.8	26.1	5.389			3.101		

Table B.7 Skeletal muscle continued...

Rat	Protein			Citrate synthase					Complex I							
				CSA.prot^{-1}					CIA.prot^{-1}					CIA.UCS^{-1}		
	P_{CON}	Mean	SD	CSA	P_{CSA}	Activity	Mean	SD	CIA	P_{CIA}	Activity	Mean	SD	Activity	Mean	SD
VN-1	1.22			1,914	1.22	1,571			26.45	24.4	1.085			0.691		
VN-2	1.15			2,228	1.15	1,936			140.9	23.0	6.122			3.163		
VN-3	1.07	1.18	0.12	2,491	1.07	2,337	1,965	333.0	207.0	21.3	9.710	6.710	3.465	4.155	3.312	1.607
VN-4	1.03			2,433	1.03	2,367			150.9	20.6	7.339			3.100		
VN-5	1.31			2,163	1.31	1,655			136.8	26.1	5.234			3.162		
VN-6	1.33			2,558	1.33	1,923			286.5	26.6	10.77			5.601		
VV-1	0.80			745.3	0.80	926			48.53	16.1	3.016			3.256		
VV-2	0.93			1,584	0.93	1,697			173.7	18.7	9.300			5.481		
VV-3	1.03	1.01	0.23	1,067	1.03	1,035	1,269	271.6	8.931	20.6	0.433	2.763	3.315	0.419	2.009	1.972
VV-4	1.05			1,307	1.05	1,251			22.87	20.9	1.094			0.874		
VV-5	0.81			1,092	0.81	1,348			19.79	16.2	1.221			0.906		
VV-6	1.42			1,930	1.42	1,355			43.20	28.5	1.517			1.119		
VC-1	2.14			4,812	2.14	2,248			173.7	42.8	4.057			1.804		
VC-2	0.64			863.4	0.64	1,349			33.20	12.8	2.593			1.923		
VC-3	0.27	0.71	0.71	815.2	0.27	3,018	2,242	600.6	63.71	5.40	11.79	5.555	3.219	3.908	2.387	0.826
VC-4	0.31			862.9	0.31	2,772			29.15	6.22	4.682			1.689		
VC-5	0.37			795.7	0.37	2,168			41.81	7.34	5.696			2.627		
VC-6	0.56			1,065	0.56	1,900			50.56	11.2	4.508			2.373		
VS-1	0.75			1,560	0.75	2,083			21.29	15.0	1.422			0.683		
VS-2	1.03			2,102	1.03	2,039			74.16	20.6	3.598			1.764		
VS-3	0.81	0.90	0.10	2,211	0.81	2,719	2,166	346.3	99.57	16.3	6.121	3.537	1.876	2.251	1.584	0.719
VS-4	0.96			1,690	0.96	1,765			25.18	19.1	1.315			0.745		
VS-5	0.94			2,288	0.94	2,428			78.85	18.9	4.183			1.723		
VS-6	0.92			1,807	0.92	1,960			84.51	18.4	4.583			2.338		
RX-1	1.02			1,273	1.02	1,246			47.90	20.4	2.344			1.881		
RX-2	0.75			1,790	0.75	2,372			14.88	15.1	0.986			0.416		
RX-3	0.88	0.94	0.38	1,843	0.88	2,100	2,015	857.7	52.08	17.6	2.966	2.766	1.549	1.413	1.520	0.704
RX-4	1.00			2,663	1.00	2,667			59.23	20.0	2.967			1.112		
RX-5	0.41			1,202	0.41	2,966			44.82	8.10	5.530			1.865		
RX-6	1.56			1,153	1.56	741			56.12	31.1	1.803			2.434		
RN-1	0.68			733.3	0.68	1,072			39.06	13.7	2.855			2.663		
RN-2	1.20			2,054	1.20	1,710			59.05	24.0	2.458			1.437		
RN-3	1.08	0.93	0.19	1,552	1.08	1,440	1,666	723.9	90.67	21.6	4.207	2.663	1.391	2.922	1.630	1.040
RN-4	0.90			1,859	0.90	2,076			57.91	17.9	3.233			1.558		
RN-5	0.92			2,613	0.92	2,843			57.72	18.4	3.140			1.104		
RN-6	0.79			676.4	0.79	853			1.317	15.9	0.083			0.097		
RV-1	0.63			636.6	0.63	1,008			43.26	12.6	3.426			3.398		
RV-2	1.16			1,695	1.16	1,458			22.11	23.3	0.951			0.652		
RV-3	0.67	1.04	0.42	706.0	0.67	1,050	1,226	411.82	1.325	13.4	0.099	1.750	1.490	0.094	1.427	1.181
RV-4	1.02			875.0	1.02	859			29.99	20.4	1.472			1.714		
RV-5	1.79			1,831	1.79	1,022			29.09	35.8	0.812			0.794		
RV-6	0.95			1,871	0.95	1,960			71.43	19.1	3.743			1.909		
RC-1	0.77			1,292	0.77	1,686			61.95	15.3	4.042			2.397		
RC-2	0.67			1,082	0.67	1,609			59.90	20.2	2.970			1.845		
RC-3	0.73	0.70	0.10	1,521	0.73	2,097	2,209	560.9	8.522	14.5	0.588	3.321	2.236	0.280	1.496	0.858
RC-4	0.73			2,004	0.73	2,741			51.55	14.6	3.526			1.286		
RC-5	0.52			1,106	0.52	2,116			26.75	15.7	1.706			0.806		
RC-6	0.80			2,410	0.80	3,006			113.7	16.0	7.094			2.360		
RS-1	0.53			2,058	0.53	3,893			117.2	10.6	11.09			2.848		
RS-2	0.87			2,027	0.87	2,325			71.17	17.4	4.080			1.755		
RS-3	0.71	0.88	0.38	1,674	0.71	2,356	2,179	935.9	68.28	14.2	4.804	4.202	3.695	2.039	1.683	0.812
RS-4	0.71			1,032	0.71	1,447			11.25	14.3	0.788			0.545		
RS-5	0.80			1,217	0.80	1,513			24.46	16.1	1.520			1.005		
RS-6	1.62			2,500	1.62	1,539			95.24	32.5	2.933			1.905		

Table B.7 Skeletal muscle continued...

Rat	Protein			Citrate synthase					Complex I							
				CSA.prot^{-1}					CIA.prot^{-1}					CIA.UCS^{-1}		
	P_{CON}	Mean	SD	CSA	P_{CSA}	Activity	Mean	SD	CIA	P_{CIA}	Activity	Mean	SD	Activity	Mean	SD
RX-E1	0.83	N/A		1,969	0.83	2,386	N/A		23.68	16.5	1.435	N/A		0.601	N/A	
RX-E2	1.02			2,706	1.02	2,641			96.01	20.5	4.684			1.774		
RV-E1	1.58			1,392	1.58	881.2			51.47	31.6	1.629			1.849		

Rats and corresponding data points that were randomly excluded from the main study are listed at the bottom of the table in grey text and designated the codes RX-E1, RX-E2 and RV-E1 for rats from dose groups RX and RV respectively. The aforementioned rats were excluded based on the random number generator of STATISTICA™, and was applied consistently for all parameter data sets. CIA = complex I activity in μmol.min^{-1}, CIA.prot^{-1} = complex I activity in terms of protein in μmol.min^{-1}.μg^{-1}, CIA.UCS^{-1} = complex I activity per units citrate synthase in nmol.min^{-1}.UCS^{-1}, CSA = citrate synthase activity in μmol.min^{-1}, CSA.prot^{-1} = citrate synthase activity in terms of protein expressed in μmol.min^{-1}.μg^{-1}, P_{CIA} = amount of protein used in reaction for complex I activity, P_{CON} = protein concentration of mitochondrial isolate in μg.μL^{-1}, P_{CSA} = amount of protein used in the reaction for citrate synthase activity, SD = standard deviation. Rats were treated with NN = no dose regimen, VX = vehicle and sacrificed, VN = vehicle and no dose, VV = vehicle and vehicle, VC = vehicle and CoQ_{10}, VS = vehicle and succinate, RX = rotenone and sacrificed, RN = rotenone and no dose, RV = rotenone and vehicle, RC = rotenone and CoQ_{10}, RS = rotenone and succinate.

Table B.8 lists the complex I, citrate synthase and protein concentration data generated from the rat main study. A volume of 10 μL from a 1:10 dilution of the mitochondrial isolate was used for assaying citrate synthase, while a volume of 5 μL was used for the successful determination of complex I activity.

Table B.8 Liver tissue complex I data generated from the rat main study

Rat	Protein			Citrate synthase					Complex I							
				CSA.prot^{-1}					CIA.prot^{-1}					CIA.UCS^{-1}		
	P_{CON}	Mean	SD	CSA	P_{CSA}	Activity	Mean	SD	CIA	P_{CIA}	Activity	Mean	SD	Activity	Mean	SD
NN-1	4.65	5.80	0.82	1,428	4.65	307.4	289.7	44.0	116.9	23.2	5.032	4.221	0.866	16.37	14.59	2.356
NN-2	7.10			1,640	7.10	231.0			143.2	35.5	4.034			17.46		
NN-3	5.88			2,020	5.88	343.6			134.4	29.4	4.573			13.31		
NN-4	5.27			1,465	5.27	277.9			104.1	26.4	3.948			14.21		
NN-5	5.87			1,920	5.87	326.9			147.2	29.4	5.012			15.33		
NN-6	6.04			1,518	6.04	251.2			82.35	30.2	2.725			10.85		
VX-1	5.95	7.10	1.01	1,685	5.95	283.2	282.3	51.2	256.3	29.7	8.618	8.212	1.446	30.43	29.78	7.184
VX-2	6.84			1,645	6.84	240.4			293.7	34.2	8.585			35.71		
VX-3	7.16			1,735	7.16	242.3			334.8	35.8	9.352			38.59		
VX-4	8.99			2,356	8.99	262.0			358.7	45.0	7.979			30.45		
VX-5	6.78			2,568	6.78	378.9			314.8	33.9	9.291			24.52		
VX-6	6.86			1,970	6.86	287.2			186.9	34.3	5.449			18.97		
VN-1	5.33	5.06	0.25	1,824	5.33	342.0	281.2	43.5	140.2	26.7	5.257	6.129	1.997	15.37	22.18	8.371
VN-2	5.39			1,262	5.39	234.0			177.7	27.0	6.594			28.18		
VN-3	5.07			1,210	5.07	238.7			77.92	25.3	3.075			12.88		
VN-4	4.94			1,506	4.94	304.8			153.3	24.7	6.210			20.37		
VN-5	4.73			1,230	4.73	259.9			218.2	23.7	9.219			35.47		
VN-6	4.92			1,515	4.92	307.9			157.9	24.6	6.417			20.84		
VV-1	4.41	4.73	0.40	1,328	4.41	301.2	291.1	32.4	112.7	22.1	5.108	6.821	1.718	16.96	23.94	7.776
VV-2	4.79			1,329	4.79	277.4			218.1	24.0	9.103			32.82		
VV-3	4.73			1,296	4.73	274.1			121.5	23.6	5.138			18.75		
VV-4	4.57			1,117	4.57	244.6			190.2	22.8	8.327			34.05		
VV-5	4.39			1,375	4.39	313.4			163.9	21.9	7.474			23.85		
VV-6	5.48			1,841	5.48	336.0			158.2	27.4	5.774			17.18		
VC-1	5.68	5.58	0.43	1,489	5.68	262.0	233.3	56.6	192.9	28.4	6.788	4.046	2.043	25.91	17.05	7.988
VC-2	6.24			1,480	6.24	237.4			128.1	31.2	4.107			17.30		
VC-3	5.33			1,082	5.33	203.2			67.64	26.6	2.540			12.50		
VC-4	5.49			995.5	5.49	181.3			26.61	27.5	0.969			5.347		
VC-5	4.98			1,643	4.98	329.9			125.6	24.9	5.044			15.29		
VC-6	5.79			1,076	5.79	185.9			139.8	29.0	4.828			25.98		

Table B.8 Liver tissue continued...

Rat	Protein			Citrate synthase					Complex I							
				CSA.prot^{-1}					CIA.prot^{-1}					CIA.UCS^{-1}		
	P_{CON}	Mean	SD	CSA	P_{CSA}	Activity	Mean	SD	CIA	P_{CIA}	Activity	Mean	SD	Activity	Mean	SD
VS-1	7.34	5.98	0.76	2,141	7.34	291.7	251.5	45.3	89.61	36.7	2.441	3.819	2.250	8.370	16.61	13.08
VS-2	5.21			1,146	5.21	220.0			110.5	26.0	4.241			19.28		
VS-3	6.12			1,665	6.12	272.1			96.57	30.6	3.156			11.60		
VS-4	6.12			1,881	6.12	307.4			92.28	30.6	3.016			9.811		
VS-5	5.46			1,056	5.46	193.6			221.8	27.3	8.129			42.00		
VS-6	5.65			1,266	5.65	224.0			54.53	28.2	1.930			8.616		
RX-1	8.23	6.95	0.94	2,916	8.23	354.2	330.18	29.20	172.9	41.2	4.200	5.45	3.769	11.86	16.72	11.82
RX-2	6.57			2,116	6.57	322.3			156.9	32.8	4.779			14.83		
RX-3	6.75			1,883	6.75	278.8			128.1	33.8	3.792			13.60		
RX-4	7.74			2,749	7.74	355.2			114.3	38.7	2.952			8.313		
RX-5	5.56			1,932	5.56	347.7			109.2	27.8	3.932			11.31		
RX-6	6.84			2,207	6.84	322.9			445.9	34.2	13.05			40.41		
RN-1	5.56	4.76	0.54	1,667	5.56	299.8	320.2	48.8	68.73	27.8	2.472	7.113	2.597	8.245	22.78	10.03
RN-2	4.47			1,334	4.47	298.0			194.0	22.4	8.671			29.10		
RN-3	4.38			1,808	4.38	412.6			156.0	21.9	7.122			17.26		
RN-4	5.32			1,687	5.32	317.1			207.2	26.6	7.789			24.57		
RN-5	4.34			1,403	4.34	323.2			141.5	21.7	6.523			20.18		
RN-6	4.48			1,213	4.48	270.8			226.3	22.4	10.10			37.31		
RV-1	6.17	5.32	1.53	2,240	6.17	363.0	310.23	58.68	101.6	30.9	3.291	5.15	3.433	9.068	16.34	10.20
RV-2	4.23			1,689	4.23	399.0			216.4	21.2	10.22			25.62		
RV-3	4.41			1,161	4.41	263.2			164.1	22.1	7.440			28.26		
RV-4	6.21			1,914	6.21	308.4			162.5	31.0	5.236			16.98		
RV-5	7.48			1,934	7.48	258.7			166.0	37.4	4.441			17.17		
RV-6	3.43			922.8	3.43	269.1			4.271	17.1	0.249			0.926		
RC-1	4.86	5.21	0.61	1,095	4.86	225.5	291.0	54.8	187.7	24.3	7.731	6.604	1.090	34.28	23.30	5.952
RC-2	5.01			1,405	5.01	280.4			147.2	25.0	5.879			20.96		
RC-3	5.58			1,758	5.58	315.2			212.5	27.9	7.618			24.17		
RC-4	5.99			1,740	5.99	290.5			205.3	30.0	6.856			23.60		
RC-5	5.57			2,132	5.57	383.0			186.0	27.8	6.681			17.44		
RC-6	4.29			1,078	4.29	251.6			104.2	21.4	4.859			19.31		
RS-1	7.49	6.18	0.88	2,022	7.49	270.1	241.2	29.6	299.9	37.4	8.010	5.747	2.277	29.66	23.76	8.290
RS-2	5.19			1,236	5.19	238.3			81.60	25.9	3.147			13.21		
RS-3	5.57			1,501	5.57	269.5			119.2	27.8	4.281			15.88		
RS-4	6.78			1,372	6.78	202.4			180.4	33.9	5.323			26.29		
RS-5	5.57			1,431	5.57	257.1			250.8	27.8	9.009			35.04		
RS-6	6.47			1,358	6.47	210.0			152.4	32.3	4.713			22.45		
RX-E1	8.44	N/A		2,468	8.44	292.5	N/A		257.4	42.2	6.100	N/A		20.86	N/A	
RX-E2	6.47			1,893	6.47	292.5			260.6	32.4	8.054			27.53		
RV-E1	3.92			1,528	3.92	390.0			150.1	19.6	7.667			19.66		

Rats and corresponding data points that were randomly excluded from the main study are listed at the bottom of the table in grey text and designated the codes RX-E1, RX-E2 and RV-E1 for rats from dose groups RX and RV respectively. The aforementioned rats were excluded based on the random number generator of STATISTICA™, and was applied consistently for all parameter data sets. CIA = complex I activity in $\mu mol.min^{-1}$, CIA.prot^{-1} = complex I activity in terms of protein in $\mu mol.min^{-1}.\mu g^{-1}$, CIA.UCS^{-1} = complex I activity per units citrate synthase in $nmol.min^{-1}.UCS^{-1}$, CSA = citrate synthase activity in $\mu mol.min^{-1}$, CSA.prot^{-1} = citrate synthase activity in terms of protein expressed in $\mu mol.min^{-1}.\mu g^{-1}$, P_{CIA} = amount of protein used in reaction for complex I activity, P_{CON} = protein concentration of mitochondrial isolate in $\mu g.\mu L^{-1}$, P_{CSA} = amount of protein used in the reaction for citrate synthase activity, SD = standard deviation. Rats were treated with NN = no dose regimen, VX = vehicle and sacrificed, VN = vehicle and no dose, VV = vehicle and vehicle, VC = vehicle and CoQ_{10}, VS = vehicle and succinate, RX = rotenone and sacrificed, RN = rotenone and no dose, RV = rotenone and vehicle, RC = rotenone and CoQ_{10}, RS = rotenone and succinate.

APPENDIX C

ANTIOXIDANT CAPACITY DATA

Antioxidant capacity data was generated from blood and all tissues investigated in the rat main study. Appendix C lists this data for heart muscle, brain tissue, skeletal muscle and liver tissue since it was required that this data be presented in terms of the protein content of each sample. Therefore, it was not necessary to present blood antioxidant capacity data, which was already presented in Section 5.3.2 of Chapter Five. Since a volume of 2 μL from all tissue preparations were used to determine antioxidant capacity, the ORAC values (μM TE) were divided by twice the protein concentrations (P_{CON}) in order to obtain the final antioxidant capacities in terms of protein ($AC.prot^{-1}$).

Heart muscle antioxidant capacity data generated from the rat main study are presented in Table C.1. Means and standard deviations for the data are also presented for each dose group.

Table C.1 Heart muscle antioxidant capacity data generated from the rat main study

Rat	Protein			AC			AC.prot^{-1}		
	P_{CON}	Mean	SD	ORAC	Mean	SD	Value	Mean	SD
NN-1	4.01	4.15	0.32	238.9	219.8	62.83	29.81	26.62	7.80
NN-2	3.61			179.1			24.81		
NN-3	4.33			275.1			31.78		
NN-4	4.08			301.9			36.96		
NN-5	4.45			186.2			20.92		
NN-6	4.44			137.4			15.46		
VX-1	4.18	4.08	0.39	171.2	345.6	175.8	20.47	43.80	24.2
VX-2	3.52			418.4			59.44		
VX-3	3.70			504.5			68.17		
VX-4	4.14			574.7			69.35		
VX-5	4.47			199.5			22.33		
VX-6	4.46			205.3			23.03		
VN-1	3.32	3.73	0.32	413.8	374.7	84.29	62.40	50.58	12.2
VN-2	3.38			400.0			59.20		
VN-3	3.71			235.9			31.82		
VN-4	3.94			309.1			39.26		
VN-5	4.08			445.7			54.58		
VN-6	3.94			443.5			56.23		
VV-1	4.99	4.72	0.54	156.2	263.9	111.5	15.65	27.83	10.2
VV-2	4.46			154.7			17.34		
VV-3	3.98			287.3			36.14		
VV-4	5.58			452.8			40.58		
VV-5	4.67			301.3			32.28		
VV-6	4.62			231.2			25.03		

Table C.1 Heart muscle continued...

Rat	Protein			AC			AC.prot^{-1}		
	P_{CON}	Mean	SD	ORAC	Mean	SD	Value	Mean	SD
VC-1	4.64	4.27	0.44	241.7	265.6	109.4	26.03	31.07	13.0
VC-2	4.01			379.8			47.33		
VC-3	4.39			403.1			45.96		
VC-4	3.85			212.9			27.65		
VC-5	3.85			110.1			14.30		
VC-6	4.89			246.0			25.17		
VS-1	3.61	4.03	1.52	272.2	213.3	83.99	37.68	27.27	10.5
VS-2	3.49			130.6			18.72		
VS-3	3.03			98.00			16.19		
VS-4	3.45			200.7			29.12		
VS-5	7.11			290.1			20.40		
VS-6	3.47			288.2			41.48		
RX-1	4.26	4.05	0.50	164.9	250.5	158.2	19.36	31.38	21.0
RX-2	4.41			364.6			41.29		
RX-3	4.08			327.6			40.17		
RX-4	3.63			467.0			64.37		
RX-5	4.62			93.01			10.07		
RX-6	3.29			85.69			13.03		
RN-1	4.20	4.19	0.30	416.1	338.3	82.43	49.58	40.44	10.0
RN-2	4.51			327.9			36.38		
RN-3	4.04			181.3			22.46		
RN-4	4.30			360.8			42.00		
RN-5	4.41			386.3			43.76		
RN-6	3.69			357.3			48.47		
RV-1	3.75	4.61	0.76	141.6	180.5	94.93	18.88	19.47	9.79
RV-2	4.32			297.3			34.43		
RV-3	5.45			294.8			27.05		
RV-4	5.57			132.4			11.89		
RV-5	4.65			154.2			16.57		
RV-6	3.94			62.89			7.982		
RC-1	3.77	3.90	0.25	322.1	223.3	91.81	42.68	28.62	12.1
RC-2	3.74			305.6			40.85		
RC-3	4.25			217.8			25.63		
RC-4	3.76			84.34			11.22		
RC-5	3.69			152.0			20.60		
RC-6	4.19			257.7			30.76		
RS-1	4.21	4.10	0.52	141.1	151.3	31.60	16.75	18.71	4.64
RS-2	3.16			161.4			25.56		
RS-3	4.02			113.6			14.14		
RS-4	4.72			160.3			16.99		
RS-5	4.34			203.6			23.44		
RS-6	4.15			127.7			15.40		
RX-E1	3.72	N/A		201.7	N/A		27.11	N/A	
RX-E2	4.67			181.9			19.45		
RV-E1	3.59			234.7			32.67		

The final antioxidant capacity data is presented in terms of protein (AC.prot^{-1}) with the units micromolar Trolox equivalents per microgram protein (μM TE.μg^{-1}). AC = antioxidant capacity, ORAC = oxygen radical absorbance capacity, P_{CON} = protein concentration, SD = standard deviation. Rats and corresponding data points that were randomly excluded from the main study are listed at the bottom of the table in grey text and designated the codes RX-E1, RX-E2 and RV-E1 for rats from dose groups RX and RV respectively. The aforementioned rats were excluded based on the random number generator of STATISTICA™, and was applied consistently for all parameter data sets. Rats were treated with NN = no dose regimen, VX = vehicle and sacrificed, VN = vehicle and no dose, VV = vehicle and vehicle, VC = vehicle and CoQ_{10}, VS = vehicle and succinate, RX = rotenone and sacrificed, RN = rotenone and no dose, RV = rotenone and vehicle, RC = rotenone and CoQ_{10}, RS = rotenone and succinate.

Table C.2 lists the brain tissue antioxidant capacity data generated from the rat main study. Descriptive statistics in the form of means and standard deviations are also presented.

Table C.2 Brain tissue antioxidant capacity data generated from the rat main study

Rat	Protein			AC			AC.prot^{-1}		
	P_{CON}	Mean	SD	ORAC	Mean	SD	Value	Mean	SD
NN-1	2.33	2.65	0.20	58.54	75.35	43.49	12.59	14.04	7.66
NN-2	2.50			22.35			4.467		
NN-3	2.69			102.6			19.05		
NN-4	2.75			33.42			6.086		
NN-5	2.75			129.7			23.61		
NN-6	2.86			105.6			18.46		
VX-1	2.26	2.21	0.54	97.31	122.6	51.66	21.54	28.14	12.29
VX-2	1.57			79.93			25.49		
VX-3	2.25			152.2			33.82		
VX-4	1.95			193.8			49.68		
VX-5	3.19			153.0			23.99		
VX-6	2.07			59.30			14.32		
VN-1	2.73	2.61	0.22	181.8	136.1	34.15	33.31	26.17	6.38
VN-2	2.79			169.8			30.40		
VN-3	2.23			134.4			30.08		
VN-4	2.66			110.8			20.84		
VN-5	2.46			126.8			25.74		
VN-6	2.79			92.75			16.65		
VV-1	2.97	2.77	0.20	57.97	83.77	42.44	9.764	14.96	6.95
VV-2	3.08			149.3			24.25		
VV-3	2.64			91.89			17.41		
VV-4	2.69			113.6			21.14		
VV-5	2.60			51.20			9.854		
VV-6	2.63			38.67			7.364		
VC-1	1.94	2.32	0.29	117.7	116.0	25.42	30.41	25.80	8.11
VC-2	2.40			132.2			27.50		
VC-3	1.98			147.4			37.26		
VC-4	2.61			96.20			18.44		
VC-5	2.59			77.22			14.90		
VC-6	2.38			125.0			26.29		
VS-1	2.45	2.40	0.53	155.5	103.7	30.27	31.78	22.51	7.99
VS-2	2.48			97.14			19.56		
VS-3	2.27			64.94			14.28		
VS-4	1.98			94.78			23.89		
VS-5	1.85			116.5			31.55		
VS-6	3.34			93.47			13.97		
RX-1	2.43	2.62	0.31	102.3	80.29	33.71	21.08	15.36	6.30
RX-2	2.62			110.5			21.07		
RX-3	2.19			59.65			13.64		
RX-4	2.90			115.5			19.93		
RX-5	2.59			32.95			6.370		
RX-6	3.02			60.84			10.06		

Table C.2 Brain tissue continued...

Rat	Protein			AC			$AC.prot^{-1}$		
	P_{CON}	Mean	SD	ORAC	Mean	SD	Value	Mean	SD
RN-1	2.67	2.72	0.13	126.0	124.3	23.09	23.63	22.74	3.61
RN-2	2.82			150.3			26.66		
RN-3	2.49			86.74			17.44		
RN-4	2.81			139.7			24.84		
RN-5	2.72			134.3			24.70		
RN-6	2.83			108.7			19.20		
RV-1	2.45	2.50	0.38	118.4	254.0	270.5	24.13	55.30	43.36
RV-2	2.81			84.31			14.98		
RV-3	2.94			144.8			24.65		
RV-4	1.84			431.1			117.0		
RV-5	2.54			257.2			50.66		
RV-6	2.43			488.2			100.3		
RC-1	2.28	2.29	0.16	126.1	90.81	32.93	27.59	19.90	7.03
RC-2	2.55			121.8			23.89		
RC-3	2.27			71.71			15.83		
RC-4	2.37			39.77			8.392		
RC-5	2.15			81.81			19.07		
RC-6	2.10			103.6			24.65		
RS-1	3.31	2.20	0.67	101.8	56.92	29.40	15.40	12.95	5.31
RS-2	2.58			26.00			5.043		
RS-3	1.64			54.11			16.53		
RS-4	1.82			65.80			18.03		
RS-5	2.31			69.89			15.16		
RS-6	1.58			23.86			7.559		
RX-E1	2.79	N/A		97.69	N/A		17.50	N/A	
RX-E2	2.87			128.4			22.38		
RV-E1	2.00			140.3			35.04		

The final antioxidant capacity data is presented in terms of protein ($AC.prot^{-1}$) with the units micromolar Trolox equivalents per microgram protein ($\mu M\ TE.\mu g^{-1}$). AC = antioxidant capacity, ORAC = oxygen radical absorbance capacity, P_{CON} = protein concentration, SD = standard deviation. Rats and corresponding data points that were randomly excluded from the main study are listed at the bottom of the table in grey text and designated the codes RX-E1, RX-E2 and RV-E1 for rats from dose groups RX and RV respectively. The aforementioned rats were excluded based on the random number generator of STATISTICA™, and was applied consistently for all parameter data sets. Rats were treated with NN = no dose regimen, VX = vehicle and sacrificed, VN = vehicle and no dose, VV = vehicle and vehicle, VC = vehicle and CoQ_{10}, VS = vehicle and succinate, RX = rotenone and sacrificed, RN = rotenone and no dose, RV = rotenone and vehicle, RC = rotenone and CoQ_{10}, RS = rotenone and succinate.

The skeletal muscle antioxidant capacity data generated from the rat main study are presented in Table C.3. The means and standard deviations for the various dose groups have also been listed.

Table C.3 Skeletal muscle antioxidant capacity data generated from the rat main study

Rat	Protein			AC			$AC.prot^{-1}$		
	P_{CON}	Mean	SD	ORAC	Mean	SD	Value	Mean	SD
NN-1	5.18	4.90	0.52	84.21	178.4	78.56	8.134	18.73	9.217
NN-2	4.55			126.2			13.87		
NN-3	5.24			244.3			23.32		
NN-4	4.42			269.5			30.49		
NN-5	5.64			115.73			10.26		
NN-6	4.37			230.3			26.33		

Table C.3 Skeletal muscle continued...

Rat	Protein			AC			AC.prot^{-1}		
	P_{CON}	Mean	SD	ORAC	Mean	SD	Value	Mean	SD
VX-1	3.76	3.90	0.45	171.71	223.3	41.34	22.83	28.65	4.014
VX-2	3.15			193.3			30.67		
VX-3	3.80			236.3			31.10		
VX-4	3.99			204.9			25.71		
VX-5	4.22			285.6			33.86		
VX-6	4.47			247.7			27.73		
VN-1	4.36	4.56	0.27	332.1	287.9	40.65	38.12	31.70	5.264
VN-2	4.48			286.3			31.94		
VN-3	4.64			225.0			24.28		
VN-4	4.22			308.4			36.51		
VN-5	4.69			256.6			27.35		
VN-6	4.98			318.8			31.98		
VV-1	5.65	5.17	0.45	222.1	208.2	61.39	19.67	20.33	6.893
VV-2	4.80			161.6			16.84		
VV-3	4.76			325.2			34.18		
VV-4	4.78			163.7			17.11		
VV-5	5.73			184.8			16.13		
VV-6	5.30			191.7			18.07		
VC-1	6.28	5.09	0.83	392.3	255.9	95.38	31.22	24.58	6.714
VC-2	4.79			288.4			30.14		
VC-3	4.65			257.0			27.64		
VC-4	4.79			197.4			20.59		
VC-5	4.11			110.2			13.39		
VC-6	5.92			290.0			24.51		
VS-1	3.71	3.86	0.13	270.2	223.5	42.92	36.38	28.92	5.640
VS-2	4.07			243.4			29.92		
VS-3	3.74			144.6			19.32		
VS-4	3.95			214.2			27.09		
VS-5	3.89			228.0			29.33		
VS-6	3.82			240.7			31.49		
RX-1	4.08	4.59	1.17	227.2	182.8	45.44	27.87	21.77	9.69
RX-2	3.10			225.6			36.37		
RX-3	4.39			142.0			16.16		
RX-4	4.01			194.6			24.23		
RX-5	5.78			192.7			16.68		
RX-6	6.18			114.9			9.30		
RN-1	4.67	4.01	0.49	235.6	208.7	60.15	25.24	25.75	5.992
RN-2	3.61			138.5			19.20		
RN-3	3.37			126.5			18.74		
RN-4	3.82			255.1			33.41		
RN-5	4.35			234.3			26.94		
RN-6	4.24			262.2			30.96		
RV-1	3.72	4.17	0.30	119.1	202.2	104.78	16.00	24.37	13.02
RV-2	4.10			271.2			33.10		
RV-3	4.43			246.7			27.84		
RV-4	3.98			347.9			43.67		
RV-5	4.56			161.6			17.73		
RV-6	4.24			66.66			7.863		

Table C.3 Skeletal muscle continued...

Rat	Protein			AC			AC.prot^{-1}		
	P_{CON}	Mean	SD	ORAC	Mean	SD	Value	Mean	SD
RC-1	4.17	3.90	0.39	168.3	181.6	51.63	20.17	23.58	7.569
RC-2	4.10			214.7			26.17		
RC-3	4.42			132.3			14.96		
RC-4	3.44			115.2			16.76		
RC-5	3.59			247.2			34.48		
RC-6	3.66			211.9			28.93		
RS-1	4.22	3.77	0.25	183.1	169.9	40.45	21.70	22.47	4.892
RS-2	3.68			125.7			17.11		
RS-3	3.50			163.1			23.27		
RS-4	3.87			208.3			26.90		
RS-5	3.77			217.3			28.81		
RS-6	3.59			122.1			17.00		
RX-E1	4.16	N/A		195.1	N/A		23.44	N/A	
RX-E2	3.47			346.4			49.97		
RV-E1	4.96			244.8			24.67		

The final antioxidant capacity data is presented in terms of protein (AC.prot^{-1}) with the units micromolar Trolox equivalents per microgram protein (μM TE.μg^{-1}). AC = antioxidant capacity, ORAC = oxygen radical absorbance capacity, P_{CON} = protein concentration, SD = standard deviation. Rats and corresponding data points that were randomly excluded from the main study are listed at the bottom of the table in grey text and designated the codes RX-E1, RX-E2 and RV-E1 for rats from dose groups RX and RV respectively. The aforementioned rats were excluded based on the random number generator of STATISTICA™, and was applied consistently for all parameter data sets. Rats were treated with NN = no dose regimen, VX = vehicle and sacrificed, VN = vehicle and no dose, VV = vehicle and vehicle, VC = vehicle and CoQ_{10}, VS = vehicle and succinate, RX = rotenone and sacrificed, RN = rotenone and no dose, RV = rotenone and vehicle, RC = rotenone and CoQ_{10}, RS = rotenone and succinate.

Liver tissue antioxidant capacity data that was generated from the rat main study are listed in Table C.4. The mean and standard deviation descriptive statistics are also presented.

Table C.4 Liver tissue antioxidant capacity data generated from the rat main study

Rat	Protein			AC			AC.prot^{-1}		
	P_{CON}	Mean	SD	ORAC	Mean	SD	Value	Mean	SD
NN-1	8.62	8.60	0.67	219.6	422.4	184.5	12.75	24.75	11.21
NN-2	8.35			345.8			20.71		
NN-3	9.50			677.9			35.67		
NN-4	8.50			367.3			21.60		
NN-5	7.55			622.8			41.23		
NN-6	9.09			300.6			16.54		
VX-1	8.99	8.26	0.75	507.4	553.3	121.2	28.21	33.35	5.836
VX-2	8.27			555.6			33.58		
VX-3	9.03			701.6			38.84		
VX-4	7.24			506.4			34.95		
VX-5	8.52			675.4			39.63		
VX-6	7.51			373.6			24.88		
VN-1	7.83	7.85	0.58	608.7	595.5	71.2	38.89	37.89	2.630
VN-2	8.11			596.8			36.82		
VN-3	6.81			515.2			37.81		
VN-4	8.05			636.5			39.54		
VN-5	7.74			516.5			33.36		
VN-6	8.55			699.3			40.92		

Table C.4 Liver tissue continued...

Rat	Protein			AC			$AC.prot^{-1}$		
	P_{CON}	Mean	SD	ORAC	Mean	SD	Value	Mean	SD
VV-1	8.04	9.43	0.76	649.6	444.6	128.5	40.41	23.97	8.828
VV-2	9.39			271.6			14.47		
VV-3	10.24			469.5			22.93		
VV-4	9.68			433.0			22.36		
VV-5	9.88			488.0			24.71		
VV-6	9.37			355.5			18.97		
VC-1	9.49	10.27	1.05	481.9	594.2	121.8	25.39	29.06	5.990
VC-2	9.07			690.0			38.02		
VC-3	9.82			615.5			31.33		
VC-4	10.60			582.3			27.46		
VC-5	10.60			436.9			20.60		
VC-6	12.02			758.8			31.57		
VS-1	6.93	7.90	1.12	458.2	564.3	74.04	33.04	35.97	4.281
VS-2	6.99			564.2			40.35		
VS-3	6.92			551.5			39.85		
VS-4	8.80			519.2			29.50		
VS-5	9.51			661.6			34.78		
VS-6	8.24			631.2			38.32		
RX-1	6.87	7.21	0.64	508.4	330.7	98.61	37.02	23.13	7.639
RX-2	6.72			312.6			23.26		
RX-3	6.31			203.2			14.56		
RX-4	6.98			325.9			24.46		
RX-5	6.66			311.7			19.18		
RX-6	8.13			322.2			20.31		
RN-1	7.93	6.20	0.44	415.6	413.9	77.10	32.66	33.30	5.107
RN-2	6.36			337.5			31.39		
RN-3	5.37			305.6			24.32		
RN-4	6.28			465.4			37.76		
RN-5	6.16			500.1			37.47		
RN-6	6.67			459.3			36.21		
RV-1	6.34	7.37	0.95	237.3	288.3	269.7	17.58	18.17	15.51
RV-2	8.88			581.9			32.75		
RV-3	8.13			665.0			40.91		
RV-4	7.06			139.0			9.847		
RV-5	7.09			58.84			4.147		
RV-6	6.31			47.71			3.781		
RC-1	6.81	7.09	0.68	519.7	446.0	71.53	38.15	31.74	6.354
RC-2	7.44			446.4			30.00		
RC-3	6.99			345.8			24.73		
RC-4	6.97			373.8			26.83		
RC-5	8.18			490.1			29.95		
RC-6	6.14			500.3			40.76		
RS-1	9.11	7.08	1.14	515.5	396.3	135.2	28.29	27.54	7.025
RS-2	5.83			260.3			22.33		
RS-3	6.77			393.9			29.07		
RS-4	7.04			447.9			31.80		
RS-5	7.43			546.9			36.83		
RS-6	6.30			213.6			16.94		

Table C.4 Liver tissue continued...

Rat	Protein			AC			$AC.prot^{-1}$		
	P_{CON}	Mean	SD	ORAC	Mean	SD	Value	Mean	SD
RX-E1	6.82	N/A		485.8	N/A		35.63	N/A	
RX-E2	6.31			310.1			24.57		
RV-E1	8.42			488.8			29.02		

The final antioxidant capacity data is presented in terms of protein ($AC.prot^{-1}$) with the units micromolar Trolox equivalents per microgram protein ($\mu M\ TE.\mu g^{-1}$). AC = antioxidant capacity, ORAC = oxygen radical absorbance capacity, P_{CON} = protein concentration, SD = standard deviation. Rats and corresponding data points that were randomly excluded from the main study are listed at the bottom of the table in grey text and designated the codes RX-E1, RX-E2 and RV-E1 for rats from dose groups RX and RV respectively. The aforementioned rats were excluded based on the random number generator of STATISTICA™, and was applied consistently for all parameter data sets. Rats were treated with NN = no dose regimen, VX = vehicle and sacrificed, VN = vehicle and no dose, VV = vehicle and vehicle, VC = vehicle and CoQ_{10}, VS = vehicle and succinate, RX = rotenone and sacrificed, RN = rotenone and no dose, RV = rotenone and vehicle, RC = rotenone and CoQ_{10}, RS = rotenone and succinate.

APPENDIX D

GLUTATHIONE CONCENTRATION DATA

Glutathione concentrations were determined successfully from blood and liver samples collected during the rat main study. The GSH/GSSG ratios were determined by assaying for total glutathione and GSSG concentrations in exclusive samples. The GSH content was subsequently determined by subtracting twice the concentration of GSSG from that of the total glutathione amount, since the oxidised is present in twice the molar concentration in living cells. Finally, the ratio of GSH to GSSG was calculated. The data presented in Table D.1 and D.2 for blood and liver tissue glutathione concentrations are listed in a maximum of four significant numbers.

Blood glutathione concentrations generated from the rat main study are presented in Table D.1. Basic statistics in the form of means and standard deviations are also listed.

Table D.1 Blood glutathione data generated from the rat main study

Rat	Total glutathione			GSSG			GSH	GSH/GSSG		
	Conc	Mean	SD	Conc	Mean	SD	Conc	Ratio	Mean	SD
NN-1	748.5	837.6	103	73.19	95.27	20.9	602.1	8.23	7.10	1.86
NN-2	873.8			85.15			703.5	8.26		
NN-3	991.8			106.2			779.4	7.34		
NN-4	814.8			83.23			648.4	7.79		
NN-5	707.9			131.5			444.8	3.38		
NN-6	888.6			92.32			703.9	7.62		
VX-1	655.7	647.5	51.3	92.80	92.4	7.61	470.1	5.07	5.07	1.07
VX-2	655.7			92.32			471.1	5.10		
VX-3	719.2			78.93			561.3	7.11		
VX-4	581.7			91.85			398.0	4.33		
VX-5	595.8			96.63			402.5	4.17		
VX-6	676.9			101.9			473.1	4.64		
VN-1	602.8	713.9	74.4	84.67	91.21	20.6	433.5	5.12	6.18	2.10
VN-2	715.6			113.8			487.9	4.29		
VN-3	676.9			56.92			563.0	9.89		
VN-4	701.5			94.72			512.1	5.41		
VN-5	817.9			87.06			643.7	7.39		
VN-6	768.5			110.0			548.5	4.99		
VV-1	715.6	732.1	45.3	126.3	125.3	6.97	463.1	3.67	3.86	0.47
VV-2	786.1			128.2			529.7	4.13		
VV-3	705.1			130.1			444.8	3.42		
VV-4	793.2			122.0			549.2	4.50		
VV-5	701.5			132.0			437.5	3.31		
VV-6	691.0			112.9			465.2	4.12		

Table D.1 Blood continued...

Rat	Total glutathione			GSSG			GSH	GSH/GSSG		
	Conc	Mean	SD	Conc	Mean	SD	Conc	Ratio	Mean	SD
VC-1	836.9	838.2	37.4	78.45	85.71	16.8	680.0	8.67	8.12	2.10
VC-2	789.0			55.97			677.1	12.1		
VC-3	822.2			99.02			624.2	6.30		
VC-4	844.3			91.37			661.6	7.24		
VC-5	833.3			87.54			658.2	7.52		
VC-6	903.3			101.9			699.5	6.87		
VS-1	774.3	832.0	37.1	118.6	127.7	14.7	537.0	4.53	4.57	0.62
VS-2	881.2			150.7			579.8	3.85		
VS-3	811.1			116.2			578.7	4.98		
VS-4	848.0			136.8			574.4	4.20		
VS-5	825.9			131.5			562.8	4.28		
VS-6	851.7			112.4			626.9	5.58		
RX-1	729.7	746.5	29.0	129.2	111.8	12.3	471.4	3.65	4.74	0.68
RX-2	740.3			91.85			556.6	6.06		
RX-3	743.8			109.1			525.7	4.82		
RX-4	786.1			124.4			537.4	4.32		
RX-5	693.2			98.54			496.1	5.03		
RX-6	755.8			115.3			525.3	4.56		
RN-1	676.9	791.4	78.0	132.0	115.4	23.2	412.8	3.13	5.12	1.75
RN-2	796.7			110.0			576.7	5.24		
RN-3	895.4			91.37			712.7	7.80		
RN-4	810.8			131.5			547.7	4.16		
RN-5	839.0			141.6			555.8	3.93		
RN-6	729.7			86.10			557.5	6.47		
RV-1	578.1	741.3	156	61.71	116.0	36.1	454.7	7.37	4.74	1.69
RV-2	863.7			141.1			581.5	4.12		
RV-3	965.9			168.4			629.2	3.74		
RV-4	539.4			109.1			321.2	2.95		
RV-5	835.5			130.6			574.3	4.40		
RV-6	687.4			119.6			448.3	3.75		
RC-1	936.5	938.3	60.1	93.28	137.8	31.9	749.9	8.04	5.15	1.83
RC-2	914.4			159.3			595.8	3.74		
RC-3	903.3			187.0			529.2	2.83		
RC-4	918.1			129.6			658.8	5.08		
RC-5	1058			129.6			798.9	6.16		
RC-6	899.6			128.2			643.2	5.02		
RS-1	980.7	978.9	116	139.2	134.4	27.7	702.3	5.05	5.53	1.71
RS-2	1018			103.3			811.0	7.85		
RS-3	1047			146.9			753.4	5.13		
RS-4	903.3			180.3			542.6	3.01		
RS-5	1128			124.4			879.5	7.07		
RS-6	796.4			112.4			571.6	5.08		
RX-E1	743.8	N/A		112.4	N/A		519.0	4.62	N/A	
RX-E2	779.1			113.8			551.4	4.84		
RV-E1	719.2			81.32			556.5	6.84		

Glutathione concentrations are listed in micromolar (μM) units. The amount of reduced glutathione (GSH) is calculated by subtracting twice the oxidised glutathione (GSSG) concentration from that of total glutathione. Conc = concentration, GSH = reduced glutathione, GSSG = oxidised glutathione, SD = standard deviation. Rats and corresponding data points that were randomly excluded from the main study are listed at the bottom of the table in grey text and designated the codes RX-E1, RX-E2 and RV-E1 for rats from dose groups RX and RV respectively. The aforementioned rats were excluded based on the random number generator of STATISTICA™, and was applied consistently for all parameter data sets. Rats were treated with NN = no dose regimen, VX = vehicle and sacrificed, VN = vehicle and no dose, VV = vehicle and vehicle, VC = vehicle and CoQ_{10}, VS = vehicle and succinate, RX = rotenone and sacrificed, RN = rotenone and no dose, RV = rotenone and vehicle, RC = rotenone and CoQ_{10}, RS = rotenone and succinate.

Liver tissue was collected and successfully assayed for glutathione concentrations, as presented in Table D.2. As with the blood data, means and standard deviations are presented for liver glutathione. It should be noted that protein concentrations were taken into account when calculating liver GSH/GSSG ratios. When assaying for total glutathione, a 1:200 dilution of the preparation was made, of which a volume of 50 μL was used in the reaction. The GSSG samples were diluted 1:30 and 50 μL also used in the assay. Therefore, taking into account the abovementioned dilution factors and volumes, the total glutathione and oxidised glutathione in terms of protein, denoted TG.prot^{-1} and OG.prot^{-1}, were calculated. Finally, the amount of GSH was determined by subtracting twice the OG.prot^{-1} value from that of TG.prot^{-1}, and the ratios calculated accordingly.

Table D.2 Liver tissue glutathione data generated from the rat main study

Rat	Protein			Total glutathione				GSSG				GSH	GSH/GSSG (in terms of protein)		
	P_{CON}	Mean	SD	TG_{CON}	TG.prot^{-1}	Mean	SD	OG_{CON}	OG.prot^{-1}	Mean	SD	RG.prot^{-1}	Ratio	Mean	SD
NN-1	8.53	8.52	0.67	585.4	274.5	243.1	17.72	12.44	0.875	11.27	1.54	272.7	311.6	305.6	15.17
NN-2	8.26			516.5	250.0			11.03	0.801			248.4	310.1		
NN-3	9.42			560.3	238.0			13.15	0.838			236.3	282.1		
NN-4	8.42			468.0	222.4			9.860	0.703			221.0	314.4		
NN-5	7.47			446.1	238.9			9.156	0.736			237.5	322.8		
NN-6	9.00			529.0	235.0			11.97	0.798			233.4	292.6		
VX-1	9.03	8.30	0.75	473.3	209.6	230.1	14.14	19.24	1.278	20.88	3.85	207.0	162.0	154.5	31.23
VX-2	8.31			476.3	229.2			18.78	1.355			226.5	167.1		
VX-3	9.07			520.6	229.6			17.63	1.166			227.2	194.8		
VX-4	7.28			438.2	240.6			23.59	1.943			236.7	121.8		
VX-5	8.56			474.8	221.9			18.55	1.300			219.3	168.6		
VX-6	7.55			471.8	250.0			27.48	2.185			245.7	112.4		
VN-1	7.99	8.01	0.58	448.9	224.8	220.5	12.33	17.40	1.307	14.24	2.32	222.2	169.9	207.6	25.51
VN-2	8.27			455.0	220.1			14.43	1.047			218.1	208.2		
VN-3	6.97			410.7	235.5			10.99	0.946			233.6	247.1		
VN-4	8.21			442.7	215.7			13.28	0.971			213.8	220.2		
VN-5	7.90			393.9	199.4			13.05	0.991			197.4	199.2		
VN-6	8.71			494.7	227.3			16.26	1.121			225.0	200.8		
VV-1	8.23	9.62	0.76	511.5	248.6	209.4	22.04	16.72	1.219	14.58	2.36	246.2	202.0	230.6	28.62
VV-2	9.58			525.2	219.3			18.09	1.133			217.0	191.5		
VV-3	10.4			493.1	189.1			12.82	0.738			187.7	254.3		
VV-4	9.87			511.5	207.2			14.66	0.891			205.4	230.6		
VV-5	10.1			500.8	199.0			12.60	0.751			197.5	263.1		
VV-6	9.56			461.1	192.9			12.60	0.791			191.4	242.0		
VC-1	10.0	10.5	0.63	494.6	197.6	201.1	28.09	14.32	0.858	13.46	1.37	195.9	228.2	262.2	51.51
VC-2	9.60			588.5	245.3			10.80	0.675			243.9	361.3		
VC-3	10.3			540.0	208.8			14.09	0.817			207.1	253.6		
VC-4	11.1			522.8	187.9			13.38	0.722			186.5	258.4		
VC-5	11.1			444.5	159.8			13.62	0.734			158.3	215.6		
VC-6	10.9			563.4	207.3			14.56	0.803			205.7	256.1		

Table D.2 Liver tissue continued...

Rat	Protein			Total glutathione				GSSG				GSH	GSH/GSSG (in terms of protein)		
	P_{CON}	Mean	SD	TG_{CON}	TG.prot^{-1}	Mean	SD	OG_{CON}	OG.prot^{-1}	Mean	SD	RG.prot^{-1}	Ratio	Mean	SD
VS-1	6.98	8.22	1.05	472.7	271.0	245.5	20.13	9.391	0.808	11.46	2.48	269.4	333.6	297.3	49.92
VS-2	8.68			525.9	242.2			9.625	0.665			240.9	362.2		
VS-3	6.96			468.0	268.9			10.33	0.890			267.1	300.0		
VS-4	8.84			513.4	232.2			15.73	1.067			230.0	215.6		
VS-5	9.55			566.6	237.2			13.15	0.826			235.6	285.3		
VS-6	8.28			458.6	221.5			10.56	0.766			220.0	287.4		
RX-1	7.08	7.06	0.53	429.0	242.3	203.7	37.32	19.24	1.630	23.46	14.6	239.0	146.7	163.8	131.3
RX-2	6.94			264.1	152.3			43.74	3.784			144.8	38.26		
RX-3	7.20			303.8	168.9			35.50	2.960			163.0	55.06		
RX-4	6.88			374.0	217.5			26.34	2.297			212.9	92.69		
RX-5	6.33			381.9	241.4			8.452	0.801			239.8	299.2		
RX-6	7.96			397.5	199.8			7.513	0.566			198.7	350.8		
RN-1	6.46	6.30	0.44	438.2	271.1	302.5	37.82	10.53	0.978	24.85	31.6	269.2	275.3	220.4	98.28
RN-2	5.48			432.1	315.5			11.91	1.304			312.9	239.9		
RN-3	6.39			426.0	266.8			11.91	1.119			264.6	236.5		
RN-4	6.27			450.4	287.5			15.11	1.447			284.6	196.7		
RN-5	6.78			516.0	304.6			10.31	0.912			302.8	331.8		
RN-6	6.44			595.4	369.5			89.31	8.315			352.9	42.4		
RV-1	6.94	7.40	0.90	410.7	236.7	251.6	31.76	34.58	2.989	20.90	11.0	230.7	77.18	180.8	90.54
RV-2	8.84			577.1	261.0			13.51	0.917			259.2	282.7		
RV-3	8.09			596.9	295.2			13.74	1.019			293.1	287.6		
RV-4	7.08			487.0	275.0			35.50	3.006			269.0	89.47		
RV-5	7.12			367.9	206.7			13.74	1.158			204.4	176.5		
RV-6	6.34			372.5	235.2			14.32	1.356			232.5	171.4		
RC-1	7.33	7.12	0.68	496.1	270.6	285.5	52.78	11.97	0.980	13.03	3.16	268.7	274.3	263.1	44.81
RC-2	7.37			419.5	227.6			9.625	0.783			226.0	288.5		
RC-3	6.92			601.0	347.2			14.32	1.241			344.7	277.8		
RC-4	6.90			475.8	275.9			10.80	0.939			274.0	291.7		
RC-5	8.11			486.8	240.0			18.55	1.371			237.2	173.0		
RC-6	6.07			533.7	351.7			12.91	1.276			349.1	273.6		
RS-1	9.07	7.08	1.13	521.2	229.8	267.4	23.64	10.80	0.714	9.665	2.78	228.4	319.7	340.1	79.49
RS-2	5.79			427.3	295.3			7.513	0.779			293.7	377.2		
RS-3	6.82			432.0	253.4			14.32	1.260			250.9	199.1		
RS-4	7.09			468.0	264.2			7.278	0.616			263.0	426.7		
RS-5	7.39			525.9	284.8			10.56	0.858			283.1	329.9		
RS-6	6.35			439.8	277.2			7.513	0.710			275.7	388.3		
RX-E1	7.03	N/A		415.3	236.2	N/A		34.12	2.911	N/A		230.3	79.13	N/A	
RX-E2	6.53			355.7	218.0			31.83	2.926			212.1	72.50		
RV-E1	8.61			552.7	256.7			9.847	0.686			255.3	372.2		

Ratios were determined from final glutathione concentrations in micromolar per microgram ($\mu M.\mu g^{-1}$) protein. The amount of reduced glutathione (GSH) was calculated by subtracting twice the oxidised glutathione (GSSG) concentration from that of total glutathione. GSH = reduced glutathione, GSSG = oxidised glutathione, OG_{CON} = concentration of oxidised glutathione in micromolar (μM), OG.prot^{-1} = oxidised glutathione concentration in terms of protein ($\mu M.\mu g^{-1}$), P_{CON} = protein concentration in microgram per microlitre ($\mu g.\mu L^{-1}$), RG.prot^{-1} = reduced glutathione in terms of protein ($\mu M.\mu g^{-1}$), TG_{CON} = concentration of total glutathione in micromolar (μM), TG.prot^{-1} = total glutathione concentration in terms of protein ($\mu M.\mu g^{-1}$), SD = standard deviation. Rats and corresponding data points that were randomly excluded from the main study are listed at the bottom of the table in grey text and designated the codes RX-E1, RX-E2 and RV-E1 for rats from dose groups RX and RV respectively. The aforementioned rats were excluded based on the random number generator of STATISTICA™, and was applied consistently for all parameter data sets. Rats were treated with NN = no dose regimen, VX = vehicle and sacrificed, VN = vehicle and no dose, VV = vehicle and vehicle, VC = vehicle and CoQ_{10}, VS = vehicle and succinate, RX = rotenone and sacrificed, RN = rotenone and no dose, RV = rotenone and vehicle, RC = rotenone and CoQ_{10}, RS = rotenone and succinate.

APPENDIX E

LACTATE AND PYRUVATE DATA

The ratio of lactate to pyruvate was determined in the rat main study from blood, heart muscle, brain tissue, skeletal muscle and liver tissue. The individual lactate and pyruvate concentrations are presented in Table E.1 to E.5. The data is presented with a maximum of four significant figures. As presented in Section 4.4.7 of Chapter Four, samples were deproteinised and hence did not require the expression of L/P ratios in terms of protein.

Blood lactate and pyruvate concentrations are presented in Table E.1. Means and standard deviation descriptive statistics are also presented for the various dose groups.

Table E.1 Blood lactate and pyruvate data generated from the rat main study

Rat	Lactate			Pyruvate			Lactate/Pyruvate		
	Conc	Mean	SD	Conc	Mean	SD	Ratio	Mean	SD
NN-1	220.2	282.3	81.93	461.0	341.0	82.36	0.478	0.906	0.429
NN-2	287.4			314.0			0.915		
NN-3	251.3			322.6			0.779		
NN-4	185.7			411.4			0.451		
NN-5	340.5			230.0			1.480		
NN-6	408.7			306.7			1.332		
VX-1	168.1	200.6	111.1	518.3	513.6	122.6	0.324	0.403	0.230
VX-2	88.88			403.7			0.220		
VX-3	256.0			342.0			0.748		
VX-4	110.8			535.9			0.207		
VX-5	392.7			621.6			0.632		
VX-6	187.4			660.0			0.284		
VN-1	544.7	262.8	180.1	317.2	478.2	118.1	1.717	0.661	0.612
VN-2	368.6			365.5			1.008		
VN-3	92.74			570.8			0.162		
VN-4	157.1			625.9			0.251		
VN-5	319.0			505.0			0.632		
VN-6	94.68			484.7			0.195		
VV-1	457.2	220.0	120.0	478.2	443.5	118.1	0.956	0.539	0.315
VV-2	186.6			373.1			0.500		
VV-3	137.4			545.9			0.252		
VV-4	221.0			244.2			0.905		
VV-5	146.0			461.9			0.316		
VV-6	171.5			557.8			0.307		
VC-1	127.1	178.9	75.29	254.7	353.9	76.01	0.499	0.542	0.321
VC-2	120.5			412.4			0.292		
VC-3	185.6			351.2			0.528		
VC-4	134.8			386.7			0.348		
VC-5	184.0			444.2			0.414		
VC-6	321.2			274.0			1.172		

Table E.1 Blood continued...

Rat	Lactate			Pyruvate			Lactate/Pyruvate		
	Conc	Mean	SD	Conc	Mean	SD	Ratio	Mean	SD
VS-1	110.6	144.6	69.81	467.4	434.2	98.58	0.237	0.355	0.227
VS-2	138.1			413.9			0.334		
VS-3	155.6			395.7			0.393		
VS-4	64.39			366.3			0.176		
VS-5	272.3			345.5			0.788		
VS-6	126.7			616.2			0.206		
RX-1	652.6	496.2	218.2	455.9	442.9	65.53	1.431	1.121	0.512
RX-2	563.3			565.7			0.996		
RX-3	712.2			200.0			1.822		
RX-4	217.7			399.7			0.545		
RX-5	605.4			442.6			1.368		
RX-6	226.3			402.5			0.562		
RN-1	476.9	514.4	235.0	314.0	495.7	101.0	1.519	1.082	0.541
RN-2	200.0			505.3			0.396		
RN-3	871.7			473.9			1.839		
RN-4	568.0			616.6			0.921		
RN-5	632.4			539.0			1.173		
RN-6	337.5			525.7			0.642		
RV-1	463.5	410.2	187.3	547.6	405.9	108.3	0.846	1.085	0.599
RV-2	284.3			242.1			1.175		
RV-3	227.7			484.2			0.470		
RV-4	711.7			334.1			2.130		
RV-5	512.5			402.1			1.274		
RV-6	261.5			425.6			0.615		
RC-1	357.5	310.3	134.1	310.9	427.7	151.7	1.150	0.765	0.304
RC-2	392.1			408.0			0.961		
RC-3	248.8			286.6			0.868		
RC-4	154.5			531.3			0.291		
RC-5	511.0			681.0			0.750		
RC-6	197.8			348.3			0.568		
RS-1	350.8	342.5	302.9	393.5	406.2	162.3	0.891	0.806	0.756
RS-2	184.6			390.3			0.473		
RS-3	17.81			125.5			0.142		
RS-4	271.8			604.4			0.450		
RS-5	910.6			401.9			2.266		
RS-6	319.2			521.3			0.612		
RX-E1	283.5	N/A		524.3	N/A		0.541	N/A	
RX-E2	526.4			571.1			0.922		
RV-E1	298.2			501.3			0.595		

Lactate and pyruvate concentrations are presented in micromole per litre ($\mu mol.L^{-1}$) concentrations. Conc = concentration, SD = standard deviation. Rats and corresponding data points that were randomly excluded from the main study are listed at the bottom of the table in grey text and designated the codes RX-E1, RX-E2 and RV-E1 for rats from dose groups RX and RV respectively. The aforementioned rats were excluded based on the random number generator of STATISTICA™, and was applied consistently for all parameter data sets. Rats were treated with NN = no dose regimen, VX = vehicle and sacrificed, VN = vehicle and no dose, VV = vehicle and vehicle, VC = vehicle and CoQ_{10}, VS = vehicle and succinate, RX = rotenone and sacrificed, RN = rotenone and no dose, RV = rotenone and vehicle, RC = rotenone and CoQ_{10}, RS = rotenone and succinate.

Table E.2 lists the heart muscle lactate and pyruvate concentrations as well as the L/P ratios generated from the rat main study. Descriptive statistics including the means and standard deviations are also presented.

Table E.2 Heart muscle lactate and pyruvate data generated from the rat main study

Rat	Lactate			Pyruvate			Lactate/Pyruvate		
	Conc	Mean	SD	Conc	Mean	SD	Ratio	Mean	SD
NN-1	1,161	983.9	110.7	44.24	39.94	5.750	26.24	25.17	5.174
NN-2	1,077			33.27			32.37		
NN-3	954.1			31.86			29.95		
NN-4	875.1			43.86			19.95		
NN-5	917.1			43.62			21.03		
NN-6	919.2			42.79			21.49		
VX-1	1,133	1,136	88.33	28.37	38.40	6.150	39.93	30.25	5.526
VX-2	1,013			34.23			29.61		
VX-3	1,123			45.24			24.83		
VX-4	1,083			42.33			25.59		
VX-5	1,269			38.90			32.62		
VX-6	1,194			41.33			28.89		
VN-1	1,048	1,117	117.0	45.82	50.58	3.488	22.88	22.17	2.660
VN-2	1,238			54.62			22.67		
VN-3	1,174			47.95			24.48		
VN-4	985.6			54.40			18.12		
VN-5	1,247			49.97			24.95		
VN-6	1,009			50.69			19.91		
VV-1	950.4	923.6	51.55	24.09	39.11	11.42	39.46	25.39	7.855
VV-2	917.8			37.86			24.24		
VV-3	877.3			33.09			26.51		
VV-4	1,014			47.97			21.14		
VV-5	886.3			35.37			25.06		
VV-6	895.7			56.31			15.91		
VC-1	1,098	1,072	148.9	49.02	47.01	4.902	22.41	23.10	4.841
VC-2	1,076			45.27			23.77		
VC-3	996.8			48.05			20.75		
VC-4	895.7			43.17			20.75		
VC-5	1,027			55.14			18.62		
VC-6	1,339			41.42			32.33		
VS-1	1,087	1,136	125.6	59.03	52.20	8.146	18.42	22.52	5.958
VS-2	1,301			46.26			28.13		
VS-3	1,276			41.42			30.81		
VS-4	1,119			47.39			23.61		
VS-5	1,036			60.72			17.05		
VS-6	997.5			58.36			17.09		
RX-1	1,043	1,061	147.1	43.85	40.54	4.566	23.77	26.48	4.937
RX-2	914.0			45.08			20.27		
RX-3	885.4			34.58			25.60		
RX-4	1,081			44.33			24.39		
RX-5	1,179			35.87			32.86		
RX-6	1,264			39.53			31.97		
RN-1	943.0	967.7	118.0	50.48	53.89	8.307	18.68	18.11	2.087
RN-2	1,069			61.10			17.50		
RN-3	1,029			46.92			21.93		
RN-4	1,084			64.53			16.80		
RN-5	773.1			43.38			17.82		
RN-6	907.7			56.90			15.95		
RV-1	926.1	970.5	119.1	30.59	41.90	9.569	30.27	23.96	5.090
RV-2	891.8			34.87			25.57		
RV-3	1,119			38.30			29.21		
RV-4	1,090			57.07			19.10		
RV-5	987.3			47.98			20.58		
RV-6	808.8			42.54			19.01		

Table E.2 Heart muscle continued...

Rat	Lactate			Pyruvate			Lactate/Pyruvate		
	Conc	Mean	SD	Conc	Mean	SD	Ratio	Mean	SD
RC-1	921.5	1,094	103.1	52.68	53.70	9.350	17.49	20.85	3.835
RC-2	1,098			54.07			20.30		
RC-3	1,102			52.14			21.14		
RC-4	1,058			37.48			28.23		
RC-5	1,228			63.69			19.28		
RC-6	1,157			62.11			18.63		
RS-1	1,290	1,026	231.0	47.00	46.54	3.780	27.45	22.40	6.255
RS-2	1,168			44.36			26.33		
RS-3	872.5			46.05			18.95		
RS-4	725.3			52.79			13.74		
RS-5	1,225			41.44			29.57		
RS-6	874.0			47.61			18.36		
RX-E1	930.2	N/A		38.79	N/A		23.98	N/A	
RX-E2	1,099			34.70			31.69		
RV-E1	767.8			40.60			18.91		

Lactate and pyruvate concentrations are presented in micromole per litre ($\mu mol.L^{-1}$) concentrations. Conc = concentration, SD = standard deviation. Rats and corresponding data points that were randomly excluded from the main study are listed at the bottom of the table in grey text and designated the codes RX-E1, RX-E2 and RV-E1 for rats from dose groups RX and RV respectively. The aforementioned rats were excluded based on the random number generator of STATISTICA™, and was applied consistently for all parameter data sets. Rats were treated with NN = no dose regimen, VX = vehicle and sacrificed, VN = vehicle and no dose, VV = vehicle and vehicle, VC = vehicle and CoQ_{10}, VS = vehicle and succinate, RX = rotenone and sacrificed, RN = rotenone and no dose, RV = rotenone and vehicle, RC = rotenone and CoQ_{10}, RS = rotenone and succinate.

Table E.3 lists the brain tissue lactate and pyruvate concentrations generated from the rat main study. Basic statistics in the form of means and standard deviations are also presented for each dose group.

Table E.3 Brain tissue lactate and pyruvate data generated from the rat main study

Rat	Lactate			Pyruvate			Lactate/Pyruvate		
	Conc	Mean	SD	Conc	Mean	SD	Ratio	Mean	SD
NN-1	631.3	605.6	34.0	15.22	13.09	2.539	41.47	47.76	9.30
NN-2	559.5			16.53			33.84		
NN-3	568.8			10.07			56.51		
NN-4	643.6			11.91			54.02		
NN-5	616.0			13.86			44.44		
NN-6	614.6			10.92			56.28		
VX-1	500.1	584.2	95.3	11.87	15.88	4.240	42.12	38.32	8.40
VX-2	535.3			10.93			48.99		
VX-3	759.7			17.25			44.04		
VX-4	602.0			16.47			36.54		
VX-5	515.6			16.04			32.16		
VX-6	592.6			22.74			26.06		
VN-1	494.6	582.1	94.0	25.93	20.92	3.217	19.08	28.60	7.21
VN-2	598.1			15.86			37.72		
VN-3	659.8			21.64			30.48		
VN-4	438.6			21.11			20.78		
VN-5	640.5			20.73			30.90		
VN-6	661.0			20.25			32.64		

Table E.3 Brain tissue continued...

Rat	Lactate			Pyruvate			Lactate/Pyruvate		
	Conc	Mean	SD	Conc	Mean	SD	Ratio	Mean	SD
VV-1	628.6	634.1	79.5	18.45	15.88	4.908	34.07	42.66	11.86
VV-2	754.3			22.65			33.30		
VV-3	636.6			13.62			46.75		
VV-4	544.1			13.85			39.28		
VV-5	686.2			18.17			37.77		
VV-6	554.9			8.57			64.78		
VC-1	613.7	539.6	84.3	16.05	16.41	2.211	38.24	33.08	4.68
VC-2	561.3			15.20			36.93		
VC-3	494.6			19.45			25.42		
VC-4	411.8			13.53			30.43		
VC-5	514.0			15.63			32.90		
VC-6	642.3			18.58			34.58		
VS-1	612.1	641.5	30.0	13.15	13.31	6.274	46.55	55.66	20.53
VS-2	612.8			25.39			24.14		
VS-3	627.6			13.43			46.73		
VS-4	690.0			10.43			66.16		
VS-5	651.9			9.464			68.88		
VS-6	654.3			8.032			81.46		
RX-1	632.3	742.8	104.6	7.254	21.98	9.795	87.17	41.5	23.5
RX-2	699.5			15.70			44.57		
RX-3	680.2			18.74			36.29		
RX-4	696.3			27.25			25.55		
RX-5	876.1			29.84			29.36		
RX-6	872.2			33.09			26.36		
RN-1	735.7	648.5	52.0	12.31	14.79	1.780	59.78	44.66	8.72
RN-2	630.9			15.28			41.30		
RN-3	645.4			13.75			46.94		
RN-4	668.3			14.30			46.72		
RN-5	578.0			15.59			37.08		
RN-6	632.9			17.52			36.11		
RV-1	679.8	629.8	50.6	13.08	15.51	3.860	51.95	42.6	10.1
RV-2	678.6			14.89			45.57		
RV-3	598.8			12.37			48.42		
RV-4	598.9			12.05			49.70		
RV-5	662.9			20.20			32.82		
RV-6	559.8			20.45			27.37		
RC-1	581.0	602.8	39.3	24.38	19.43	6.075	23.83	33.82	10.75
RC-2	546.5			11.36			48.11		
RC-3	657.3			18.42			35.69		
RC-4	609.9			25.11			24.29		
RC-5	632.4			24.15			26.19		
RC-6	589.6			13.16			44.82		
RS-1	737.4	653.4	60.0	19.90	18.15	7.277	37.06	46.87	34.70
RS-2	648.4			17.20			37.69		
RS-3	653.8			27.23			24.01		
RS-4	592.8			20.04			29.58		
RS-5	703.3			19.55			35.97		
RS-6	584.6			5.002			116.9		
RX-E1	675.1	N/A		14.9	N/A		45.19	N/A	
RX-E2	894.4			29.0			30.81		
RV-E1	625.3			24.8			25.18		

Lactate and pyruvate concentrations are presented in micromole per litre ($\mu mol.L^{-1}$) concentrations. Conc = concentration, SD = standard deviation. Rats and corresponding data points that were randomly excluded from the main study are listed at the bottom of the table in grey text and designated the codes RX-E1, RX-E2 and RV-E1 for rats from dose groups RX and RV respectively. The aforementioned rats were excluded based on the random number generator of STATISTICA™, and was applied consistently for all parameter data sets. Rats were treated with NN = no dose regimen, VX = vehicle and sacrificed, VN = vehicle and no dose, VV = vehicle and vehicle, VC = vehicle and CoQ_{10}, VS = vehicle and succinate, RX = rotenone and sacrificed, RN = rotenone and no dose, RV = rotenone and vehicle, RC = rotenone and CoQ_{10}, RS = rotenone and succinate.

The skeletal muscle lactate and pyruvate data generated from the rat main study are presented in Table E.4. These concentrations are listed with corresponding means and standard deviations for each dose group.

Table E.4 Skeletal muscle lactate and pyruvate data generated from the rat main study

Rat	Lactate			Pyruvate			Lactate/Pyruvate		
	Conc	Mean	SD	Conc	Mean	SD	Ratio	Mean	SD
NN-1	1,701	1,481	203.4	14.86	13.96	6.932	114.5	128.2	56.20
NN-2	1,560			8.017			194.6		
NN-3	1,478			7.934			186.3		
NN-4	1,441			12.38			116.5		
NN-5	1,111			26.82			41.41		
NN-6	1,596			13.76			116.0		
VX-1	1,202	1,532	241.2	15.08	18.27	3.573	79.71	86.51	22.25
VX-2	1,447			15.95			90.68		
VX-3	1,353			22.97			58.87		
VX-4	1,851			14.66			126.2		
VX-5	1,706			21.77			78.38		
VX-6	1,636			19.21			85.15		
VN-1	1,463	1,514	201.7	7.903	16.58	4.707	185.1	101.4	44.09
VN-2	1,464			17.95			81.56		
VN-3	1,659			17.67			93.88		
VN-4	1,316			22.25			59.14		
VN-5	1,843			17.09			107.8		
VN-6	1,342			16.64			80.63		
VV-1	1,933	1,709	180.1	16.51	17.43	4.099	117.1	104.2	31.75
VV-2	1,450			23.98			60.48		
VV-3	1,575			19.22			81.94		
VV-4	1,795			13.18			136.2		
VV-5	1,841			13.20			139.4		
VV-6	1,662			18.48			89.94		
VC-1	1,340	1,555	183.6	18.56	18.23	5.228	72.19	93.56	36.06
VC-2	1,778			16.60			107.1		
VC-3	1,551			23.48			66.04		
VC-4	1,496			21.45			69.77		
VC-5	1,767			20.60			85.75		
VC-6	1,400			8.725			160.5		
VS-1	1,382	1,546	181.2	15.96	16.20	10.45	86.56	156.8	155.8
VS-2	1,662			19.42			85.59		
VS-3	1,644			15.62			105.2		
VS-4	1,257			8.531			147.3		
VS-5	1,692			3.616			468.0		
VS-6	1,641			34.02			48.23		
RX-1	1,430	1,661	246.4	15.74	18.40	6.042	90.82	98.0	33.9
RX-2	1,570			22.38			70.14		
RX-3	1,839			26.47			69.48		
RX-4	1,403			13.86			101.2		
RX-5	2,039			21.55			94.62		
RX-6	1,685			10.40			162.0		
RN-1	1,401	1,502	171.8	20.26	12.75	4.487	69.16	129.3	42.29
RN-2	1,281			9.219			138.9		
RN-3	1,472			15.41			95.54		
RN-4	1,554			8.123			191.3		
RN-5	1,793			12.60			142.4		
RN-6	1,509			10.92			138.2		

Table E.4 Skeletal muscle continued...

Rat	Lactate			Pyruvate			Lactate/Pyruvate		
	Conc	Mean	SD	Conc	Mean	SD	Ratio	Mean	SD
RV-1	1,873	1,668	221.4	25.23	18.62	5.005	74.24	93.8	22.4
RV-2	1,793			13.32			134.6		
RV-3	1,260			12.11			104.0		
RV-4	1,644			19.29			85.23		
RV-5	1,631			20.48			79.68		
RV-6	1,805			21.31			84.71		
RC-1	2,479	1,664	429.0	12.46	18.79	4.996	198.9	99.05	53.96
RC-2	1,198			22.72			52.75		
RC-3	1,533			19.68			77.87		
RC-4	1,571			24.25			64.79		
RC-5	1,655			20.75			79.76		
RC-6	1,549			12.88			120.2		
RS-1	1,850	1,395	270.2	11.46	16.59	3.188	161.4	89.58	37.66
RS-2	1,375			18.42			74.62		
RS-3	1,318			13.75			95.85		
RS-4	1,144			18.18			62.92		
RS-5	1,544			18.46			83.62		
RS-6	1,137			19.25			59.09		
RX-E1	1,359	N/A		25.63	N/A		53.01	N/A	
RX-E2	1,823			15.01			121.5		
RV-E1	2,440			15.81			154.3		

Lactate and pyruvate concentrations are presented in micromole per litre ($\mu mol.L^{-1}$) concentrations. Conc = concentration, SD = standard deviation. Rats and corresponding data points that were randomly excluded from the main study are listed at the bottom of the table in grey text and designated the codes RX-E1, RX-E2 and RV-E1 for rats from dose groups RX and RV respectively. The aforementioned rats were excluded based on the random number generator of STATISTICA™, and was applied consistently for all parameter data sets. Rats were treated with NN = no dose regimen, VX = vehicle and sacrificed, VN = vehicle and no dose, VV = vehicle and vehicle, VC = vehicle and CoQ_{10}, VS = vehicle and succinate, RX = rotenone and sacrificed, RN = rotenone and no dose, RV = rotenone and vehicle, RC = rotenone and CoQ_{10}, RS = rotenone and succinate.

Table E.5 lists the liver lactate and pyruvate concentrations generated from the rat main study. Descriptive statistics in the form of means and standard deviations are also presented.

Table E.5 Liver tissue lactate and pyruvate data generated from the rat main study

Rat	Lactate			Pyruvate			Lactate/Pyruvate		
	Conc	Mean	SD	Conc	Mean	SD	Ratio	Mean	SD
NN-1	378.5	369.4	61.97	33.88	47.83	14.49	11.17	8.482	3.072
NN-2	417.5			44.69			9.343		
NN-3	451.9			47.29			9.556		
NN-4	327.8			66.26			4.947		
NN-5	278.9			63.33			4.403		
NN-6	361.7			31.53			11.47		
VX-1	408.0	487.4	52.48	30.88	30.39	9.576	13.21	17.43	5.758
VX-2	559.0			32.38			17.27		
VX-3	493.2			18.56			26.57		
VX-4	519.9			34.69			14.99		
VX-5	452.4			21.00			21.54		
VX-6	492.1			44.81			10.98		
VN-1	313.5	436.5	110.8	38.31	41.54	12.10	8.183	11.50	4.684
VN-2	556.9			37.55			14.83		
VN-3	485.8			49.05			9.905		
VN-4	479.5			31.03			15.45		
VN-5	500.0			31.06			16.10		
VN-6	283.2			62.24			4.550		

Table E.5 Liver tissue continued...

Rat	Lactate			Pyruvate			Lactate/Pyruvate		
	Conc	Mean	SD	Conc	Mean	SD	Ratio	Mean	SD
VV-1	358.5	325.7	37.69	27.59	43.38	12.19	13.00	7.986	2.551
VV-2	296.1			39.54			7.489		
VV-3	296.3			36.89			8.031		
VV-4	386.4			63.89			6.047		
VV-5	310.6			46.27			6.713		
VV-6	306.2			46.12			6.640		
VC-1	551.6	463.4	232.2	64.54	38.79	18.33	8.546	12.49	3.491
VC-2	296.0			34.50			8.579		
VC-3	369.4			23.73			15.57		
VC-4	286.0			18.51			15.46		
VC-5	381.7			34.25			11.15		
VC-6	895.6			57.22			15.65		
VS-1	541.7	428.3	96.12	31.58	31.26	7.507	17.15	14.43	4.836
VS-2	343.2			30.75			11.16		
VS-3	405.4			37.49			10.81		
VS-4	402.4			17.65			22.80		
VS-5	549.8			38.83			14.16		
VS-6	327.7			31.26			10.48		
RX-1	772.3	507.9	262.4	28.16	39.44	12.93	27.42	14.02	8.010
RX-2	302.3			39.05			7.743		
RX-3	248.3			56.15			4.422		
RX-4	290.0			21.42			13.54		
RX-5	838.7			49.08			17.09		
RX-6	596.0			42.77			13.93		
RN-1	405.2	408.4	100.1	45.17	40.94	4.329	8.971	10.03	2.550
RN-2	351.0			38.51			9.114		
RN-3	605.6			40.06			15.12		
RN-4	336.5			38.71			8.693		
RN-5	358.6			35.96			9.975		
RN-6	393.5			47.21			8.336		
RV-1	367.0	301.5	72.92	50.34	36.22	10.20	7.290	8.889	3.611
RV-2	291.3			27.98			10.41		
RV-3	369.6			23.82			15.52		
RV-4	219.7			32.73			6.711		
RV-5	210.0			36.91			5.689		
RV-6	351.3			45.53			7.715		
RC-1	728.6	500.4	130.1	36.59	49.02	11.05	19.91	11.14	5.393
RC-2	472.1			47.85			9.865		
RC-3	498.4			57.33			8.695		
RC-4	380.4			54.55			6.973		
RC-5	376.8			62.22			6.056		
RC-6	545.8			35.58			15.34		
RS-1	636.9	471.7	147.1	55.40	36.71	13.81	11.50	15.30	10.22
RS-2	644.6			18.54			34.77		
RS-3	284.4			41.76			6.811		
RS-4	398.3			47.43			8.397		
RS-5	494.2			28.54			17.32		
RS-6	371.8			28.57			13.01		
RX-E1	403.3	N/A		29.23	N/A		13.80	N/A	
RX-E2	258.0			25.38			10.16		
RV-E1	297.2			36.82			8.071		

Lactate and pyruvate concentrations are presented in micromole per litre ($\mu mol.L^{-1}$) concentrations. Conc = concentration, SD = standard deviation. Rats and corresponding data points that were randomly excluded from the main study are listed at the bottom of the table in grey text and designated the codes RX-E1, RX-E2 and RV-E1 for rats from dose groups RX and RV respectively. The aforementioned rats were excluded based on the random number generator of STATISTICA™, and was applied consistently for all parameter data sets. Rats were treated with NN = no dose regimen, VX = vehicle and sacrificed, VN = vehicle and no dose, VV = vehicle and vehicle, VC = vehicle and CoQ_{10}, VS = vehicle and succinate, RX = rotenone and sacrificed, RN = rotenone and no dose, RV = rotenone and vehicle, RC = rotenone and CoQ_{10}, RS = rotenone and succinate.

APPENDIX F

ADENYLATE DATA

The ATP/ADP ratios were successfully determined from blood, heart muscle, skeletal muscle and liver tissue preparations of the rat main study. As with the preparation of samples for the lactate and pyruvate assays, adenylate samples were deproteinised and thus did not require that protein concentrations be determined. Total adenylates (ATP + ADP) were initially determined, followed by the concentration of ATP in two separate assays. Therefore, the concentration of ADP was calculated by subtracting the ATP value from that of the total adenylate concentration. Finally, the ratios of ATP to ADP were determined. Data is presented with no more than four significant numbers.

Table F.1 lists the blood adenylate data and final ATP/ADP ratios generated from the rat main study. Descriptive statistics in the form of means and standard deviations are also presented.

Table F.1 Blood adenylate data generated from the rat main study

Rat	Total adenylates			ATP			ADP	ATP/ADP		
	Conc	Mean	SD	Conc	Mean	SD	Conc	Ratio	Mean	SD
NN-1	325.4	292.9	31.63	164.0	158.9	11.11	161.4	1.017	1.239	0.309
NN-2	240.6			153.3			87.27	1.757		
NN-3	269.1			152.0			117.1	1.298		
NN-4	305.9			148.4			157.4	0.943		
NN-5	309.3			156.9			152.4	1.030		
NN-6	307.3			178.9			128.4	1.393		
VX-1	221.0	188.2	30.71	119.7	110.0	9.237	101.3	1.182	1.795	1.293
VX-2	174.8			96.8			77.99	1.241		
VX-3	184.1			110.6			73.50	1.505		
VX-4	215.1			105.7			109.4	0.966		
VX-5	146.1			117.3			28.74	4.082		
VX-6	---			---			---	---		
VN-1	172.2	173.3	19.60	134.9	117.9	15.66	37.29	3.618	2.252	0.776
VN-2	153.9			102.0			51.87	1.967		
VN-3	188.4			127.5			60.90	2.094		
VN-4	---			---			---	---		
VN-5	154.5			100.5			53.95	1.863		
VN-6	197.3			124.7			72.65	1.716		
VV-1	232.2	207.1	26.99	210.3	179.0	24.94	21.96	9.575	12.058	13.600
VV-2	---			---			---	---		
VV-3	193.2			162.2			30.96	5.239		
VV-4	169.3			164.7			4.574	36.01		
VV-5	208.1			156.2			51.90	3.010		
VV-6	232.8			201.5			31.24	6.451		

Table F.1 Blood continued...

Rat	Total adenylates			ATP			ADP	ATP/ADP		
	Conc	Mean	SD	Conc	Mean	SD	Conc	Ratio	Mean	SD
VC-1	268.2	280.5	37.93	151.4	146.9	11.54	116.7	1.297	1.140	0.223
VC-2	232.8			134.9			97.98	1.377		
VC-3	262.7			144.8			117.9	1.228		
VC-4	281.4			132.4			149.0	0.888		
VC-5	291.4			159.7			131.7	1.213		
VC-6	346.3			157.9			188.4	0.838		
VS-1	125.8	195.8	45.19	72.47	121.3	25.99	53.32	1.359	3.113	4.271
VS-2	226.5			125.0			101.5	1.232		
VS-3	222.7			114.2			108.5	1.052		
VS-4	233.5			140.7			92.75	1.518		
VS-5	152.4			140.5			11.89	11.818		
VS-6	214.0			134.8			79.26	1.701		
RX-1	---	204.7	57.16	---	100.0	19.97	---	---	1.142	0.561
RX-2	186.1			124.6			61.45	2.028		
RX-3	155.0			80.13			74.88	1.070		
RX-4	155.2			84.27			70.97	1.187		
RX-5	284.4			93.41			191.0	0.489		
RX-6	242.9			117.4			125.5	0.936		
RN-1	147.5	149.2	13.99	99.85	105.7	8.662	47.67	2.095	2.626	0.831
RN-2	124.4			96.02			28.42	3.379		
RN-3	146.6			108.9			37.66	2.892		
RN-4	158.9			107.3			51.58	2.080		
RN-5	152.9			120.4			32.43	3.713		
RN-6	165.0			101.5			63.48	1.599		
RV-1	170.1	219.0	34.97	150.9	140.1	10.00	19.18	7.866	2.727	2.584
RV-2	249.9			141.3			108.6	1.301		
RV-3	195.7			140.7			55.04	2.556		
RV-4	221.7			150.6			71.11	2.118		
RV-5	211.0			129.7			81.22	1.598		
RV-6	265.4			127.3			138.1	0.922		
RC-1	266.1	244.2	24.51	127.7	121.0	10.91	138.4	0.923	0.989	0.094
RC-2	256.2			126.5			129.7	0.975		
RC-3	250.8			116.2			134.6	0.864		
RC-4	261.6			135.9			125.8	1.080		
RC-5	228.0			112.8			115.2	0.980		
RC-6	202.1			106.6			95.6	1.115		
RS-1	231.4	209.4	53.01	140.9	111.4	25.56	90.46	1.558	3.229	5.459
RS-2	149.9			140.1			9.766	14.35		
RS-3	281.5			100.8			180.6	0.558		
RS-4	203.6			88.69			114.9	0.772		
RS-5	242.0			116.5			125.5	0.929		
RS-6	148.3			81.15			67.2	1.208		
RX-E1	---	N/A		---	N/A		---	---	N/A	
RX-E2	278.9			87.50			191.4	0.457		
RV-E1	195.4			181.2			14.25	12.72		

Adenylate concentrations are listed in micromole per litre ($\mu mol.L^{-1}$). The concentration of ADP was calculated by subtracting the amount of ATP from that of the total adenylate concentration. '---' = missing data due to unsuccessful assaying of the sample, ADP = adenosine diphosphate, ATP = adenosine triphosphate, Conc = concentration, SD = standard deviation. Rats and corresponding data points that were randomly excluded from the main study are listed at the bottom of the table in grey text and designated the codes RX-E1, RX-E2 and RV-E1 for rats from dose groups RX and RV respectively. The aforementioned rats were excluded based on the random number generator of STATISTICA™, and was applied consistently for all parameter data sets. Rats were treated with NN = no dose regimen, VX = vehicle and sacrificed, VN = vehicle and no dose, VV = vehicle and vehicle, VC = vehicle and CoQ_{10}, VS = vehicle and succinate, RX = rotenone and sacrificed, RN = rotenone and no dose, RV = rotenone and vehicle, RC = rotenone and CoQ_{10}, RS = rotenone and succinate.

Total adenylates and ATP concentrations generated from skeletal muscle during the rat main study are presented in Table F.2. Means and standard deviations for the respective rat groups were in addition included.

Table F.2 Heart muscle adenylate data generated from the rat main study

Rat	Total adenylates			ATP			ADP	ATP/ADP		
	Conc	Mean	SD	Conc	Mean	SD	Conc	Ratio	Mean	SD
NN-1	396.0	313.7	56.08	285.6	235.6	49.82	110.4	2.588	3.570	2.304
NN-2	310.1			276.3			33.84	8.164		
NN-3	257.0			192.2			64.89	2.961		
NN-4	357.0			276.3			80.74	3.422		
NN-5	251.8			171.3			80.49	2.128		
NN-6	310.0			211.7			98.28	2.154		
VX-1	225.7	253.2	28.39	165.8	156.8	25.27	59.90	2.768	1.730	0.608
VX-2	260.4			143.0			117.4	1.218		
VX-3	256.4			137.7			118.7	1.160		
VX-4	273.4			172.4			101.0	1.707		
VX-5	214.1			127.1			87.02	1.461		
VX-6	288.9			194.6			94.28	2.064		
VN-1	196.9	209.2	21.49	120.9	150.9	20.45	76.07	1.589	3.064	1.720
VN-2	240.6			175.1			65.50	2.674		
VN-3	191.6			134.5			57.07	2.357		
VN-4	232.6			150.8			81.83	1.842		
VN-5	198.2			155.8			42.32	3.683		
VN-6	195.4			168.4			27.00	6.240		
VV-1	165.7	260.7	53.40	94.9	196.9	52.99	70.80	1.340	9.494	17.144
VV-2	325.0			233.5			91.47	2.553		
VV-3	277.5			212.3			65.16	3.259		
VV-4	285.1			207.5			77.60	2.674		
VV-5	264.6			192.5			72.07	2.671		
VV-6	246.2			240.7			5.414	44.47		
VC-1	254.7	252.1	28.28	213.0	205.0	27.69	41.69	5.109	4.875	2.271
VC-2	270.4			243.8			26.64	9.150		
VC-3	286.5			215.2			71.27	3.020		
VC-4	264.6			209.6			55.09	3.804		
VC-5	222.1			184.9			37.15	4.978		
VC-6	214.5			163.3			51.22	3.188		
VS-1	332.6	283.6	36.96	236.2	204.3	30.51	96.40	2.450	2.636	0.597
VS-2	281.7			210.9			70.87	2.975		
VS-3	279.3			219.6			59.65	3.682		
VS-4	229.6			154.5			75.08	2.058		
VS-5	262.5			181.5			80.98	2.241		
VS-6	315.9			223.2			92.63	2.410		
RX-1	254.0	268.9	78.51	178.0	201.29	54.74	75.99	2.342	3.327	1.392
RX-2	365.7			266.0			99.77	2.666		
RX-3	248.3			211.4			36.85	5.737		
RX-4	318.1			229.5			88.55	2.592		
RX-5	---			---			---	---		
RX-6	158.4			121.5			36.84	3.299		
RN-1	286.3	252.1	52.40	214.8	177.3	45.27	71.56	3.001	2.349	0.498
RN-2	268.3			188.2			80.11	2.349		
RN-3	287.1			208.9			78.20	2.672		
RN-4	261.0			184.8			76.16	2.427		
RN-5	147.7			89.74			58.00	1.547		
RN-6	262.0			177.5			84.49	2.101		

Table F.2 Heart muscle continued...

Rat	Total adenylates			ATP			ADP	ATP/ADP		
	Conc	Mean	SD	Conc	Mean	SD	Conc	Ratio	Mean	SD
RV-1	280.5	274.9	77.02	215.2	220.8	63.07	65.35	3.293	7.963	8.815
RV-2	195.9			188.4			7.424	25.39		
RV-3	282.6			175.4			107.2	1.637		
RV-4	301.4			238.6			62.80	3.799		
RV-5	399.0			338.1			60.90	5.552		
RV-6	189.9			169.1			20.84	8.113		
RC-1	248.2	253.9	32.29	208.4	179.4	35.25	39.80	5.235	2.718	1.393
RC-2	251.0			187.3			63.70	2.940		
RC-3	256.8			171.3			85.42	2.006		
RC-4	197.6			114.0			83.62	1.363		
RC-5	280.0			209.9			70.15	2.992		
RC-6	290.1			185.3			104.8	1.769		
RS-1	231.1	268.2	44.42	163.0	195.7	45.55	68.06	2.395	2.797	0.917
RS-2	274.2			220.5			53.65	4.110		
RS-3	262.7			169.0			93.71	1.803		
RS-4	323.2			251.8			71.41	3.526		
RS-5	207.9			137.0			70.91	1.932		
RS-6	310.2			233.0			77.23	3.017		
RX-E1	291.5	N/A		197.7	N/A		93.77	2.108	N/A	
RX-E2	299.8			237.6			62.15	3.823		
RV-E1	251.7			200.6			51.11	3.925		

Adenylate concentrations are listed in micromole per litre ($\mu mol.L^{-1}$). The concentration of ADP was calculated by subtracting the amount of ATP from that of the total adenylate concentration. '---' = missing data due to unsuccessful assaying of the sample, ADP = adenosine diphosphate, ATP = adenosine triphosphate, Conc = concentration, SD = standard deviation. Rats and corresponding data points that were randomly excluded from the main study are listed at the bottom of the table in grey text and designated the codes RX-E1, RX-E2 and RV-E1 for rats from dose groups RX and RV respectively. The aforementioned rats were excluded based on the random number generator of STATISTICA™, and was applied consistently for all parameter data sets. Rats were treated with NN = no dose regimen, VX = vehicle and sacrificed, VN = vehicle and no dose, VV = vehicle and vehicle, VC = vehicle and CoQ_{10}, VS = vehicle and succinate, RX = rotenone and sacrificed, RN = rotenone and no dose, RV = rotenone and vehicle, RC = rotenone and CoQ_{10}, RS = rotenone and succinate.

Skeletal muscle adenylate data generated from the rat main study are presented in Table F.3. Basic descriptive statistics are presented for the corresponding rat groups.

Table F.3 Skeletal muscle adenylate data generated from the rat main study

Rat	Total adenylates			ATP			ADP	ATP/ADP		
	Conc	Mean	SD	Conc	Mean	SD	Conc	Ratio	Mean	SD
NN-1	852.1	798.2	107.6	754.2	656.3	107.4	97.93	7.702	5.181	2.193
NN-2	903.1			672.2			230.8	2.912		
NN-3	593.6			450.3			143.3	3.143		
NN-4	793.6			704.2			89.45	7.873		
NN-5	802.7			645.8			156.9	4.116		
NN-6	844.0			710.9			133.2	5.338		
VX-1	807.5	745.5	75.70	666.6	619.0	91.25	140.9	4.731	5.612	2.972
VX-2	781.9			601.8			180.1	3.341		
VX-3	628.0			484.7			143.3	3.382		
VX-4	773.5			709.3			64.14	11.06		
VX-5	807.7			705.8			102.0	6.920		
VX-6	674.6			545.8			128.8	4.239		

Table F.3 Skeletal muscle continued...

Rat	Total adenylates			ATP			ADP	ATP/ADP		
	Conc	Mean	SD	Conc	Mean	SD	Conc	Ratio	Mean	SD
VN-1	724.8	718.4	77.35	635.8	632.7	82.56	89.03	7.141	8.255	3.638
VN-2	737.5			617.7			119.8	5.156		
VN-3	565.0			488.5			76.48	6.387		
VN-4	742.9			627.6			115.4	5.440		
VN-5	772.2			709.1			63.15	11.23		
VN-6	768.1			717.5			50.61	14.18		
VV-1	562.8	699.9	80.98	459.4	575.9	79.30	103.3	4.446	4.833	1.203
VV-2	806.7			672.0			134.8	4.986		
VV-3	748.9			641.5			107.4	5.975		
VV-4	687.7			515.8			171.9	3.001		
VV-5	697.1			565.5			131.5	4.300		
VV-6	696.5			601.0			95.57	6.288		
VC-1	866.7	754.8	99.64	617.5	582.5	87.33	249.2	2.478	3.511	0.906
VC-2	595.4			433.2			162.2	2.671		
VC-3	685.5			542.2			143.2	3.786		
VC-4	819.7			655.1			164.7	3.978		
VC-5	754.6			576.7			177.9	3.242		
VC-6	806.8			670.3			136.5	4.912		
VS-1	947.3	851.1	54.66	696.4	676.3	44.06	250.8	2.777	4.051	0.992
VS-2	780.0			590.3			189.6	3.113		
VS-3	847.0			716.8			130.3	5.502		
VS-4	845.2			684.1			161.0	4.248		
VS-5	858.9			690.4			168.5	4.097		
VS-6	828.3			679.6			148.7	4.570		
RX-1	758.8	740.7	93.32	637.3	632.0	93.36	121.5	5.244	6.148	2.097
RX-2	759.0			662.1			96.95	6.829		
RX-3	818.0			669.2			148.8	4.497		
RX-4	794.6			722.0			72.66	9.937		
RX-5	756.7			650.6			106.0	6.137		
RX-6	557.0			450.8			106.2	4.246		
RN-1	760.7	757.0	15.92	683.1	673.4	18.57	77.63	8.799	8.175	1.154
RN-2	726.6			648.9			77.71	8.350		
RN-3	770.5			685.7			84.88	8.078		
RN-4	763.4			671.4			92.00	7.297		
RN-5	754.1			655.0			99.05	6.613		
RN-6	766.8			696.6			70.27	9.912		
RV-1	530.2	696.4	158.5	406.0	561.8	135.6	124.2	3.268	6.417	7.133
RV-2	711.3			678.9			32.42	20.94		
RV-3	532.2			405.4			126.8	3.196		
RV-4	698.8			542.6			156.2	3.474		
RV-5	749.1			612.9			136.1	4.502		
RV-6	957.2			724.8			232.4	3.119		
RC-1	795.7	791.0	56.39	605.0	595.2	70.49	190.8	3.171	3.236	1.051
RC-2	868.5			724.3			144.2	5.022		
RC-3	753.0			559.1			193.9	2.884		
RC-4	771.2			605.8			165.4	3.663		
RC-5	841.0			549.8			291.1	1.889		
RC-6	716.6			527.3			189.3	2.785		
RS-1	712.3	779.8	41.92	484.6	614.6	73.23	227.7	2.128	3.939	1.166
RS-2	793.7			658.0			135.7	4.847		
RS-3	825.9			689.7			136.2	5.063		
RS-4	752.2			580.6			171.6	3.384		
RS-5	813.6			627.7			185.9	3.376		
RS-6	781.0			647.3			133.8	4.838		

Table F.3 Skeletal muscle continued...

Rat	Total adenylates			ATP			ADP	ATP/ADP		
	Conc	Mean	SD	Conc	Mean	SD	Conc	Ratio	Mean	SD
RX-E1	631.1	N/A		586.1	N/A		45.03	13.02	N/A	
RX-E2	738.8			657.4			81.34	8.083		
RV-E1	685.7			532.1			153.6	3.464		

Adenylate concentrations are listed in micromole per litre ($\mu mol.L^{-1}$). The concentration of ADP was calculated by subtracting the amount of ATP from that of the total adenylate concentration. ADP = adenosine diphosphate, ATP = adenosine triphosphate, Conc = concentration, SD = standard deviation. Rats and corresponding data points that were randomly excluded from the main study are listed at the bottom of the table in grey text and designated the codes RX-E1, RX-E2 and RV-E1 for rats from dose groups RX and RV respectively. The aforementioned rats were excluded based on the random number generator of STATISTICA™, and was applied consistently for all parameter data sets. Rats were treated with NN = no dose regimen, VX = vehicle and sacrificed, VN = vehicle and no dose, VV = vehicle and vehicle, VC = vehicle and CoQ_{10}, VS = vehicle and succinate, RX = rotenone and sacrificed, RN = rotenone and no dose, RV = rotenone and vehicle, RC = rotenone and CoQ_{10}, RS = rotenone and succinate.

The final adenylate data set generated from the rat main study is presented in Table F.4, namely liver tissue adenylates. Descriptive statistics in the form of means and standard deviations are presented for the corresponding dose groups.

Table F.4 Liver tissue adenylate data generated from the rat main study

Rat	Total adenylates			ATP			ADP	ATP/ADP		
	Conc	Mean	SD	Conc	Mean	SD	Conc	Ratio	Mean	SD
NN-1	274.9	267.1	44.33	215.1	223.3	32.36	59.78	3.598	6.204	3.205
NN-2	272.0			212.7			59.38	3.582		
NN-3	260.4			217.9			42.59	5.116		
NN-4	255.7			235.0			20.72	11.34		
NN-5	338.9			278.6			60.29	4.622		
NN-6	200.7			180.6			20.15	8.963		
VX-1	207.9	253.0	38.40	191.5	209.7	30.21	16.39	11.68	5.612	3.015
VX-2	233.4			190.9			42.51	4.491		
VX-3	251.4			198.9			52.51	3.788		
VX-4	252.5			200.8			51.70	3.885		
VX-5	249.4			205.9			43.54	4.728		
VX-6	323.3			270.3			53.03	5.097		
VN-1	167.4	182.4	17.93	164.2	174.7	19.75	3.139	52.33	34.69	21.59
VN-2	---			---			---	---		
VN-3	202.2			197.4			4.802	41.12		
VN-4	---			---			---	---		
VN-5	---			---			---	---		
VN-6	177.6			162.3			15.29	10.61		
VV-1	189.2	258.5	45.30	166.5	215.6	31.41	22.78	7.309	5.810	2.552
VV-2	246.1			198.3			47.74	4.154		
VV-3	305.5			243.9			61.58	3.960		
VV-4	312.4			249.3			63.08	3.952		
VV-5	251.8			229.6			22.26	10.32		
VV-6	246.0			206.1			39.87	5.170		
VC-1	218.4	226.4	44.53	187.1	184.1	30.17	31.32	5.974	5.773	4.151
VC-2	298.6			226.4			72.12	3.140		
VC-3	216.0			180.7			35.38	5.106		
VC-4	183.7			136.4			47.27	2.885		
VC-5	184.4			172.0			12.39	13.89		
VC-6	257.2			201.9			55.37	3.646		

Table F.4 Liver tissue continued...

Rat	Total adenylates			ATP			ADP	ATP/ADP		
	Conc	Mean	SD	Conc	Mean	SD	Conc	Ratio	Mean	SD
VS-1	285.4	239.5	62.47	224.2	186.5	38.72	61.20	3.664	11.46	19.89
VS-2	298.8			229.5			69.28	3.313		
VS-3	269.1			176.8			92.32	1.915		
VS-4	128.3			125.9			2.419	52.04		
VS-5	214.1			167.1			47.00	3.556		
VS-6	241.2			195.4			45.81	4.265		
RX-1	564.7	220.0	172.6	512.6	182.3	164.6	52.10	9.838	5.177	3.177
RX-2	173.1			145.1			27.94	5.193		
RX-3	144.1			85.99			58.09	1.480		
RX-4	207.5			156.9			50.57	3.103		
RX-5	107.7			83.56			24.10	3.467		
RX-6	123.3			109.6			13.73	7.980		
RN-1	164.1	161.6	31.53	113.8	110.4	26.40	50.27	2.264	2.947	2.164
RN-2	159.3			137.9			21.43	6.432		
RN-3	---			---			---	---		
RN-4	128.6			100.1			28.56	3.504		
RN-5	143.7			70.95			72.77	0.975		
RN-6	212.2			129.3			82.83	1.562		
RV-1	148.5	189.1	41.18	103.7	132.0	44.72	44.85	2.312	2.664	1.570
RV-2	207.1			153.2			53.90	2.843		
RV-3	252.4			183.6			68.82	2.668		
RV-4	147.2			92.85			54.31	1.710		
RV-5	170.4			81.65			88.79	0.920		
RV-6	208.9			176.9			31.99	5.530		
RC-1	168.8	207.8	35.11	118.0	139.0	36.29	50.80	2.324	2.185	0.806
RC-2	256.5			180.0			76.58	2.350		
RC-3	238.4			163.1			75.26	2.168		
RC-4	215.0			146.9			68.16	2.154		
RC-5	175.3			77.83			97.52	0.798		
RC-6	192.7			148.0			44.67	3.313		
RS-1	146.4	194.5	38.36	112.6	160.9	33.28	33.74	3.338	5.434	2.327
RS-2	212.3			162.0			50.30	3.220		
RS-3	213.3			189.6			23.73	7.989		
RS-4	232.3			196.0			36.31	5.399		
RS-5	145.3			130.0			15.25	8.527		
RS-6	217.3			174.9			42.35	4.131		
RX-E1	140.7	N/A		134.5	N/A		6.250	21.52	N/A	
RX-E2	194.8			132.7			62.10	2.137		
RV-E1	212.7			153.7			58.97	2.606		

Adenylate concentrations are listed in micromole per litre ($\mu mol.L^{-1}$). The concentration of ADP was calculated by subtracting the amount of ATP from that of the total adenylate concentration. '---' = missing data due to unsuccessful assaying of the sample, ADP = adenosine diphosphate, ATP = adenosine triphosphate, Conc = concentration, SD = standard deviation. Rats and corresponding data points that were randomly excluded from the main study are listed at the bottom of the table in grey text and designated the codes RX-E1, RX-E2 and RV-E1 for rats from dose groups RX and RV respectively. The aforementioned rats were excluded based on the random number generator of STATISTICA™, and was applied consistently for all parameter data sets. Rats were treated with NN = no dose regimen, VX = vehicle and sacrificed, VN = vehicle and no dose, VV = vehicle and vehicle, VC = vehicle and CoQ_{10}, VS = vehicle and succinate, RX = rotenone and sacrificed, RN = rotenone and no dose, RV = rotenone and vehicle, RC = rotenone and CoQ_{10}, RS = rotenone and succinate.

APPENDIX G

PYRIDINE DATA

The NAD/NADH ratios were determined successfully from blood, skeletal muscle and liver tissue preparations of the rat main study, as presented in Tables G.1 to G.3 respectively. Two separate assays were performed for the determination of total pyridines (NAD + NADH) and of NADH only. The concentration of NAD was subsequently determined by subtracting the amount of NADH from that of the total pyridine concentration. Finally, the ratio of NAD to NADH was calculated. Pyridine data is presented in Appendix G with a maximum of four significant numbers.

Table G.1 lists the blood pyridine data generated from the rat main study. The mean and standard deviation for corresponding data sets are also presented.

Table G.1 Blood pyridine data generated from the rat main study

Rat	Total pyridines			NADH			NAD	NAD/NADH		
	Conc	Mean	SD	Conc	Mean	SD	Conc	Ratio	Mean	SD
NN-1	2.444	2.299	0.273	2.086	1.827	0.217	0.358	0.172	0.262	0.102
NN-2	---			---			---	---		
NN-3	2.679			1.914			0.765	0.400		
NN-4	2.173			1.889			0.284	0.150		
NN-5	1.963			1.506			0.457	0.303		
NN-6	2.235			1.741			0.494	0.284		
VX-1	2.279	2.603	0.453	2.035	2.002	0.201	0.244	0.120	0.296	0.141
VX-2	2.186			1.709			0.477	0.279		
VX-3	2.221			1.919			0.302	0.158		
VX-4	2.640			1.965			0.674	0.343		
VX-5	3.221			2.326			0.895	0.385		
VX-6	3.070			2.058			1.012	0.492		
VN-1	1.942	2.058	0.174	1.547	1.610	0.184	0.395	0.256	0.286	0.121
VN-2	2.291			1.709			0.581	0.340		
VN-3	2.244			1.814			0.430	0.237		
VN-4	2.035			1.372			0.663	0.483		
VN-5	1.849			1.442			0.407	0.282		
VN-6	1.988			1.779			0.209	0.118		
VV-1	1.988	2.357	0.346	1.837	1.936	0.185	0.151	0.082	0.220	0.161
VV-2	2.279			2.233			0.047	0.021		
VV-3	1.942			1.721			0.221	0.128		
VV-4	2.791			2.047			0.744	0.364		
VV-5	2.616			1.965			0.651	0.331		
VV-6	2.523			1.814			0.709	0.391		

Table G.1 Blood continued...

Rat	Total pyridines			NADH			NAD	NAD/NADH		
	Conc	Mean	SD	Conc	Mean	SD	Conc	Ratio	Mean	SD
VC-1	2.333	2.193	0.524	1.914	1.809	0.367	0.420	0.219	0.207	0.097
VC-2	1.765			1.654			0.111	0.067		
VC-3	1.914			1.543			0.370	0.240		
VC-4	2.469			1.827			0.642	0.351		
VC-5	3.037			2.469			0.568	0.230		
VC-6	1.642			1.444			0.198	0.137		
VS-1	2.358	2.785	1.012	2.086	2.079	0.819	0.272	0.130	0.386	0.294
VS-2	2.185			1.728			0.457	0.264		
VS-3	2.679			2.074			0.605	0.292		
VS-4	2.148			1.136			1.012	0.891		
VS-5	---			---			---	---		
VS-6	4.556			3.370			1.185	0.352		
RX-1	2.151	1.817	0.517	1.872	1.574	0.467	0.279	0.149	0.160	0.058
RX-2	2.012			1.872			0.140	0.075		
RX-3	2.070			1.779			0.291	0.163		
RX-4	1.953			1.581			0.372	0.235		
RX-5	0.901			0.765			0.136	0.177		
RX-6	---			---			---	---		
RN-1	1.721	1.953	0.337	1.326	1.370	0.277	0.395	0.298	0.461	0.321
RN-2	1.721			1.047			0.674	0.644		
RN-3	2.512			1.767			0.744	0.421		
RN-4	1.640			1.465			0.174	0.119		
RN-5	2.174			1.081			1.093	1.011		
RN-6	1.953			1.535			0.419	0.273		
RV-1	2.349	1.678	0.699	1.884	1.349	0.524	0.465	0.247	0.231	0.085
RV-2	1.733			1.326			0.407	0.307		
RV-3	---			---			---	---		
RV-4	---			---			---	---		
RV-5	0.953			0.837			0.116	0.139		
RV-6	---			---			---	---		
RC-1	2.062	2.235	0.257	1.926	1.866	0.297	0.136	0.071	0.208	0.117
RC-2	2.395			1.951			0.444	0.228		
RC-3	2.506			2.309			0.198	0.086		
RC-4	1.901			1.568			0.333	0.213		
RC-5	2.481			1.951			0.531	0.272		
RC-6	2.062			1.494			0.568	0.380		
RS-1	2.148	2.062	0.270	1.333	1.390	0.628	0.815	0.611	1.106	1.919
RS-2	2.383			0.432			1.951	4.514		
RS-3	1.975			1.864			0.111	0.060		
RS-4	2.148			2.037			0.111	0.055		
RS-5	---			---			---	---		
RS-6	1.654			1.284			0.370	0.288		
RX-E1	1.965	N/A		1.628	N/A		0.337	0.207	N/A	
RX-E2	2.081			1.488			0.593	0.398		
RV-E1	1.721			1.500			0.221	0.147		

Pyridine concentrations are listed in micromolar concentrations (μM). The concentration of NAD was calculated by subtracting the amount of NADH from that of the total pyridine concentration. '---' = missing data due to unsuccessful assaying of the sample, Conc = concentration, NAD = oxidised nicotinamide adenine dinucleotide, NADH = reduced nicotinamide adenine dinucleotide, SD = standard deviation. Rats and corresponding data points that were randomly excluded from the main study are listed at the bottom of the table in grey text and designated the codes RX-E1, RX-E2 and RV-E1 for rats from dose groups RX and RV respectively. The aforementioned rats were excluded based on the random number generator of STATISTICA™, and was applied consistently for all parameter data sets. Rats were treated with NN = no dose regimen, VX = vehicle and sacrificed, VN = vehicle and no dose, VV = vehicle and vehicle, VC = vehicle and CoQ_{10}, VS = vehicle and succinate, RX = rotenone and sacrificed, RN = rotenone and no dose, RV = rotenone and vehicle, RC = rotenone and CoQ_{10}, RS = rotenone and succinate.

Skeletal muscle pyridine data generated from the rat main study are presented in Table G.2. The descriptive statistics in the form of means and standard deviations are listed for each dose group. In addition to the pyridine data, protein concentrations were generated and the final pyridine data presented in terms of protein. Ten microlitres of the skeletal muscle preparations were used for the assaying of total pyridine concentrations and the reduced form, namely NADH. Therefore, the total pyridine and reduced pyridine (NADH) concentrations in terms of protein, namely $TP.prot^{-1}$ and $RP.prot^{-1}$, were obtained by multiplying the respective protein concentration (P_{CON}) value by the sample volume of 10 μL, and dividing the total and reduced pyridine concentrations (TP_{CON} and RP_{CON}) by this value. It should be noted the TP_{CON} and RP_{CON} are listed in micromolar concentrations, thus the $TP.prot^{-1}$ and $RP.prot^{-1}$ values were multiplied by a 10^3 to obtain amounts in nanomolar concentrations. Oxidised NAD concentrations ($OP.prot^{-1}$) were subsequently calculated and the NAD/NADH ratios determined accordingly.

Table G.2 Skeletal muscle pyridine data generated from the rat main study

Rat	Protein			Total pyridine				NADH				NAD	NAD/NADH (in terms of protein)		
	P_{CON}	Mean	SD	TP_{CON}	$TP.prot^{-1}$	Mean	SD	RP_{CON}	$RP.prot^{-1}$	Mean	SD	$OP.prot^{-1}$	Ratio	Mean	SD
NN-1	9.16	67.76	12.8	6.277	68.53	67.76	12.8	1.404	15.33	29.11	12.0	53.19	3.47	1.711	1.33
NN-2	8.76			6.426	73.36			1.468	16.76			56.60	3.38		
NN-3	8.44			4.638	54.96			2.489	29.50			25.46	0.86		
NN-4	9.30			4.723	50.81			2.766	29.75			21.06	0.71		
NN-5	7.85			5.787	73.72			2.830	36.05			37.67	1.05		
NN-6	9.37			7.979	85.19			4.426	47.25			37.94	0.80		
VX-1	7.99	95.62	13.5	7.277	91.02	95.62	13.5	2.191	27.41	35.91	13.6	63.61	2.32	1.854	0.68
VX-2	9.22			9.723	105.4			2.894	31.37			74.05	2.36		
VX-3	11.8			12.66	107.0			4.553	38.48			68.51	1.78		
VX-4	8.89			9.745	109.6			5.489	61.72			47.84	0.78		
VX-5	7.88			6.511	82.59			1.851	23.48			59.11	2.52		
VX-6	8.19			6.404	78.15			2.702	32.97			45.18	1.37		
VN-1	7.28	116.5	47.8	14.53	199.7	116.5	47.8	6.000	82.45	65.24	19.3	117.2	1.42	0.804	0.59
VN-2	8.48			8.745	103.1			5.766	67.97			35.12	0.52		
VN-3	7.92			6.851	86.46			4.000	50.48			35.98	0.71		
VN-4	8.39			10.53	125.6			4.000	47.68			77.87	1.63		
VN-5	9.19			5.468	59.48			4.553	49.52			9.951	0.20		
VN-6	8.55			10.66	124.7			7.979	93.35			31.37	0.34		
VV-1	9.25	83.16	17.3	9.745	105.3	83.16	17.3	3.191	34.49	32.16	7.18	70.83	2.05	1.659	0.62
VV-2	8.36			5.745	68.68			2.191	26.20			42.48	1.62		
VV-3	8.22			6.489	78.91			2.064	25.10			53.81	2.14		
VV-4	8.92			8.681	97.28			3.872	43.40			53.89	1.24		
VV-5	9.09			8.085	88.96			2.489	27.39			61.57	2.25		
VV-6	10.2			6.085	59.80			3.702	36.38			23.42	0.64		
VC-1	11.3	55.91	14.1	7.872	69.47	55.91	14.1	2.872	25.35	28.50	11.2	44.12	1.74	1.076	0.46
VC-2	10.9			7.064	64.65			4.766	43.62			21.03	0.48		
VC-3	10.4			4.149	39.74			2.000	19.16			20.58	1.07		
VC-4	10.1			3.830	38.06			1.596	15.86			22.20	1.40		
VC-5	9.73			5.383	55.32			2.617	26.89			28.42	1.06		
VC-6	11.0			7.489	68.22			4.404	40.12			28.10	0.70		

Table G.2 Skeletal muscle continued...

Rat	Protein			Total pyridine				NADH				NAD	NAD/NADH (in terms of protein)		
	P_{CON}	Mean	SD	TP_{CON}	$TP.prot^{-1}$	Mean	SD	RP_{CON}	$RP.prot^{-1}$	Mean	SD	$OP.prot^{-1}$	Ratio	Mean	SD
VS-1	8.84	64.15	17.2	6.766	76.54	64.15	17.2	1.915	21.66	30.59	10.62	54.88	2.53	1.249	0.89
VS-2	9.13			6.234	68.27			2.574	28.20			40.08	1.42		
VS-3	9.38			7.000	74.65			3.447	36.76			37.89	1.03		
VS-4	9.31			2.787	29.94			2.298	24.69			5.257	0.21		
VS-5	9.82			6.532	66.54			2.255	22.97			43.56	1.90		
VS-6	9.94			6.851	68.94			4.894	49.25			19.70	0.40		
RX-1	6.98	82.75	28.5	6.085	87.21	82.75	28.5	2.383	34.15	36.45	23.1	53.06	1.55	2.145	1.91
RX-2	7.29			7.596	104.2			3.447	47.29			56.92	1.20		
RX-3	7.23			5.957	82.39			3.319	45.91			36.49	0.79		
RX-4	8.51			10.23	120.3			5.915	69.54			50.78	0.73		
RX-5	7.83			3.277	41.86			0.489	6.252			35.61	5.70		
RX-6	8.75			5.298	60.52			1.362	15.56			44.97	2.89		
RN-1	7.84	104.0	21.0	10.30	131.3	104.0	21.0	6.170	78.68	51.66	20.5	52.64	0.67	1.143	0.46
RN-2	7.87			8.213	104.3			2.872	36.49			67.85	1.86		
RN-3	8.17			7.362	90.10			3.489	42.70			47.39	1.11		
RN-4	7.02			8.979	127.9			5.404	77.00			50.93	0.66		
RN-5	8.72			7.426	85.12			3.468	39.76			45.37	1.14		
RN-6	7.89			6.745	85.43			2.787	35.31			50.13	1.42		
RV-1	9.06	73.43	25.0	3.170	34.97	73.43	25.0	2.106	23.24	35.92	9.6	11.74	0.51	1.113	0.82
RV-2	9.31			4.617	49.58			3.915	42.04			7.541	0.18		
RV-3	8.91			7.617	85.53			4.362	48.98			36.55	0.75		
RV-4	7.59			6.872	90.56			2.298	30.28			60.28	1.99		
RV-5	8.81			7.362	83.54			3.617	41.05			42.50	1.04		
RV-6	7.75			7.468	96.40			2.319	29.93			66.46	2.22		
RC-1	9.26	43.77	17.9	2.170	23.44	43.77	17.9	0.787	8.50	26.88	12.6	14.94	1.76	0.763	0.58
RC-2	9.09			3.979	43.79			2.872	31.62			12.18	0.39		
RC-3	9.00			5.660	62.89			4.000	44.45			18.44	0.41		
RC-4	9.21			2.000	21.73			1.702	18.49			3.236	0.18		
RC-5	8.59			4.277	49.80			2.085	24.28			25.52	1.05		
RC-6	8.97			5.468	60.95			3.043	33.92			27.04	0.80		
RS-1	10.3	97.65	32.4	8.404	81.75	97.65	32.4	6.277	61.06	59.90	23.6	20.70	0.34	0.728	0.68
RS-2	8.51			8.319	97.72			5.255	61.73			35.99	0.58		
RS-3	8.97			10.62	118.4			3.426	38.19			80.17	2.10		
RS-4	8.91			3.915	43.95			2.745	30.81			13.14	0.43		
RS-5	9.46			10.04	106.2			6.723	71.10			35.10	0.49		
RS-6	8.99			12.40	137.9			8.681	96.52			41.40	0.43		
RX-E1	6.03	N/A		1.553	1.553	N/A		0.851	14.12	N/A		11.65	0.82	N/A	
RX-E2	6.78			6.681	6.681			2.170	31.99			66.49	2.08		
RV-E1	8.01			4.681	4.681			2.277	28.41			30.01	1.06		

Ratios were determined from final pyridine concentrations in nanomolar per microgram ($nM.\mu g^{-1}$) protein. The concentration of NAD was calculated by subtracting the amount of NADH from that of the total pyridine concentration. P_{CON} = protein concentration in terms of microgram per microlitre ($\mu g.\mu L^{-1}$), NAD = oxidised nicotinamide adenine dinucleotide, NADH = reduced nicotinamide adenine dinucleotide, $OP.prot^{-1}$ = oxidised pyridine concentration in terms of protein in nanomolar per microgram ($nM.\mu g^{-1}$) protein, RP_{CON} = reduced pyridine concentration in micromolar (μM), $RP.prot^{-1}$ = reduced pyridine concentration in terms of protein in nanomolar per microgram ($nM.\mu g^{-1}$) protein, SD = standard deviation, TP_{CON} = total pyridine concentration in micromolar (μM), $TP.prot^{-1}$ = total pyridine concentration in terms of protein in nanomolar per microgram ($nM.\mu g^{-1}$) protein. Rats and corresponding data points that were randomly excluded from the main study are listed at the bottom of the table in grey text and designated the codes RX-E1, RX-E2 and RV-E1 for rats from dose groups RX and RV respectively. The aforementioned rats were excluded based on the random number generator of STATISTICA™, and was applied consistently for all parameter data sets. Rats were treated with NN = no dose regimen, VX = vehicle and sacrificed, VN = vehicle and no dose, VV = vehicle and vehicle, VC = vehicle and CoQ_{10}, VS = vehicle and succinate, RX = rotenone and sacrificed, RN = rotenone and no dose, RV = rotenone and vehicle, RC = rotenone and CoQ_{10}, RS = rotenone and succinate.

Table G.3 lists the liver tissue pyridine data generated from the rat main study. Mean and standard deviation statistics are also presented. Protein concentrations were also required for the determination of liver NAD/NADH ratios. Since 100 μL was used when assaying the total and reduced pyridine sample preparations, this factor was incorporated into the calculation of $TP.prot^{-1}$ and $RP.prot^{-1}$ values. Finally, the $OP.prot^{-1}$ concentrations and NAD/NADH ratios were calculated accordingly.

Table G.3 Liver tissue pyridine data generated from the rat main study

Rat	Protein			Total pyridine				NADH				NAD	NAD/NADH (in terms of protein)		
	P_{CON}	Mean	SD	TP_{CON}	$TP.prot^{-1}$	Mean	SD	RP_{CON}	$RP.prot^{-1}$	Mean	SD	$OP.prot^{-1}$	Ratio	Mean	SD
NN-1	4.21	4.05	0.26	0.929	2.207	2.466	0.773	0.327	0.777	0.551	0.317	1.429	1.839	10.19	15.40
NN-2	4.28			1.383	3.231			0.106	0.247			2.985	12.10		
NN-3	4.12			1.404	3.411			0.296	0.718			2.693	3.750		
NN-4	4.15			0.538	1.298			0.306	0.738			0.560	0.759		
NN-5	3.56			0.876	2.462			0.275	0.771			1.690	2.192		
NN-6	4.01			0.876	2.187			0.021	0.053			2.134	40.50		
VX-1	3.41	3.26	0.32	0.571	1.675	2.839	0.773	0.391	1.148	1.399	0.305	0.527	0.459	1.026	0.375
VX-2	3.38			0.803	2.373			0.423	1.249			1.124	0.900		
VX-3	2.67			0.962	3.594			0.507	1.896			1.698	0.896		
VX-4	3.14			1.173	3.736			0.518	1.649			2.087	1.265		
VX-5	3.56			1.057	2.971			0.412	1.159			1.812	1.564		
VX-6	3.42			0.919	2.684			0.444	1.296			1.388	1.071		
VN-1	3.71	3.37	0.33	1.035	2.793	3.150	0.460	0.412	1.111	1.290	0.458	1.681	1.513	1.678	0.889
VN-2	3.43			0.951	2.775			0.718	2.097			0.678	0.324		
VN-3	2.79			1.025	3.676			0.296	1.061			2.615	2.464		
VN-4	3.58			0.972	2.715			0.317	0.885			1.830	2.067		
VN-5	3.50			1.131	3.226			0.549	1.568			1.658	1.058		
VN-6	3.21			1.194	3.715			0.328	1.019			2.696	2.645		
VV-1	4.00	3.62	0.34	0.549	1.374	1.932	0.329	0.296	0.740	1.091	0.236	0.634	0.857	0.816	0.380
VV-2	3.24			0.697	2.153			0.275	0.848			1.305	1.538		
VV-3	3.68			0.771	2.098			0.444	1.207			0.891	0.738		
VV-4	3.36			0.655	1.952			0.423	1.259			0.693	0.550		
VV-5	3.40			0.592	1.743			0.402	1.183			0.560	0.474		
VV-6	4.04			0.919	2.275			0.528	1.307			0.967	0.740		
VC-1	4.47	3.93	0.43	0.370	0.827	1.592	0.406	0.285	0.638	0.667	0.346	0.189	0.296	2.159	2.194
VC-2	4.22			0.729	1.728			0.106	0.250			1.477	5.900		
VC-3	3.48			0.570	1.638			0.243	0.698			0.940	1.348		
VC-4	3.37			0.602	1.788			0.391	1.161			0.627	0.541		
VC-5	3.88			0.781	2.015			0.359	0.926			1.089	1.176		
VC-6	4.15			0.644	1.553			0.137	0.331			1.222	3.692		
VS-1	5.22	4.26	0.52	0.950	1.821	2.262	0.641	0.317	0.607	0.700	0.385	1.214	2.000	2.770	1.649
VS-2	4.23			1.362	3.223			0.581	1.374			1.849	1.345		
VS-3	4.08			0.824	2.021			0.169	0.414			1.606	3.875		
VS-4	3.62			1.024	2.828			0.327	0.904			1.924	2.129		
VS-5	4.23			0.644	1.524			0.243	0.575			0.949	1.652		
VS-6	4.21			0.908	2.155			0.137	0.326			1.829	5.615		

Table G.3 Liver tissue continued...

Rat	Protein			Total pyridine				NADH				NAD	NAD/NADH (in terms of protein)		
	P_{CON}	Mean	SD	TP_{CON}	TP.prot^{-1}	Mean	SD	RP_{CON}	RP.prot^{-1}	Mean	SD	OP.prot^{-1}	Ratio	Mean	SD
RX-1	2.93	3.55	0.63	1.934	6.593	7.961	3.448	0.507	1.729	2.037	0.563	4.864	2.812	2.826	0.916
RX-2	2.98			2.832	9.510			0.782	2.626			6.884	2.622		
RX-3	3.39			4.480	13.21			0.898	2.649			10.56	3.988		
RX-4	3.69			1.860	5.035			0.750	2.031			3.004	1.479		
RX-5	3.65			3.474	9.528			0.739	2.027			7.501	3.700		
RX-6	4.64			1.805	3.890			0.538	1.160			2.730	2.353		
RN-1	3.20	2.79	0.37	3.983	12.47	15.78	5.169	0.275	0.860	2.061	1.115	11.61	13.50	8.470	5.249
RN-2	2.19			1.817	8.296			0.433	1.978			6.319	3.195		
RN-3	2.58			5.177	20.07			1.025	3.972			16.09	4.052		
RN-4	3.08			6.826	22.13			0.613	1.987			20.14	10.14		
RN-5	2.90			4.015	13.86			0.718	2.480			11.38	4.588		
RN-6	2.81			5.008	17.85			0.306	1.092			16.76	15.34		
RV-1	3.76	3.39	0.30	2.483	6.603	8.383	4.749	0.666	1.770	1.686	0.748	4.833	2.730	4.793	4.209
RV-2	3.24			1.205	3.721			0.486	1.502			2.220	1.478		
RV-3	3.45			1.205	3.496			0.581	1.687			1.810	1.073		
RV-4	3.49			5.251	15.05			0.465	1.332			13.71	10.30		
RV-5	3.49			3.011	8.632			0.275	0.787			7.845	9.962		
RV-6	2.89			3.695	12.80			0.876	3.036			9.765	3.217		
RC-1	3.93	3.75	0.26	1.869	4.751	5.523	2.438	0.190	0.483	1.103	0.570	4.268	8.833	4.909	3.017
RC-2	3.80			1.204	3.166			0.190	0.500			2.666	5.333		
RC-3	3.75			1.879	5.012			0.486	1.295			3.717	2.870		
RC-4	3.48			1.130	3.247			0.475	1.366			1.882	1.378		
RC-5	4.11			3.716	9.037			0.412	1.001			8.036	8.026		
RC-6	3.42			2.713	7.925			0.676	1.974			5.952	3.016		
RS-1	4.46	3.76	0.46	1.362	3.056	4.871	2.222	0.348	0.782	1.144	0.299	2.274	2.909	3.208	1.152
RS-2	3.12			1.869	5.988			0.359	1.150			4.838	4.206		
RS-3	3.89			1.647	4.237			0.538	1.385			2.852	2.059		
RS-4	3.80			1.299	3.421			0.306	0.807			2.615	3.241		
RS-5	3.89			1.415	3.638			0.475	1.222			2.416	1.978		
RS-6	3.41			3.030	8.886			0.517	1.517			7.369	4.857		
RX-E1	3.75	N/A		1.511	1.511	N/A		1.194	3.184	N/A		0.845	0.265	N/A	
RX-E2	3.57			1.733	1.733			0.475	1.333			3.526	2.644		
RV-E1	2.93			2.039	2.039			0.518	1.767			5.194	2.939		

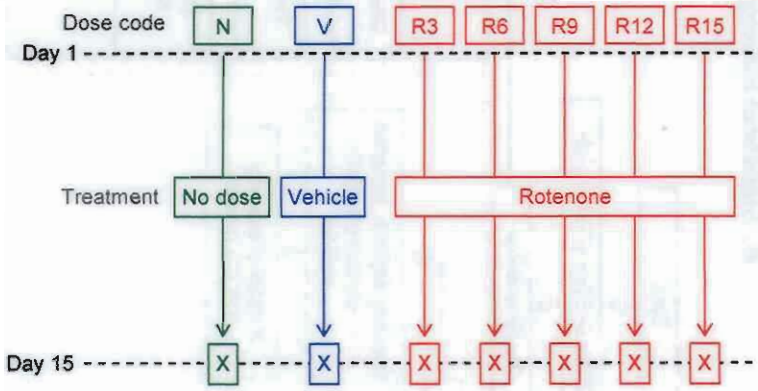
Ratios were determined from final pyridine concentrations in nanomolar per microgram (nM.μg^{-1}) protein. The concentration of NAD was calculated by subtracting the amount of NADH from that of the total pyridine concentration. P_{CON} = protein concentration in terms of microgram per microlitre (μg.μL^{-1}), NAD = oxidised nicotinamide adenine dinucleotide, NADH = reduced nicotinamide adenine dinucleotide, OP.prot^{-1} = oxidised pyridine concentration in terms of protein in nanomolar per microgram (nM.μg^{-1}) protein, RP_{CON} = reduced pyridine concentration in micromolar (μM), RP.prot^{-1} = reduced pyridine concentration in terms of protein in nanomolar per microgram (nM.μg^{-1}) protein, SD = standard deviation, TP_{CON} = total pyridine concentration in micromolar (μM), TP.prot^{-1} = total pyridine concentration in terms of protein in nanomolar per microgram (nM.μg^{-1}) protein. Rats and corresponding data points that were randomly excluded from the main study are listed at the bottom of the table in grey text and designated the codes RX-E1, RX-E2 and RV-E1 for rats from dose groups RX and RV respectively. The aforementioned rats were excluded based on the random number generator of STATISTICA™, and was applied consistently for all parameter data sets. Rats were treated with NN = no dose regimen, VX = vehicle and sacrificed, VN = vehicle and no dose, VV = vehicle and vehicle, VC = vehicle and CoQ_{10}, VS = vehicle and succinate, RX = rotenone and sacrificed, RN = rotenone and no dose, RV = rotenone and vehicle, RC = rotenone and CoQ_{10}, RS = rotenone and succinate.

QUICK REFERENCE

Evaluation of the effects of coenzyme Q10 and succinate in a rotenone-induced complex I deficient rat model

Marco Alessandrini
2006

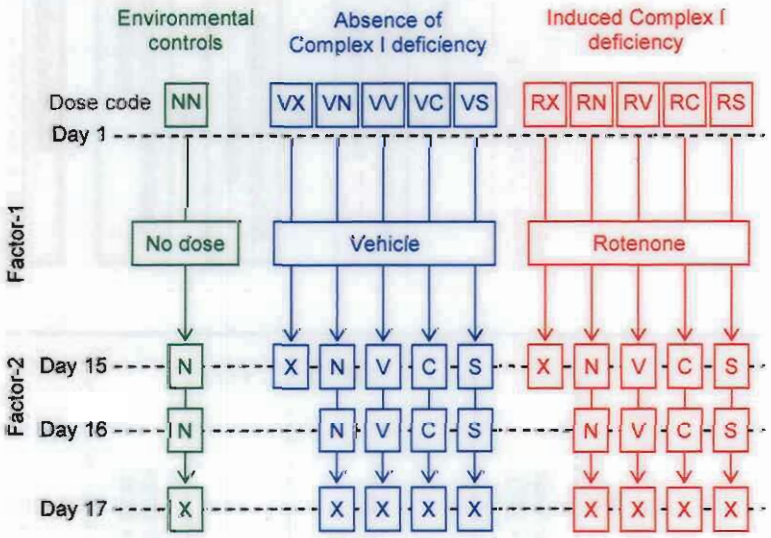
1. Rat PILOT Study Design (Figure 4.1, page 46)



Treatment of Rats

N = no dose
V = vehicle
R3 = rotenone 3 $mg.kg^{-1}.day^{-1}$
R6 = rotenone 6 $mg.kg^{-1}.day^{-1}$
R9 = rotenone 9 $mg.kg^{-1}.day^{-1}$
R12 = rotenone 12 $mg.kg^{-1}.day^{-1}$
R15 = rotenone 15 $mg.kg^{-1}.day^{-1}$

2. Rat MAIN Study Design (Figure 4.2, page 47)



Factors

Factor-1 = dose regimens received from days 1 to 14
Factor-2 = dose regimens received on days 15 and 16

Treatment of Rats

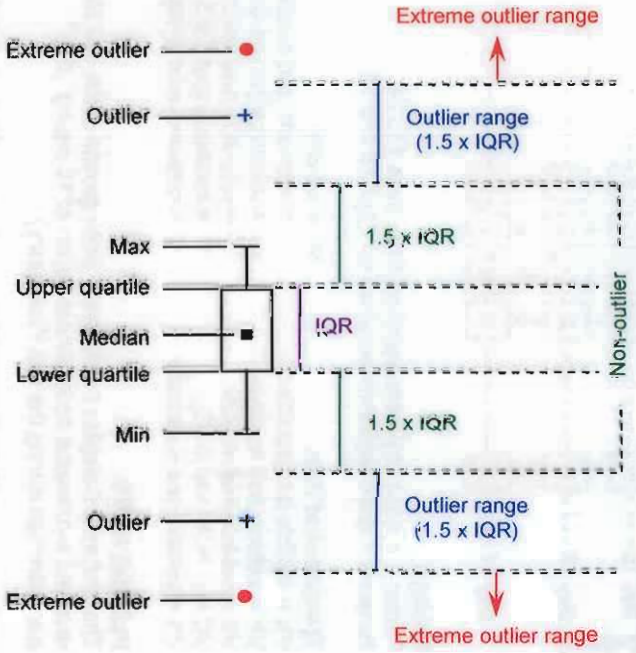
NN = no dose
VX = vehicle and sacrificed
RX = rotenone and sacrificed
VN = vehicle and no dose
RN = rotenone and no dose
VV = vehicle and vehicle
RV = rotenone and vehicle
VC = vehicle and CoQ_{10}
RC = rotenone and CoQ_{10}
VS = vehicle and succinate
RS = rotenone and succinate

PLEASE NOTE

The 'Induced Complex I deficiency' dose groups of the Rat Main Study received a rotenone dose concentration of 15 $mg.kg^{-1}.day^{-1}$ (as optimised during the Rat Pilot Study).

3. **Box-whisker plot** and data ranges

(Figure 4.4, page 61)



4. **Statistical Strategy** for Rat PILOT and MAIN studies

(Figure 4.3, page 60)

